N.M. Patrikalakis
C. Chryssostomidis

Theoretical and Experimental Prediction of the Response of a Marine Riser Model in a Uniform Stream

MIT Sea Grant Program

Massachusetts Institute of Technology
Cambridge
Massachusetts 02139

Report Number
MITSG 83-15
August 1983

THEORETICAL AND EXPERIMENTAL PREDICTION OF THE RESPONSE OF A MARINE RISER MODEL IN A UNIFORM STREAM

by

N. M. Patrikalakis

and

C. Chryssostomidis

MIT Sea Grant Report No. 83-15

August, 1983

ABSTRACT

The objective of this report is to provide:

1. A method for predicting the response of a riser in a uniform stream based on rigid cylinder experimental results.

2. An analysis of the experimental results obtained from a 3 m flexible riser model subjected to excitation from a uniform stream which is constant with depth and of speed between 100 and 465 mm/s.

3. A comparison of the experimental results from the flexible model with theoretical predictions of the response based on rigid cylinder experimental results.

ACKNOWLEDGEMENTS

Funding for this research was obtained from the MIT Sea Grant College Program, Conoco, Inc. and Gulf Oil Company. All experiments were performed at the Laboratory for Hydrodynamics of the National Technical University of Athens, Greece. K. Ho helped in the preparation of the figures of this report. The typed manuscript was prepared by P. McSweeney.

RELATED SEA GRANT REPORTS

1. "Theoretical and Experimental Prediction of the Response of a Marine Riser Model Subjected to Sinusoid Excitation of its Top End with Amplitude Equal to Two Diameters", C. Chryssostomidis, N. M. Patrikalakis and E. A. Vrakas, MIT Sea Grant Report No. 83-2, March 1983.

2. "Theoretical and Experimental Prediction of the Response of a Marine Riser Model Subjected to Sinusoid Excitation of its Top End with Amplitude of Two Diameters Parallel to a Uniform Stream of Speed Equal to 120 mm/s", C. Chryssostomidis and N. M. Patrikalakis, MIT Sea Grant Report No. 83-3, March 1983.

3. "Theoretical and Experimental Prediction of the Response of a Marine Riser Model Subjected to Sinusoid Excitation of its Top End with Amplitude of Two Diameters Parallel to a Uniform Stream of Speed Equal to 240 mm/s", C. Chryssostomidis and N. M. Patrikalakis, MIT Sea Grant Report No. 83-4, March 1983.

4. "Theoretical and Experimental Prediction of the Response of a Marine Riser Model Subjected to Sinusoid Excitation of its Top End with Amplitude of Two Diameters Orthogonal to a Uniform Stream of Speed Equal to 120 mm/s", N. M. Patrikalakis and C. Chryssostomidis, MIT Sea Grant Report No. 83-5, March 1983.

5. "Theoretical and Experimental Prediction of the Response of a Marine Riser Model Subjected to Sinusoid Excitation of its Top End with Amplitude of Two Diameters Orthogonal to a Uniform Stream of Speed Equal to 240 mm/s", N. M. Patrikalakis and C. Chryssostomidis, MIT Sea Grant Report No. 83-6, March 1983.

6. "Theoretical and Experimental Prediction of the Response of a Marine Riser Model Subjected to Sinusoid Excitation of its Top End Orthogonal to a Uniform Stream of Speed Equal to 42 mm/s", N. M. Patrikalakis and C. Chryssostomidis, MIT Sea Grant Report No. 83-18, August 1983.

7. "Theoretical and Experimental Prediction of the Response of a Marine Riser Model Subjected to Sinusoid Excitation of its Top End Parallel to a Uniform Stream", C. Chryssostomidis and N. M. Patrikalakis, MIT Sea Grant Report No. 83-19, August 1983.

8. "Theoretical and Experimental Prediction of the Response of a Marine Riser Model Subjected to Sinusoid Excitation of its Top End", C. Chryssostomidis and N. M. Patrikalakis, MIT Sea Grant Report No. 83-20, August 1983.

9. "Theoretical and Experimental Prediction of the Response of a Marine Riser Model Subjected to Sinusoid Excitation of its Top End Orthogonal to a Uniform Stream", N. M. Patrikalakis and C. Chryssostomidis, MIT Sea Grant Report No. 83-21, August 1983.

TABLE OF CONTENTS

Page Number

LIST OF TABLES

LIST OF FIGURES

1. PREDICTION OF THE RESPONSE OF A FLEXIBLE CYLINDER IN A UNIFORM STREAM USING RIGID CYLINDER EXPERIMENTS

1.1 Introduction

In this study we develop a method for the theoretical prediction of the static and lift responses of a flexible cylinder in a uniform stream. This method is based on rigid cylinder experimental results and assumes the following:

- There is no dynamic response parallel to the stream, and
- The dynamic response orthogonal to the stream is monochromatic.

A quantification of the validity of these assumptions can be found in Section 3 of this report where the results of our theoretical method are compared with experimental data obtained from a 3m flexible riser model.

Our theoretical method of prediction is based on an explicit relation between lift force and motion derived from experiments involving rigid cylinders forced to oscillate sinusoidally orthogonally to a uniform stream; see, for example, Mercier (1973) and Sarpkaya (1977a). When the frequency of imposed oscillation, $\hat{\omega}$, is within the range of synchronism, the measured lift force is practically monochromatic with frequency $\hat{\omega}$. The range of synchronism between the frequency of vortex "shedding" and oscillation is shown in Figure A-1. Within

this range, the measured lift force $F^X(\hat{t})$ is, usually, related to the cylinder motion, $x\sin\hat{\omega}\hat{t}$, by the following equation:

$$F^X(\hat{t}) = \rho A_e L c_m x\hat{\omega}^2 \sin\hat{\omega}\hat{t} - (4/3\pi)\,\rho D_e L c_d x^2\hat{\omega}^2 \cos\hat{\omega}\hat{t} \qquad (1)$$

where:

$F^X(\hat{t})$ denotes the measured overall lift force acting on the rigid cylinder of length, L, and outer (effective) diameter, D_e.

ρ is the fluid density

A_e $= \rho D_e^2/4$

The symbols c_m and c_d denote the experimentally determined added mass and drag coefficients.

For smooth cylinders, c_m and c_d depend upon the non-dimensional amplitude, x/D_e; the reduced velocity, $U^*=V_c/fD_e$; Reynolds number, $Re=V_cD_e/\nu$; the aspect ratio, $\lambda=L/D_e$ and end geometry. V_c denotes the stream speed, $f=\hat{\omega}/2\pi$ and ν is the kinematic viscosity of the fluid. In most rigid cylinder experiments the cylinder is fitted with circular end plates which are known to enhance the spanwise correlation of the hydrodynamic force, King (1977). Measured values for $c_M=c_m+1$ and c_d can be found in Figures A-2 and A-3, respectively as a function of U* parametrically with respect to x/D_e, taken from Mercier (1973). The Reynolds number in Mercier's experiments varied between 4,000 and 32,000, while most experiments were performed at Re=8,000. Mercier used cylinders fitted with end plates and aspect

ratios, λ=7 and 14, and measured the overall hydrodynamic force but did not provide estimates of its spanwise correlation. Information about the spanwise correlation in similar experiments can be found in Toebes (1969) and King (1977). By comparing Figures A-1 and A-3, we see that within the range of synchronism the drag coefficient becomes negative for small amplitudes, x/D_e, which implies that transfer of energy from the stream to a flexible cylinder is possible. Mercier (1973) also presented measured estimates of the overall average drag coefficient, c_D=Average Drag/0.5 $\rho D_e V_c^2 L$, as a function of $S_o=1/U^*$, parametrically with respect to x/D_e, see Figure A-4.

Outside the range of synchronism, the measured lift force in rigid cylinder experiments is no longer monochromatic, Moeller and Leehey (1982). Measurement of lift force components at frequencies other than the frequency of imposed oscillation cannot be used to predict response of flexible cylinders because there is no rigid cylinder motion at these other frequencies to relate lift force with motion, Patrikalakis (1983). Equation (1), however, can still be used to relate measured lift force at frequency, $\hat{\omega}$, to motion, $x\sin\hat{\omega}\hat{t}$.

The method described in this report can be extended to predict the dynamic response of a flexible cylinder parallel to a uniform stream, using, for example, the rigid cylinder results of Verley and Moe (1979). In addition, the method can provide estimates of the dynamic response of a flexible cylinder placed in a constant stream extending only over part of the length of the cylinder. For this case, the rigid cylinder results of Sarpkaya (1977b) need to be also employed. The details of

our method to predict static and lift responses of a flexible cylinder in a uniform stream are presented in the next Section. The particular geometry of an exploration riser is used as an example for the development of our method.

1.2 Static and Lift Responses of a Riser in a Uniform Stream

As shown in Patrikalakis (1983), the use of linear structural restoring forces is an acceptable approximation for the study of flexural oscillations of risers under the following basic assumptions: 1) low excited flexural modes, 2) small flexural displacements compared to the length, and 3) the presence of a slip joint. The outer geometry of the riser surface is assumed to be uniform, of effective diameter D_e. This is a good approximation due to the presence of uniform buoyancy modules over most of the length of the riser.

Under these assumptions, the governing partial differential equation for the lift motion, $\hat{u}(\hat{Z},\hat{t})$, is:

$$-EI\hat{u}_{\hat{Z}\hat{Z}\hat{Z}\hat{Z}} + [(We\ \hat{Z} + Pe(0))\hat{u}_{\hat{Z}}]_{\hat{Z}} + F^X(\hat{Z},\hat{t}) = M\hat{u}_{\hat{t}\hat{t}} - \Delta^X \qquad (2)$$

where

EI	denotes the bending rigidity
We	the average effective weight per unit length
Pe(0)	the effective overpull at the lower end, $\hat{Z}=0$
$F^X(\hat{Z},\hat{t})$	the hydrodynamic force per unit length orthogonal to the stream

M the average mass per unit length of the riser

Δ^X the structural damping force per unit length orthogonal to the stream

$\hat{Z}$ the elevation above the lower end of the riser

$\hat{t}$ the time, and

subscripts $\hat{Z}$ and $\hat{t}$ denote partial derivatives.

As stated in the previous Section, we will assume that the lift response is monochromatic. This means that the solutions of equation (2)

$$\hat{u}(\hat{Z},\hat{t}) = \mathrm{Im}[\hat{g}(\hat{Z})e^{i\hat{\omega}\hat{t}}] \tag{3}$$

where

$\mathrm{Im}[.]$ denotes the imaginary part

$\hat{g}(\hat{Z})$ is an unknown complex function of $\hat{Z}$, and

$\hat{\omega}$ is an unknown circular frequency of lift motion.

In all subsequent analysis omission of the superscript (^) from $\hat{g}$, $\hat{t}$, $\hat{u}$, $\hat{Z}$ and $\hat{\omega}$ will denote nondimensional quantities. Displacements are nondimensionalized with respect to D_e. $\hat{Z}$ is nondimensionalized with respect to the overall length of the riser, L. The time constant used in the nondimensionalization of time and response frequency is:

$$\tau_o = L[(M+A_e\rho)/Pe(0)]^{1/2} \tag{4}$$

Using equations (1) to (4), the governing equation describing the sinusoid lift response of a riser in a uniform stream can be brought to the following convenient nondimensional form:

$$-\varepsilon g''''+[(\mu Z+1)g']' + \frac{\omega^2(m+c_m)}{m+1} g = \frac{16}{3\pi^2} \frac{c_d i\omega^2}{(m+1)} |g|g + i\omega \sum_{n=1}^{\infty} c_n \Phi_n(Z) g_n \quad (5)$$

where

$$g_n = \int_0^1 \Phi_n(Z)g(Z)dZ \quad (6)$$

$$\varepsilon = EI/Pe(0)L^2 \quad (7)$$

$$\mu = WeL/Pe(0) \quad (8)$$

$$m = M/\rho A_e \quad (9)$$

$$c_n = \hat{c}_n L[(M+A_e\rho)Pe(0)]^{-1/2} \quad (10)$$

$\hat{c}_n$ denotes the structural damping coefficient for the nth flexural mode, n=1,2,3 ..., and

( )' denotes the derivative with respect to Z.

The boundary conditions assumed are zero displacement and curvature at both ends. This gives:

$$g(0) = g(1) = g''(0) = g''(1) = 0 \quad (11)$$

The orthonormalized eigenfunction $\Phi_n(Z)$ in equations (5) and (6), and the corresponding nondimensional eigenvalue σ_n defined with $c_m=1$ are the solution of equations (12) to (14), Patrikalakis (1983):

$$-\varepsilon\Phi_n'''' + [(\mu Z+1)\Phi_n']' + \sigma_n^2\Phi_n = 0 \tag{12}$$

$$\Phi_n(0) = \Phi_n(1) = \Phi_n''(0) = \Phi_n''(1) = 0 \tag{13}$$

$$\int_0^1 \Phi_p(Z)\Phi_q(Z)\, dZ = \delta_{pq} \tag{14}$$

where $\delta_{pq} = 1$ if $p = q$ and $\delta_{pq} = 0$, otherwise.

From equations (4) and (5) we see that the dimensional "natural frequencies" $\hat{\omega}_n=\sigma_n/\tau_o$.

We recognize that equations (5) and (11) define a nonlinear integrodifferential eigenvalue problem which can be brought to the form of an infinite set of nonlinear simultaneous equations:

$$(\sigma_p^2+i\omega c_p - \frac{m\omega^2}{m+1})g_p = \frac{\omega^2}{m+1}\sum_{k=1}^{\infty} g_k c_m^{pk} - \frac{16i\omega^2}{3\pi^2(m+1)}\sum_{k=1}^{\infty} g_k c_d^{pk} \tag{15}$$

where $p = 1,2\ldots,$

$$c_m^{pk} = \int_0^1 c_m(Z)\, \Phi_p(Z)\, \Phi_k(Z)\, dZ \tag{16}$$

$$C_d^{pk} = \int_0^1 c_d(Z)|g(Z)|\Phi_p(Z)\Phi_k(Z)dZ, \text{ and} \tag{17}$$

$$g(Z) = \sum_{n=1}^{\infty} g_n \Phi_n(Z) \tag{18}$$

In our solution, the coefficients $c_m(Z)$ and $c_d(Z)$ are non-linear functions of $|g(Z)|$ and U^*, where $U^* = 2\pi V_c \tau_o / \omega D_e$. No Reynolds number effects are included because no data is available. Equation (15) is obtained by

- Substituting equation (18) into equation (5),
- Simplifying the resulting equation with the aid of equations (12) to (14),
- Multiplying the resulting simplified equation by $\Phi_k(Z)$ and integrating from 0 to 1.

It is convenient to rewrite equation (15) in the following form:

$$\left[\frac{(m+1)}{U^{*2}_J}\left(\frac{\sigma_p}{\sigma_J}\right)^2 + \frac{i}{\pi}(m+1)\delta_p \frac{\sigma_p}{\sigma_J}\frac{1}{U^* U^*_J} - \frac{m}{U^{*2}}\right] g_p$$

$$= \frac{1}{U^{*2}} \sum_{k=1}^{\infty} g_k C_m^{pk} - \frac{16i}{3\pi^2}\frac{1}{U^{*2}} \sum_{k=1}^{\infty} g_k C_d^{pk} \tag{19}$$

valid for $p = 1,2\ldots$, where δ_p is a logarithmic decrement defined by:

$$\delta_p = \pi c_p / \sigma_p \tag{20}$$

and $U^*_J = 2\pi V_c \tau_o / \sigma_J D_e$, where J is a positive index, such that g_J is real.

Note that if g(Z) is expanded as shown in (18), then it is always possible to arrange for one of the g_n's to be real by an appropriate shift of the time origin in equation (3).

If the spectral expansion (18) is truncated as:

$$g(Z) \simeq \sum_{n=Q}^{N} \Phi_n(Z) g_n \qquad (21)$$

then equation (19) provides 2(N-Q+1) simultaneous equations for 2(N-Q+1) unknowns: U^*, g_n (n=Q,Q+1,...N), where g_n is complex except for n=J for which g_n is real, as explained before. The solution pair (g(Z);U*) depends upon:

1) The structural characteristics of the riser:

   m the mass to displaced fluid mass ratio

   σ_p the nondimensional "natural frequencies", p=1,2...

   δ_p the logarithmic decrement for the pth flexural mode, p=1,2..., which is proportional to the ratio of the structural damping force at the pth mode to the corresponding inertia force.

2) The product $U_J \sigma_J$, which is proportional to $\tau_o/(D_e/V_c)$.

3) The hydrodynamic parameters controlling c_m and c_d.

Monomodal solutions of (19) are investigated in this report. The order (J) of the mode used in the present solution scheme is selected a priori:

$$g(Z) \simeq g_J \Phi_J(Z) \tag{22}$$

where $g_J \geq 0$.

If we let:

$$\hat{C}_m = \int_0^1 c_m(Z)\Phi_J^2(Z)dZ \tag{23}$$

$$\hat{C}_d = \int_0^1 c_d(Z)|\Phi_J^3(Z)|dZ \tag{24}$$

then equation (19) provides the following two simultaneous nonlinear equations for U* and nonzero values of g_J:

$$\frac{m+\hat{C}_m}{U^{*2}} = \frac{m+1}{U^{*2}_J} \tag{25}$$

$$\frac{g_J\hat{C}_d}{U^*} = -\frac{3\pi}{16}(m+1)\frac{\delta_J}{U^*_J} \tag{26}$$

It can be verified that the expression of $\hat{C}_m$ given by equation (23) satisfies the following equation:

$$\int_0^L d\hat{Z} \int_0^{2\pi/\hat{\omega}} d\hat{t}\ \{\rho A_e \hat{u}_{\hat{t}\hat{t}}[\hat{C}_m - c_m(\hat{Z})]\}^2 = \text{minimum}$$

Thus, $\hat{C}_m$ corresponds to an overall mean square best fit of the local added mass force distribution. Rewriting equation (25) as

$$\omega = \sigma_J/\tau \tag{27}$$

where

$$\tau = L[(M+\hat{C}_m A_e \rho)/Pe(0)]^{1/2} \tag{28}$$

we see that the response frequency is equal to the square root of the restoring to the inertia force. This is valid in general for the "limit cycle" response of all mechanical systems when there is no external excitation at a fixed characteristic frequency. "Mechanical system" in our case means the combination of the flexible cylinder and flowing fluid and the inertia force, therefore, includes both structural inertial forces and added mass forces. Equation (26) expresses the energy balance between the energy generated and dissipated by the flow, see equation (24), and the energy dissipated due to structural losses. Equations (23) and (24) and numerical values from Figures A-2 and A-3 indicate the insensitivity of the response to local phenomena, particularly forces from portions of the length where the response amplitude is very small, e.g., near the nodes of motion.

Inspection of Figure A-3 and the fact that $\delta_J>0$, leads to the conclusion that equation (26) admits solutions for g_J less than approximately 1, and reduced velocities U* near 5. In order for (22) to be a reasonable approximation of the general solution, the above

implies that U^*_J should also be close to 5. The above conclusions are also substantiated from experiments involving flexible cylinders, King (1977) and Vandiver (1983).

The numerical solution of (25) and (26) with direct iteration, i.e. by solving (25) for U* and (26) for g_J, is not expected to work because of the large derivatives of c_m and c_d in the area of interest, see Dahlquist and Björck (1974). Good approximations of the solution can be obtained as follows. We define an increasing sequence of likely reduced velocities $U^*=U^*_i$, i=1,2,...m for each of which we solve (25) and (26) separately for g_J. The solutions can be isolated easily by bisection. If $g_J^{(1i)}$ and $g_J^{(2i)}$ are the solutions of (25) and (26) respectively for a fixed U^*_i, the sequence $d_i=g_J^{(1i)}-g_J^{(2i)}$ can be examined to determine the index j for which $d_j d_{j+1}\leq 0$. If d_j or $d_{j+1}=0$, the solution concludes. If not, the estimate $\hat{U}^*=(1+\psi)^{-1}U^*_{j+1}+\psi(1+\psi)^{-1}U^*_j$, where $\psi=|d_{j+1}/d_j|$ and a corresponding estimate for g_J at U* is found from one of the equations. If the sequence U^*_i is closely spaced, then the procedure suggested above isolates the solution with good approximation.

Once an estimate of the lift response is available, Figure A-4 provides estimates of the local average drag coefficients, $c_D(Z)$, which can be employed to estimate the static response. In our solution, the average drag coefficient is a nonlinear function of $|g(Z)|$ and U*. As before, no Reynolds number effects are included

because no data is available. The nondimensional static displacement, $v(Z)$, is, therefore, the solution of the following boundary value problem, Patrikalakis (1983):

$$-\varepsilon v'''' + [(\mu Z+1)v']' + F^{Y}(Z) = 0 \qquad (29)$$

with boundary conditions

$$v(0) = v(1) = v''(0) = v''(1) = 0 \qquad (30)$$

where $F^{Y}(Z)$ is defined by:

$$F^{Y}(Z) = c_{D}(Z)\, \kappa\, \lambda$$

where

$$\lambda = L/D_{e}$$

$$\kappa = 0.5\rho D_{e} L V_{c}^{2}/Pe(0)$$

Equations (29) and (30) can be solved in terms of Airy functions or by finite differences. Our solution uses finite differences.

An interesting extension of our solution scheme is to investigate multimode solutions of equations (19). This extension will not affect our present predictions of maximum lift responses, which are already good as the results of Section 3 indicate. However, the

extended capability for multimode solutions should prove useful in estimating the response when more than one mode is excited.

Before concluding this Section we should mention that it is possible to estimate a relation between lift force and motion using spring mounted rigid cylinder experiments in which the cylinder is permitted to respond orthogonally to a uniform stream; see for example, Dean et al. (1977). For the range of velocities for which the response motion of the spring mounted cylinder is monochromatic, the estimates of the relation between lift force and motion derived from rigid cylinder and spring mounted rigid cylinder experiments are similar. Sarpkaya (1977a), for example, has calculated the maximum response amplitude of a rigid, spring mounted cylinder permitted to respond orthogonally to a uniform stream using his forced motion data. He found that the calculated values underpredict the measured maximum amplitudes by no more than 21%. This can be partially explained because Reynolds number, aspect ratios and end conditions were not scaled exactly. The method of prediction of motion of a spring mounted rigid cylinder using forced motion rigid cylinder results, described in Sarpkaya (1977a) - involving time integration - can be simplified if the monochromatic character of lift motion is invoked a priori. For completeness, this simplified approach is developed in Appendix B of this report.

2. A DESCRIPTION OF THE RISER MODEL

Our model is made up of an aluminum tube covered externally with a sealing material. The overall model characteristics are:

- Length between ball joints (L) = 3.000 m
- Aluminum tube I.D. (D_i) = 10.92 mm
- Aluminum tube O.D. (D_o) = 12.61 mm
- External sealing (effective) diameter (D_e) = 15.3 mm
- Average mass per unit length (M) = 0.327 kg/m
- Average effective weight per unit length (We) = 1.378 N/m
- Effective overpull at the lower ball joint (Pe(0)) = 1.72 N
- Bending stiffness of a cross section (EI) = 37.6 Nm^2

The inside of the aluminum tube is filled with a glycerin solution in water of density approximately equal to 900 kg/m^3. At the ends of the model there are ball joints which minimize the end bending moments. Above the upper ball joint there is a slip joint, which is designed to minimize tension variations due to flexural motions. The riser model is also designed so it can be tensioned to the desired tension. The first four "natural frequencies" of the model in water are approximately equal to 1.57, 6.06, 13.54 and 24.02 Hz, respectively. These have been determined theoretically using c_m=1. The first two "natural frequencies" have been also verified from a decay test in quiescent water, where the initial amplitude of the response was of the order of 1/10 of the effective diameter.

The model is instrumented at ten equidistant locations, 1-10, each with two strain gauge full bridges installed on the outer surface of the aluminum tube, designed to isolate bending from tension and to measure bending strains on two orthogonal directions A and B. In the vertical static equilibrium condition, planes A and B are parallel and orthogonal to the centerline of the towing tank, respectively. The actual location of each branch of the bending bridges is at approximately 9.80 degrees from planes A and B. The numbering of the bridges begins at the upper end, while their elevation is measured from the axis of the lower ball joint. The first and last bending bridges are L/11 from the axes of the top and bottom ball joints, respectively, and the separation between bending bridges is L/11. For example, bridge A6 measures bending strains created by deflections in plane A at elevation Z=5L/11 from the axis of the lower ball joint. In addition, the model is instrumented at two extra positions, T1 and T2, 101 mm from the axes of each ball joint, with specially designed full bridges isolating tension from bending. Tension bridge T2 is at the lower end of the model. Finally, the model is instrumented at an additional location, Q1, 1773 mm from the upper ball joint, with a full torsion bridge. The mass per unit length of a single wire is 0.198 grams/m, while the total mass of all wires for all 23 full bridges is approximately 2.73% of the total model mass. Their total volume is approximately equal to 5.32 cm^3. The four wires of each bridge are braided to avoid interference and are sent internally to the lower end of the model.

The top end of the model is capable of being oscillated by a DC motor driven by a signal generator and controlled by a tachometer measuring angular velocities and a linear variable differential transducer, LVDT, measuring displacements. The rotational motion of the motor is converted to linear motion via a specially designed rack anti-backlash pinion system. During the experiments, measurements from a number of strain bridges and the LVDT were made simultaneously and were recorded digitally. Using the torque bridge, it was observed that the structural torsion was negligible, see Chapter III of Patrikalakis (1983). It was estimated analytically, and also confirmed by the tension bridge measurements, that the tension variation during the experiments was small, approximately 5% of the effective tension. Therefore, even for the lowest excited mode, the ratio of the change of restoring force due to tension variation to the overall restoring force is very small (0.3%). This implies that the assumption of constant effective tension with time is an acceptable approximation for theoretical estimates of the response.

From calibration experiments in air, it was found that the logarithmic decrement representing the structural damping force is a nonlinear function of the modal amplitude. For the first mode, our estimate for the logarithmic decrement representing the structural damping force in water, δ_1, is given by $\delta_1=A+B^3/(\alpha_1^3+C^3)$, where A=0.0664, B=0.1989, C=0.3533, and α_1 is the amplitude of the first mode in effective diameters. The corresponding estimate for the

second mode, δ_2, is given by $\delta_2=D+E^3/(\alpha_2^3+F^3)$, where D=0.0404, E=0.0431, F=0.1186 and α_2 is the amplitude of the second mode. The range of α_1 used to estimate δ_1 is between 0.17 and 1.28 D_e and the range of α_2 used to estimate δ_2 is between 0.11 and 0.26 D_e. Our experiments in air also revealed that when the upper end of the model was oscillated in a certain plane, some flexural response orthogonal to this plane existed. This happens because our model was not rotationally uniform. When the response was primarily at the first mode, it was estimated that the flexural response orthogonal to the direction of excitation was not larger than approximately 12% of the response in the plane of applied oscillation. It was felt that such an imperfection would not substantially affect the experimental results in water.

3. PRESENTATION OF EXPERIMENTAL AND THEORETICAL RESULTS

The experiments presented in this report involve excitation of our riser model from a uniform stream which is constant with depth and of speed V_c between 100 and 465 mm/s. The measured values of V_c studied are shown in Table 3.1 together with our estimates of the variability of V_c during each of our experiments. In each experiment, the current speed was achieved by accelerating the towing carriage from rest to the desired value of V_c. The water temperature for all experiments analyzed in this report is 15^oC. Additional information for our experimental results can be found in Table 3.2. During our experiments, simultaneous measurements of bending strains in planes A and B at elevations Z=2L/11, 4L/11, 5L/11 and 8L/11 were recorded digitally. For experiments 110 and 111, digital signals from all bridges; and for experiment 98, the digital signal from bridge B3 were accidentally destroyed.

The experimental and theoretical results reported here include plots of

1. The root mean square measured dynamic bending strains as a function of the response frequency and the measured static bending strains.
2. The measured and theoretical predictions of the bending strains parallel and orthogonal to the stream.
3. The measured maximum bending strains parallel and orthogonal to the stream and independent of direction.
4. Indicative partial synchronous time traces of measured bending strains from four bridges.

EXPERIMENT IDENTIFICATION NUMBER	NOMINAL CURRENT SPEED V_c(mm/s)	MAXIMUM MEASURED CURRENT SPEED V_{max}(mm/s)	MINIMUM MEASURED CURRENT SPEED V_{min}(mm/s)	VARIABILITY $\frac{V_{max}-V_{min}}{V_c} \times 100$
96	100	102.3	99.8	2.50
98	105	105.9	104.4	1.43
100	110	111.1	109.6	1.36
102	115	117.3	115.7	1.39
104	120	121.1	119.2	1.58
106	125	125.9	124.3	1.28
114	130	133.3	131.1	1.69
108	135	137.7	134.7	2.22
113	140	141.5	139.1	1.71
110	150	150.7	147.6	2.07
111	170	173.6	169.9	2.18
109	190	191.0	187.5	1.84
107	210	214.8	211.7	1.48
105	220	224.0	219.4	2.09
103	230	232.1	227.7	1.91
101	240	243.0	239.4	1.50
99	250	252.3	248.8	1.40
97	300	302.4	298.7	1.23
95	350	354.2	347.7	1.86
112	385	387.8	381.8	1.56
115	410	412.6	407.5	1.24
116	430	432.2	428.9	0.77
117	465	465.9	462.0	0.84

Table 3-1 Experiment Identification and Measured Current Speeds

EXPERIMENT IDENTIFICATION NUMBER	NOMINAL CURRENT SPEED V_c(mm/s)	Re= $V_c D_e/\nu$	MEASUREMENT TIME SPAN (SECONDS)	MEASURED PRIMARY LIFT RESPONSE FREQUENCY f_r(Hz)	MEASURED $U^*= V_c/f_r D_e$
96	100	1340	34.10	1.377	4.747
98	105	1410	34.10	1.230	5.580
100	110	1480	34.10	1.318	5.455
102	115	1540	34.10	1.318	5.703
104	120	1610	34.10	1.318	5.951
106	125	1680	34.10	1.348	6.061
114	130	1750	34.10	1.289	6.592
108	135	1810	34.10	1.318	6.695
113	140	1880	34.10	1.318	6.943
110	150	2010	29*	1.64*	5.99*
111	170	2280	29*	1.96*	5.67*
109	190	2550	34.10	2.080	5.970
107	210	2820	34.10	2.109	6.508
105	220	2950	34.10	2.139	6.722
103	230	3090	34.10	2.139	7.028
101	240	3220	34.10	2.139	7.334
99	250	3360	34.10	2.168	7.537
97	300	4030	34.10	NOT PERIODIC	
95	350	4700	34.10	NOT PERIODIC	
112	385	5170	34.10	NOT PERIODIC	
115	410	5500	17.05	NOT PERIODIC	
116	430	5770	17.05	NOT PERIODIC	
117	465	6240	17.05	4.688	6.483

*Experimental estimates were made based on the T-Figures.

Table 3-2 Description of Experiments and Information for the Measured Lift Response

The root mean square measured bending strains as a function of the response frequency from all bridges in experiment 96 and from bridges A9, A7 and A3 of experiment 102 were omitted because they were very small. For experiments 110 and 111, the time traces of measured bending strains were used to provide estimates of the primary lift response frequency, and the amplitude of bending strain parallel and orthogonal to the stream.

The root mean square responses have been calculated using standard FFT codes from the International Mathematical and Statistical Library (1981) on an IBM 370/168 computer. The root mean square response is the square root of the product of the power spectral density of the response times the effective bandwidth B_e employed in the Fourier analysis of the results. The root mean square rather than the magnitude of the power spectral density was selected for presentation because, in most cases, the experimental response was practically periodic. The logarithmic representation of the power spectral density was not selected because it tends to visually exaggerate the significance of smaller components, which are not important in this problem. For each major peak of the root mean square plots, the root mean square value of the response is shown. This is computed as the square root of the sum of the squares of the rms response strains at discrete frequencies, B_e Hz apart, in the neighborhood of each peak. In addition, the overall dynamic root mean square value of the response is shown together with the static bending strain response. The Fourier and maxima calculations were performed using the record length shown

in Table 3-2. The nomenclature used in the Figures and Tables 3-1 to 3-2 is defined below:

The experiment number corresponds to the numbering system employed during the performance of the experiments. BE is the effective bandwidth B_e employed in the Fourier analysis in Hz. VC is the nominal stream speed V_c in mm/s. FR is the primary lift response frequency f_r in Hz. A/DE is the ratio of the amplitude A of the excitation of the top end divided by the effective diameter D_e, which is zero for all experiments reported here. U_r^* is the response reduced velocity defined by $U_r^* = V_c/f_r D_e$ and $Re = V_c D_e/\nu$, where ν is the kinematic viscosity of fresh water.

The Figures of root mean square measured bending strains are referred to by the experiment identification number and the bridge name. The Figures showing the measured and theoretical predictions and maxima are referred to by the experiment identification number and the plane name. Figures showing the time traces are referred to by the experiment identification number and the letter T (trace).

Table 3.3 provides information about the theoretical prediction of the lift response at f_r and of the static response in plane A. The theoretical estimates of f_r and of the amplitude of motion in plane B are obtained as described in Section 1.2 of this report. Our present prediction of lift response is monomodal. For velocities less or equal to 150 mm/s, we used the first mode and for velocities greater or equal to 300 mm/s the second. Under the assumption of monomodal response, we have been unable to find a nontrivial solution for the

EXPERIMENT IDENTIFICATION NUMBER	U_1^*	U_2^*	$\hat{C}_m$	$\hat{C}_d^*$	$\hat{e}_D$	100δ	CALCULATED α	CALCULATED f_r	CALCULATED U_r^*
96	4.16	1.08	2.121	-0.325	1.40	9.17	0.644	1.325	4.932
98	4.37	1.13	2.011	-0.233	1.50	8.12	0.786	1.344	5.105
100	4.58	1.19	1.788	-0.200	1.60	7.82	0.855	1.386	5.188
102	4.79	1.24	1.513	-0.185	1.60	7.74	0.877	1.443	5.211
104	5.00	1.29	1.267	-0.173	1.60	7.67	0.896	1.500	5.230
106	5.20	1.35	1.050	-0.162	1.65	7.61	0.914	1.556	5.250
114	5.41	1.40	0.864	-0.151	1.70	7.55	0.937	1.610	5.277
108	5.62	1.46	0.706	-0.141	1.70	7.47	0.966	1.660	5.314
113	5.83	1.51	0.578	-0.130	1.70	7.38	1.005	1.705	5.367
	5.83	1.51	0.559	0	1.70	0	1.072	1.712	5.346
110	6.24	1.62	0.440	-0.119	1.75	7.28	1.057	1.757	5.579
111	7.08	1.83	---	---	0.97	---	---	---	---
109	7.91	2.05	---	---	0.97	---	---	---	---
107	8.74	2.27	---	---	0.96	---	---	---	---
105	9.16	2.37	---	---	0.95	---	---	---	---
103	9.58	2.48	---	---	0.95	---	---	---	---
101	9.99	2.59	---	---	0.95	---	---	---	---
99	10.41	2.70	---	---	0.94	---	---	---	---
97	12.49	3.24	2.704	-0.340	1.20	4.30	0.310	4.771	4.110
95	14.57	3.78	2.423	-0.194	1.30	4.10	0.501	4.929	4.642
112	16.03	4.15	2.068	-0.132	1.40	4.06	0.698	5.151	4.885
115	17.07	4.42	1.956	-0.104	1.55	4.05	0.872	5.228	5.126
116	17.90	4.64	1.673	-0.097	1.60	4.05	0.902	5.437	5.169
117	19.36	5.02	1.220	-0.087	1.65	4.05	0.933	5.833	5.210

Table 3-3 Information for the Theoretical Predictions for Lift and Static Responses

response in plane B for stream velocities above 150 and less than 300 mm/s. From the results of our experiments, we observe that, as the speed increases, the spanwise maximum lift response attains local maxima at certain speeds. These local maxima occur when the lift response is essentially monomodal and monochromatic. Our theoretical procedure is based on these assumptions and therefore, our estimates of the maximum lift response are good. This can be verified from the results of our experiments. For speeds on either side of the speeds that correspond to the local maxima, the prediction is not as good. This occurs because the lift response at these speeds is no longer monomodal and monochromatic, and because of increased correlation effects, King (1977), Sarpkaya (1979).

For all experiments with stream speeds less or equal to 150 mm/s or greater or equal to 300 mm/s, the theoretical predictions of Table 3-3 are derived from the results of Mercier (1973). The rigid cylinder derived hydrodynamic coefficients c_m, c_d and c_D, employed in the determination of $\hat{C}_m$, $\hat{C}_d^*$, and $\hat{c}_D$ of Table 3-3 are shown in Figures A-2, A-3 and A-4 respectively. The value of C_d^* is defined by

$$\hat{C}_d^* = \hat{C}_d \Big/ \int_0^1 |\Phi_J^3(Z)| dZ$$

which for $\Phi_J(Z) = \sqrt{2} \sin(J\pi Z)$ leads to $C_d^* = 3\pi \sqrt{2}\, \hat{C}_d/16$ where $\hat{C}_d$ is defined by equation (24). Sinusoid mode shapes are excellent approximations of the actual mode shapes of our model.

The Reynolds number in Mercier's experiments used to derive C_m, C_d and c_D was, for the most part, equal to 8000. The amplitude-to-diameter ratio of the imposed motion was less than 1.3 for c_d and c_m and less than 1.5 for c_D. In the computation of $\hat{C}_m$, $\hat{C}_d^*$ and $\hat{c}_D$ no Reynolds number correction was included and linear extrapolation was used for amplitude-to-diameter ratios outside the domain of existing data. The average drag coefficient used, $\hat{c}_D$, corresponds to the average calculated motion in the B plane. In Table 3-3, the symbol "α" denotes the amplitude of the first or the second mode in D_e, and δ the logarithmic decrement for structural damping used.

For all experiments with stream speeds greater than 150 mm/s and less than 300 mm/s, the theoretical prediction of the average drag coefficient $\hat{c}_D$ shown in Table 3-3 is derived from Figure A-5 taken from Bishop and Hassan (1964). With available rigid cylinder results we cannot estimate the amplitude of dynamic response in plane A. However, when the response in plane B is periodic, the dynamic response in plane A is primarily at f_r and 2 f_r, which is in agreement with rigid cylinder measurements.

A summary of the results for the response in plane B is shown in Figures 96B, 98B, 100B, 102B, 104B, 106B, 114B, 108B, 113B, 110B, 111B, 109B, 107B, 105B, 103B, 101B, 99B, 97B, 95B, 112B, 115B, 116B and 117B. These include the theoretical and measured dynamic response strain at the corresponding values of f_r, and the maximum

measured dynamic response strain in plane B. Our theoretical estimate of the maximum response in plane B is the same as our estimate of the dynamic lift response at f_r. For all estimates of the lift response the structural damping characteristics of the model described in Section 2 of this report were used. These are based on the amplitude of the first or second mode, α, shown in Table 3-3. For experiment 113, the value of δ=0 was also used. This resulted in a 6.6% increase of the calculated amplitude of lift response. This estimate quantifies the statement made in Section 2 that the structural damping force in our model was much smaller than the fluid drag force.

A summary of the results for the response in plane A is shown in Figures 96A, 98A, 100A, 102A, 104A, 106A, 114A, 108A, 113A, 110A, 111A, 109A, 107A, 105A, 103A, 101A, 99A, 97A, 95A, 112A, 115A, 116A, and 117A. These include the theoretical and measured static response strain; the maximum measured dynamic response strain; the maximum measured dynamic response strain independent of plane; and our present theoretical estimate of the maximum response strain independent of plane. The latter is computed as the square root of the sum of the squares of the static strain and of the maximum dynamic response strain in plane B.

EXPERIMENT 96

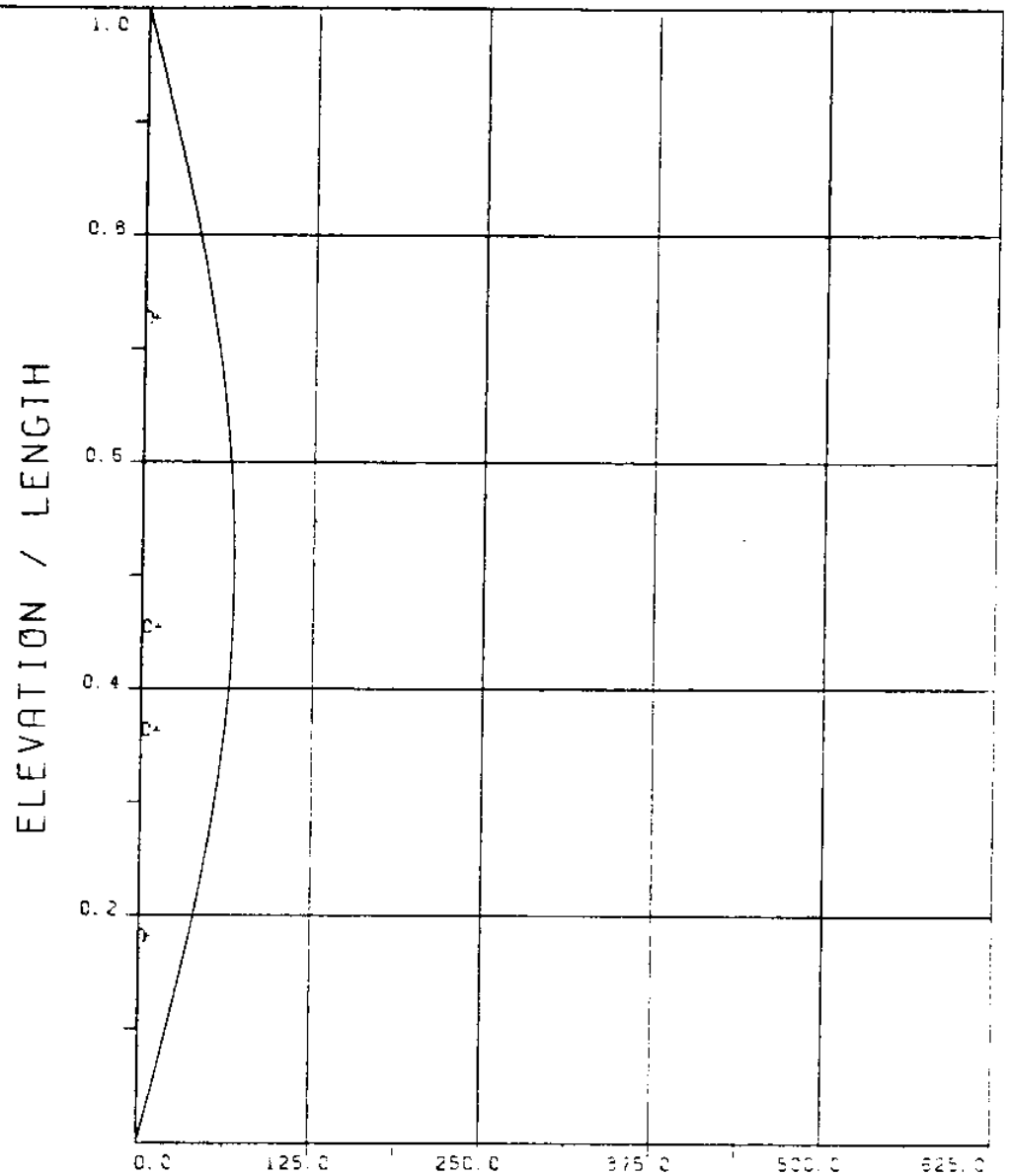

EXPERIMENT NUMBER 96

VC=100 A/DE=0.00

DYNAMIC RESPONSE AT F=FR IN PLANE B

——— THEORY o o o EXPERIMENT

MAXIMUM DYNAMIC RESPONSE IN PLANE B

——— THEORY + + + EXPERIMENT

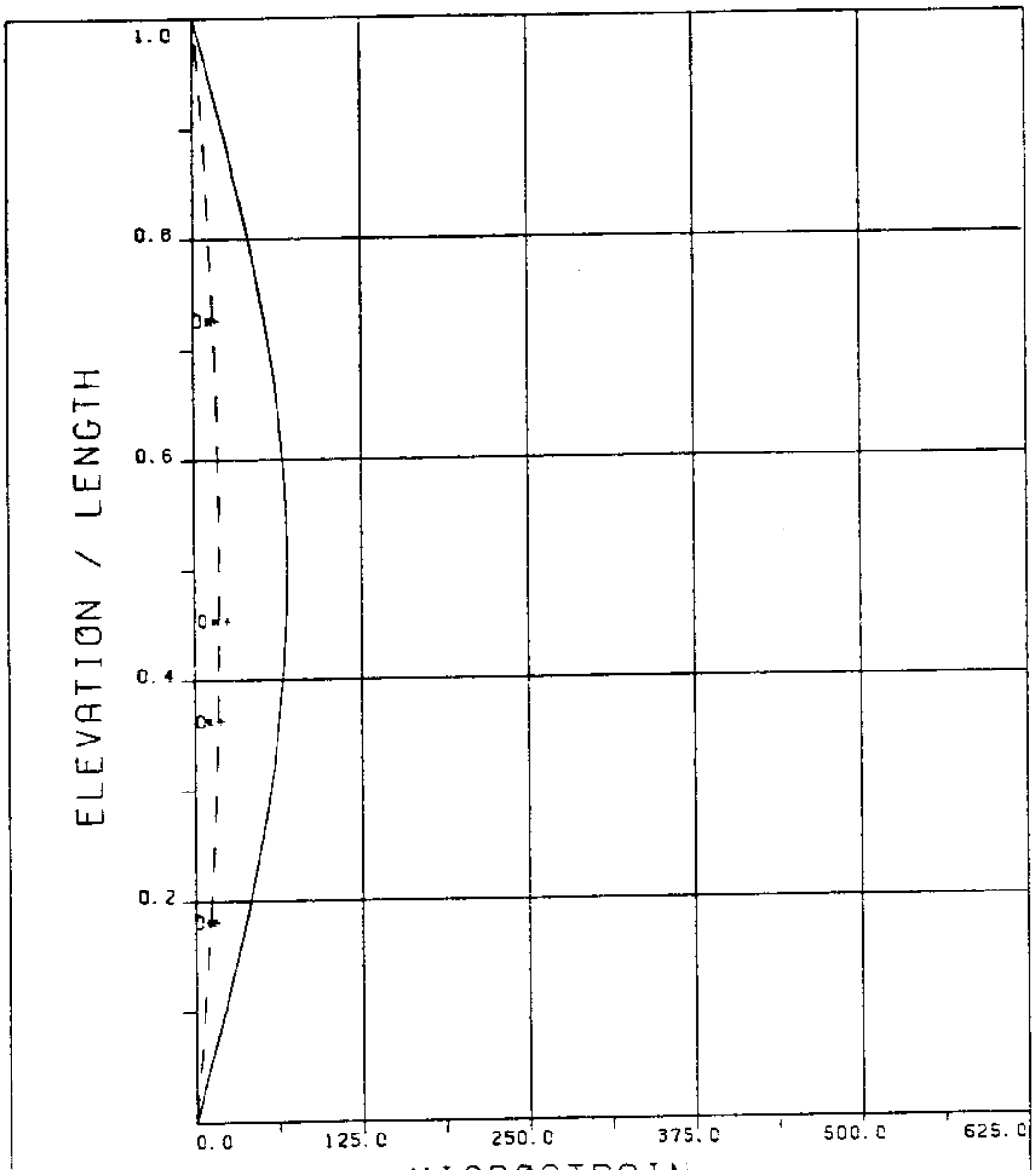

EXPERIMENT NUMBER 96

VC=100 A/DE=0.00

STATIC RESPONSE IN PLANE A

----- THEORY * * * EXPERIMENT

MAXIMUM DYNAMIC RESPONSE IN PLANE A

o o o EXPERIMENT

MAXIMUM RESPONSE

_____ THEORY + + + EXPERIMENT

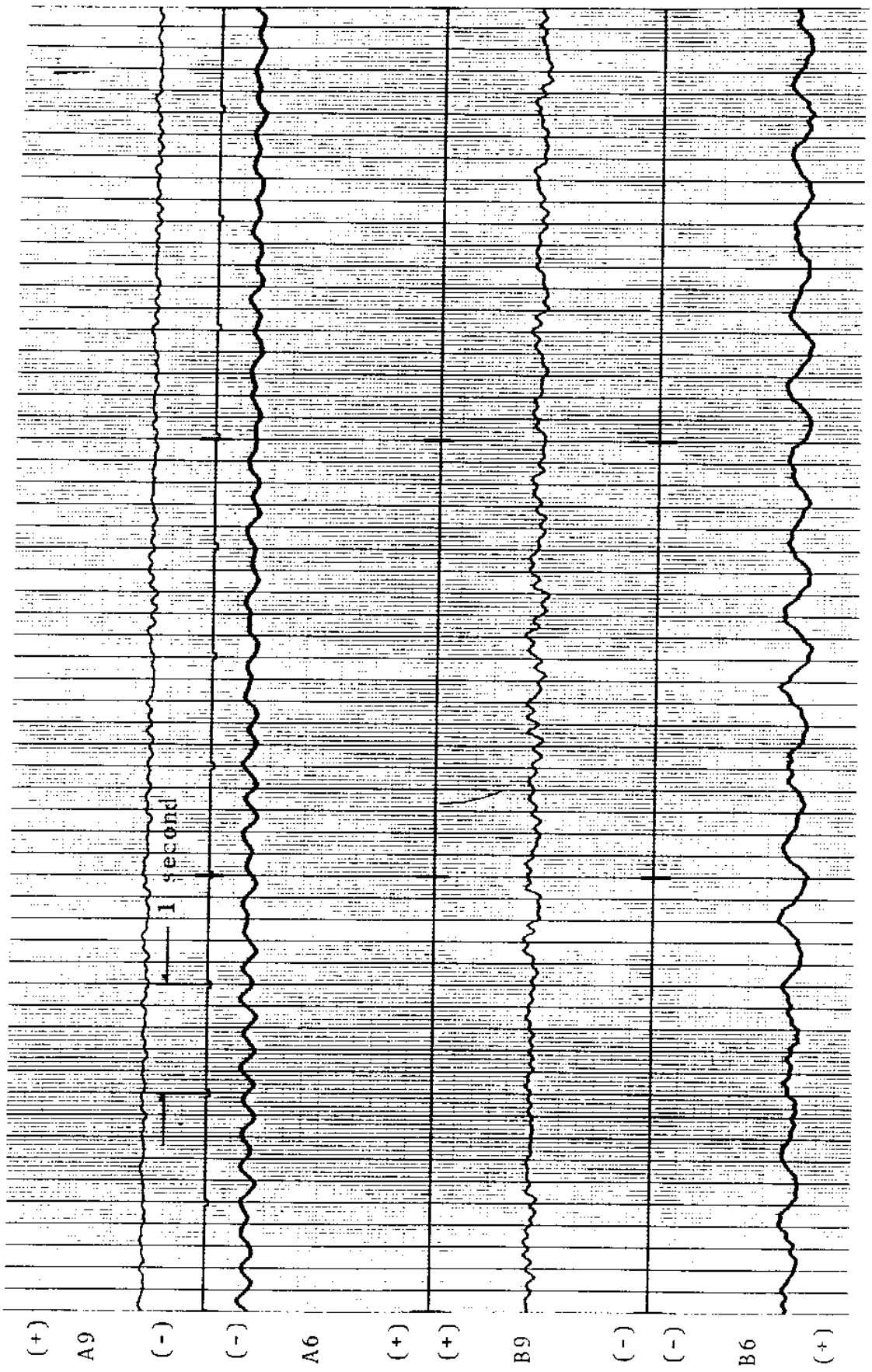

FIGURE 96Ta: ALL BRIDGES: 0.8 MICROSTRAIN/DIVISION

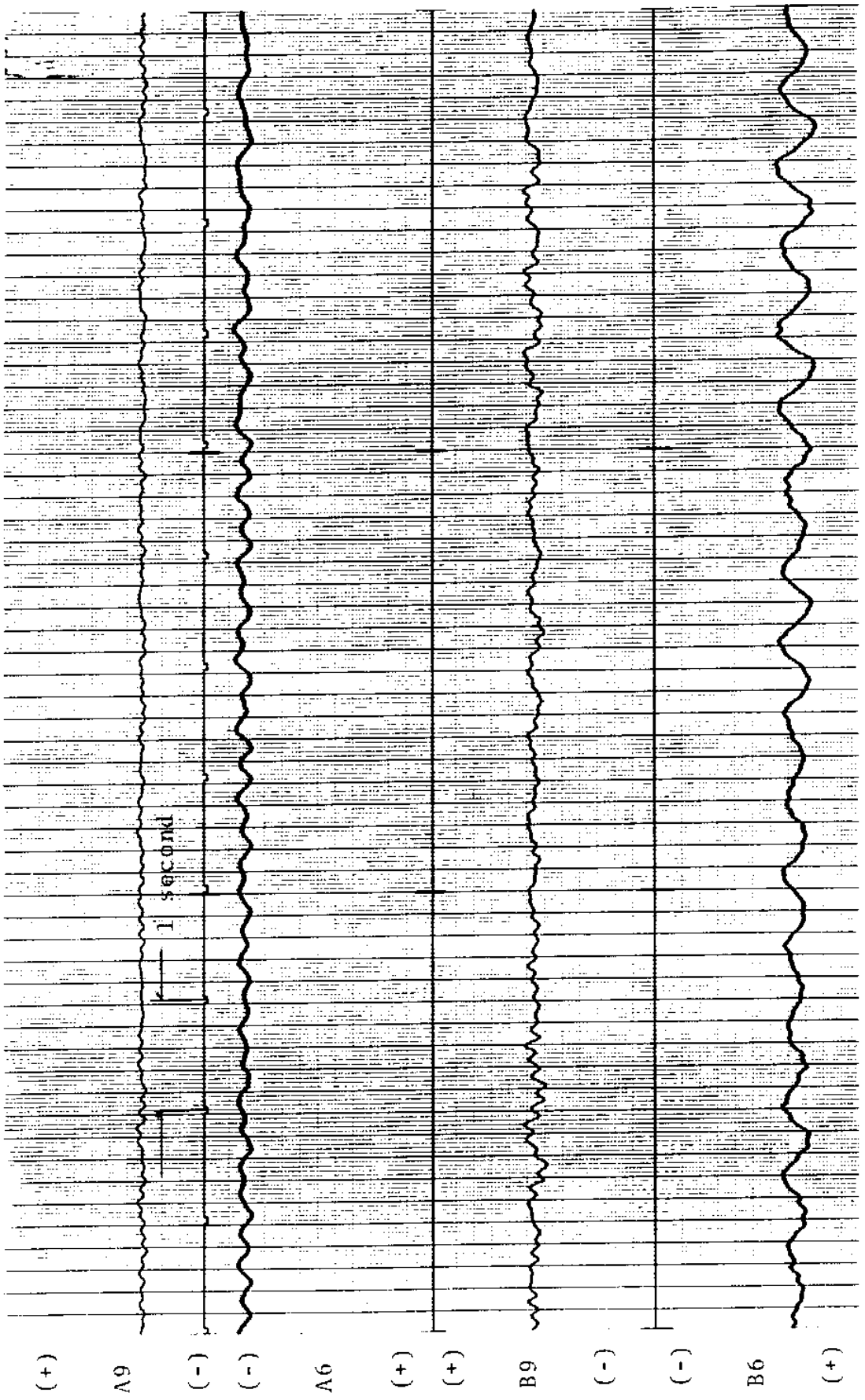

FIGURE 96Tb: ALL BRIDGES: 0.8 MICROSTRAIN/DIVISION

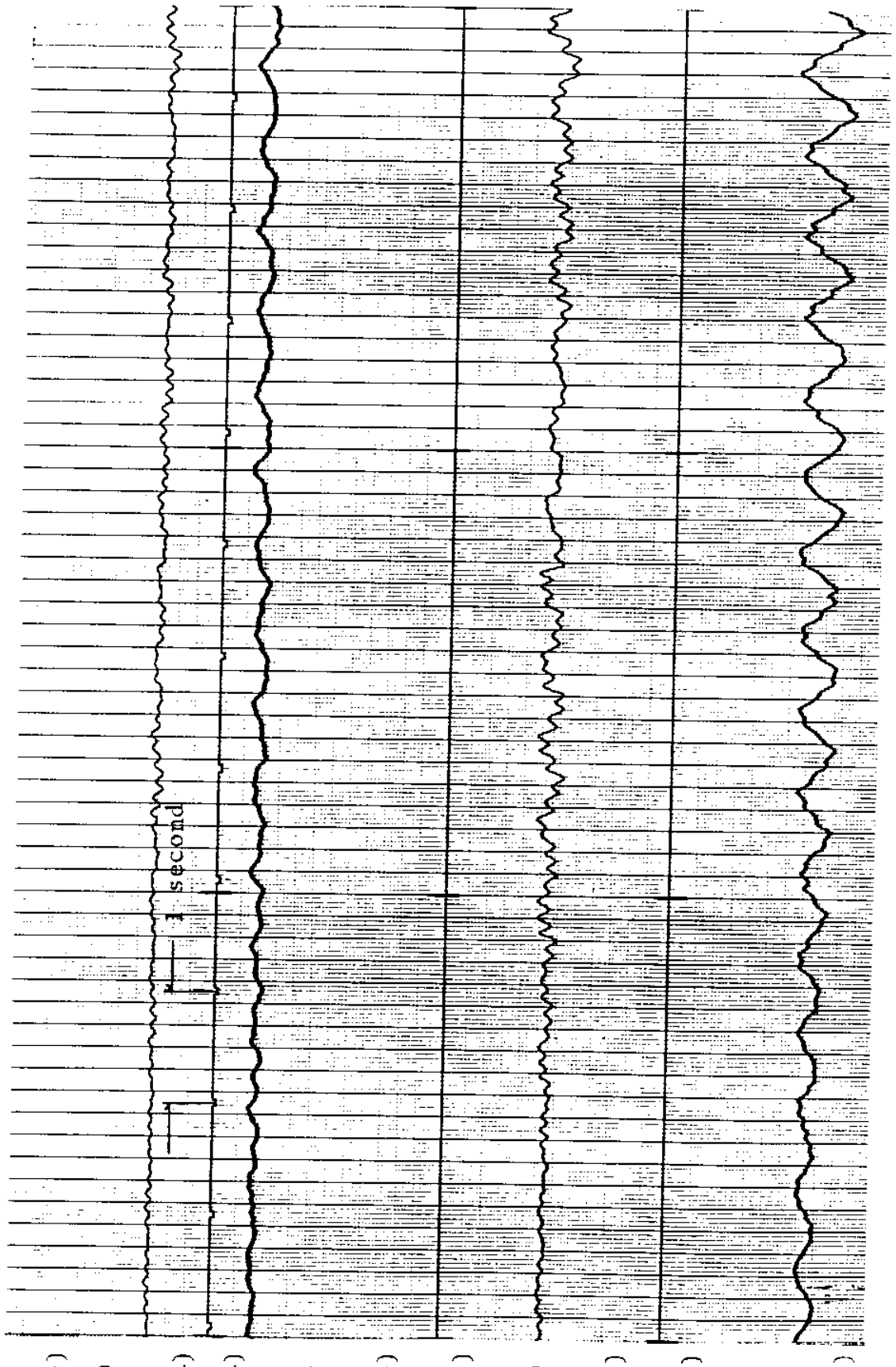

FIGURE 96Tc: ALL BRIDGES: 0.8 MICROSTRAIN/DIVISION

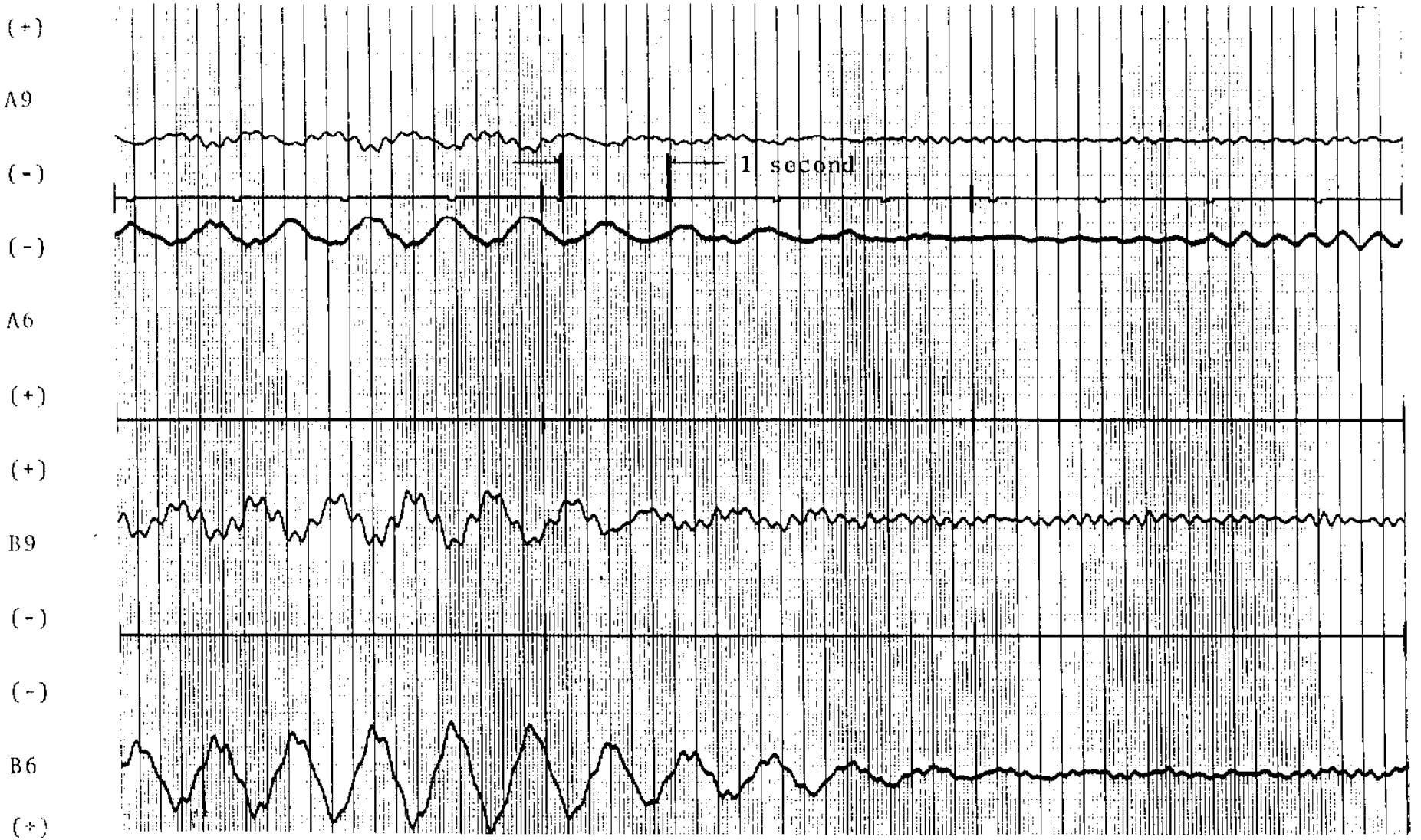

FIGURE 96Td: ALL BRIDGES: 0.8 MICROSTRAIN/DIVISION

EXPERIMENT 98

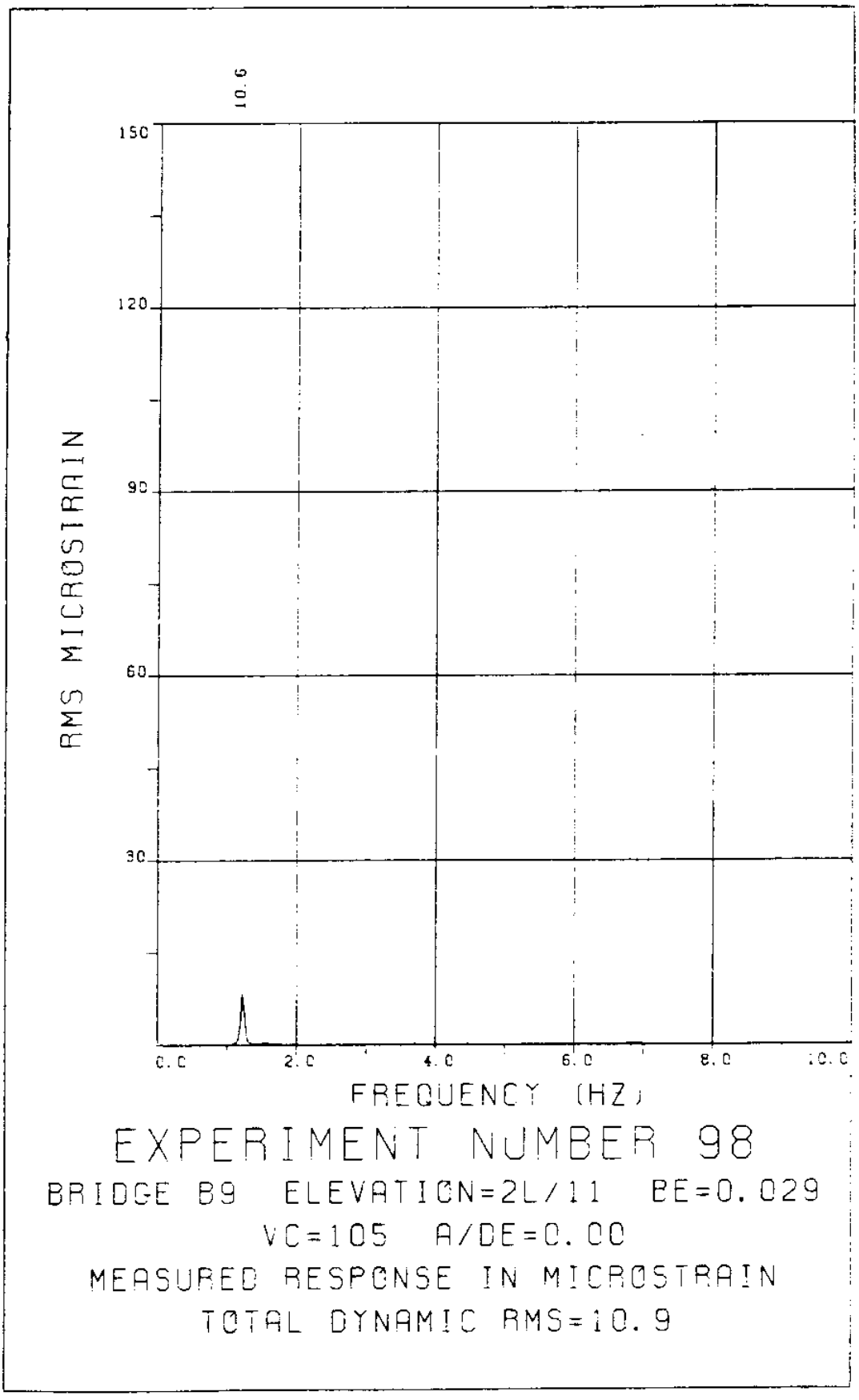

EXPERIMENT NUMBER 98

BRIDGE B9 ELEVATION=2L/11 BE=0.029

VC=105 A/DE=0.00

MEASURED RESPONSE IN MICROSTRAIN

TOTAL DYNAMIC RMS=10.9

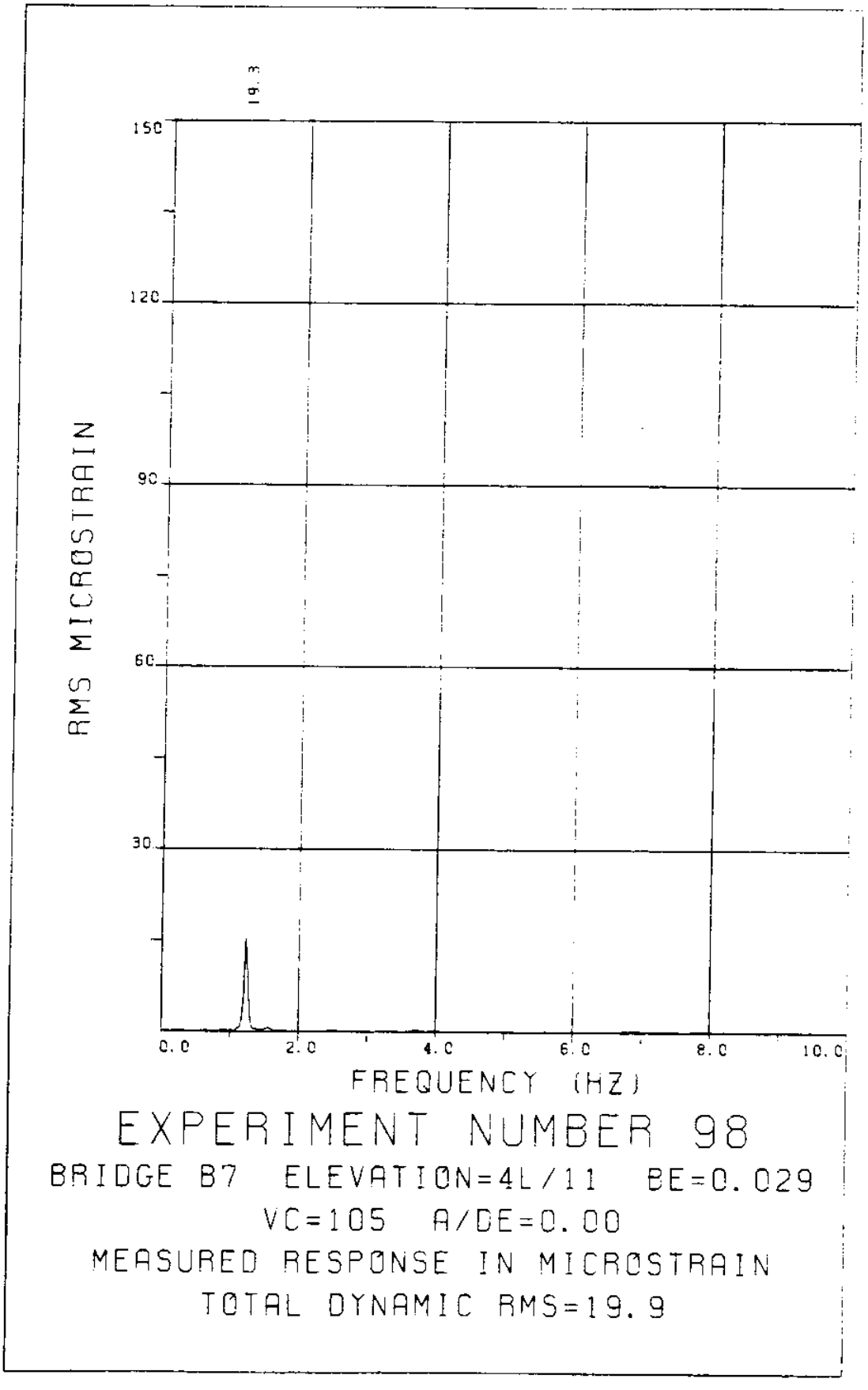
19.3
150
120
90
60
30
RMS MICROSTRAIN
0.0
2.0
4.0
6.0
8.0
10.0
FREQUENCY (HZ)
EXPERIMENT NUMBER 98
BRIDGE B7 ELEVATION=4L/11 BE=0.029
VC=105 A/DE=0.00
MEASURED RESPONSE IN MICROSTRAIN
TOTAL DYNAMIC RMS=19.9

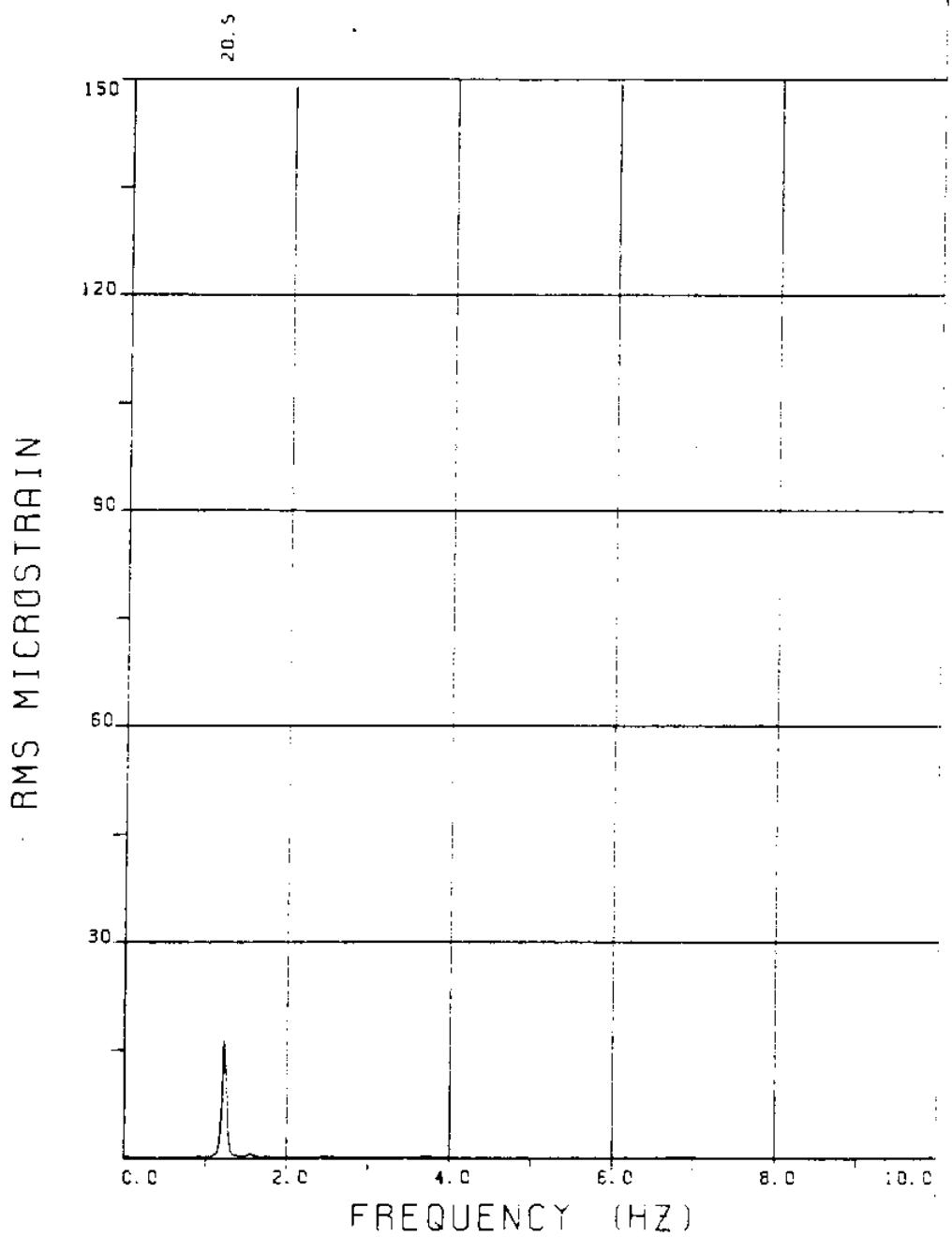

EXPERIMENT NUMBER 98

BRIDGE B6 ELEVATION=5L/11 BE=0.029

VC=350 A/DE=0.00

MEASURED RESPONSE IN MICROSTRAIN

TOTAL DYNAMIC RMS=21.2

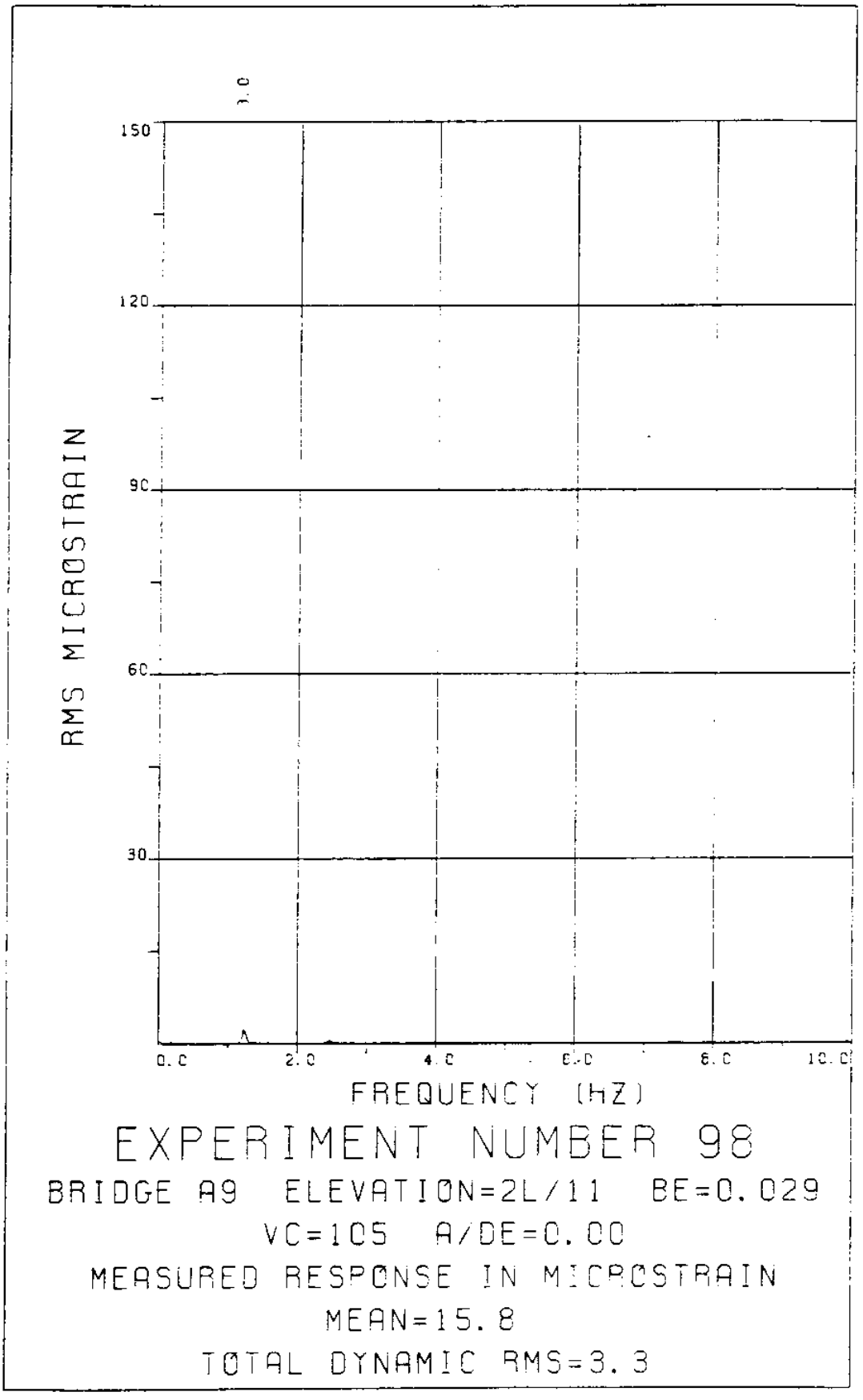
RMS MICROSTRAIN
150
120
90
60
30
0.0
2.0
4.0
6.0
8.0
10.0
FREQUENCY (HZ)
EXPERIMENT NUMBER 98
BRIDGE A9 ELEVATION=2L/11 BE=0.029
VC=105 A/DE=0.00
MEASURED RESPONSE IN MICROSTRAIN
MEAN=15.8
TOTAL DYNAMIC RMS=3.3

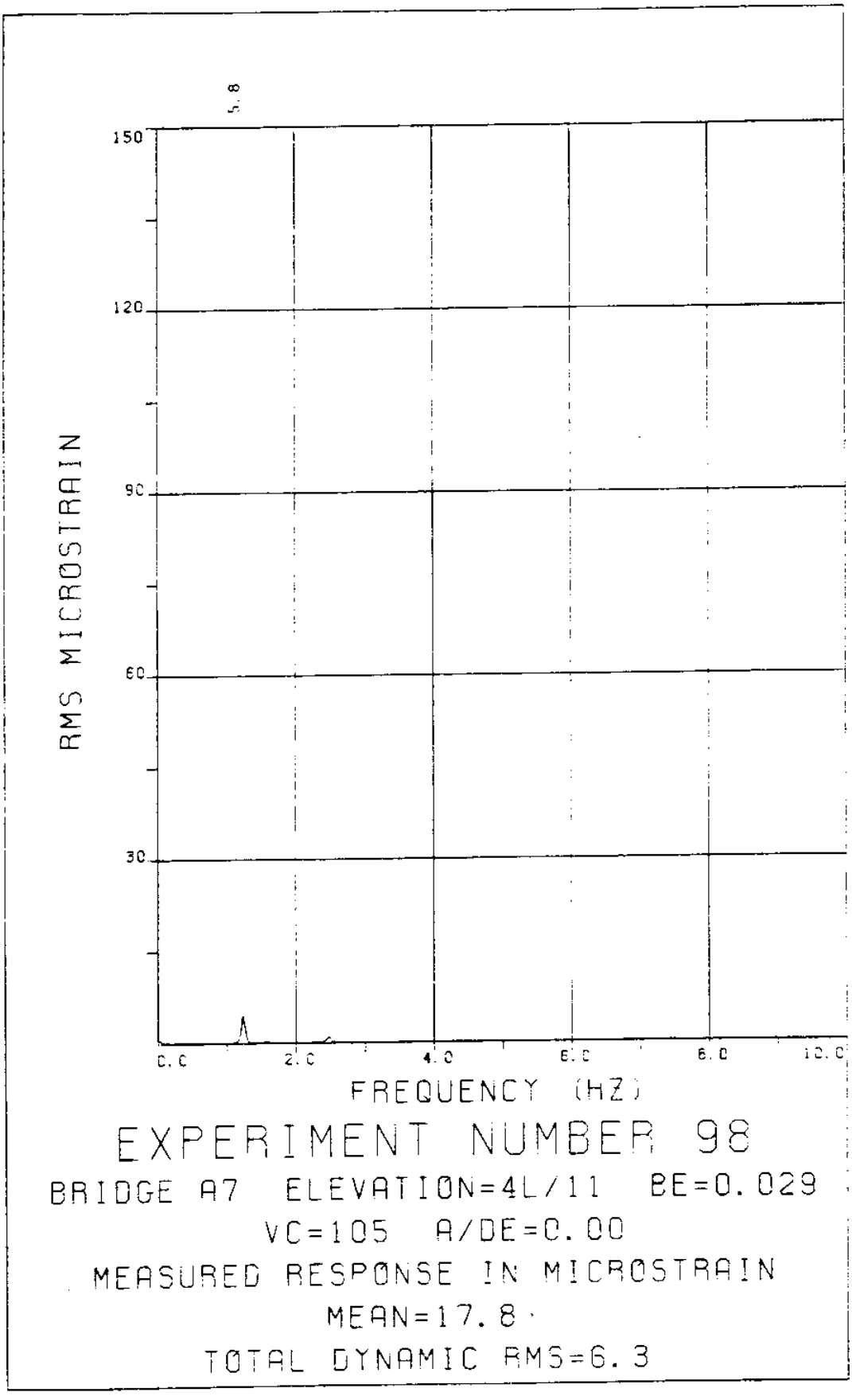
RMS MICROSTRAIN
150
120
90
60
30
0.0
2.0
4.0
6.0
8.0
10.0
FREQUENCY (HZ)
EXPERIMENT NUMBER 98
BRIDGE A7 ELEVATION=4L/11 BE=0.029
VC=105 A/DE=0.00
MEASURED RESPONSE IN MICROSTRAIN
MEAN=17.8
TOTAL DYNAMIC RMS=6.3

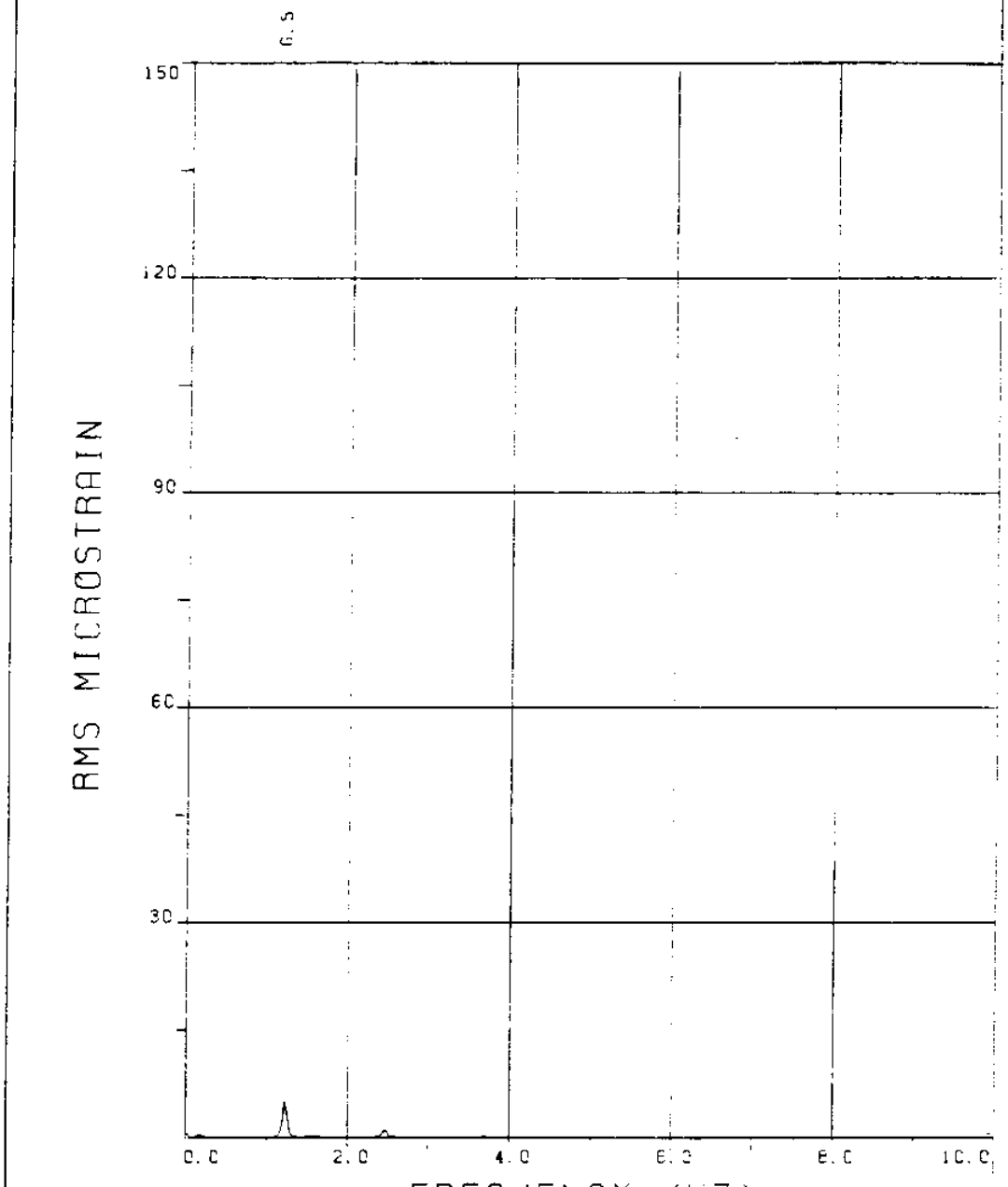

EXPERIMENT NUMBER 98

BRIDGE A6 ELEVATION=5L/11 BE=0.029

VC=105 A/DE=0.00

MEASURED RESPONSE IN MICROSTRAIN

MEAN=23.3

TOTAL DYNAMIC RMS=7.1

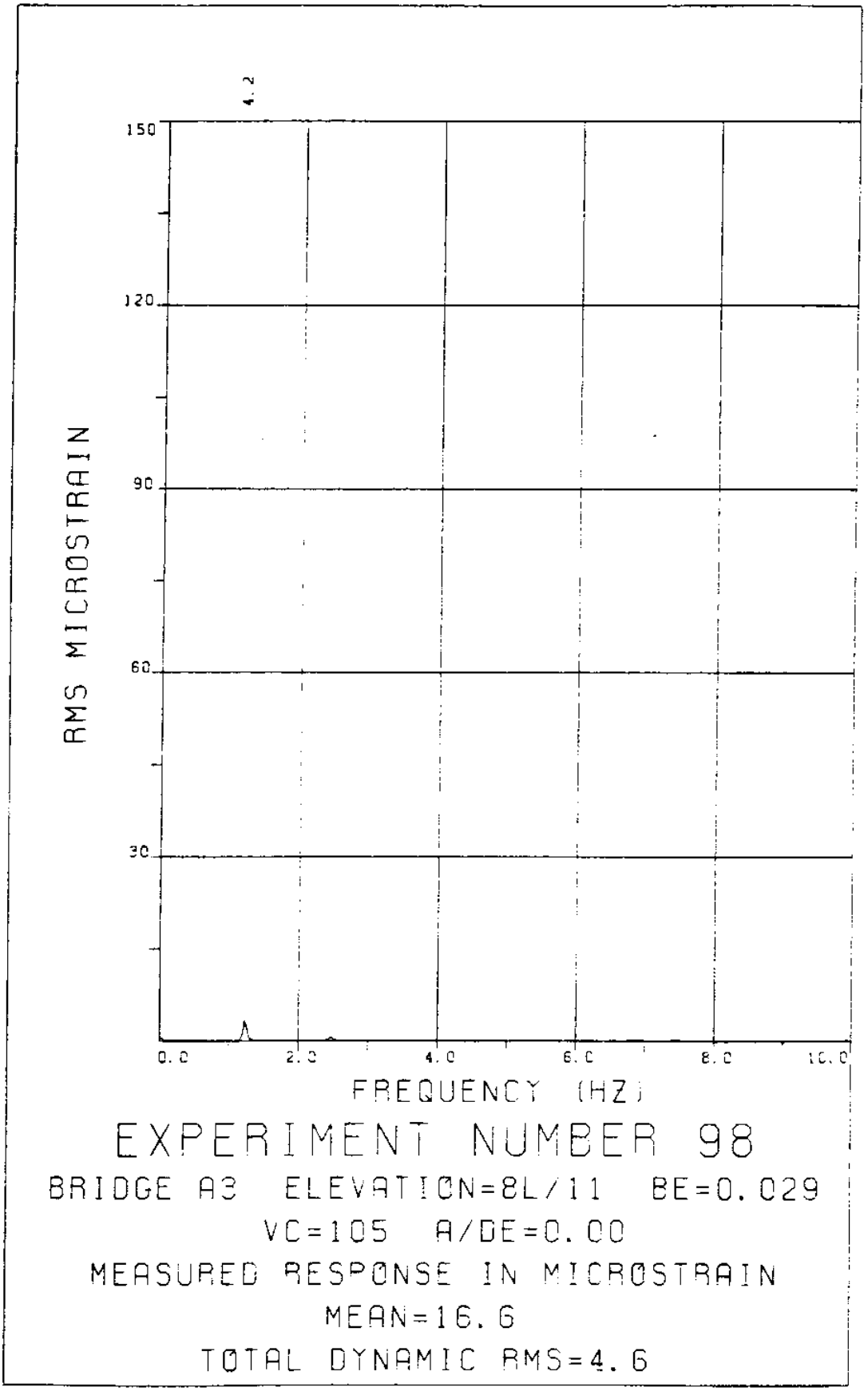
4.2
150
120
90
60
30
RMS MICROSTRAIN
0.0
2.0
4.0
6.0
8.0
10.0
FREQUENCY (HZ)
EXPERIMENT NUMBER 98
BRIDGE A3 ELEVATION=8L/11 BE=0.029
VC=105 A/DE=0.00
MEASURED RESPONSE IN MICROSTRAIN
MEAN=16.6
TOTAL DYNAMIC RMS=4.6

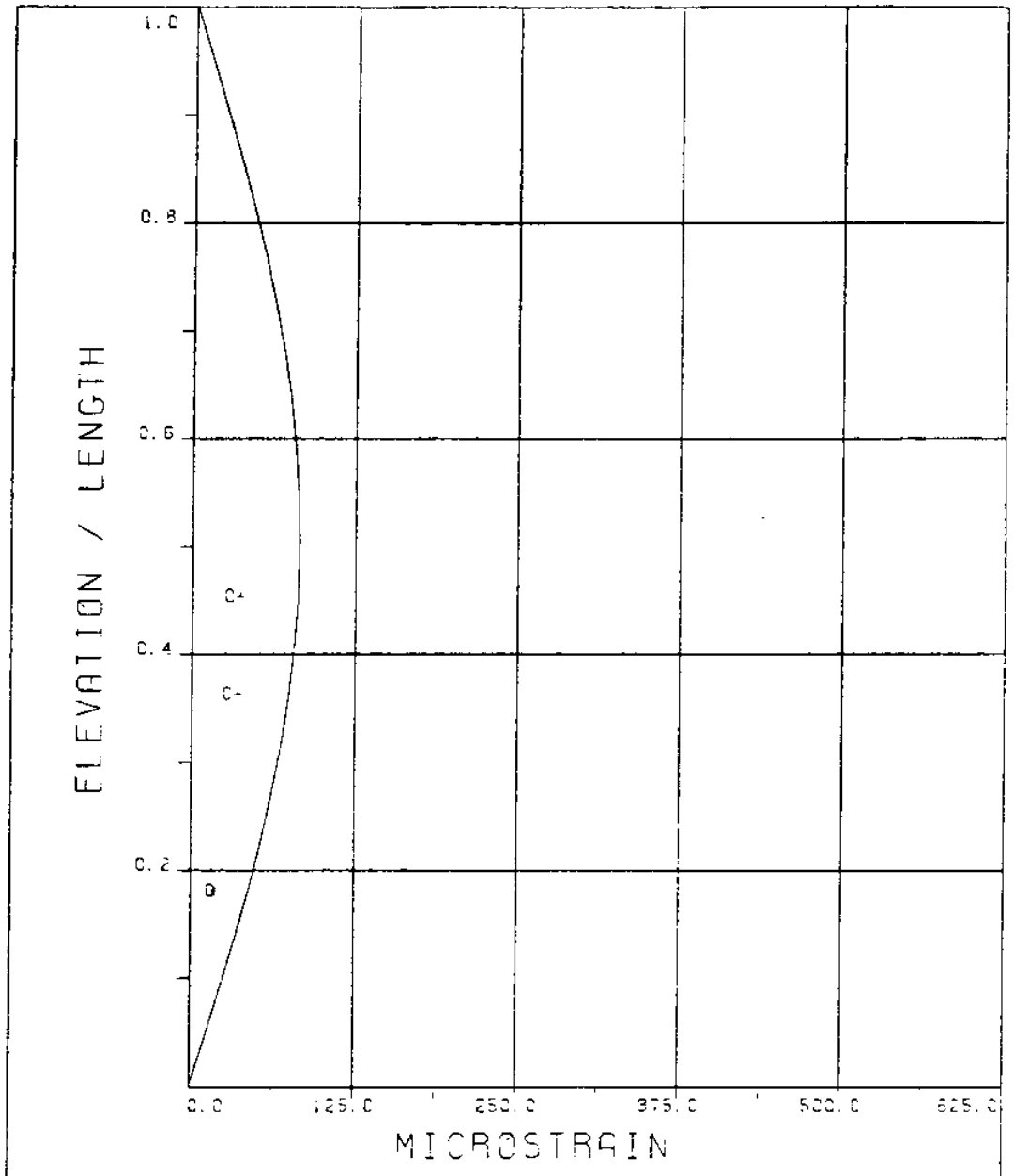

EXPERIMENT NUMBER 98

VC=105 A/DE=0.00

DYNAMIC RESPONSE AT F=FR IN PLANE B

——— THEORY o o o EXPERIMENT

MAXIMUM DYNAMIC RESPONSE IN PLANE B

——— THEORY + + + EXPERIMENT

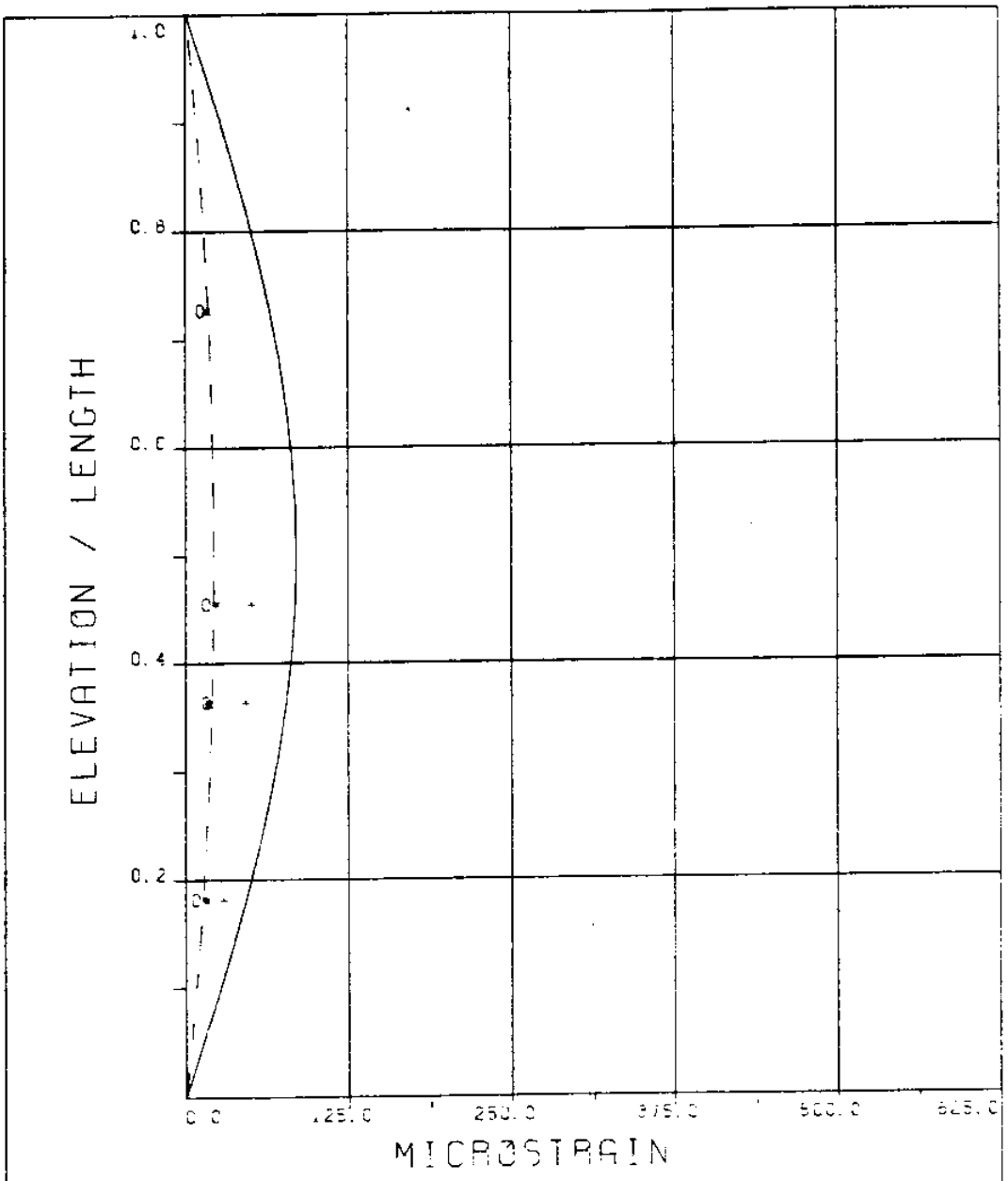

EXPERIMENT NUMBER 93

VC=105 A/DE=0.00

STATIC RESPONSE IN PLANE A

----- THEORY * * * EXPERIMENT

MAXIMUM DYNAMIC RESPONSE IN PLANE A

o o o EXPERIMENT

MAXIMUM RESPONSE

——— THEORY + + + EXPERIMENT

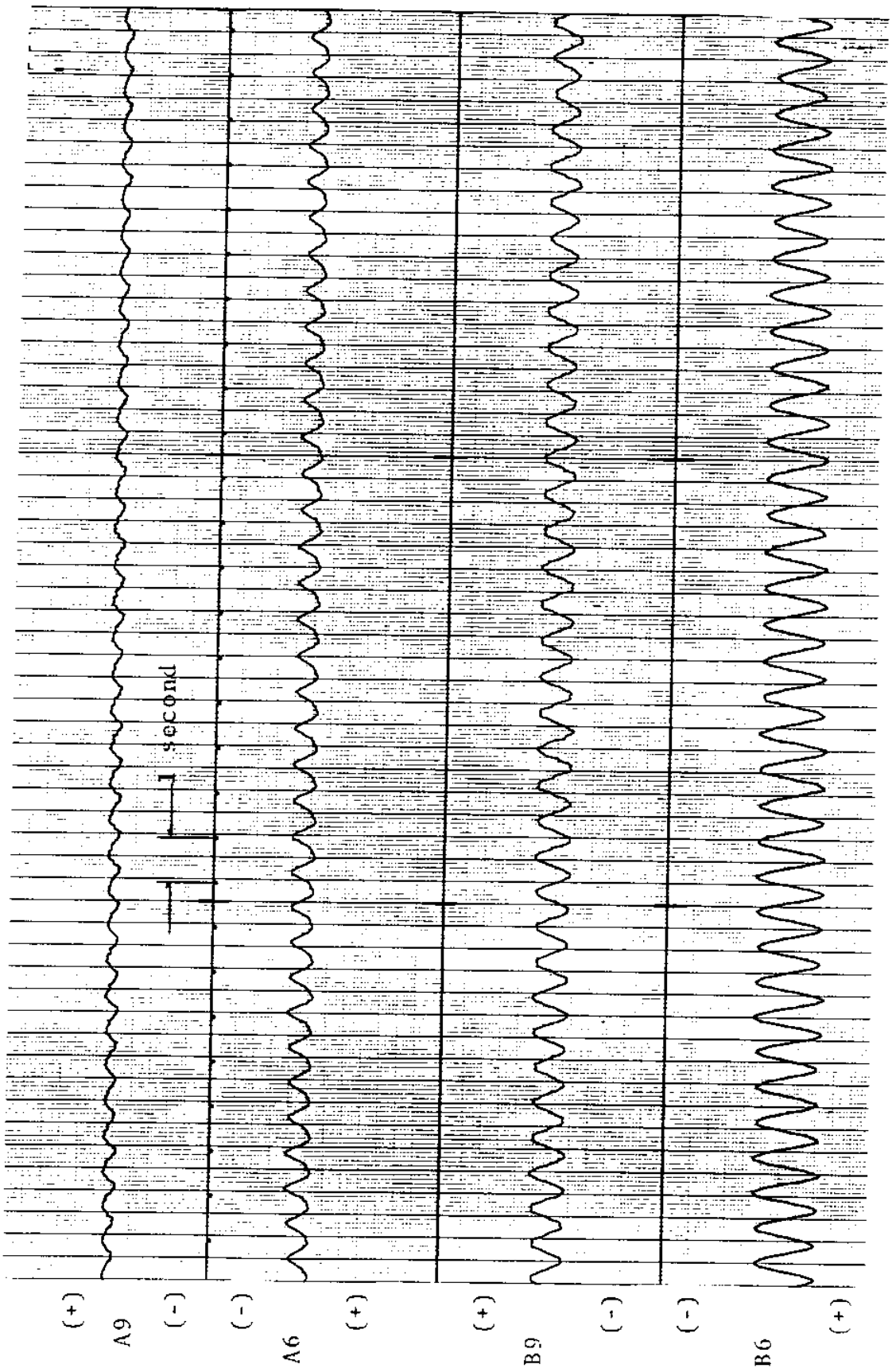

FIGURE 98T: ALL BRIDGES: 3.8 MICROSTRAIN/DIVISION

EXPERIMENT 100

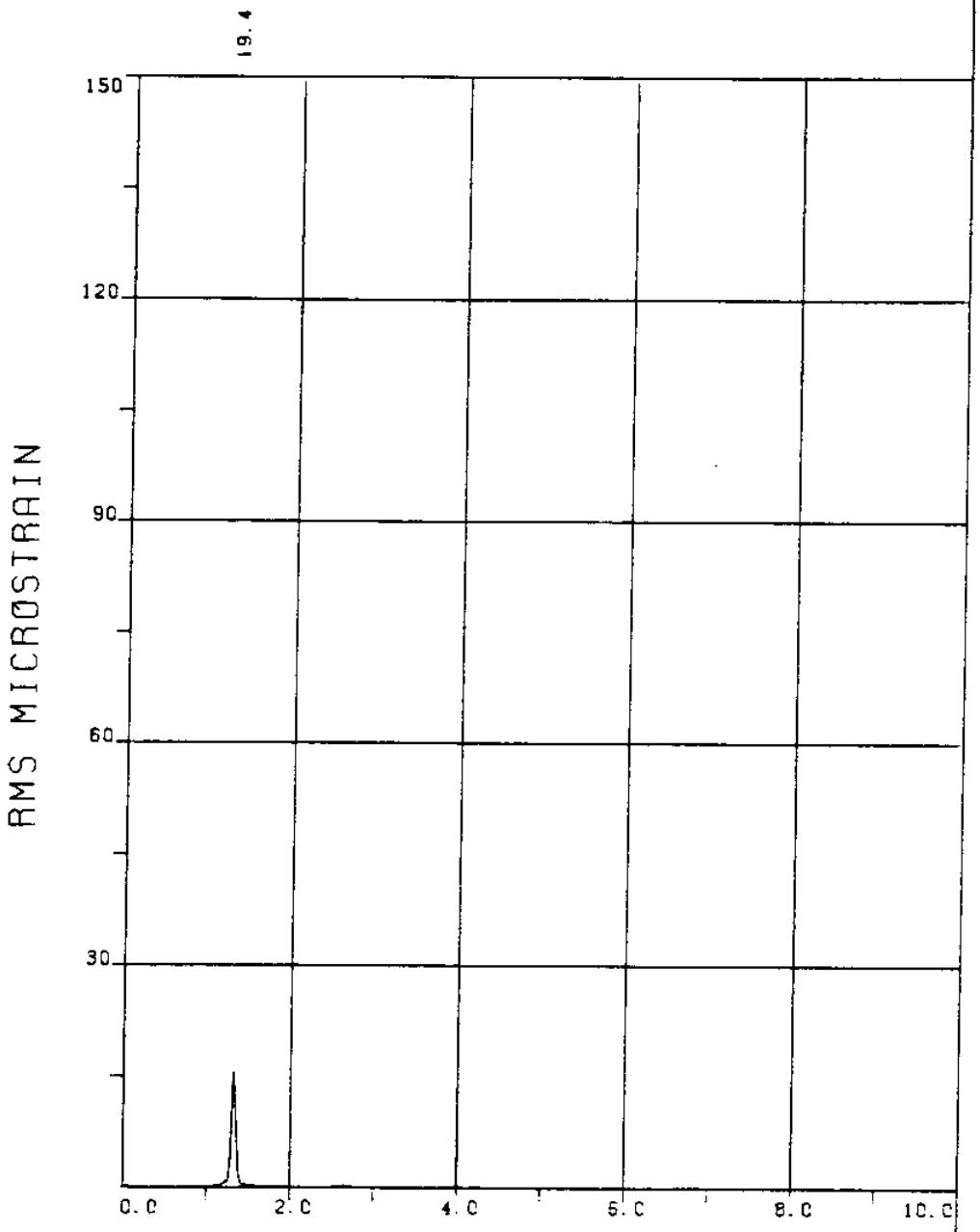

EXPERIMENT NUMBER 100

BRIDGE B9 ELEVATION=2L/11 BE=0.029

VC=110 A/DE=0.00

MEASURED RESPONSE IN MICROSTRAIN

TOTAL DYNAMIC RMS=19.4

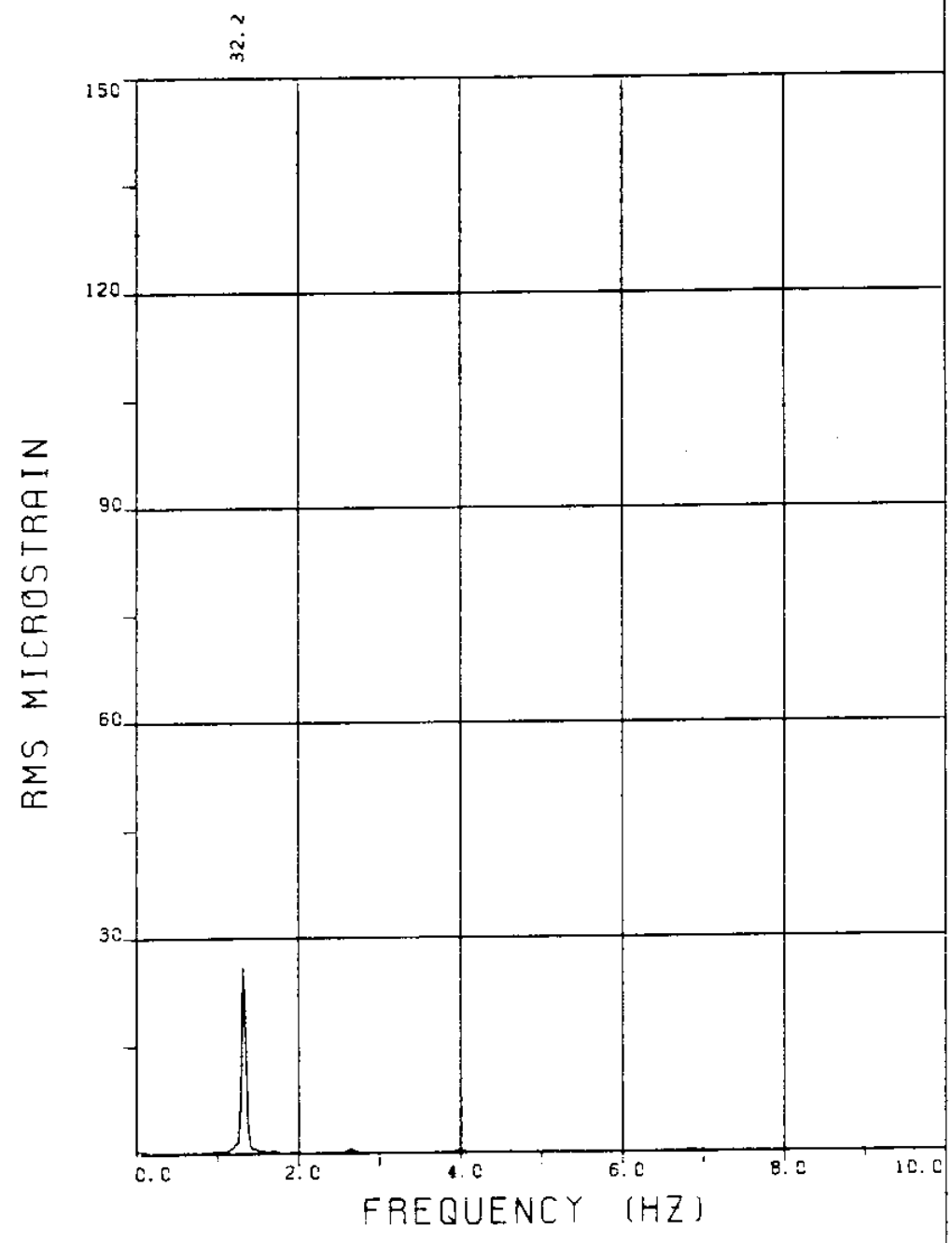

EXPERIMENT NUMBER 100

BRIDGE B7 ELEVATION=4L/11 BE=0.029

VC=110 A/DE=0.00

MEASURED RESPONSE IN MICROSTRAIN

TOTAL DYNAMIC RMS=32.2

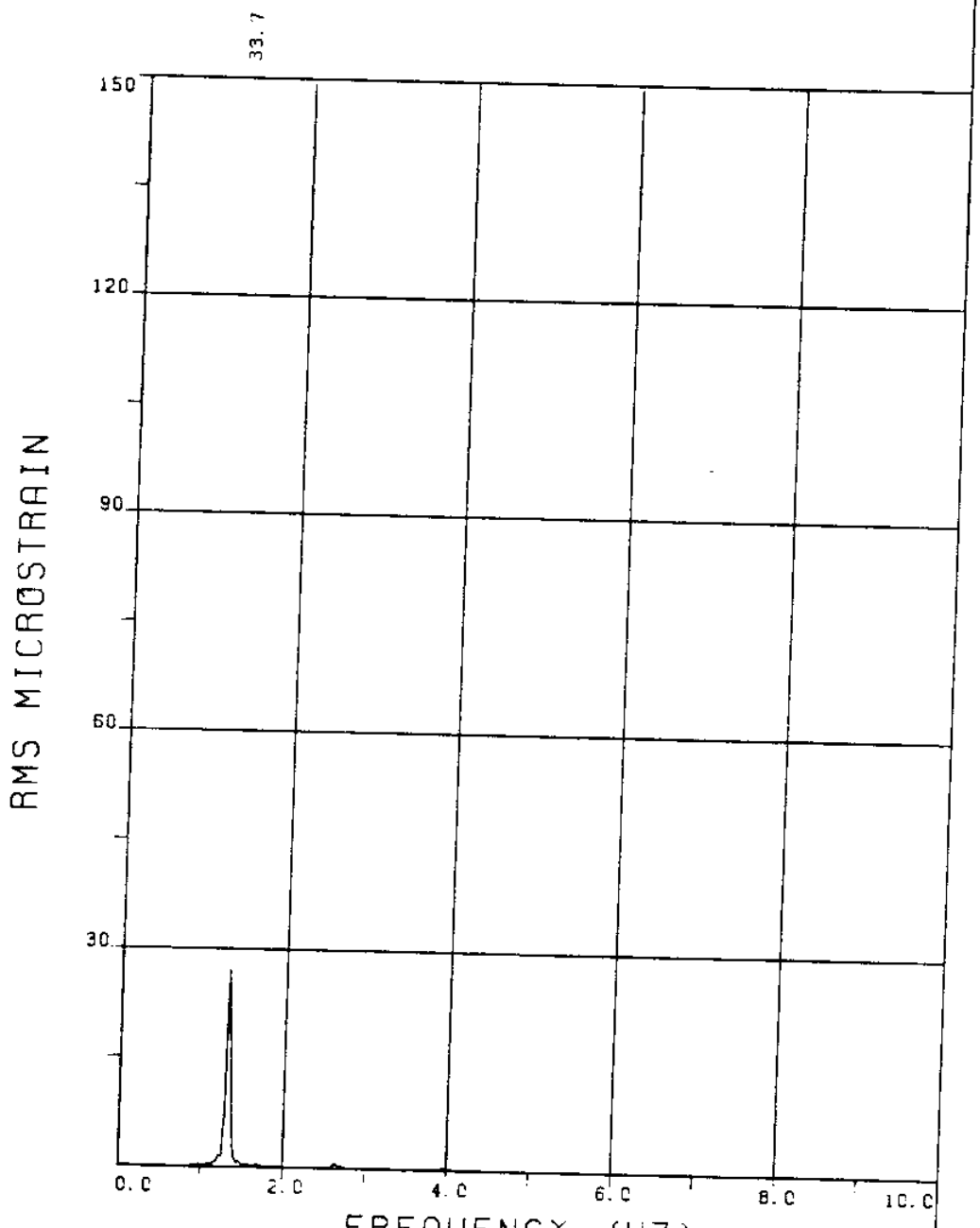

EXPERIMENT NUMBER 100

BRIDGE B6 ELEVATION=5L/11 BE=0.029

VC=110 A/DE=0.00

MEASURED RESPONSE IN MICROSTRAIN

TOTAL DYNAMIC RMS=33.7

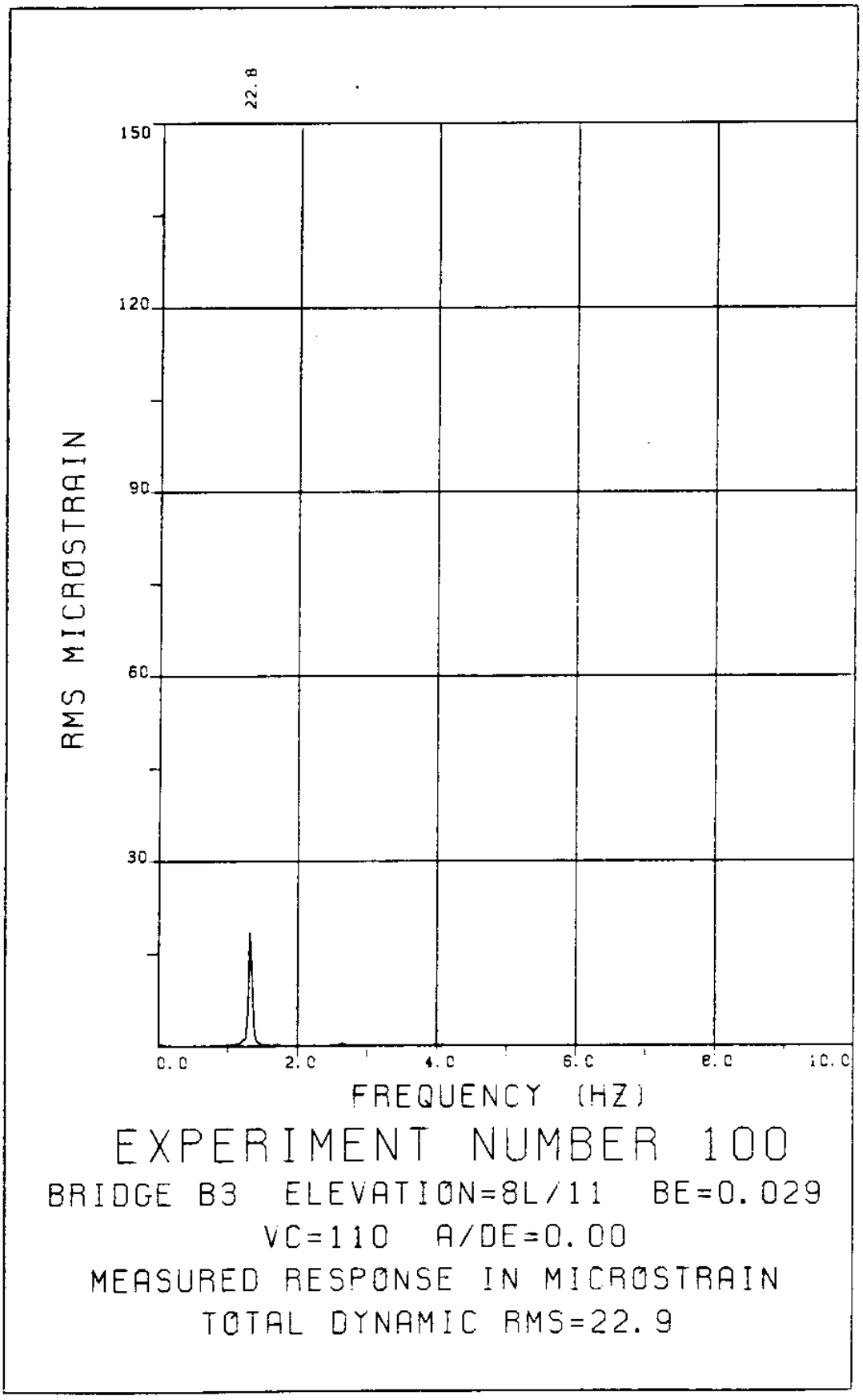

EXPERIMENT NUMBER 100

BRIDGE B3 ELEVATION=8L/11 BE=0.029

VC=110 A/DE=0.00

MEASURED RESPONSE IN MICROSTRAIN

TOTAL DYNAMIC RMS=22.9

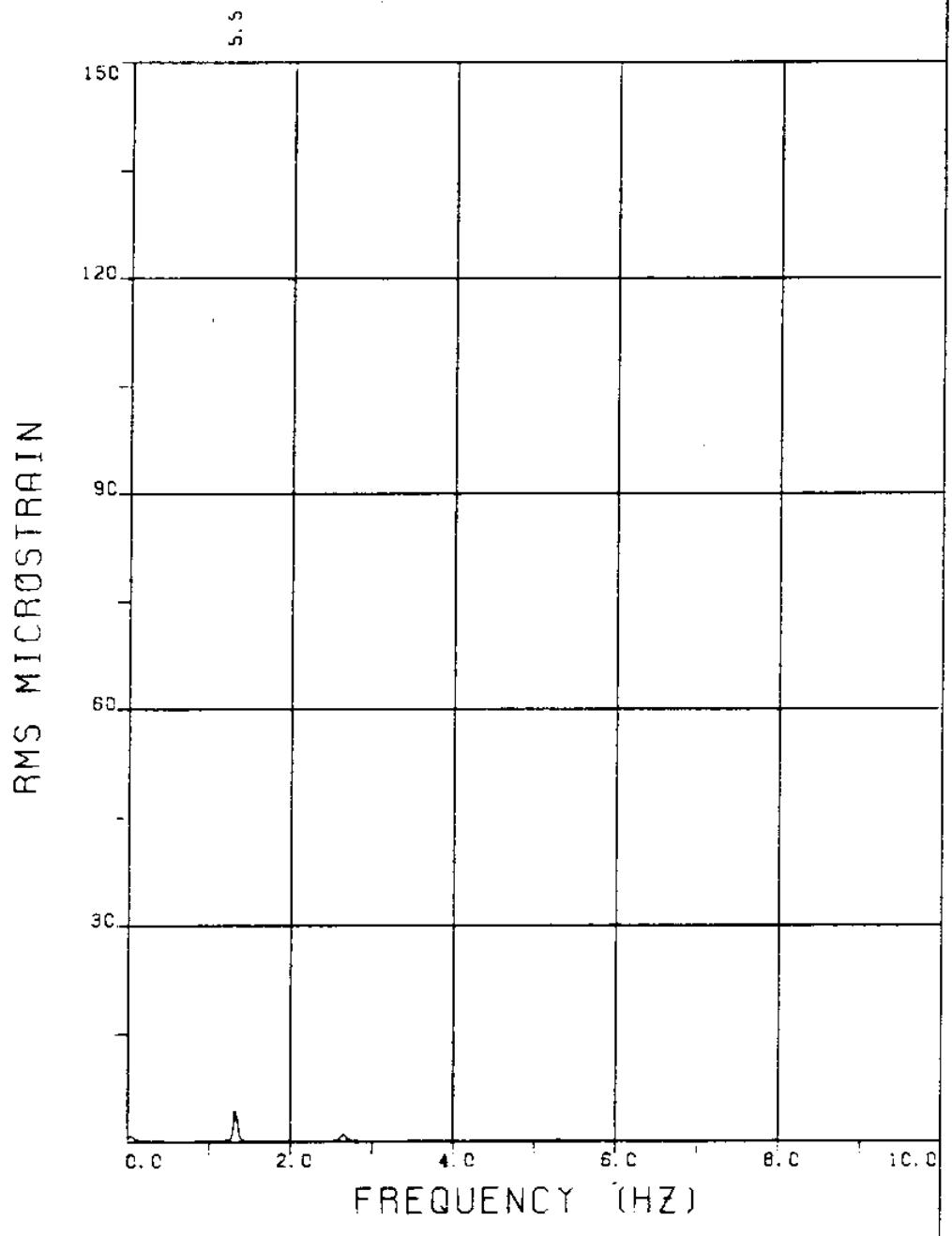

EXPERIMENT NUMBER 100

BRIDGE A9 ELEVATION=2L/11 BE=0.029

VC=110 A/DE=0.00

MEASURED RESPONSE IN MICROSTRAIN

MEAN=20.8

TOTAL DYNAMIC RMS=5.9

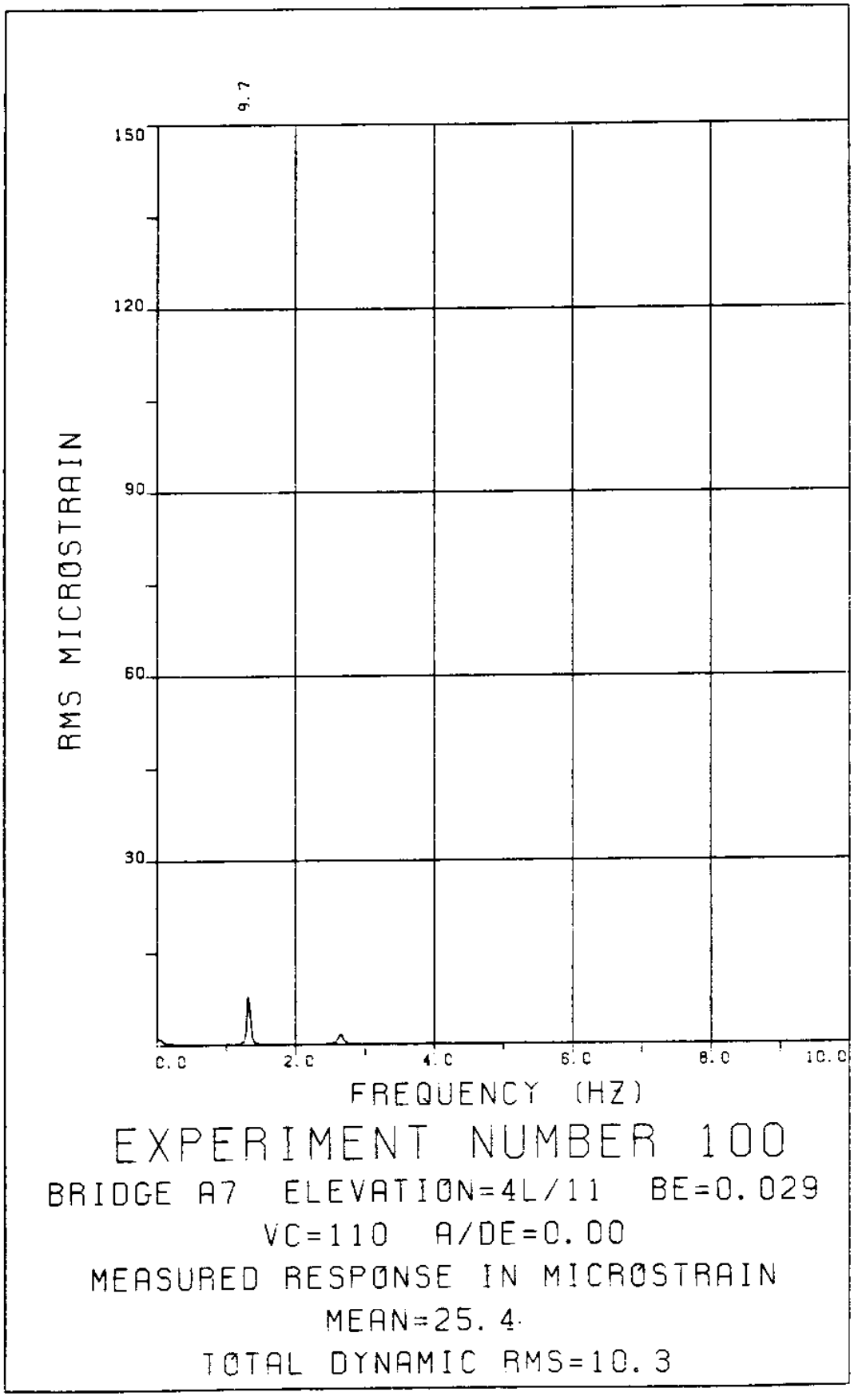
9.7
150
120
90
60
30
RMS MICROSTRAIN
0.0
2.0
4.0
6.0
8.0
10.0
FREQUENCY (HZ)
EXPERIMENT NUMBER 100
BRIDGE A7 ELEVATION=4L/11 BE=0.029
VC=110 A/DE=0.00
MEASURED RESPONSE IN MICROSTRAIN
MEAN=25.4
TOTAL DYNAMIC RMS=10.3

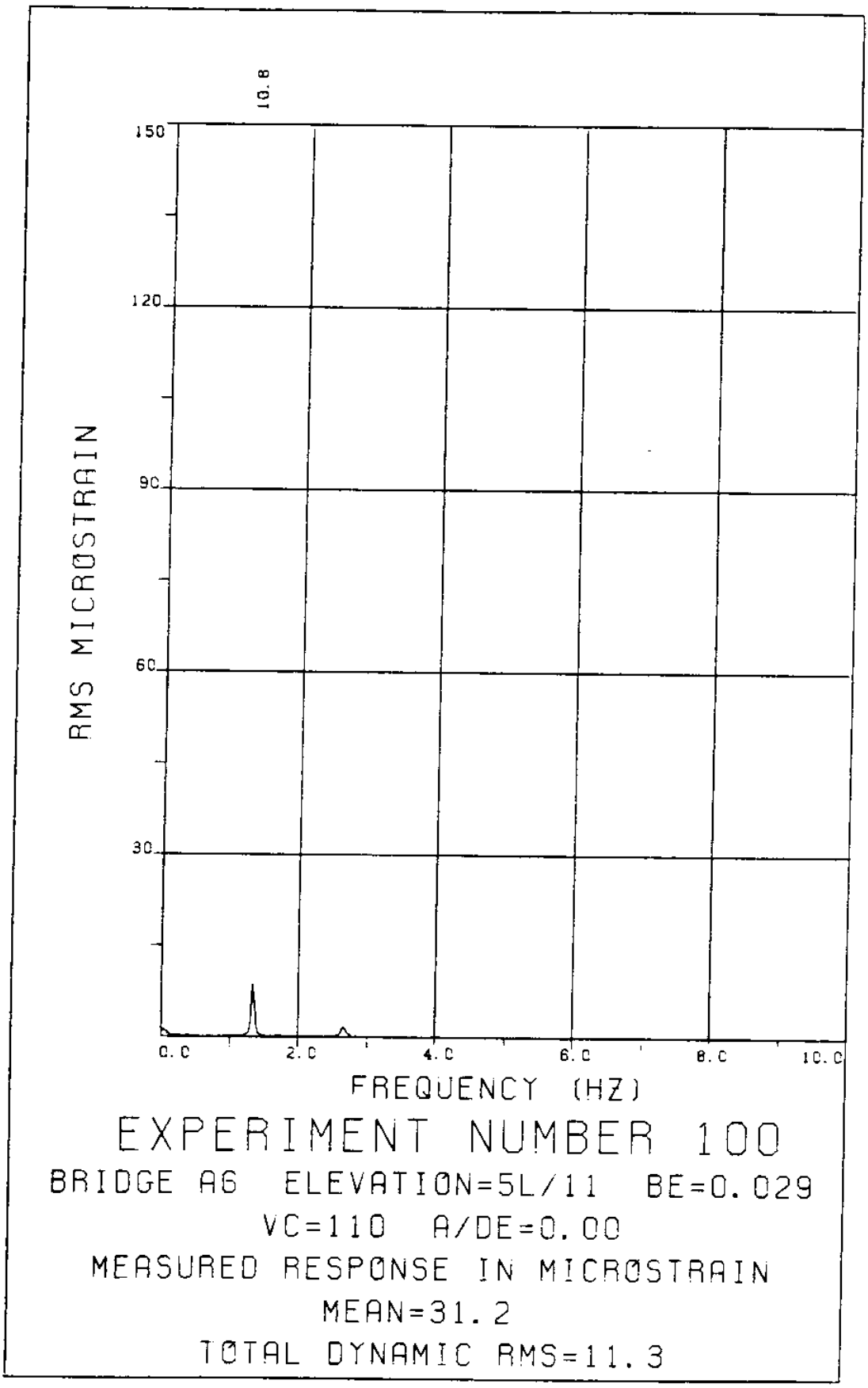

EXPERIMENT NUMBER 100

BRIDGE A6 ELEVATION=5L/11 BE=0.029

VC=110 A/DE=0.00

MEASURED RESPONSE IN MICROSTRAIN

MEAN=31.2

TOTAL DYNAMIC RMS=11.3

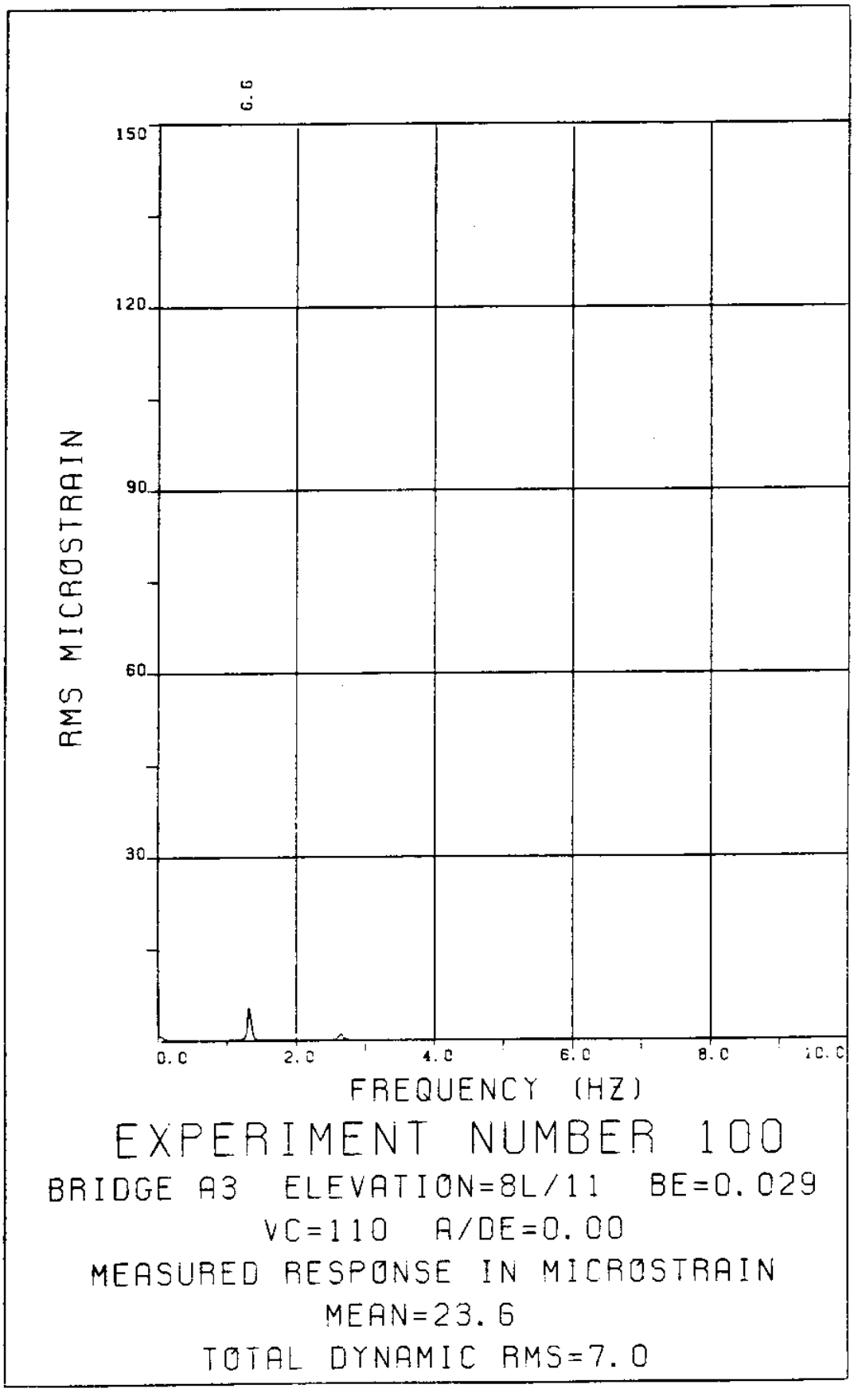
G.G
150
120
90
60
30
RMS MICROSTRAIN
0.0
2.0
4.0
6.0
8.0
10.0
FREQUENCY (HZ)
EXPERIMENT NUMBER 100
BRIDGE A3 ELEVATION=8L/11 BE=0.029
VC=110 A/DE=0.00
MEASURED RESPONSE IN MICROSTRAIN
MEAN=23.6
TOTAL DYNAMIC RMS=7.0

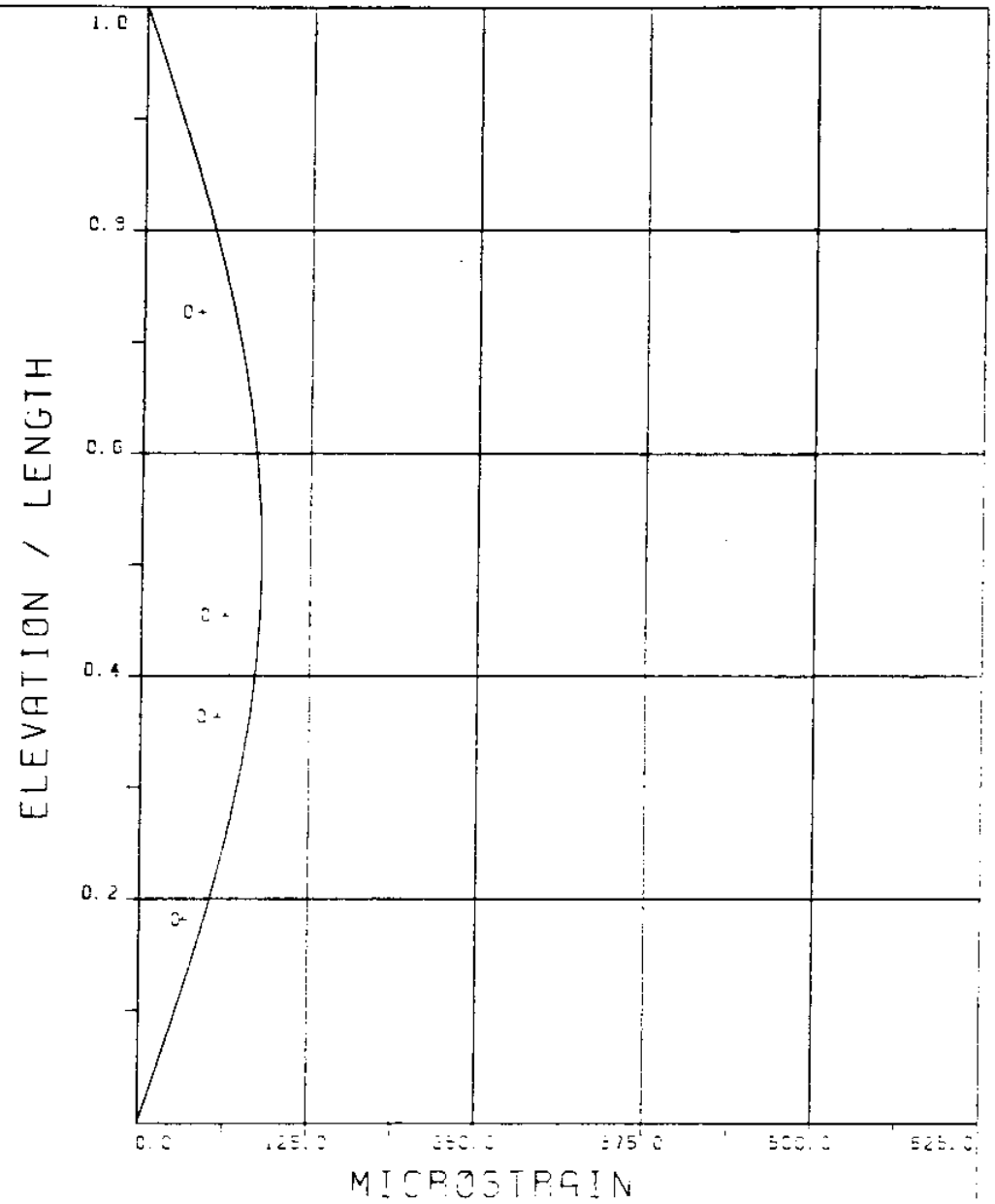

EXPERIMENT NUMBER 100

VC=110 A/DE=0.00

DYNAMIC RESPONSE AT F=FR IN PLANE B

——— THEORY o o o EXPERIMENT

MAXIMUM DYNAMIC RESPONSE IN PLANE B

——— THEORY + + + EXPERIMENT

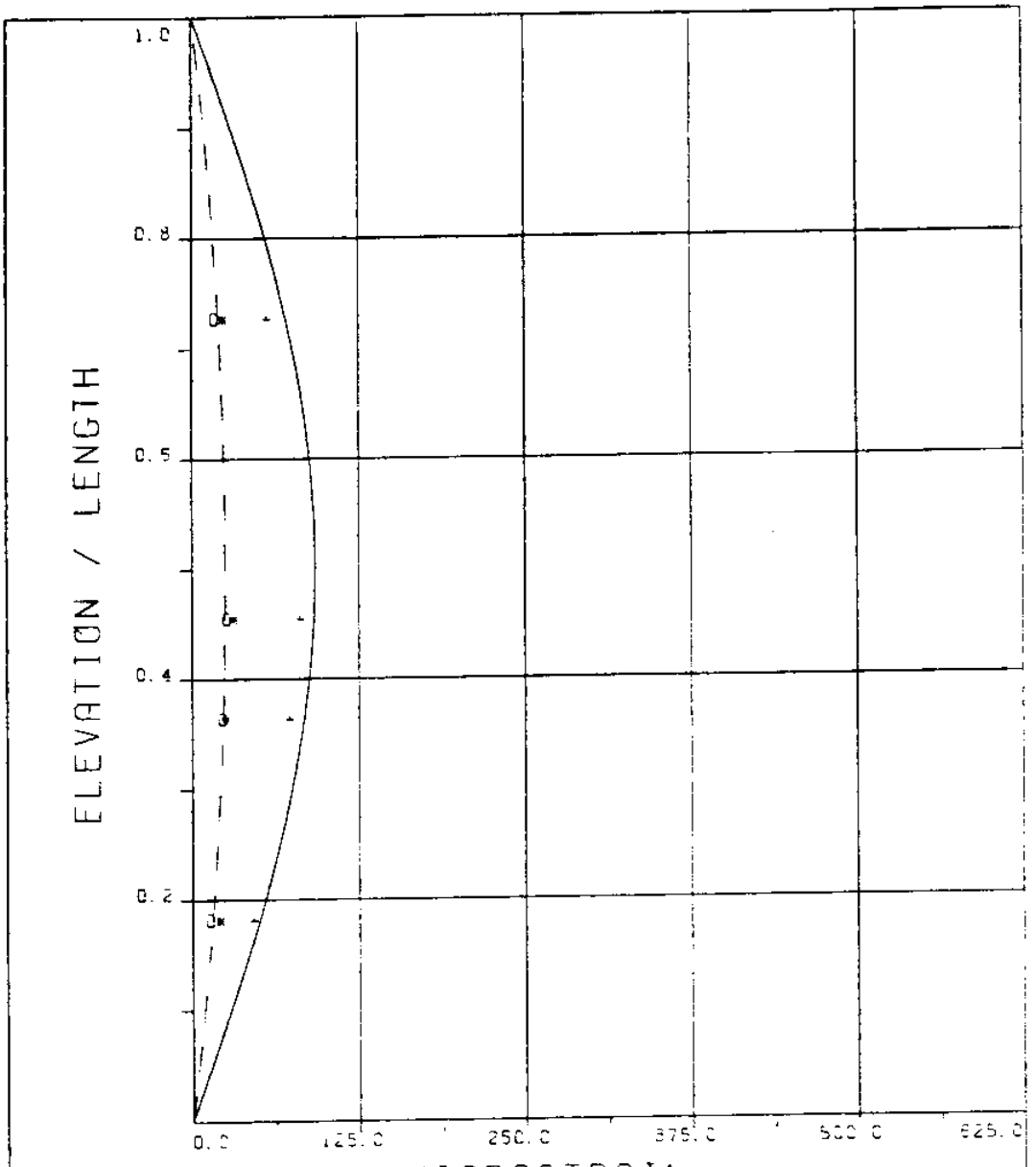

EXPERIMENT NUMBER 100

VC=110 A/DE=0.00

STATIC RESPONSE IN PLANE A

----- THEORY * * * EXPERIMENT

MAXIMUM DYNAMIC RESPONSE IN PLANE A

o o o EXPERIMENT

MAXIMUM RESPONSE

_____ THEORY + + + EXPERIMENT

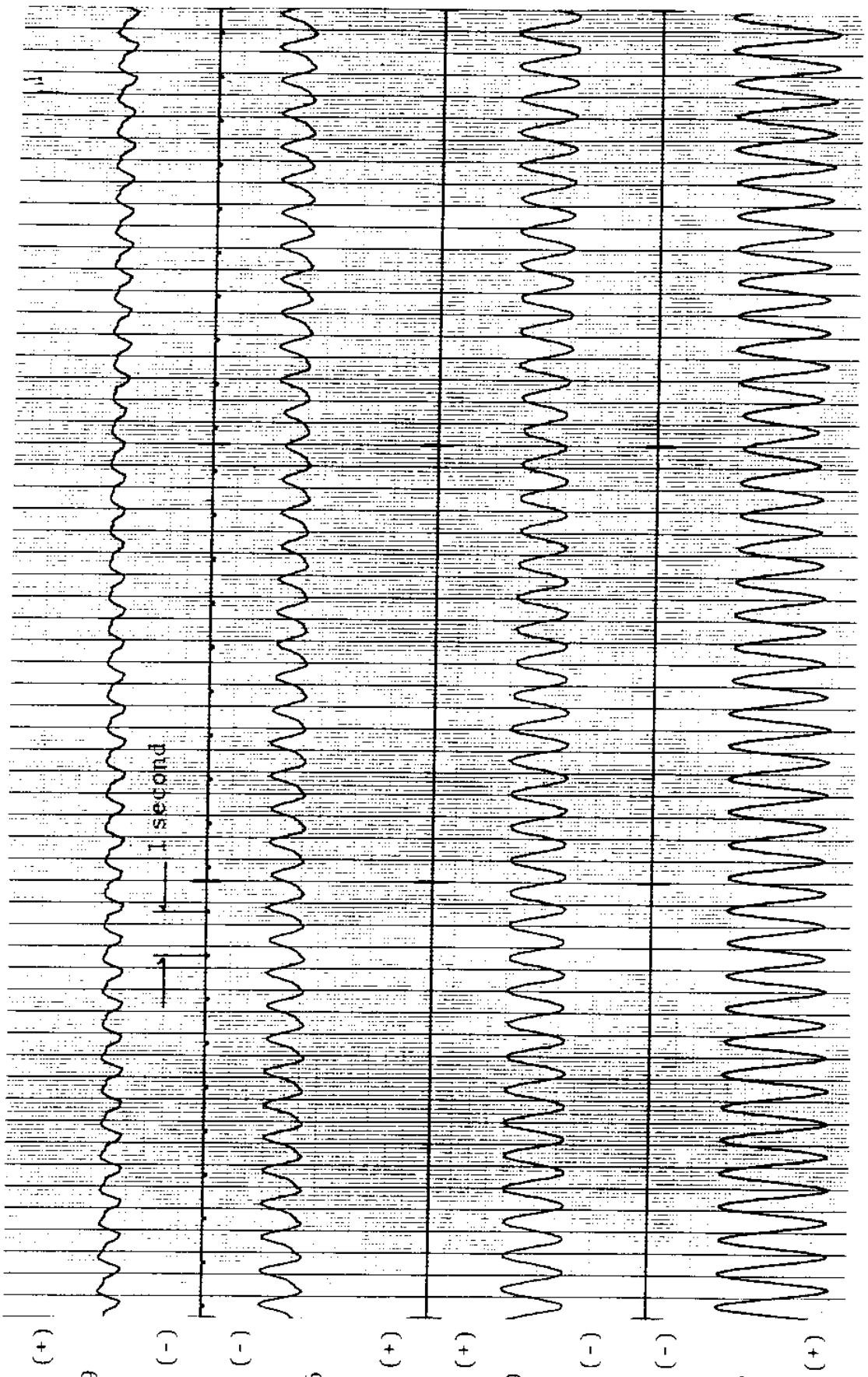

FIGURE 100T: ALL BRIDGES: 3.8 MICROSTRAIN/DIVISION

EXPERIMENT 102

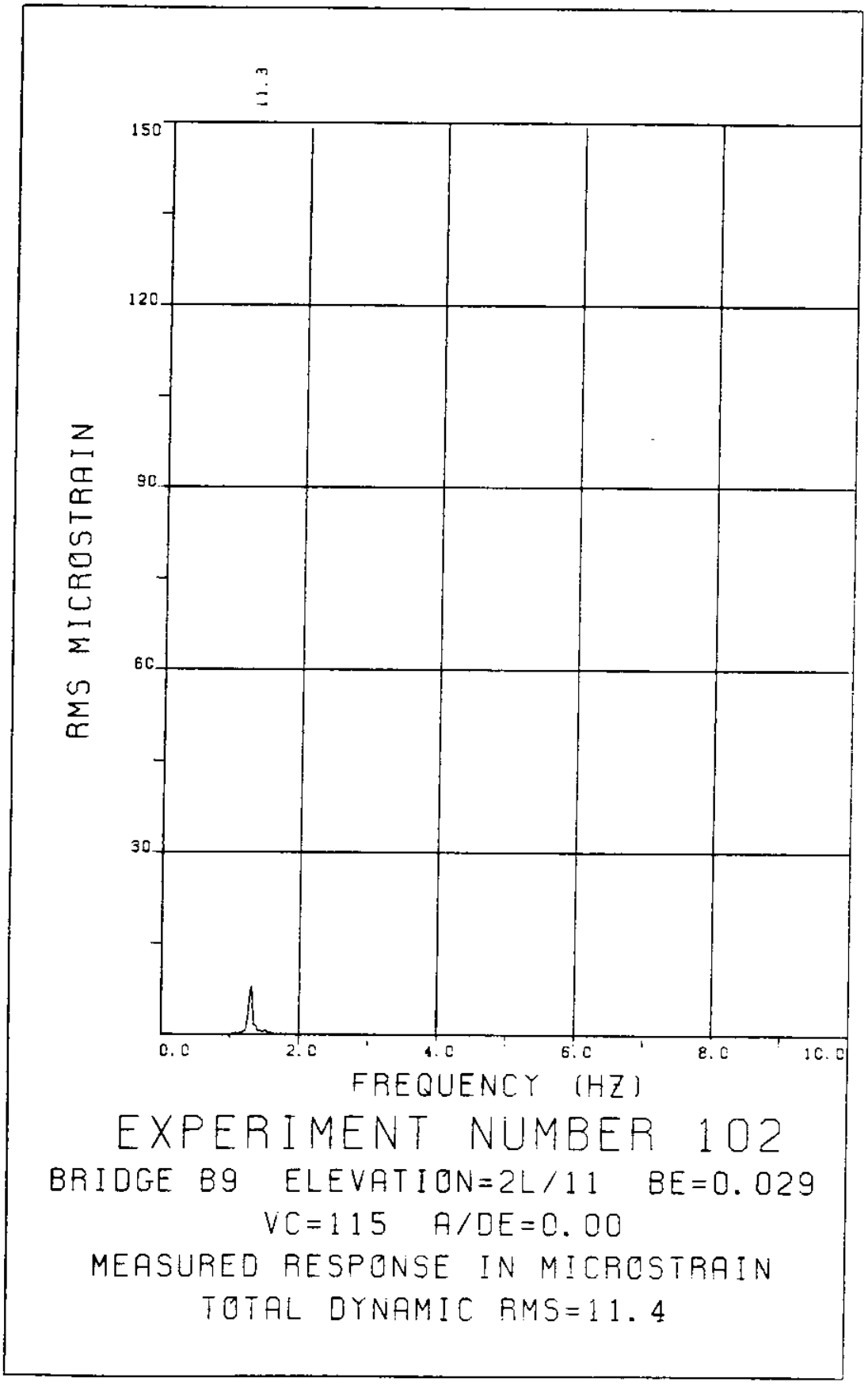

EXPERIMENT NUMBER 102

BRIDGE B9 ELEVATION=2L/11 BE=0.029

VC=115 A/DE=0.00

MEASURED RESPONSE IN MICROSTRAIN

TOTAL DYNAMIC RMS=11.4

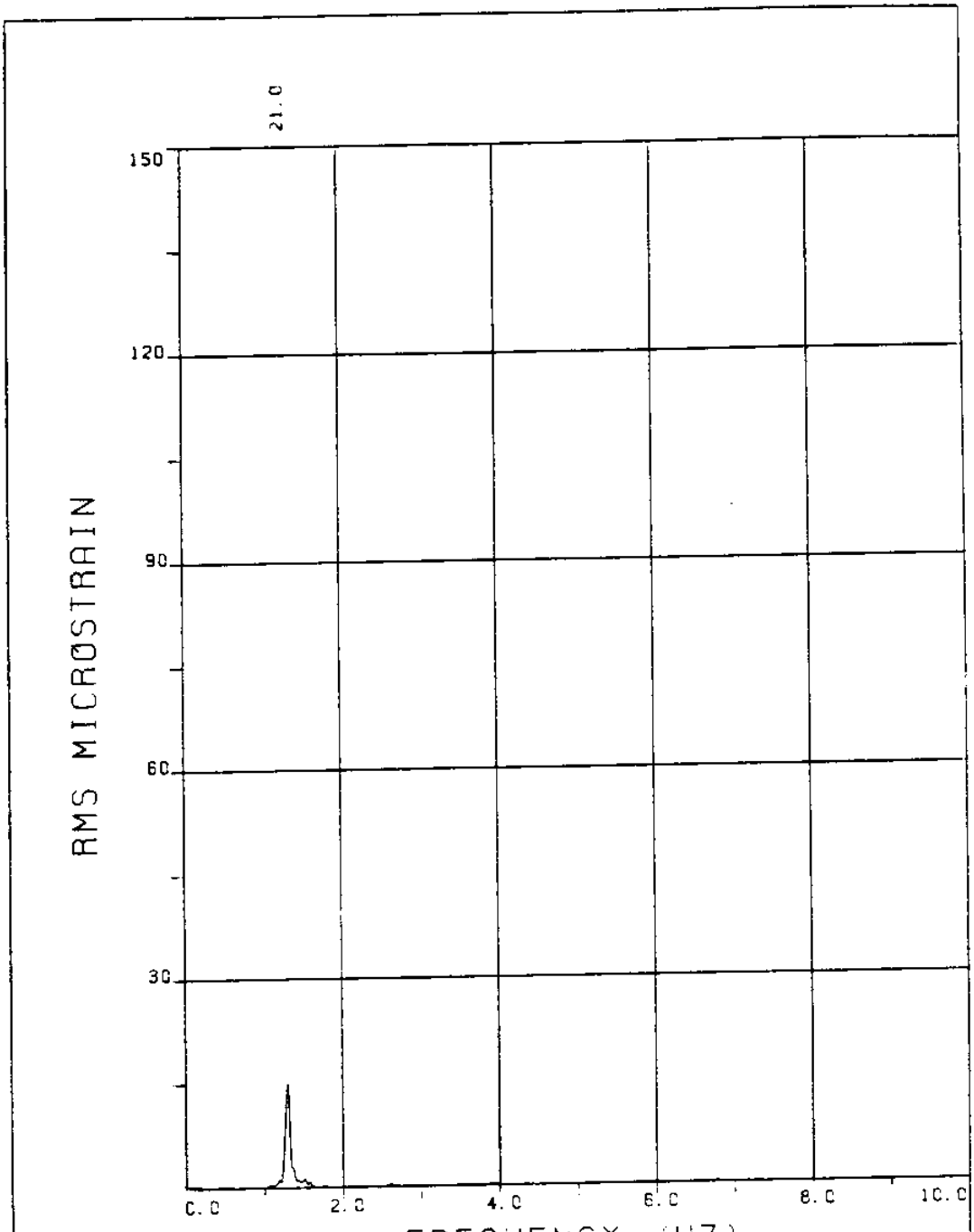

EXPERIMENT NUMBER 102

BRIDGE 87 ELEVATION=4L/11 BE=0.029

VC=115 A/DE=0.00

MEASURED RESPONSE IN MICROSTRAIN

TOTAL DYNAMIC RMS=21.1

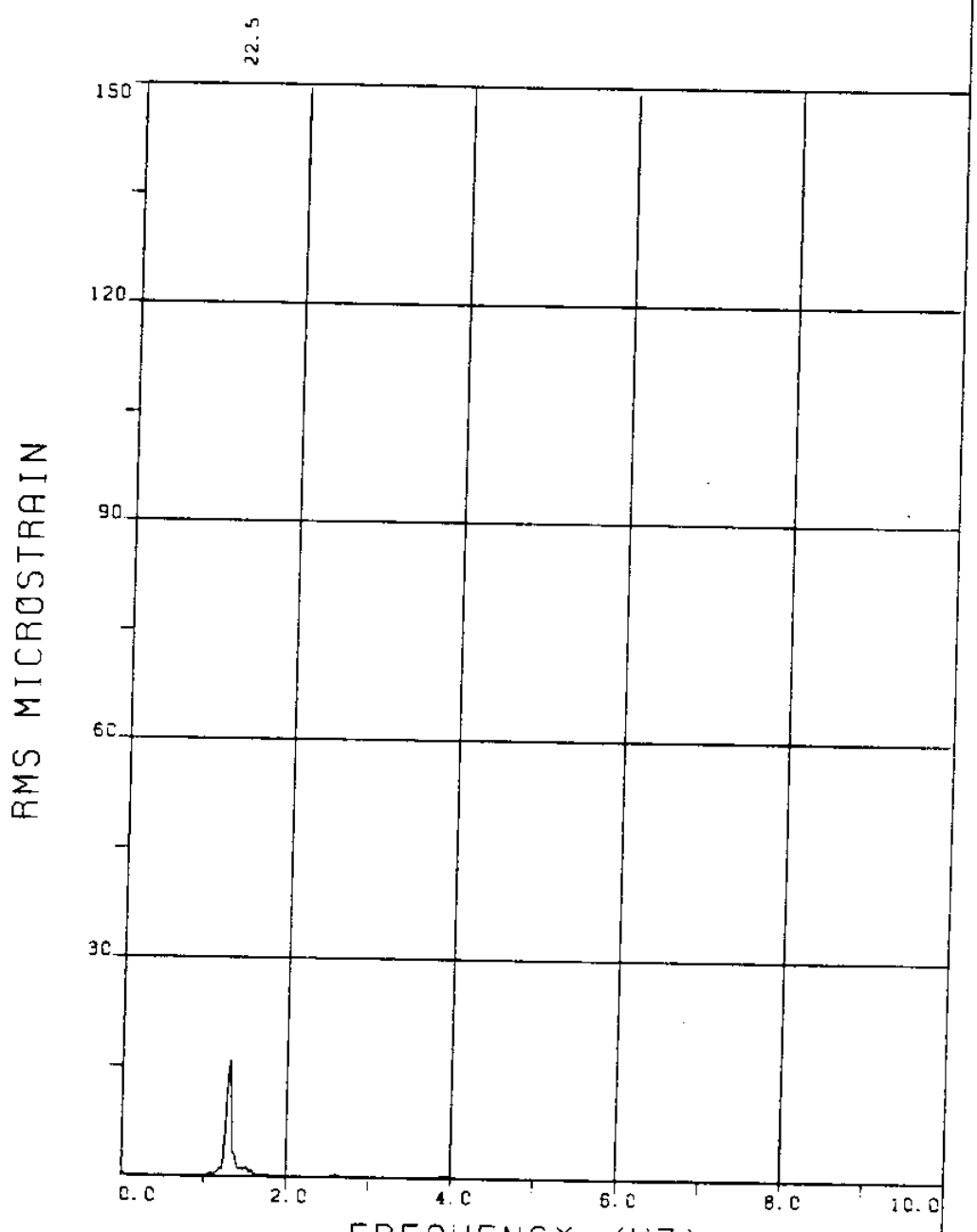

EXPERIMENT NUMBER 102

BRIDGE B6 ELEVATION=5L/11 BE=0.029

VC=115 A/DE=0.00

MEASURED RESPONSE IN MICROSTRAIN

TOTAL DYNAMIC RMS=22.5

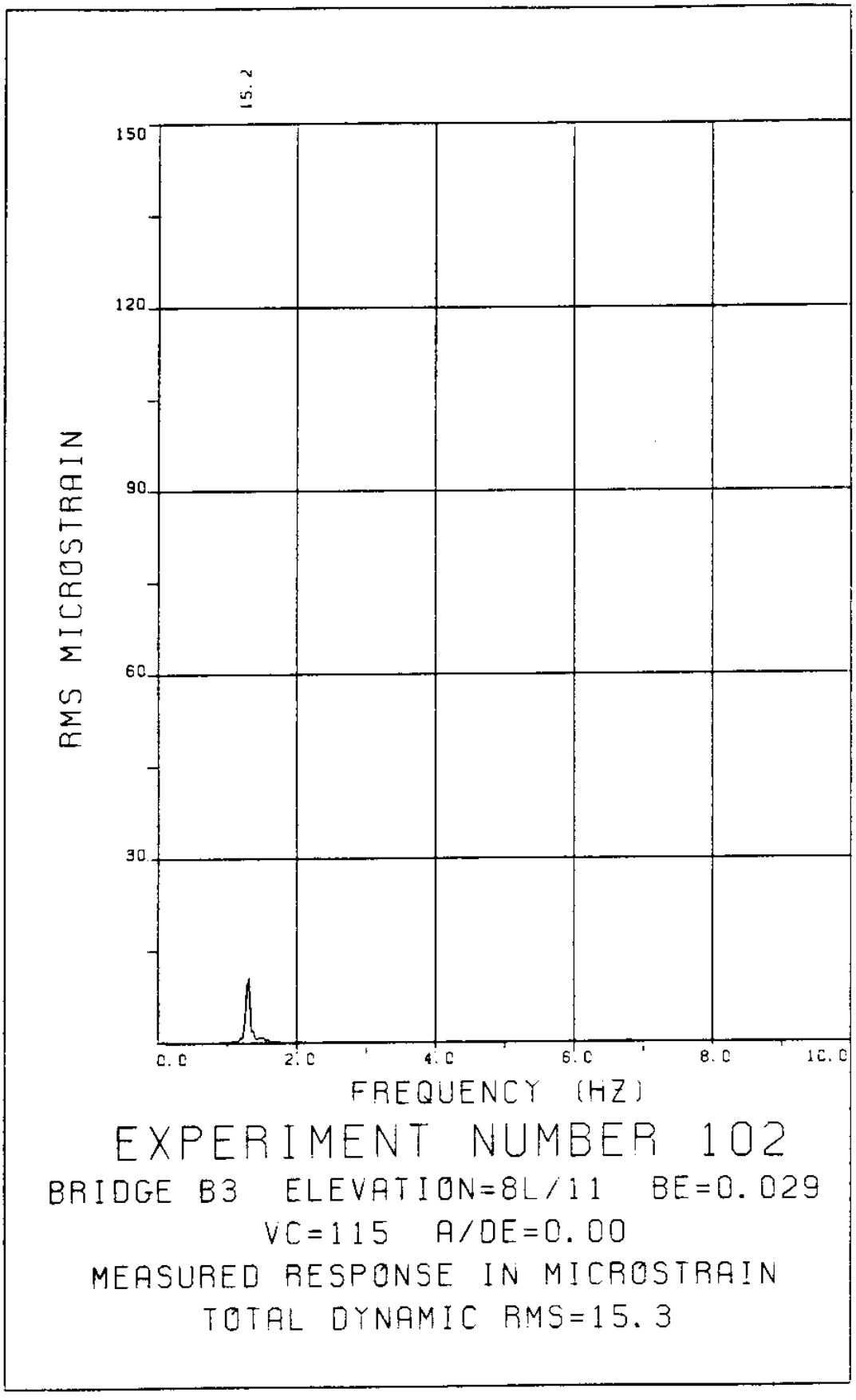

EXPERIMENT NUMBER 102

BRIDGE B3 ELEVATION=8L/11 BE=0.029

VC=115 A/DE=0.00

MEASURED RESPONSE IN MICROSTRAIN

TOTAL DYNAMIC RMS=15.3

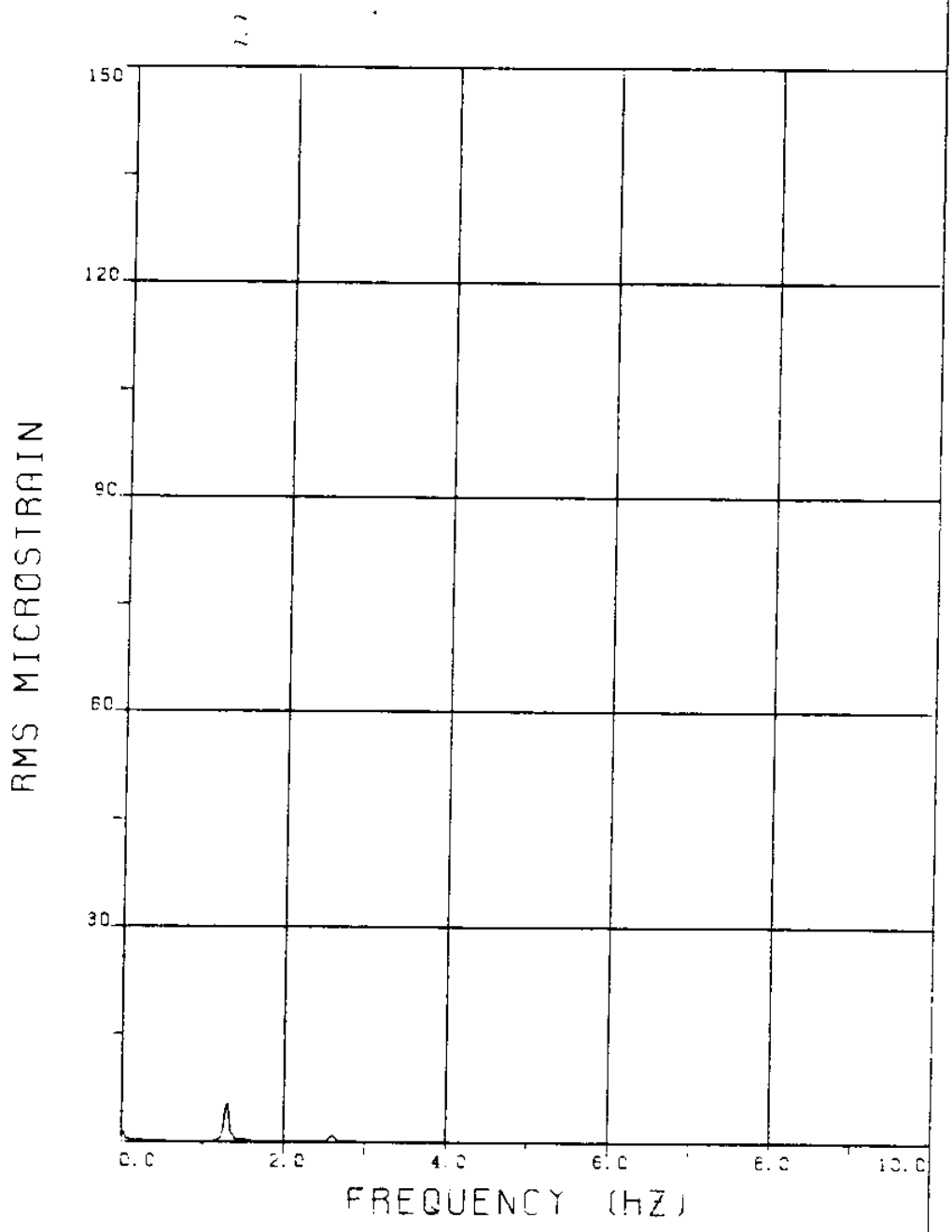

EXPERIMENT NUMBER 102

BRIDGE A6 ELEVATION=5L/11 BE=0.029

VC=115 A/DE=0.00

MEASURED RESPONSE IN MICROSTRAIN

MEAN=23.8

TOTAL DYNAMIC RMS=8.1

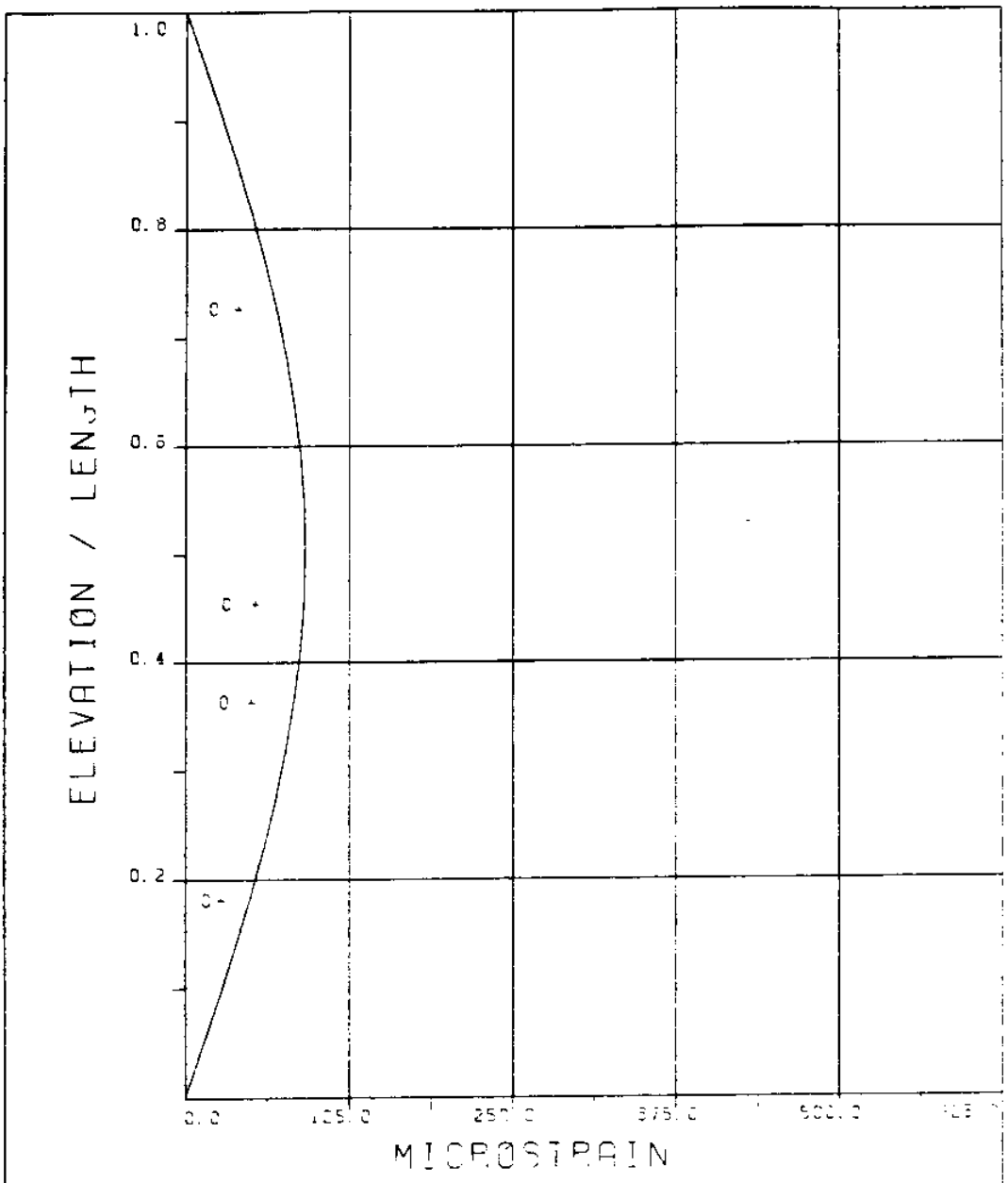

EXPERIMENT NUMBER 102

VC=115 A/DE=0.00

DYNAMIC RESPONSE AT F=FR IN PLANE B

——— THEORY o o o EXPERIMENT

MAXIMUM DYNAMIC RESPONSE IN PLANE B

——— THEORY + + + EXPERIMENT

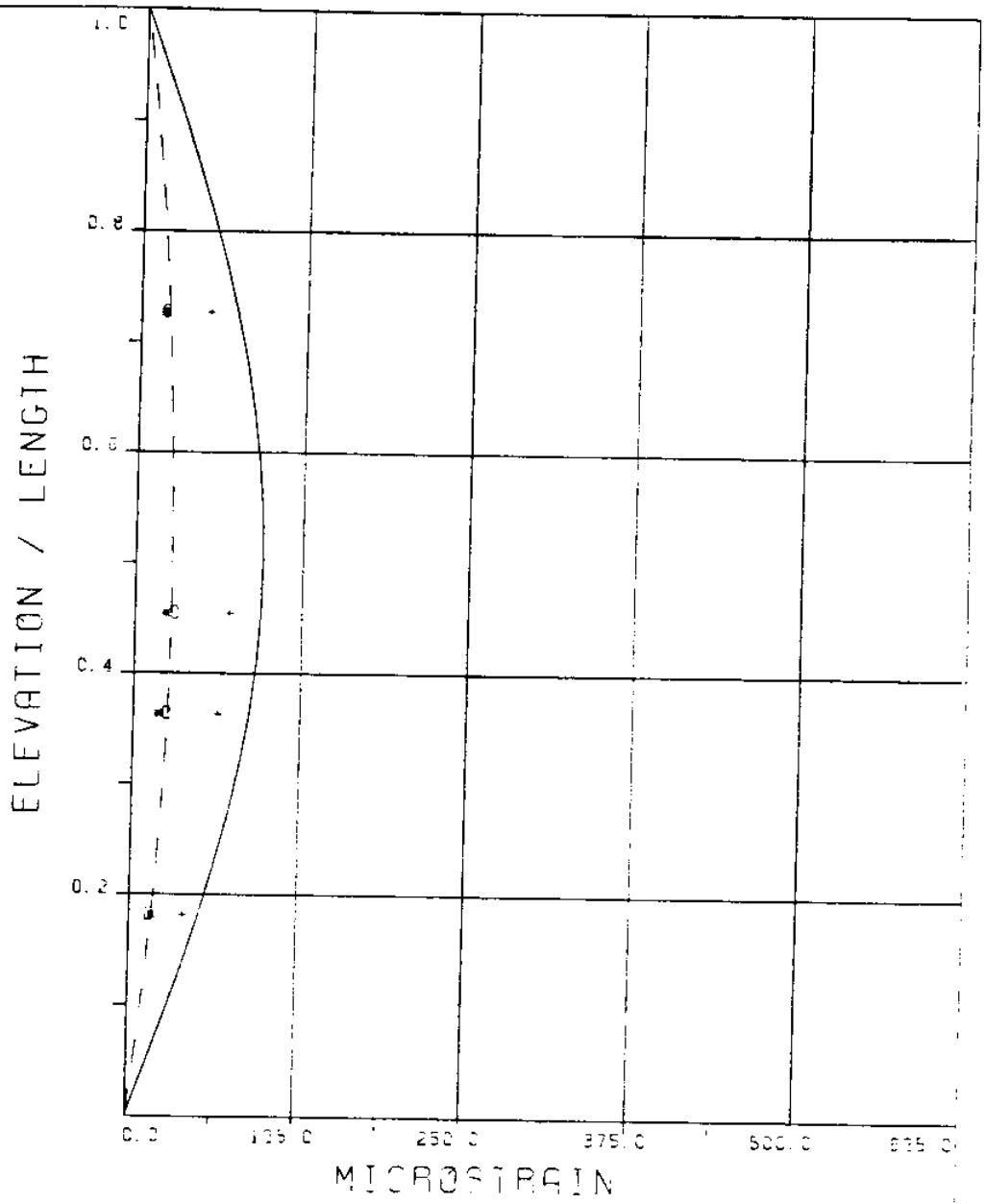

EXPERIMENT NUMBER 102

VC=115 A/DE=0.00

STATIC RESPONSE IN PLANE A

----- THEORY * * * EXPERIMENT

MAXIMUM DYNAMIC RESPONSE IN PLANE A

o o o EXPERIMENT

MAXIMUM RESPONSE

_____ THEORY + + + EXPERIMENT

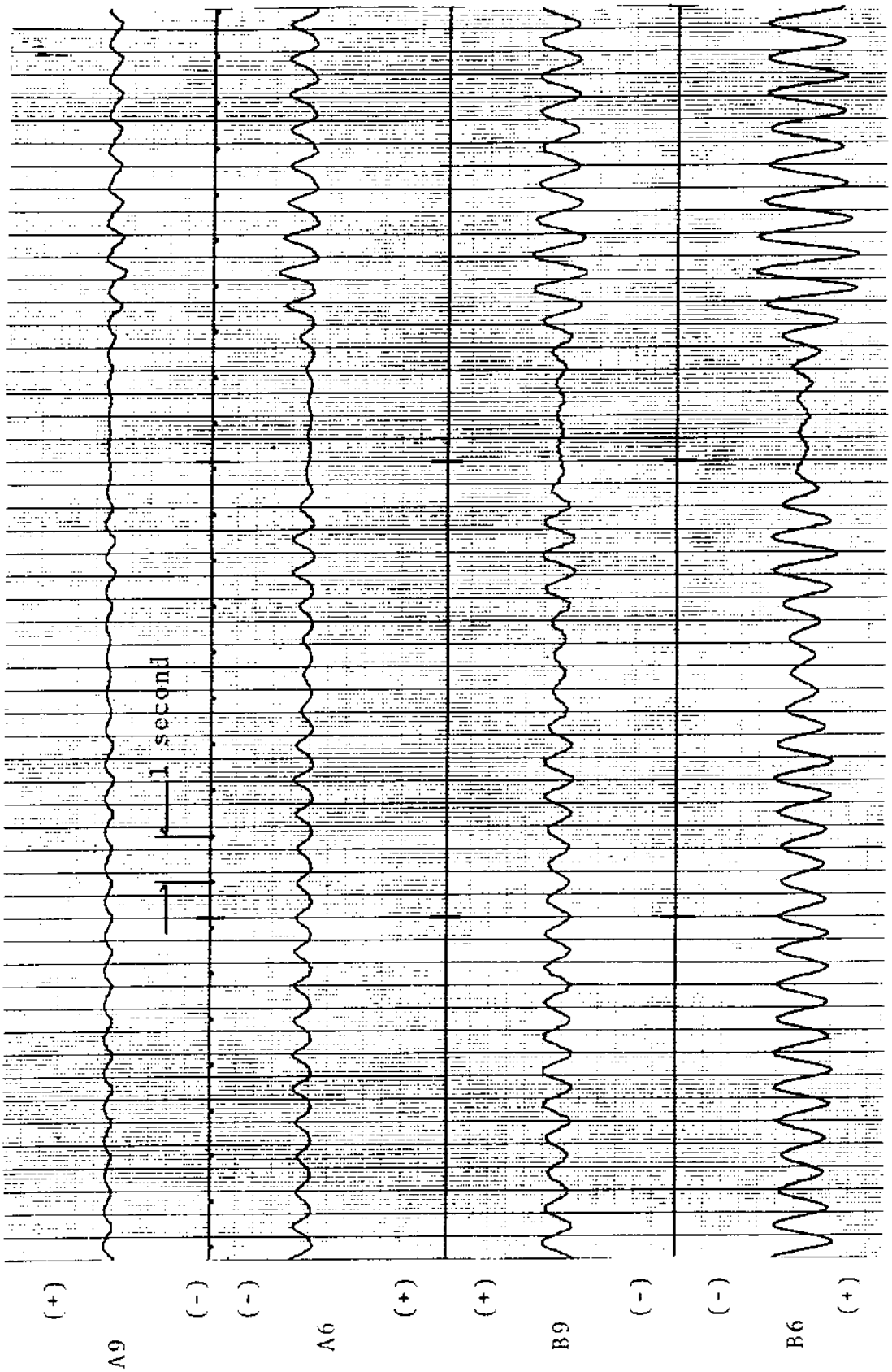

FIGURE 102Ta: ALL BRIDGES: 3.8 MICROSTRAIN/DIVISION

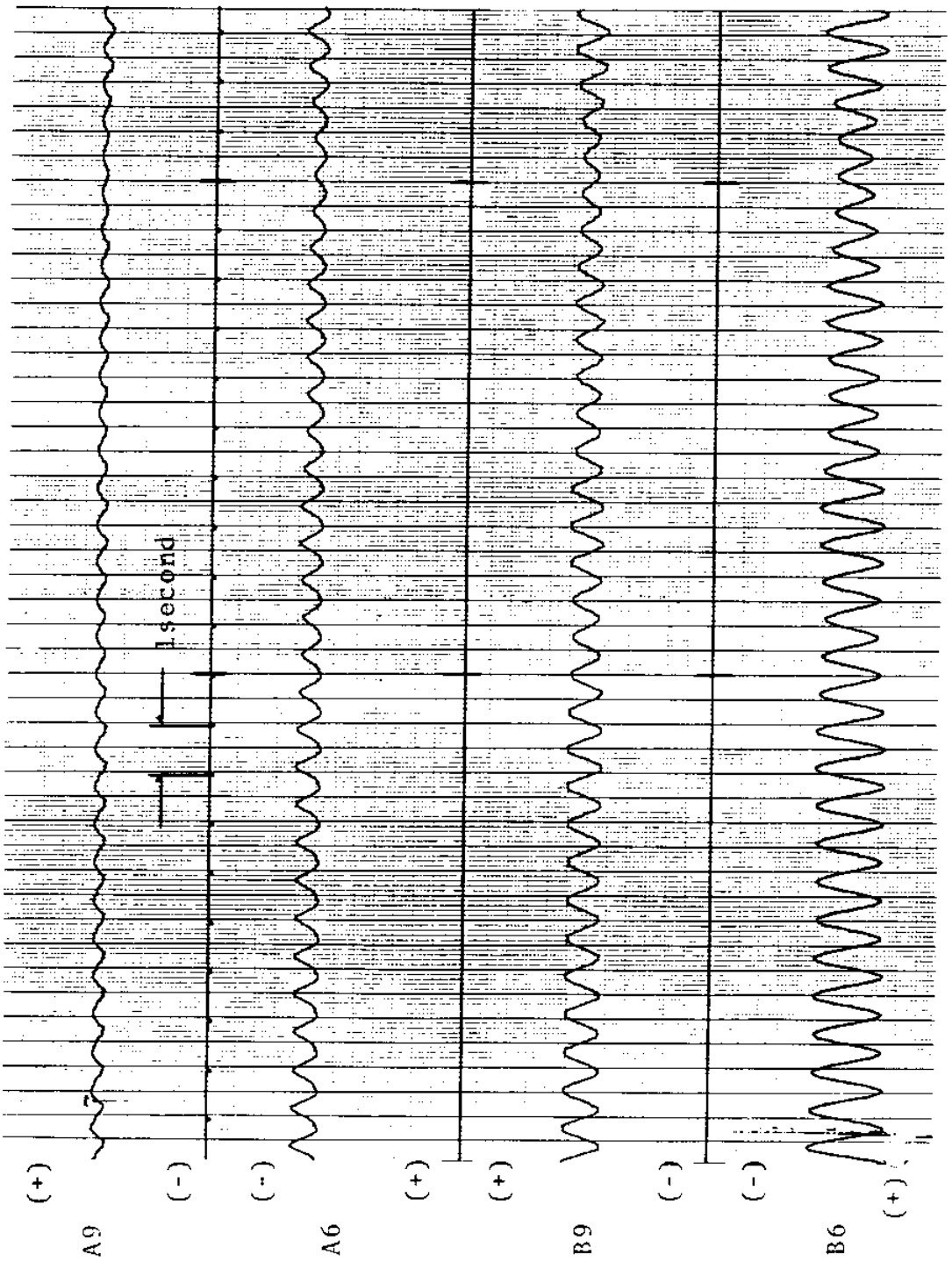

FIGURE 102Tb: ALL BRIDGES: 3.8 MICROSTRAIN/DIVISION

EXPERIMENT 104

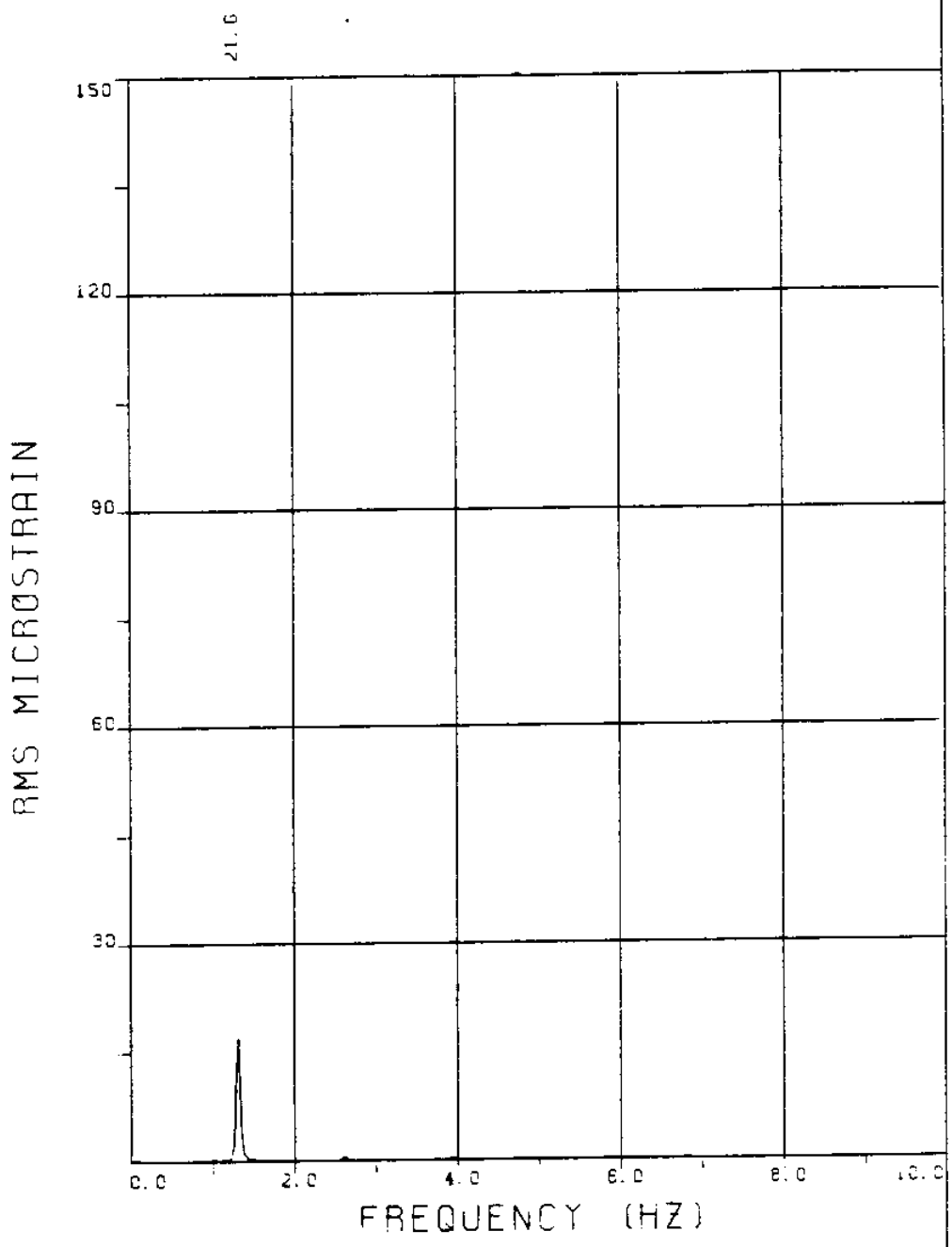

EXPERIMENT NUMBER 104

BRIDGE B9 ELEVATION=2L/11 BE=0.029

VC=120 A/DE=0.00

MEASURED RESPONSE IN MICROSTRAIN

TOTAL DYNAMIC RMS=21.7

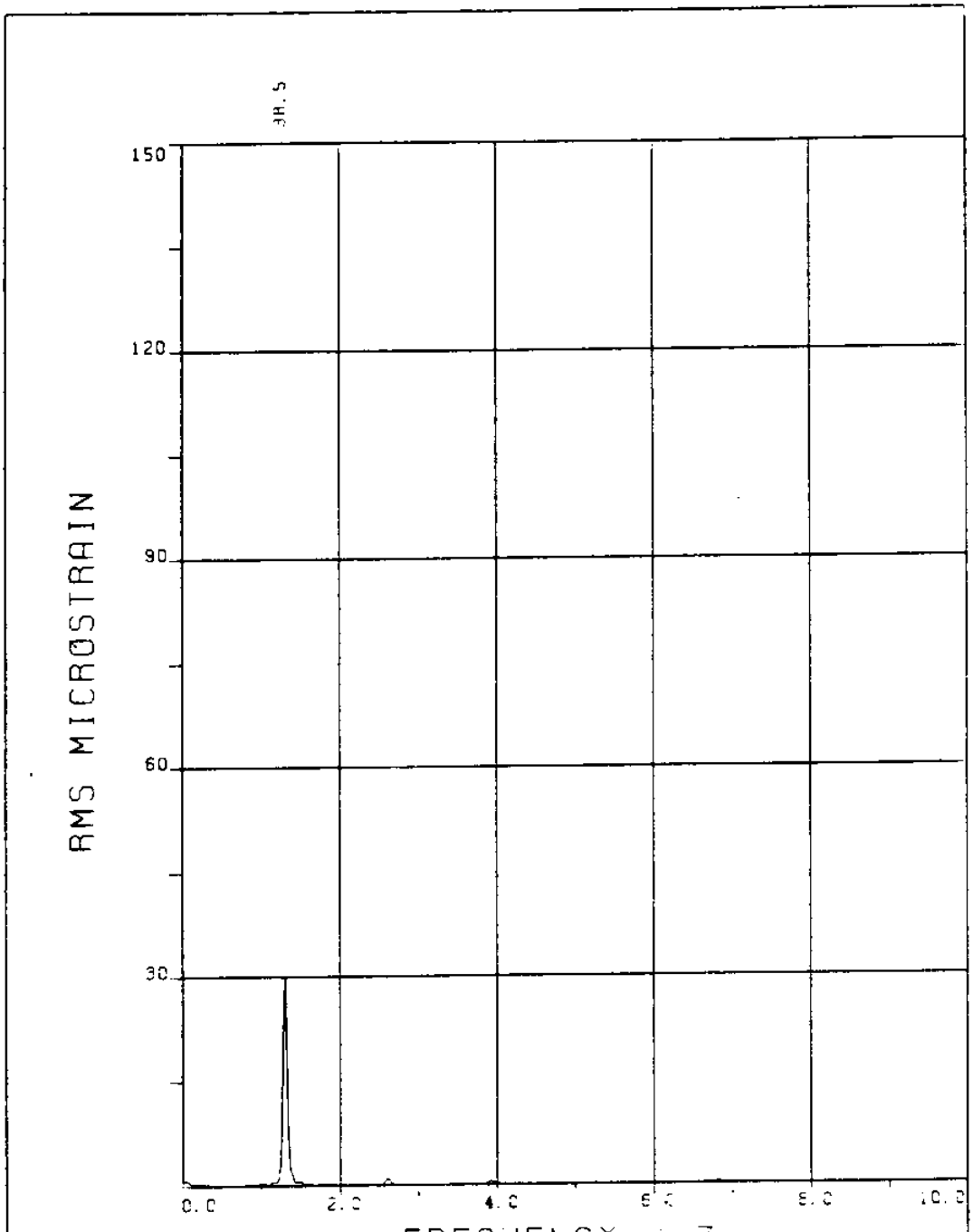

EXPERIMENT NUMBER 104

BRIDGE B7 ELEVATION=4L/11 BE=0.029

VC=120 A/DE=0.00

MEASURED RESPONSE IN MICROSTRAIN

TOTAL DYNAMIC RMS=38.6

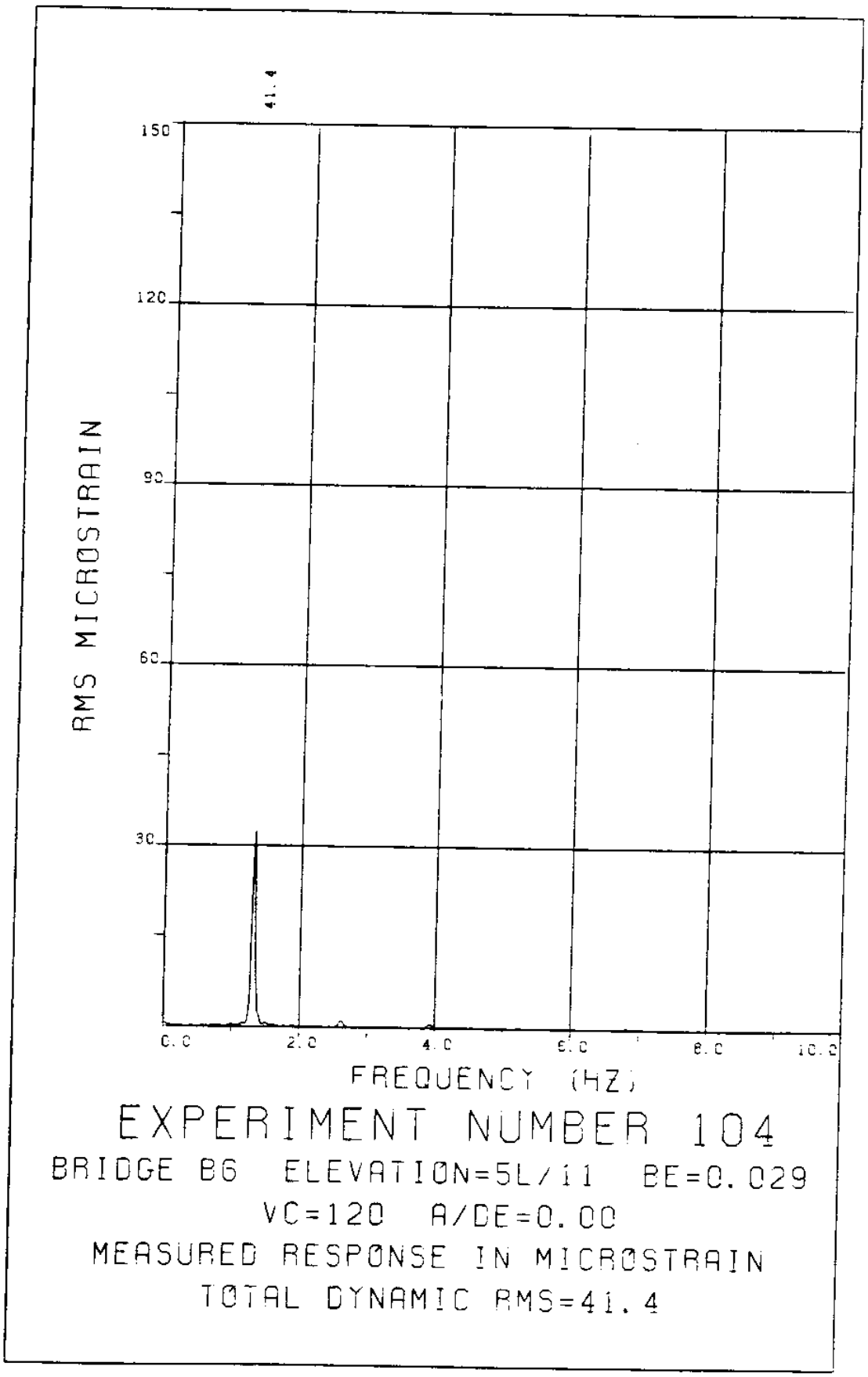

EXPERIMENT NUMBER 104

BRIDGE B6 ELEVATION=5L/11 BE=0.029

VC=120 A/DE=0.00

MEASURED RESPONSE IN MICROSTRAIN

TOTAL DYNAMIC RMS=41.4

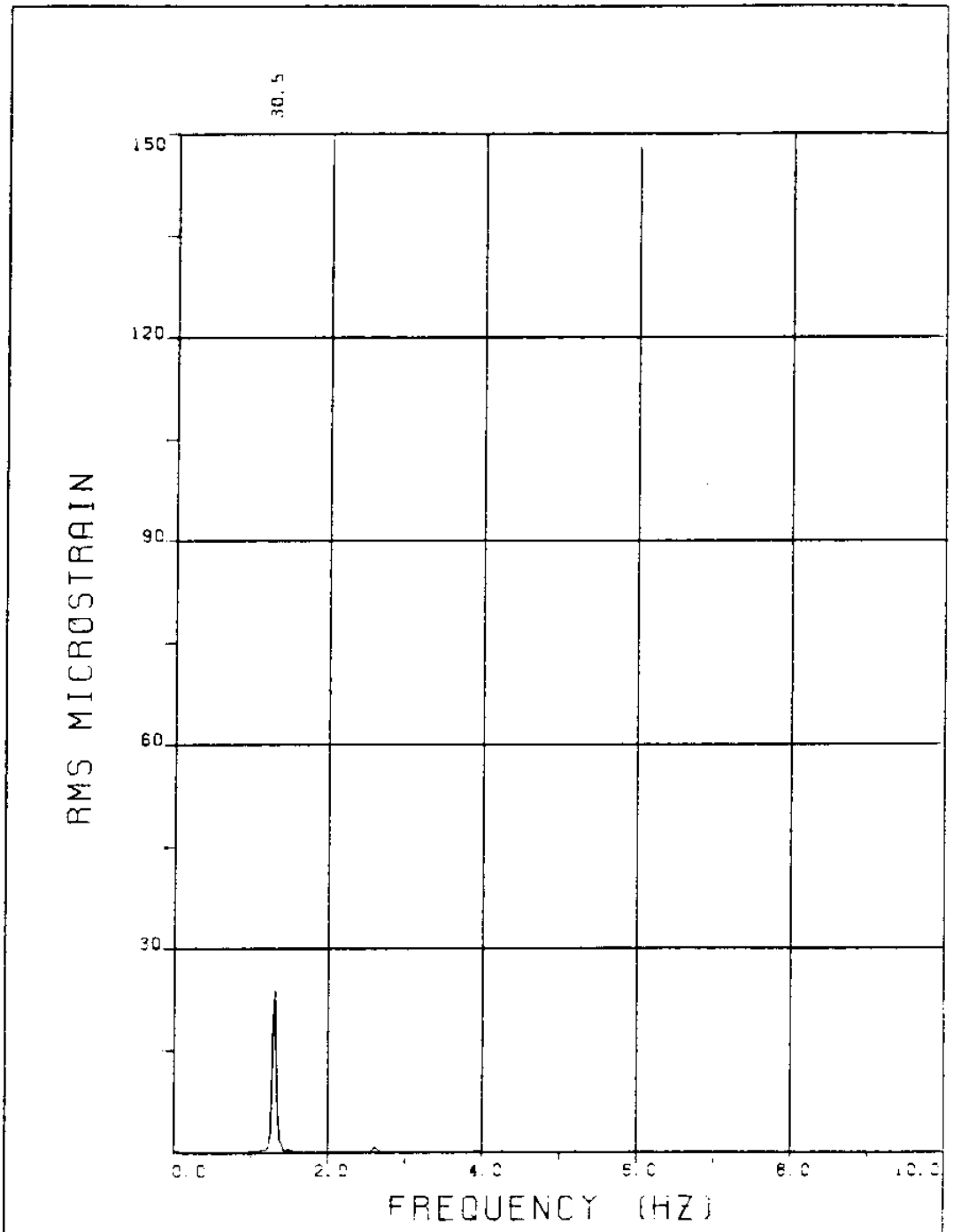

EXPERIMENT NUMBER 104

BRIDGE B3 ELEVATION=8L/11 BE=0.029

VC=120 A/DE=0.00

MEASURED RESPONSE IN MICROSTRAIN

TOTAL DYNAMIC RMS=30.6

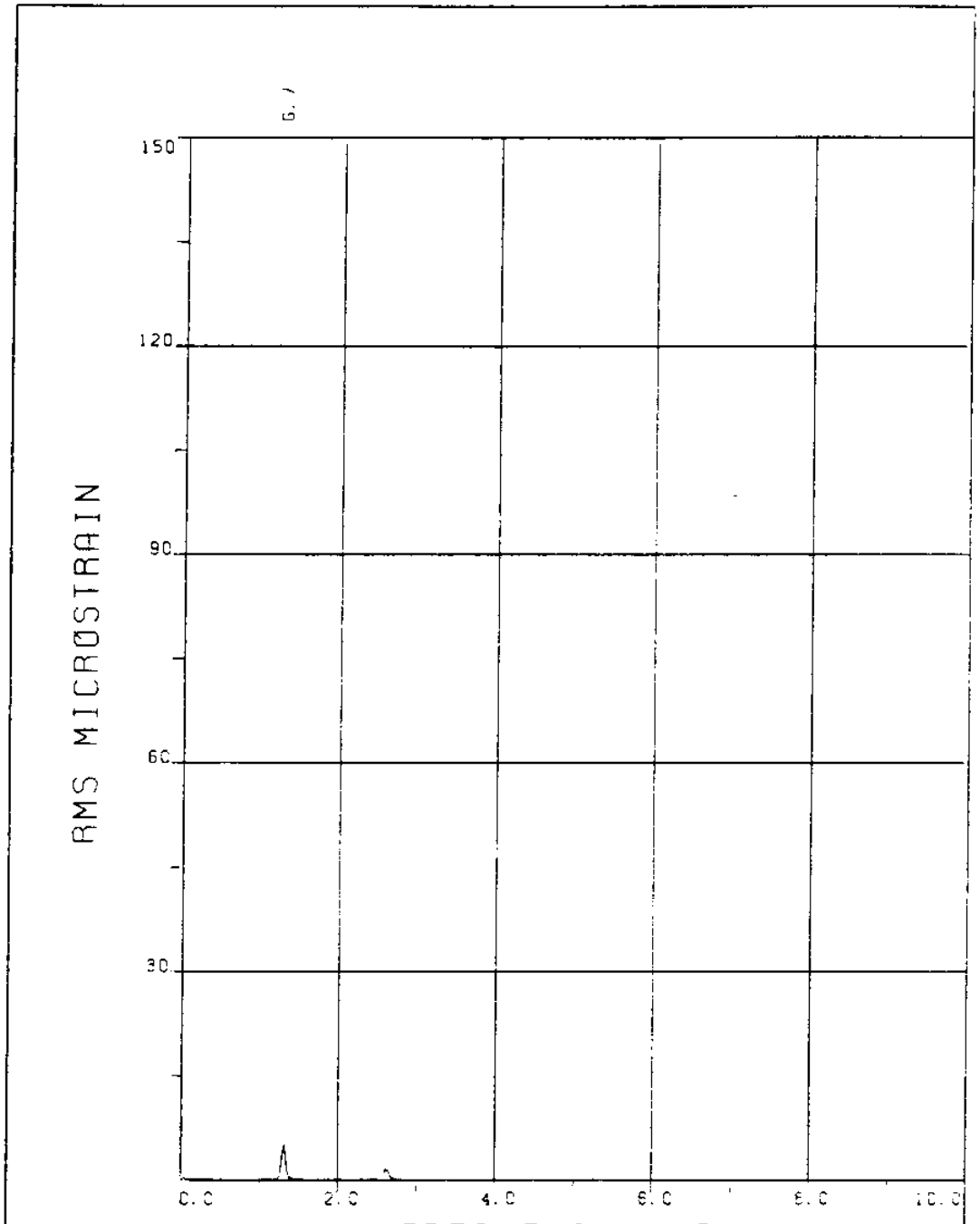

EXPERIMENT NUMBER 104

BRIDGE A9 ELEVATION=2L/11 BE=0.029

VC=120 A/DE=0.00

MEASURED RESPONSE IN MICROSTRAIN

MEAN=22.1

TOTAL DYNAMIC RMS=7.1

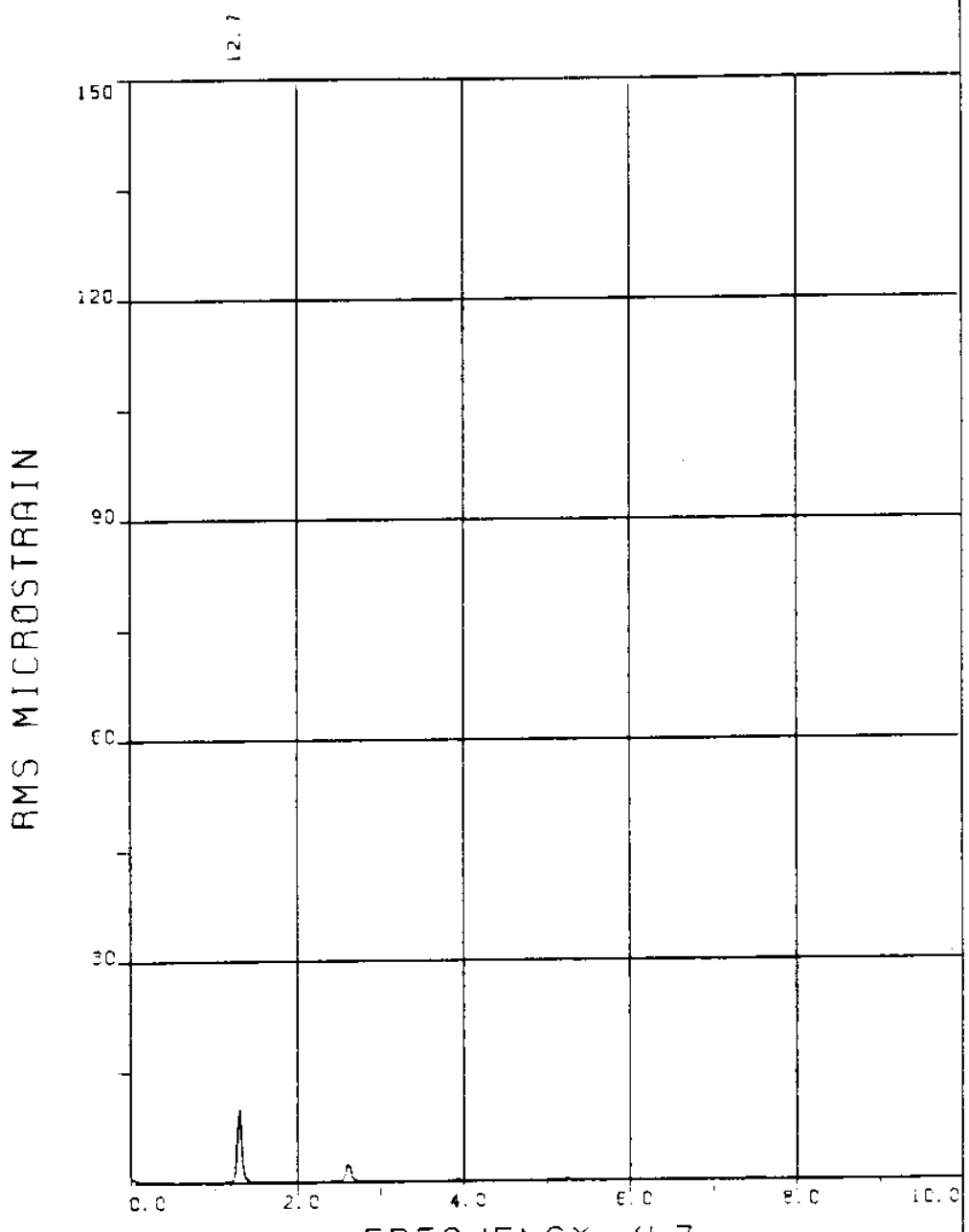

EXPERIMENT NUMBER 104

BRIDGE A7 ELEVATION=4L/11 BE=0.029

VC=120 A/DE=0.00

MEASURED RESPONSE IN MICROSTRAIN

MEAN=26.9

TOTAL DYNAMIC RMS=13.3

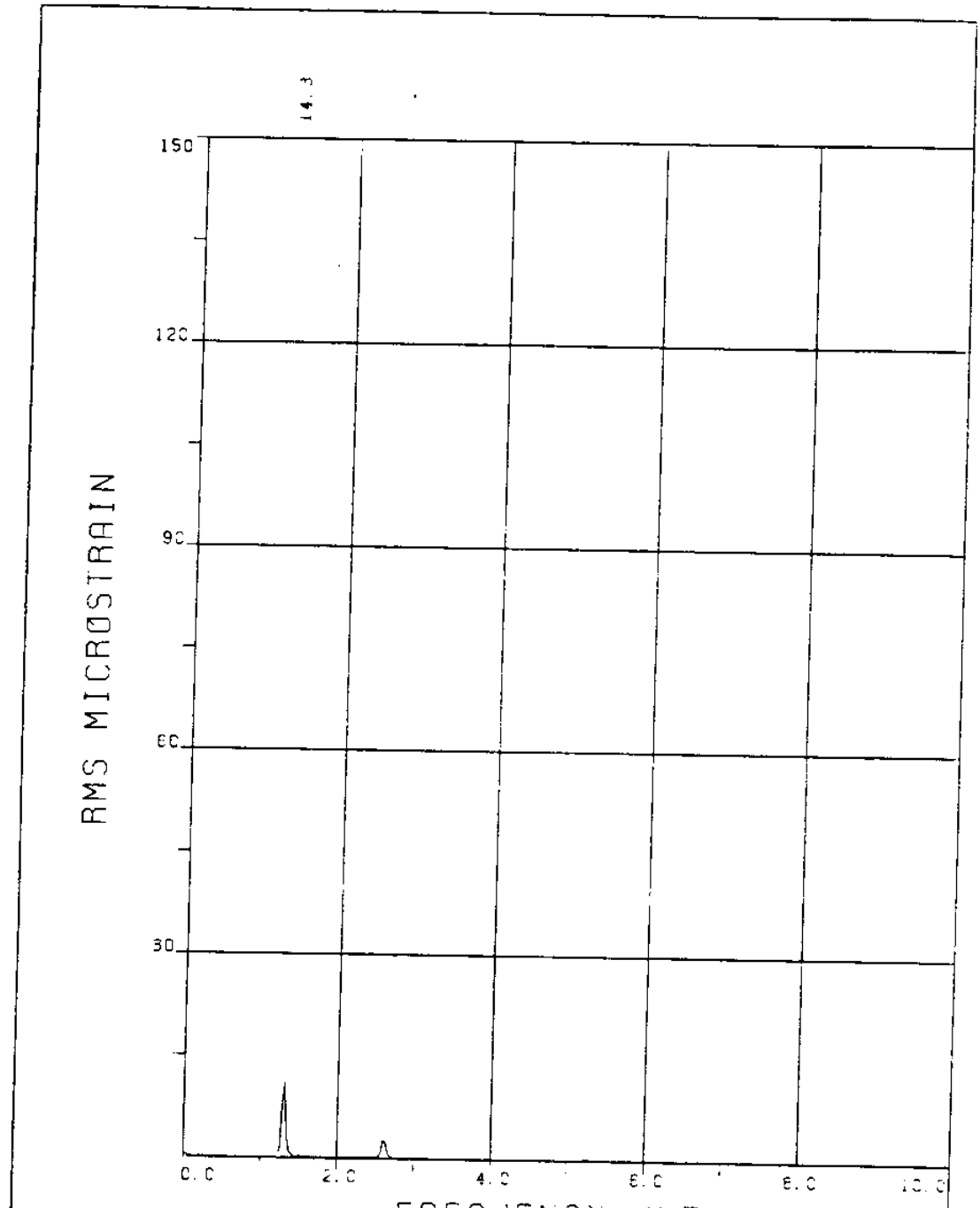

EXPERIMENT NUMBER 104

BRIDGE A6 ELEVATION=5L/11 BE=0.029

VC=120 A/DE=0.00

MEASURED RESPONSE IN MICROSTRAIN

MEAN=31.9

TOTAL DYNAMIC RMS=14.8

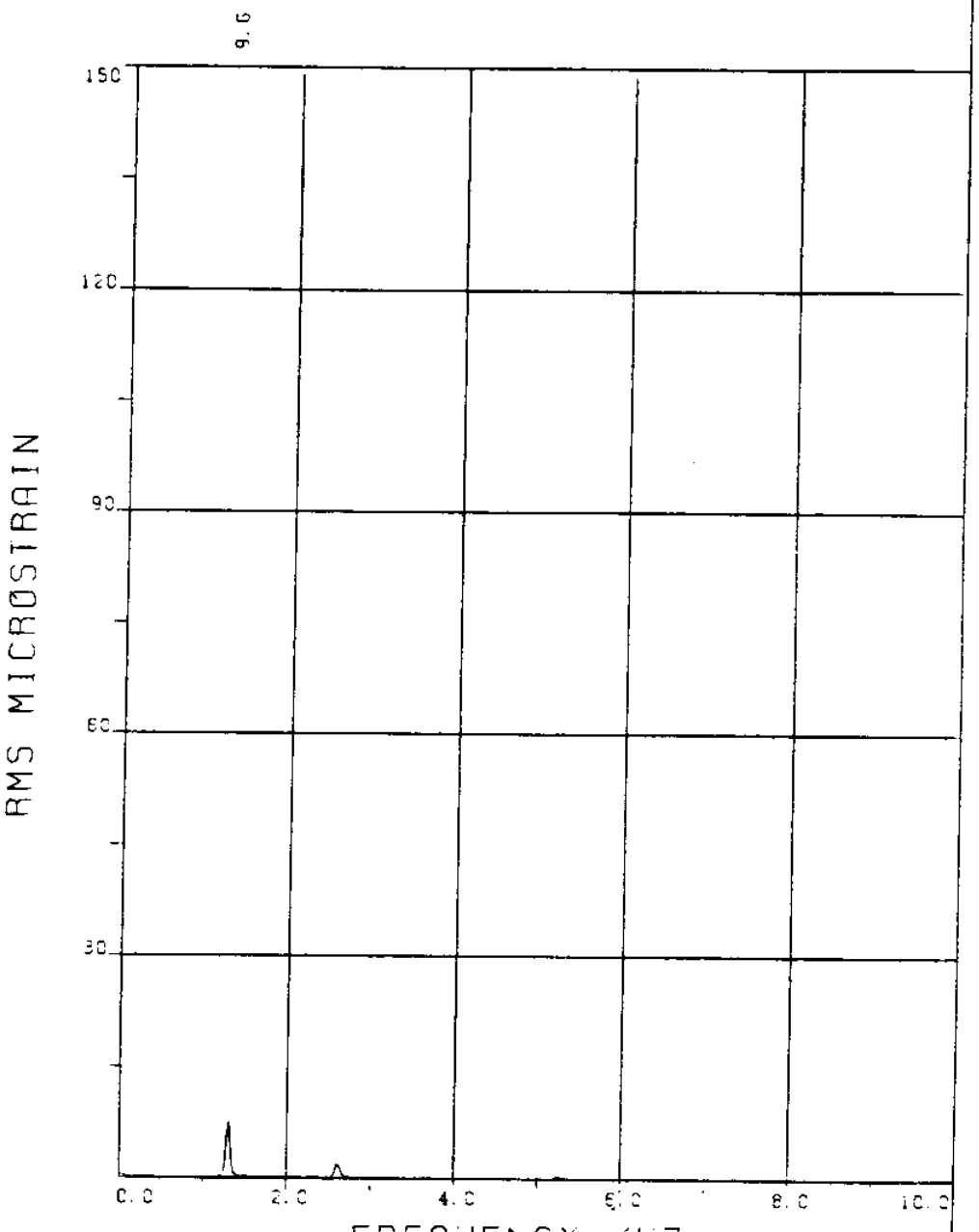

EXPERIMENT NUMBER 104

BRIDGE A3 ELEVATION=8L/11 BE=0.029

VC=120 A/DE=0.00

MEASURED RESPONSE IN MICROSTRAIN

MEAN=25.3.

TOTAL DYNAMIC RMS=10.1

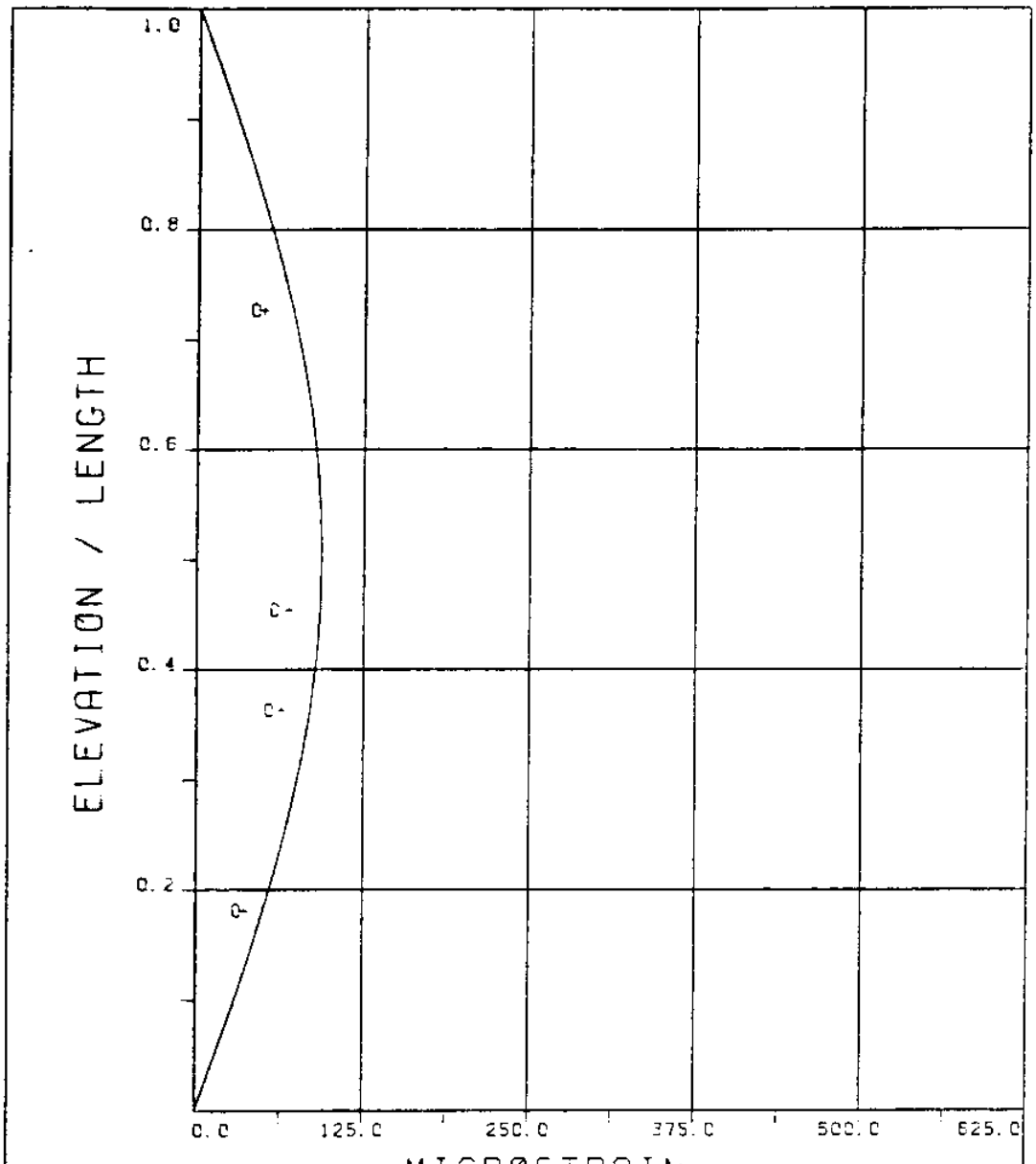

EXPERIMENT NUMBER 104

VC=120 A/DE=0.00

DYNAMIC RESPONSE AT F=FR IN PLANE B

_____ THEORY o o o EXPERIMENT

MAXIMUM DYNAMIC RESPONSE IN PLANE B

_____ THEORY + + + EXPERIMENT

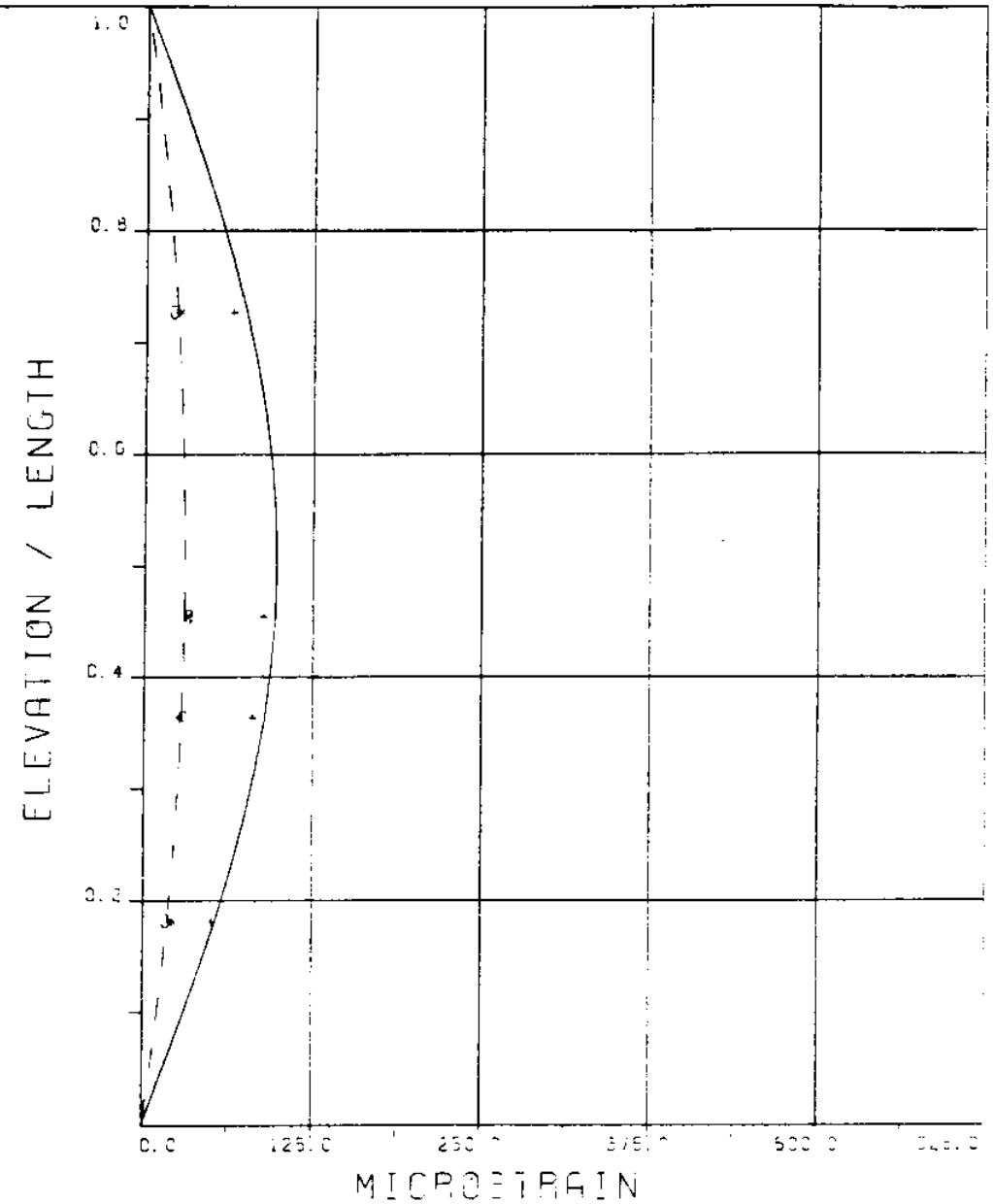

EXPERIMENT NUMBER 104

VC=120 A/DE=0.00

STATIC RESPONSE IN PLANE A

----- THEORY * * * EXPERIMENT

MAXIMUM DYNAMIC RESPONSE IN PLANE A

o o o EXPERIMENT

MAXIMUM RESPONSE

_____ THEORY + + + EXPERIMENT

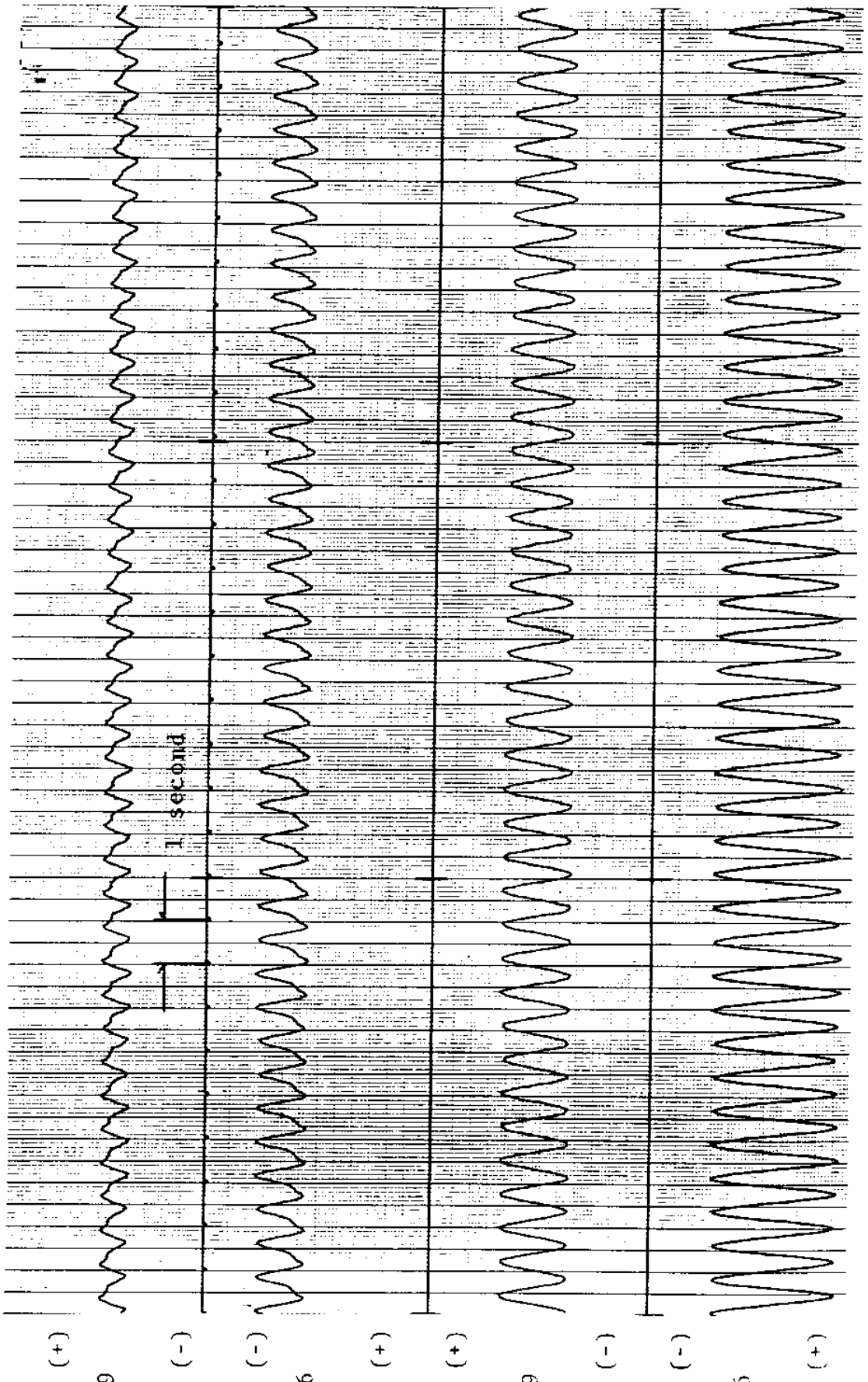

FIGURE 104T: ALL BRIDGES: 3.8 MICROSTRAIN/DIVISION

EXPERIMENT 106

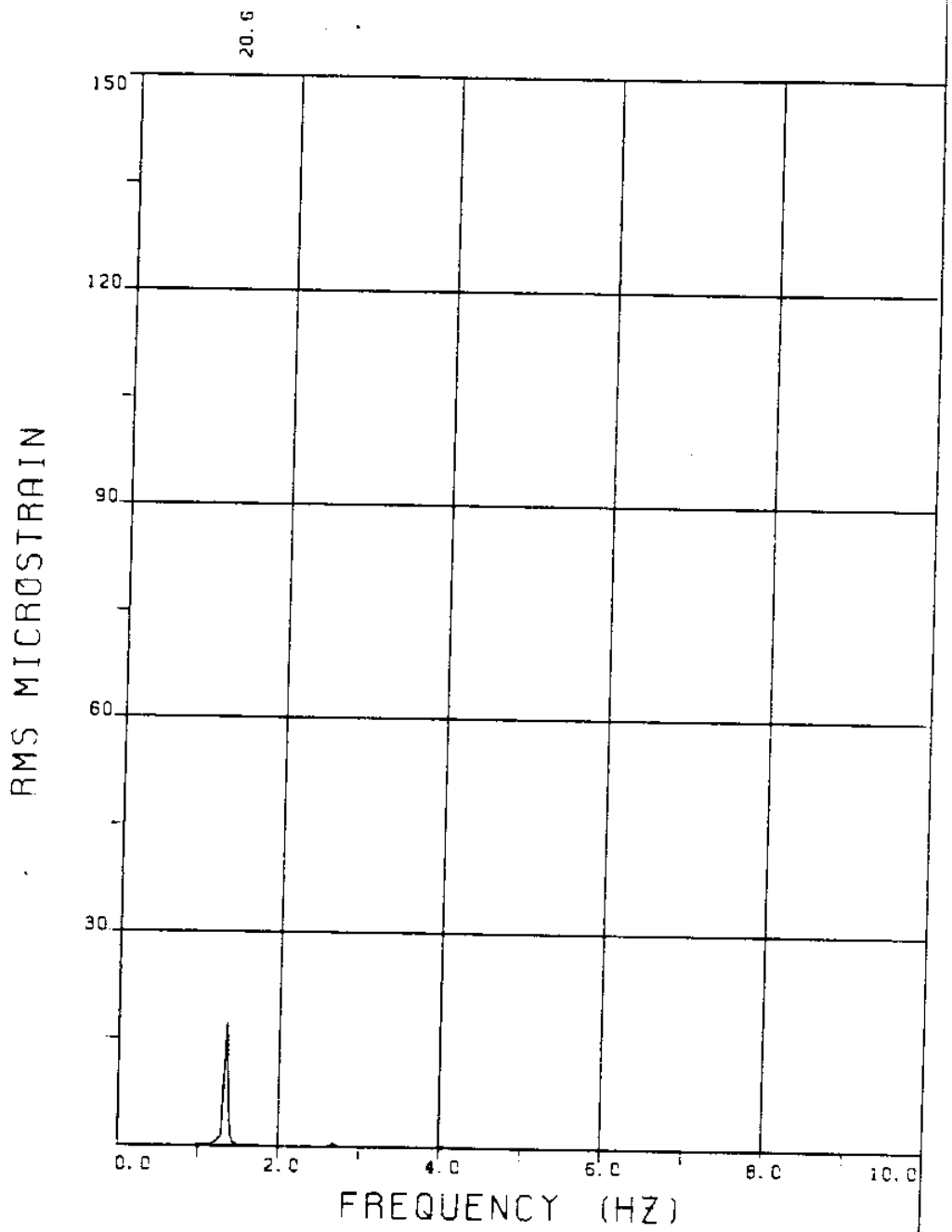

EXPERIMENT NUMBER 106

BRIDGE B9 ELEVATION=2L/11 BE=0.029

VC=125 A/DE=0.00

MEASURED RESPONSE IN MICROSTRAIN

TOTAL DYNAMIC RMS=20.7

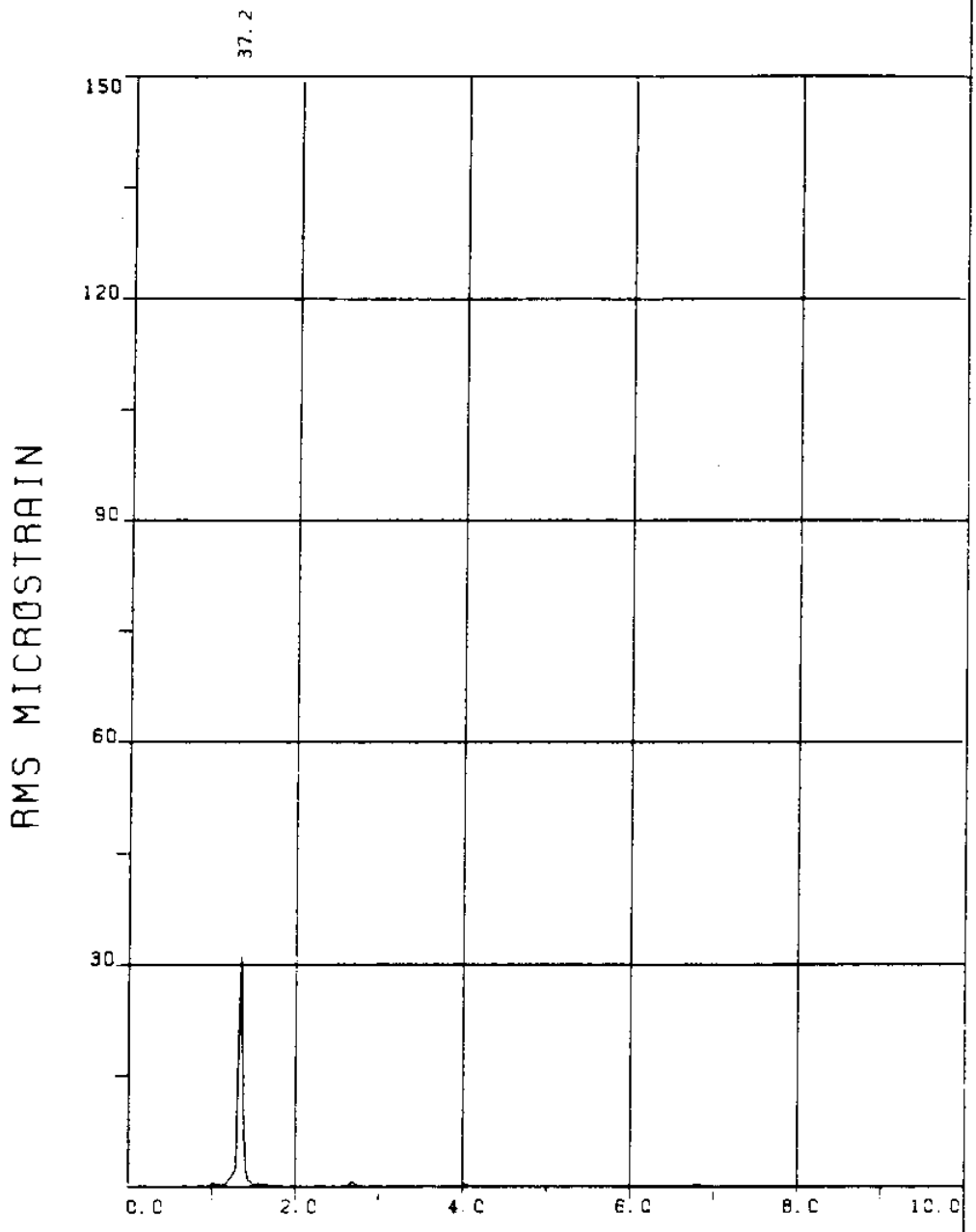

EXPERIMENT NUMBER 106

BRIDGE B7 ELEVATION=4L/11 BE=0.029

VC=125 A/DE=0.00

MEASURED RESPONSE IN MICROSTRAIN

TOTAL DYNAMIC RMS=37.2

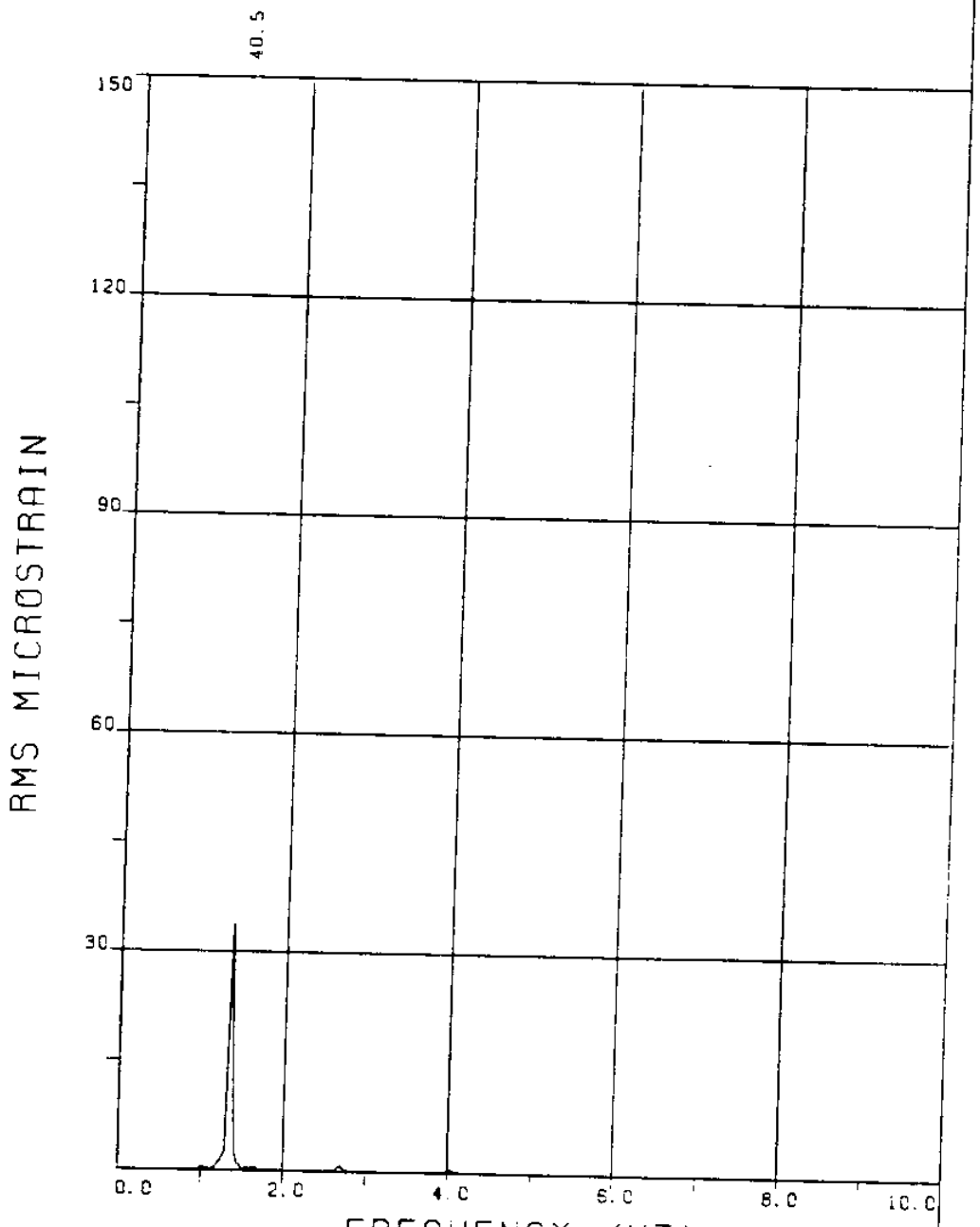

EXPERIMENT NUMBER 106

BRIDGE B6 ELEVATION=5L/11 BE=0.029

VC=125 A/DE=0.00

MEASURED RESPONSE IN MICROSTRAIN

TOTAL DYNAMIC RMS=40.5

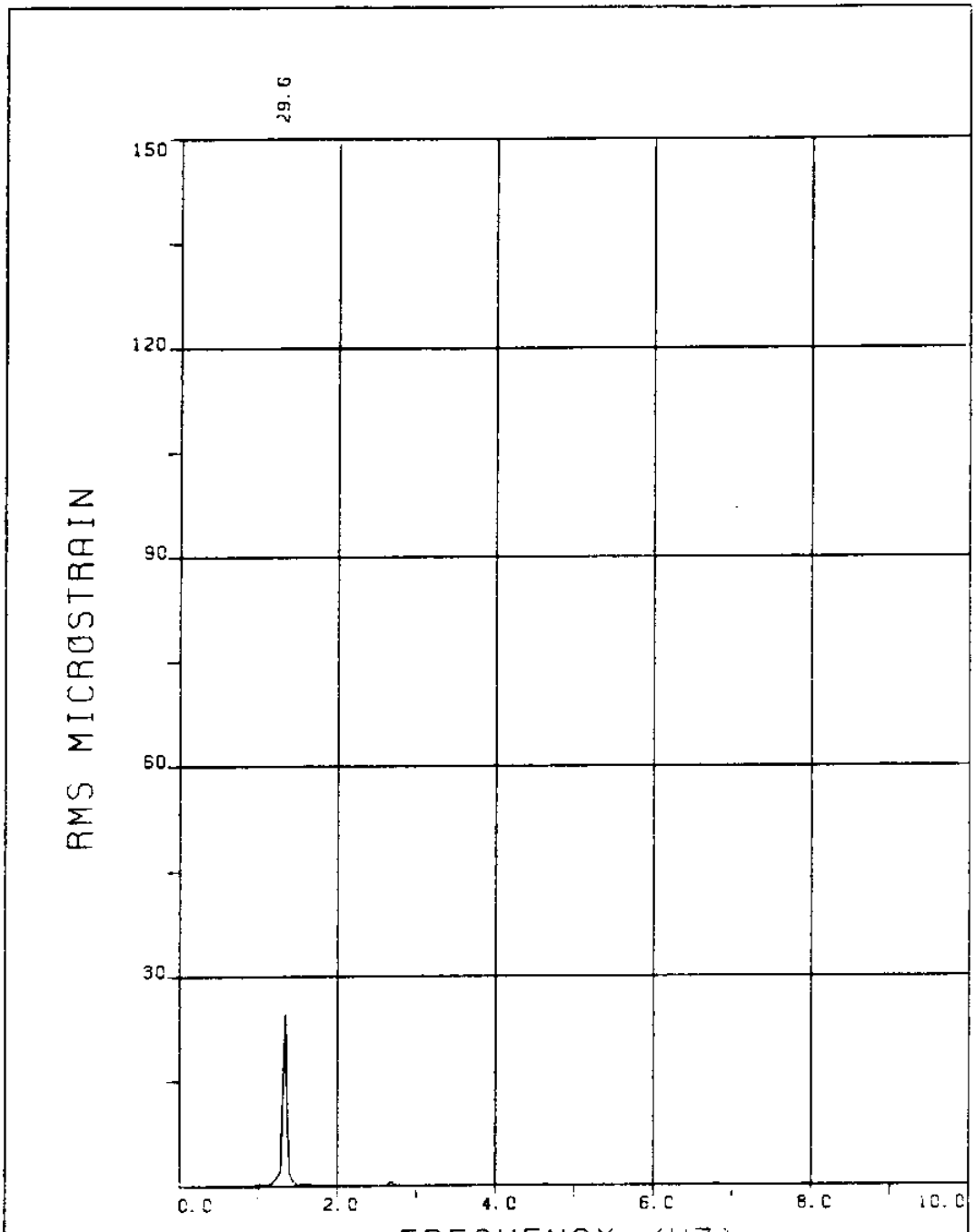

EXPERIMENT NUMBER 106

BRIDGE B3 ELEVATION=8L/11 BE=0.029

VC=125 A/DE=0.00

MEASURED RESPONSE IN MICROSTRAIN

TOTAL DYNAMIC RMS=29.6

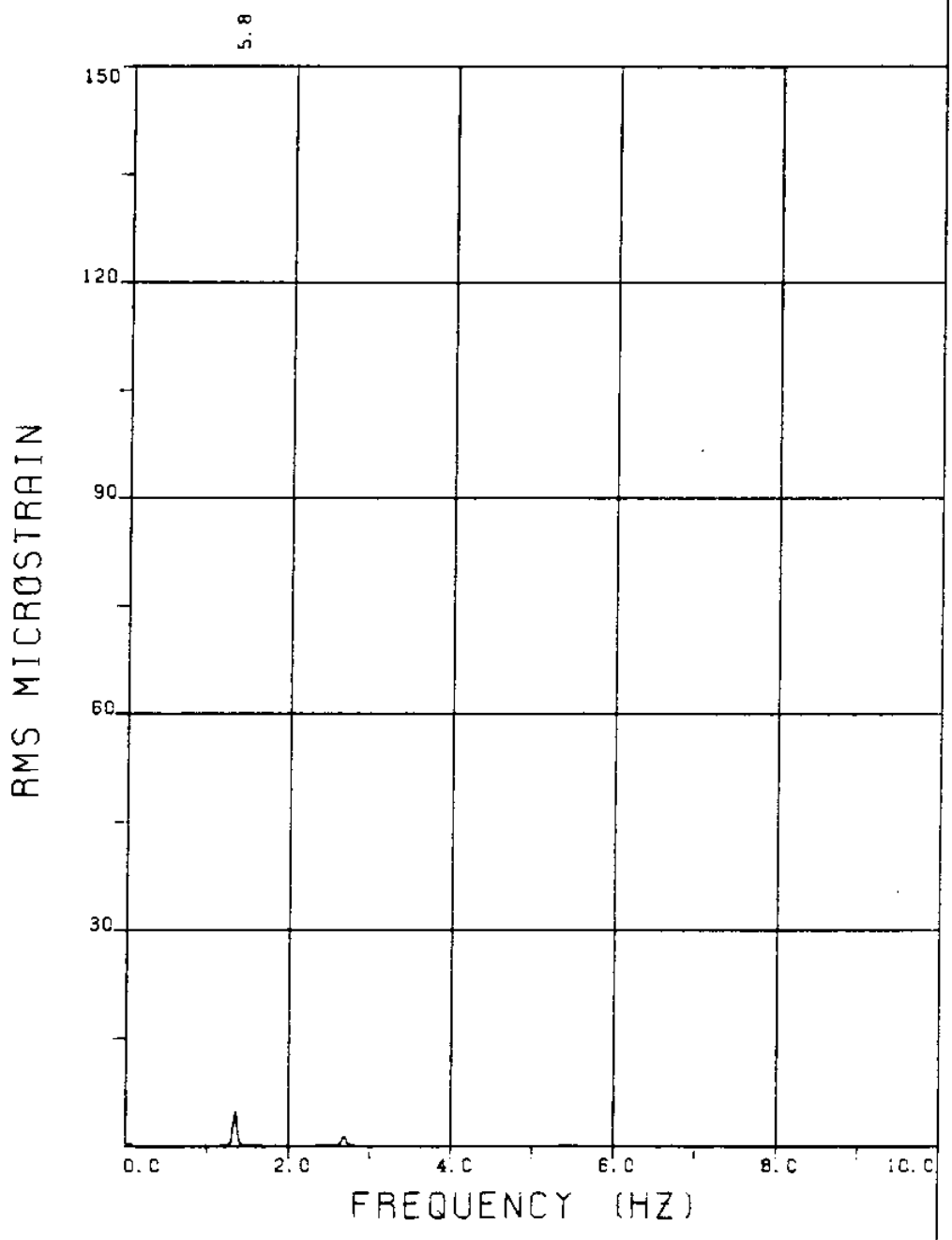

EXPERIMENT NUMBER 106

BRIDGE A9 ELEVATION=2L/11 BE=0.029

VC=125 A/DE=0.00

MEASURED RESPONSE IN MICROSTRAIN

MEAN=21.5

TOTAL DYNAMIC RMS=6.2

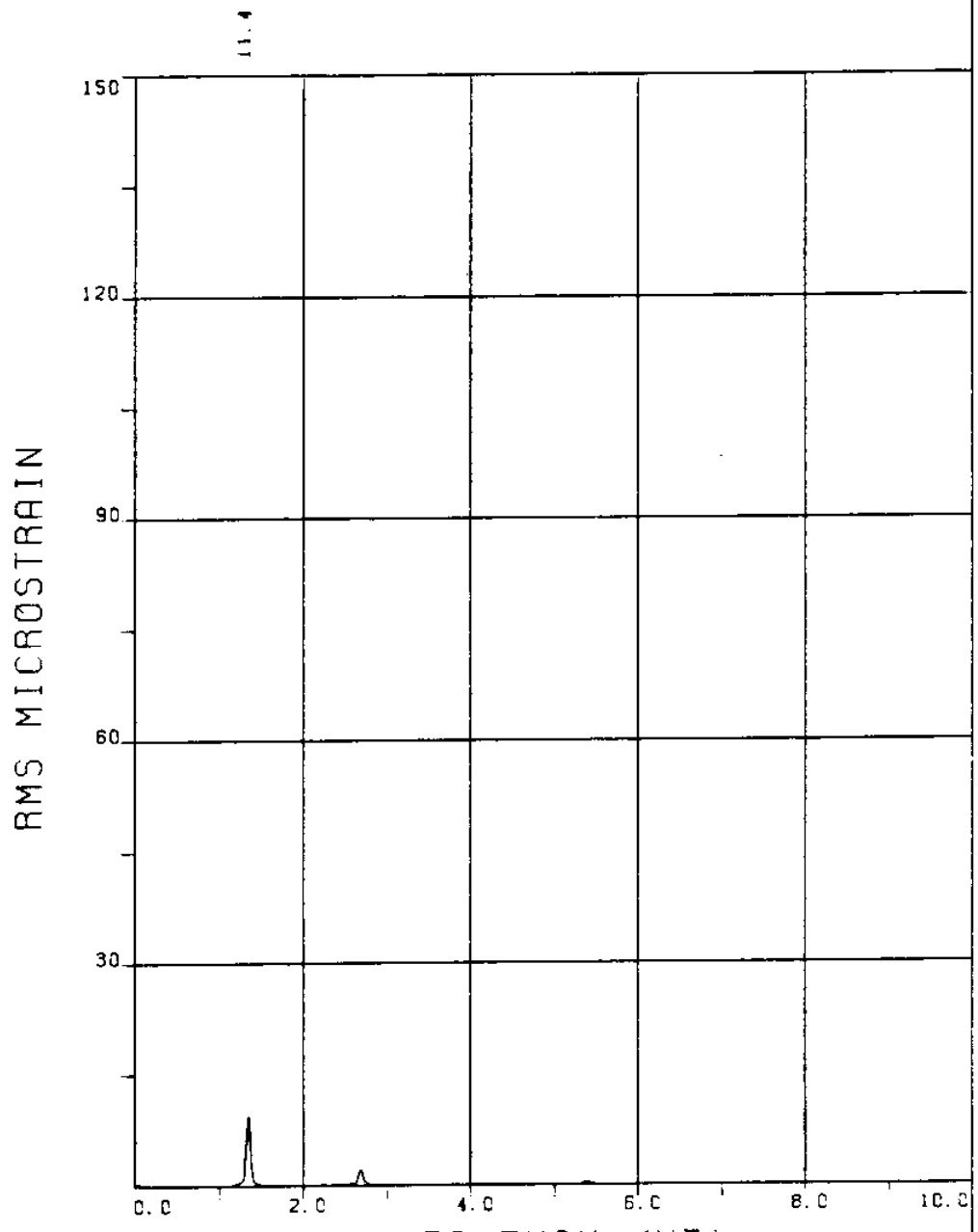

EXPERIMENT NUMBER 106

BRIDGE A7 ELEVATION=4L/11 BE=0.029

VC=125 A/DE=0.00

MEASURED RESPONSE IN MICROSTRAIN

MEAN=28.5

TOTAL DYNAMIC RMS=11.8

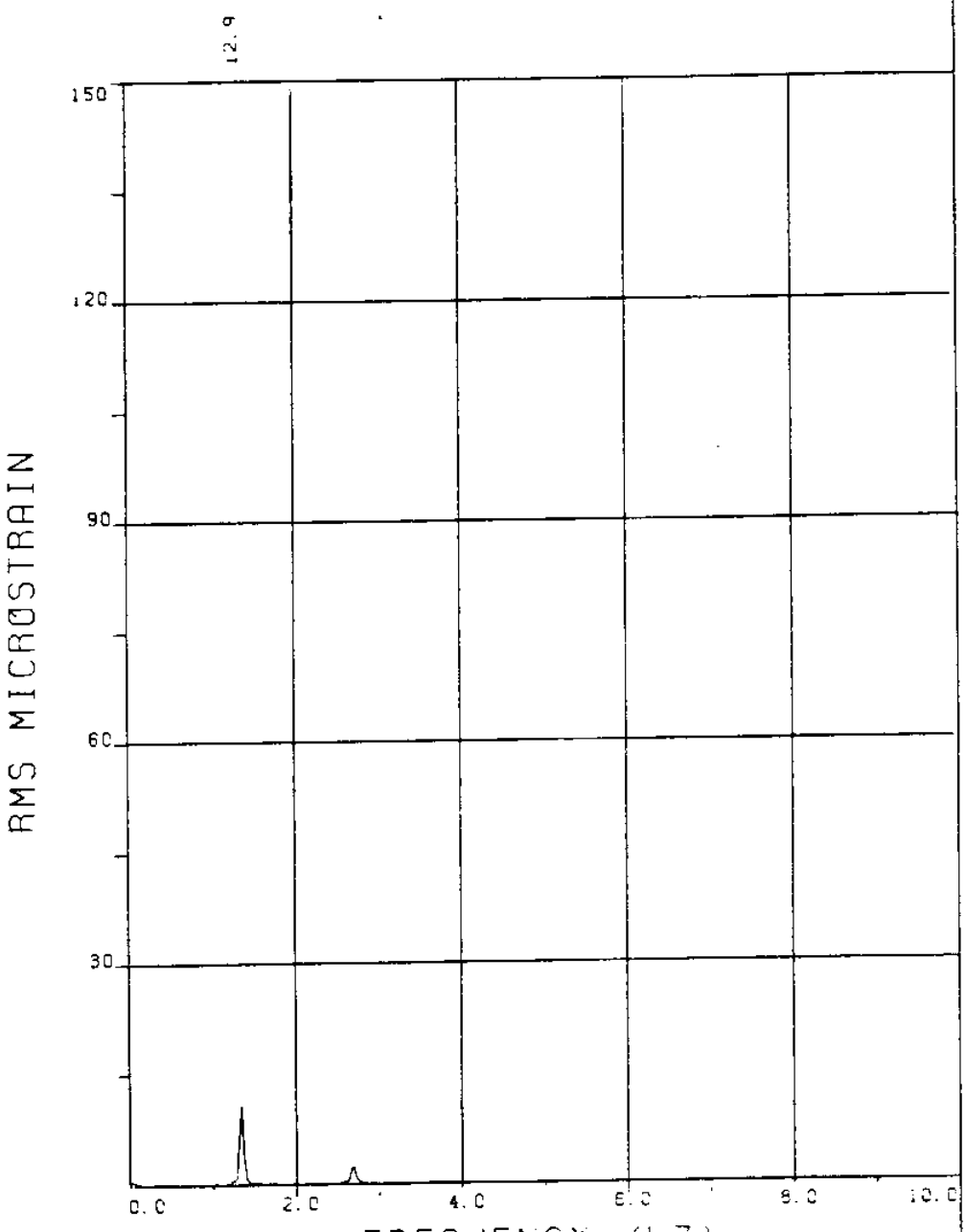

EXPERIMENT NUMBER 106

BRIDGE A6 ELEVATION=5L/11 BE=0.029

VC=125 A/DE=0.00

MEASURED RESPONSE IN MICROSTRAIN

MEAN=34.2

TOTAL DYNAMIC RMS=13.4

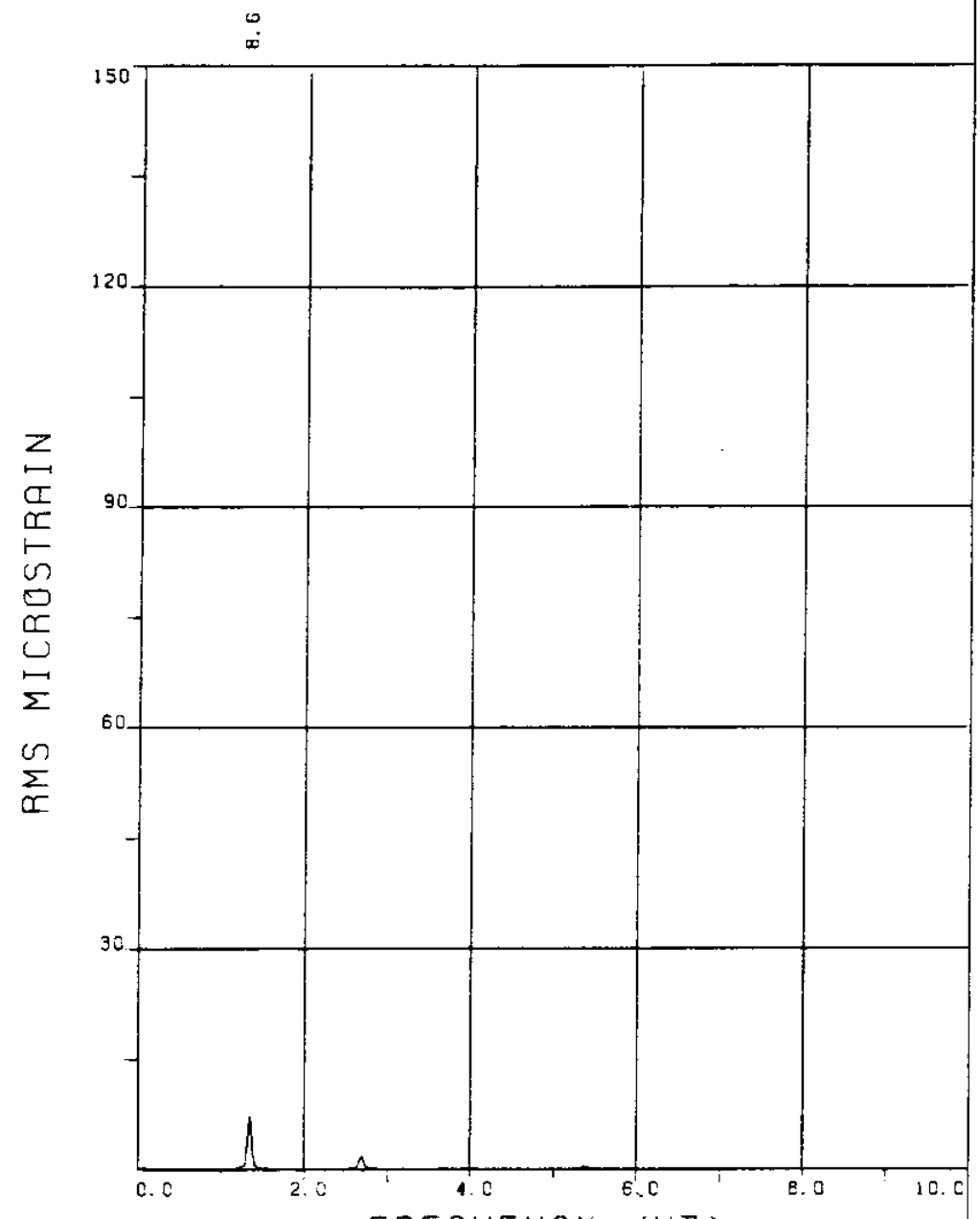

EXPERIMENT NUMBER 106

BRIDGE A3 ELEVATION=8L/11 BE=0.029

VC=125 A/DE=0.00

MEASURED RESPONSE IN MICROSTRAIN

MEAN=22.6

TOTAL DYNAMIC RMS=9.0

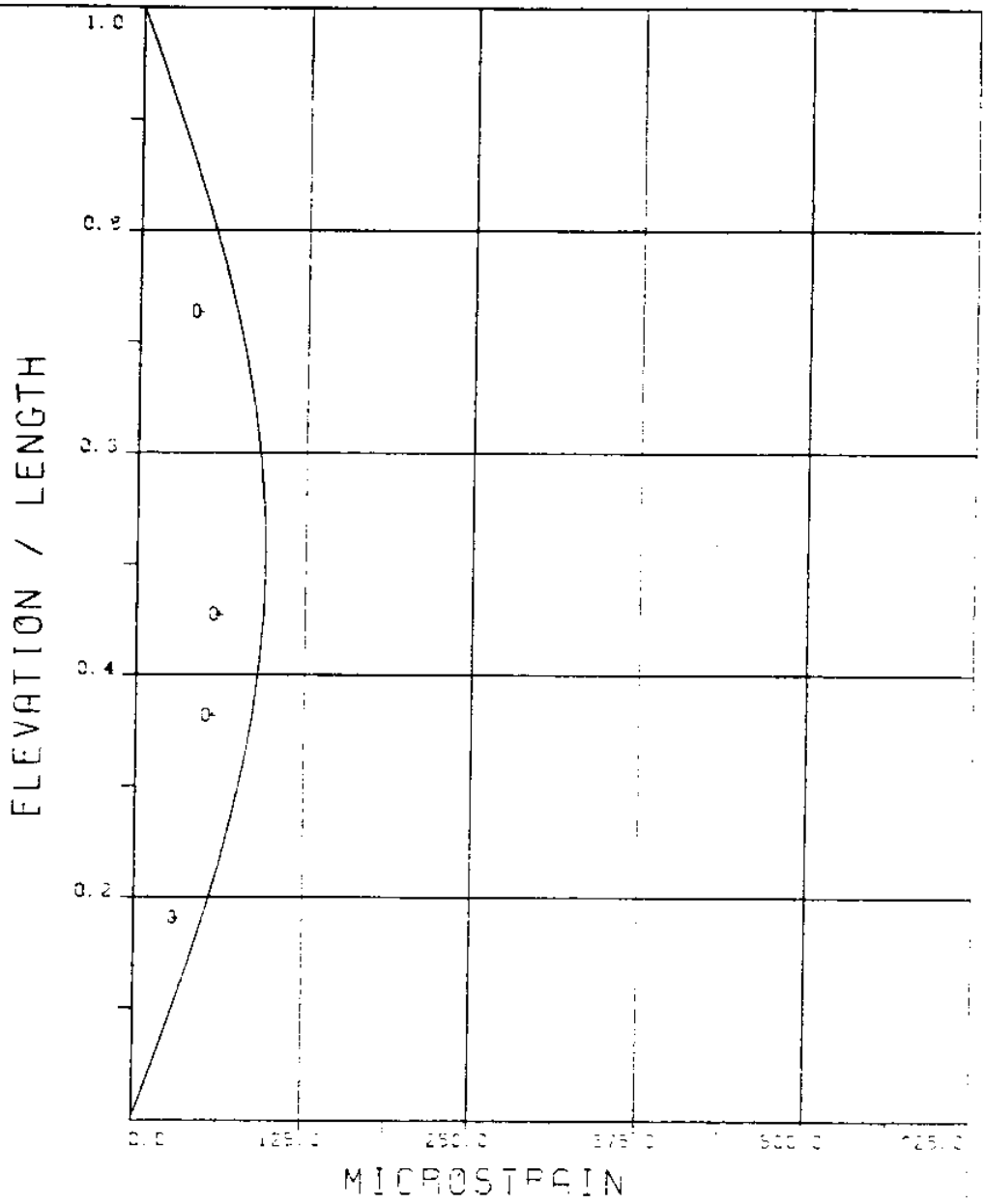

EXPERIMENT NUMBER 106

VC=125 A/DE=0.00

DYNAMIC RESPONSE AT F=FR IN PLANE B

——— THEORY o o o EXPERIMENT

MAXIMUM DYNAMIC RESPONSE IN PLANE B

——— THEORY + + + EXPERIMENT

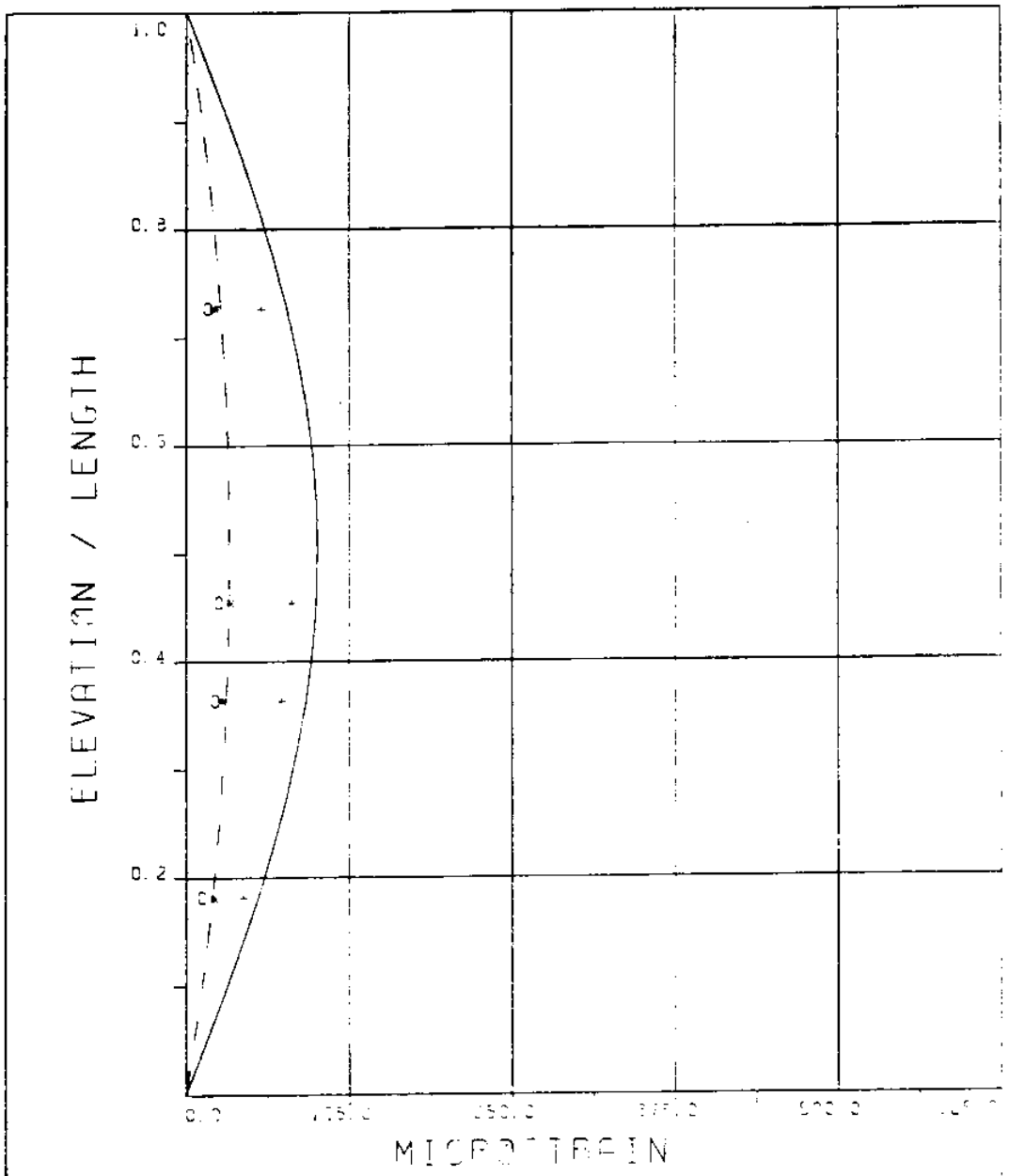

EXPERIMENT NUMBER 106

VC=125 A/DE=0.00

STATIC RESPONSE IN PLANE A

----- THEORY * * * EXPERIMENT

MAXIMUM DYNAMIC RESPONSE IN PLANE A

o o o EXPERIMENT

MAXIMUM RESPONSE

_____ THEORY + + + EXPERIMENT

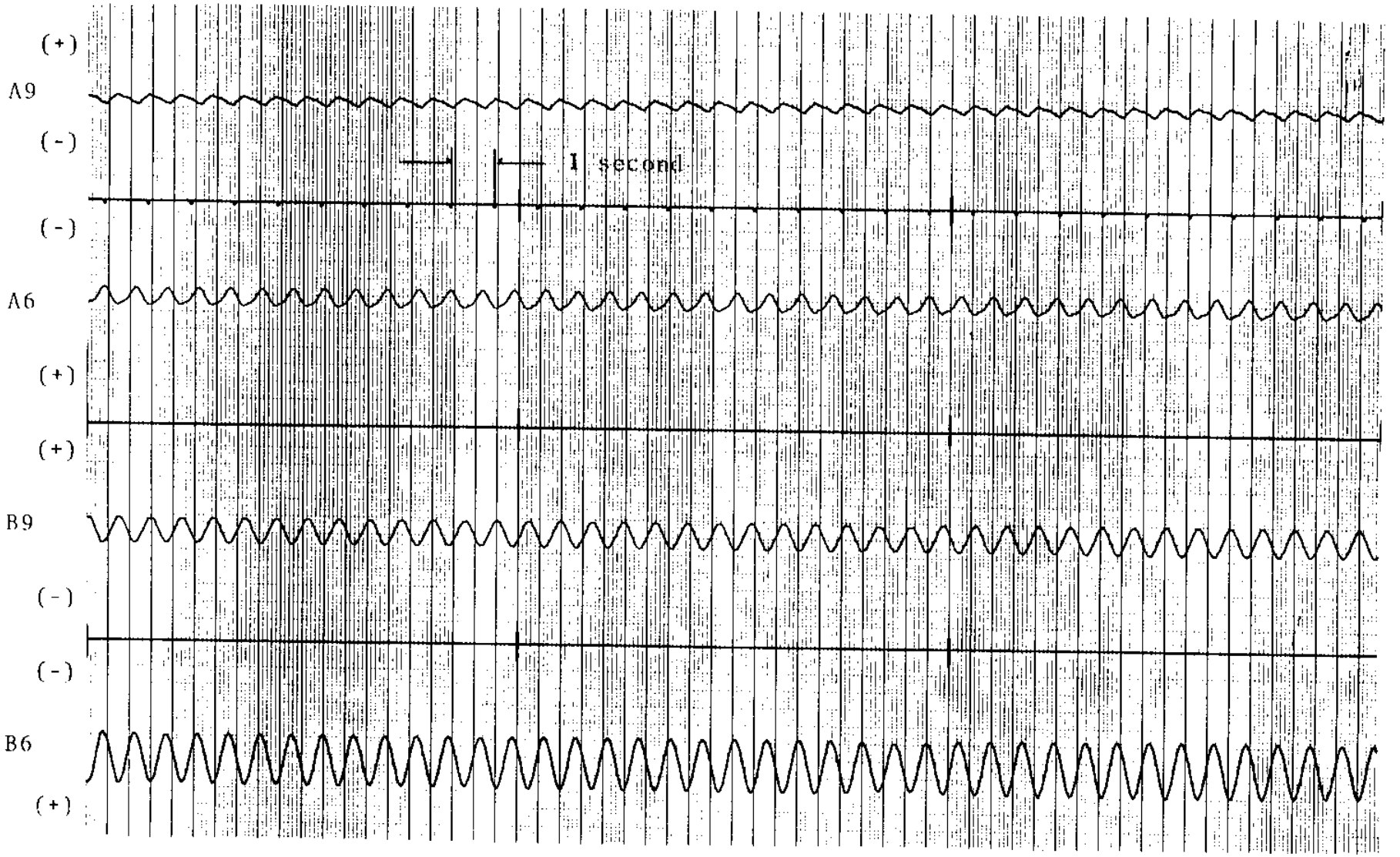

FIGURE 106T: ALL BRIDGES: 7.6 MICROSTRAIN/DIVISION

EXPERIMENT 114

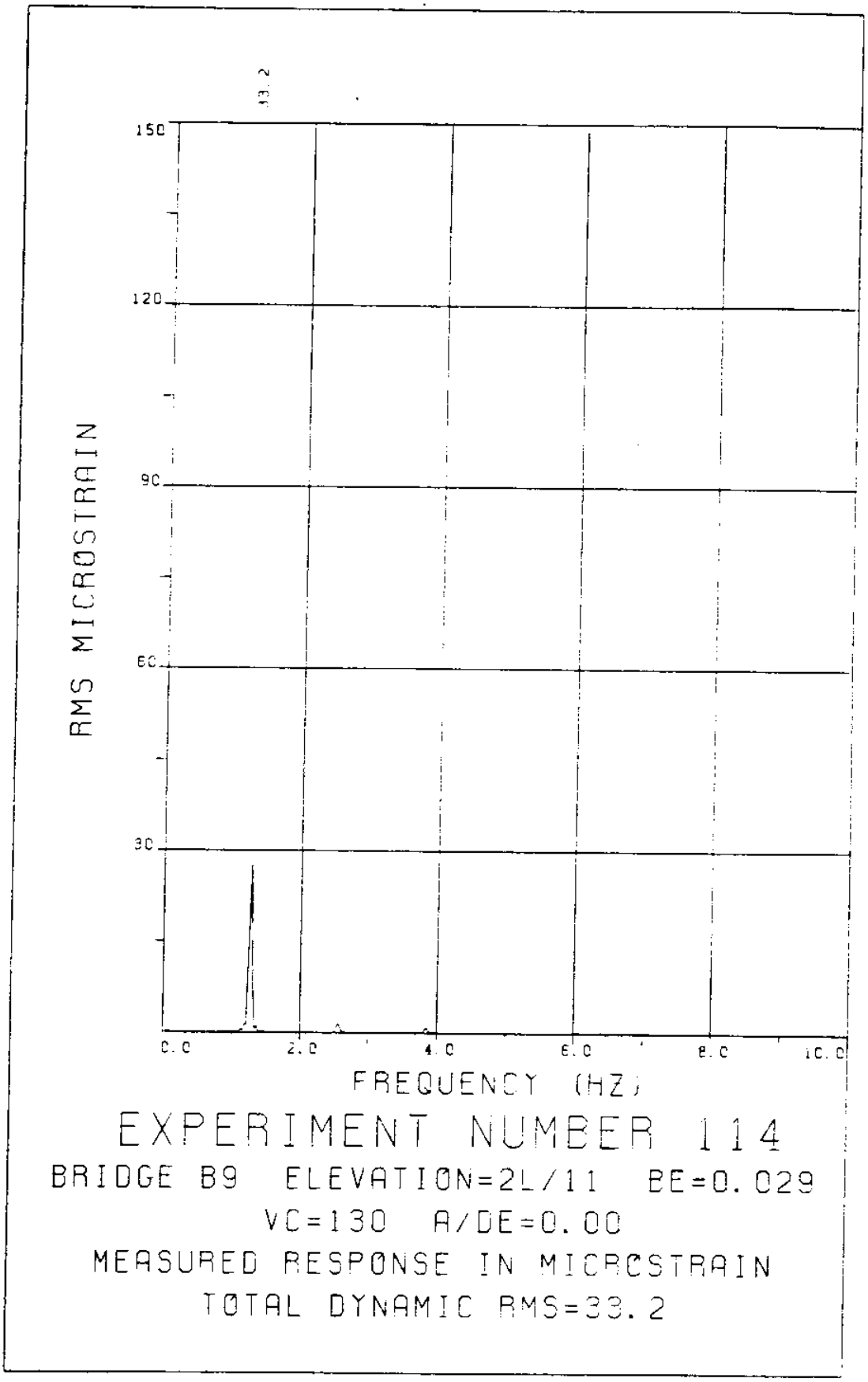
33.2
150
120
90
60
30
RMS MICROSTRAIN
0.0
2.0
4.0
6.0
8.0
10.0
FREQUENCY (HZ)
EXPERIMENT NUMBER 114
BRIDGE B9 ELEVATION=2L/11 BE=0.029
VC=130 A/DE=0.00
MEASURED RESPONSE IN MICROSTRAIN
TOTAL DYNAMIC RMS=33.2

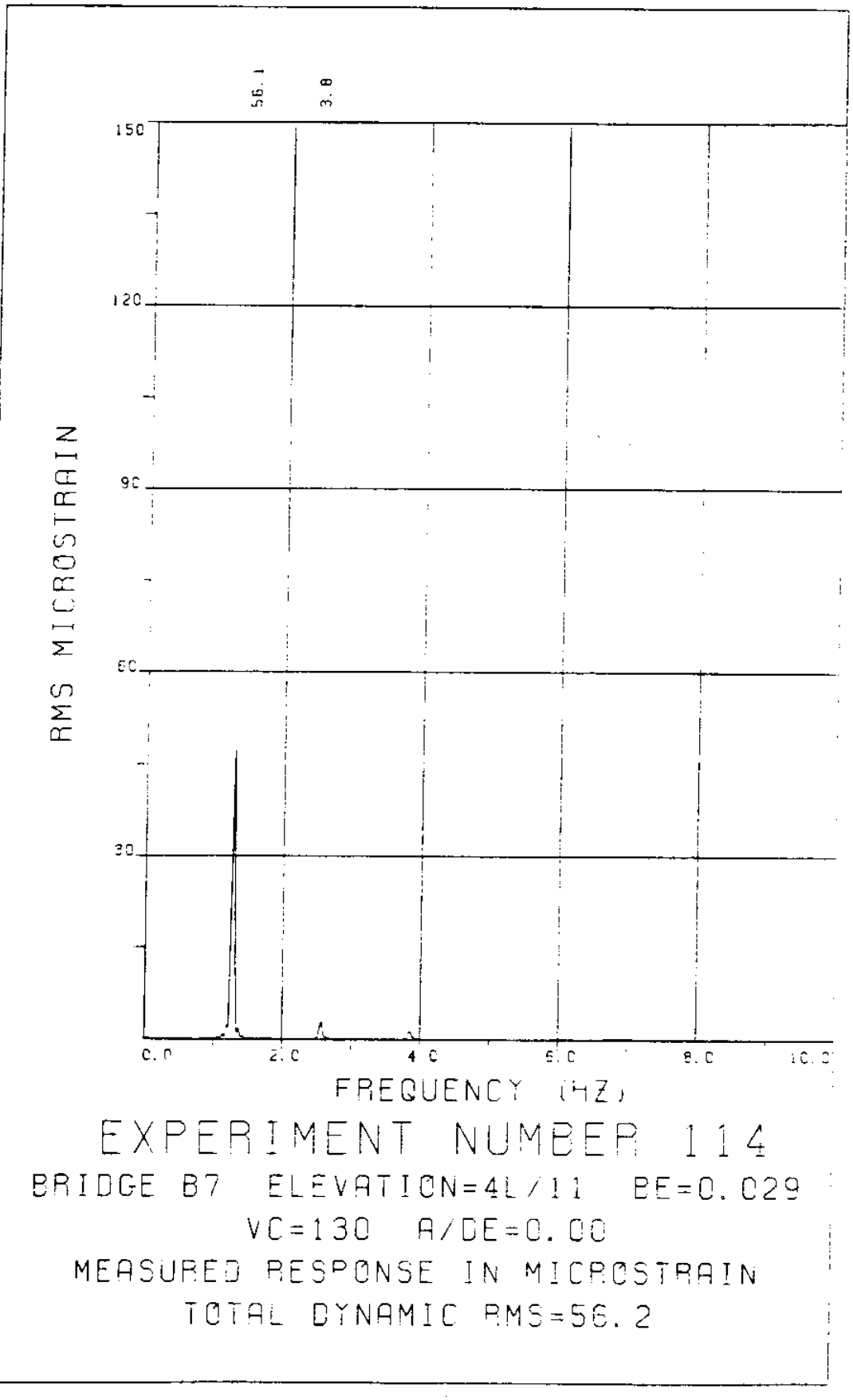

EXPERIMENT NUMBER 114

BRIDGE B7 ELEVATION=4L/11 BE=0.029

VC=130 A/DE=0.00

MEASURED RESPONSE IN MICROSTRAIN

TOTAL DYNAMIC RMS=56.2

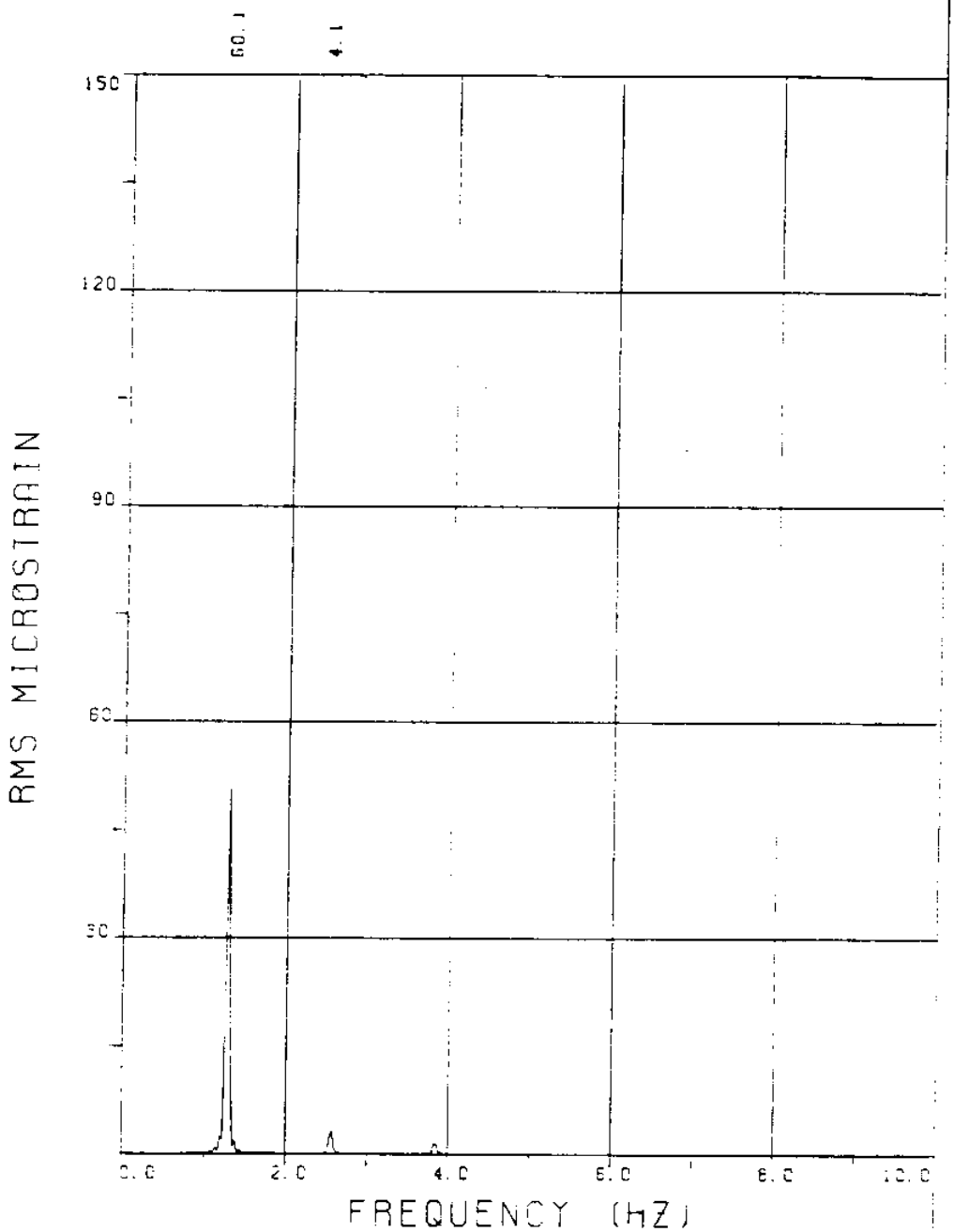

EXPERIMENT NUMBER 114

BRIDGE B6 ELEVATION=5L/11 BE=0.029

VC=130 A/DE=0.00

MEASURED RESPONSE IN MICROSTRAIN

TOTAL DYNAMIC RMS=60.1

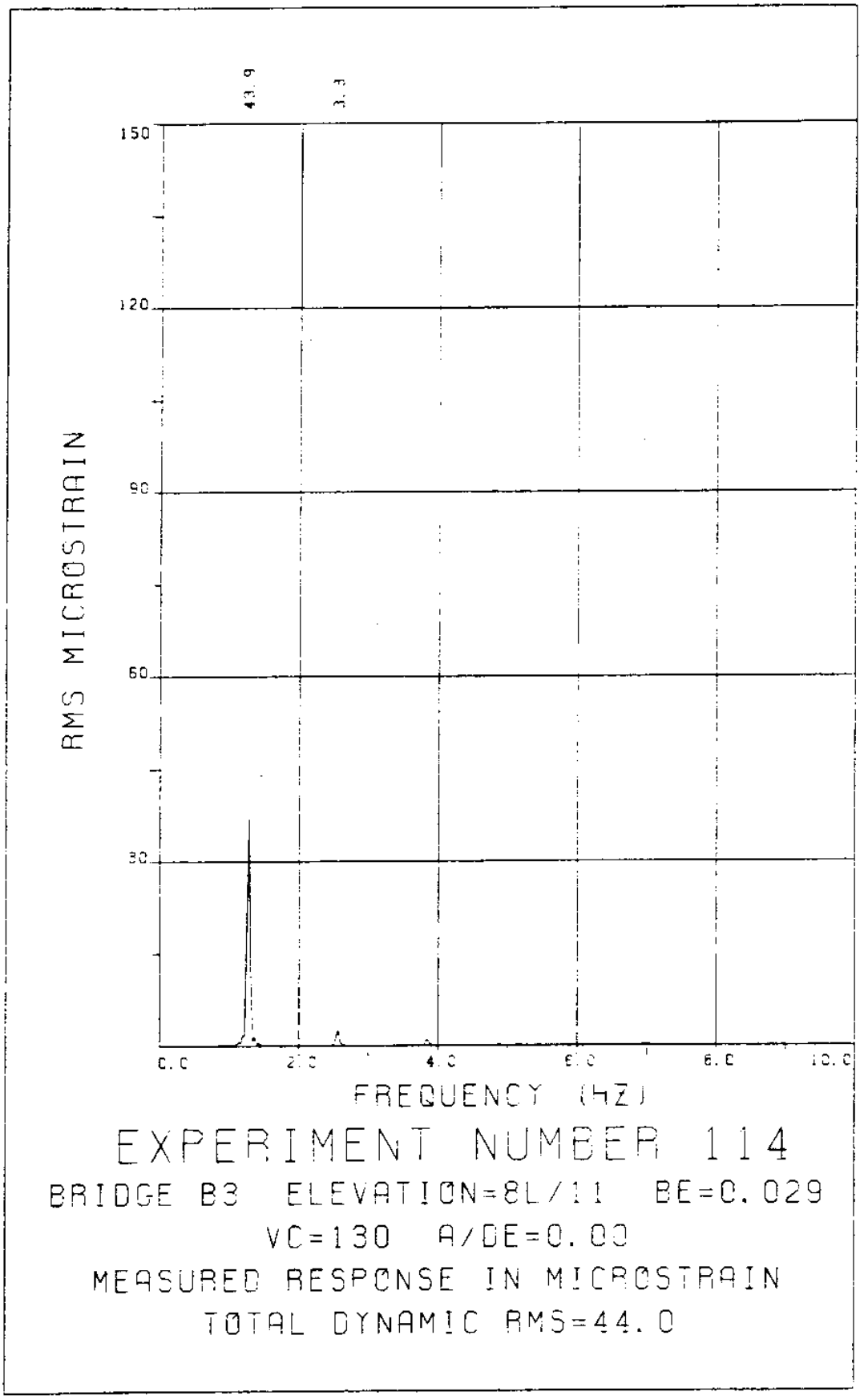
43.9
3.3
150
120
90
60
30
RMS MICROSTRAIN
0.0
2.0
4.0
6.0
8.0
10.0
FREQUENCY (HZ)
EXPERIMENT NUMBER 114
BRIDGE B3 ELEVATION=8L/11 BE=0.029
VC=130 A/DE=0.00
MEASURED RESPONSE IN MICROSTRAIN
TOTAL DYNAMIC RMS=44.0

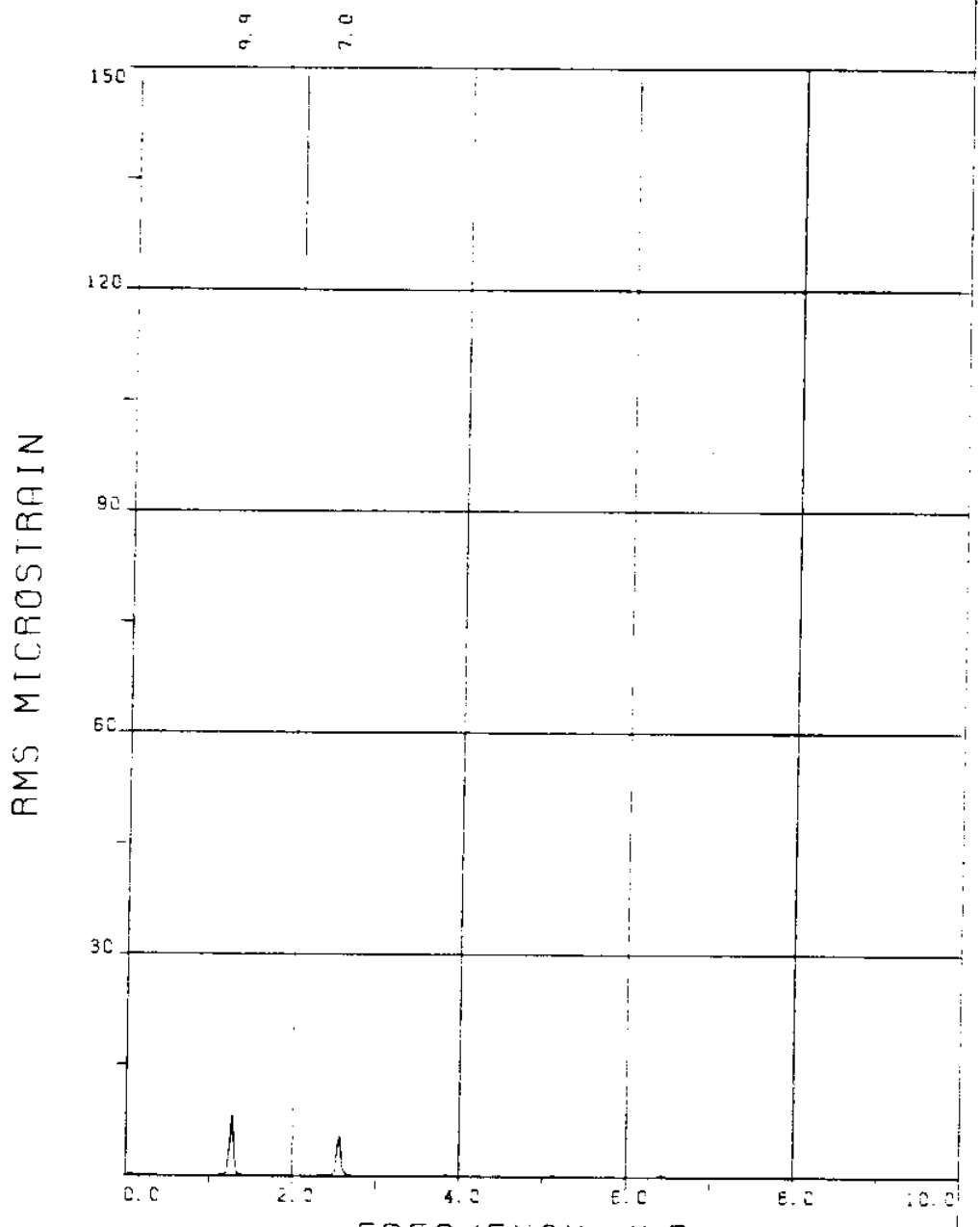

EXPERIMENT NUMBER 114

BRIDGE A9 ELEVATION=2L/11 BE=0.029

VC=130 A/DE=0.00

MEASURED RESPONSE IN MICROSTRAIN

MEAN=30.3

TOTAL DYNAMIC RMS=12.2

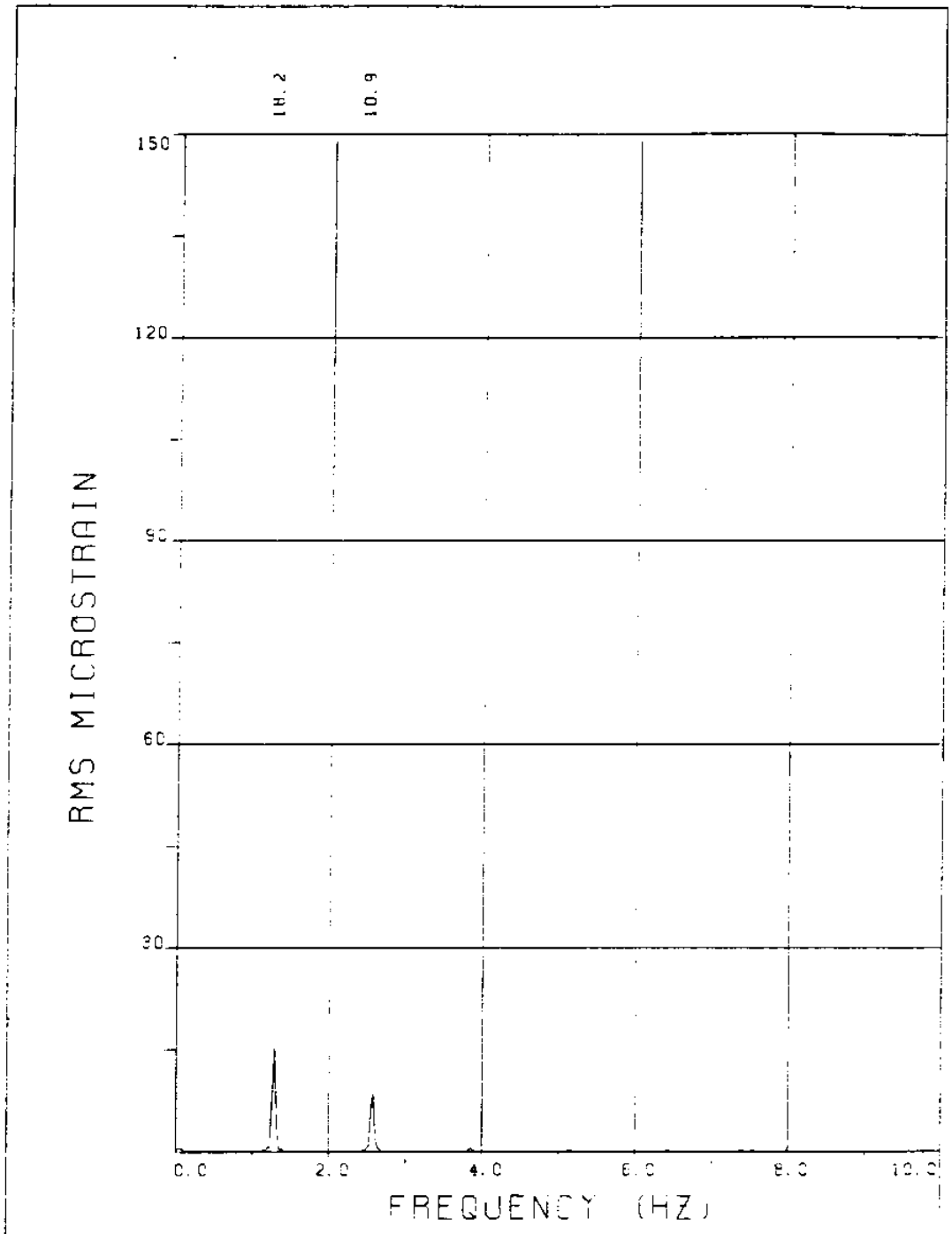

EXPERIMENT NUMBER 114

BRIDGE 97 ELEVATION=4L/11 BE=0.029

VC=130 A/DE=0.00

MEASURED RESPONSE IN MICROSTRAIN

MEAN=42.6

TOTAL DYNAMIC RMS=21.4

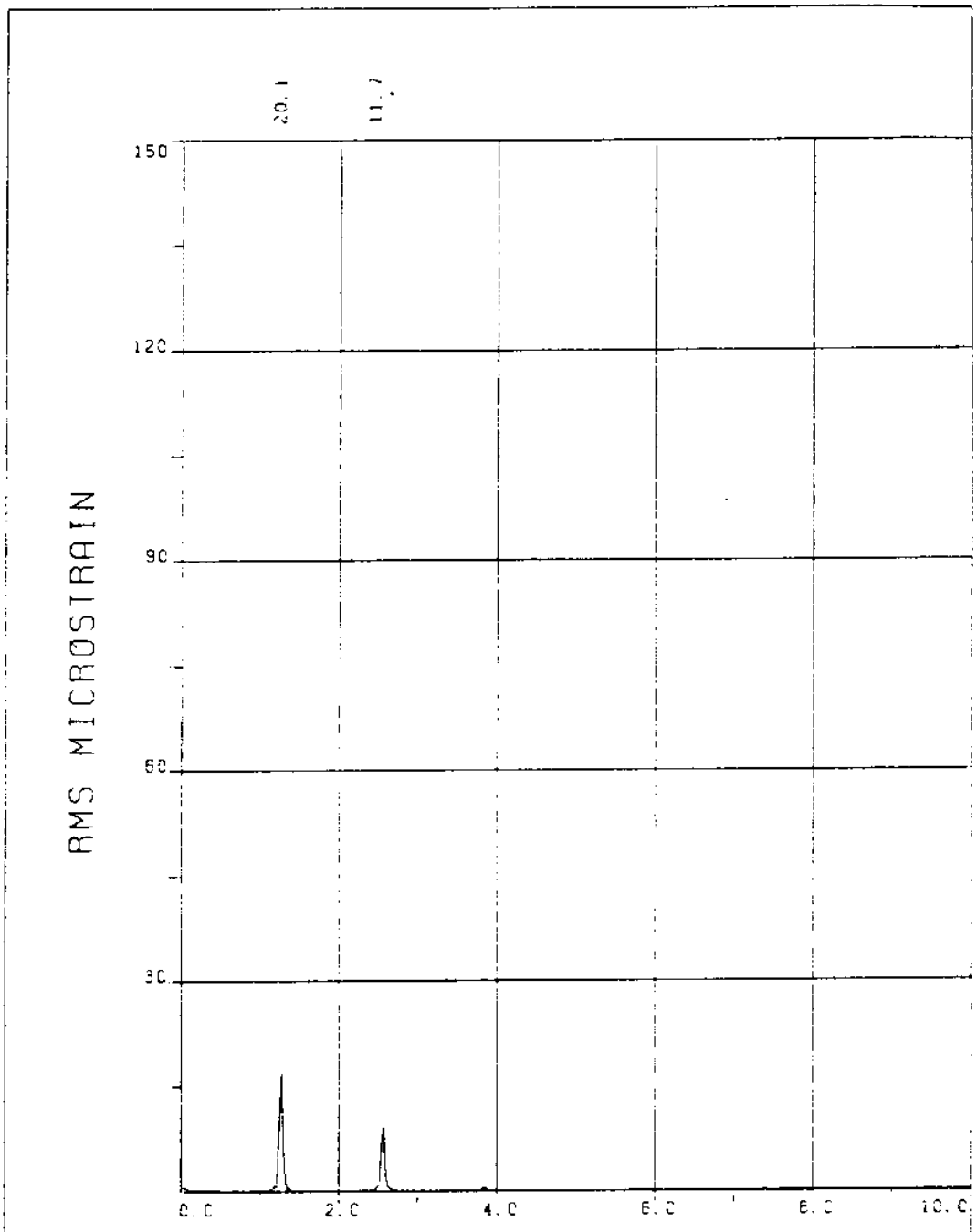

EXPERIMENT NUMBER 114

BRIDGE A6 ELEVATION=SL/11 BE=0.029

VC=130 A/DE=0.00

MEASURED RESPONSE IN MICROSTRAIN

MEAN=48.5

TOTAL DYNAMIC RMS=23.4

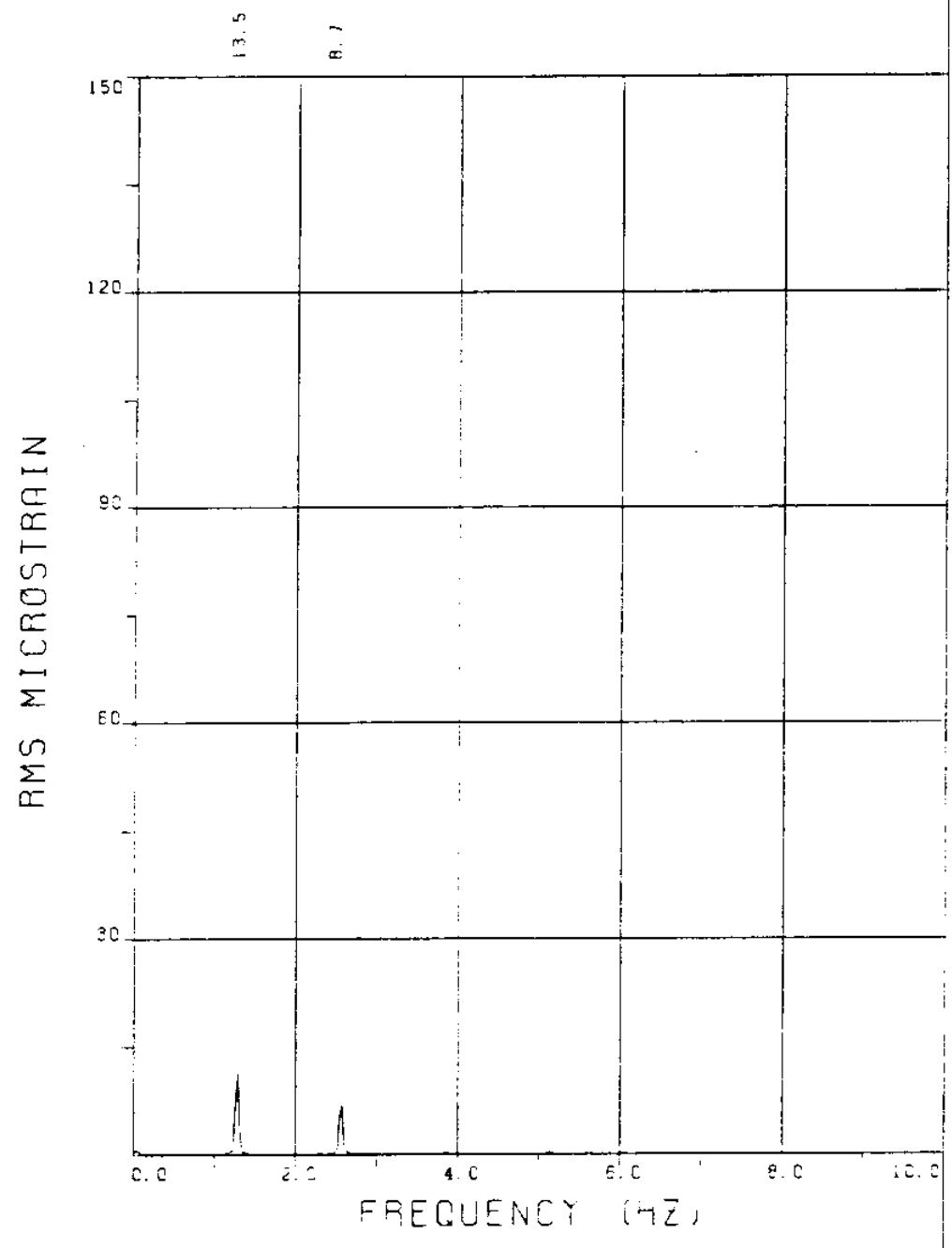

EXPERIMENT NUMBER 114

BRIDGE A3 ELEVATION=8L/11 BE=0.029

VC=130 A/DE=0.00

MEASURED RESPONSE IN MICROSTRAIN

MEAN=34.8

TOTAL DYNAMIC RMS=16.2

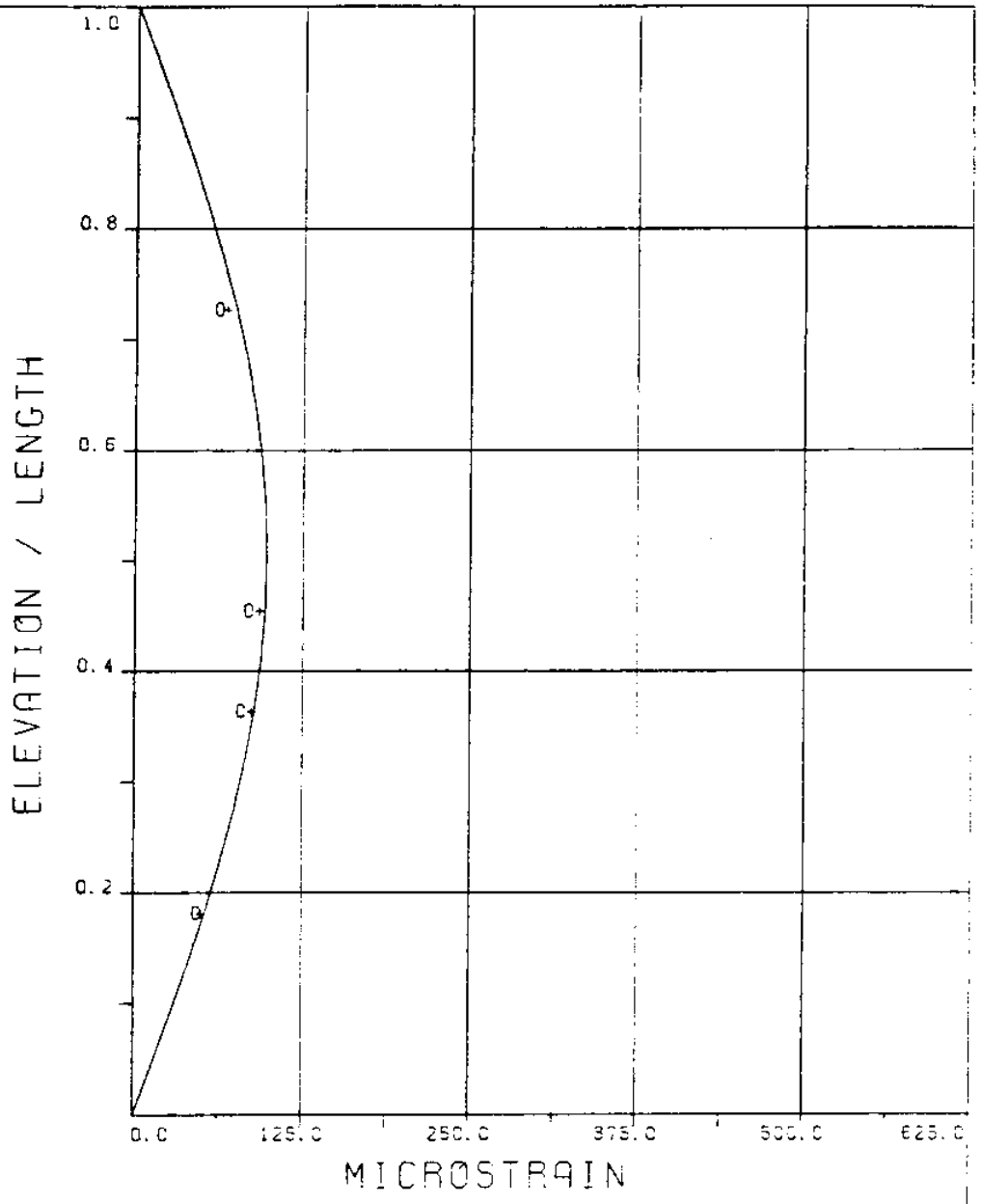

EXPERIMENT NUMBER 114

VC=130 A/DE=0.00

DYNAMIC RESPONSE AT F=FR IN PLANE B

——— THEORY o o o EXPERIMENT

MAXIMUM DYNAMIC RESPONSE IN PLANE B

——— THEORY + + + EXPERIMENT

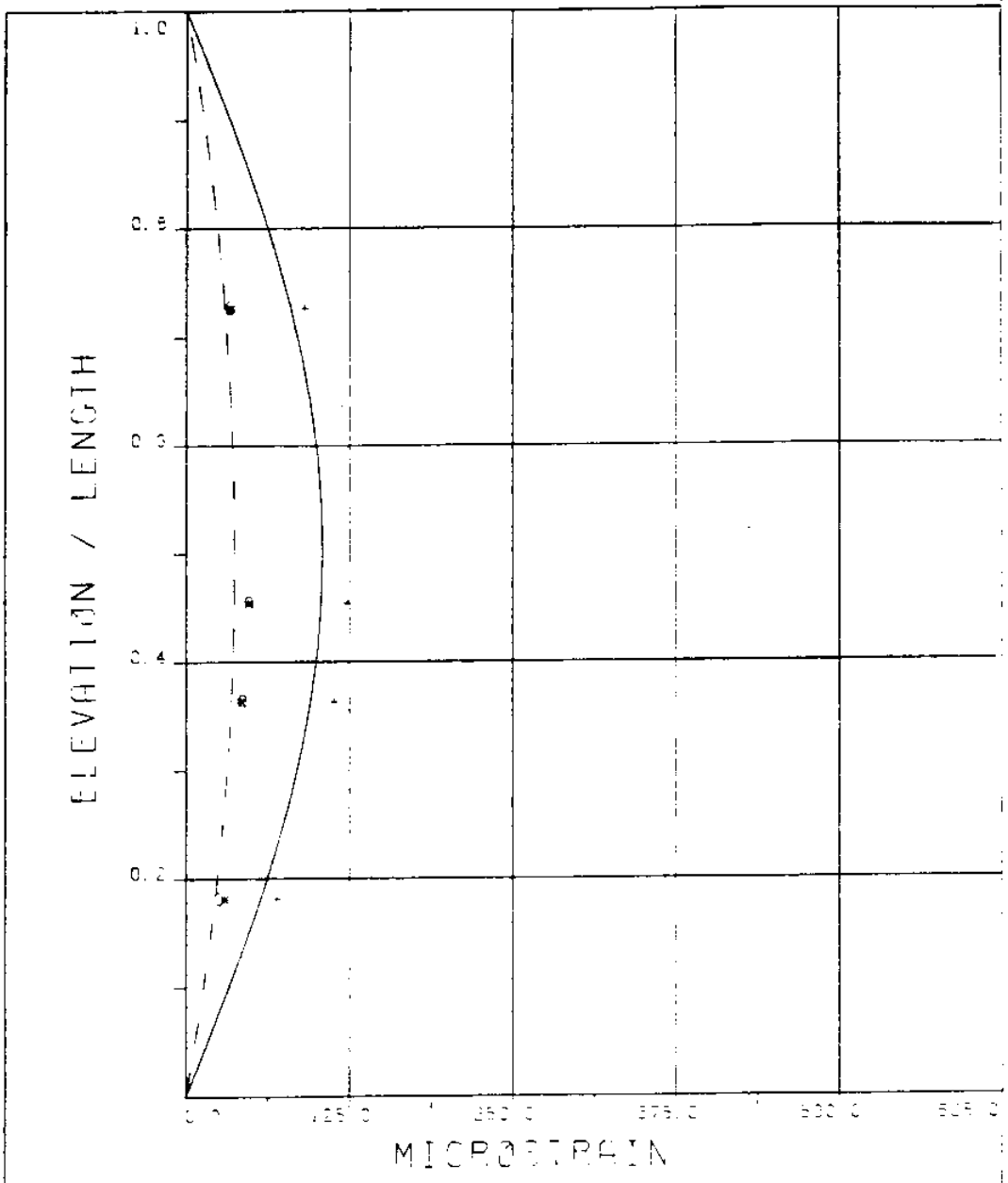

EXPERIMENT NUMBER 114

VC=130 A/DE=0.00

STATIC RESPONSE IN PLANE A

----- THEORY * * * EXPERIMENT

MAXIMUM DYNAMIC RESPONSE IN PLANE A

o o o EXPERIMENT

MAXIMUM RESPONSE

_____ THEORY + + + EXPERIMENT

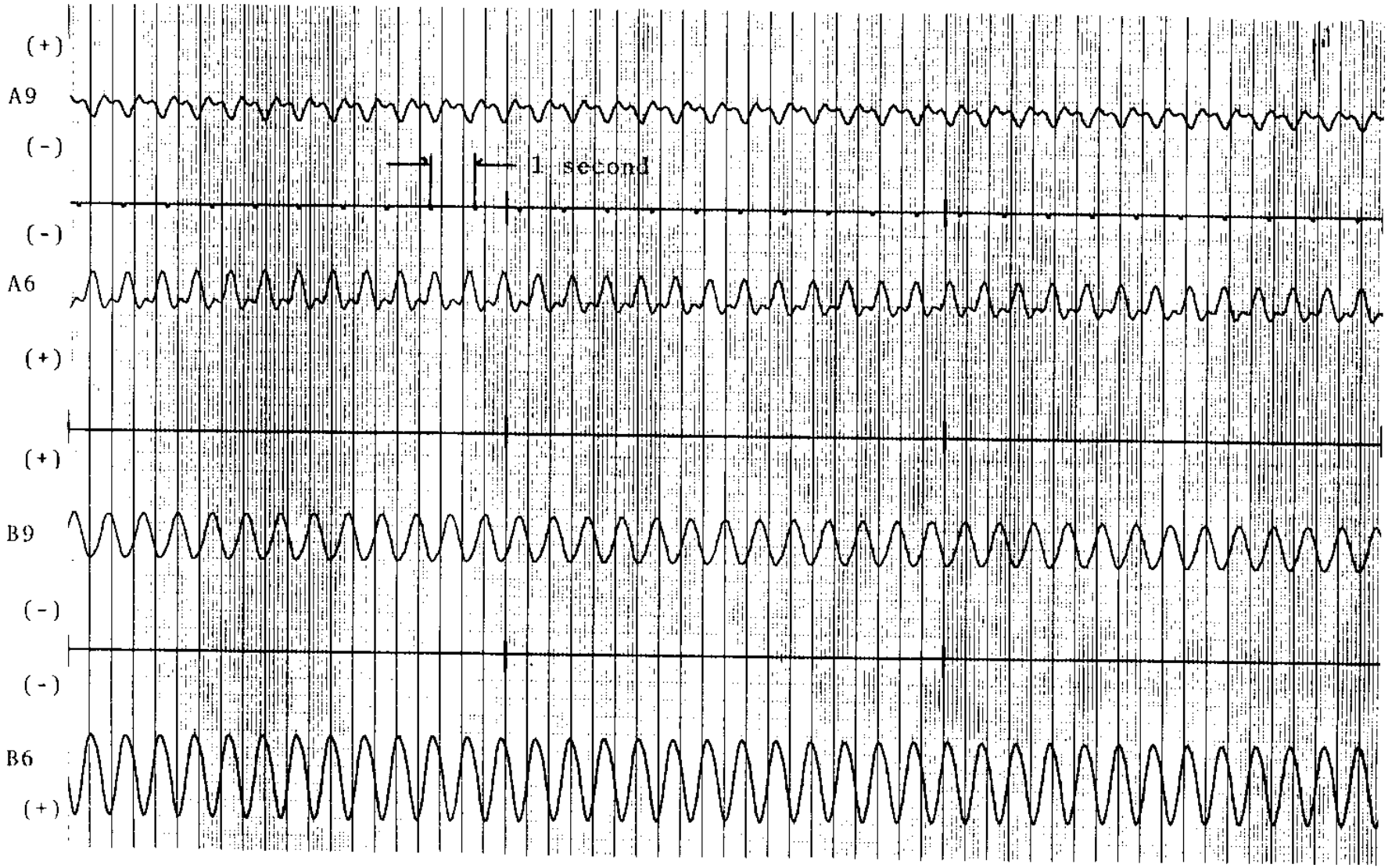

FIGURE 114Ta: ALL BRIDGES: 7.6 MICROSTRAIN/DIVISION

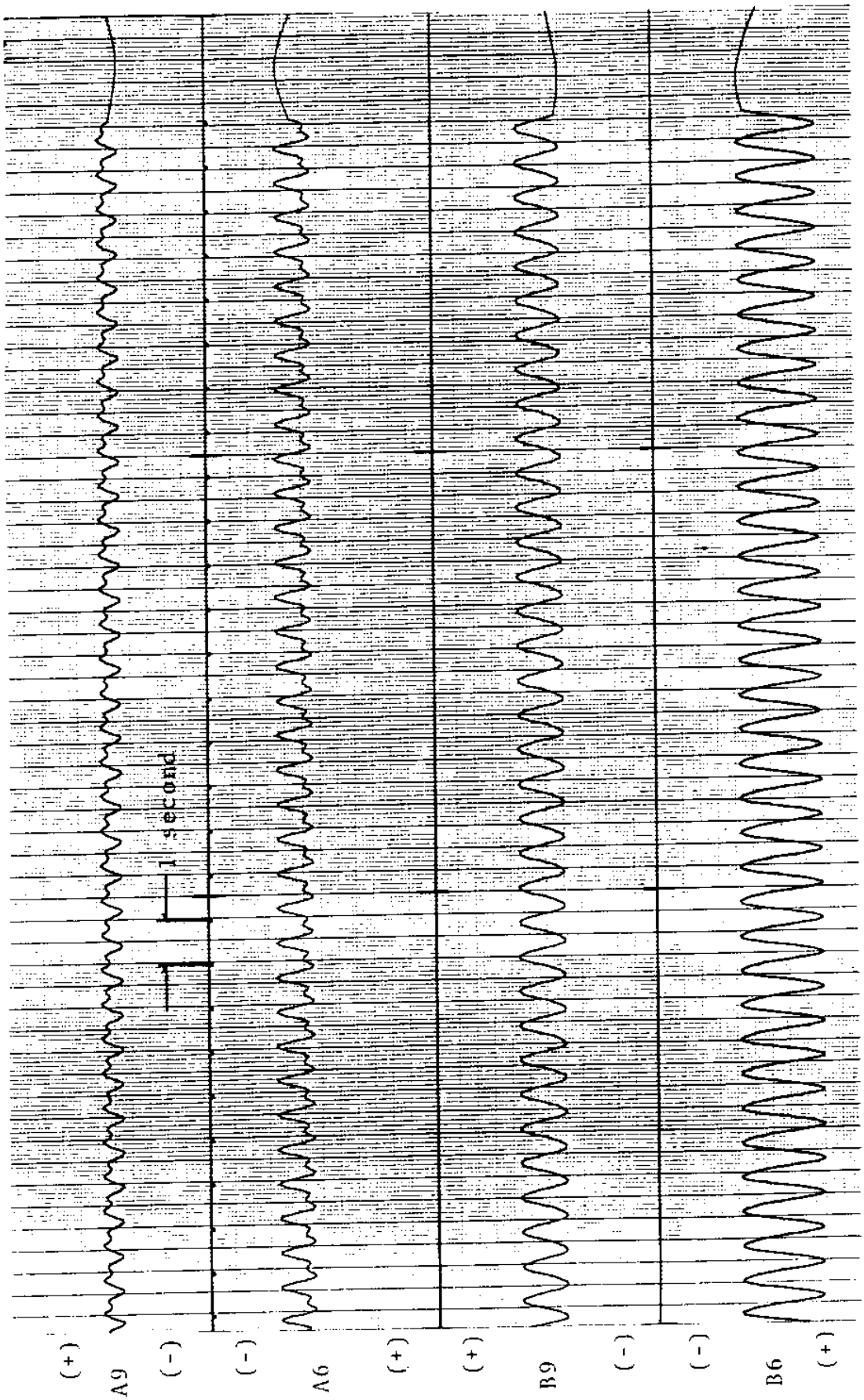

FIGURE 114Tb: ALL BRIDGES: 7.6 MICROSTRAIN/DIVISION

EXPERIMENT 108

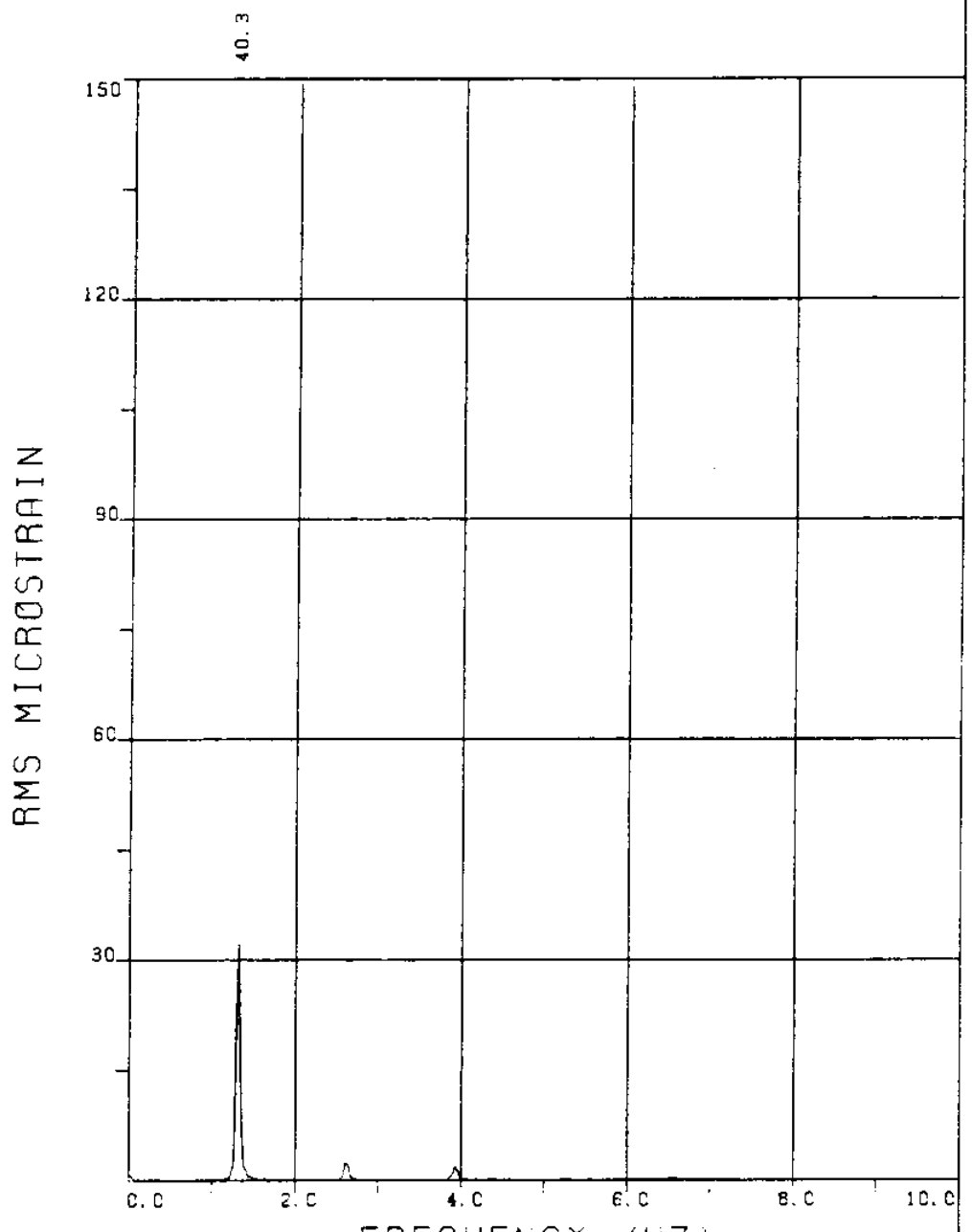

EXPERIMENT NUMBER 108

BRIDGE B9 ELEVATION=2L/11 BE=0.029

VC=135 A/DE=0.00

MEASURED RESPONSE IN MICROSTRAIN

TOTAL DYNAMIC RMS=40.5

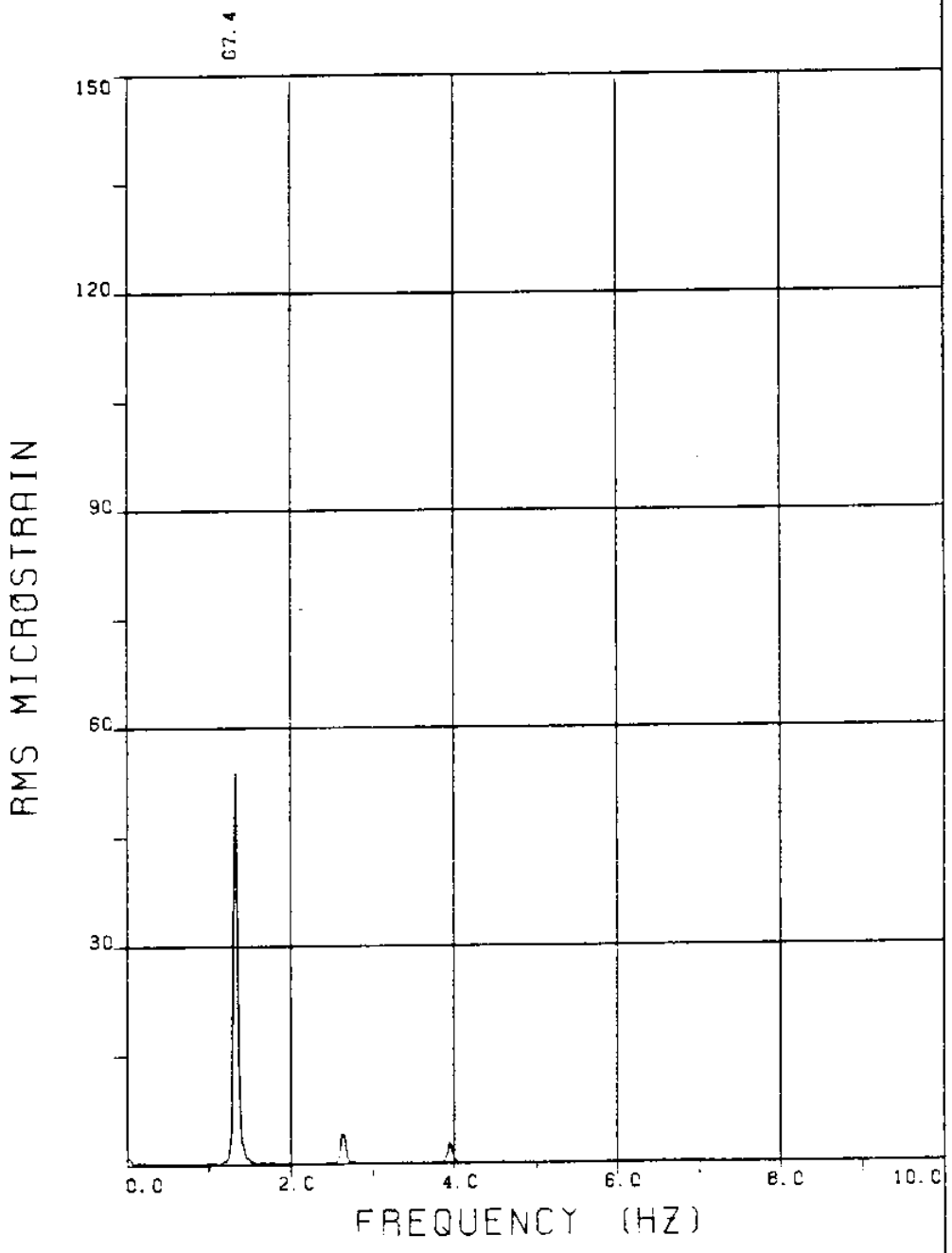

EXPERIMENT NUMBER 108

BRIDGE B7 ELEVATION=4L/11 BE=0.029

VC=135 A/DE=0.00

MEASURED RESPONSE IN MICROSTRAIN

TOTAL DYNAMIC.RMS=67.8

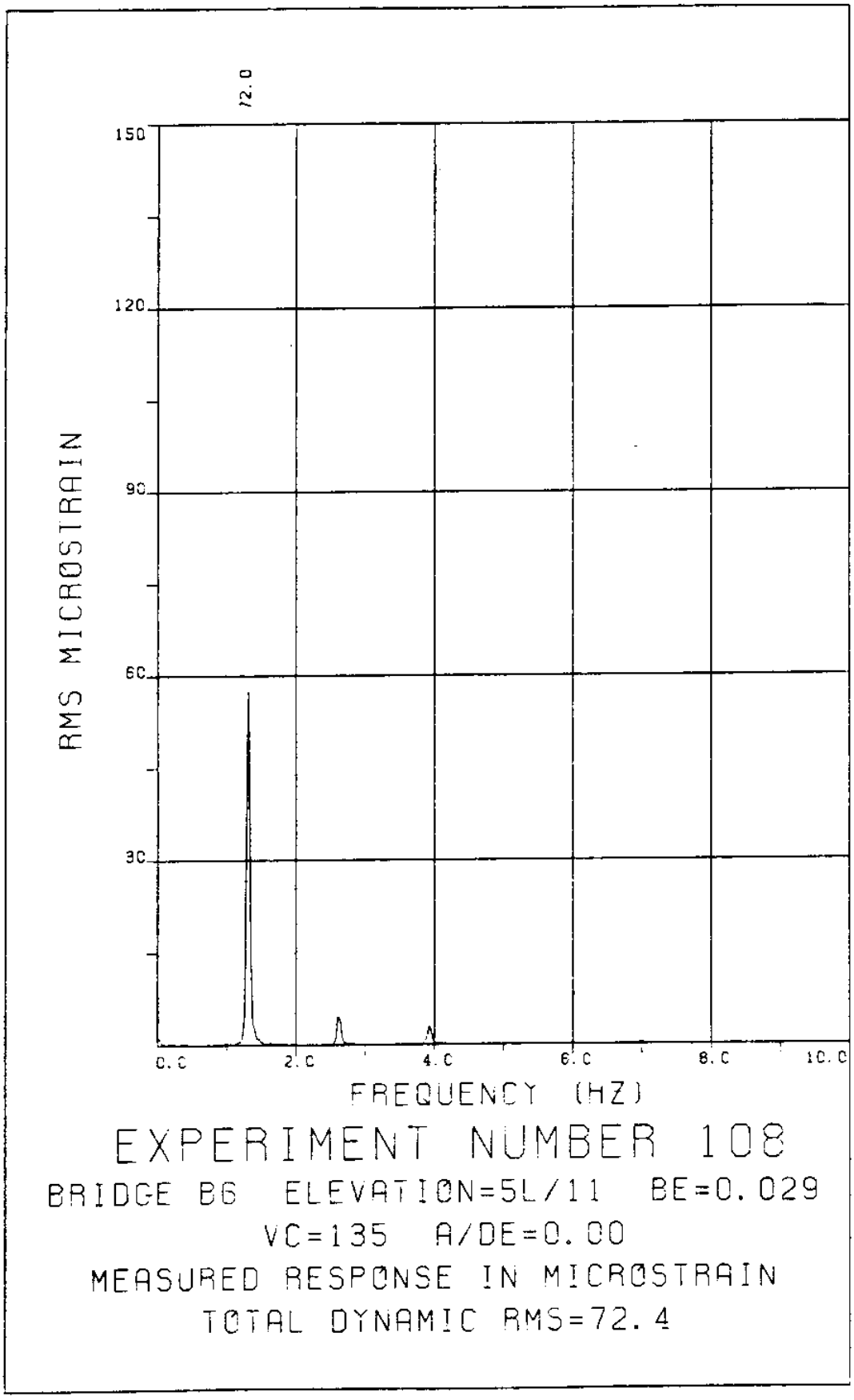

EXPERIMENT NUMBER 108

BRIDGE B6 ELEVATION=5L/11 BE=0.029

VC=135 A/DE=0.00

MEASURED RESPONSE IN MICROSTRAIN

TOTAL DYNAMIC RMS=72.4

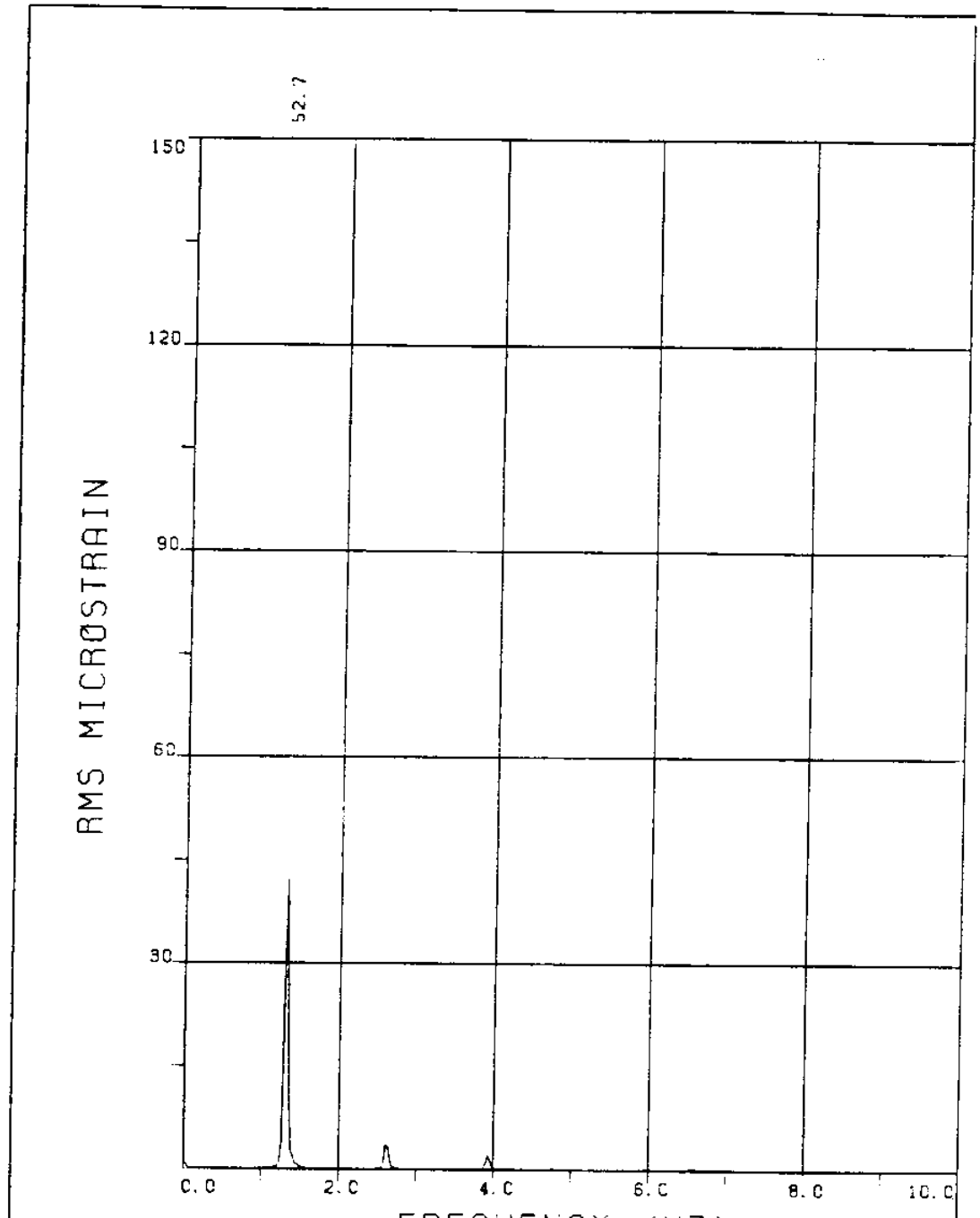

EXPERIMENT NUMBER 108

BRIDGE B3 ELEVATION=8L/11 BE=0.029

VC=135 A/DE=0.00

MEASURED RESPONSE IN MICROSTRAIN

TOTAL DYNAMIC RMS=53.0

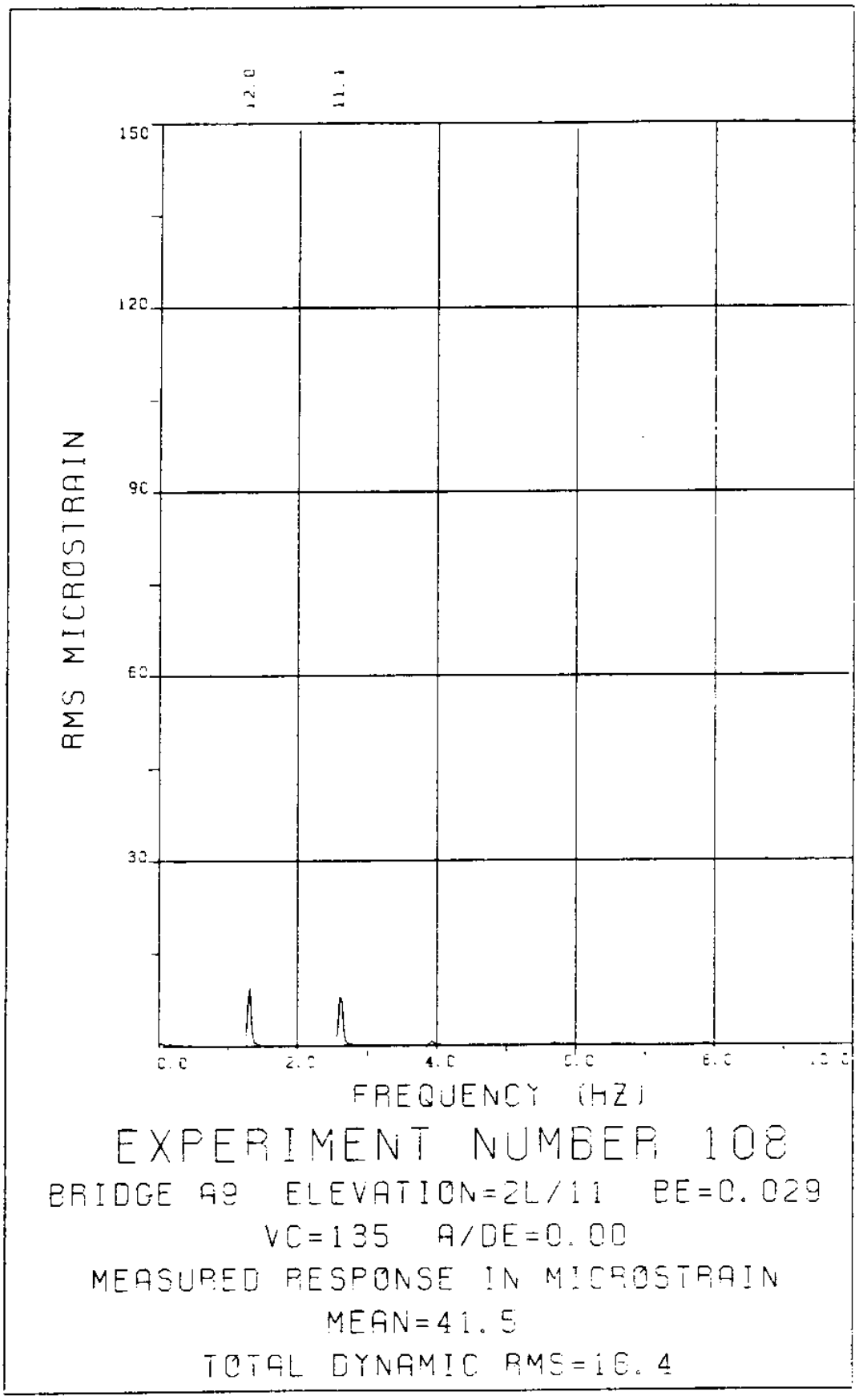
12.0
11.1
150
120
90
60
30
RMS MICROSTRAIN
0.0
2.0
4.0
6.0
8.0
FREQUENCY (HZ)
EXPERIMENT NUMBER 108
BRIDGE A8 ELEVATION=2L/11 BE=0.029
VC=135 A/DE=0.00
MEASURED RESPONSE IN MICROSTRAIN
MEAN=41.5
TOTAL DYNAMIC RMS=16.4

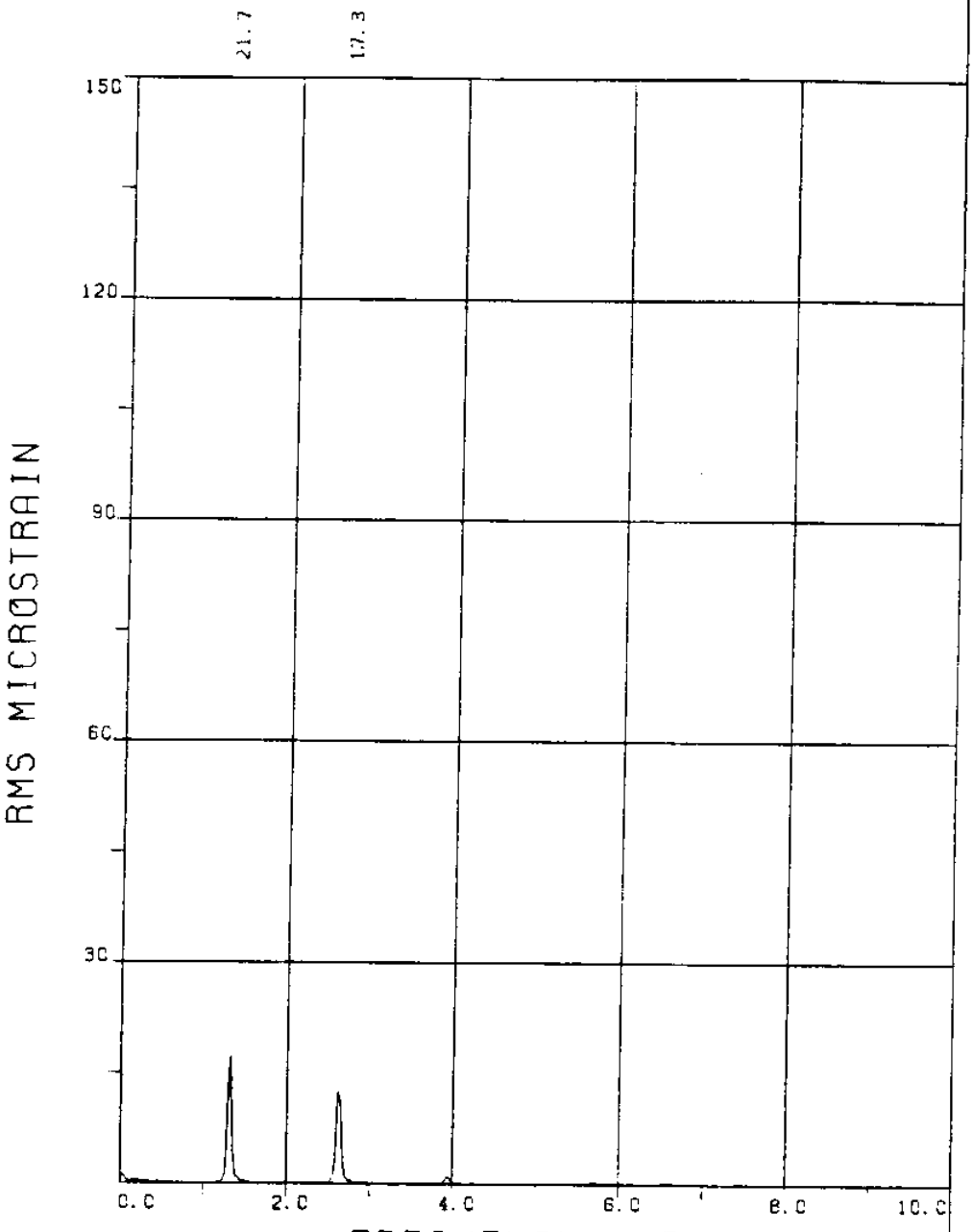

EXPERIMENT NUMBER 108

BRIDGE A7 ELEVATION=4L/11 BE=0.029

VC=135 A/DE=0.00

MEASURED RESPONSE IN MICROSTRAIN

MEAN=60.2

TOTAL DYNAMIC RMS=27.9

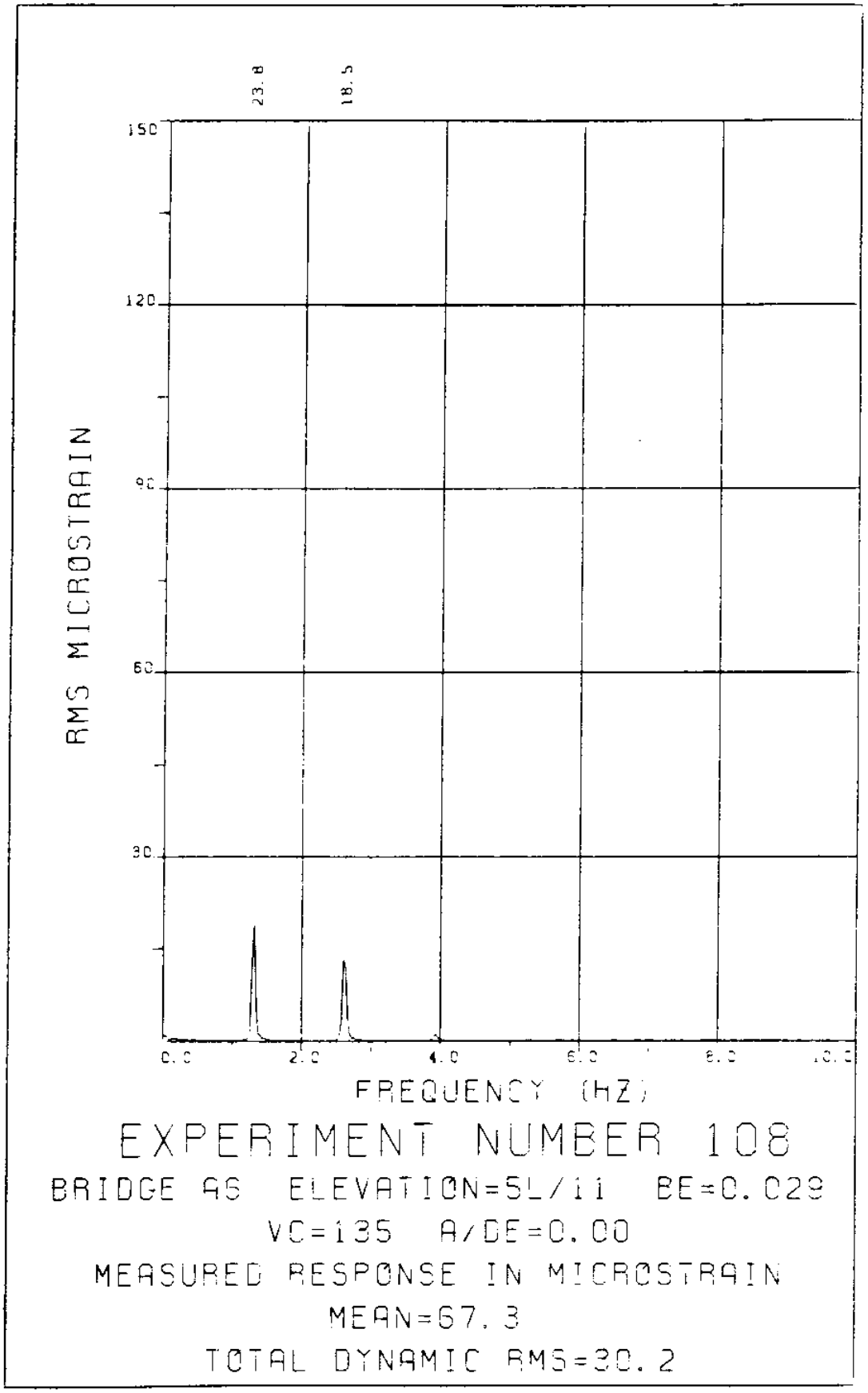
23.8
18.5
150
120
90
60
30
RMS MICROSTRAIN
0.0
2.0
4.0
6.0
8.0
10.0
FREQUENCY (HZ)
EXPERIMENT NUMBER 108
BRIDGE A6 ELEVATION=5L/11 BE=0.029
VC=135 A/DE=0.00
MEASURED RESPONSE IN MICROSTRAIN
MEAN=67.3
TOTAL DYNAMIC RMS=30.2

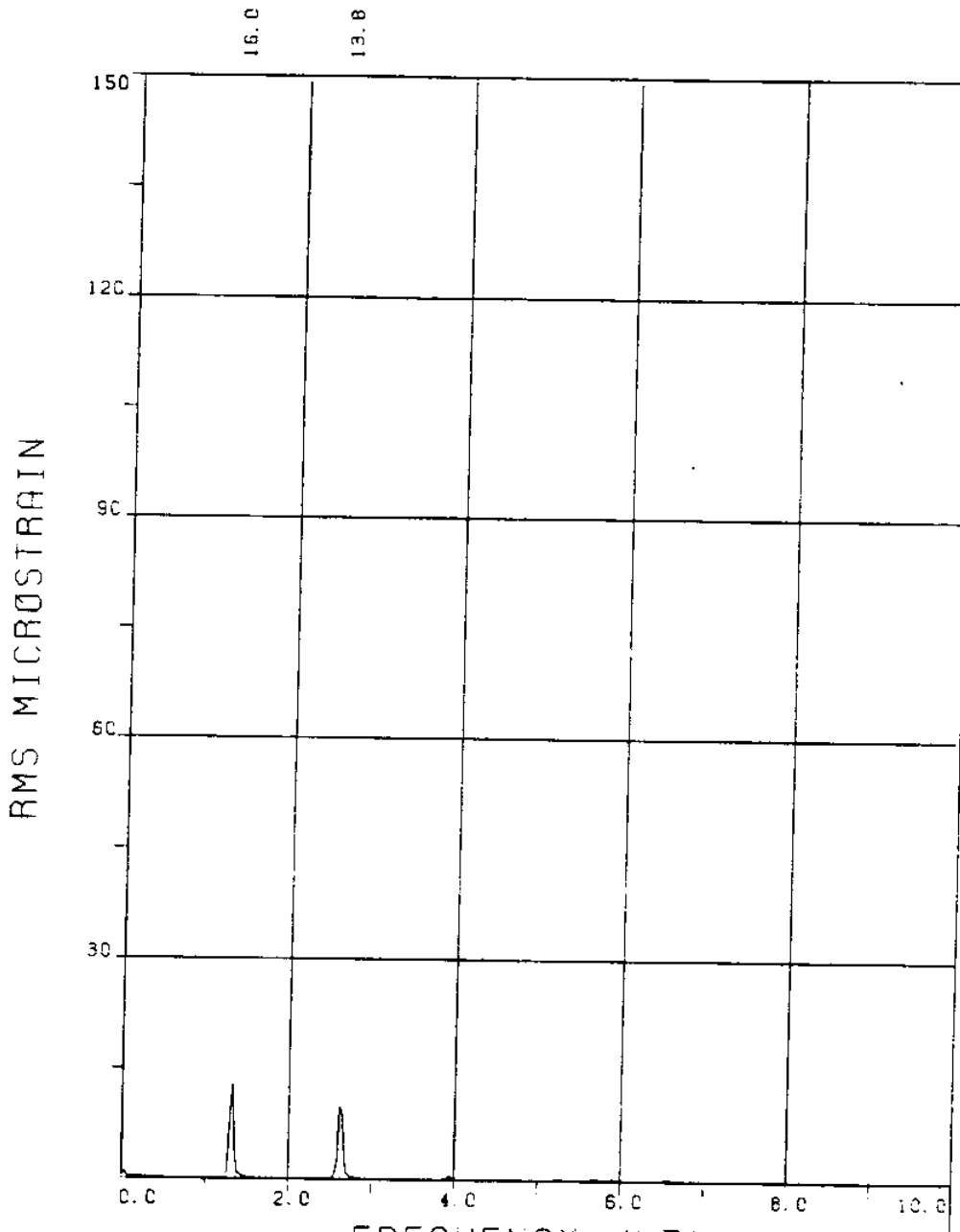

EXPERIMENT NUMBER 108

BRIDGE A3 ELEVATION=8L/11 BE=0.029

VC=135 A/DE=0.00

MEASURED RESPONSE IN MICROSTRAIN

MEAN=49.0

TOTAL DYNAMIC RMS=21.2

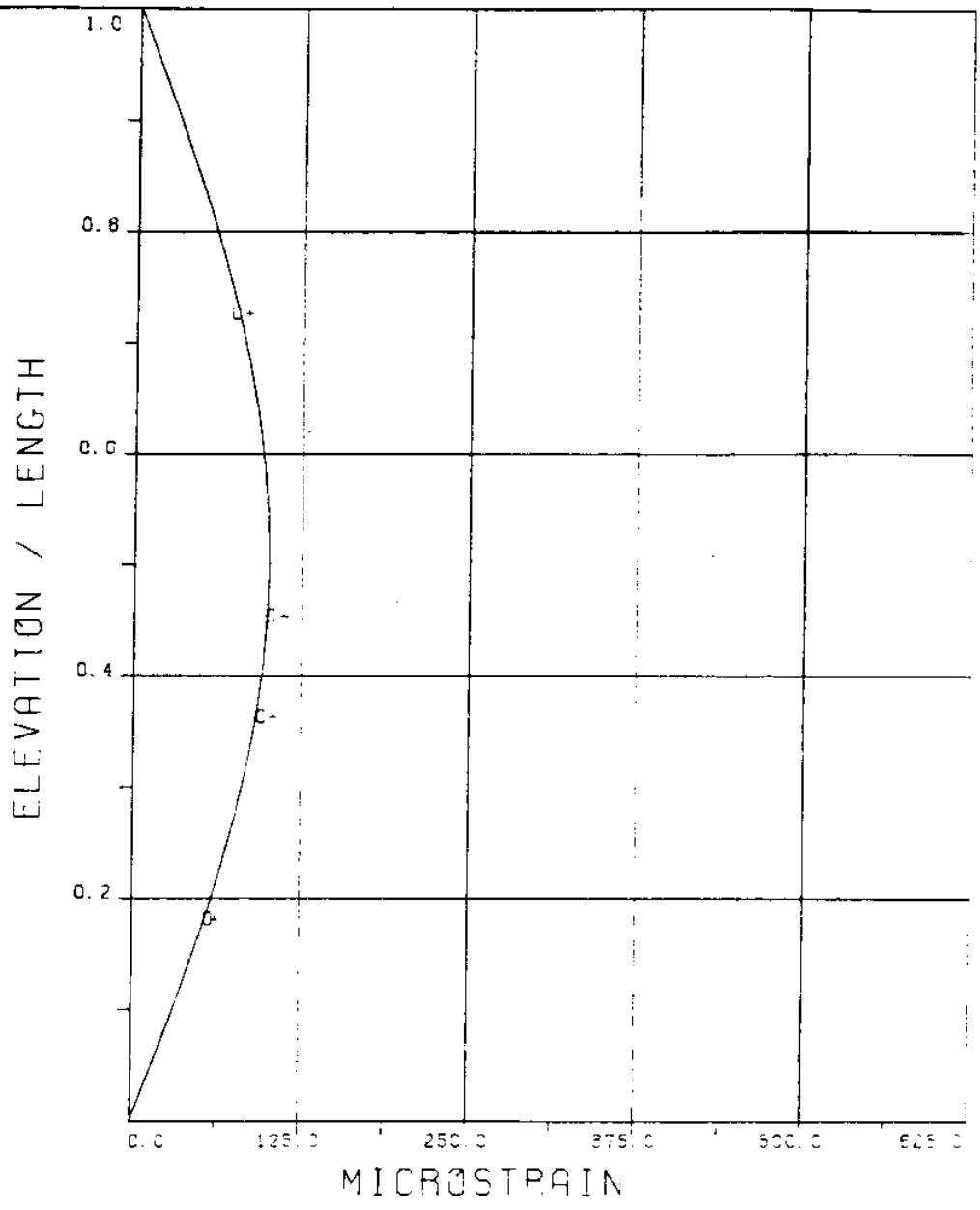

EXPERIMENT NUMBER 108

VC=135 A/DE=0.00

DYNAMIC RESPONSE AT F=FR IN PLANE B

——— THEORY o o o EXPERIMENT

MAXIMUM DYNAMIC RESPONSE IN PLANE B

——— THEORY + + + EXPERIMENT

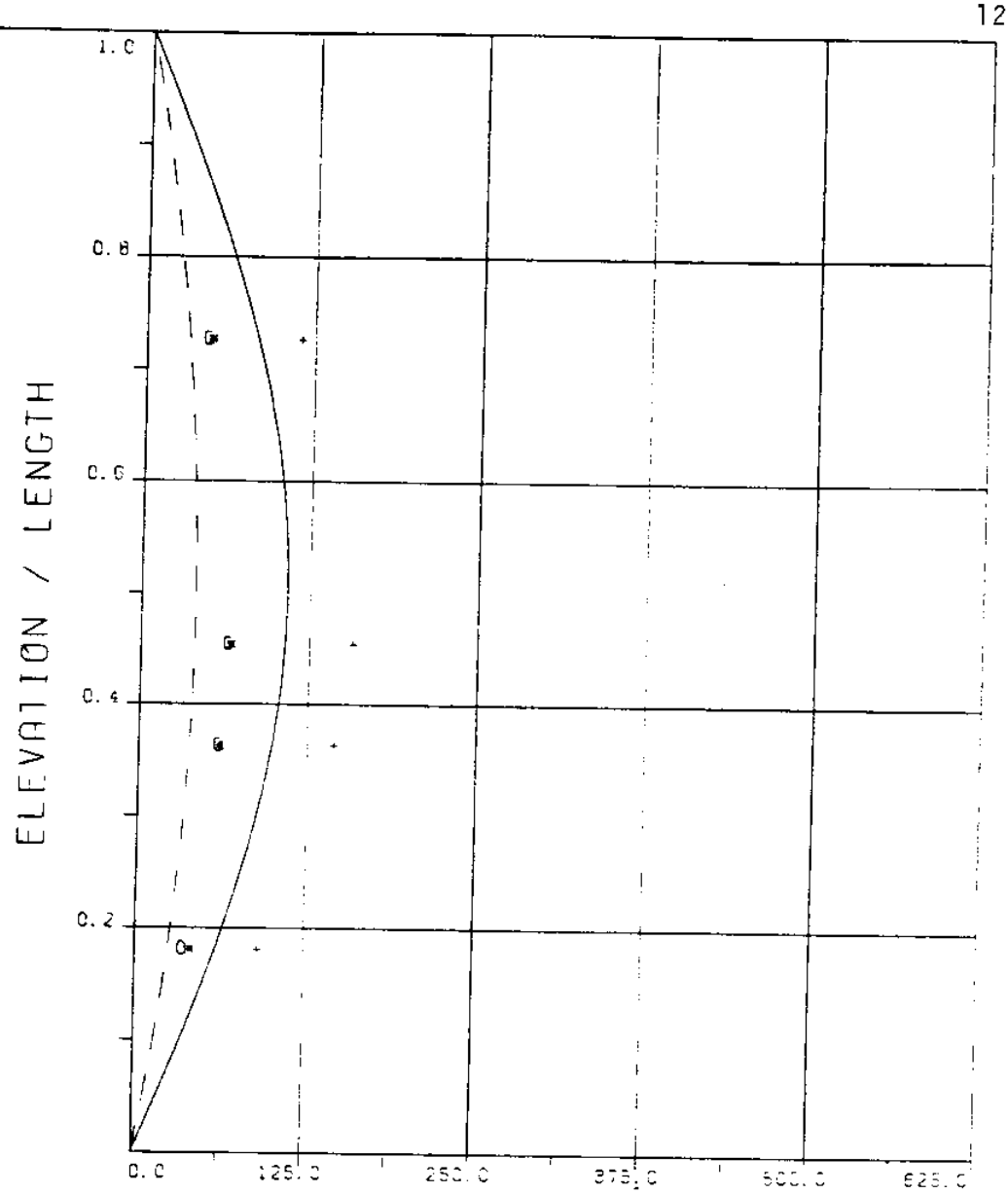

EXPERIMENT NUMBER 108

VC=135 A/DE=0.00

STATIC RESPONSE IN PLANE A

----- THEORY * * * EXPERIMENT

MAXIMUM DYNAMIC RESPONSE IN PLANE A

o o o EXPERIMENT

MAXIMUM RESPONSE

_____ THEORY + + + EXPERIMENT

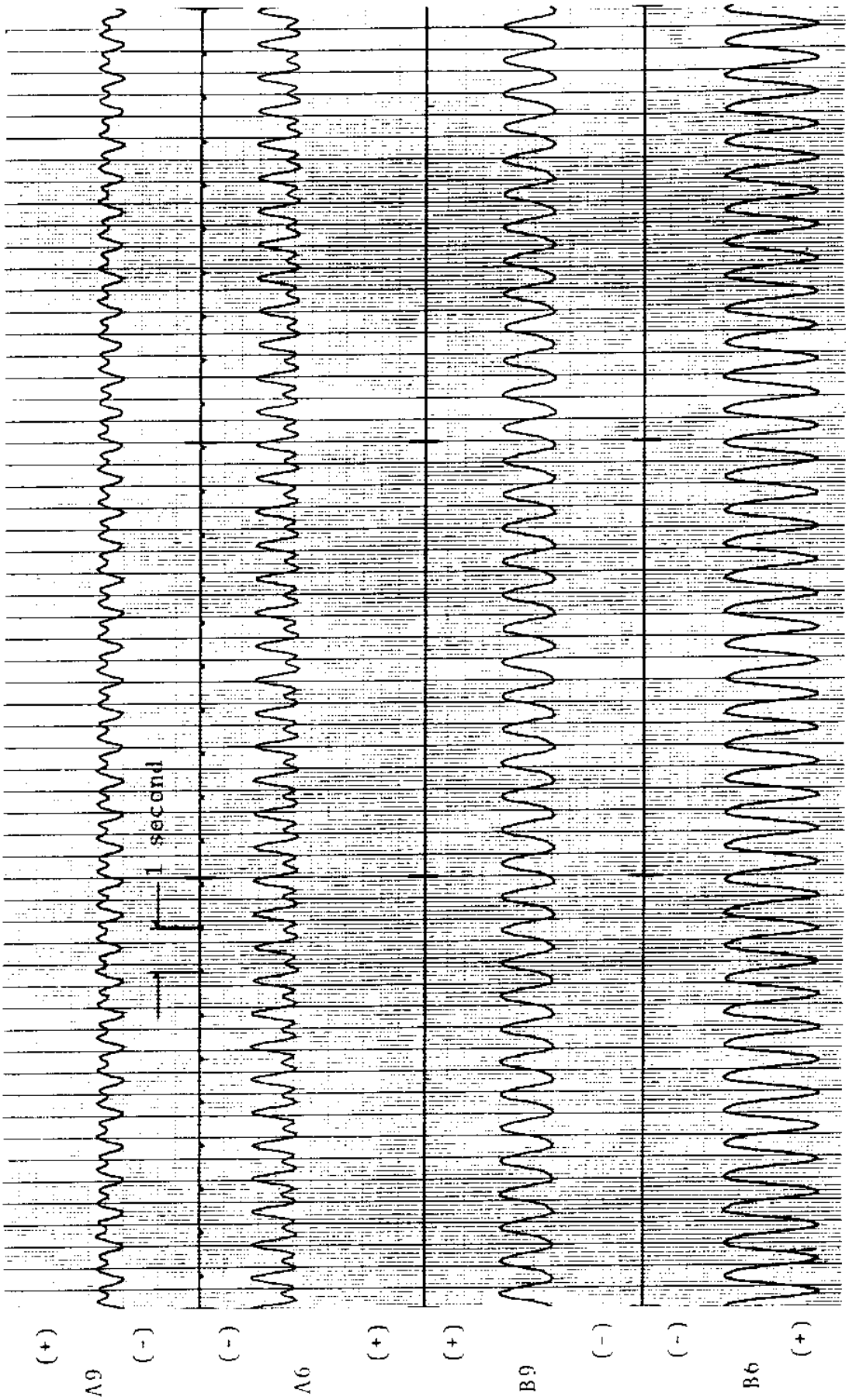

FIGURE 108T: ALL BRIDGES: 7.6 MICROSTRAIN/DIVISION

EXPERIMENT 113

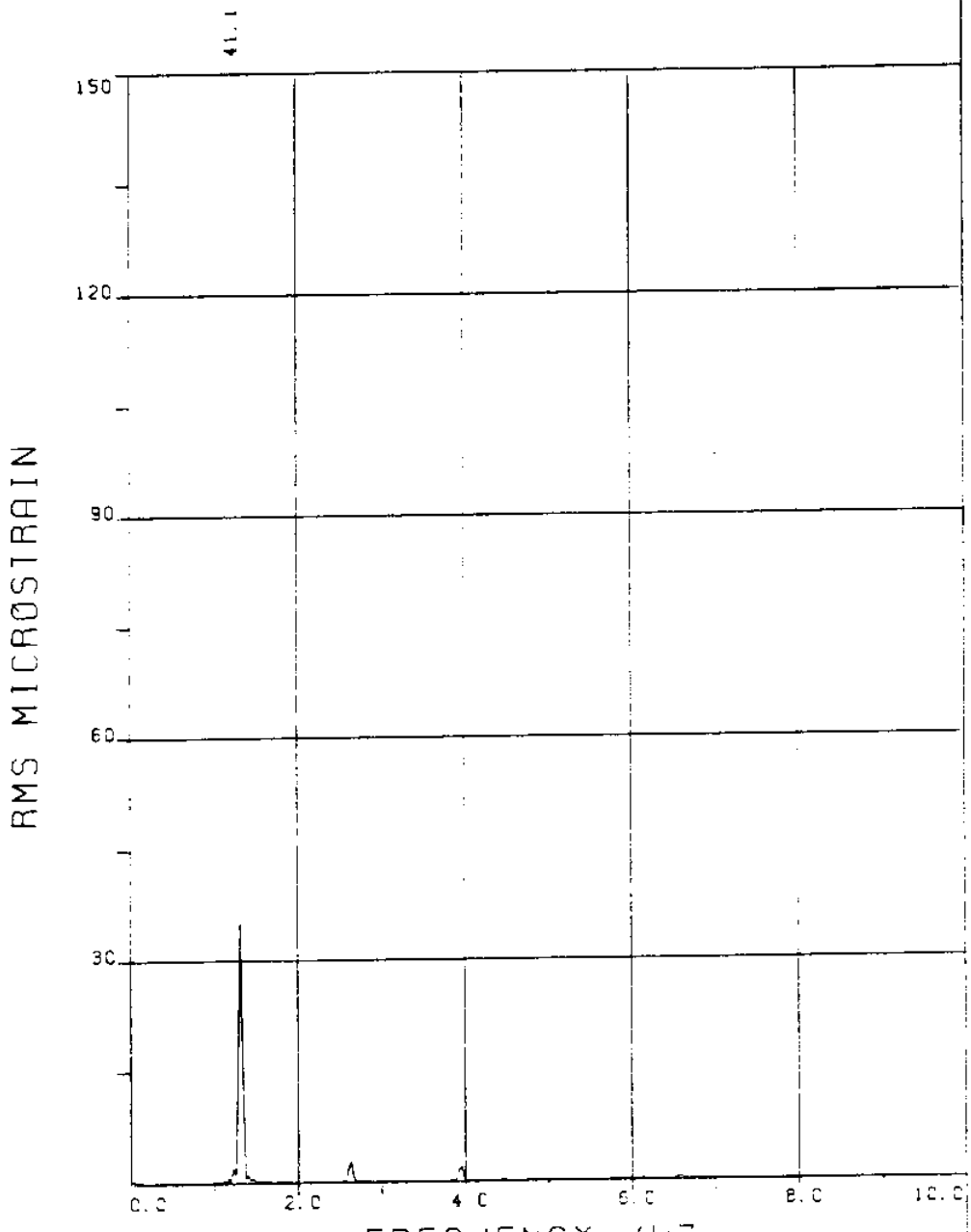

EXPERIMENT NUMBER 113

BRIDGE B9 ELEVATION=2L/11 BE=0.029

VC=140 A/DE=0.00

MEASURED RESPONSE IN MICROSTRAIN

TOTAL DYNAMIC RMS=41.2

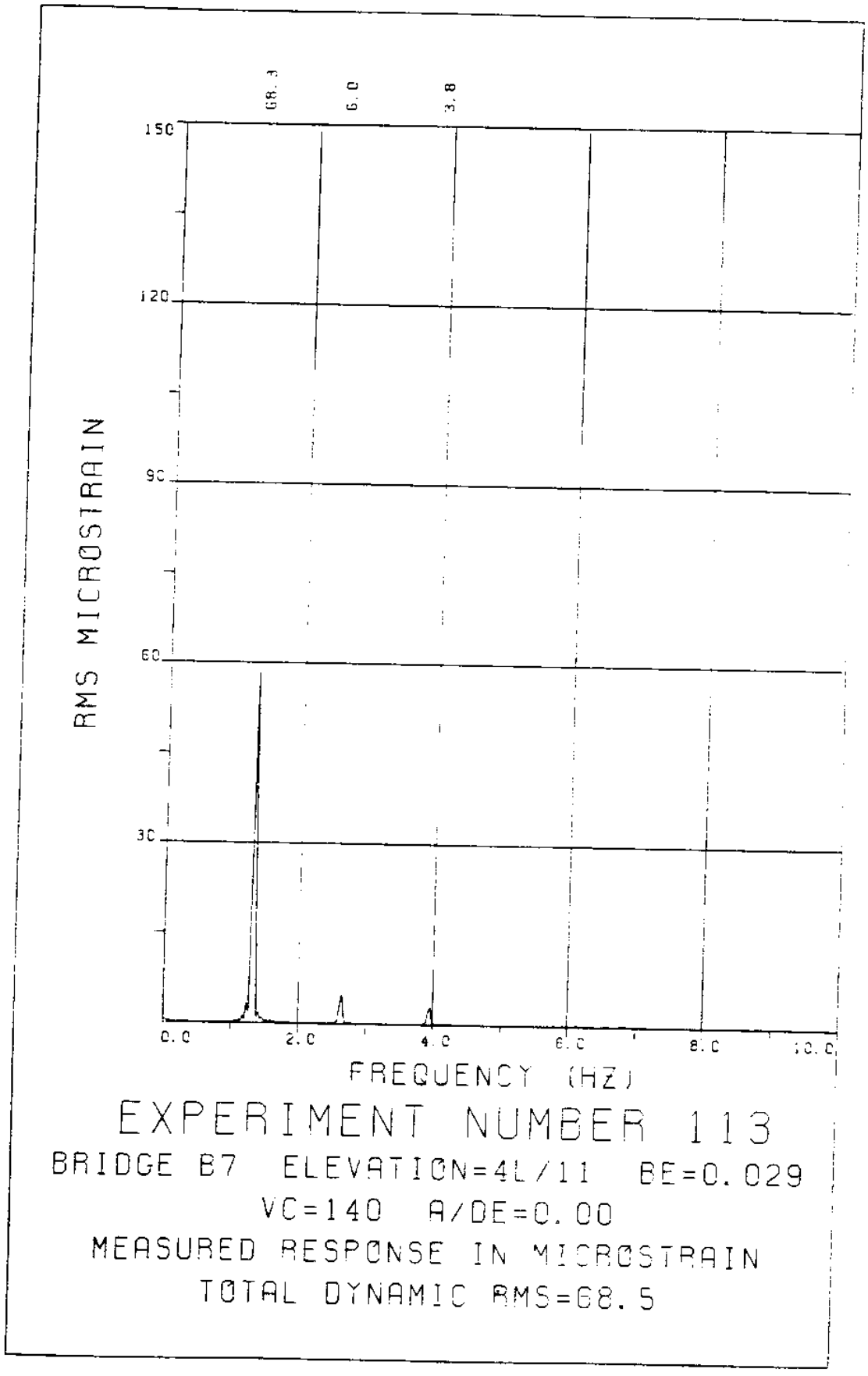

EXPERIMENT NUMBER 113

BRIDGE B7 ELEVATION=4L/11 BE=0.029

VC=140 A/DE=0.00

MEASURED RESPONSE IN MICROSTRAIN

TOTAL DYNAMIC RMS=68.5

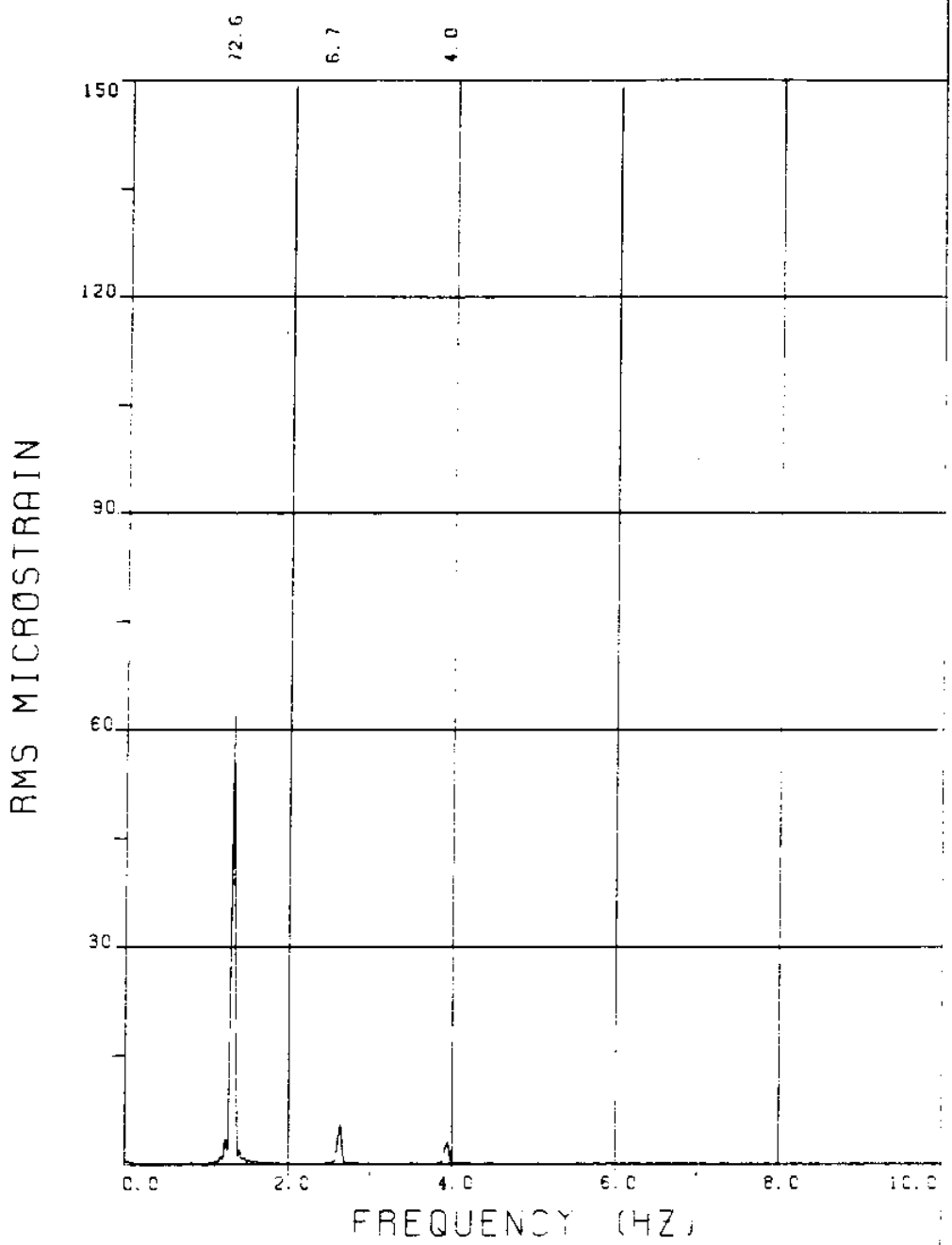

EXPERIMENT NUMBER 113

BRIDGE BG ELEVATION=5L/11 BE=0.029

VC=140 A/DE=0.00

MEASURED RESPONSE IN MICROSTRAIN

TOTAL DYNAMIC RMS=72.9

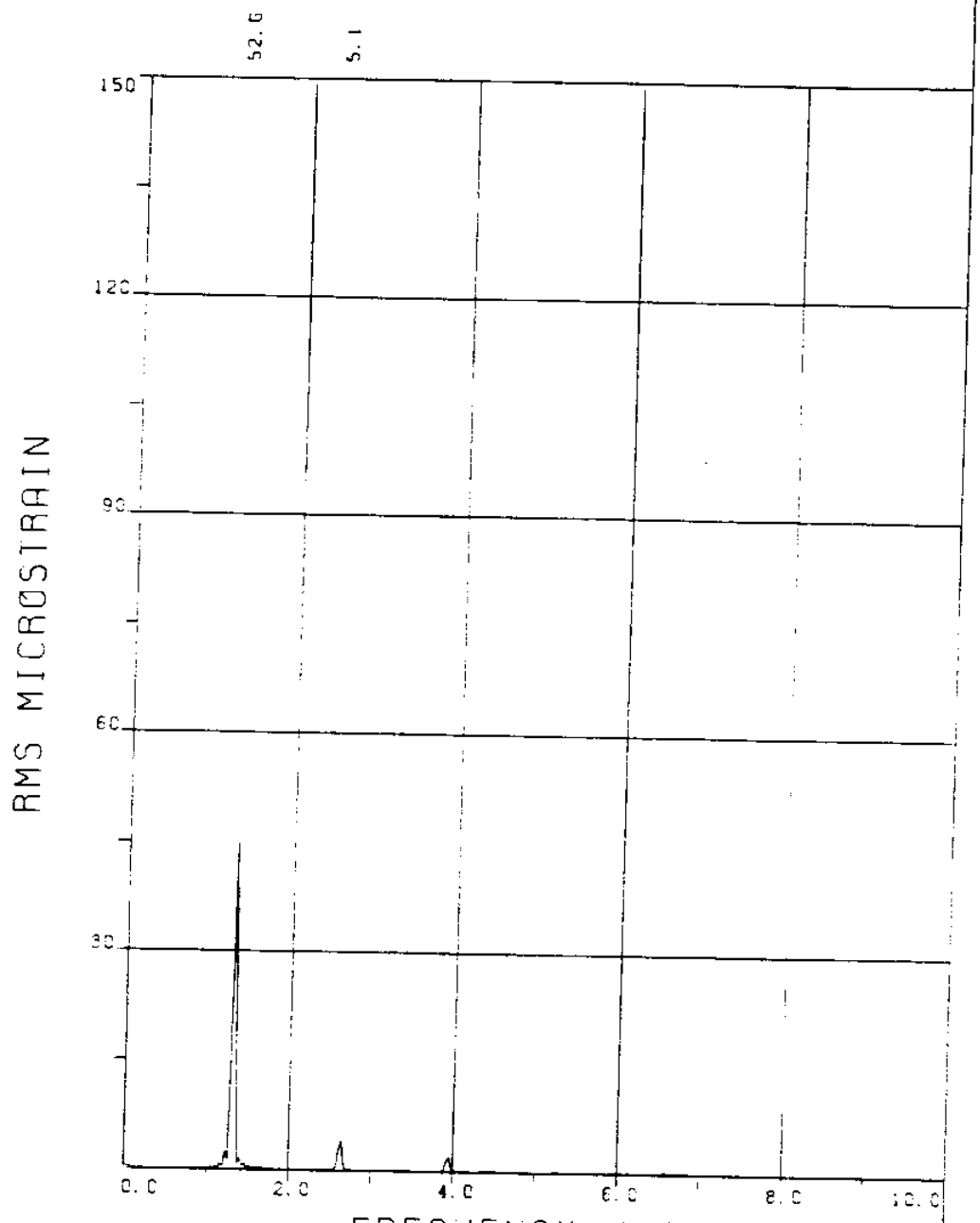

EXPERIMENT NUMBER 113

BRIDGE B3 ELEVATION=8L/11 BE=0.029

VC=140 A/DE=0.00

MEASURED RESPONSE IN MICROSTRAIN

TOTAL DYNAMIC RMS=53.0

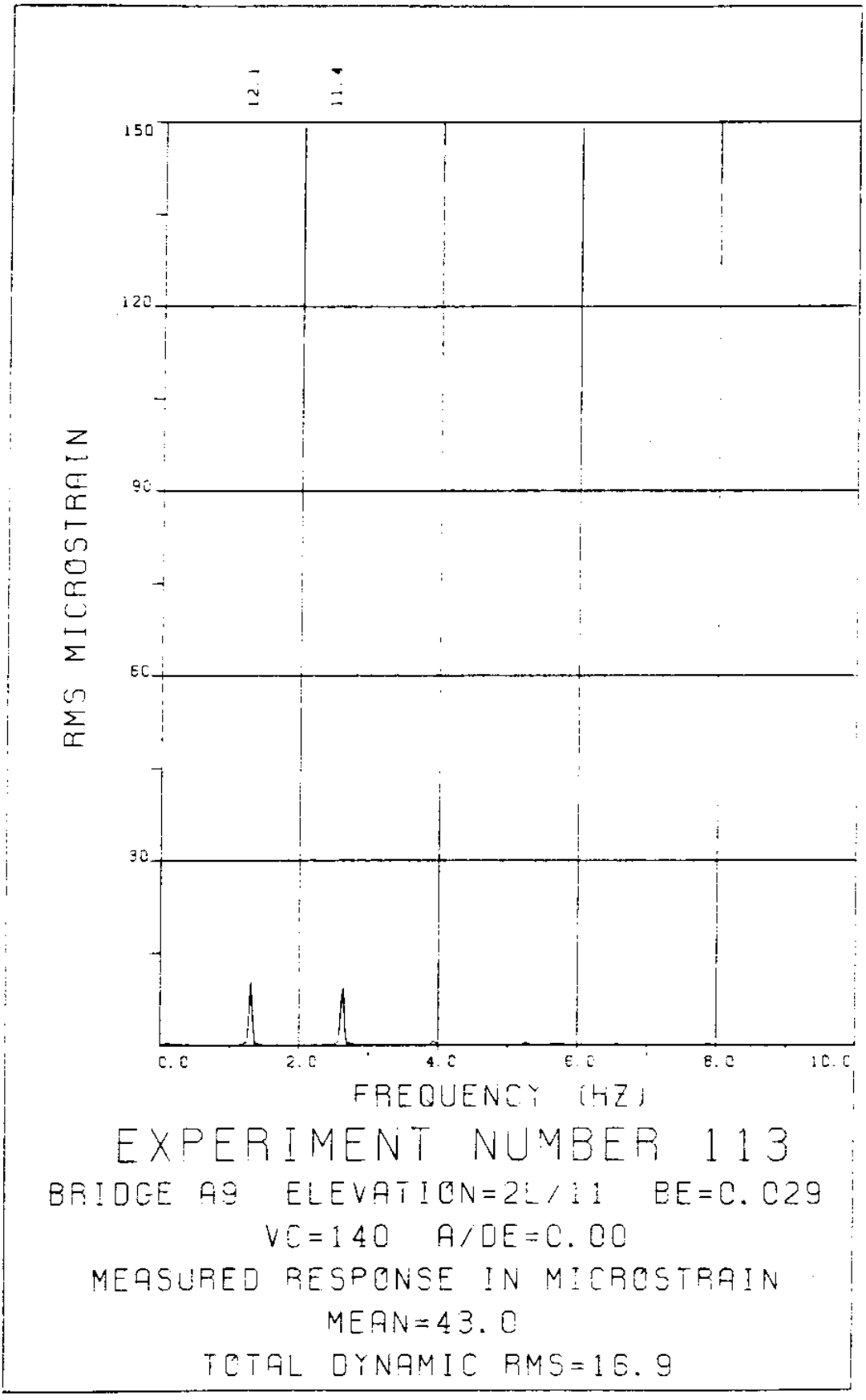
12.1
11.4
150
120
90
60
30
RMS MICROSTRAIN
0.0
2.0
4.0
6.0
8.0
10.0
FREQUENCY (HZ)
EXPERIMENT NUMBER 113
BRIDGE A9 ELEVATION=2L/11 BE=0.029
VC=140 A/DE=0.00
MEASURED RESPONSE IN MICROSTRAIN
MEAN=43.0
TOTAL DYNAMIC RMS=16.9

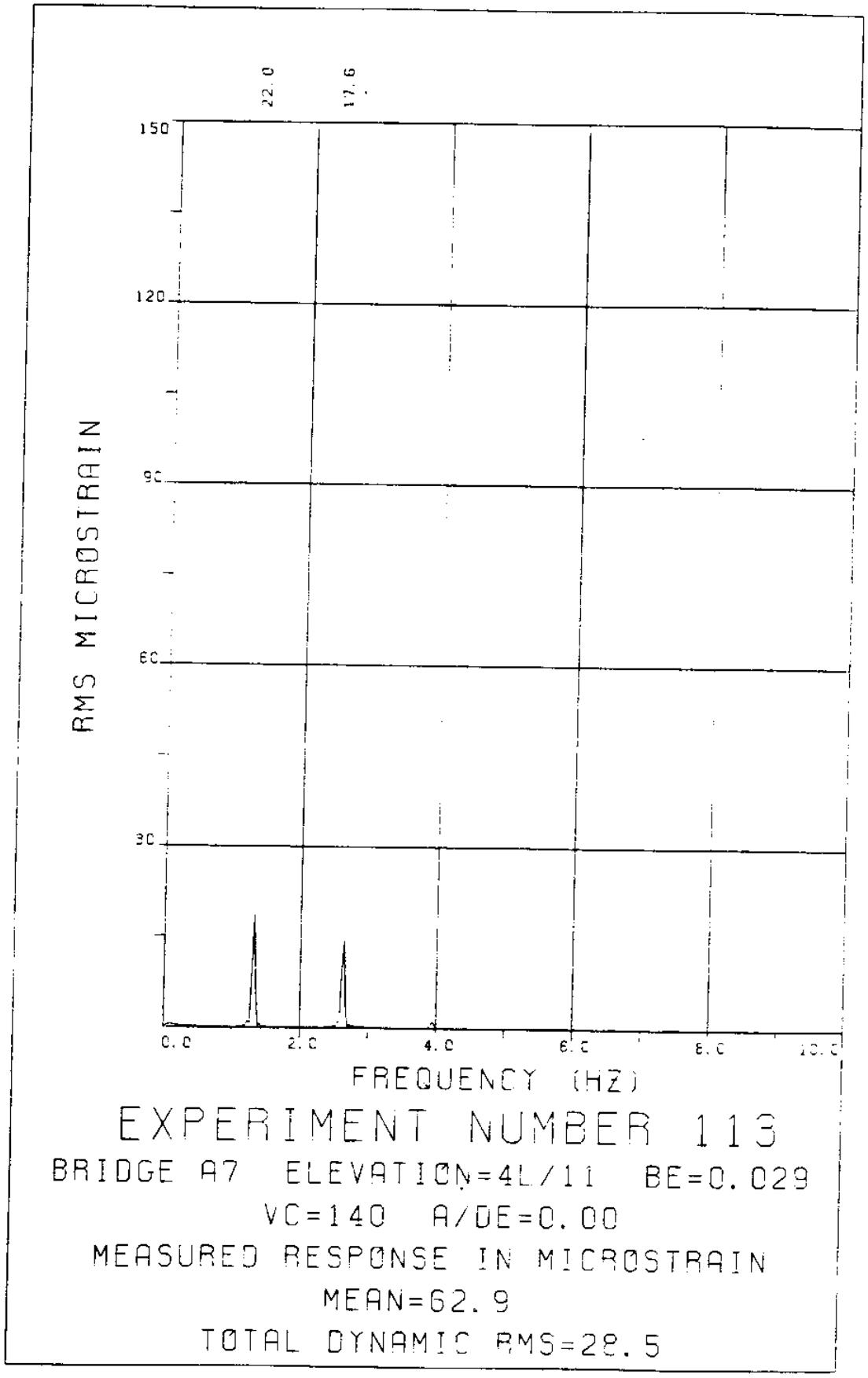
22.0
17.6
150
120
90
60
30
RMS MICROSTRAIN
0.0
2.0
4.0
6.0
8.0
10.0
FREQUENCY (HZ)
EXPERIMENT NUMBER 113
BRIDGE A7 ELEVATION=4L/11 BE=0.029
VC=140 A/DE=0.00
MEASURED RESPONSE IN MICROSTRAIN
MEAN=62.9
TOTAL DYNAMIC RMS=28.5

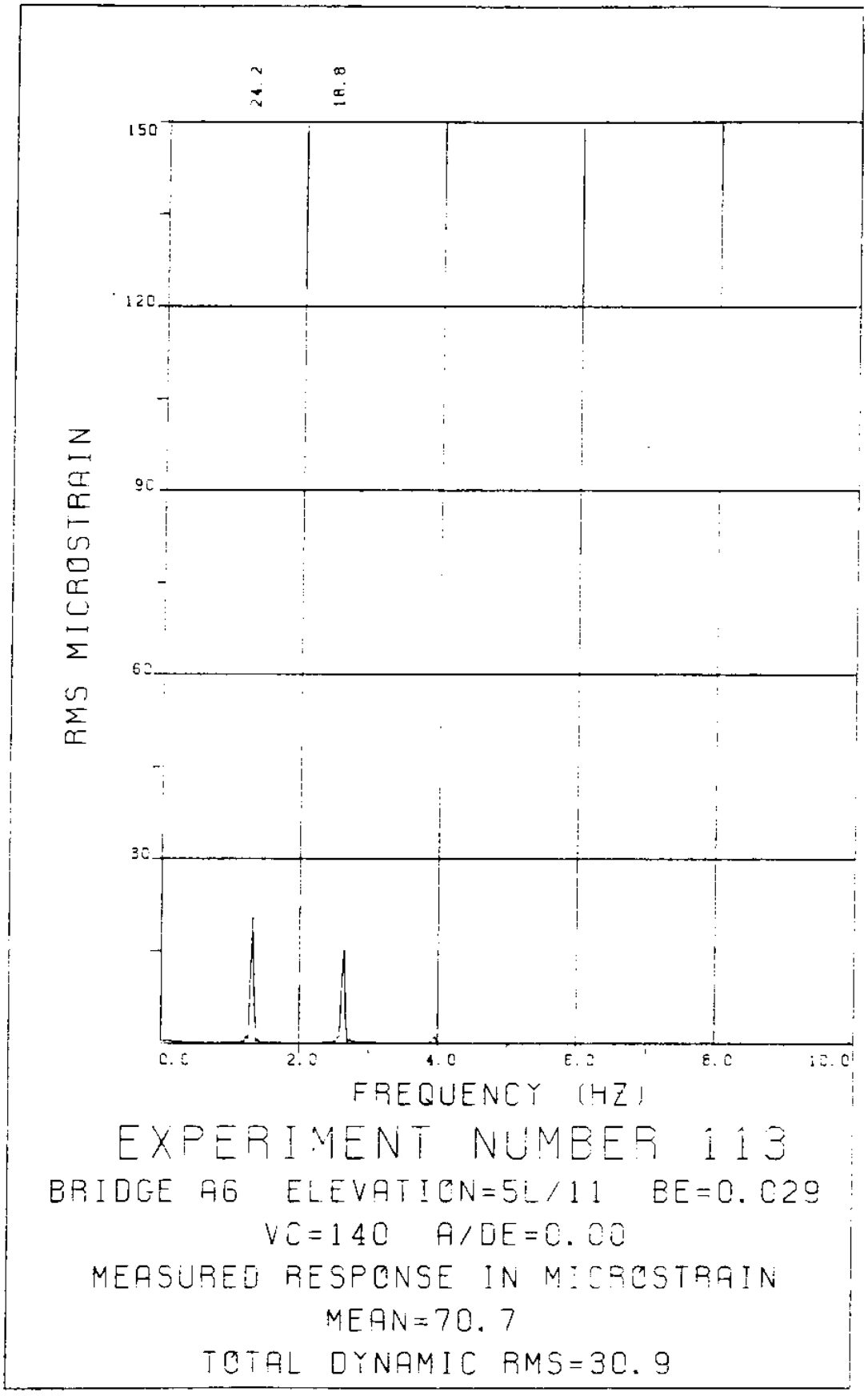

EXPERIMENT NUMBER 113

BRIDGE A6 ELEVATION=5L/11 BE=0.029

VC=140 A/DE=0.00

MEASURED RESPONSE IN MICROSTRAIN

MEAN=70.7

TOTAL DYNAMIC RMS=30.9

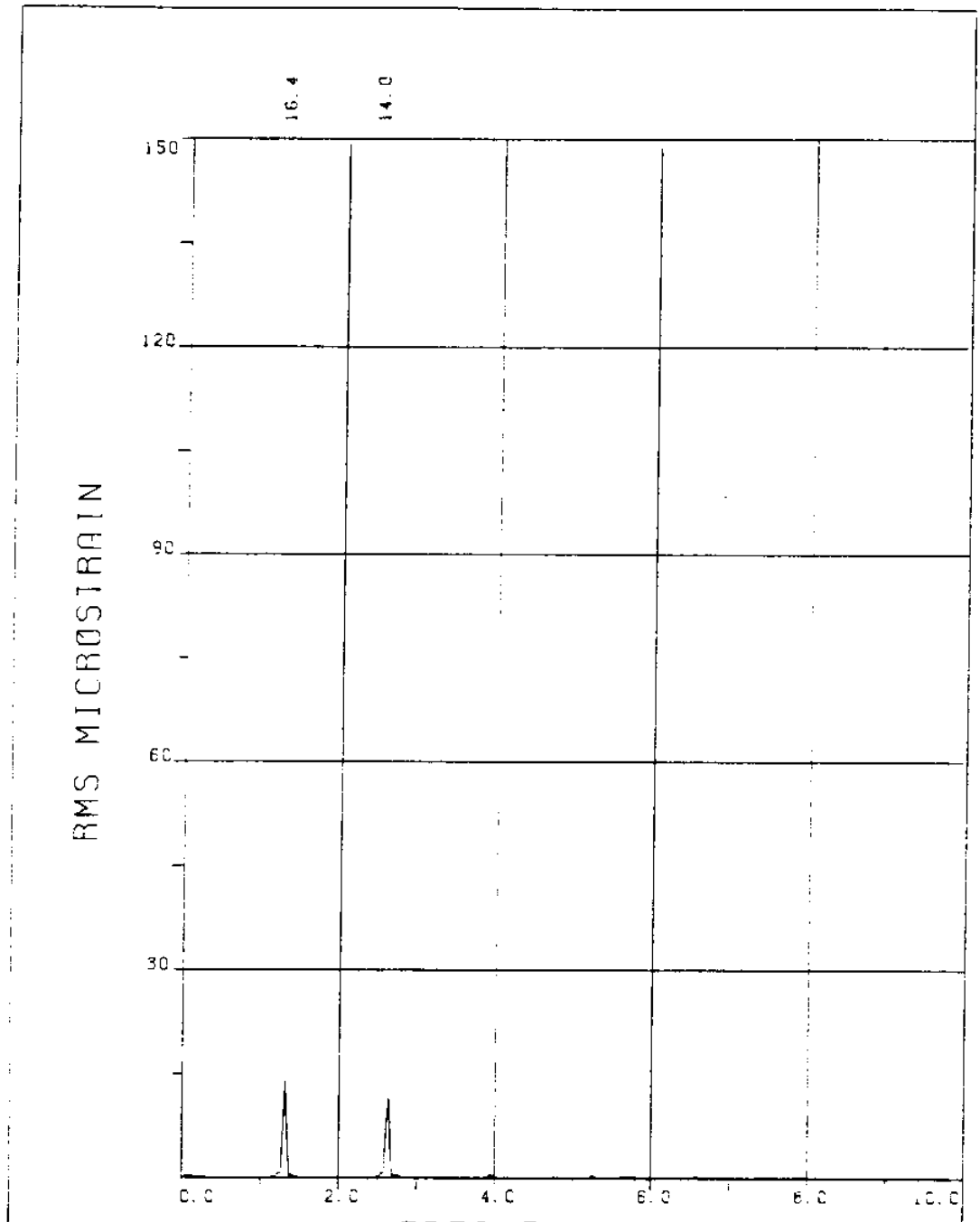

EXPERIMENT NUMBER 113

BRIDGE A3 ELEVATION=8L/11 BE=0.029

VC=140 A/DE=0.00

MEASURED RESPONSE IN MICROSTRAIN

MEAN=51.2

TOTAL DYNAMIC RMS=21.8

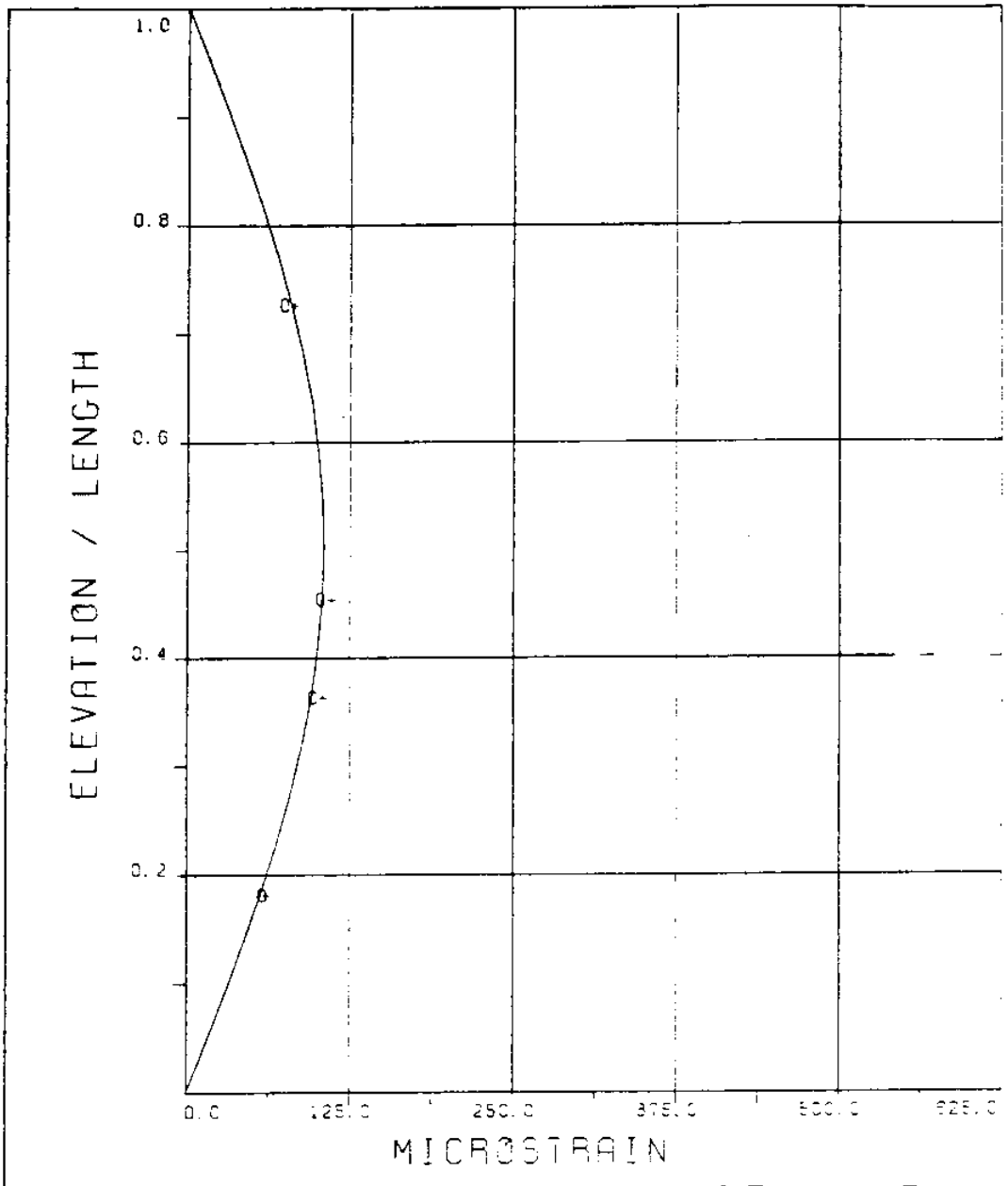

EXPERIMENT NUMBER 113

VC=140 A/DE=0.00

DYNAMIC RESPONSE AT F=FR IN PLANE B

_____ THEORY c c c EXPERIMENT

MAXIMUM DYNAMIC RESPONSE IN PLANE B

_____ THEORY + + + EXPERIMENT

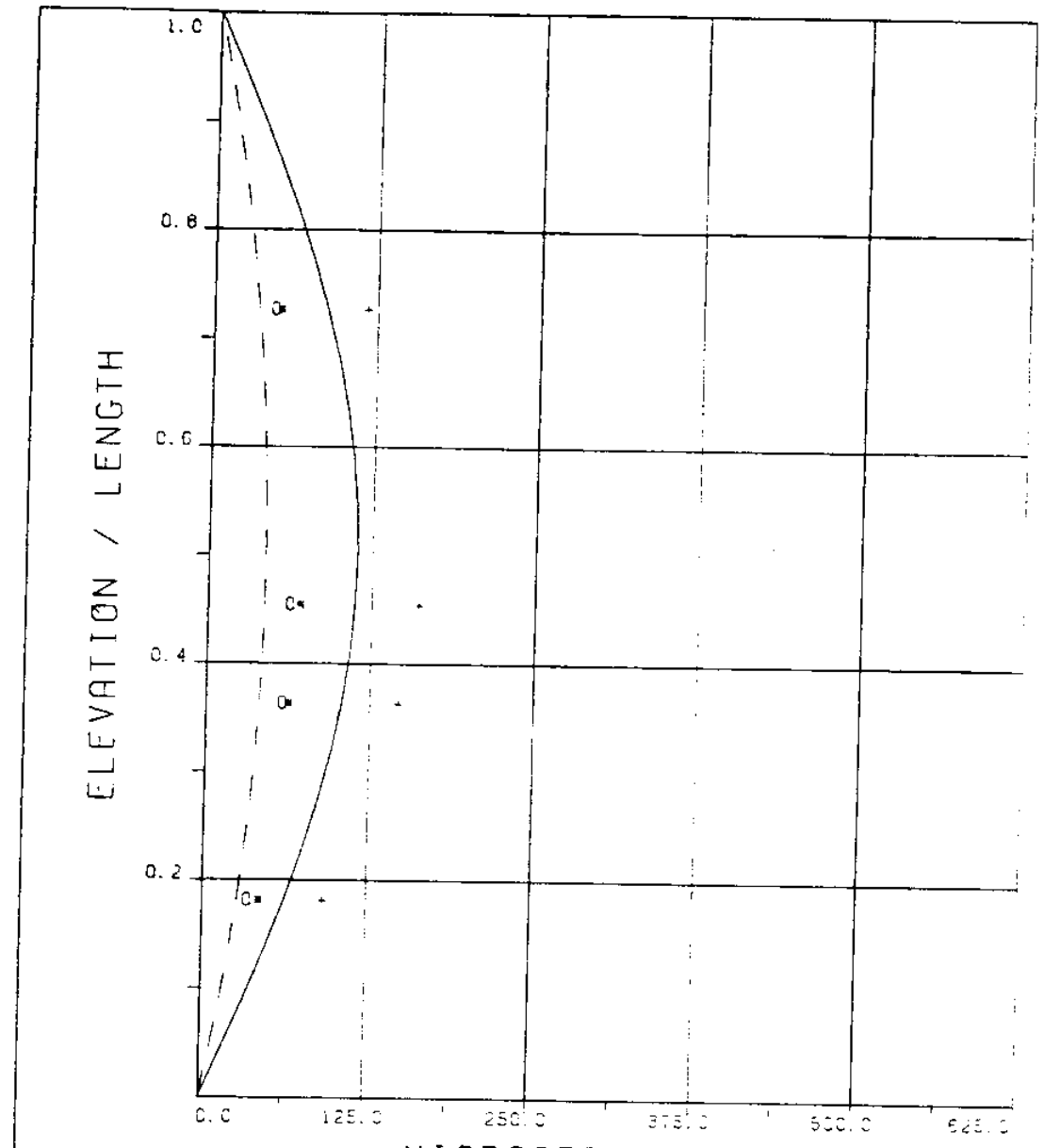

EXPERIMENT NUMBER 113

Vc=140 A/DE=0.00

STATIC RESPONSE IN PLANE A

----- THEORY * * * EXPERIMENT

MAXIMUM DYNAMIC RESPONSE IN PLANE A

o o o EXPERIMENT

MAXIMUM RESPONSE

——— THEORY + + + EXPERIMENT

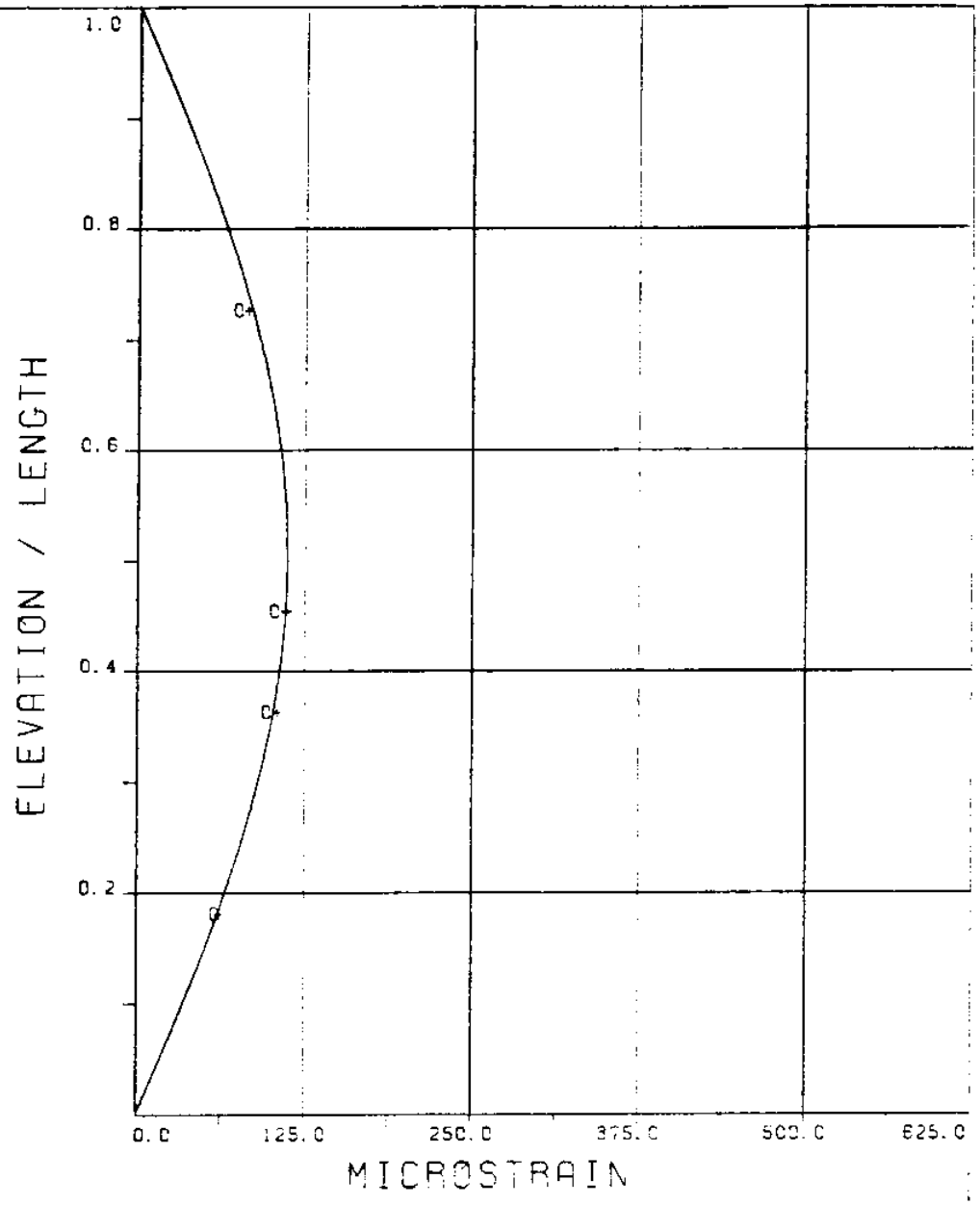

EXPERIMENT NUMBER 113

VC=140 A/DE=0.00

DYNAMIC RESPONSE AT F=FR IN PLANE B

——— THEORY o o o EXPERIMENT

MAXIMUM DYNAMIC RESPONSE IN PLANE B

——— THEORY + + + EXPERIMENT

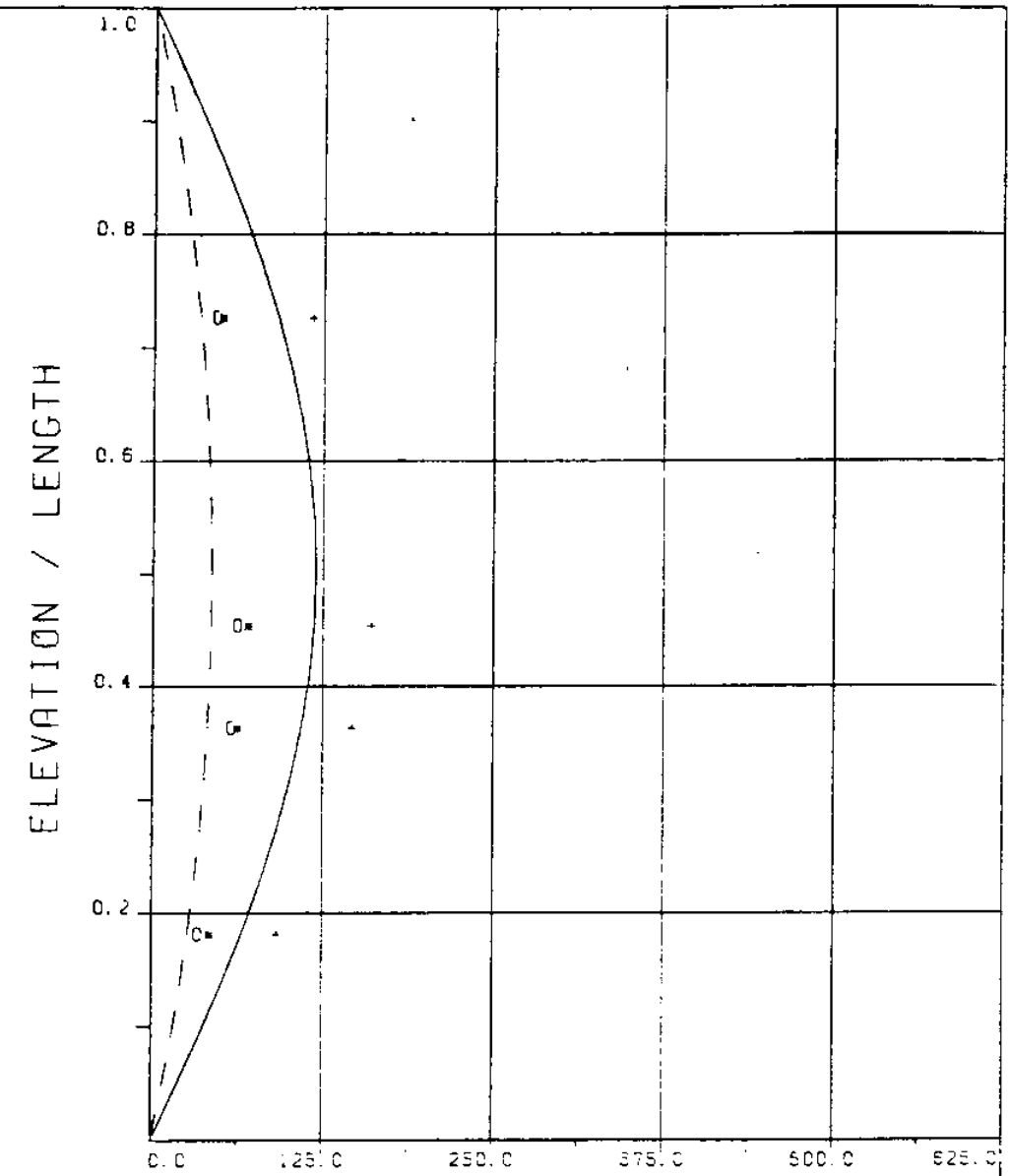

EXPERIMENT NUMBER 113

VC=140 A/DE=0.00

STATIC RESPONSE IN PLANE A

----- THEORY * * * EXPERIMENT

MAXIMUM DYNAMIC RESPONSE IN PLANE A

o o o EXPERIMENT

MAXIMUM RESPONSE

_____ THEORY + + + EXPERIMENT

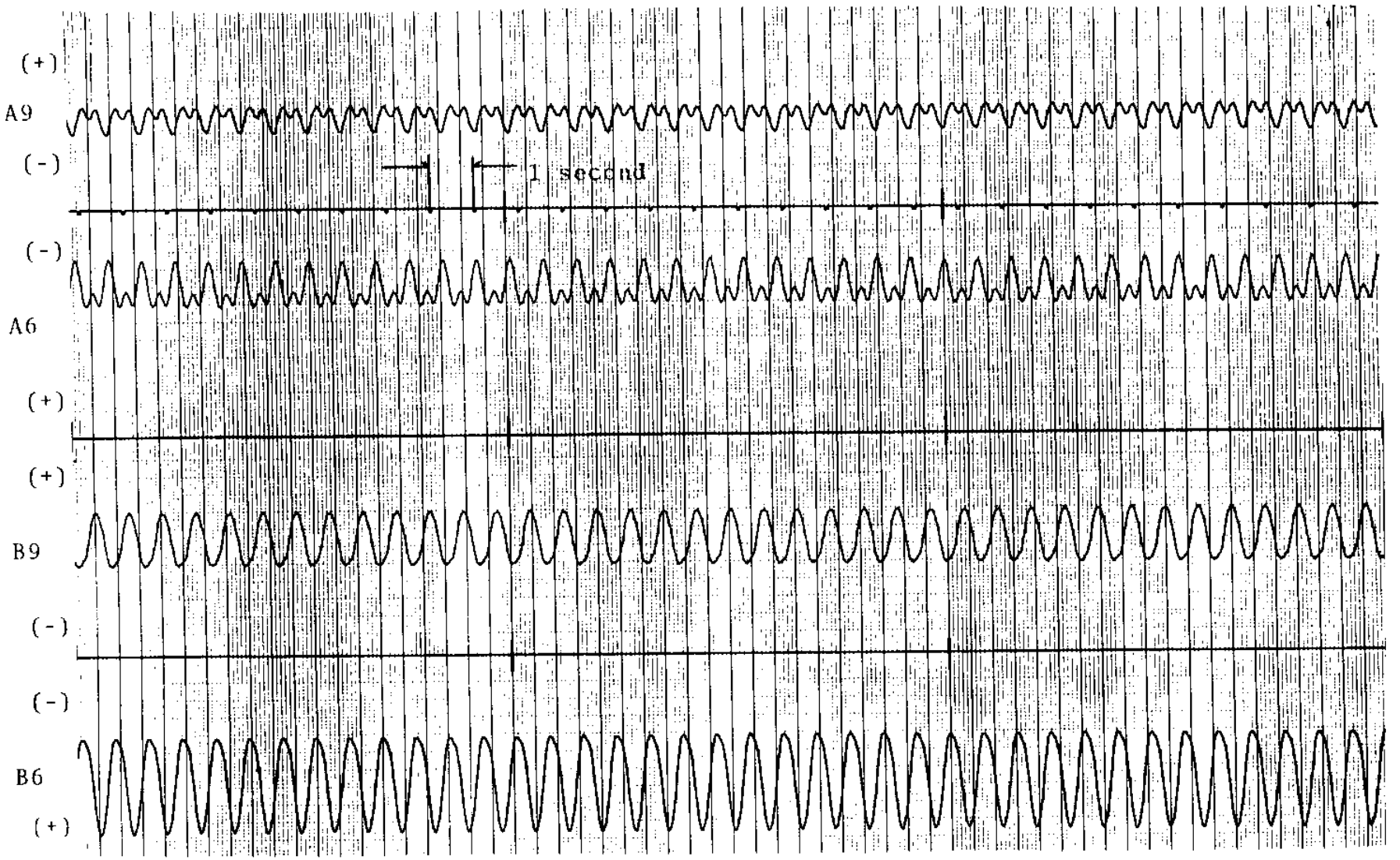

Figure 113T: ALL BRIDGES: 7.6 MICROSTRAIN/DIVISION

EXPERIMENT 110

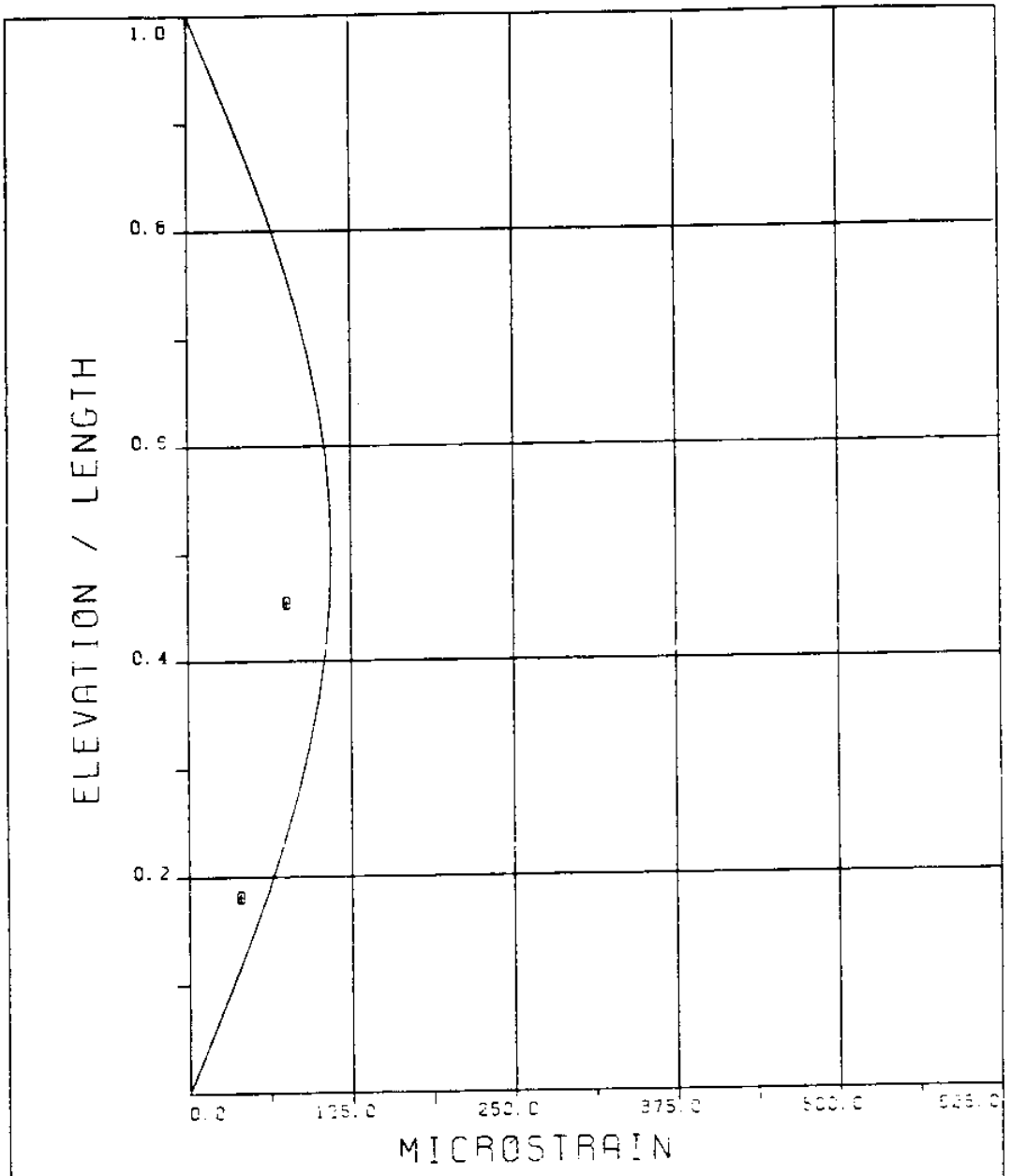

EXPERIMENT NUMBER 110

VC=150 A/DE=0.00

DYNAMIC RESPONSE AT F=FR IN PLANE B

——— THEORY o o o EXPERIMENT

MAXIMUM DYNAMIC RESPONSE IN PLANE B

——— THEORY + + + EXPERIMENT

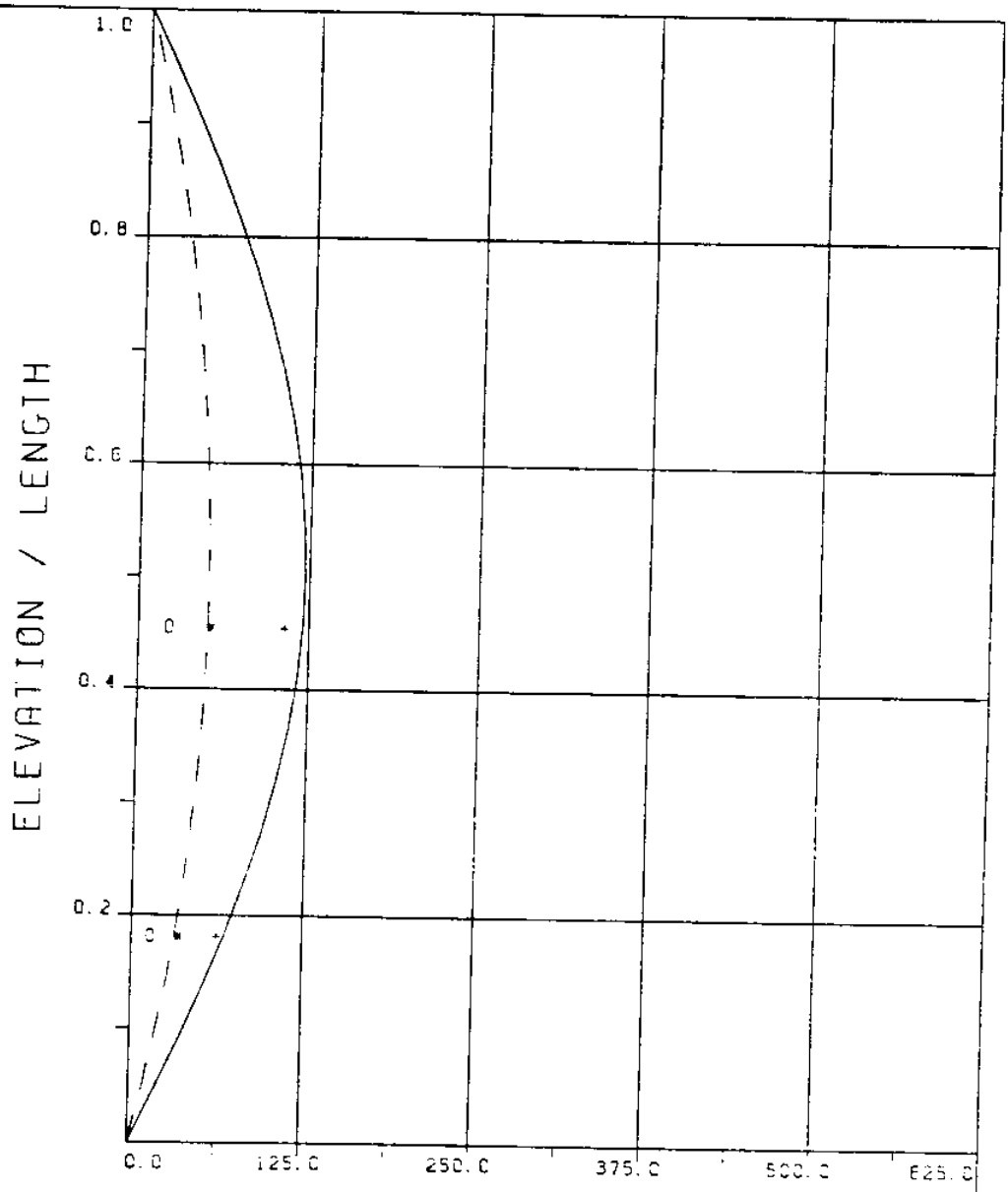

EXPERIMENT NUMBER 110

VC=150 A/DE=0.00

STATIC RESPONSE IN PLANE A

----- THEORY * * * EXPERIMENT

MAXIMUM DYNAMIC RESPONSE IN PLANE A

o o o EXPERIMENT

MAXIMUM RESPONSE

——— THEORY + + + EXPERIMENT

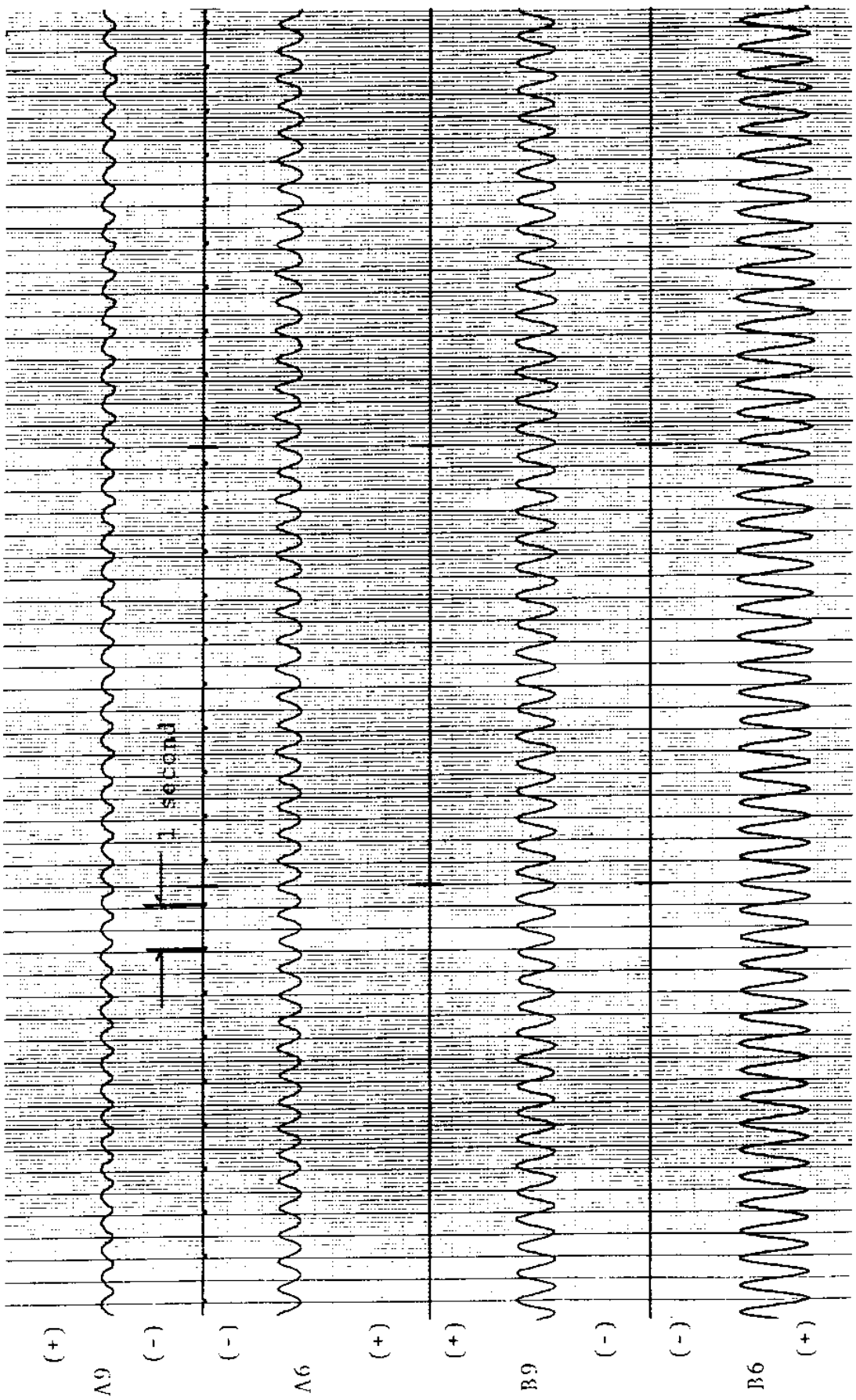

FIGURE 110T: ALL BRIDGES 7.6 MICROSTRAIN/DIVISION

EXPERIMENT III

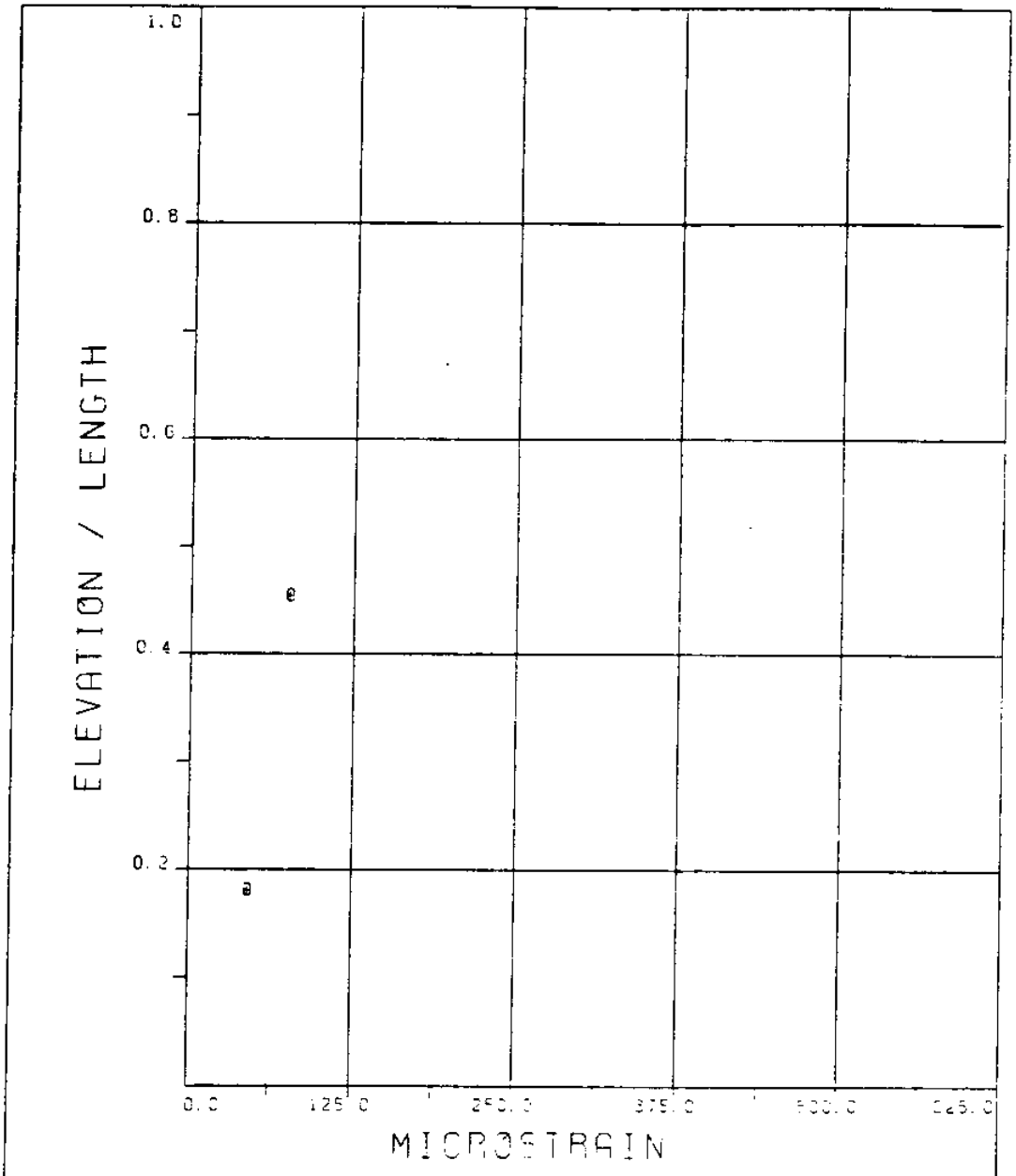

EXPERIMENT NUMBER 111

VC=170 A/DE=0.00

DYNAMIC RESPONSE AT F=FR IN PLANE B

o o o EXPERIMENT

MAXIMUM DYNAMIC RESPONSE IN PLANE B

+ + + EXPERIMENT

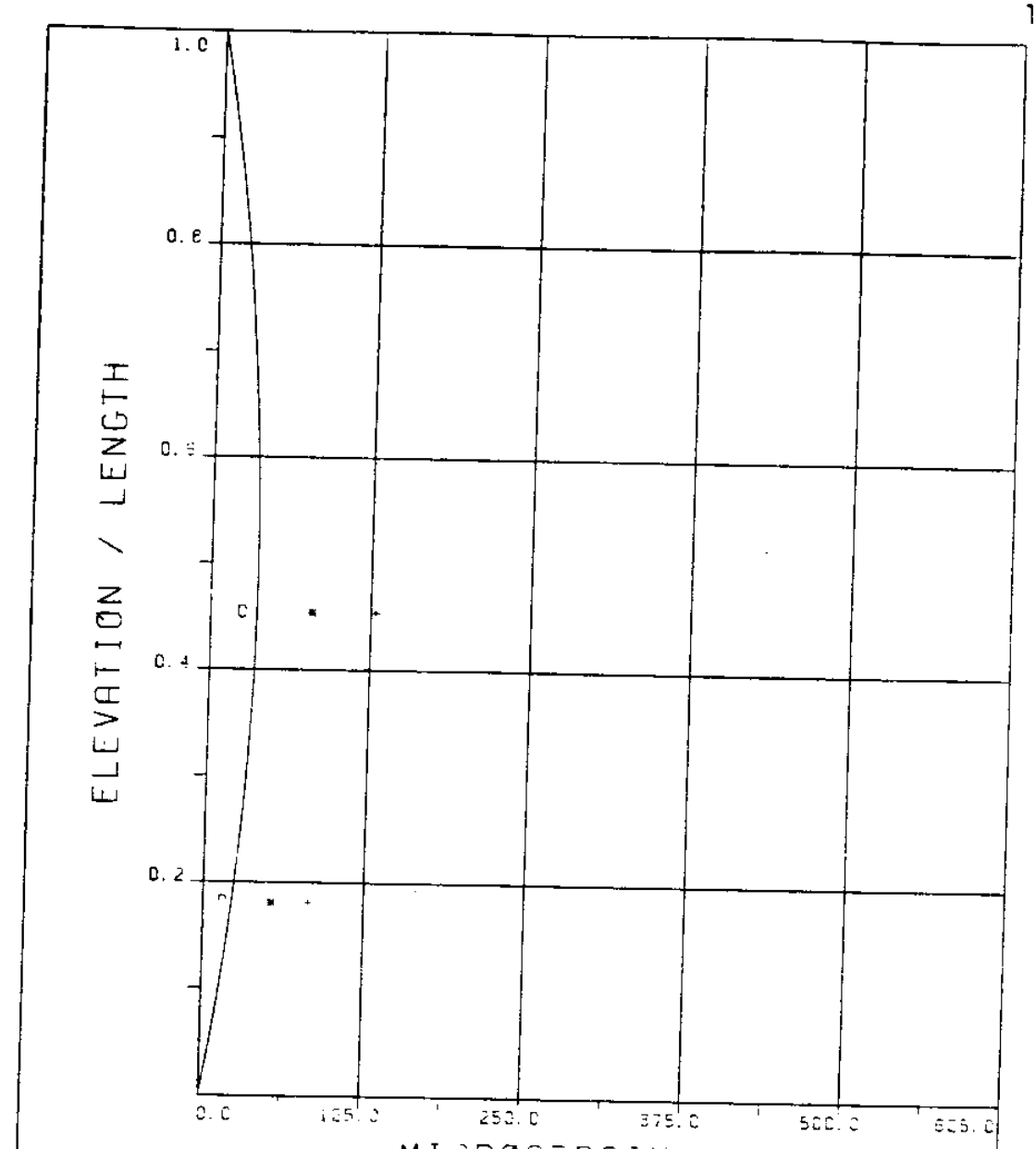

EXPERIMENT NUMBER 111

VC=170 A/DE=0.00

STATIC RESPONSE IN PLANE A

——— THEORY * * * EXPERIMENT

MAXIMUM DYNAMIC RESPONSE IN PLANE A

o o o EXPERIMENT

MAXIMUM RESPONSE

——— THEORY + + + EXPERIMENT

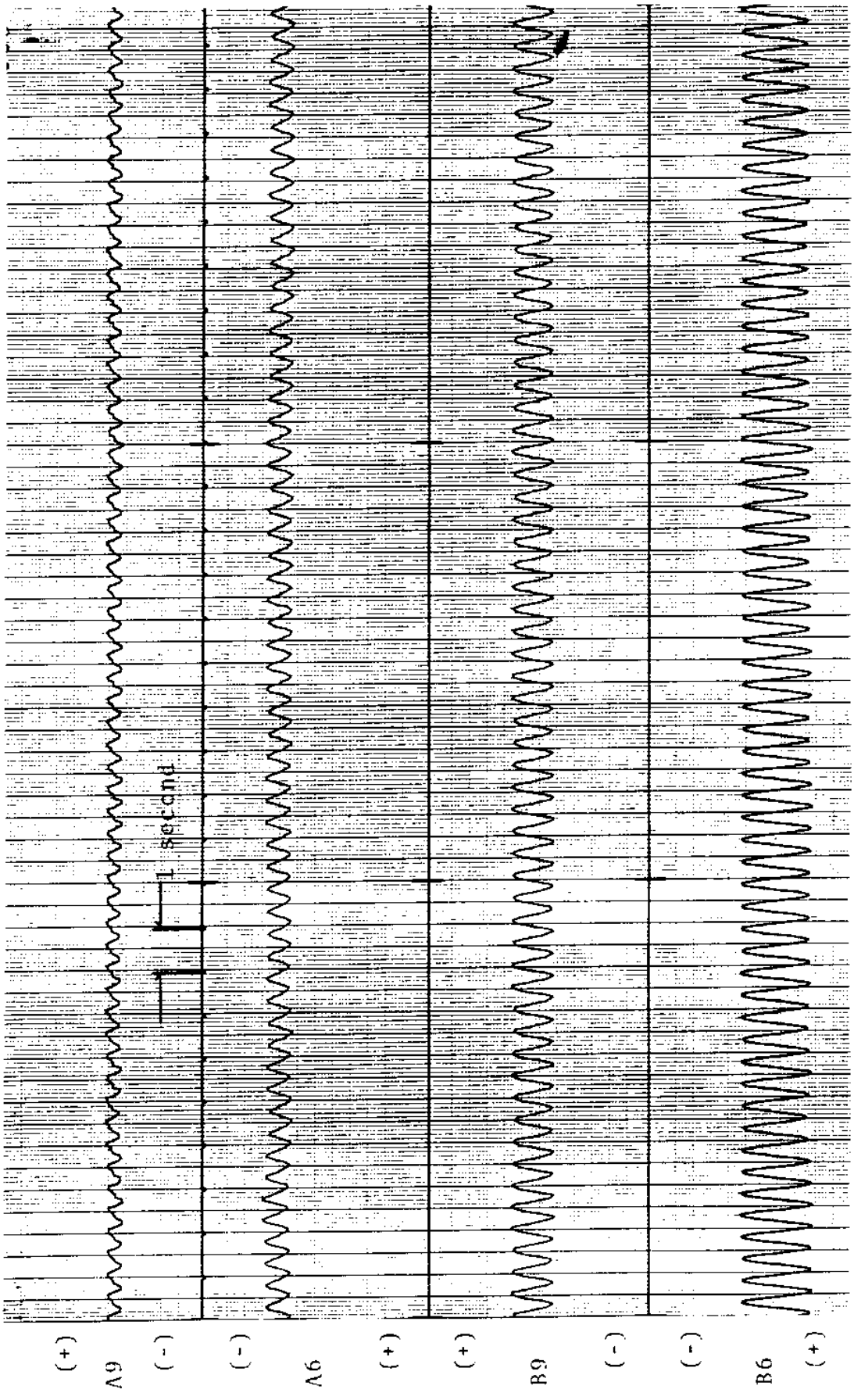

FIGURE 111T: ALL BRIDGES: 7.6 MICROSTRAIN/DIVISION

EXPERIMENT 109

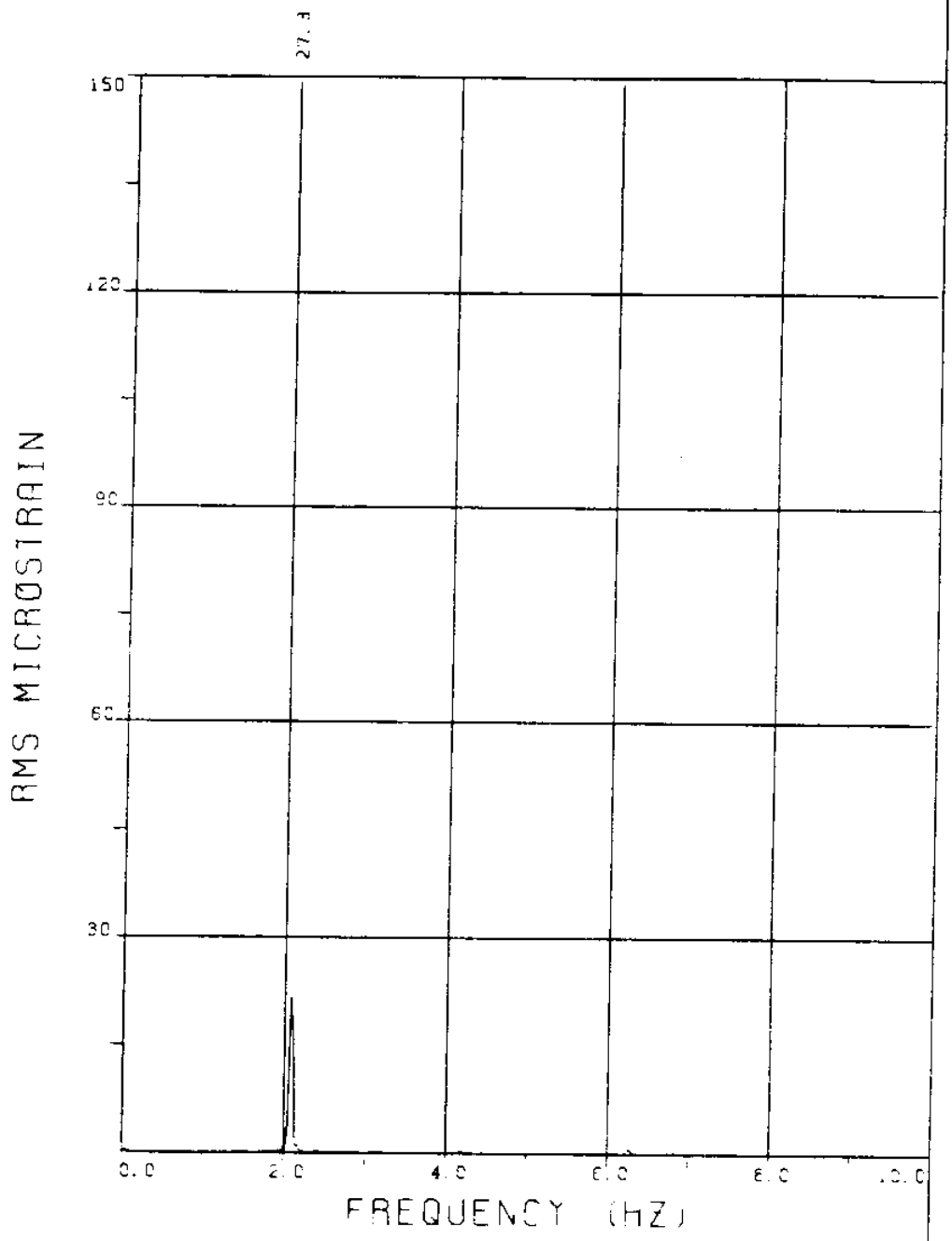

EXPERIMENT NUMBER 109

BRIDGE 89 ELEVATION=2L/11 BE=0.029

VC=190 A/DE=0.00

MEASURED RESPONSE IN MICROSTRAIN

TOTAL DYNAMIC RMS=27.4

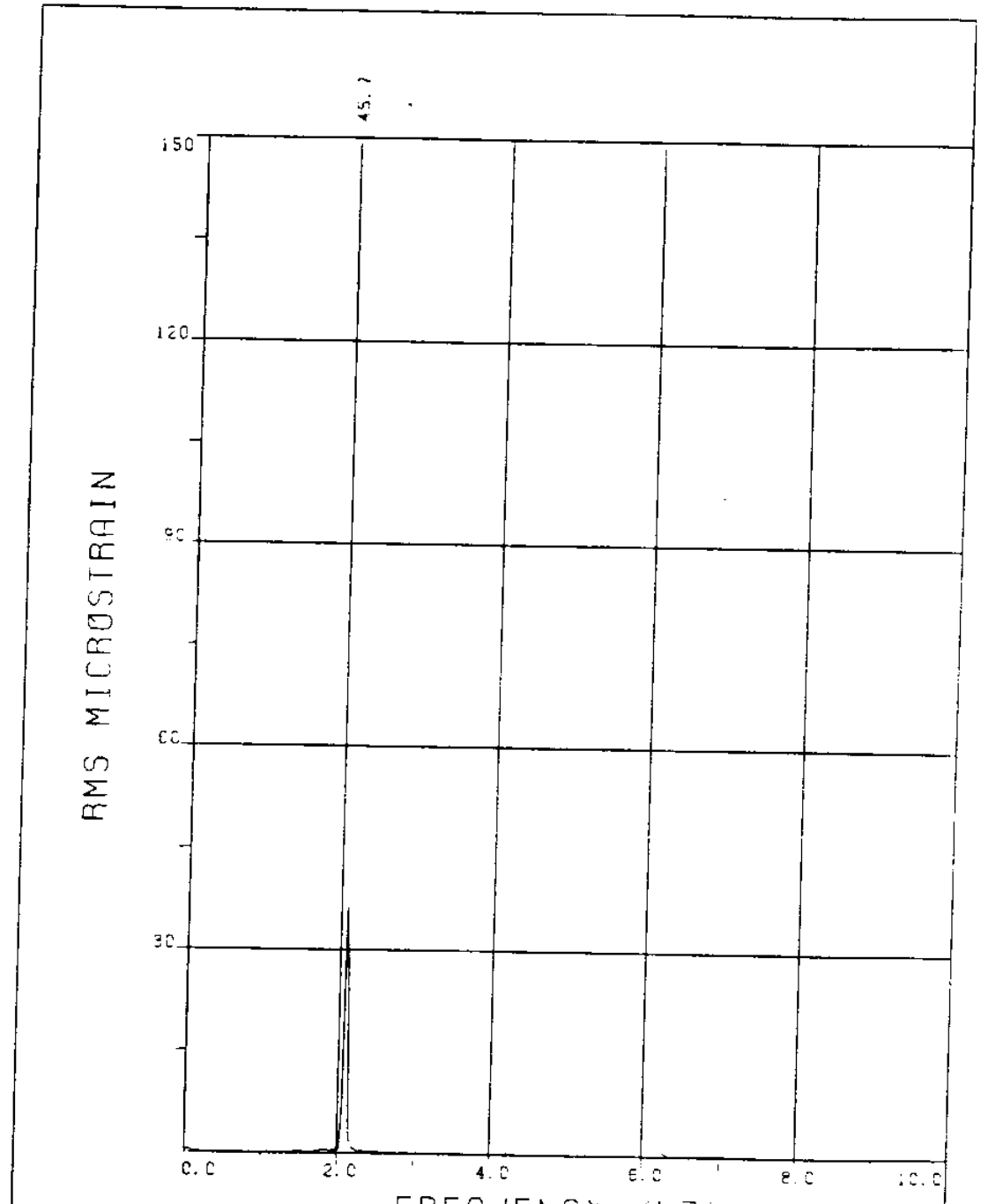

EXPERIMENT NUMBER 109

BRIDGE B7 ELEVATION=4L/11 BE=0.029

VC=190 A/DE=0.00

MEASURED RESPONSE IN MICROSTRAIN

TOTAL DYNAMIC RMS=45.8

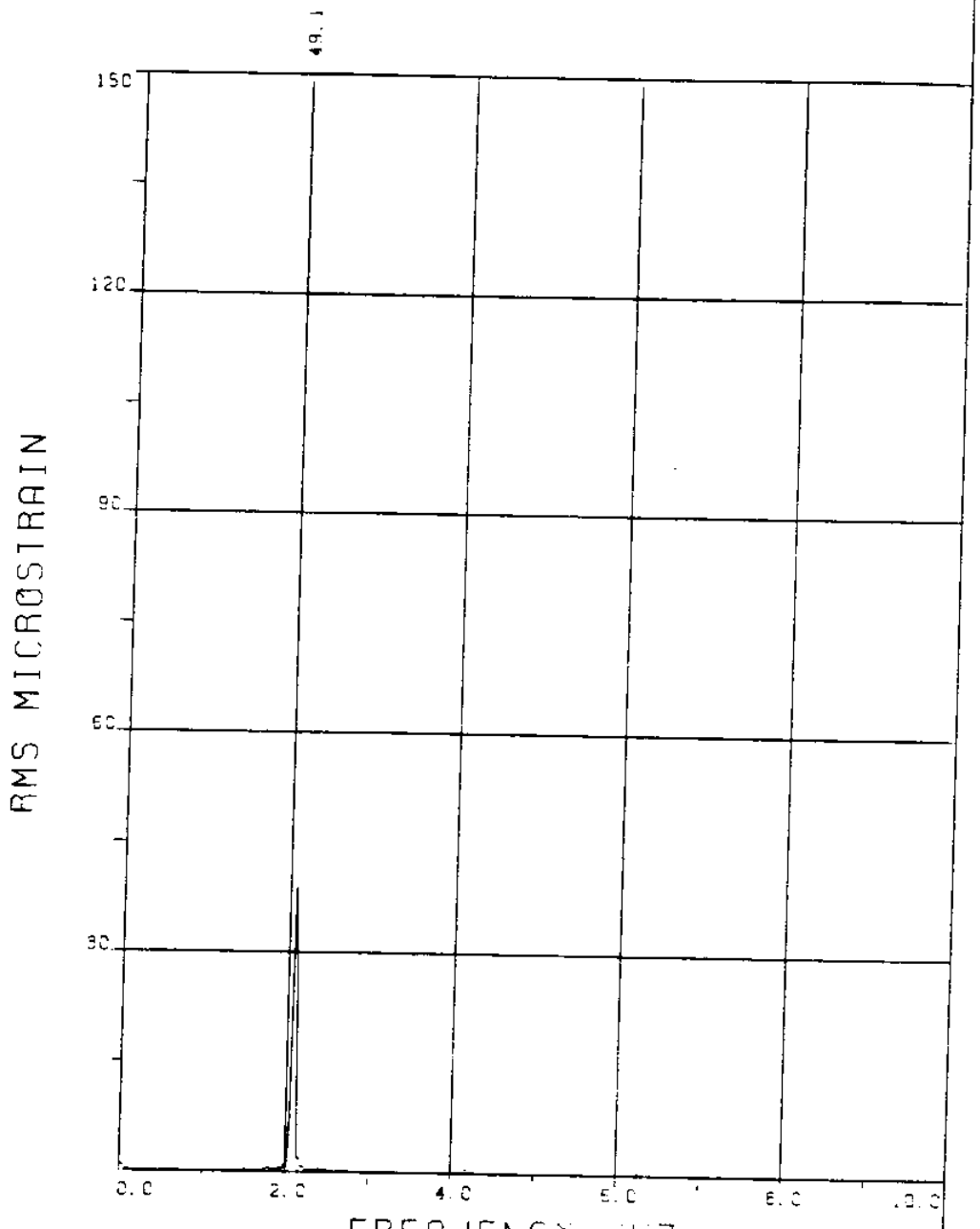

EXPERIMENT NUMBER 109

BRIDGE B6 ELEVATION=SL/11 BE=0.029

VC=190 A/DE=0.00

MEASURED RESPONSE IN MICROSTRAIN

TOTAL DYNAMIC RMS=49.1

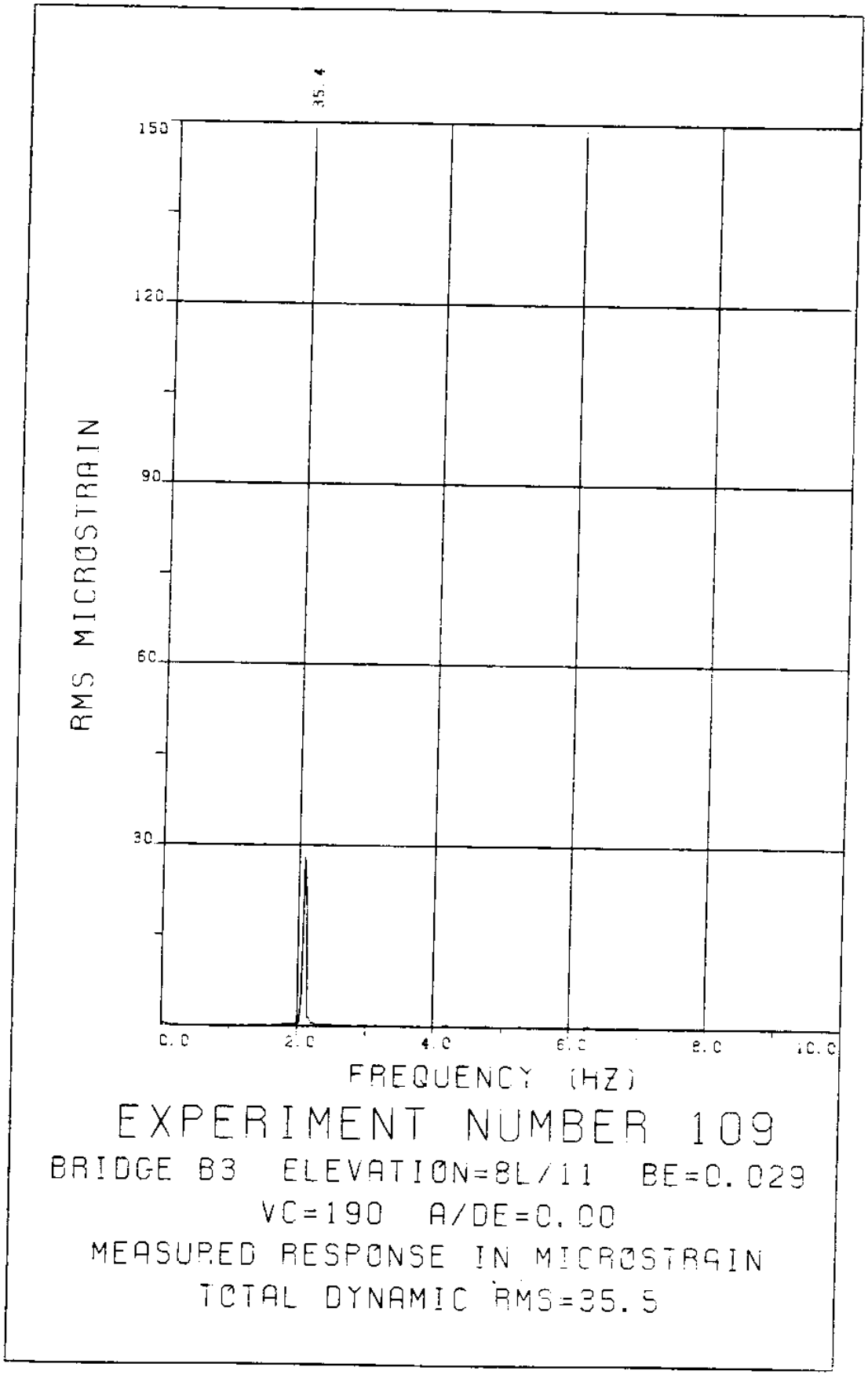
35.4
150
120
90
60
30
RMS MICROSTRAIN
0.0
2.0
4.0
6.0
8.0
10.0
FREQUENCY (HZ)
EXPERIMENT NUMBER 109
BRIDGE B3 ELEVATION=8L/11 BE=0.029
VC=190 A/DE=0.00
MEASURED RESPONSE IN MICROSTRAIN
TOTAL DYNAMIC RMS=35.5

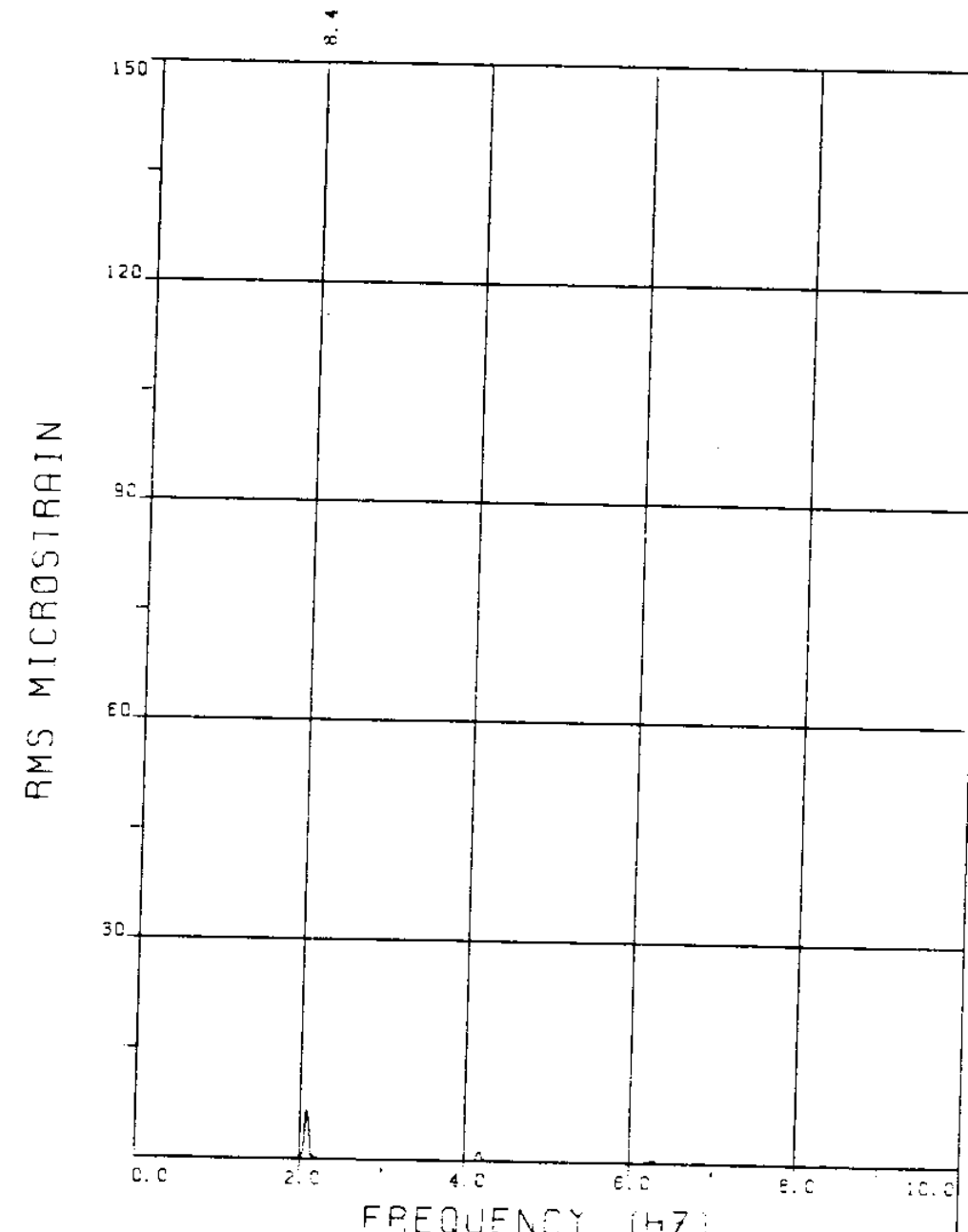

EXPERIMENT NUMBER 109

BRIDGE A9 ELEVATION=2L/11 BE=0.029

VC=190 A/DE=0.00

MEASURED RESPONSE IN MICROSTRAIN

MEAN=52.3

TOTAL DYNAMIC RMS=8.7

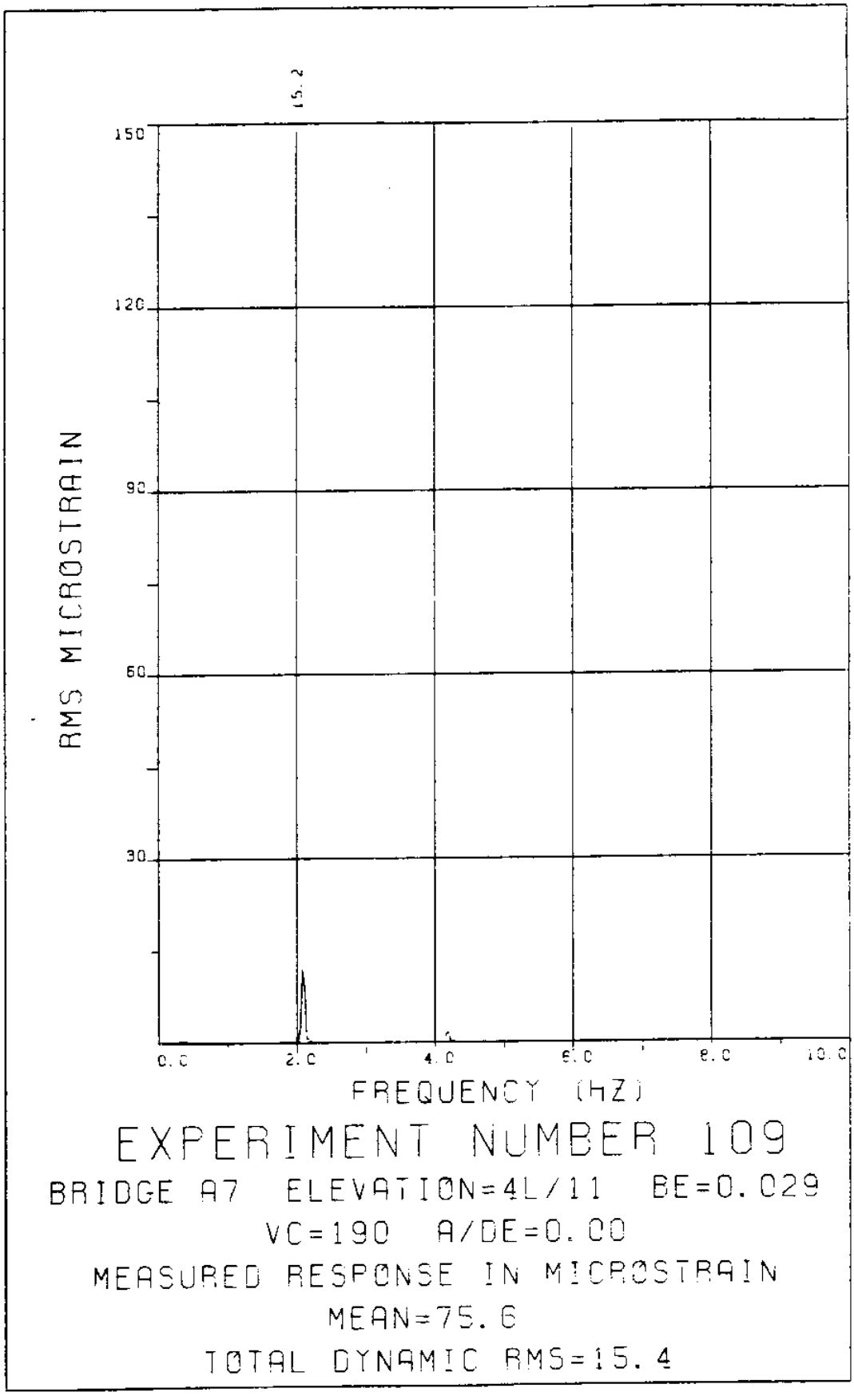
15.2
150
120
90
60
30
RMS MICROSTRAIN
0.0
2.0
4.0
6.0
8.0
10.0
FREQUENCY (HZ)
EXPERIMENT NUMBER 109
BRIDGE A7 ELEVATION=4L/11 BE=0.029
VC=190 A/DE=0.00
MEASURED RESPONSE IN MICROSTRAIN
MEAN=75.6
TOTAL DYNAMIC RMS=15.4

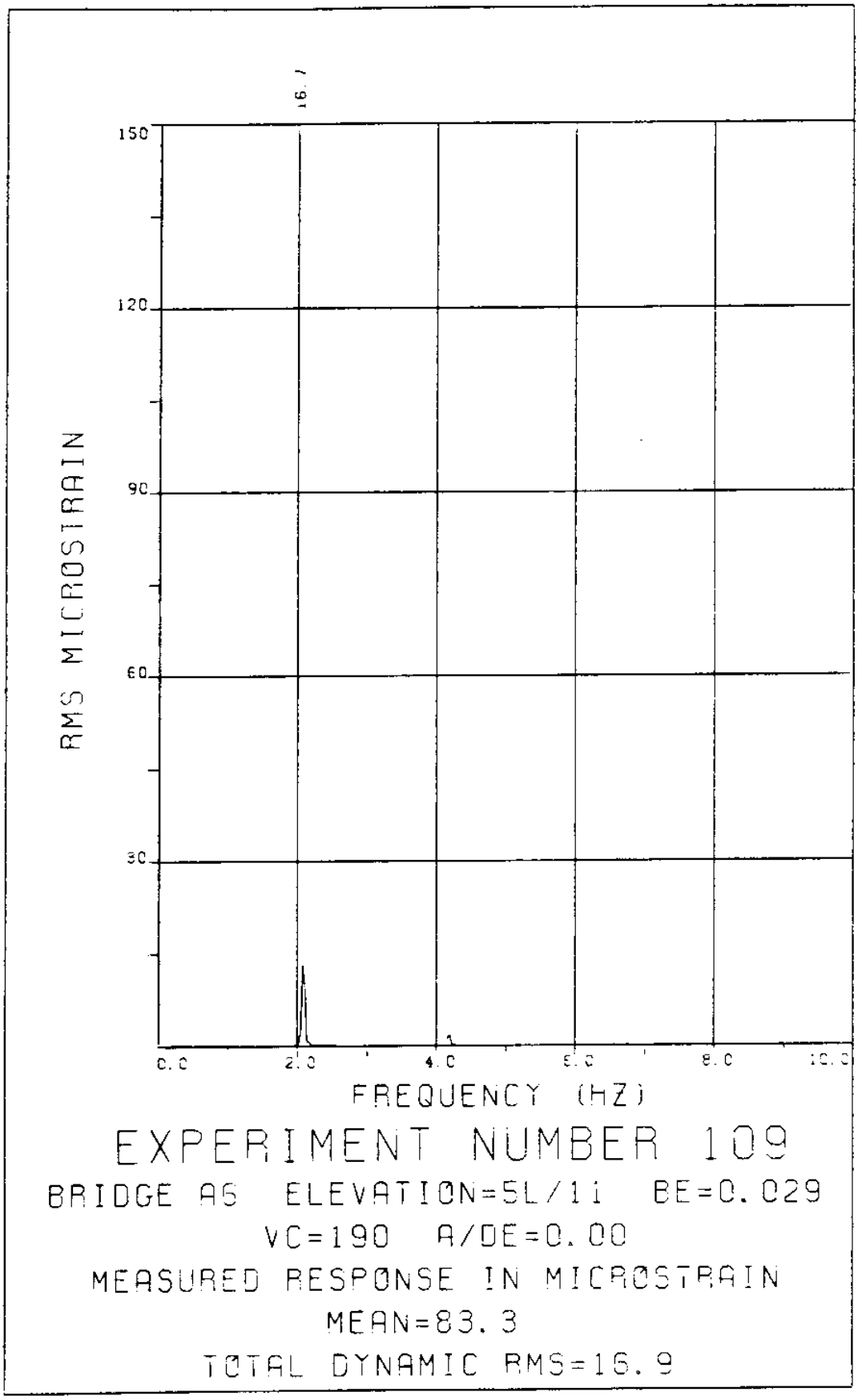
16.7
150
120
90
60
30
RMS MICROSTRAIN
0.0
2.0
4.0
6.0
8.0
10.0
FREQUENCY (HZ)
EXPERIMENT NUMBER 109
BRIDGE A6 ELEVATION=5L/11 BE=0.029
VC=190 A/DE=0.00
MEASURED RESPONSE IN MICROSTRAIN
MEAN=83.3
TOTAL DYNAMIC RMS=16.9

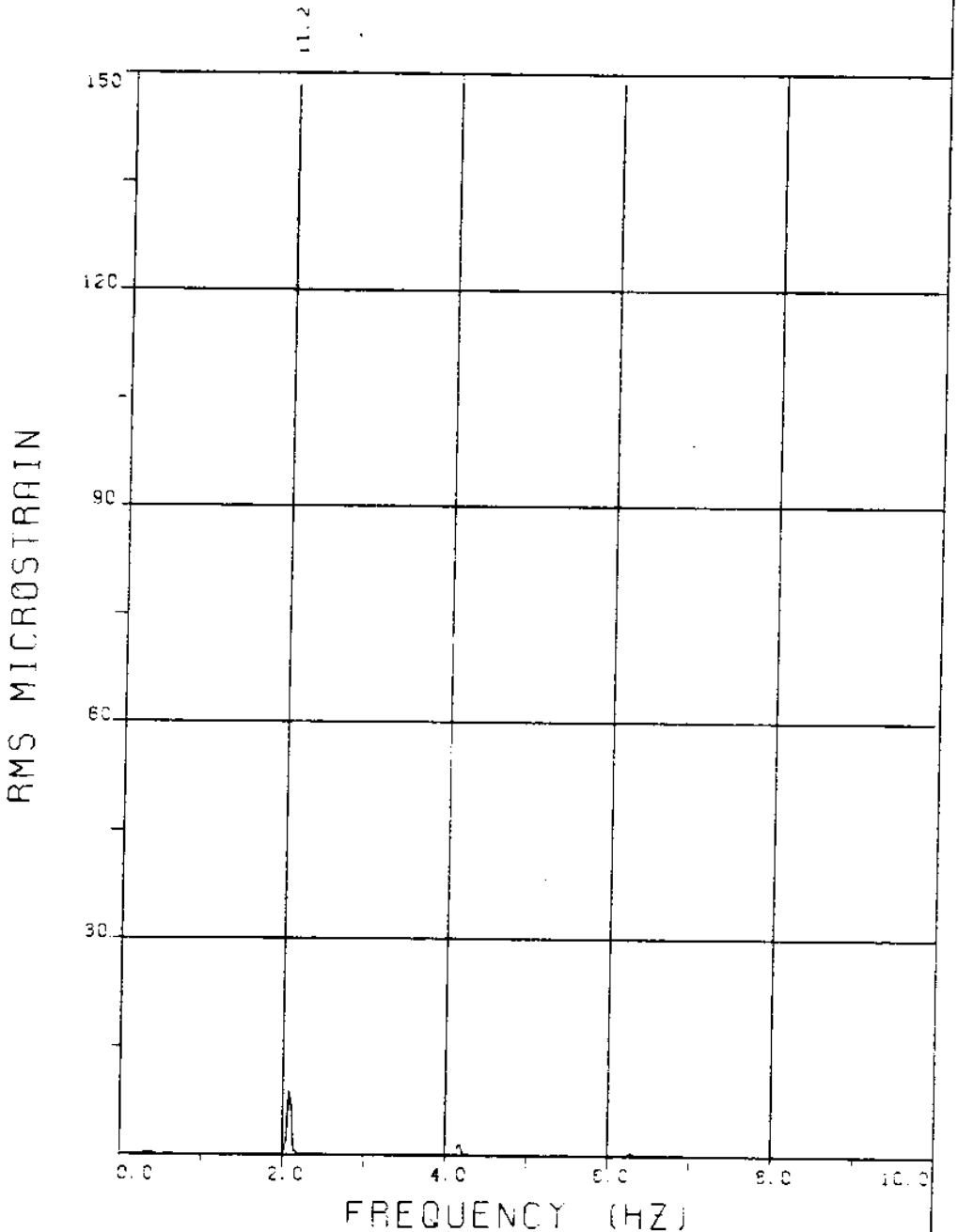

EXPERIMENT NUMBER 109

BRIDGE A3 ELEVATION=8L/11 BE=0.029

VC=190 A/DE=0.00

MEASURED RESPONSE IN MICROSTRAIN

MEAN=61.8

TOTAL DYNAMIC RMS=11.4

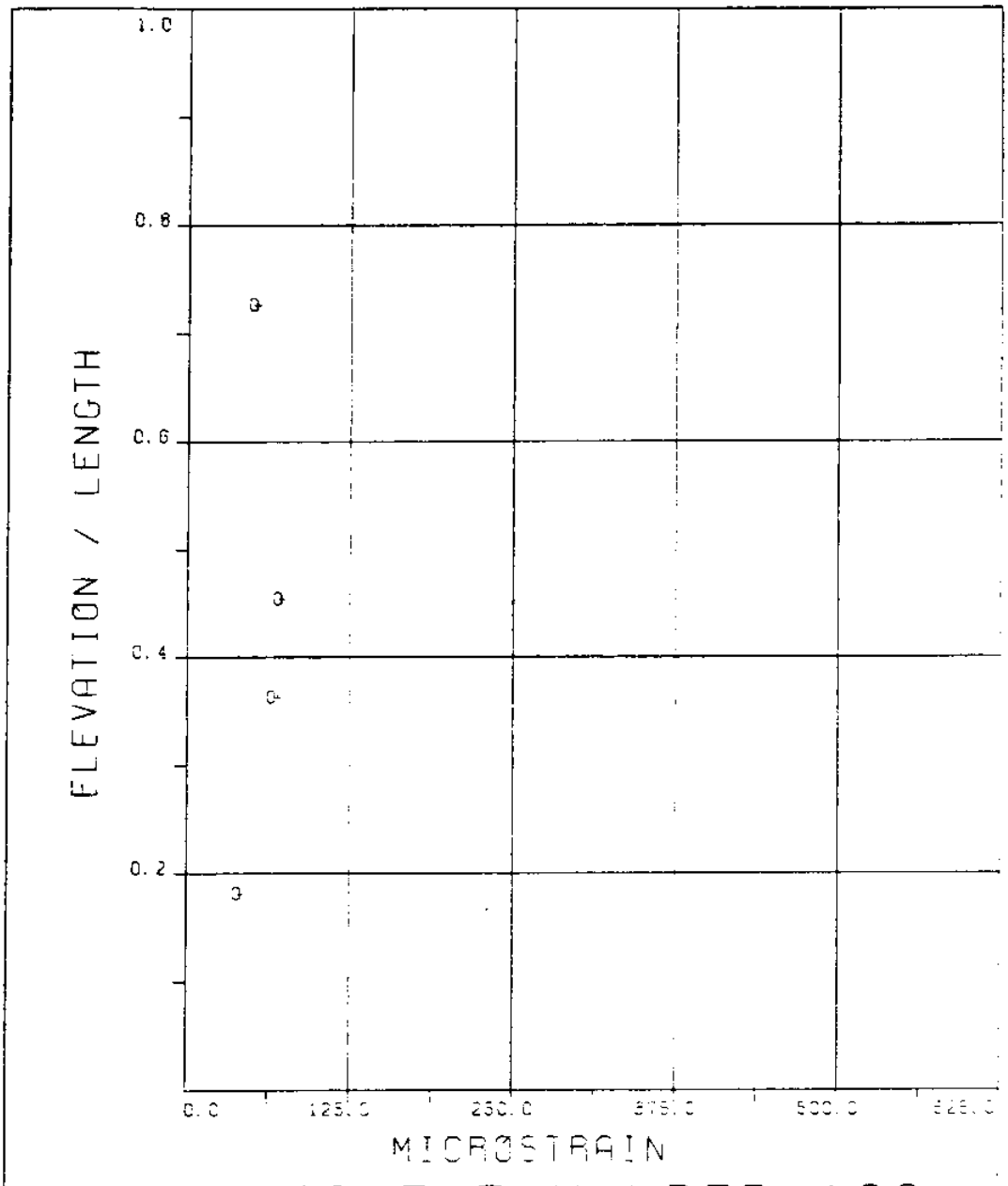

EXPERIMENT NUMBER 109

VC=190 A/DE=0.00

DYNAMIC RESPONSE AT F=FR IN PLANE B

o o o EXPERIMENT

MAXIMUM DYNAMIC RESPONSE IN PLANE B

+ + + EXPERIMENT

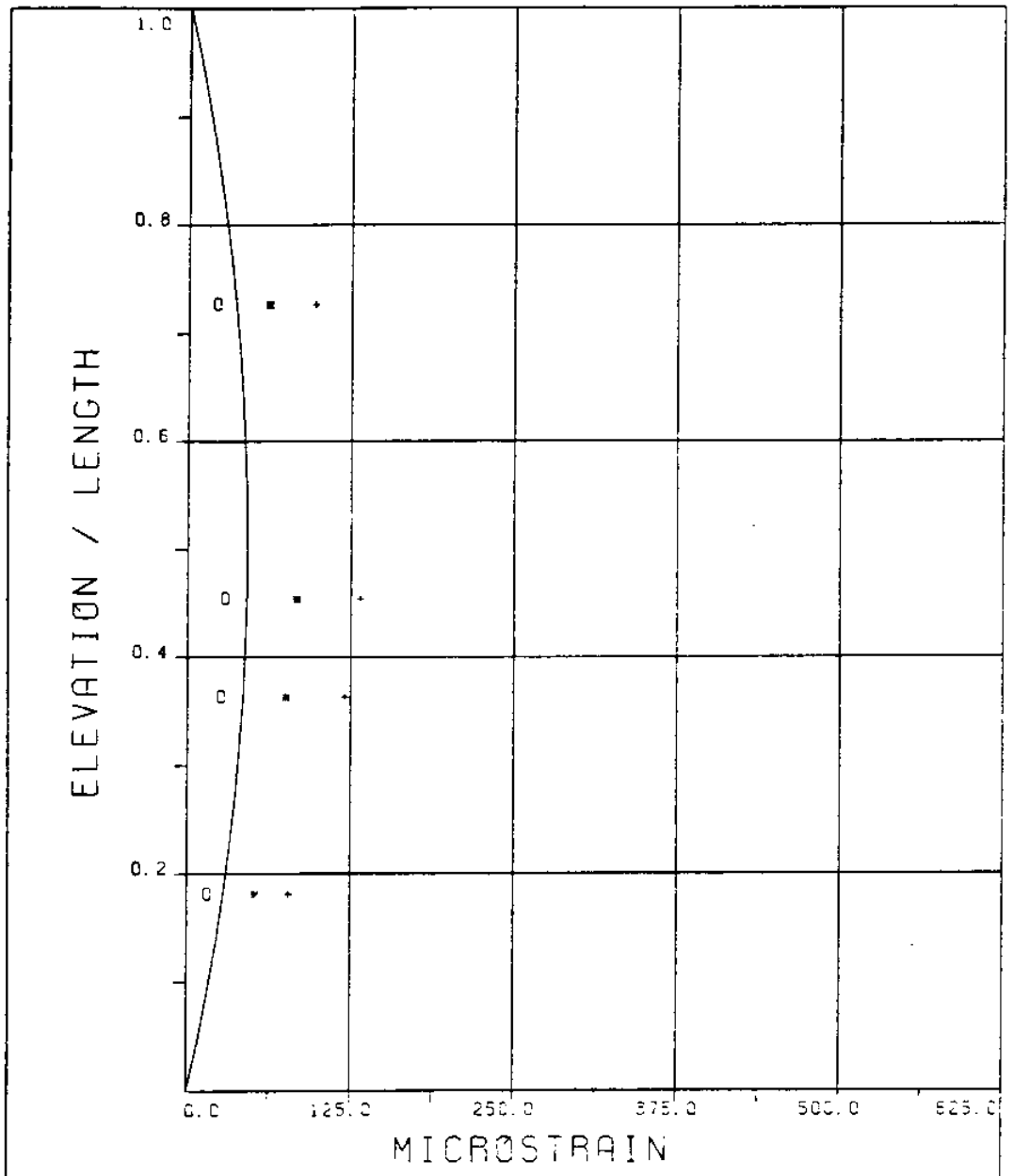

EXPERIMENT NUMBER 109

VC=190 A/DE=0.00

STATIC RESPONSE IN PLANE A

——— THEORY * * * EXPERIMENT

MAXIMUM DYNAMIC RESPONSE IN PLANE A

o o o EXPERIMENT

MAXIMUM RESPONSE

——— THEORY + + + EXPERIMENT

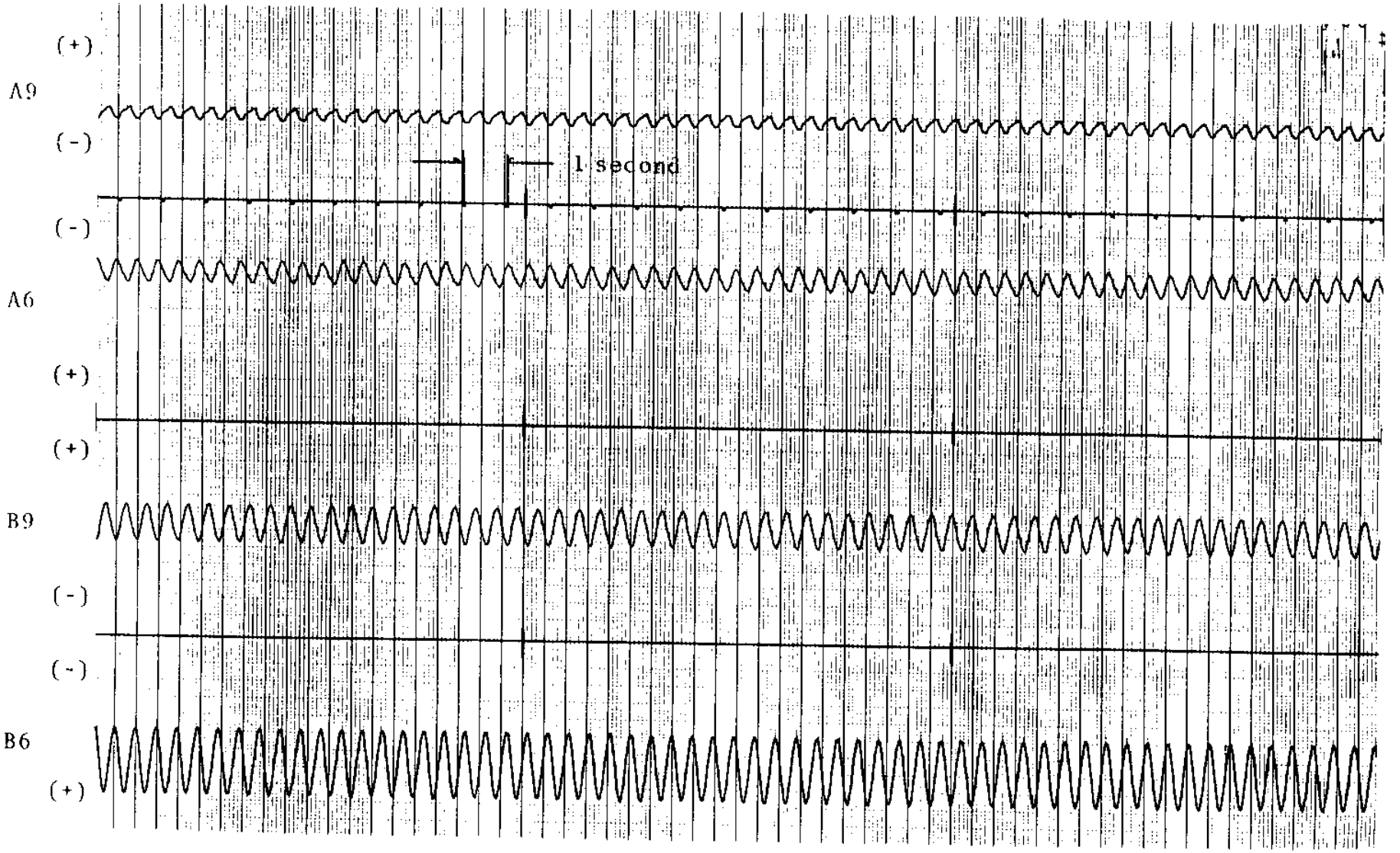

FIGURE 109T: ALL BRIDGES 7.6 MICROSTRAIN/DIVISION

EXPERIMENT 107

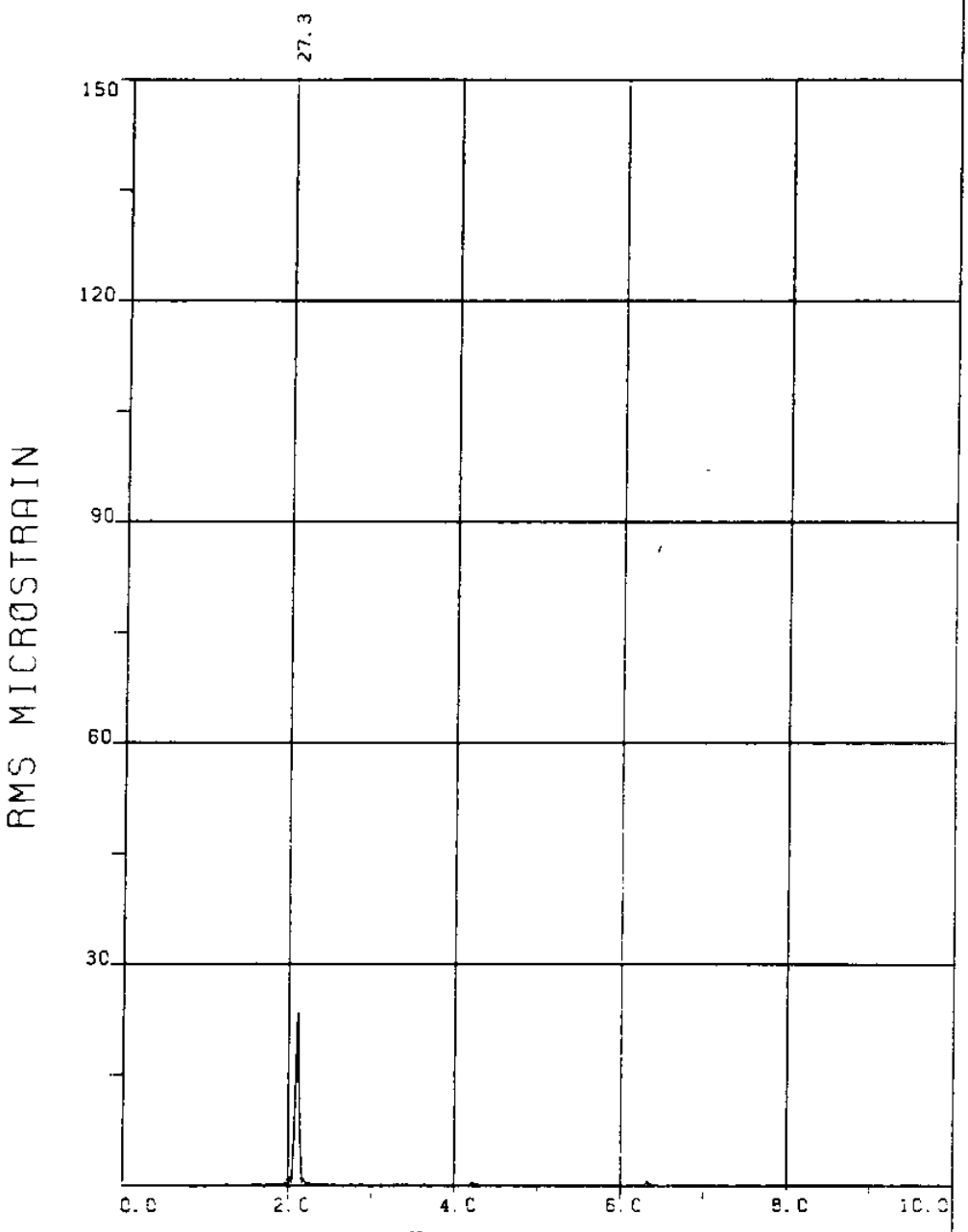

EXPERIMENT NUMBER 107

BRIDGE B9 ELEVATION=2L/11 BE=0.029

VC=210 A/DE=0.00

MEASURED RESPONSE IN MICROSTRAIN

TOTAL DYNAMIC RMS=27.4

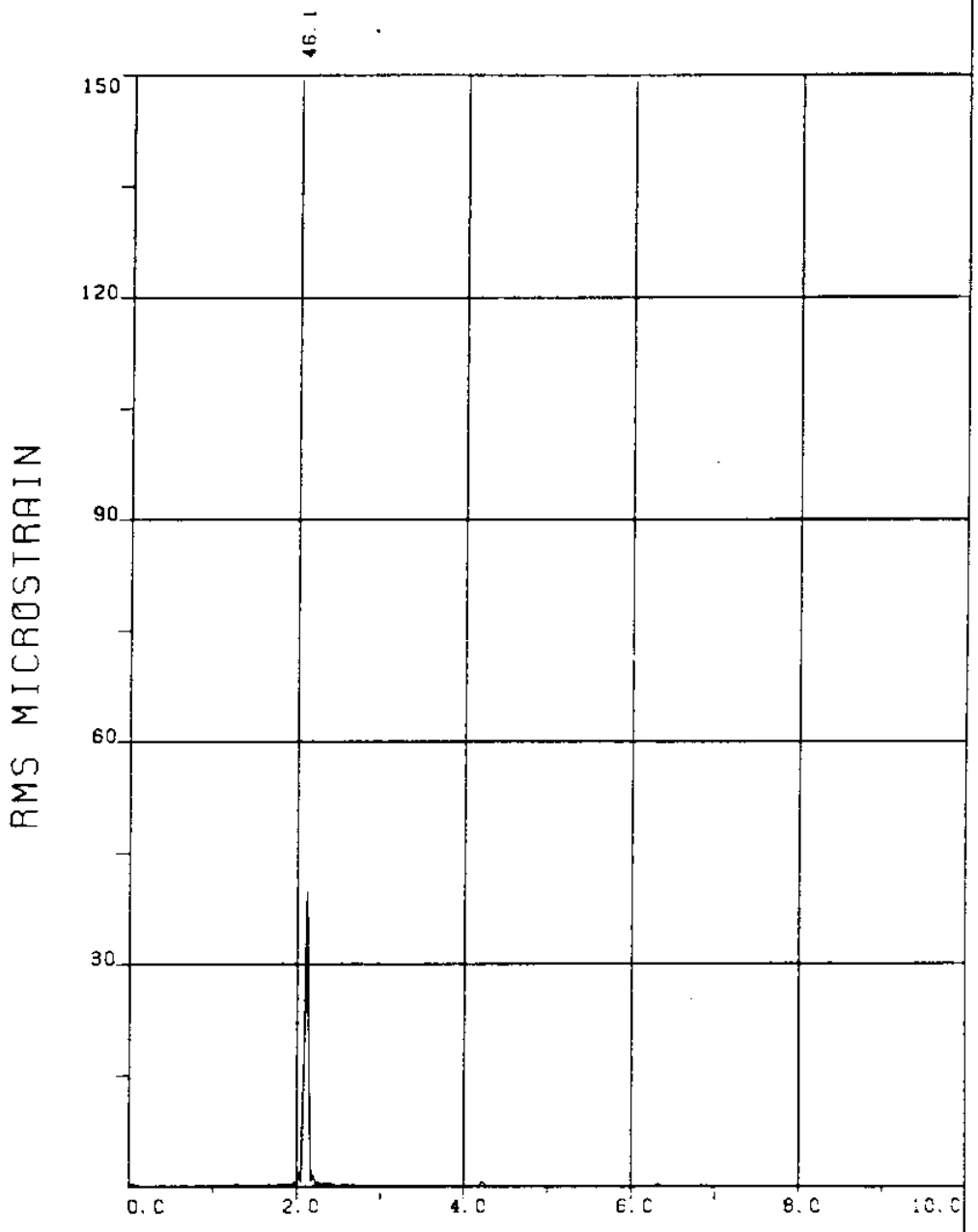

EXPERIMENT NUMBER 107

BRIDGE B7 ELEVATION=4L/11 BE=0.029

VC=210 A/DE=0.00

MEASURED RESPONSE IN MICROSTRAIN

TOTAL DYNAMIC RMS=46.1

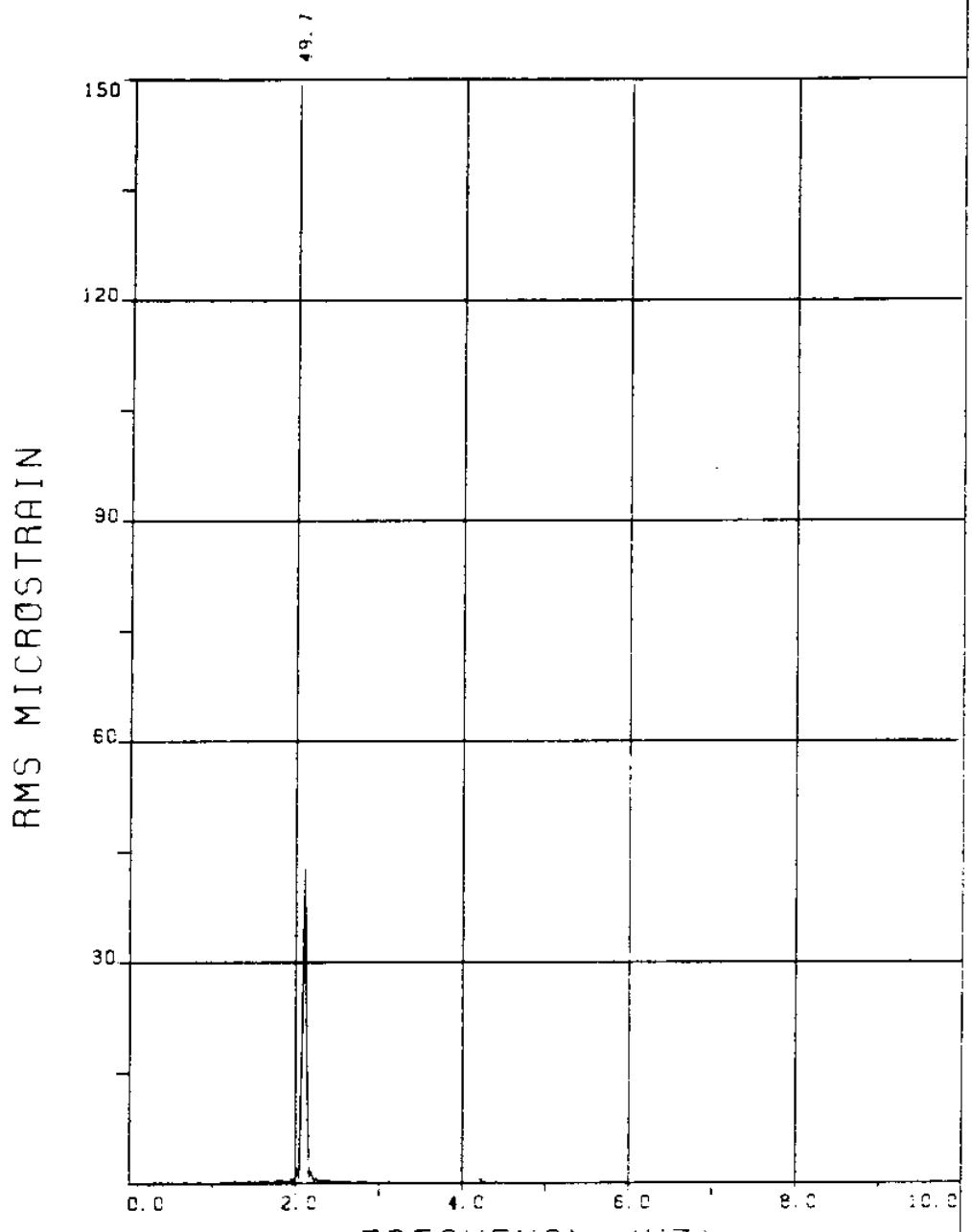

EXPERIMENT NUMBER 107

BRIDGE B6 ELEVATION=5L/11 BE=0.029

VC=210 A/DE=0.00

MEASURED RESPONSE IN MICROSTRAIN

TOTAL DYNAMIC RMS=49.7

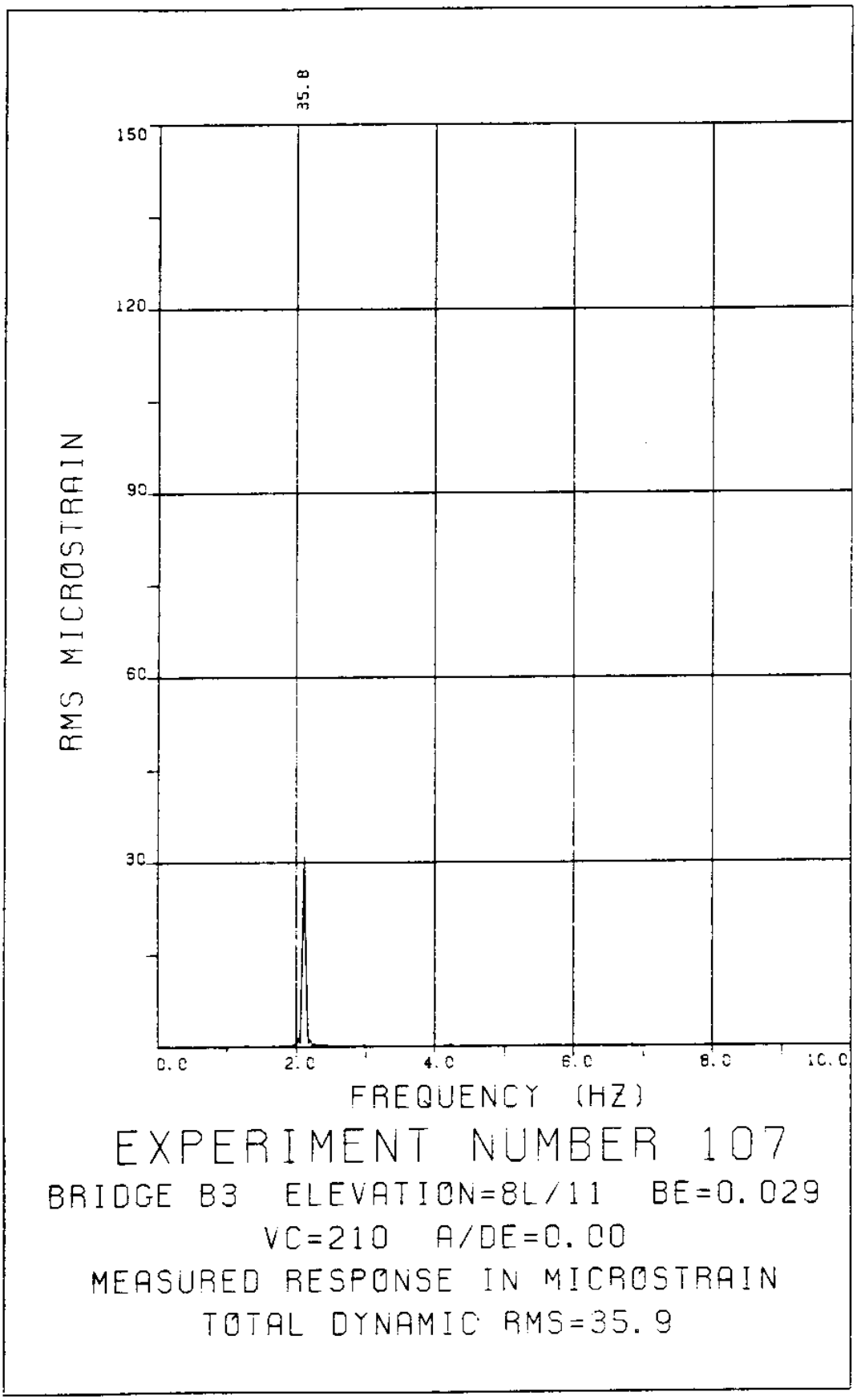
35.8
150
120
90
60
30
RMS MICROSTRAIN
0.0
2.0
4.0
6.0
8.0
10.0
FREQUENCY (HZ)
EXPERIMENT NUMBER 107
BRIDGE B3 ELEVATION=8L/11 BE=0.029
VC=210 A/DE=0.00
MEASURED RESPONSE IN MICROSTRAIN
TOTAL DYNAMIC RMS=35.9

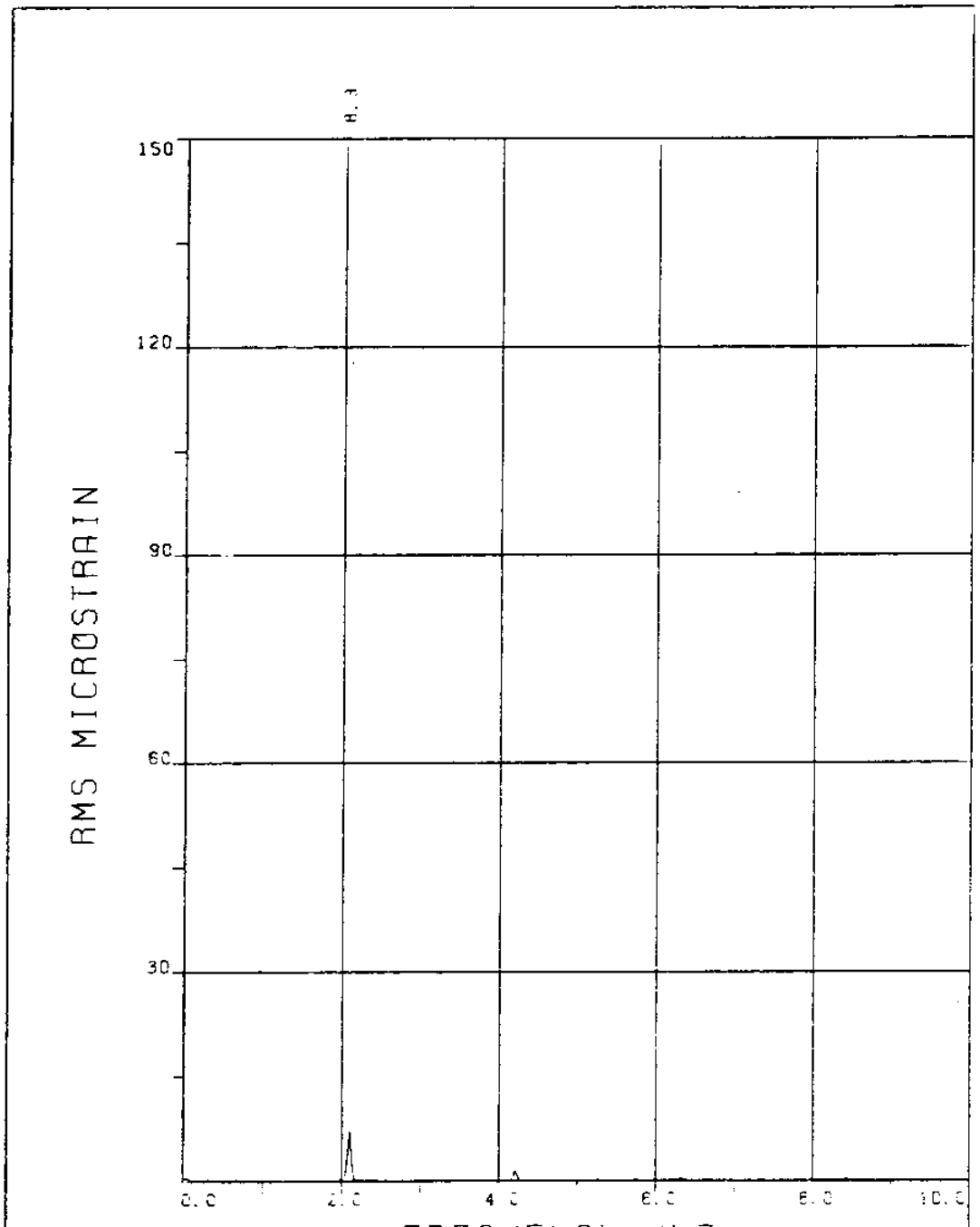

EXPERIMENT NUMBER 107

BRIDGE A9 ELEVATION=2L/11 BE=0.029

VC=210 A/DE=0.00

MEASURED RESPONSE IN MICROSTRAIN

MEAN=57.3

TOTAL DYNAMIC RMS=8.6

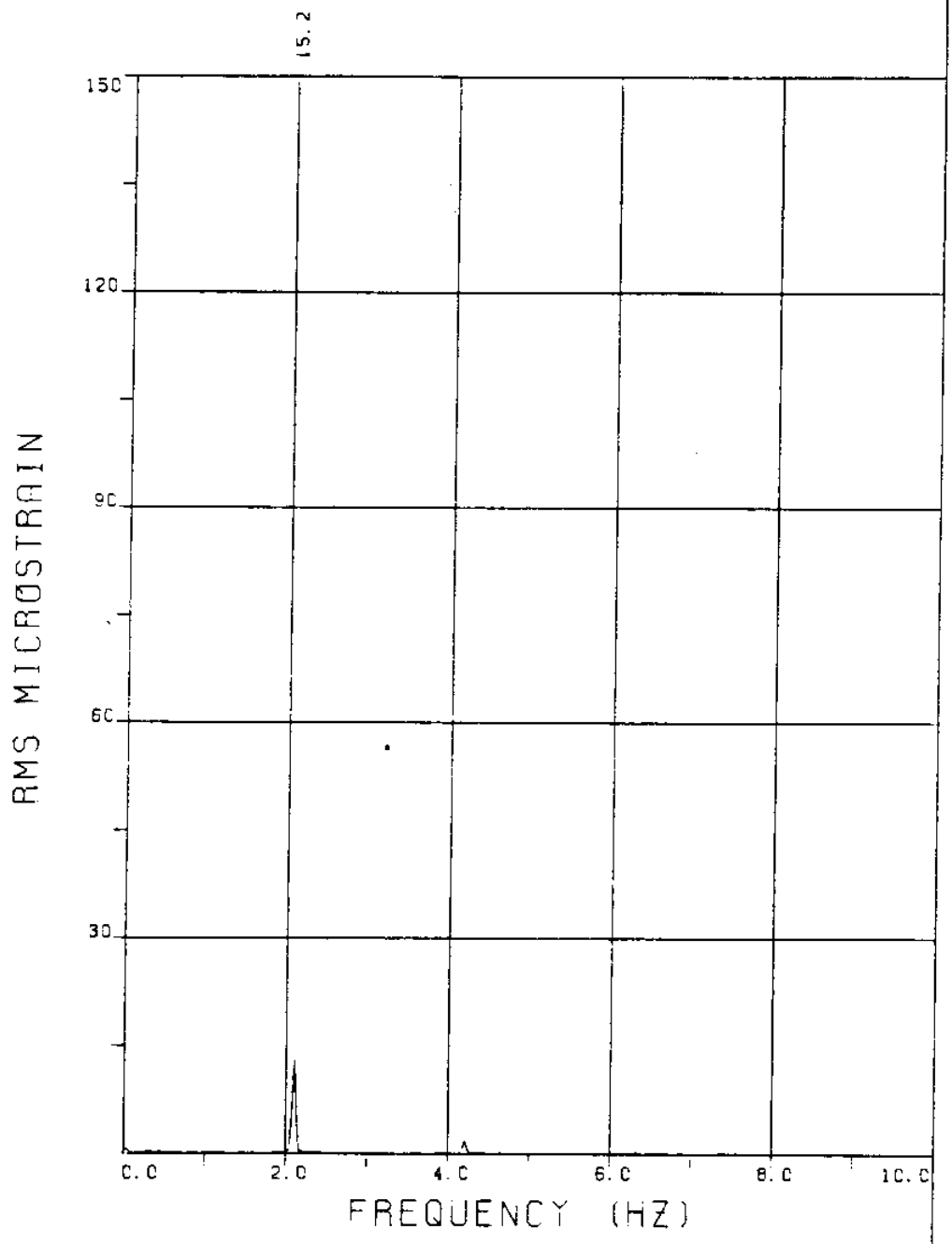

EXPERIMENT NUMBER 107

BRIDGE A7 ELEVATION=4L/11 BE=0.029

VC=210 A/DE=0.00

MEASURED RESPONSE IN MICROSTRAIN

MEAN=83.0

TOTAL DYNAMIC RMS=15.4

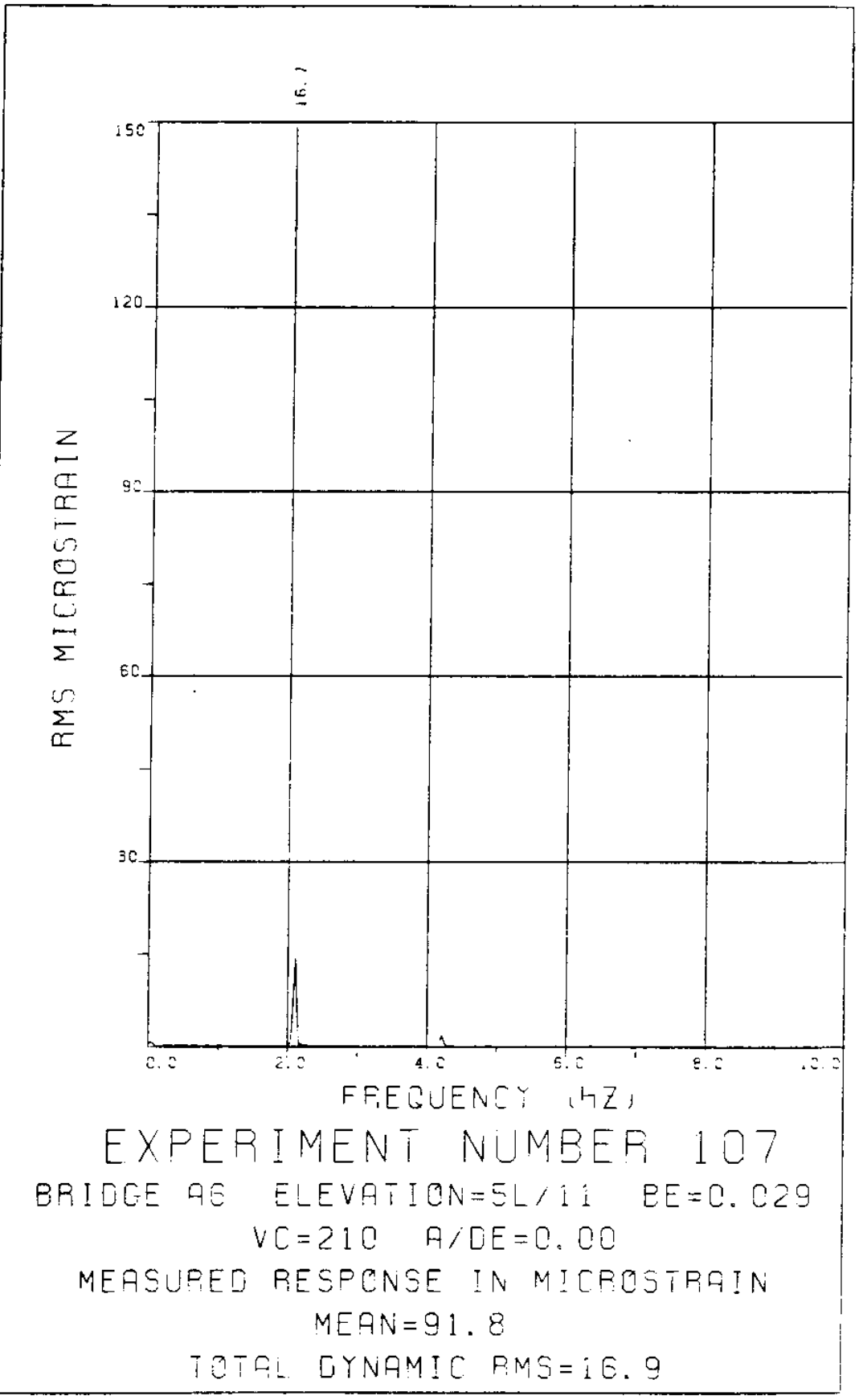
16.7
150
120
90
60
30
RMS MICROSTRAIN
0.0
2.0
4.0
6.0
8.0
10.0
FREQUENCY (HZ)
EXPERIMENT NUMBER 107
BRIDGE 96 ELEVATION=SL/11 BE=0.029
VC=210 A/DE=0.00
MEASURED RESPONSE IN MICROSTRAIN
MEAN=91.8
TOTAL DYNAMIC RMS=16.9

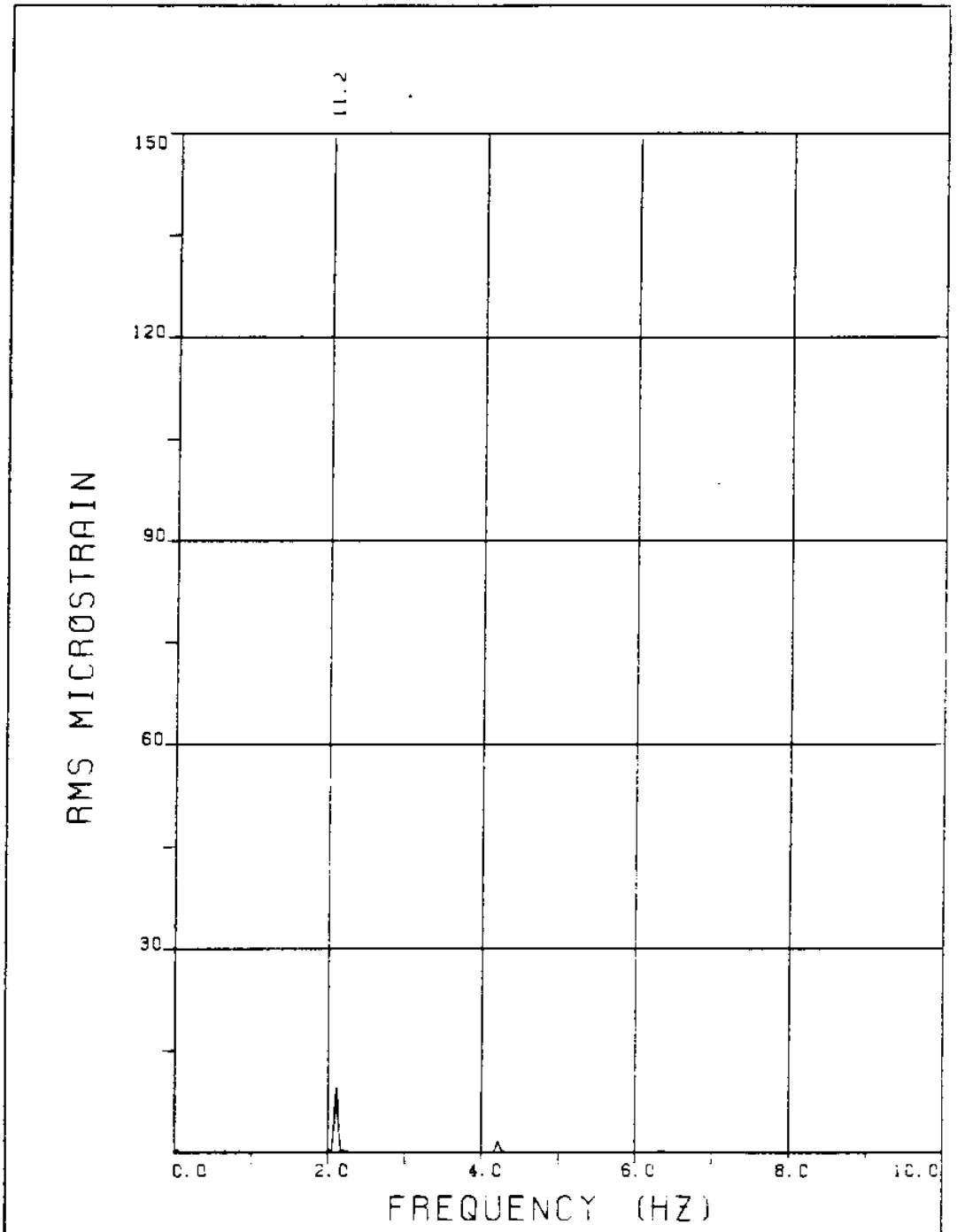

EXPERIMENT NUMBER 107

BRIDGE A3 ELEVATION=8L/11 BE=0.029

VC=210 A/DE=0.00

MEASURED RESPONSE IN MICROSTRAIN

MEAN=67.2

TOTAL DYNAMIC RMS=11.4

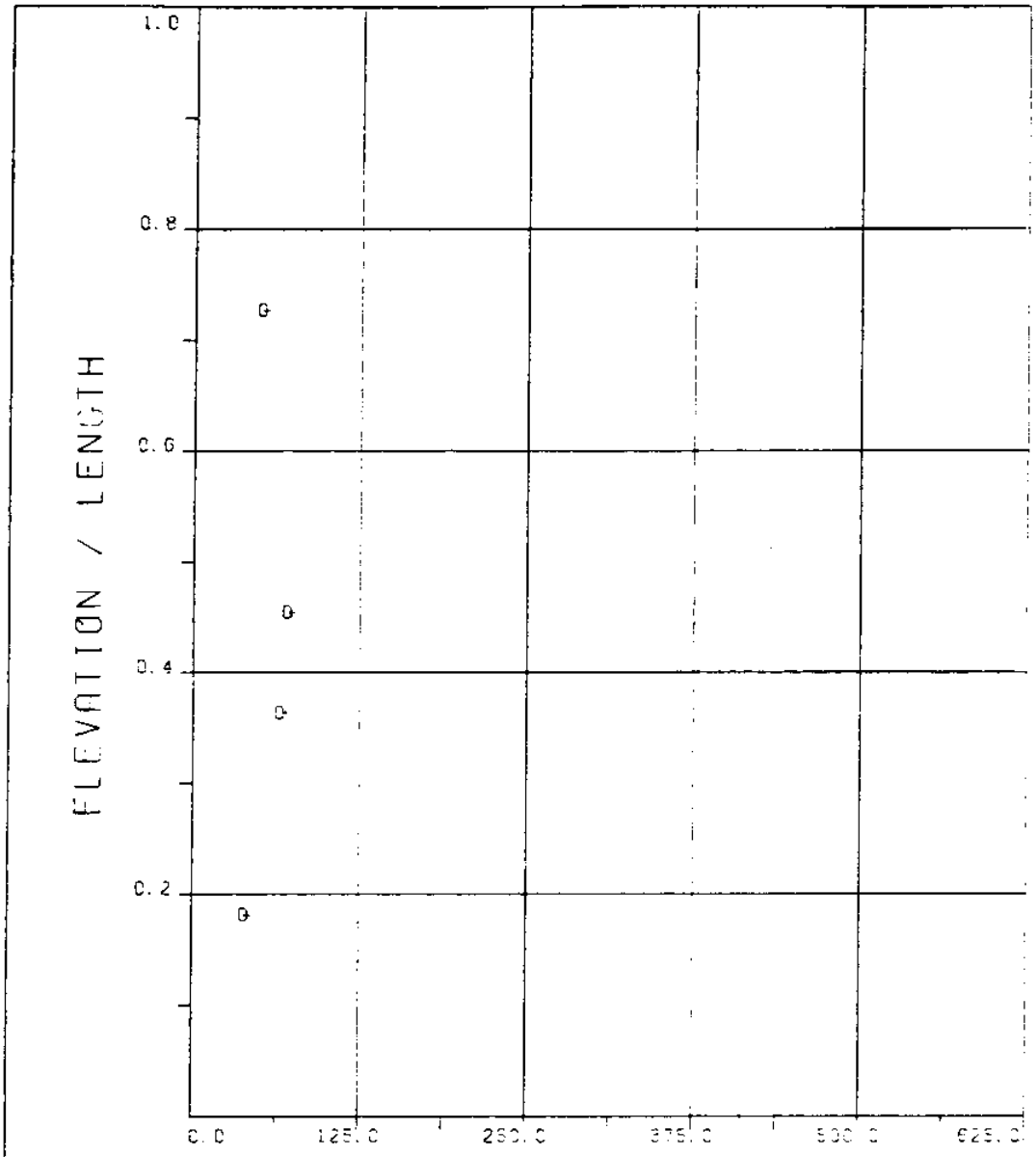

EXPERIMENT NUMBER 107

VC=210 A/DE=0.00

DYNAMIC RESPONSE AT F=FR IN PLANE B

o o o EXPERIMENT

MAXIMUM DYNAMIC RESPONSE IN PLANE B

+ + + EXPERIMENT

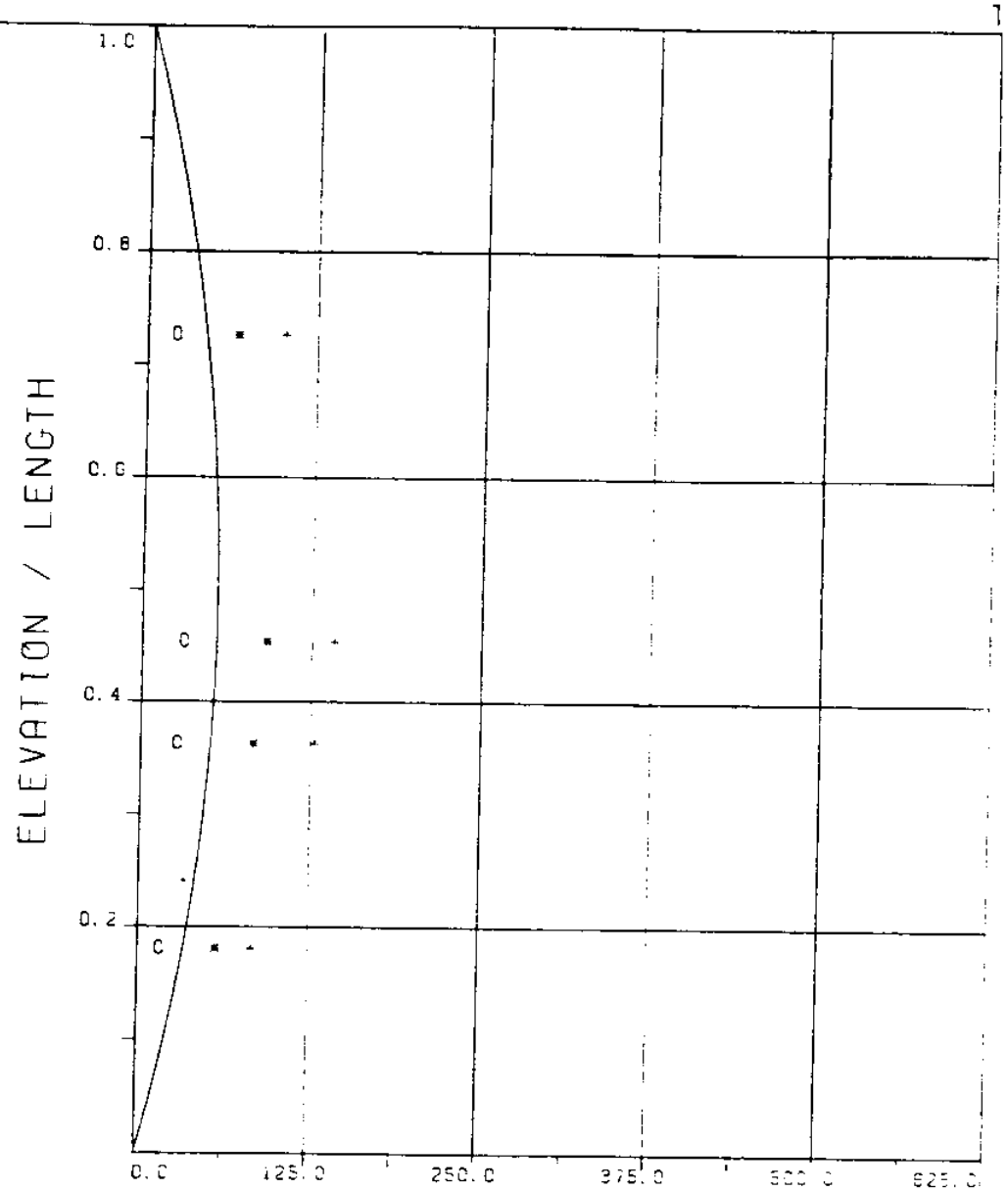

EXPERIMENT NUMBER 107

VC=210 A/DE=0.00

STATIC RESPONSE IN PLANE A

——— THEORY * * * EXPERIMENT

MAXIMUM DYNAMIC RESPONSE IN PLANE A

o o o EXPERIMENT

MAXIMUM RESPONSE

——— THEORY + + + EXPERIMENT

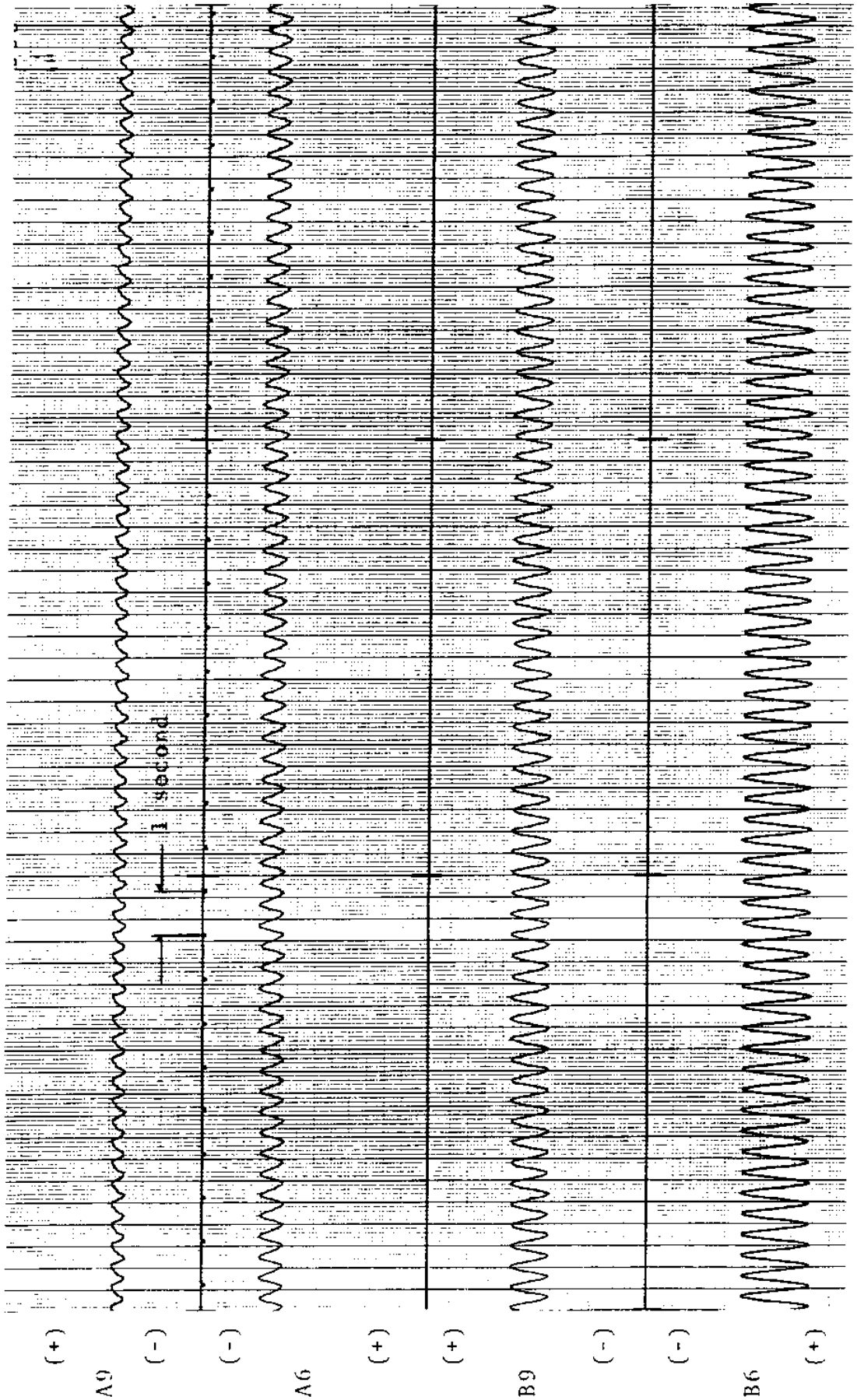

FIGURE 107T: ALL BRIDGES: 7.6 MICROSTRAIN/DIVISION

EXPERIMENT 105

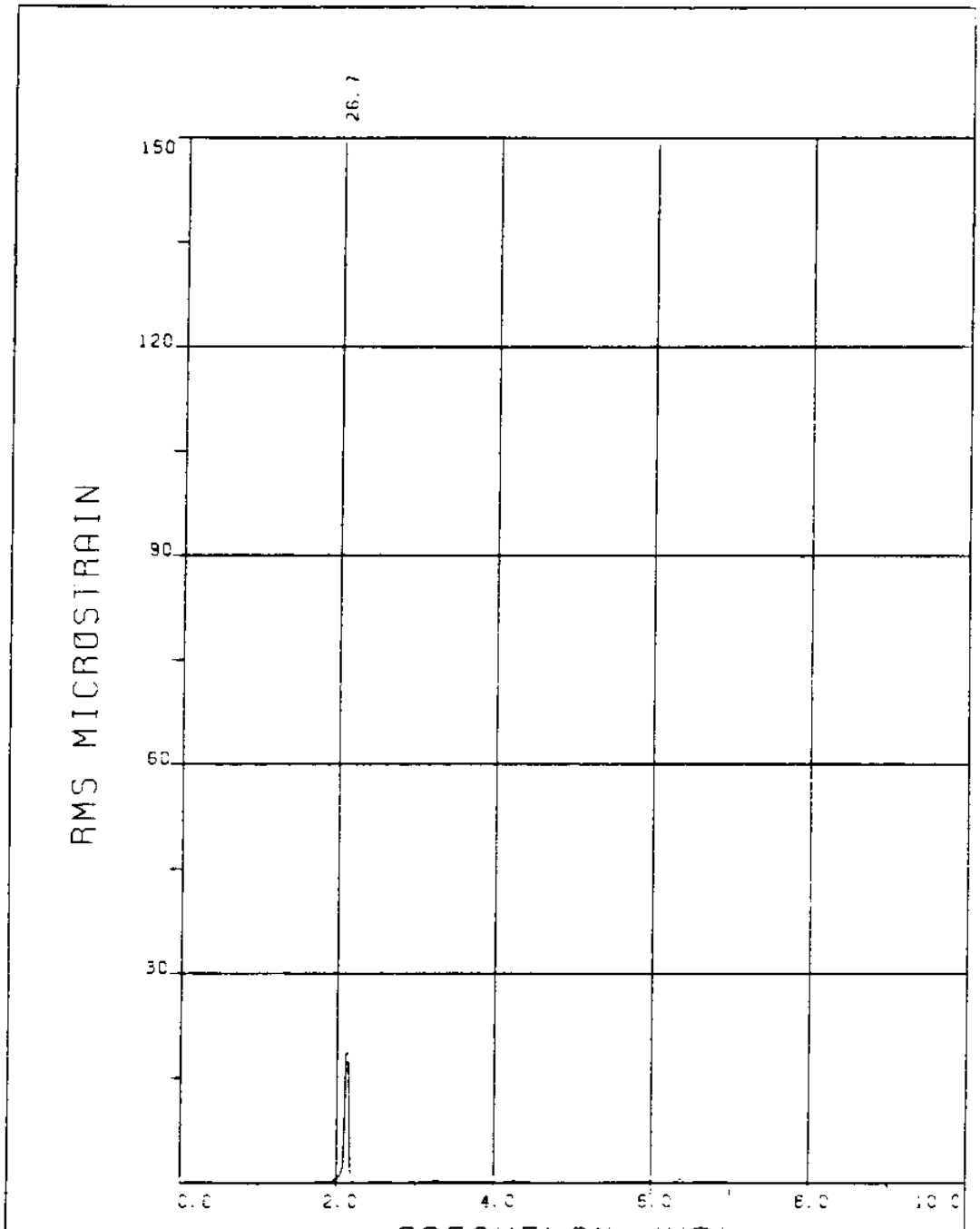

EXPERIMENT NUMBER 105

BRIDGE B9 ELEVATION=2L/11 BE=0.029

VC=220 A/DE=0.00

MEASURED RESPONSE IN MICROSTRAIN

TOTAL DYNAMIC RMS=26.7

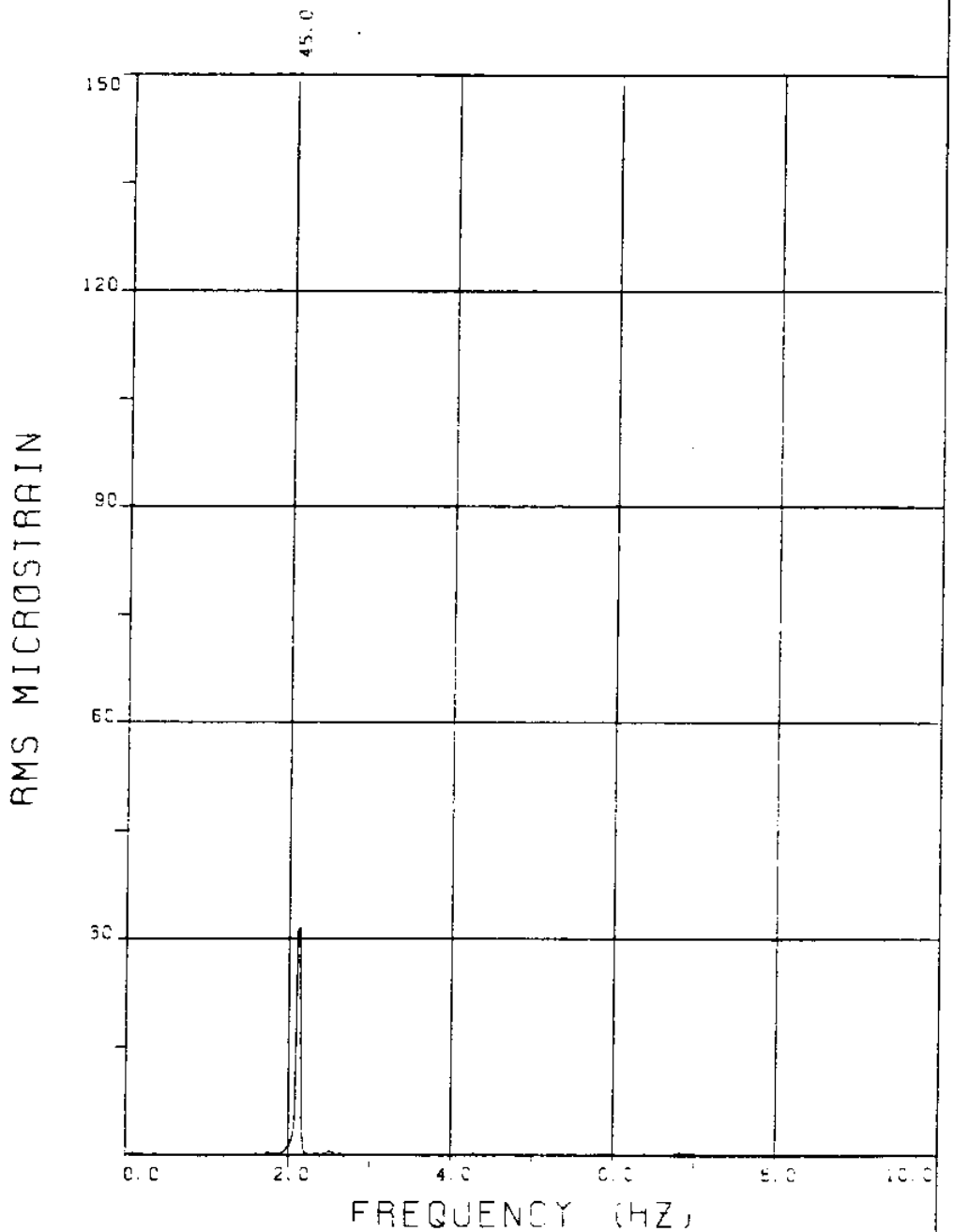

EXPERIMENT NUMBER 105

BRIDGE B7 ELEVATION=41/11 BE=0.029

VC=220 A/DE=0.00

MEASURED RESPONSE IN MICROSTRAIN

TOTAL DYNAMIC RMS=45.1

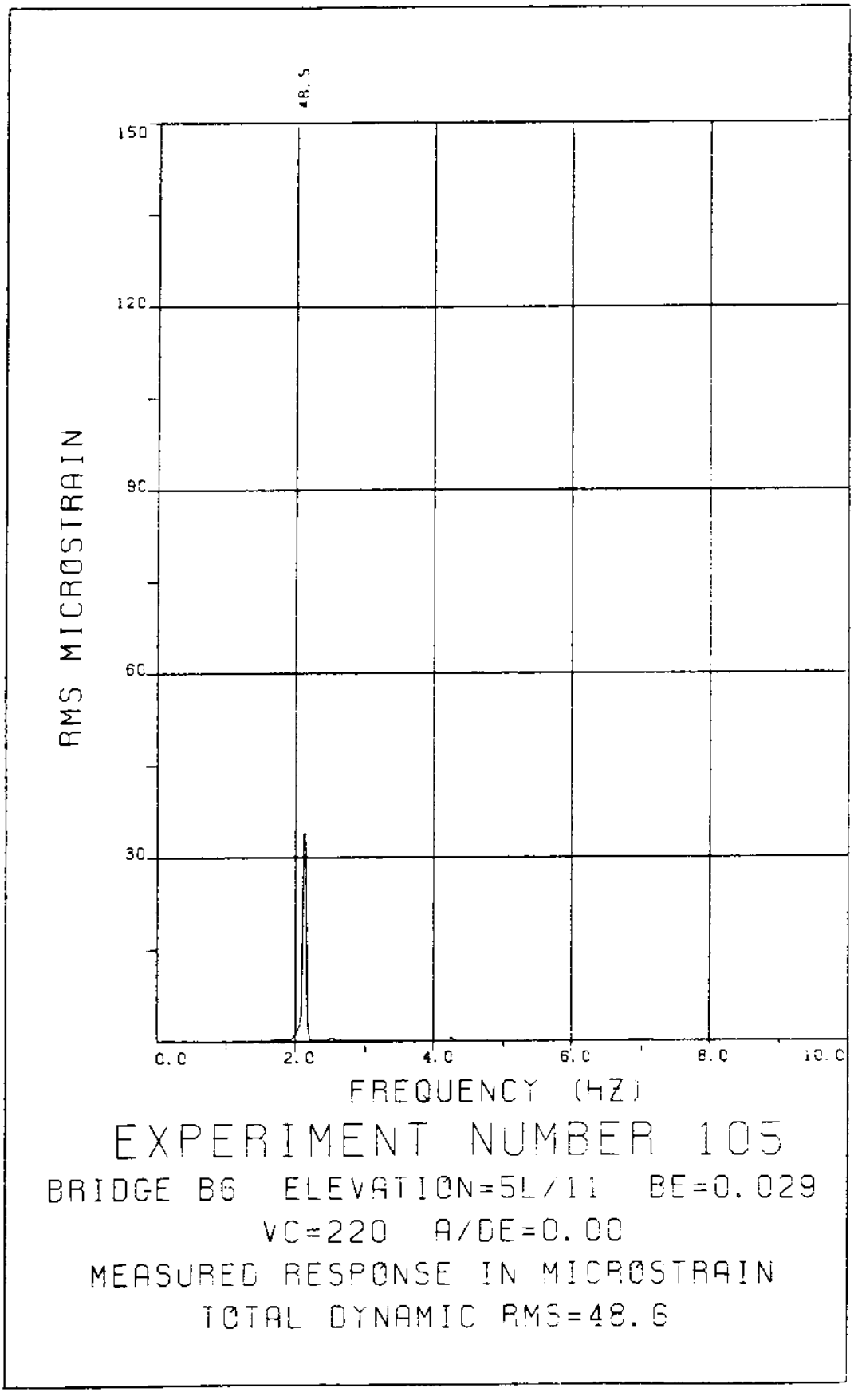
48.5
150
120
90
60
30
RMS MICROSTRAIN
0.0
2.0
4.0
6.0
8.0
10.0
FREQUENCY (HZ)
EXPERIMENT NUMBER 105
BRIDGE B6 ELEVATION=5L/11 BE=0.029
VC=220 A/DE=0.00
MEASURED RESPONSE IN MICROSTRAIN
TOTAL DYNAMIC RMS=48.6

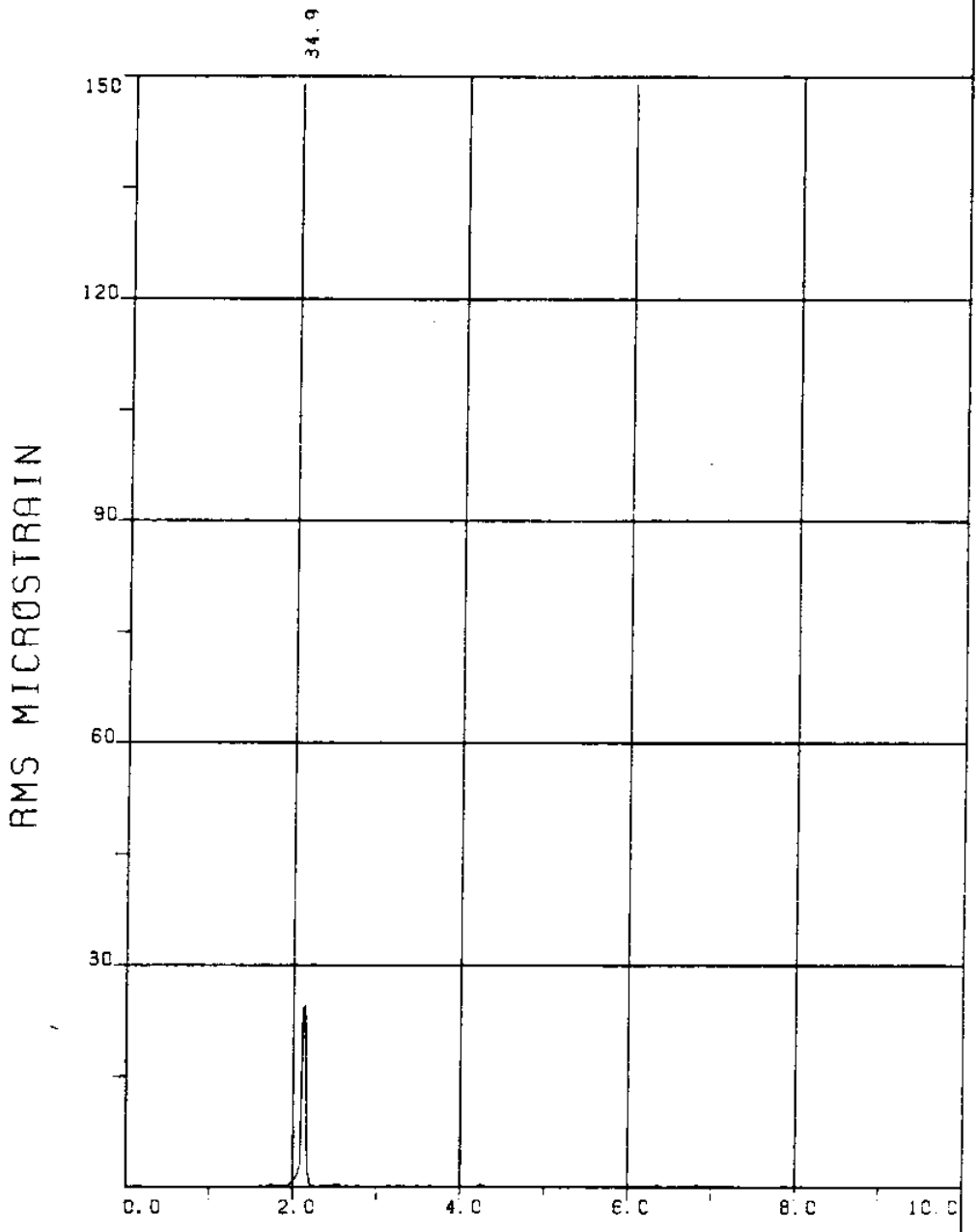

EXPERIMENT NUMBER 105

BRIDGE B3 ELEVATION=8L/11 BE=0.029

VC=220 A/DE=0.00

MEASURED RESPONSE IN MICROSTRAIN

TOTAL DYNAMIC RMS=34.9

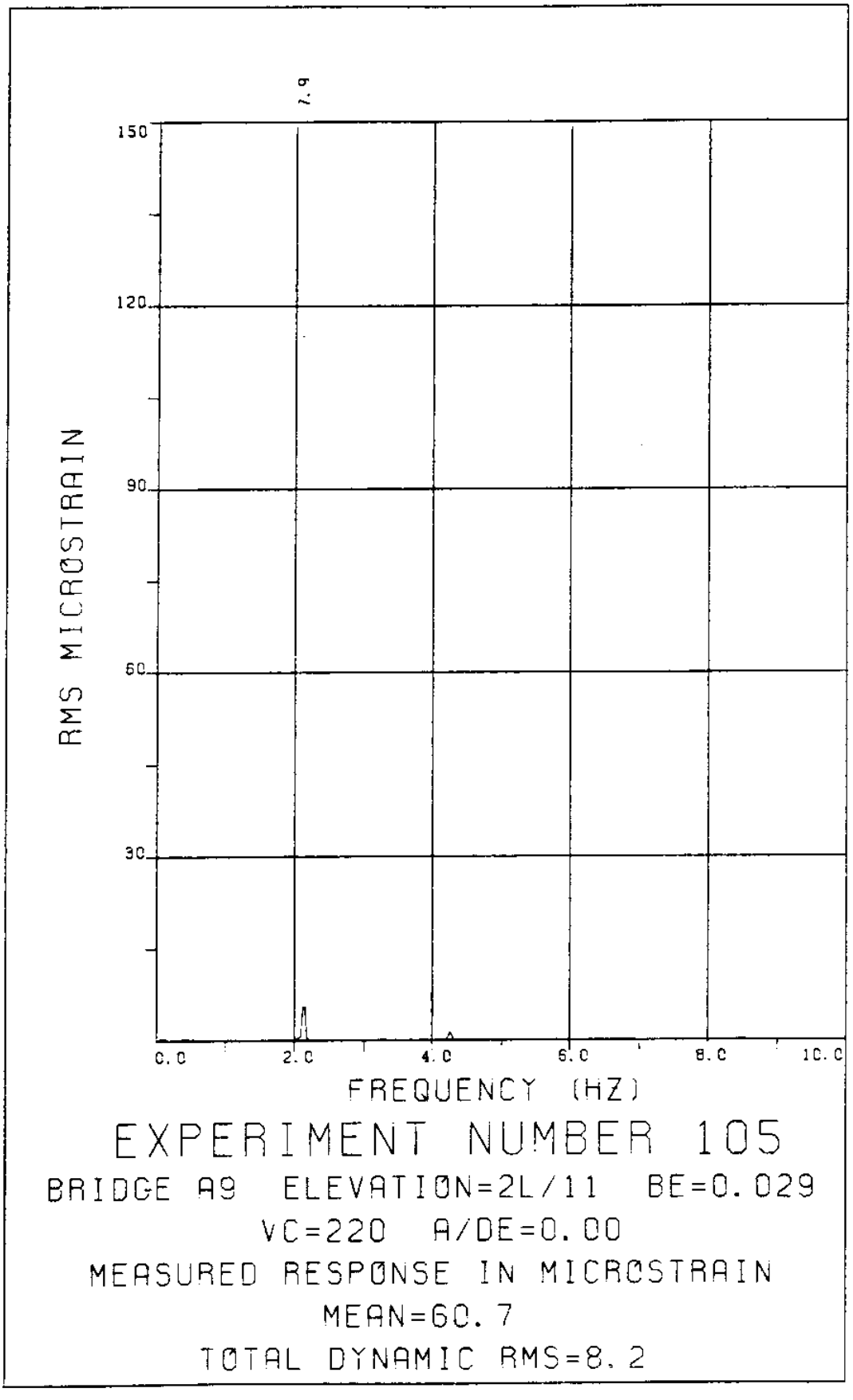

EXPERIMENT NUMBER 105

BRIDGE A9 ELEVATION=2L/11 BE=0.029

VC=220 A/DE=0.00

MEASURED RESPONSE IN MICROSTRAIN

MEAN=60.7

TOTAL DYNAMIC RMS=8.2

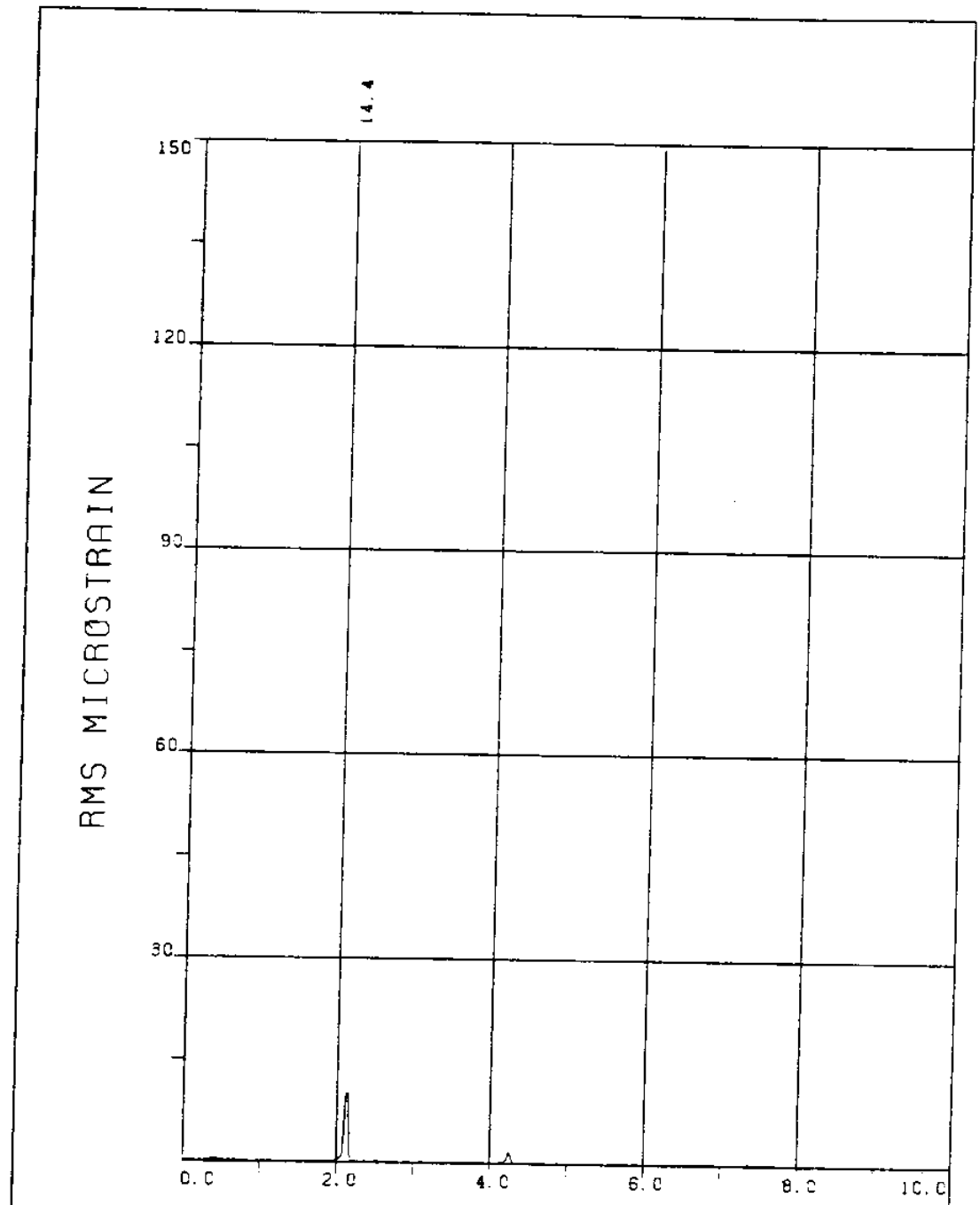

EXPERIMENT NUMBER 105

BRIDGE A7 ELEVATION=4L/11 BE=0.029

VC=220 A/DE=0.00

MEASURED RESPONSE IN MICROSTRAIN

MEAN=87.6

TOTAL DYNAMIC RMS=14.6

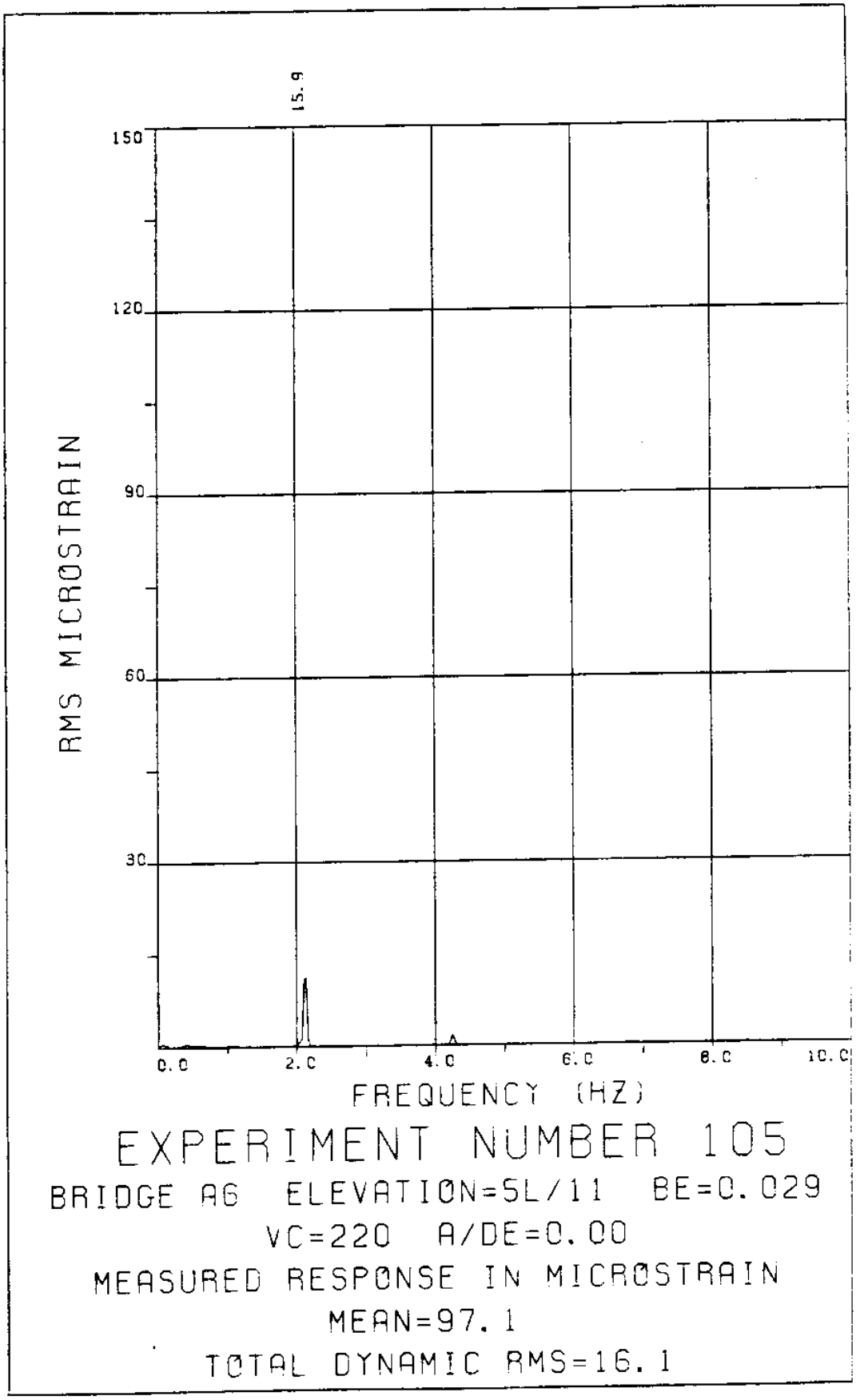

EXPERIMENT NUMBER 105

BRIDGE A6 ELEVATION=SL/11 BE=0.029

VC=220 A/DE=0.00

MEASURED RESPONSE IN MICROSTRAIN

MEAN=97.1

TOTAL DYNAMIC RMS=16.1

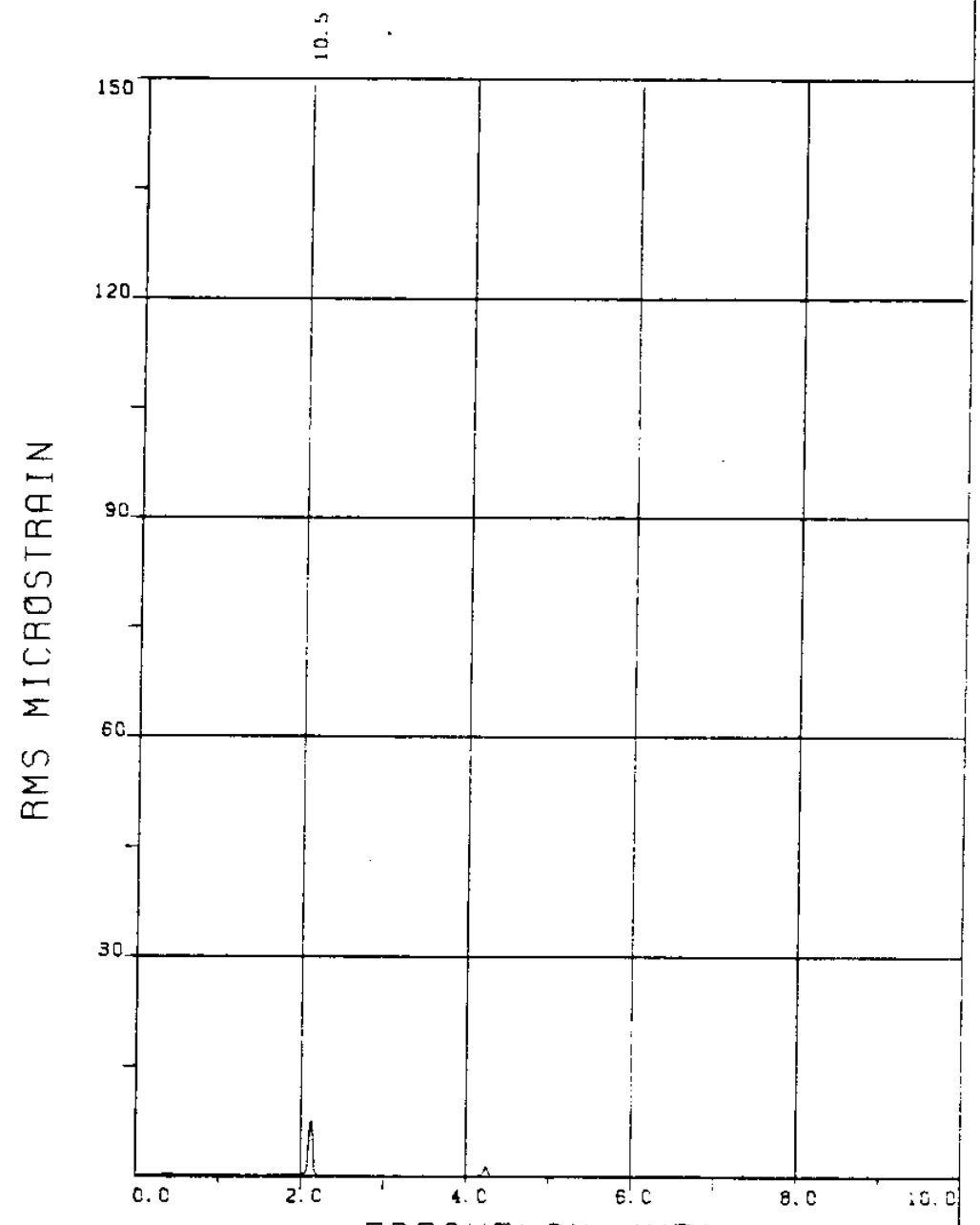

EXPERIMENT NUMBER 105

BRIDGE A3 ELEVATION=8L/11 BE=0.029

VC=220 A/DE=0.00

MEASURED RESPONSE IN MICROSTRAIN

MEAN=71.2

TOTAL DYNAMIC RMS=10.7

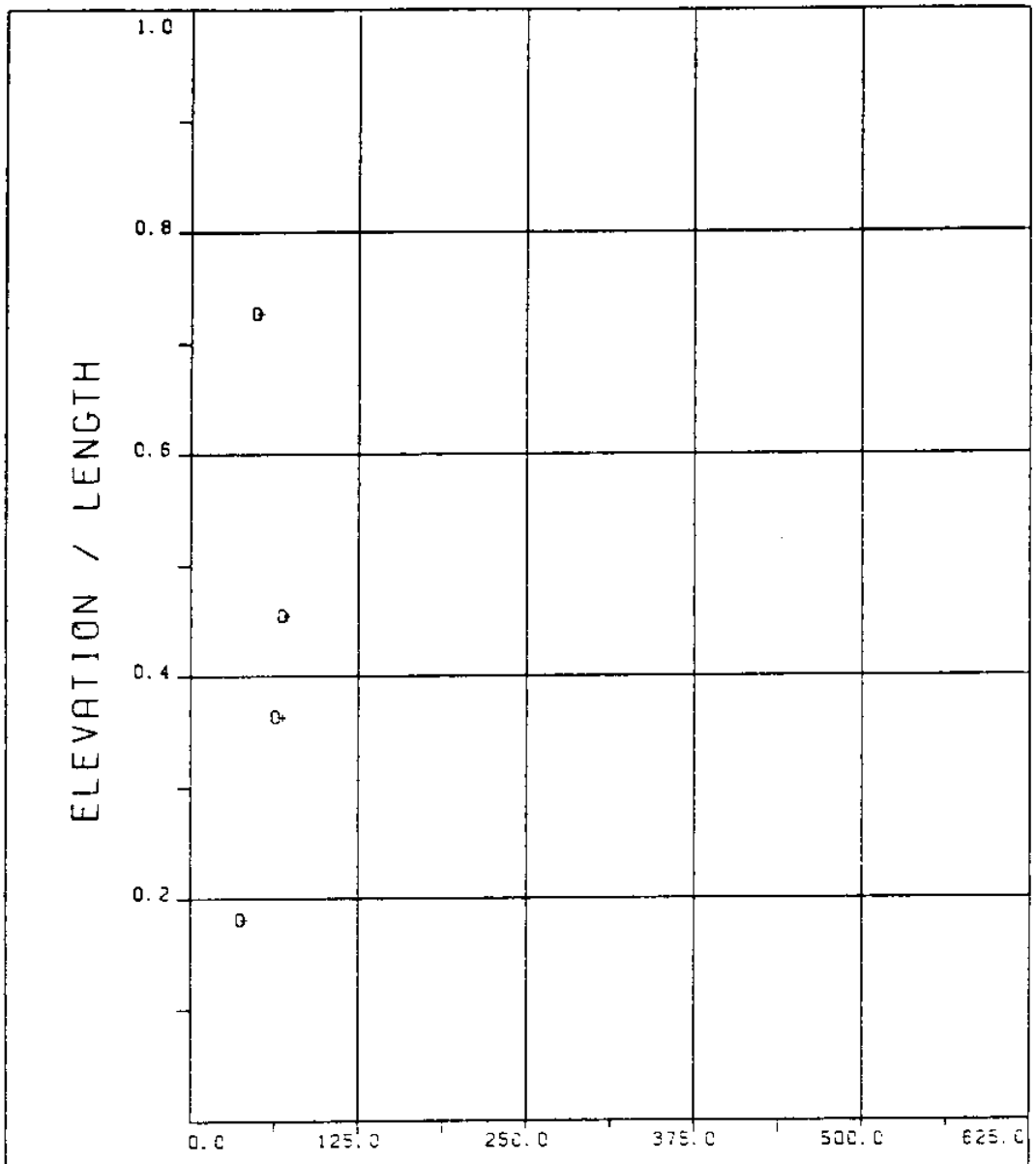

EXPERIMENT NUMBER 105

VC=220 A/DE=0.00

DYNAMIC RESPONSE AT F=FR IN PLANE B

o o o EXPERIMENT

MAXIMUM DYNAMIC RESPONSE IN PLANE B

+ + + EXPERIMENT

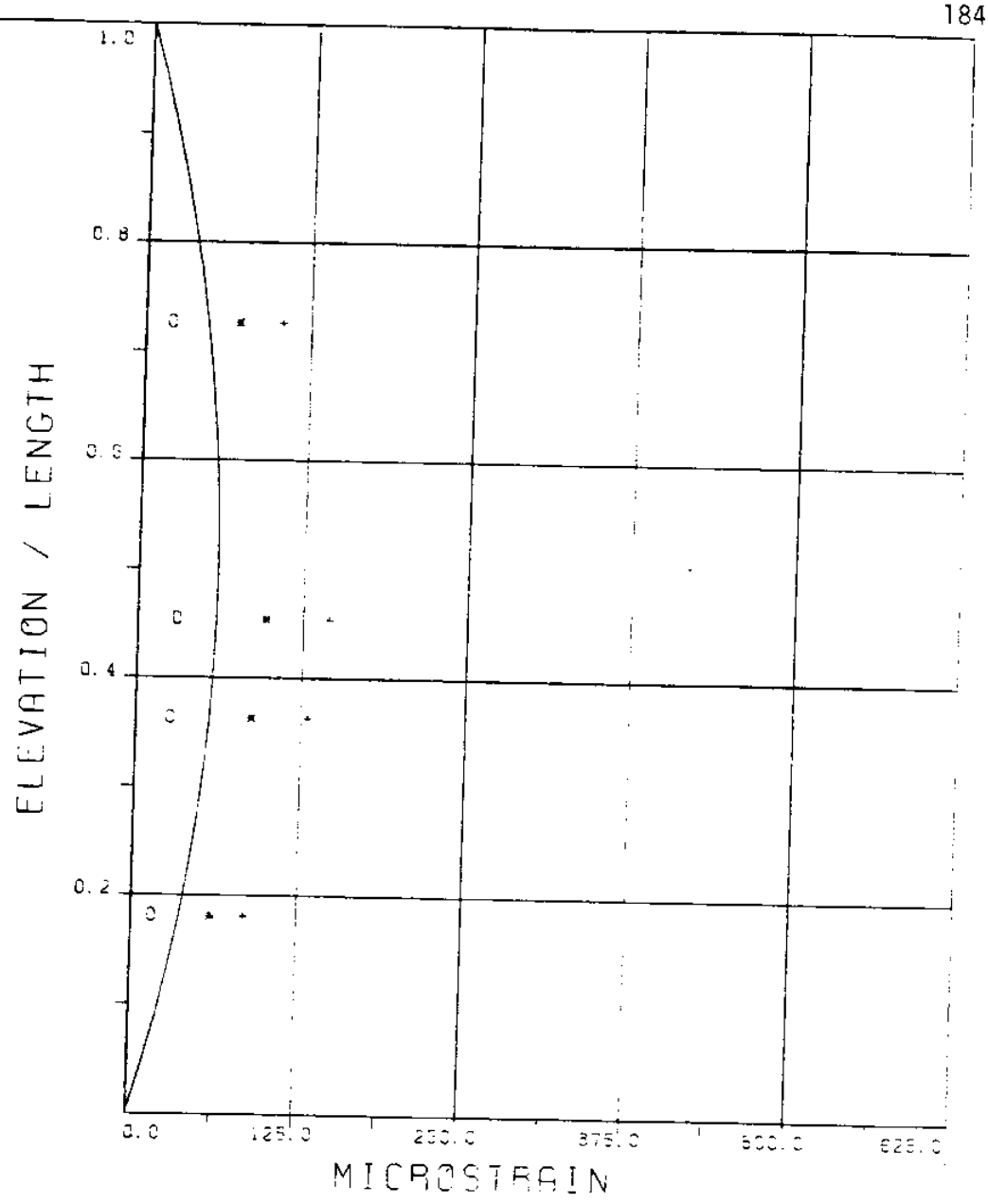

EXPERIMENT NUMBER 105

VC=220 A/DE=0.00

STATIC RESPONSE IN PLANE A

——— THEORY * * * EXPERIMENT

MAXIMUM DYNAMIC RESPONSE IN PLANE A

o o o EXPERIMENT

MAXIMUM RESPONSE

——— THEORY + + + EXPERIMENT

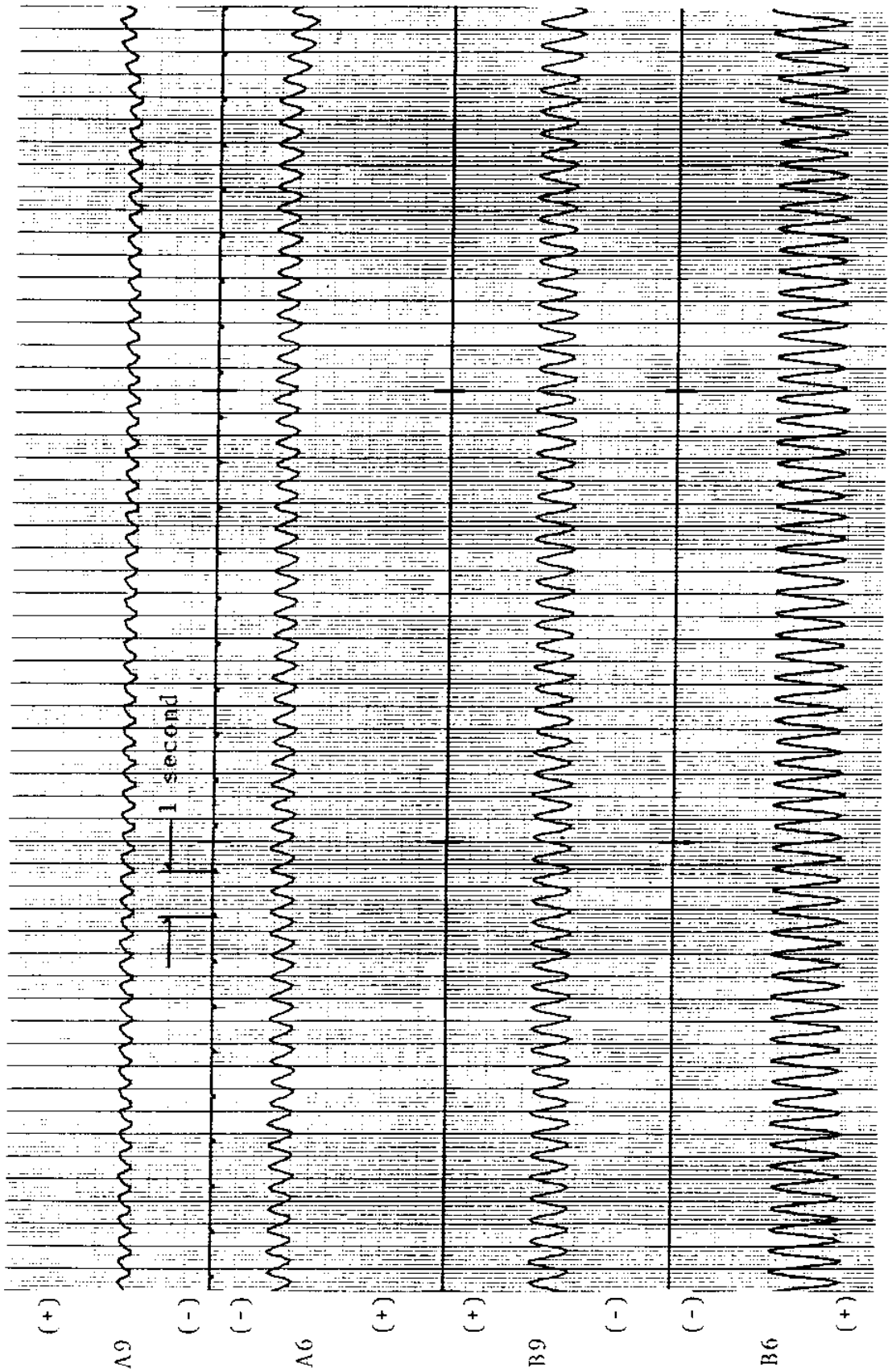

FIGURE 105T: ALL BRIDGES: 7.6 MICROSTRAIN/DIVISION

EXPERIMENT 103

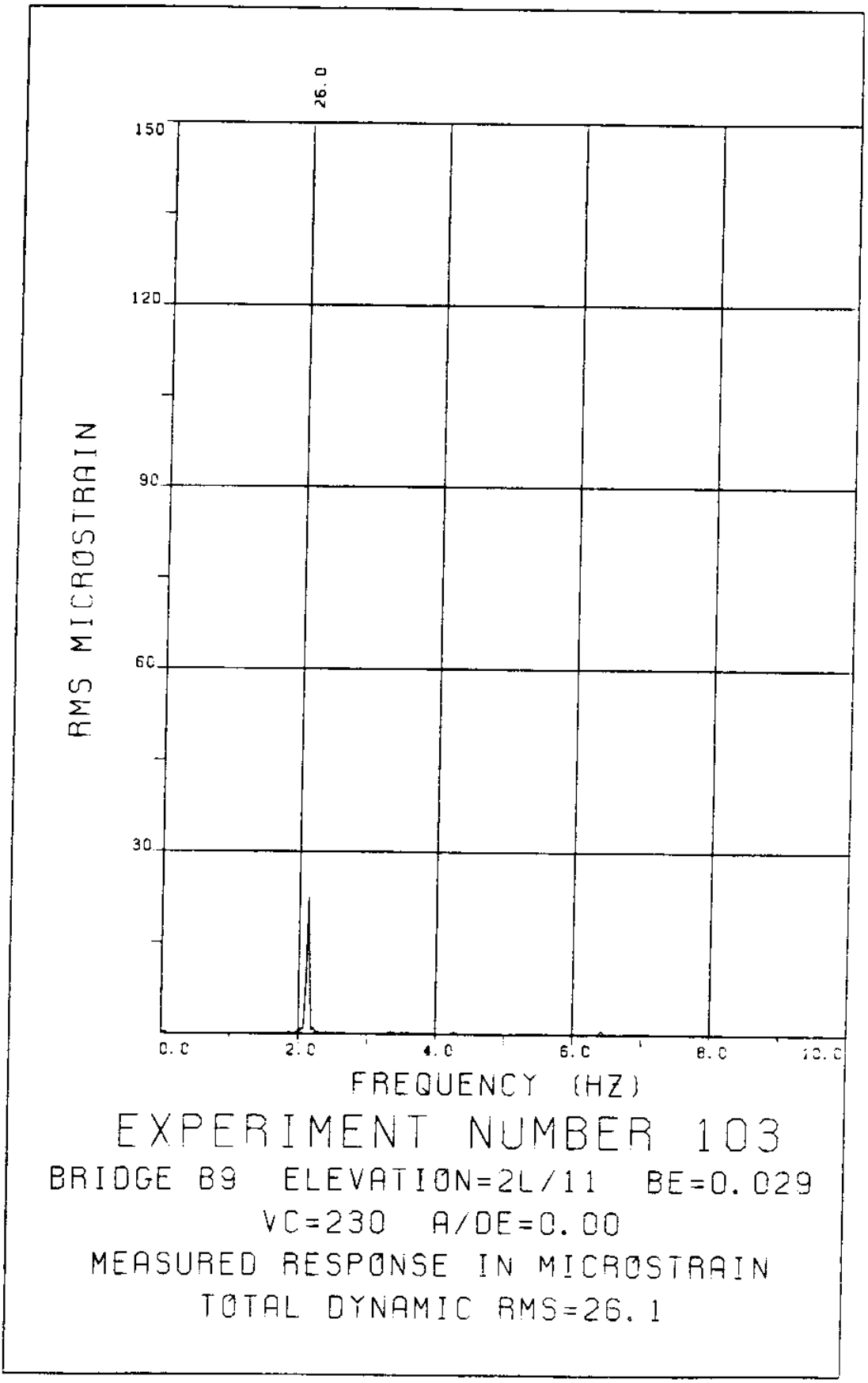
26.0
150
120
90
60
30
RMS MICROSTRAIN
0.0
2.0
4.0
6.0
8.0
10.0
FREQUENCY (HZ)
EXPERIMENT NUMBER 103
BRIDGE B9 ELEVATION=2L/11 BE=0.029
VC=230 A/DE=0.00
MEASURED RESPONSE IN MICROSTRAIN
TOTAL DYNAMIC RMS=26.1

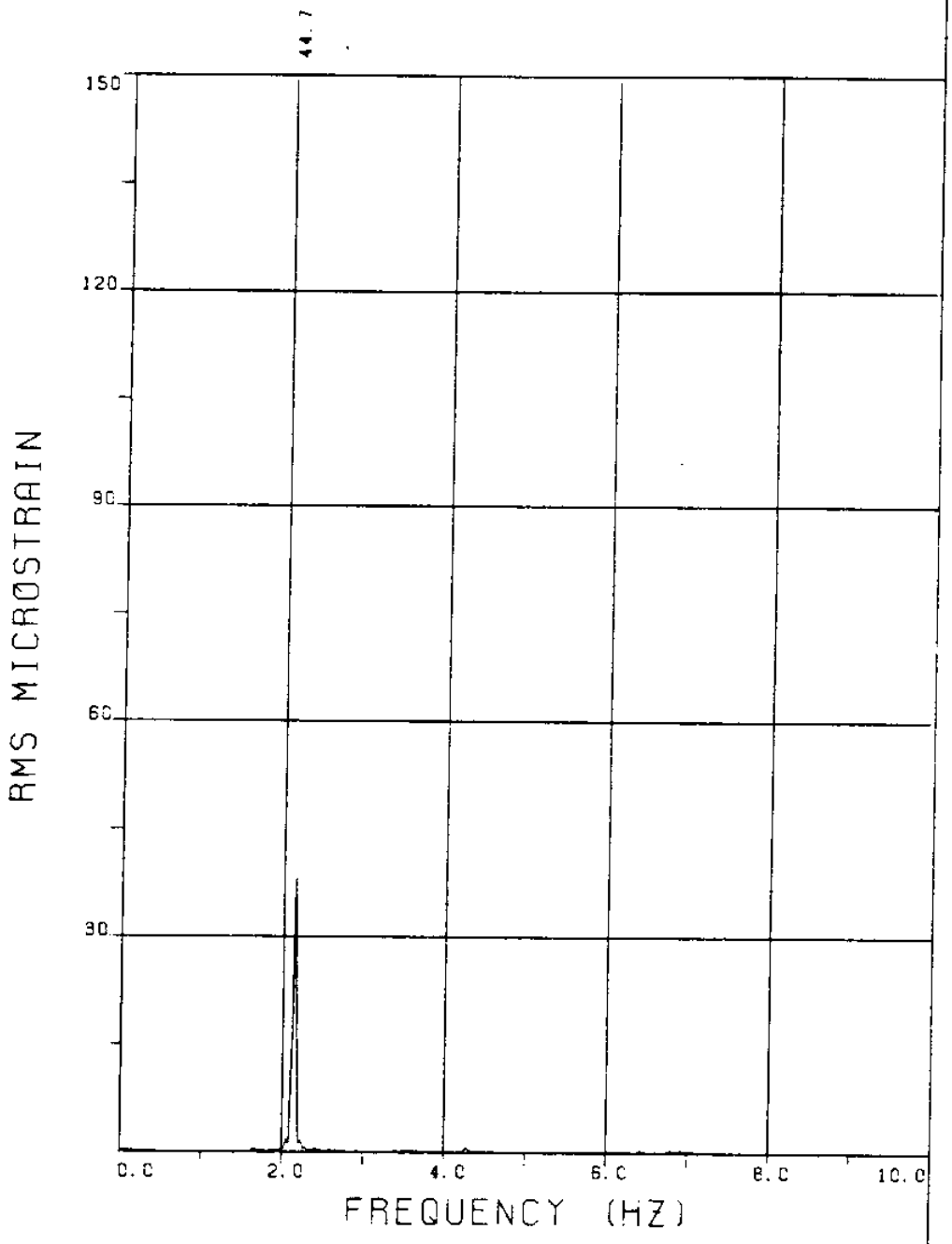

EXPERIMENT NUMBER 103

BRIDGE B7 ELEVATION=4L/11 BE=0.029

VC=230 A/DE=0.00

MEASURED RESPONSE IN MICROSTRAIN

TOTAL DYNAMIC RMS=44.7

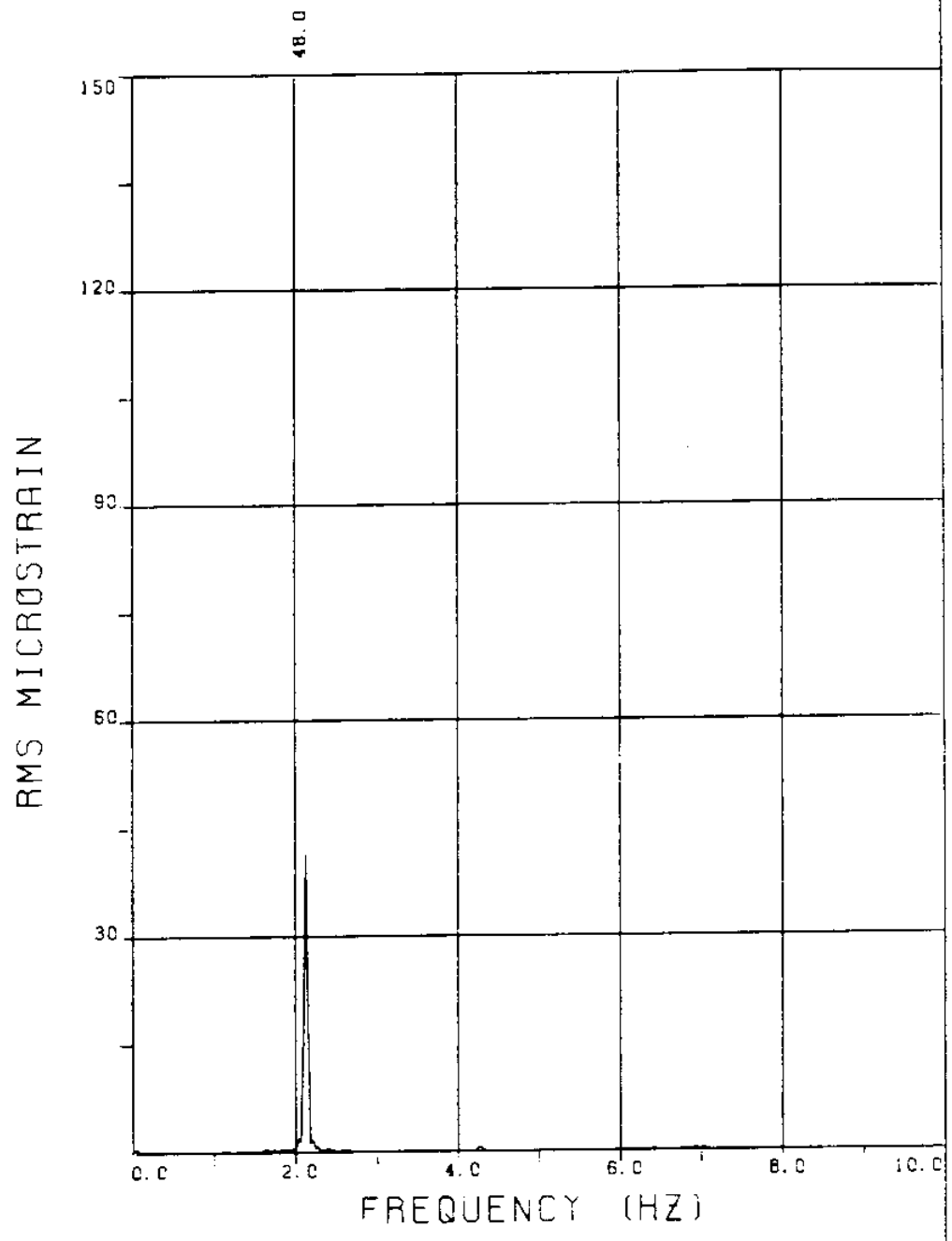

EXPERIMENT NUMBER 103

BRIDGE B6 ELEVATION=5L/11 BE=0.029

VC=230 A/DE=0.00

MEASURED RESPONSE IN MICROSTRAIN

TOTAL DYNAMIC RMS=48.0

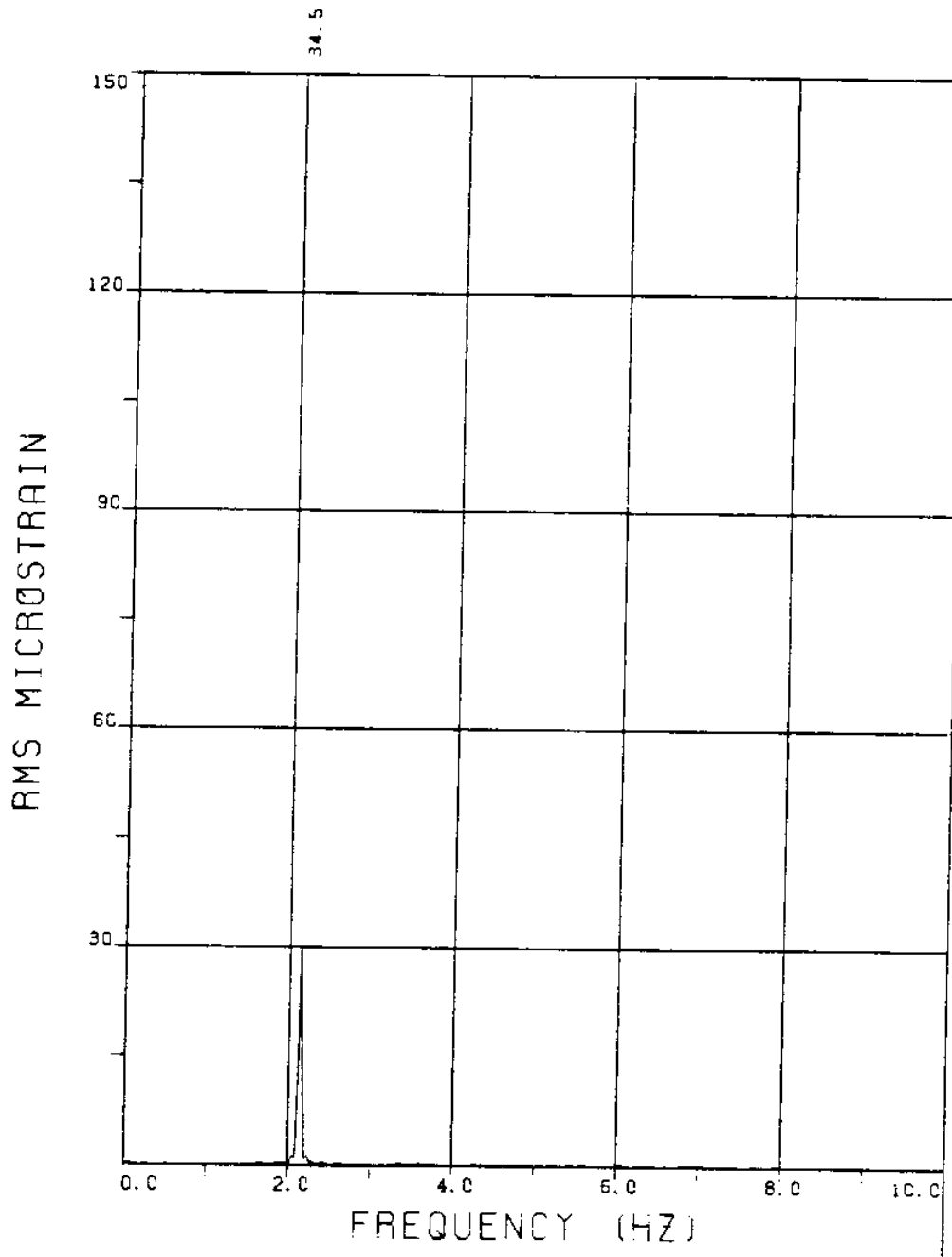

EXPERIMENT NUMBER 103

BRIDGE B3 ELEVATION=8L/11 BE=0.029

VC=230 A/DE=0.00

MEASURED RESPONSE IN MICROSTRAIN

TOTAL DYNAMIC RMS=34.5

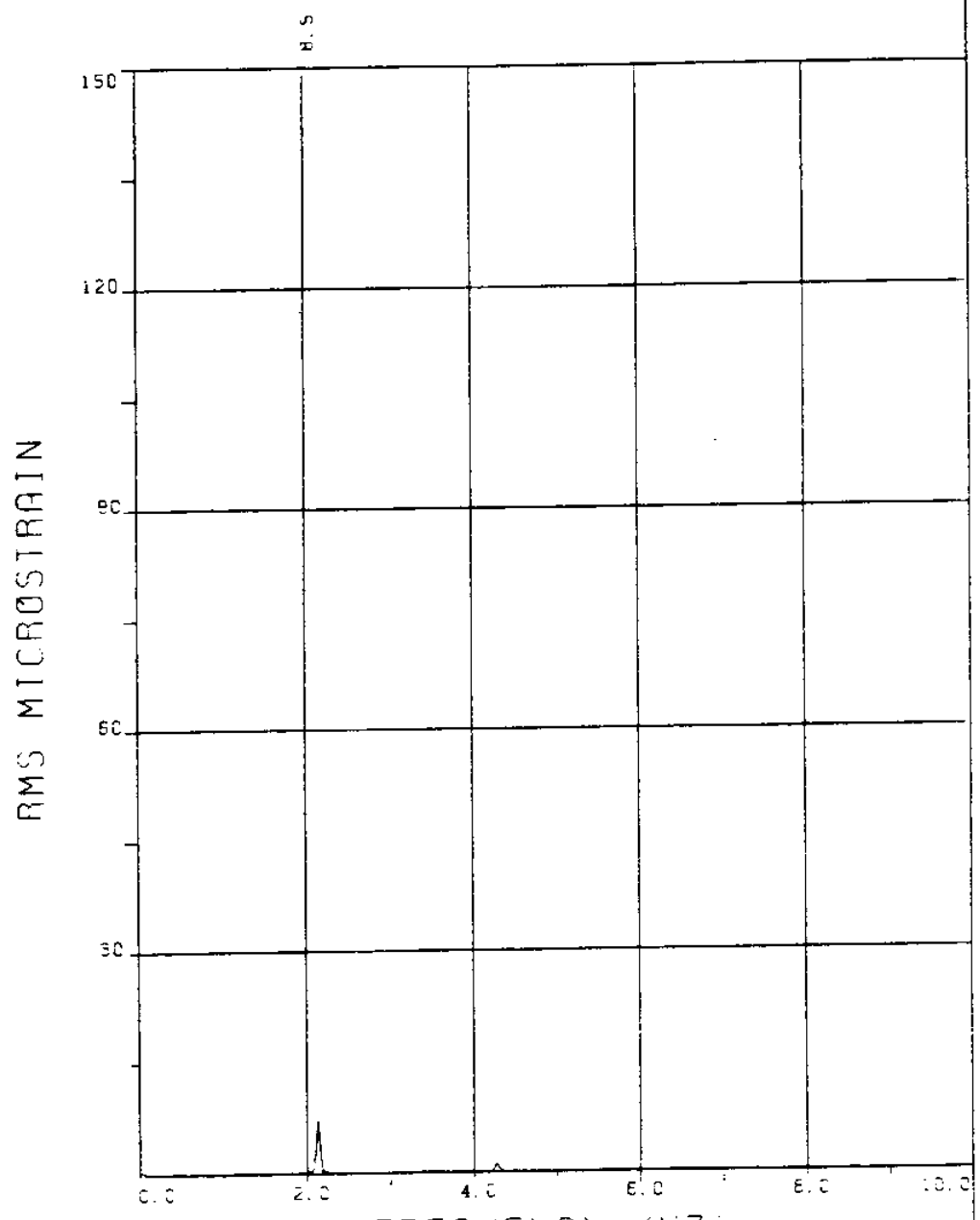

EXPERIMENT NUMBER 103

BRIDGE A9 ELEVATION=2L/11 BE=0.029

VC=230 A/DE=0.00

MEASURED RESPONSE IN MICROSTRAIN

MEAN=64.4

TOTAL DYNAMIC RMS=8.7

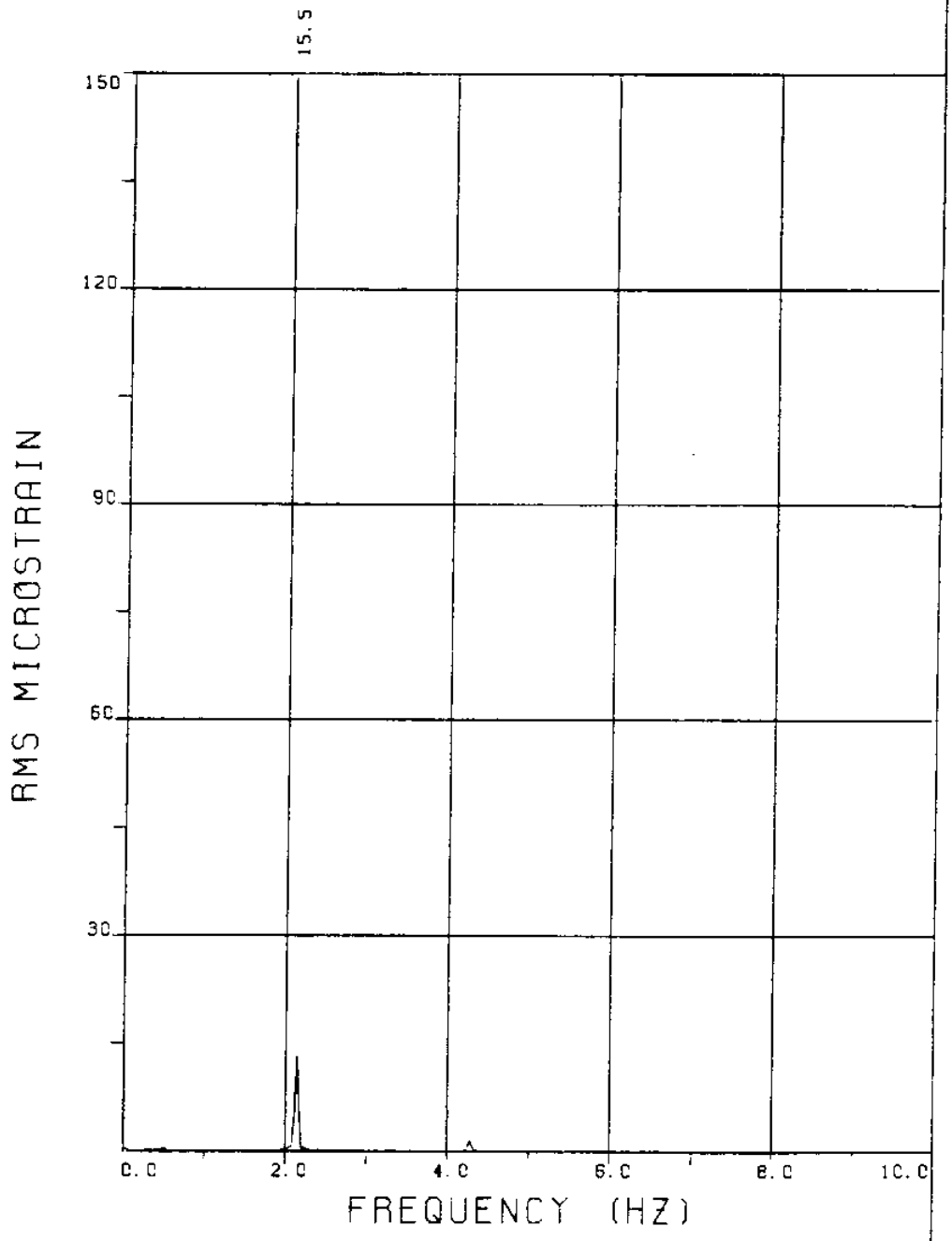

EXPERIMENT NUMBER 103

BRIDGE A7 ELEVATION=4L/11 BE=0.029

VC=230 A/DE=0.00

MEASURED RESPONSE IN MICROSTRAIN

MEAN=91.5

TOTAL DYNAMIC RMS=15.6

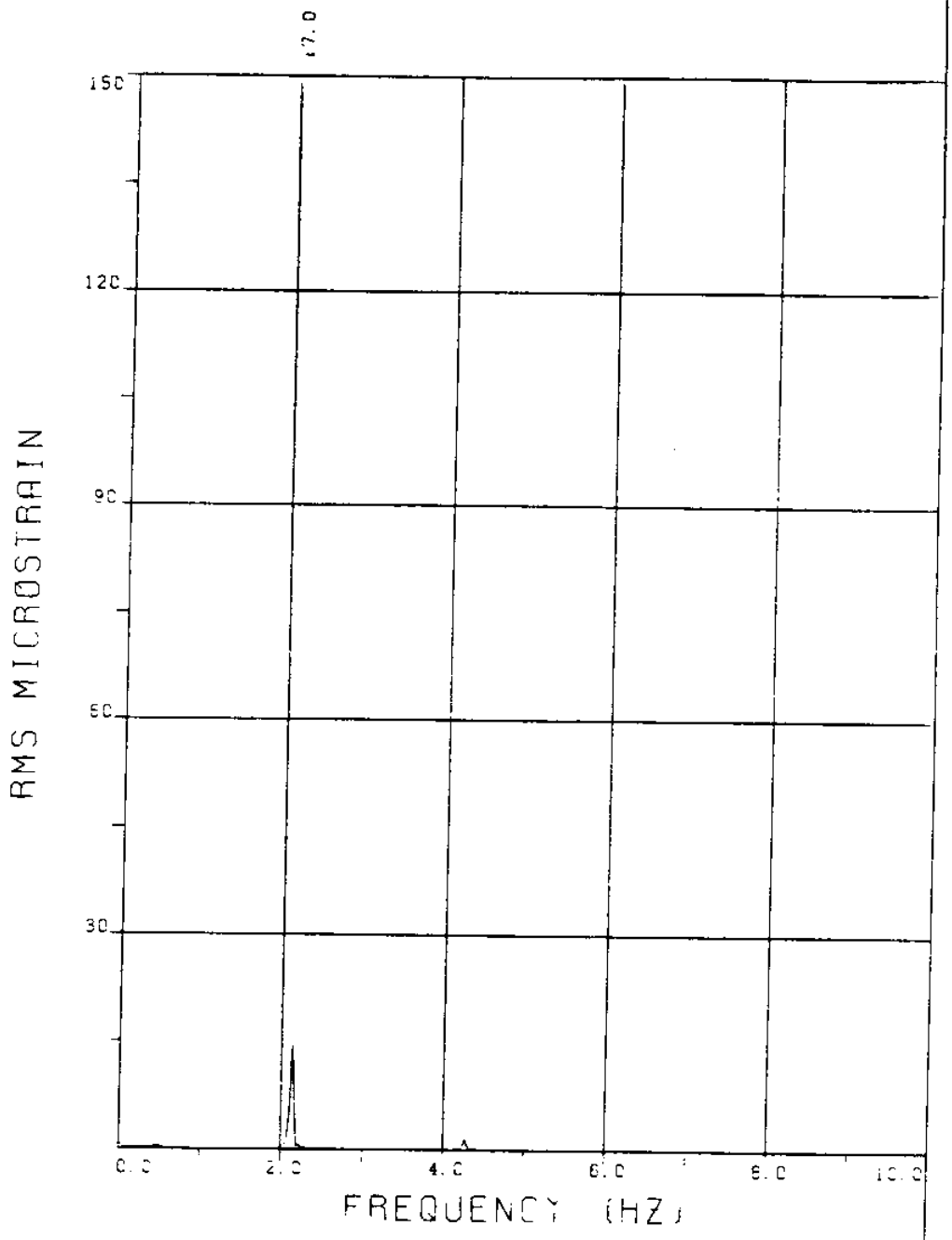

EXPERIMENT NUMBER 103

BRIDGE 96 ELEVATION=SL/11 BE=0.029

VC=230 A/DE=0.00

MEASURED RESPONSE IN MICROSTRAIN

MEAN=100.6

TOTAL DYNAMIC RMS=17.2

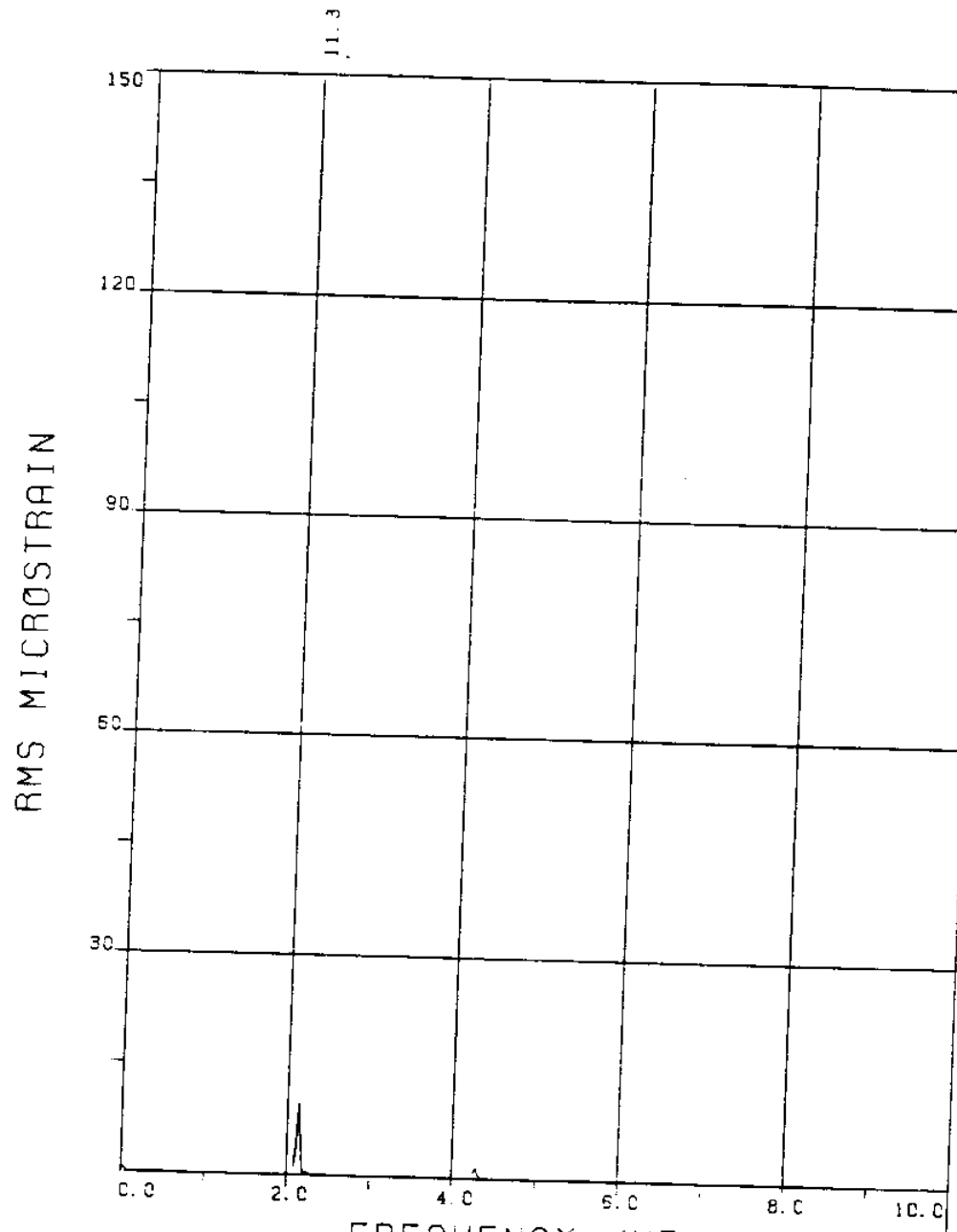

EXPERIMENT NUMBER 103

BRIDGE A3 ELEVATION=8L/11 BE=0.029

VC=230 A/DE=0.00

MEASURED RESPONSE IN MICROSTRAIN

MEAN=78.4

TOTAL DYNAMIC RMS=11.5

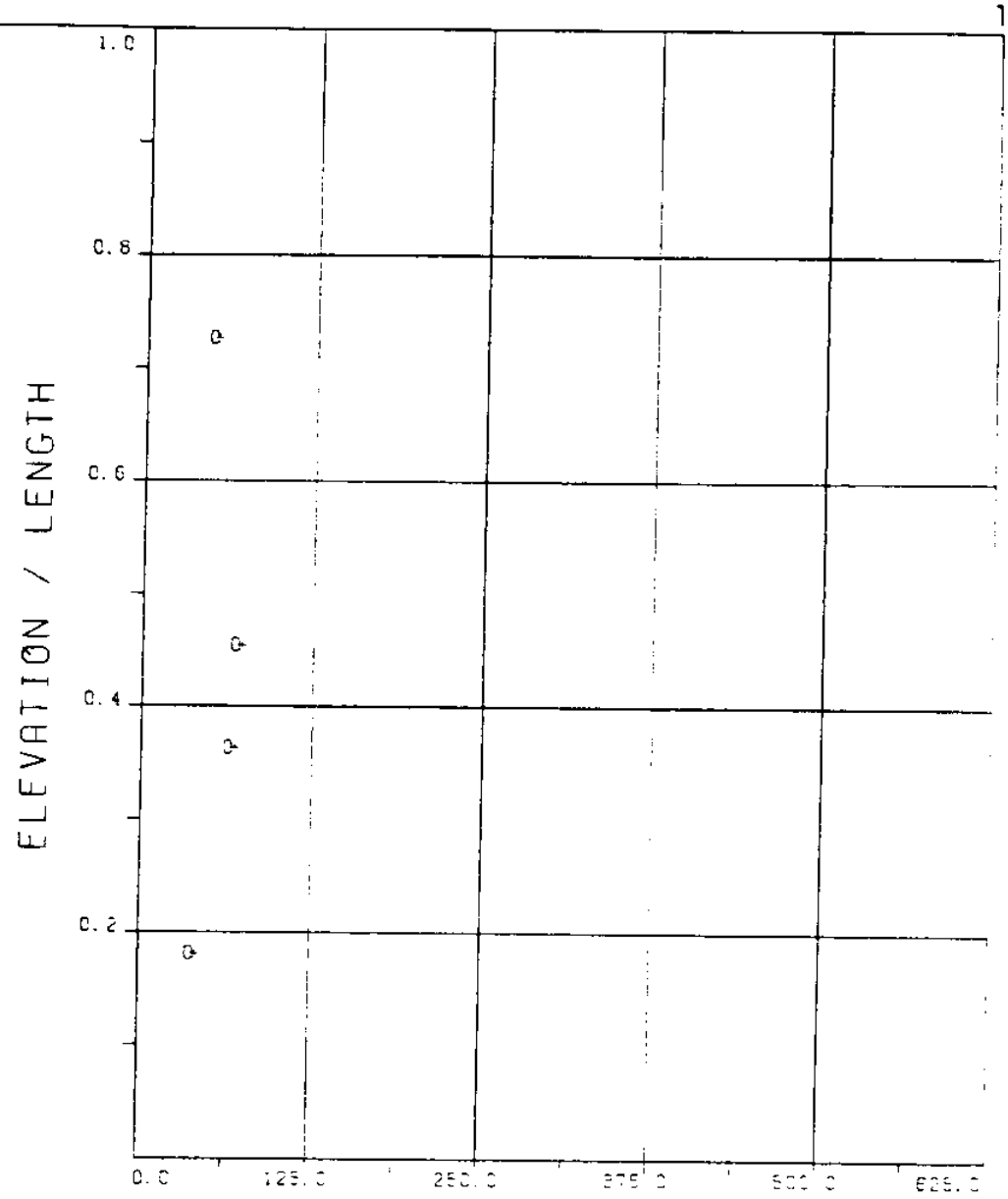

EXPERIMENT NUMBER 103

VC=230 A/DE=0.00

DYNAMIC RESPONSE AT F=FR IN PLANE B

o o o EXPERIMENT

MAXIMUM DYNAMIC RESPONSE IN PLANE B

+ + + EXPERIMENT

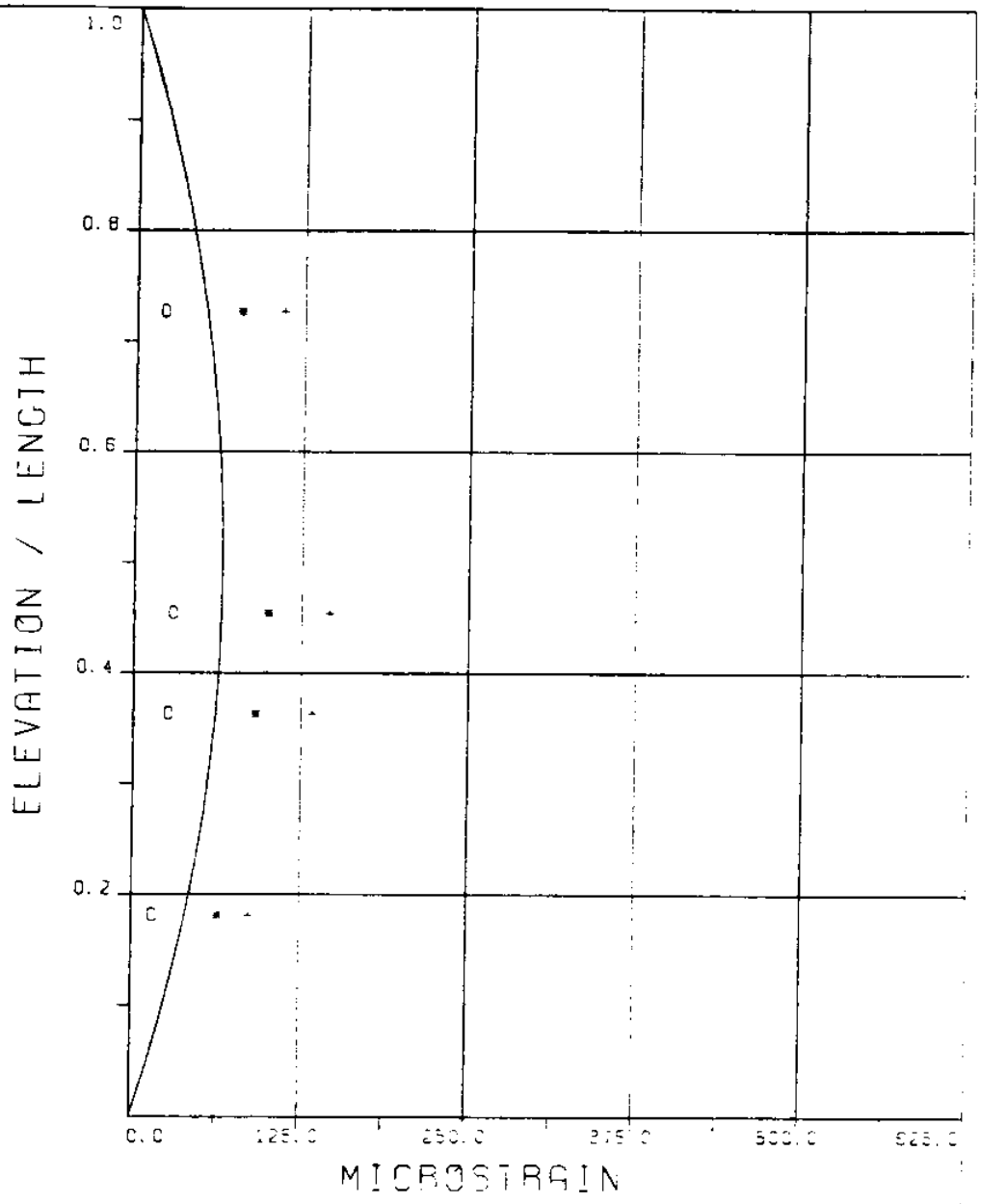

EXPERIMENT NUMBER 103

VC=230 A/DE=0.00

STATIC RESPONSE IN PLANE A

——— THEORY * * * EXPERIMENT

MAXIMUM DYNAMIC RESPONSE IN PLANE A

o o o EXPERIMENT

MAXIMUM RESPONSE

——— THEORY + + + EXPERIMENT

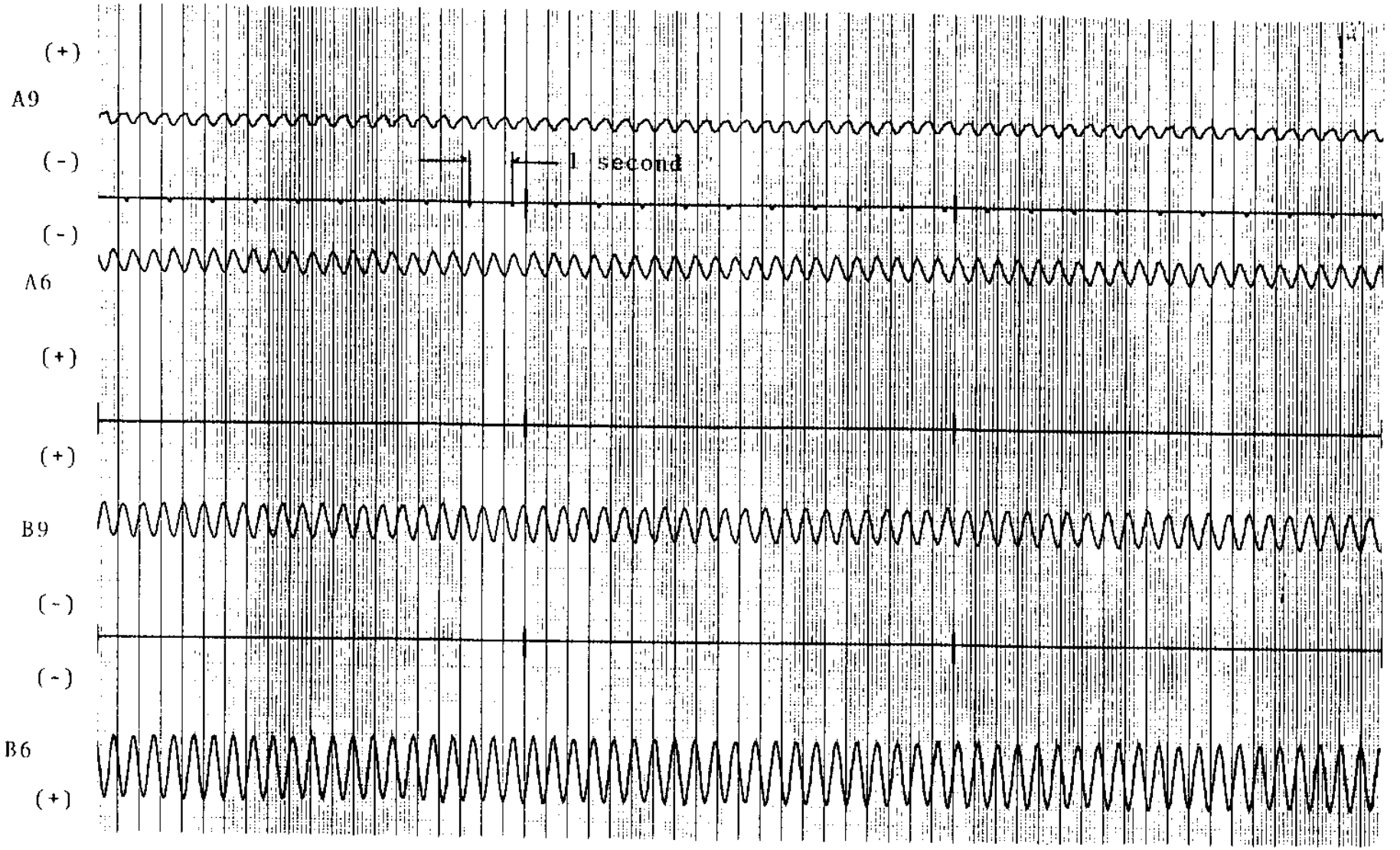

FIGURE 103T: ALL BRIDGES: 7.6 MICROSTRAIN/DIVISION

EXPERIMENT 101

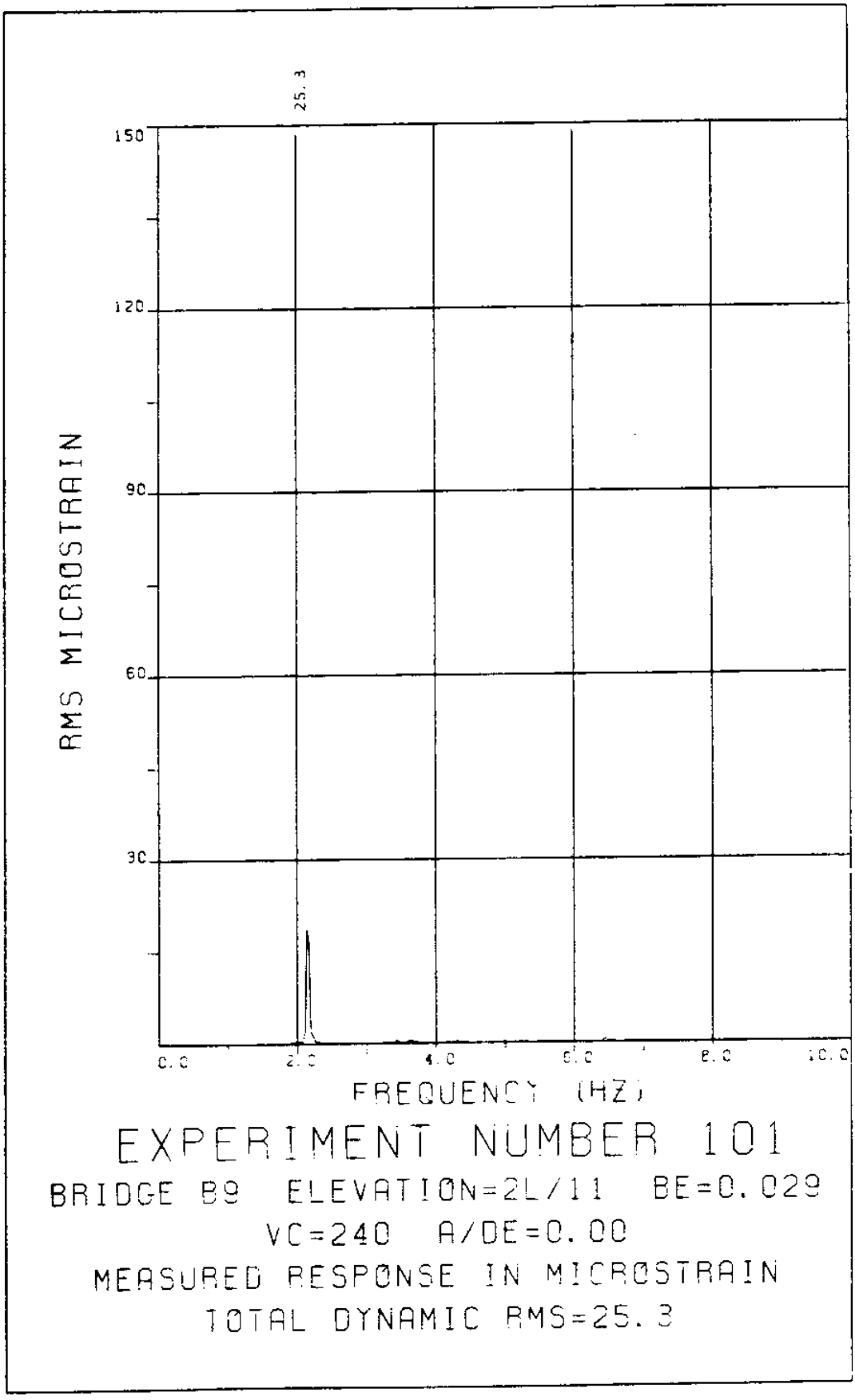
25.3
150
120
90
60
30
RMS MICROSTRAIN
0.0
2.0
4.0
6.0
8.0
10.0
FREQUENCY (HZ)
EXPERIMENT NUMBER 101
BRIDGE B9 ELEVATION=2L/11 BE=0.029
VC=240 A/DE=0.00
MEASURED RESPONSE IN MICROSTRAIN
TOTAL DYNAMIC RMS=25.3

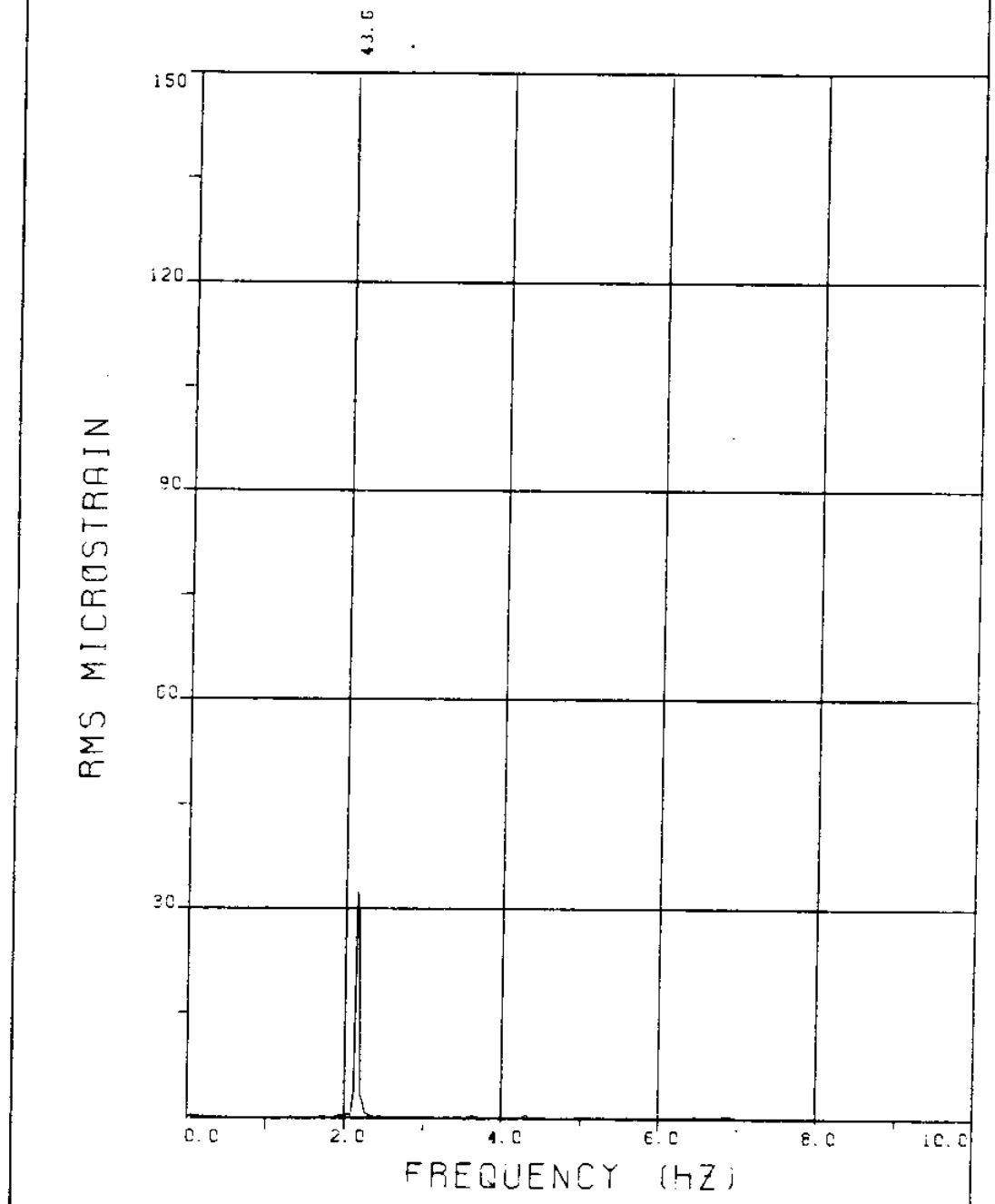

EXPERIMENT NUMBER 101

BRIDGE B7 ELEVATION=4L/11 BE=0.029

VC=240 A/DE=0.00

MEASURED RESPONSE IN MICROSTRAIN

TOTAL DYNAMIC RMS=43.7

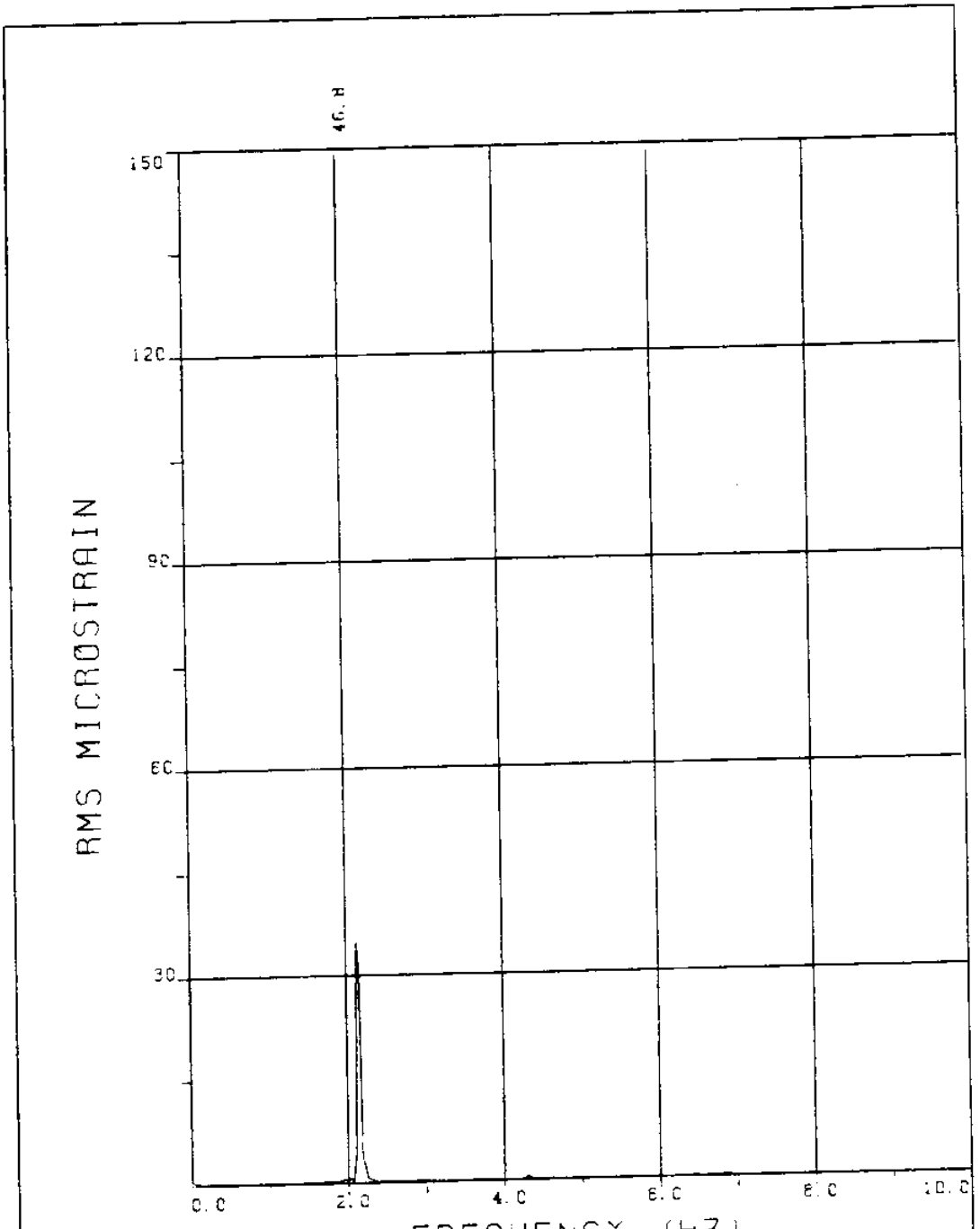

EXPERIMENT NUMBER 101

BRIDGE B6 ELEVATION=5L/11 BE=0.029

VC=240 A/DE=0.00

MEASURED RESPONSE IN MICROSTRAIN

TOTAL DYNAMIC RMS=46.9

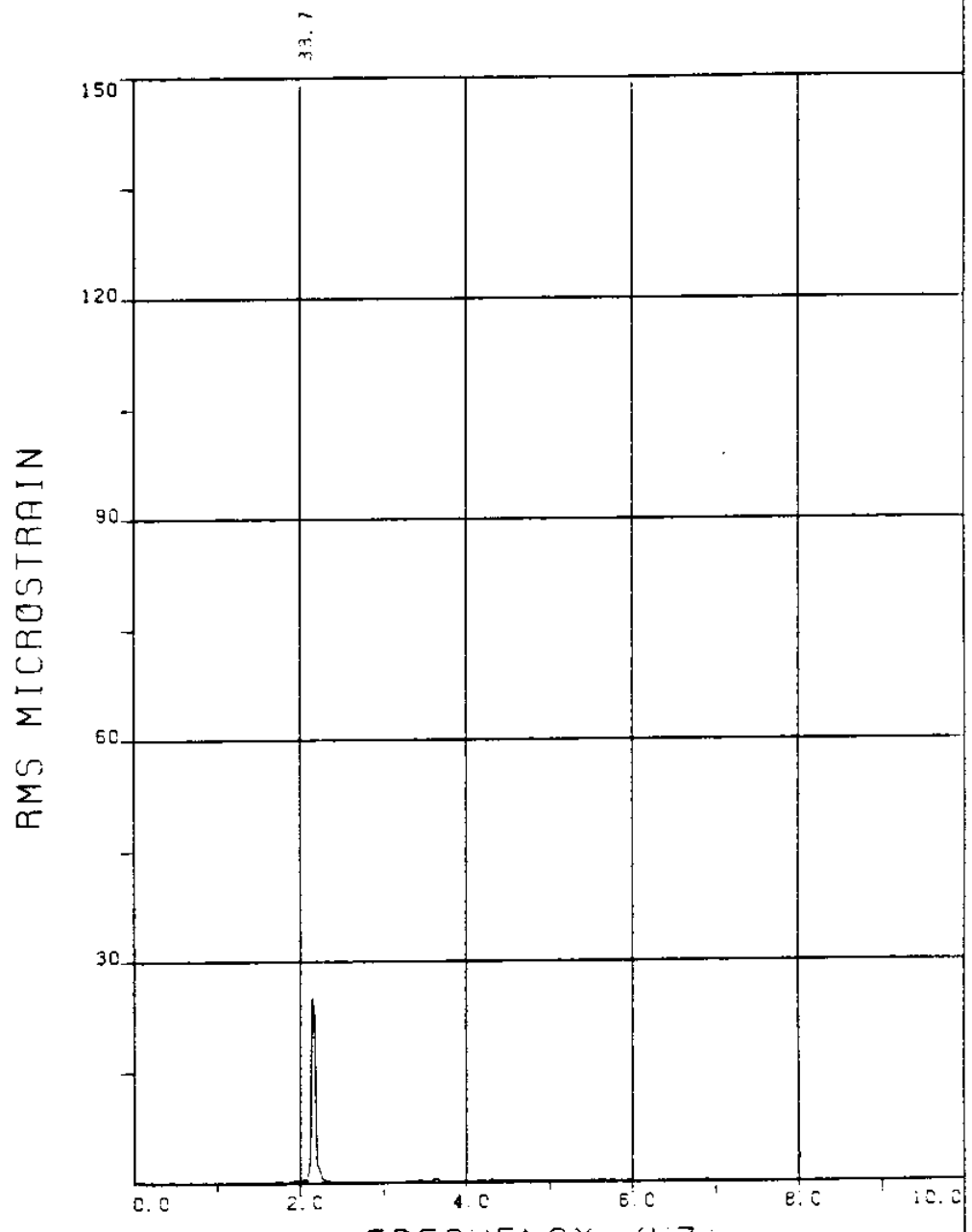

EXPERIMENT NUMBER 101

BRIDGE B3 ELEVATION=8L/11 BE=0.029

VC=240 A/DE=0.00

MEASURED RESPONSE IN MICROSTRAIN

TOTAL DYNAMIC RMS=33.8

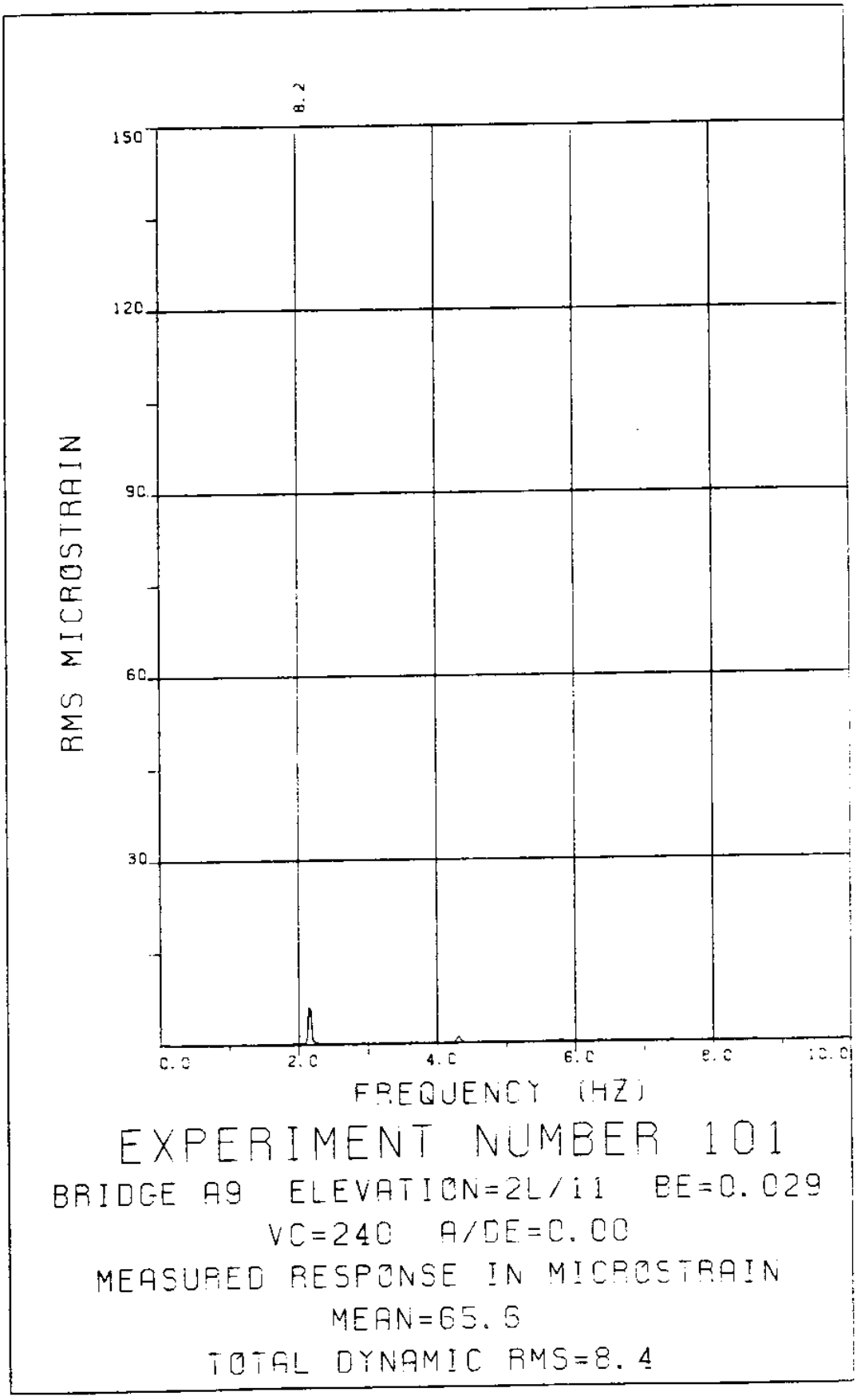
8.2
150
120
90
60
30
RMS MICROSTRAIN
0.0
2.0
4.0
6.0
8.0
10.0
FREQUENCY (HZ)
EXPERIMENT NUMBER 101
BRIDGE A9 ELEVATION=2L/11 BE=0.029
VC=240 A/DE=0.00
MEASURED RESPONSE IN MICROSTRAIN
MEAN=65.6
TOTAL DYNAMIC RMS=8.4

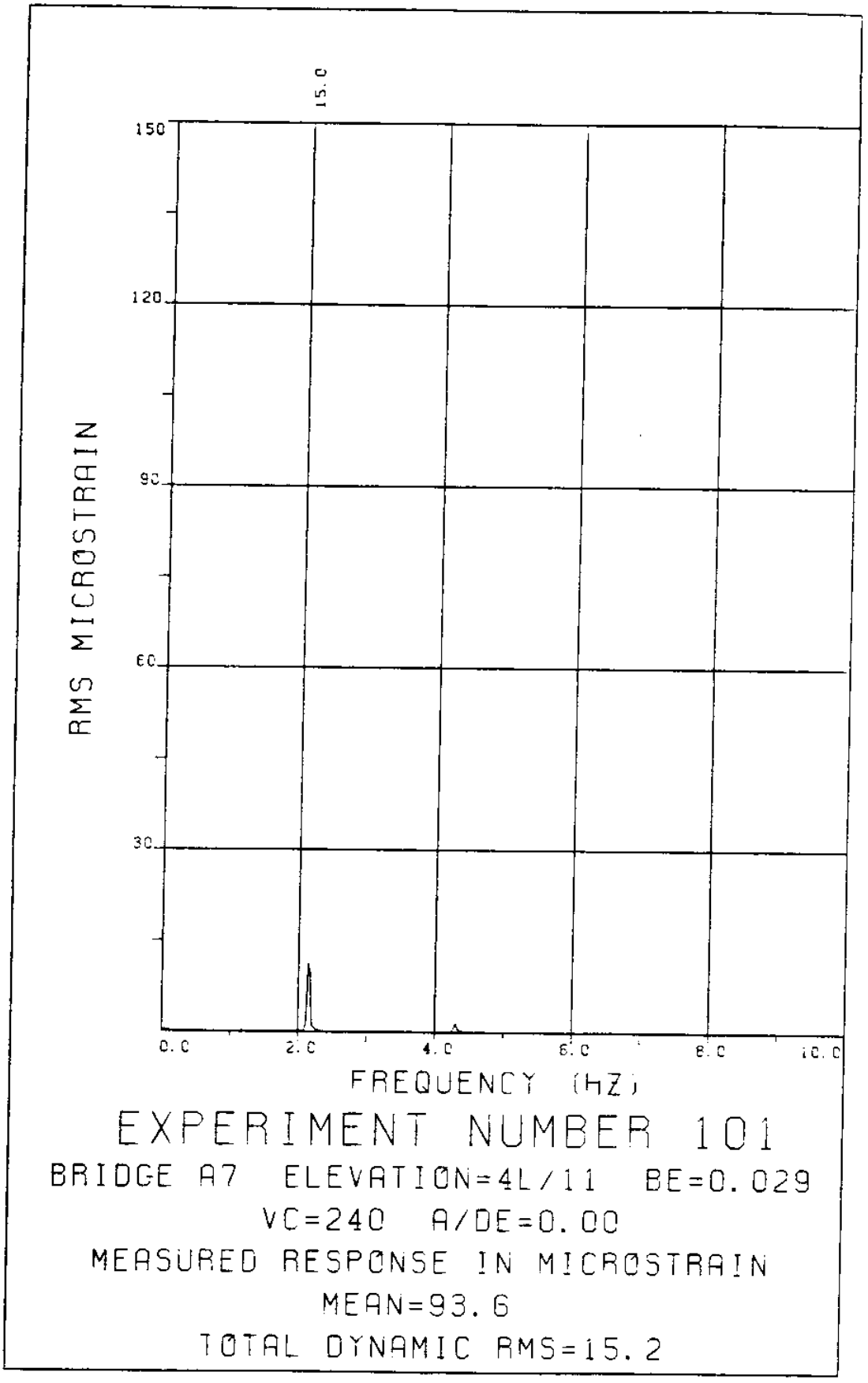

EXPERIMENT NUMBER 101

BRIDGE A7 ELEVATION=4L/11 BE=0.029

VC=240 A/DE=0.00

MEASURED RESPONSE IN MICROSTRAIN

MEAN=93.6

TOTAL DYNAMIC RMS=15.2

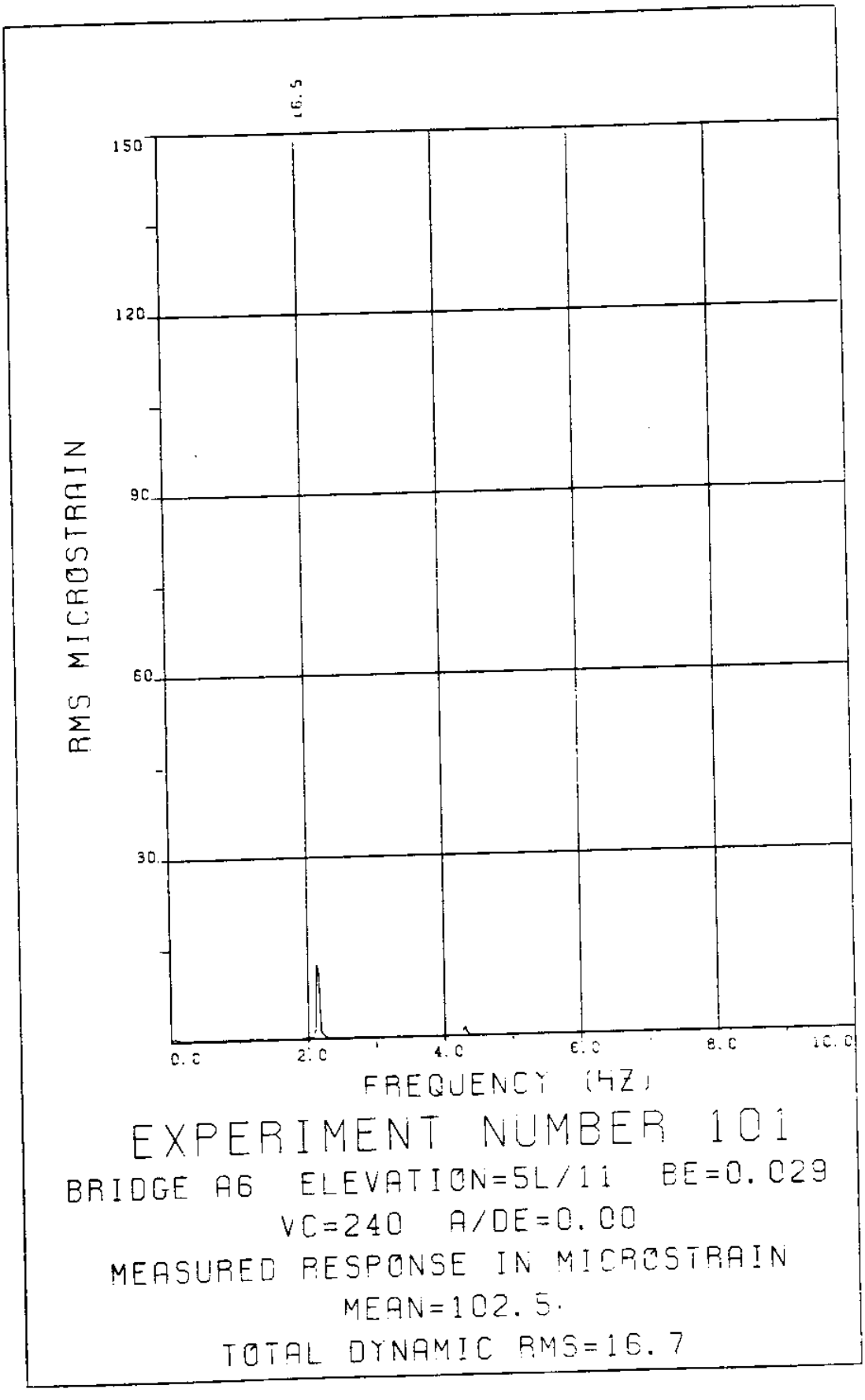
16.5
150
120
90
60
30
RMS MICROSTRAIN
0.0
2.0
4.0
6.0
8.0
10.0
FREQUENCY (HZ)
EXPERIMENT NUMBER 101
BRIDGE A6 ELEVATION=5L/11 BE=0.029
VC=240 A/DE=0.00
MEASURED RESPONSE IN MICROSTRAIN
MEAN=102.5
TOTAL DYNAMIC RMS=16.7

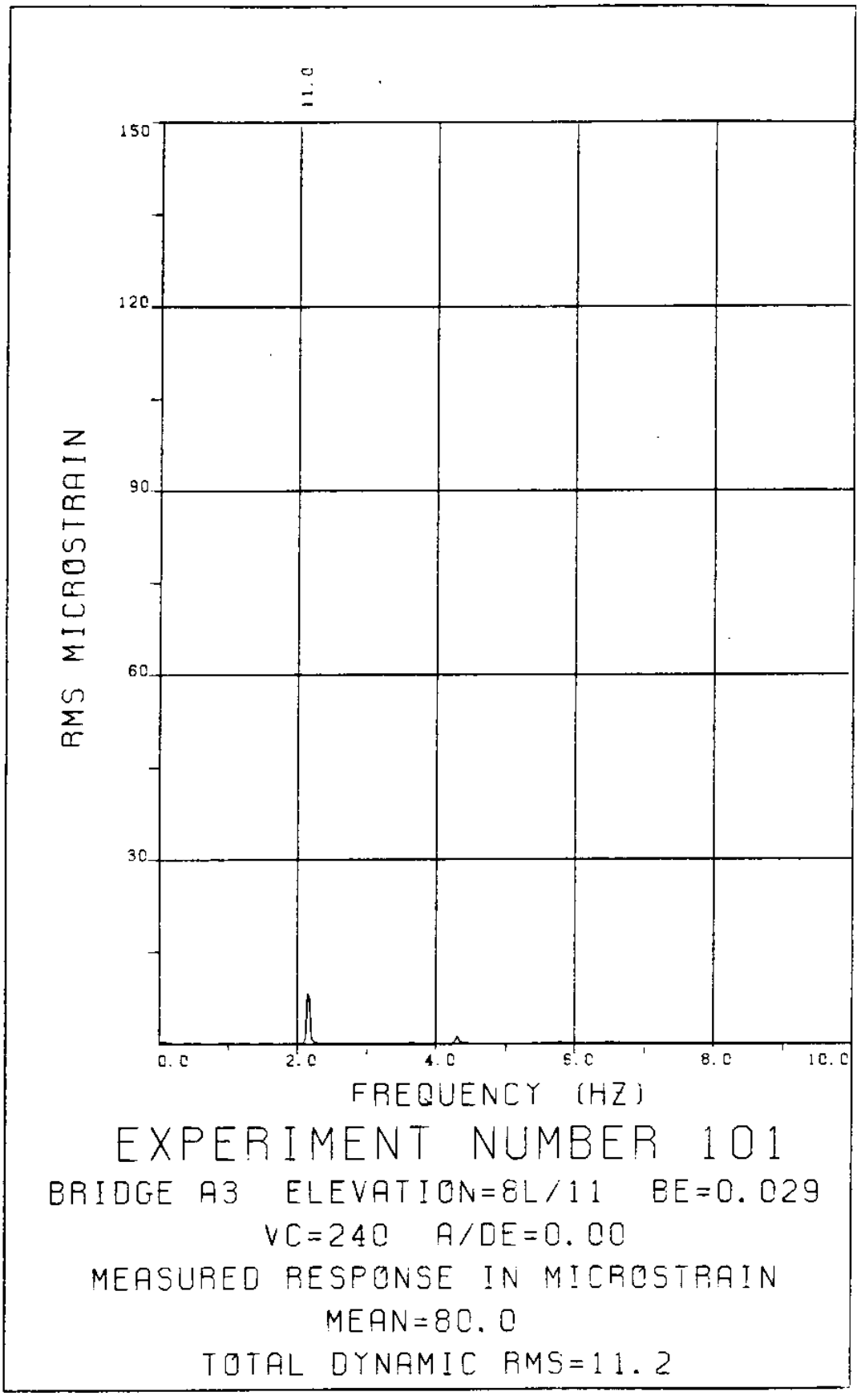

EXPERIMENT NUMBER 101

BRIDGE A3 ELEVATION=8L/11 BE=0.029

VC=240 A/DE=0.00

MEASURED RESPONSE IN MICROSTRAIN

MEAN=80.0

TOTAL DYNAMIC RMS=11.2

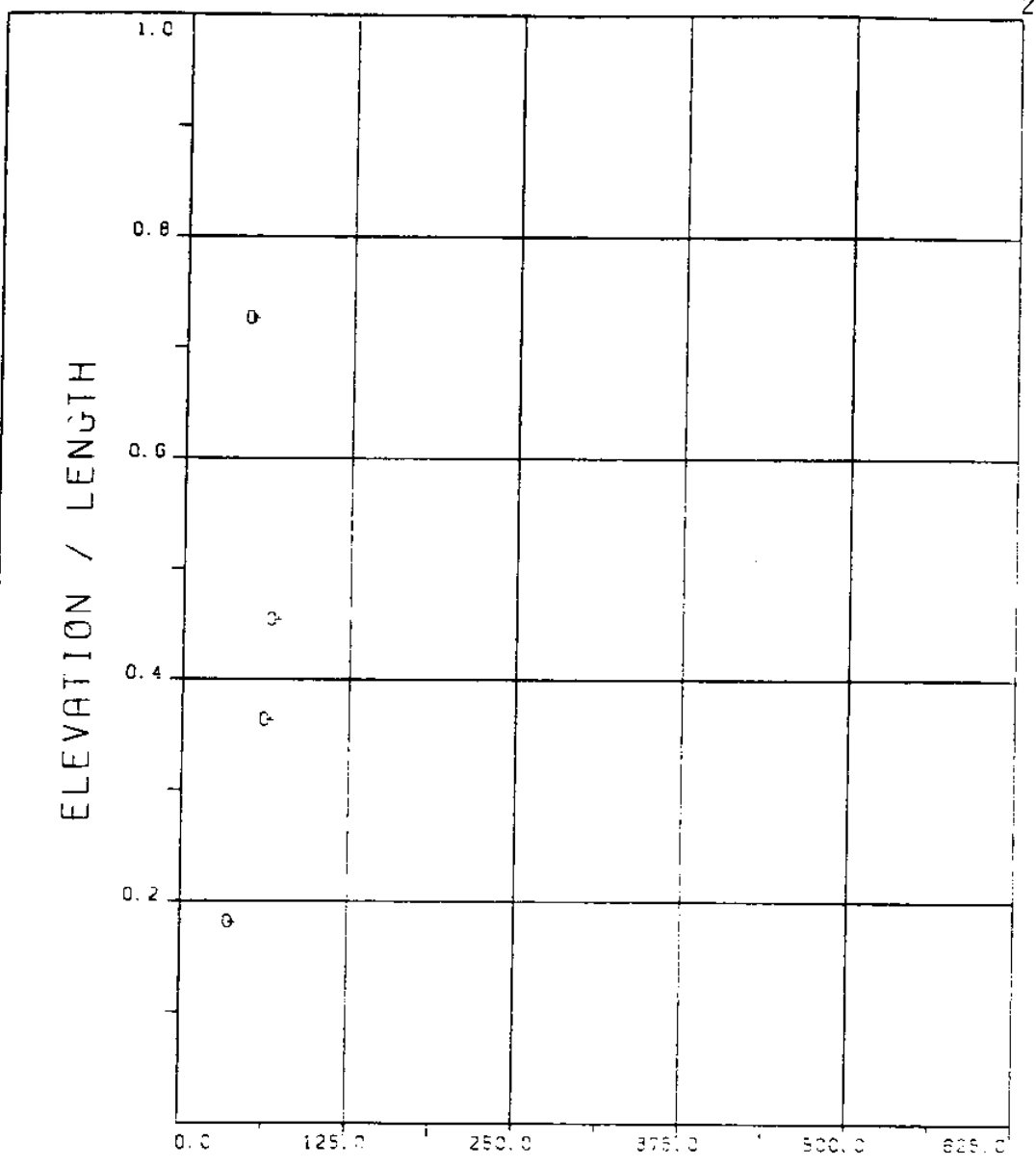

EXPERIMENT NUMBER 101

VC=240 A/DE=0.00

DYNAMIC RESPONSE AT F=FR IN PLANE B
o o o EXPERIMENT

MAXIMUM DYNAMIC RESPONSE IN PLANE B
+ + + EXPERIMENT

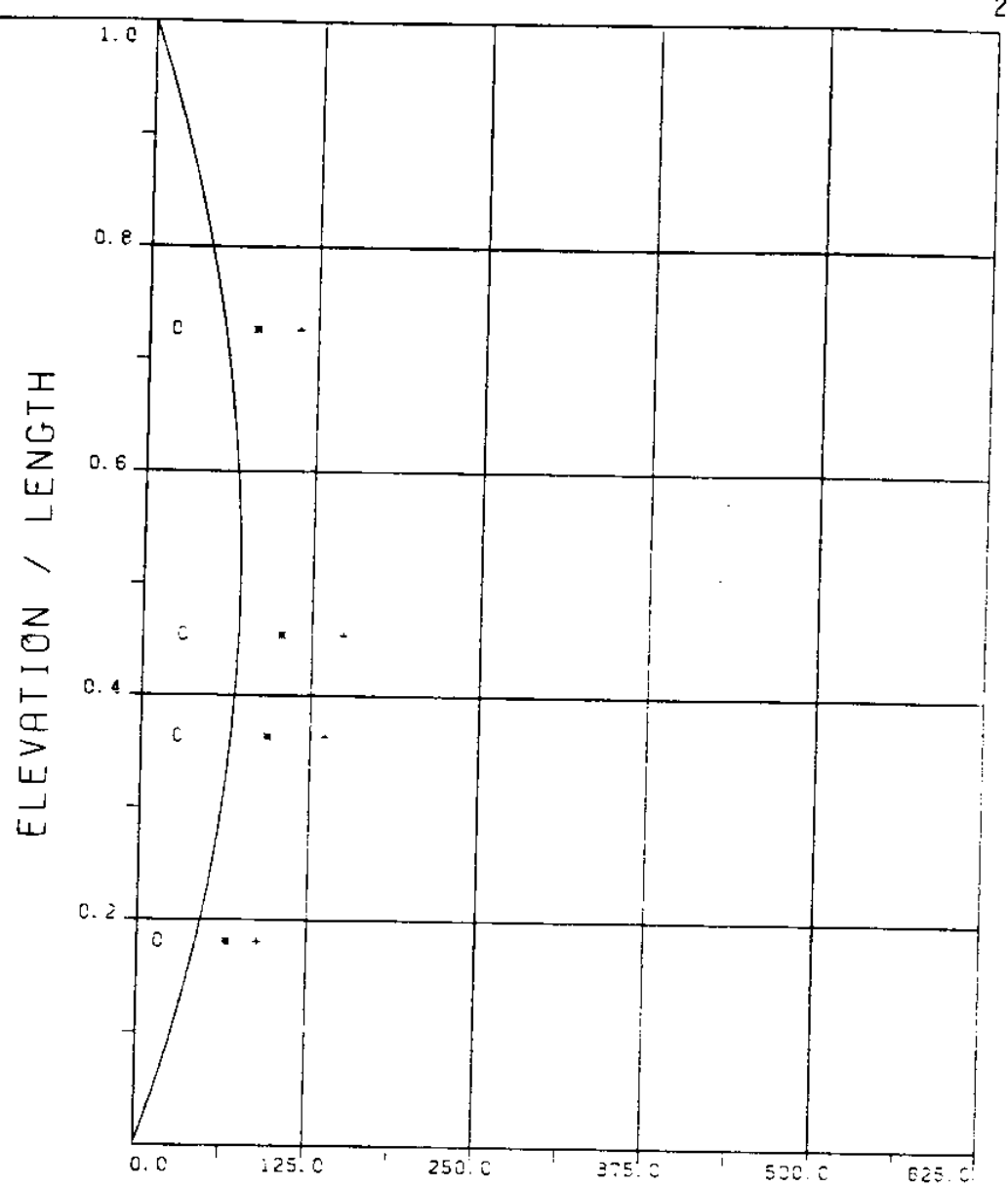

EXPERIMENT NUMBER 101

VC=240 A/DE=0.00

STATIC RESPONSE IN PLANE A

——— THEORY * * * EXPERIMENT

MAXIMUM DYNAMIC RESPONSE IN PLANE A

o o o EXPERIMENT

MAXIMUM RESPONSE

——— THEORY + + + EXPERIMENT

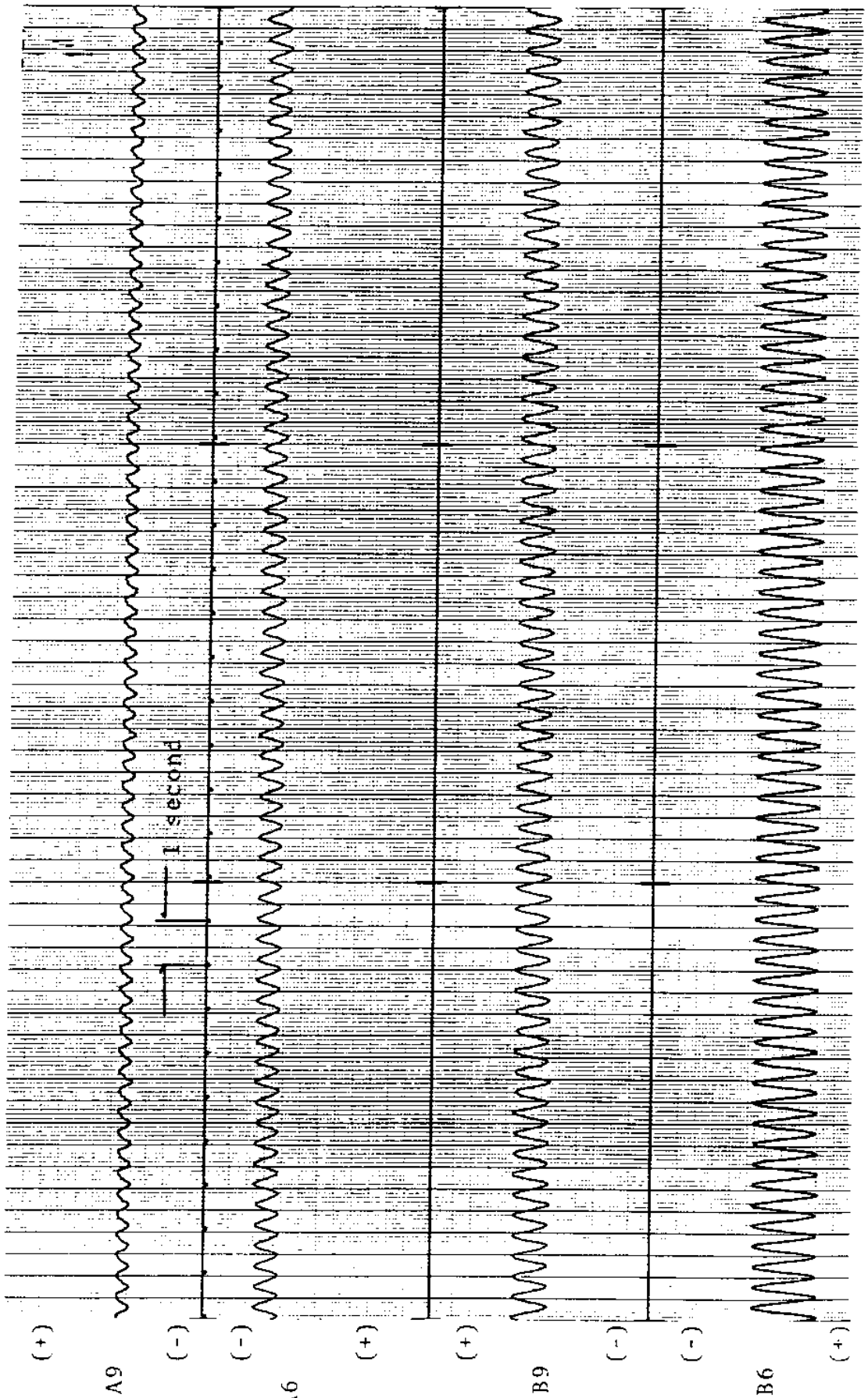

FIGURE 101T: ALL BRIDGES: 7.6 MICROSTRAIN/DIVISION

EXPERIMENT 99

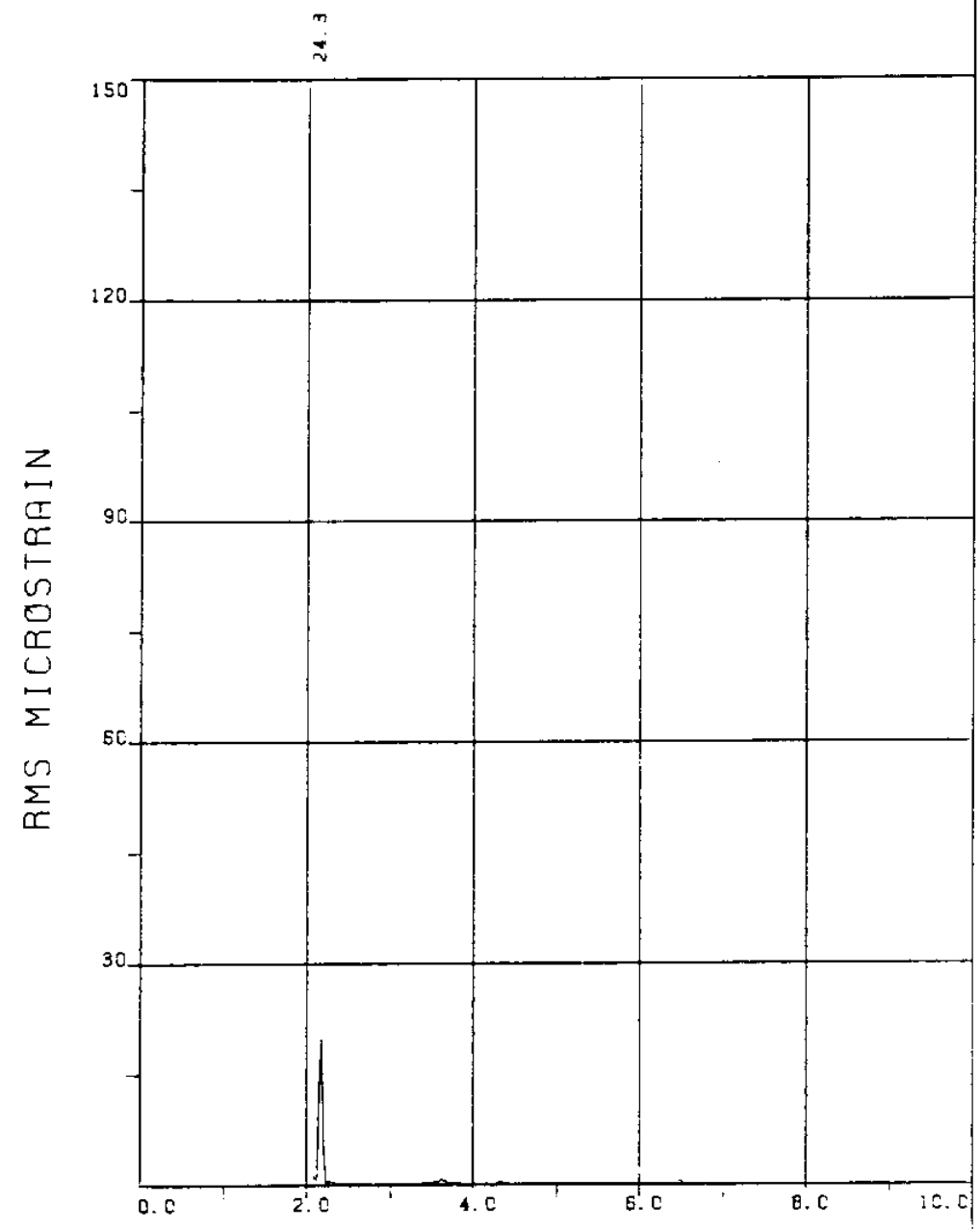

EXPERIMENT NUMBER 99

BRIDGE B9 ELEVATION=2L/11 BE=0.029

VC=250 A/DE=0.00

MEASURED RESPONSE IN MICROSTRAIN

TOTAL DYNAMIC RMS=24.4

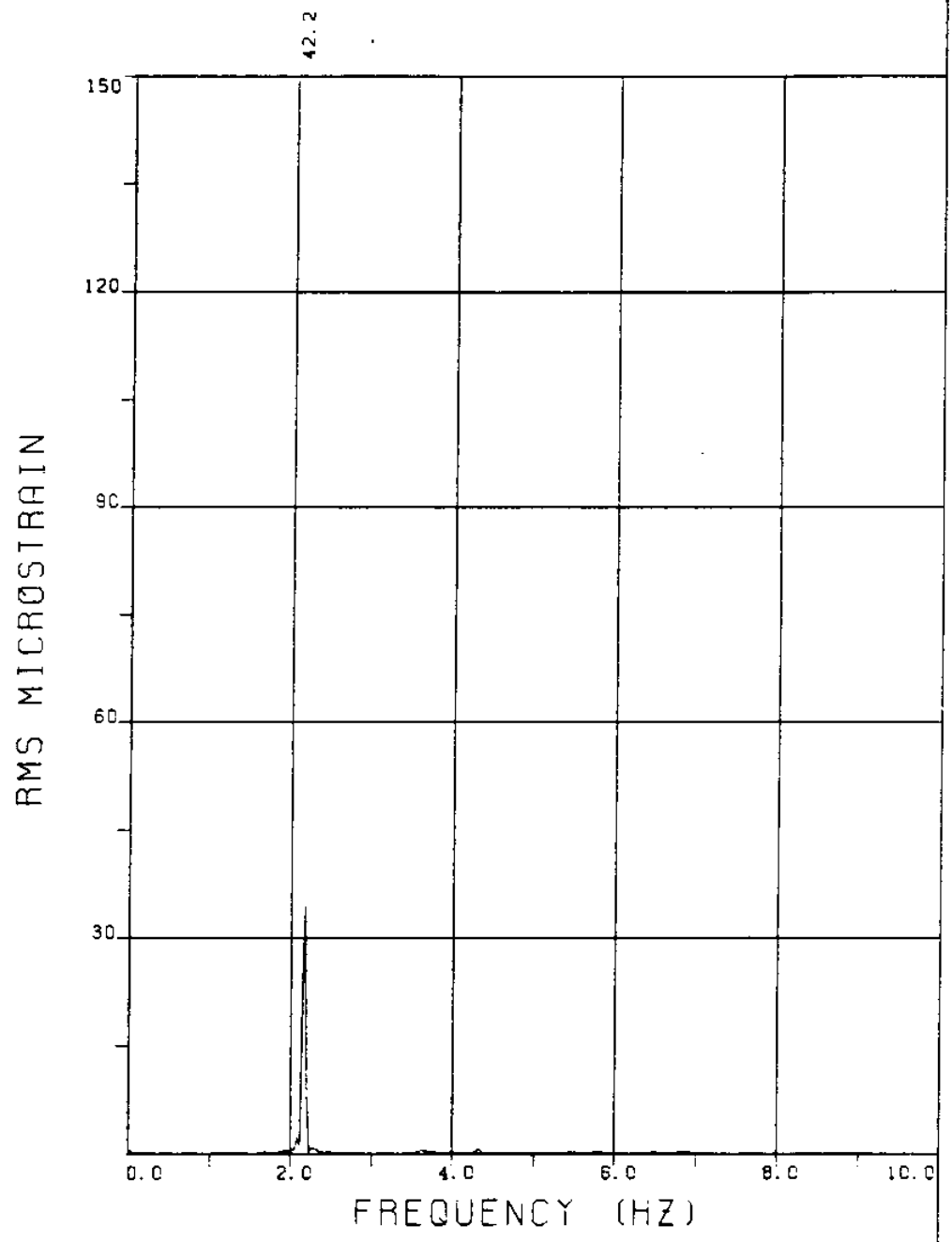

EXPERIMENT NUMBER 99

BRIDGE B7 ELEVATION=4L/11 BE=0.029

VC=250 A/DE=0.00

MEASURED RESPONSE IN MICROSTRAIN

TOTAL DYNAMIC RMS=42.2

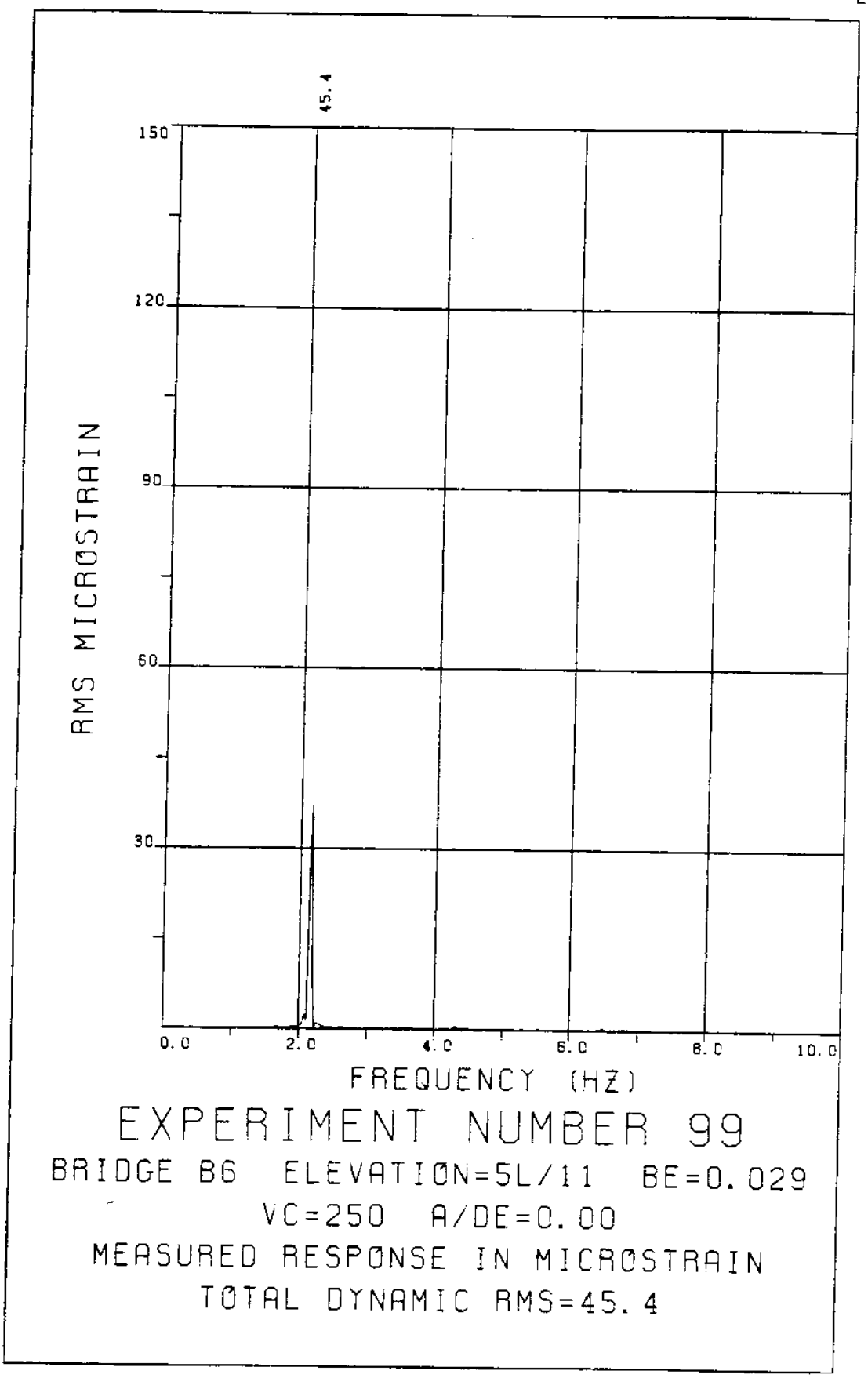

EXPERIMENT NUMBER 99

BRIDGE B6 ELEVATION=5L/11 BE=0.029

VC=250 A/DE=0.00

MEASURED RESPONSE IN MICROSTRAIN

TOTAL DYNAMIC RMS=45.4

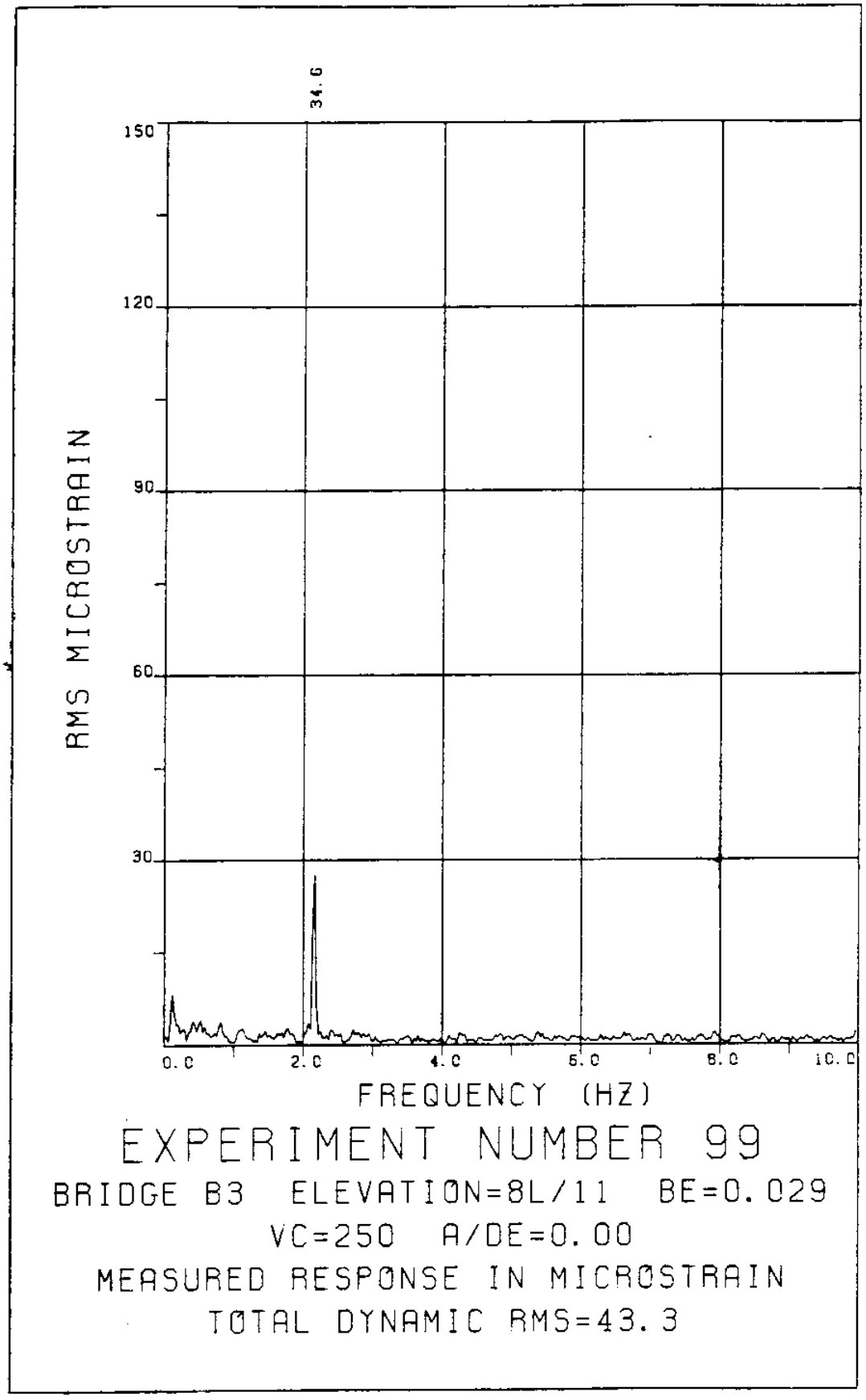

EXPERIMENT NUMBER 99

BRIDGE B3 ELEVATION=8L/11 BE=0.029

VC=250 A/DE=0.00

MEASURED RESPONSE IN MICROSTRAIN

TOTAL DYNAMIC RMS=43.3

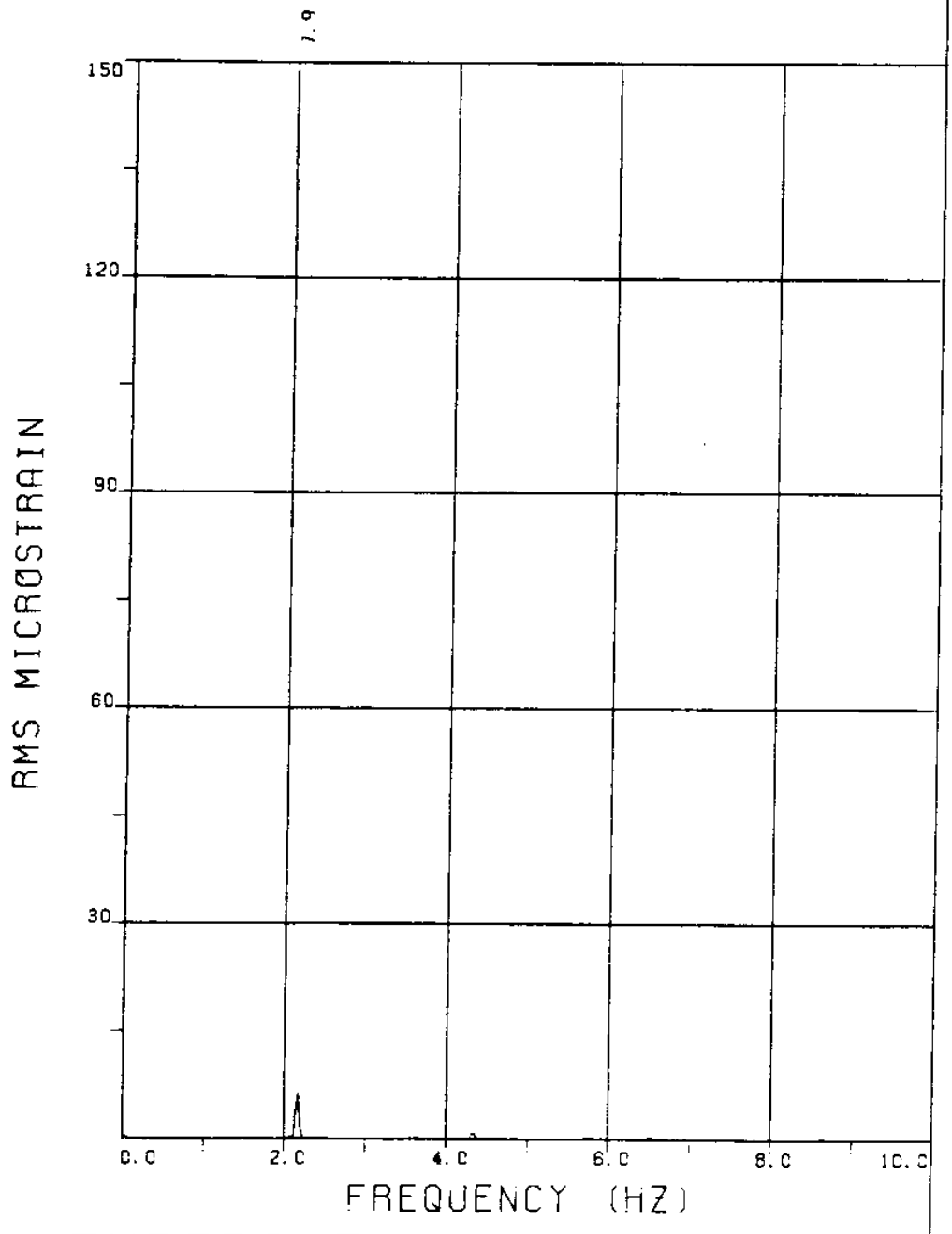

EXPERIMENT NUMBER 99

BRIDGE A9 ELEVATION=2L/11 BE=0.029

VC=250 A/DE=0.00

MEASURED RESPONSE IN MICROSTRAIN

MEAN=67.8

TOTAL DYNAMIC RMS=8.1

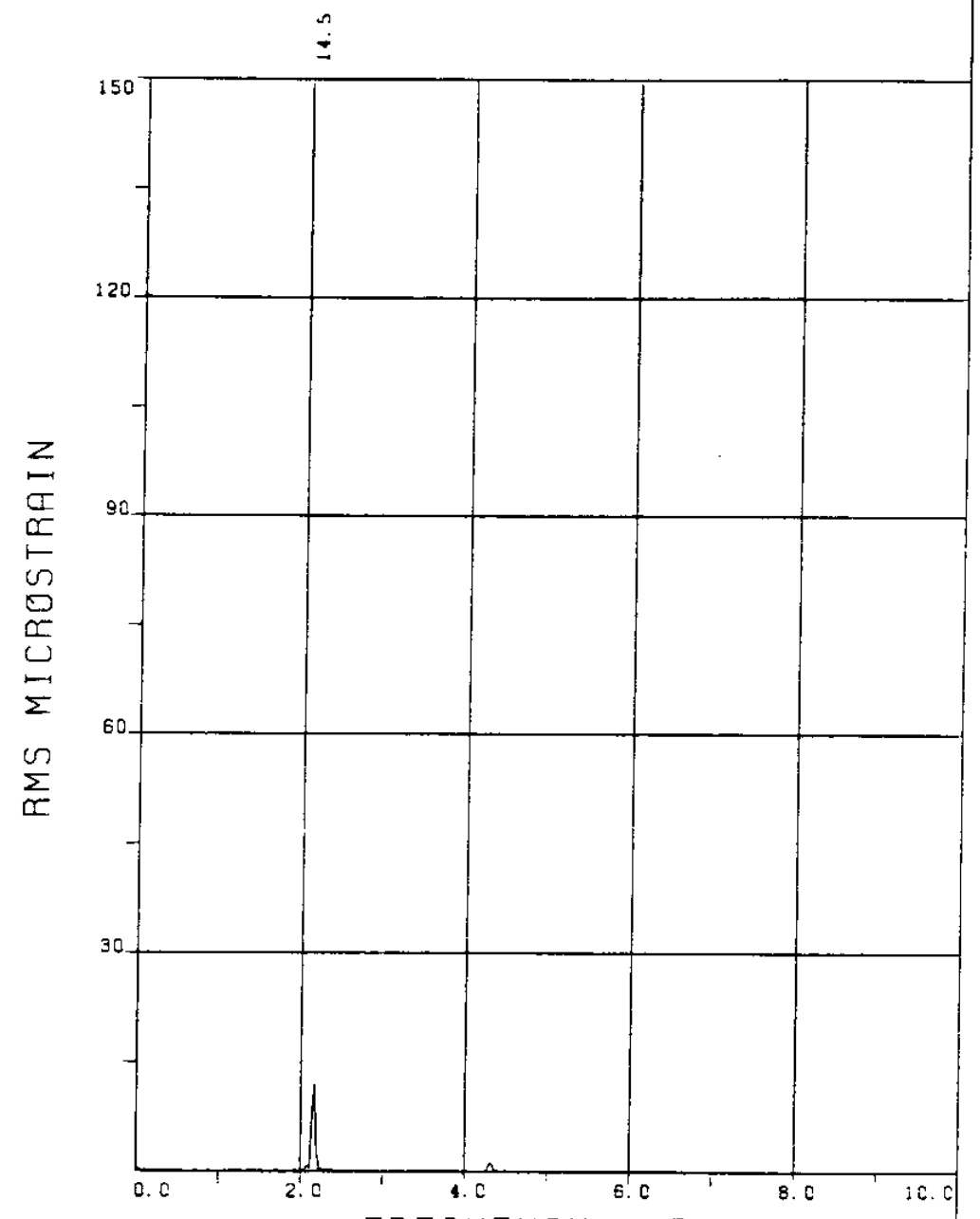

EXPERIMENT NUMBER 99

BRIDGE A7 ELEVATION=4L/11 BE=0.029

VC=250 A/DE=0.00

MEASURED RESPONSE IN MICROSTRAIN

MEAN=95.5

TOTAL DYNAMIC RMS=14.7

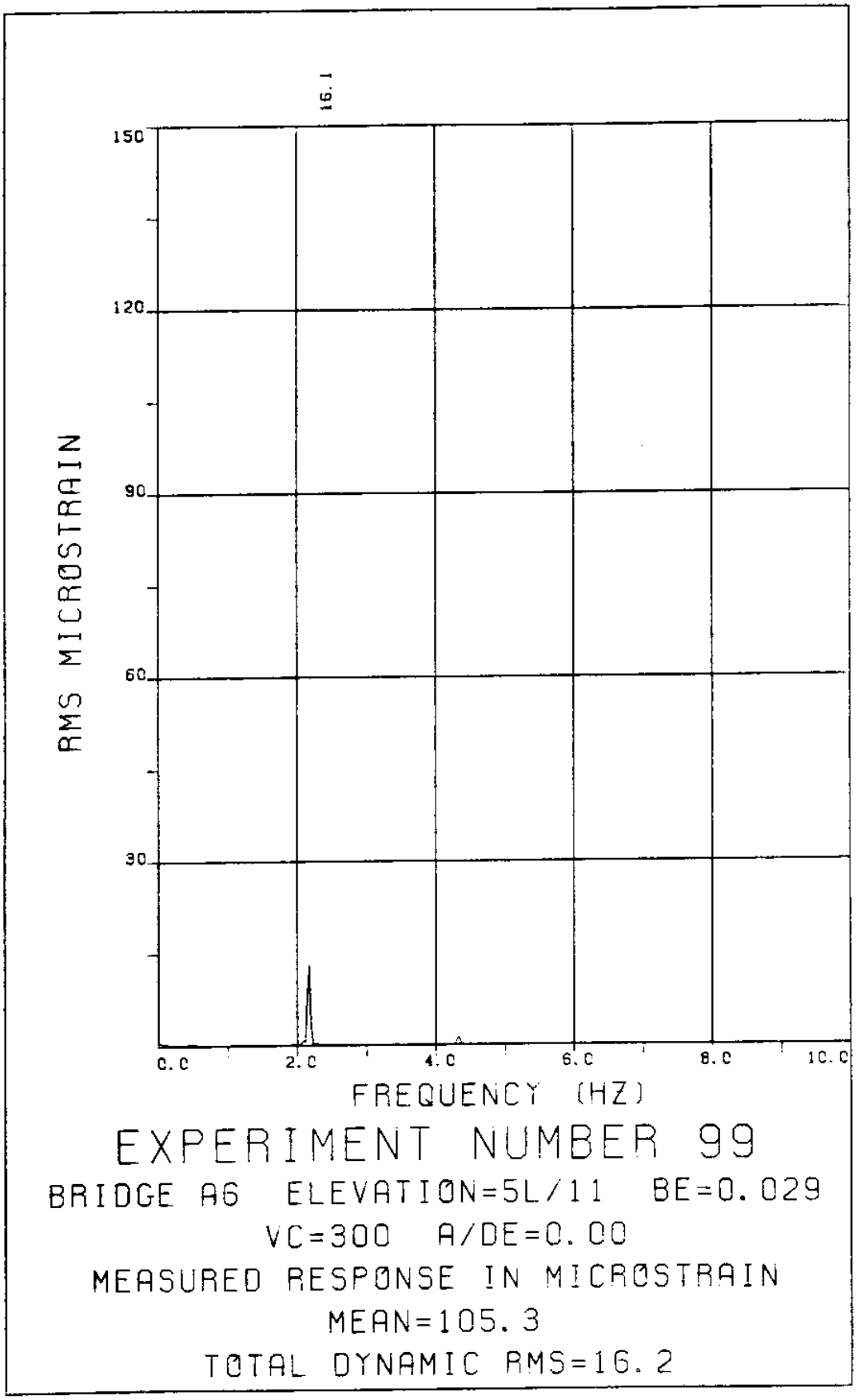

EXPERIMENT NUMBER 99

BRIDGE A6 ELEVATION=5L/11 BE=0.029

VC=300 A/DE=0.00

MEASURED RESPONSE IN MICROSTRAIN

MEAN=105.3

TOTAL DYNAMIC RMS=16.2

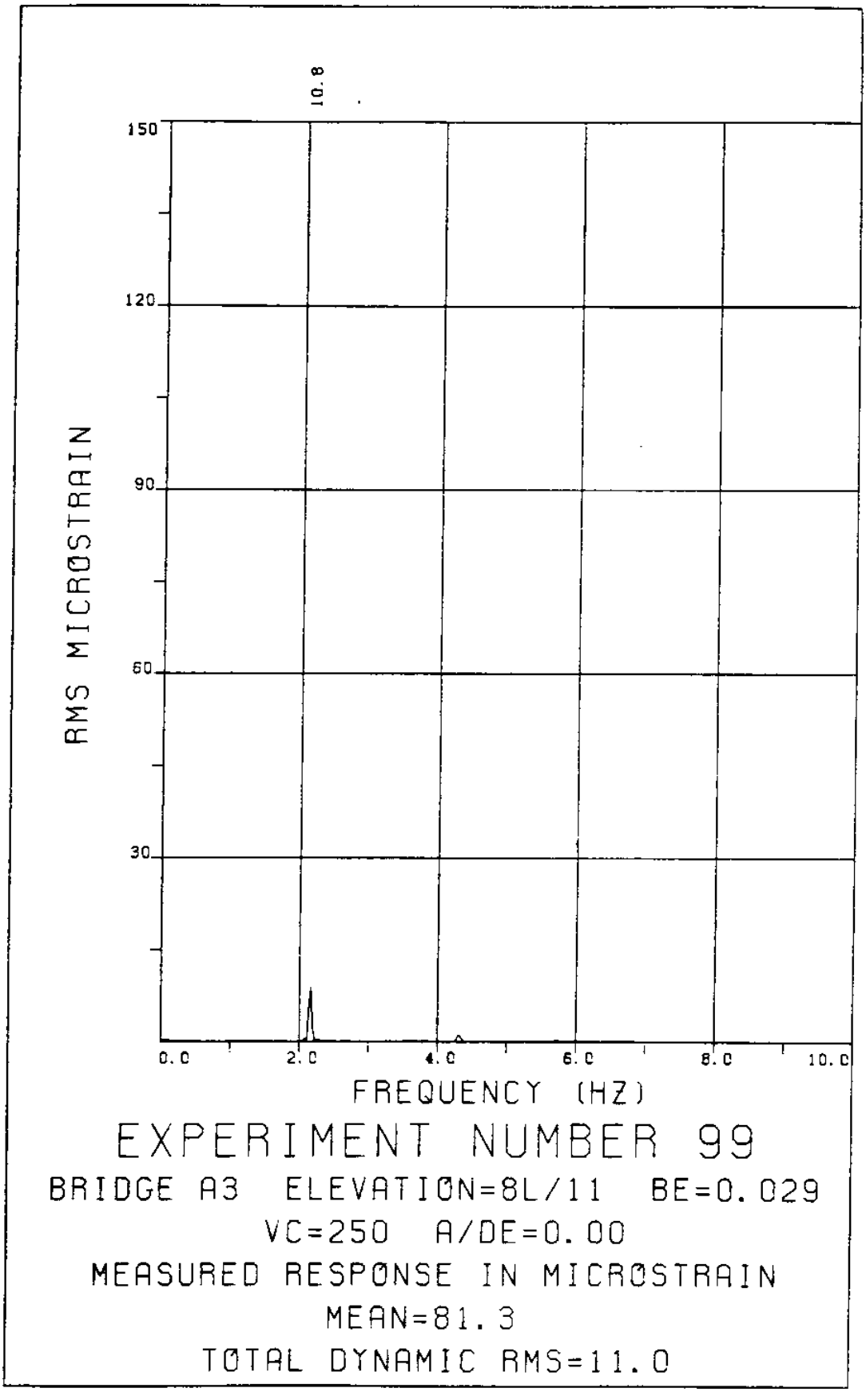
10.8
150
120
90
60
30
RMS MICROSTRAIN
0.0
2.0
4.0
6.0
8.0
10.0
FREQUENCY (HZ)
EXPERIMENT NUMBER 99
BRIDGE A3 ELEVATION=8L/11 BE=0.029
VC=250 A/DE=0.00
MEASURED RESPONSE IN MICROSTRAIN
MEAN=81.3
TOTAL DYNAMIC RMS=11.0

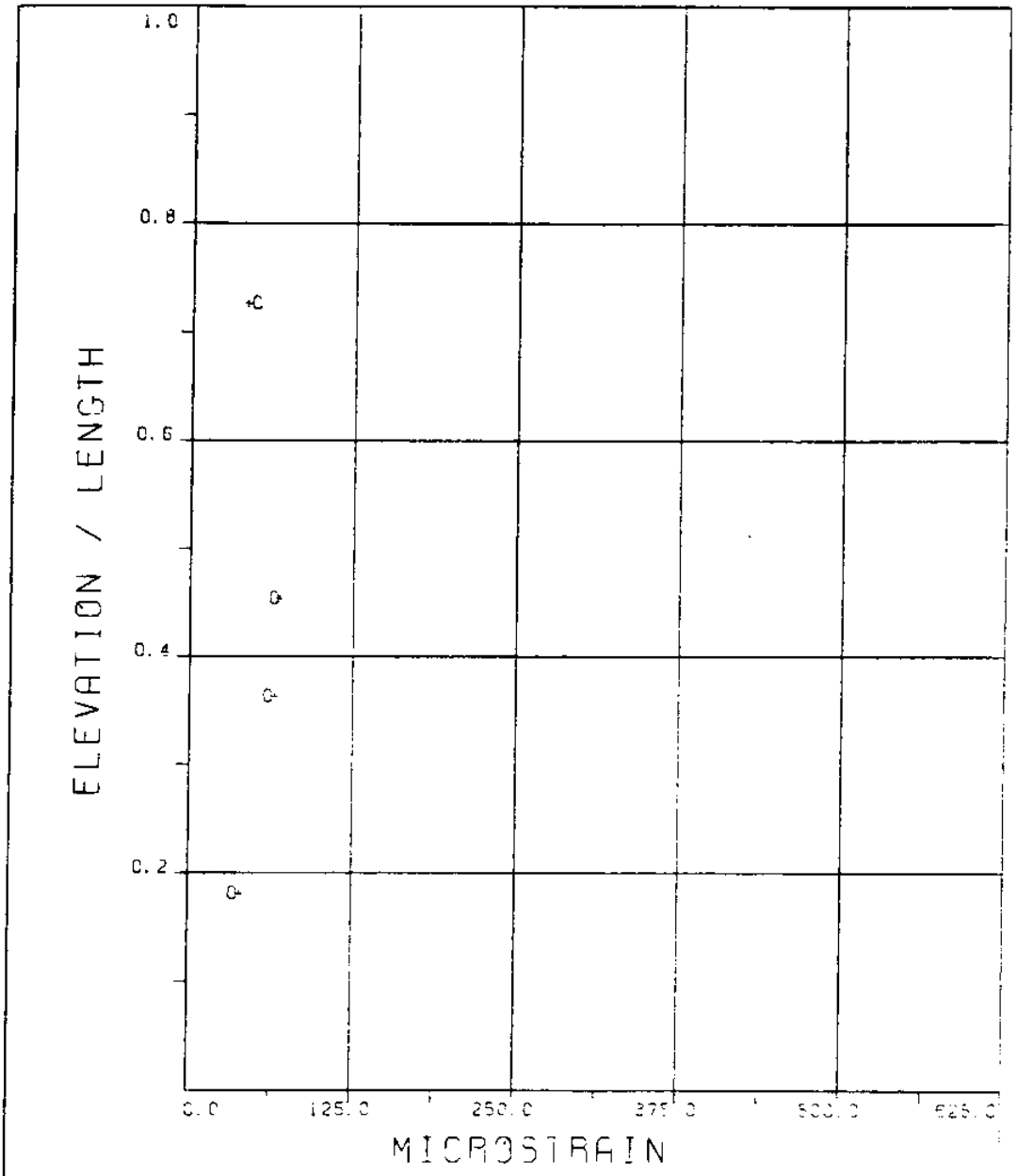

EXPERIMENT NUMBER 99

VC=250 S/DE=0.00

DYNAMIC RESPONSE AT F=FR IN PLANE B
o o o EXPERIMENT

MAXIMUM DYNAMIC RESPONSE IN PLANE B
+ + + EXPERIMENT

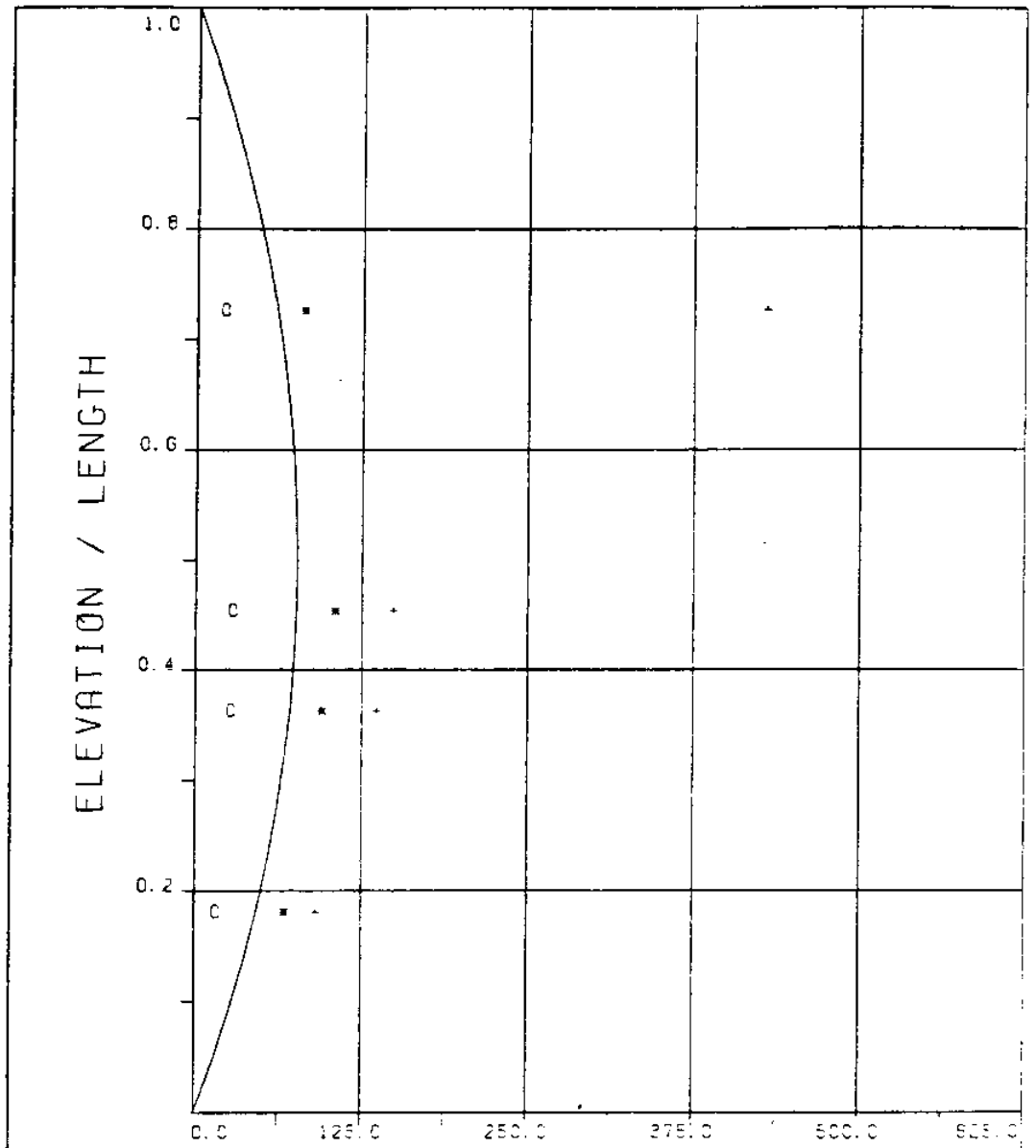

EXPERIMENT NUMBER 93

VC=250 A/DE=0.00

STATIC RESPONSE IN PLANE A

_____ THEORY * * * EXPERIMENT

MAXIMUM DYNAMIC RESPONSE IN PLANE A

o o o EXPERIMENT

MAXIMUM RESPONSE

_____ THEORY + + + EXPERIMENT

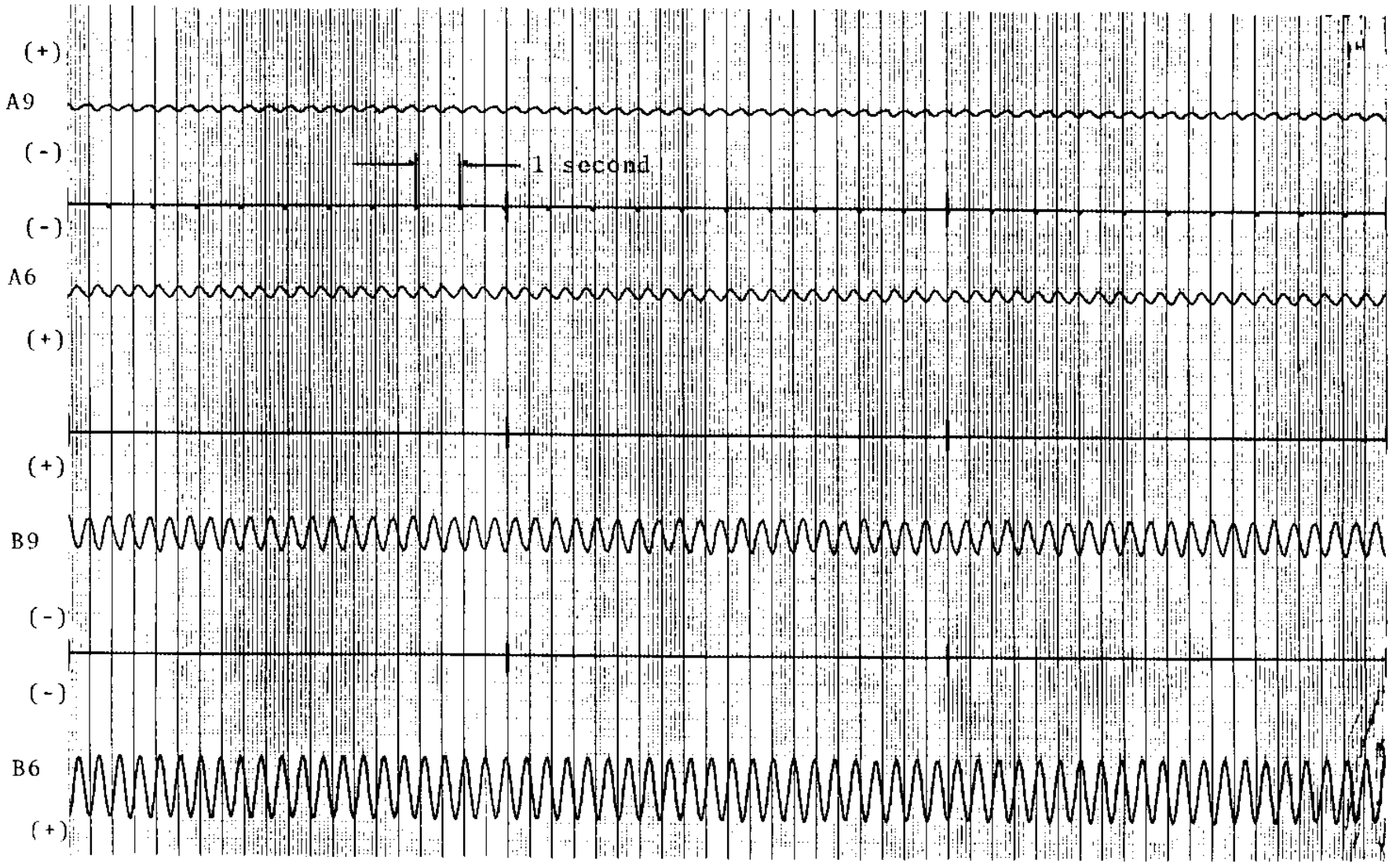

FIGURE 99T: A BRIDGES: 15.3 MICROSTRAIN/DIVISION;
B BRIDGES: 7.6 MICROSTRAIN/DIVISION

EXPERIMENT 97

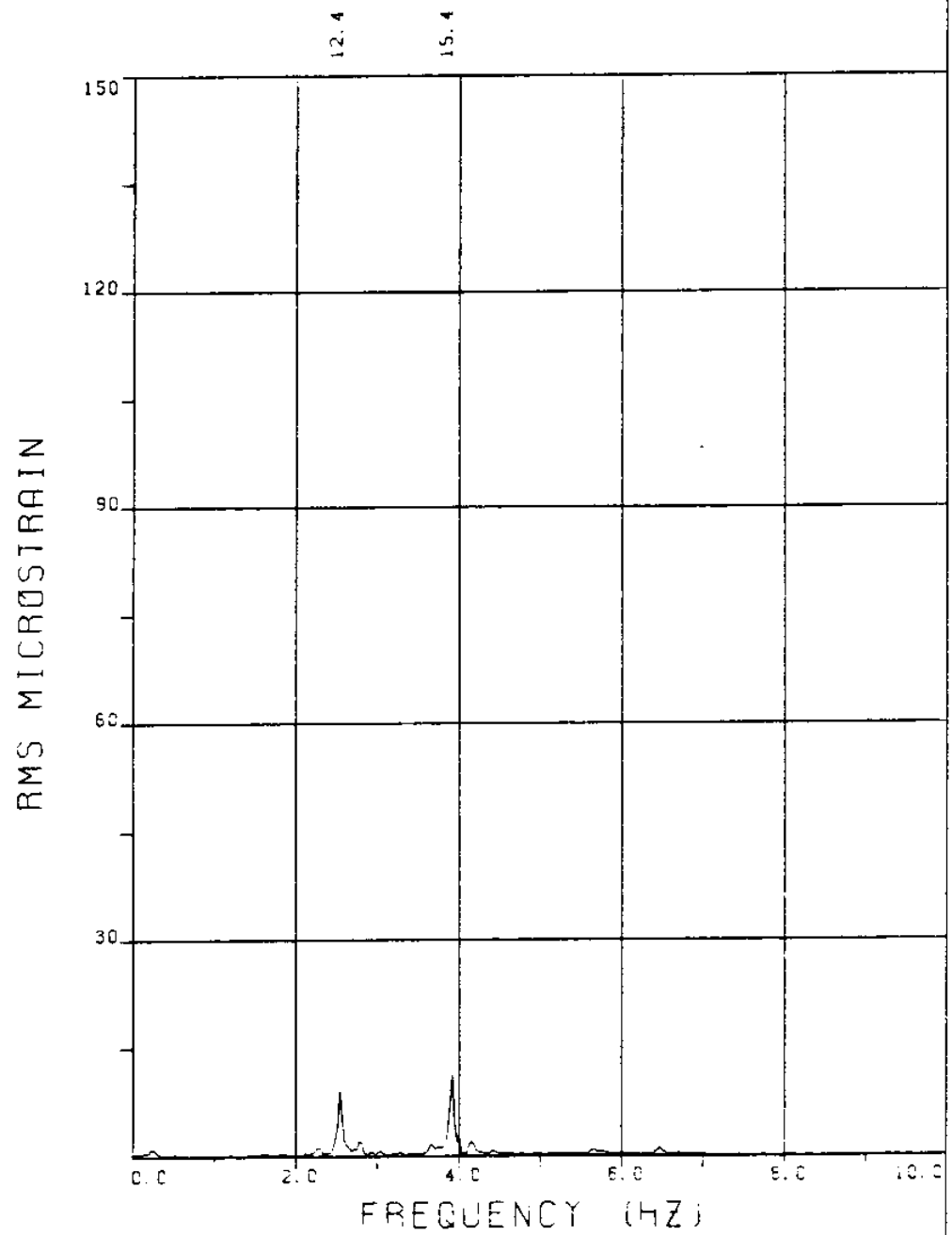

EXPERIMENT NUMBER 97

BRIDGE B9 ELEVATION=2L/11 BE=0.029

VC=300 A/DE=0.00

MEASURED RESPONSE IN MICROSTRAIN

TOTAL DYNAMIC RMS=20.2

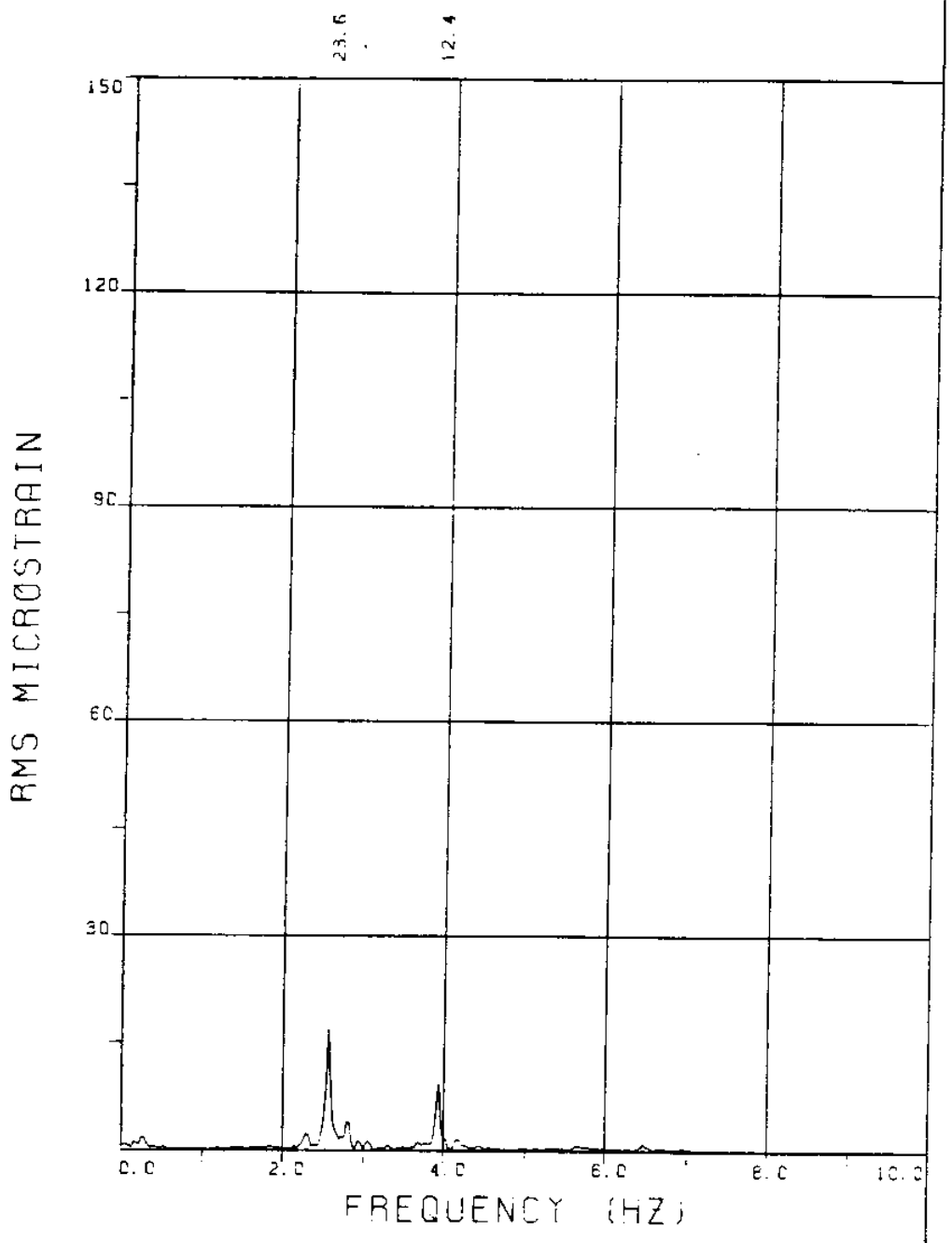

EXPERIMENT NUMBER 97

BRIDGE B7 ELEVATION=4L/11 BE=0.029

VC=300 A/DE=0.00

MEASURED RESPONSE IN MICROSTRAIN

TOTAL DYNAMIC RMS=27.2

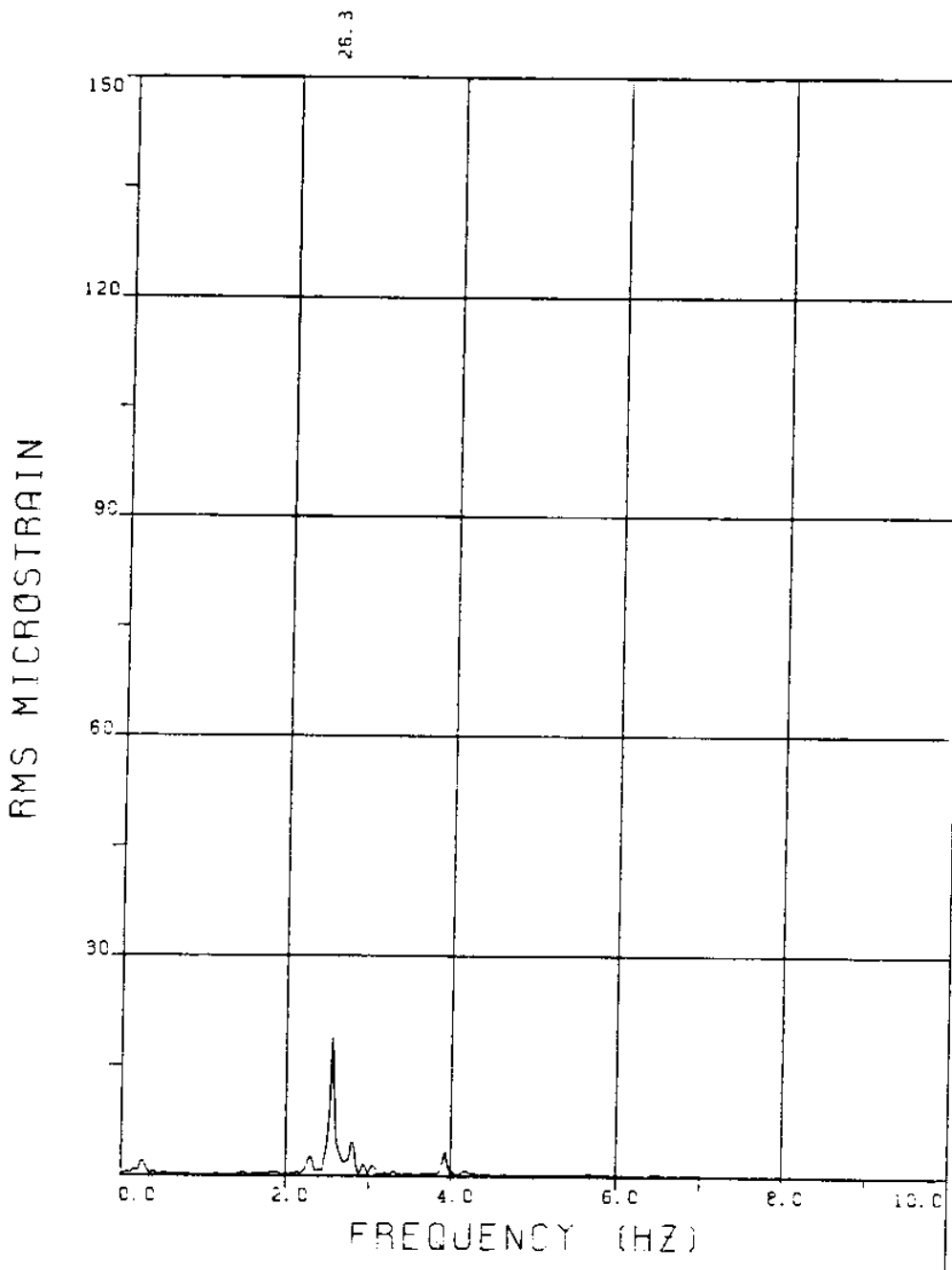

EXPERIMENT NUMBER 97

BRIDGE B6 ELEVATION=5L/11 BE=0.029

VC=300 A/DE=0.00

MEASURED RESPONSE IN MICROSTRAIN

TOTAL DYNAMIC RMS=27.1

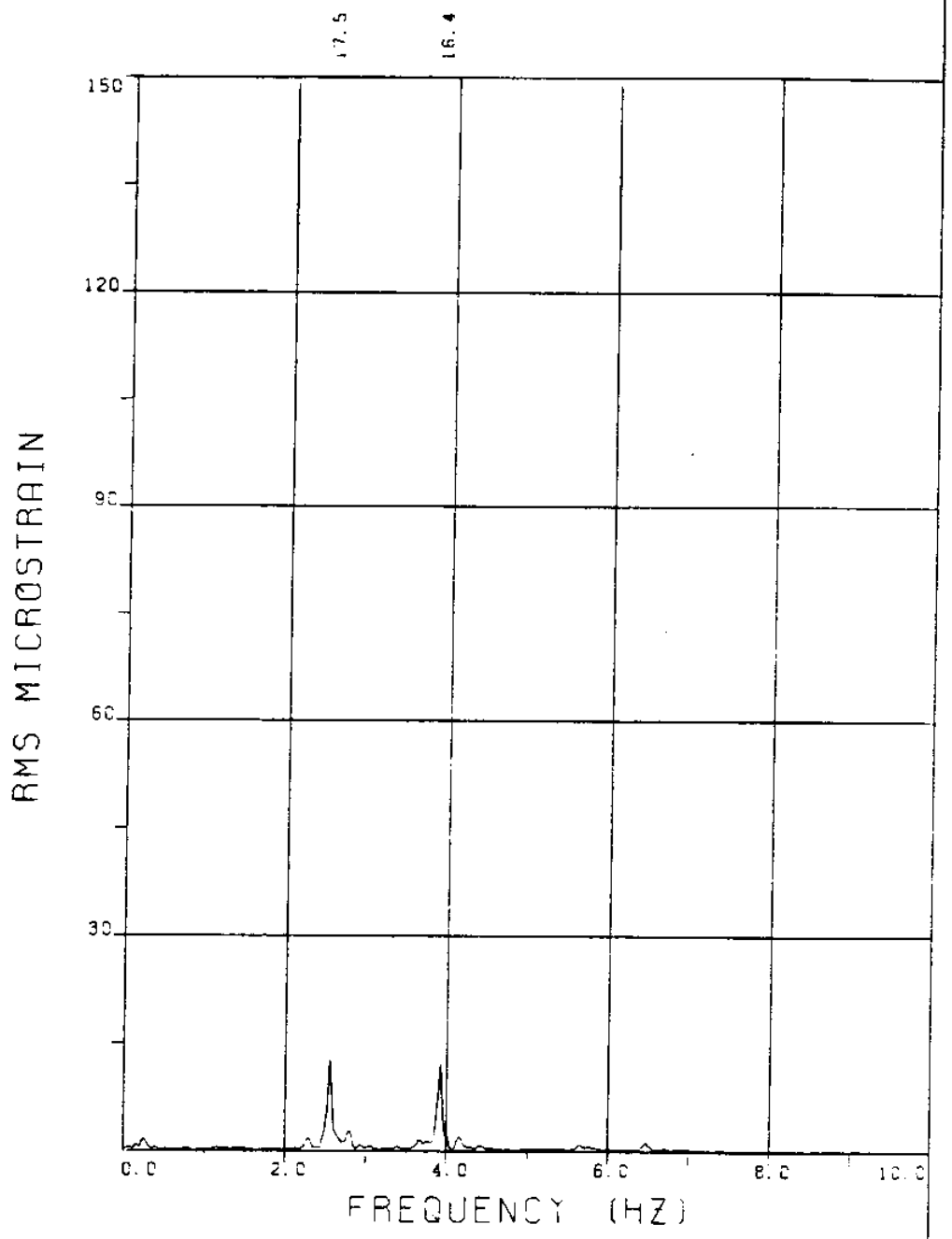

EXPERIMENT NUMBER 97

BRIDGE B3 ELEVATION=8L/11 BE=0.029

VC=300 A/DE=0.00

MEASURED RESPONSE IN MICROSTRAIN

TOTAL DYNAMIC RMS=24.5

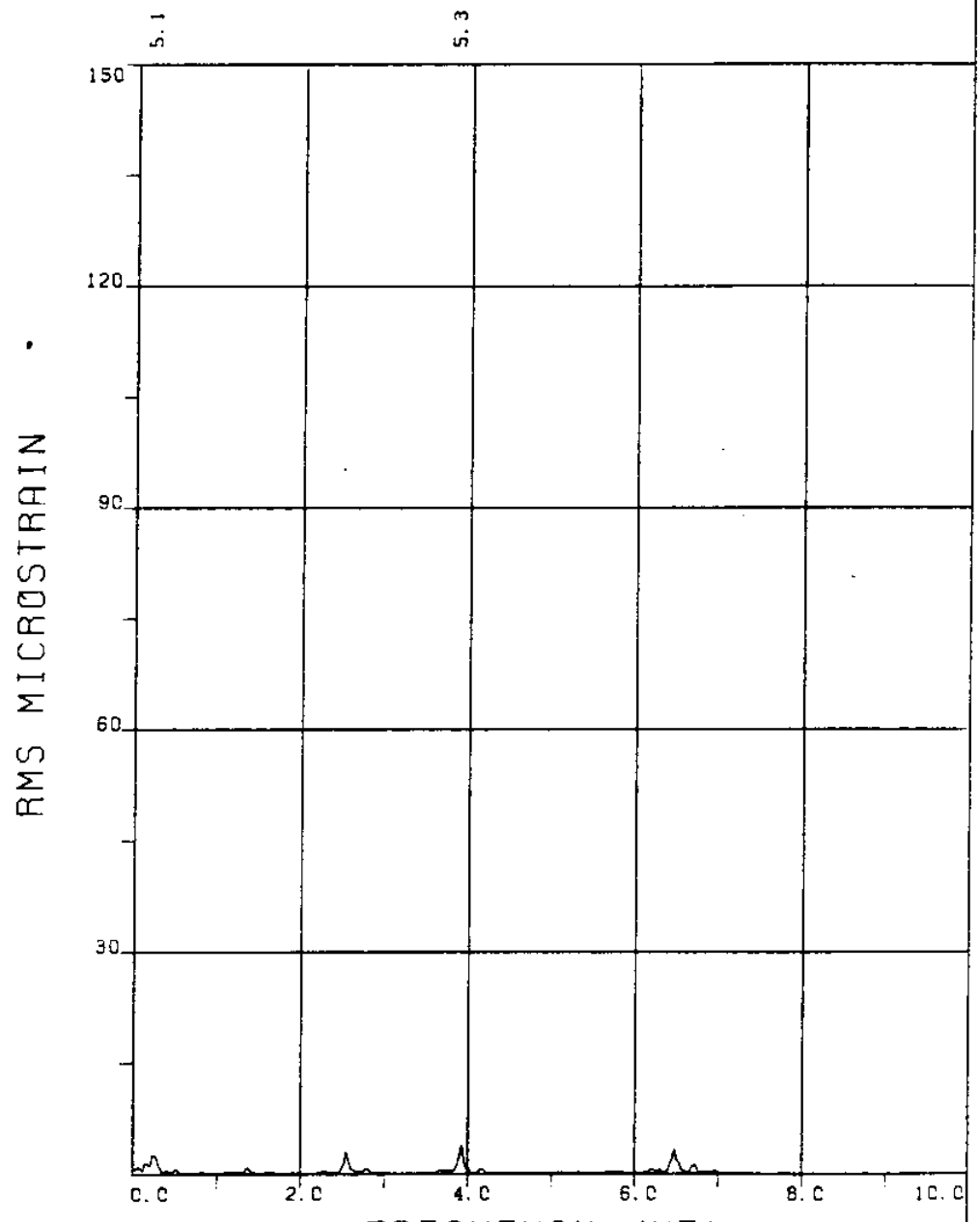

EXPERIMENT NUMBER 97

BRIDGE A9 ELEVATION=2L/11 BE=0.029

VC=300 A/DE=0.00

MEASURED RESPONSE IN MICROSTRAIN

MEAN=95.2

TOTAL DYNAMIC RMS=10.3

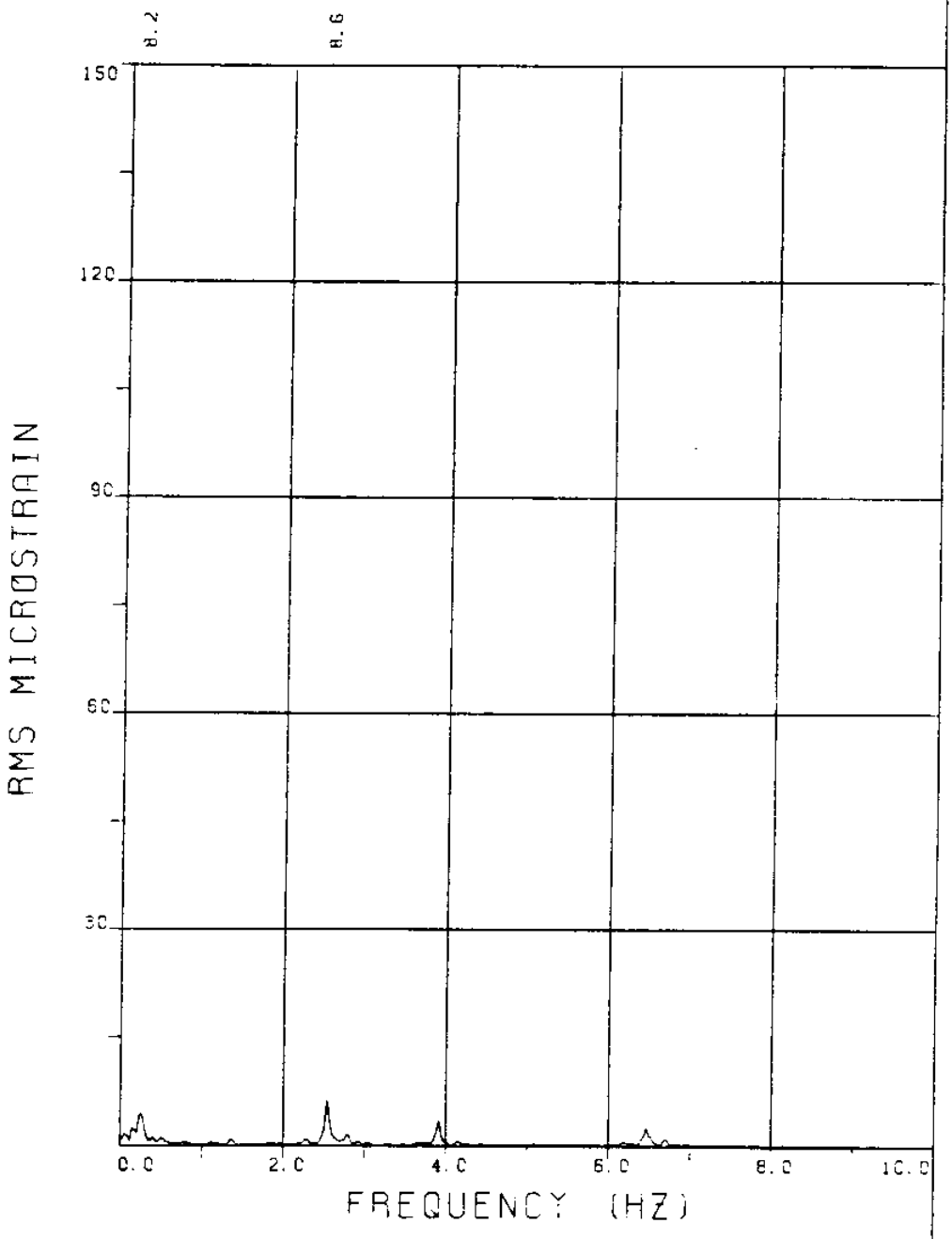

EXPERIMENT NUMBER 97

BRIDGE A7 ELEVATION=4L/11 BE=0.029

VC=300 A/DE=0.00

MEASURED RESPONSE IN MICROSTRAIN

MEAN=134.7

TOTAL DYNAMIC RMS=13.6

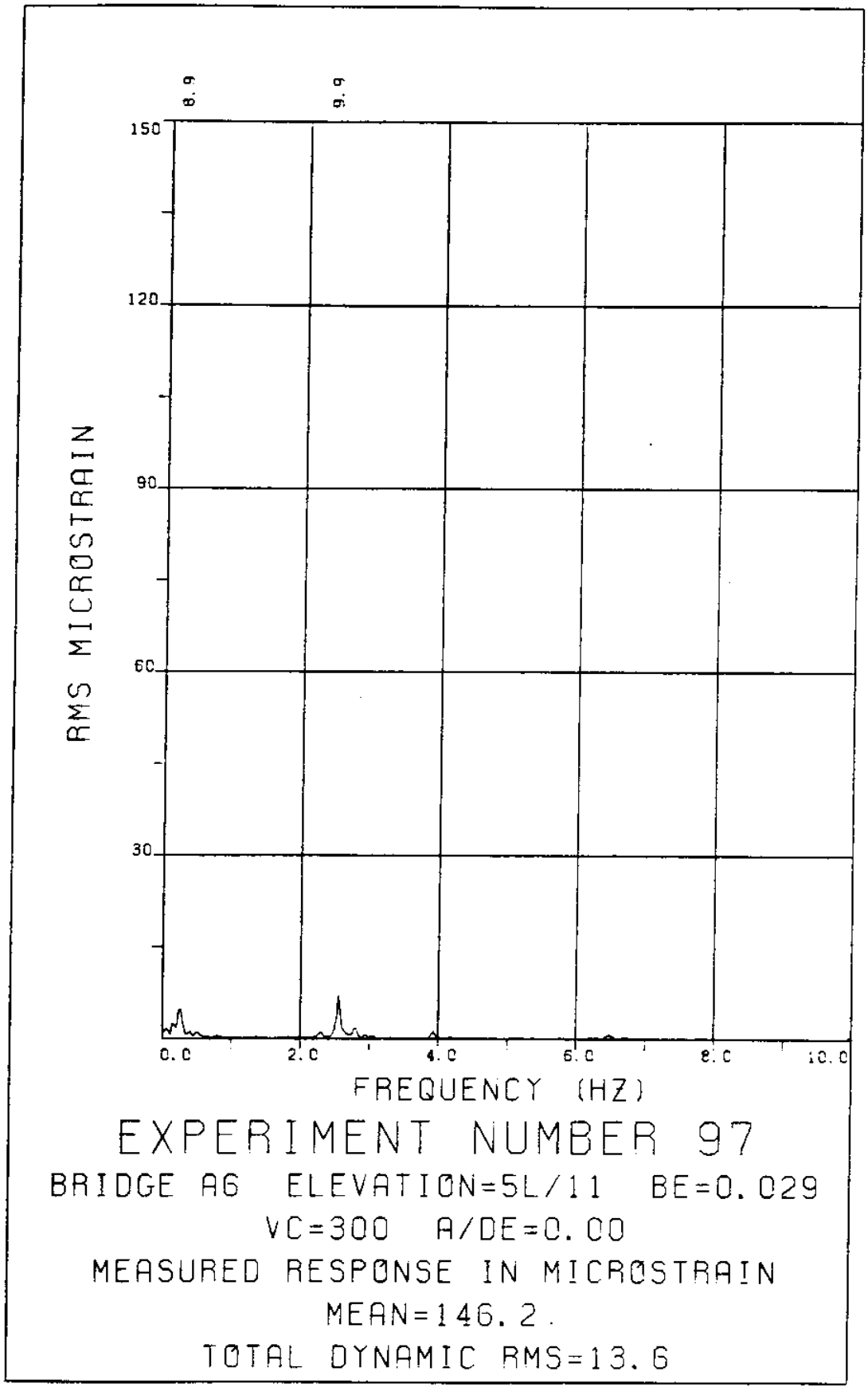

EXPERIMENT NUMBER 97

BRIDGE A6 ELEVATION=5L/11 BE=0.029

VC=300 A/DE=0.00

MEASURED RESPONSE IN MICROSTRAIN

MEAN=146.2.

TOTAL DYNAMIC RMS=13.6

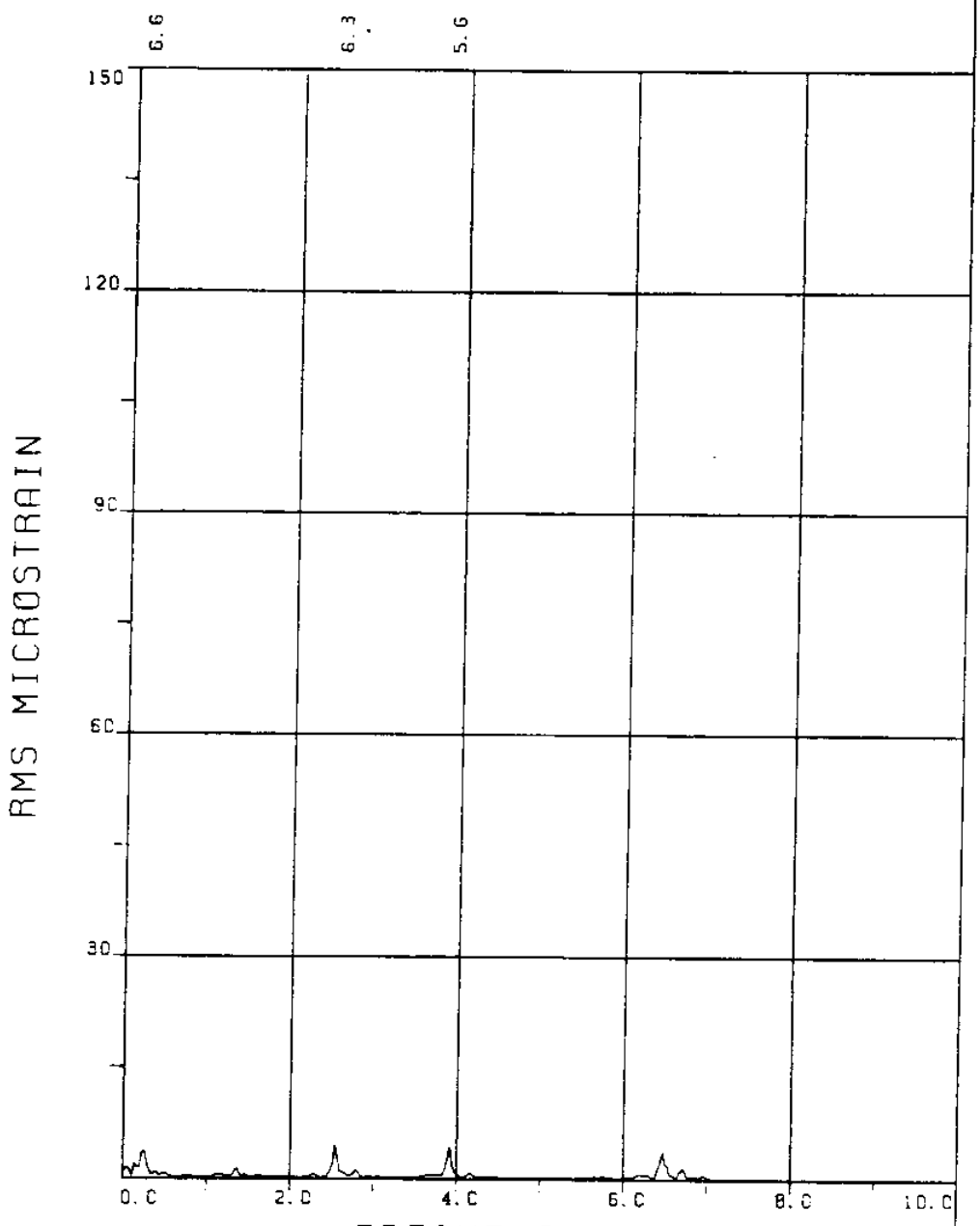

EXPERIMENT NUMBER 97

BRIDGE A3 ELEVATION=8L/11 BE=0.029

VC=300 A/DE=0.00

MEASURED RESPONSE IN MICROSTRAIN

MEAN=114.3

TOTAL DYNAMIC RMS=12.7

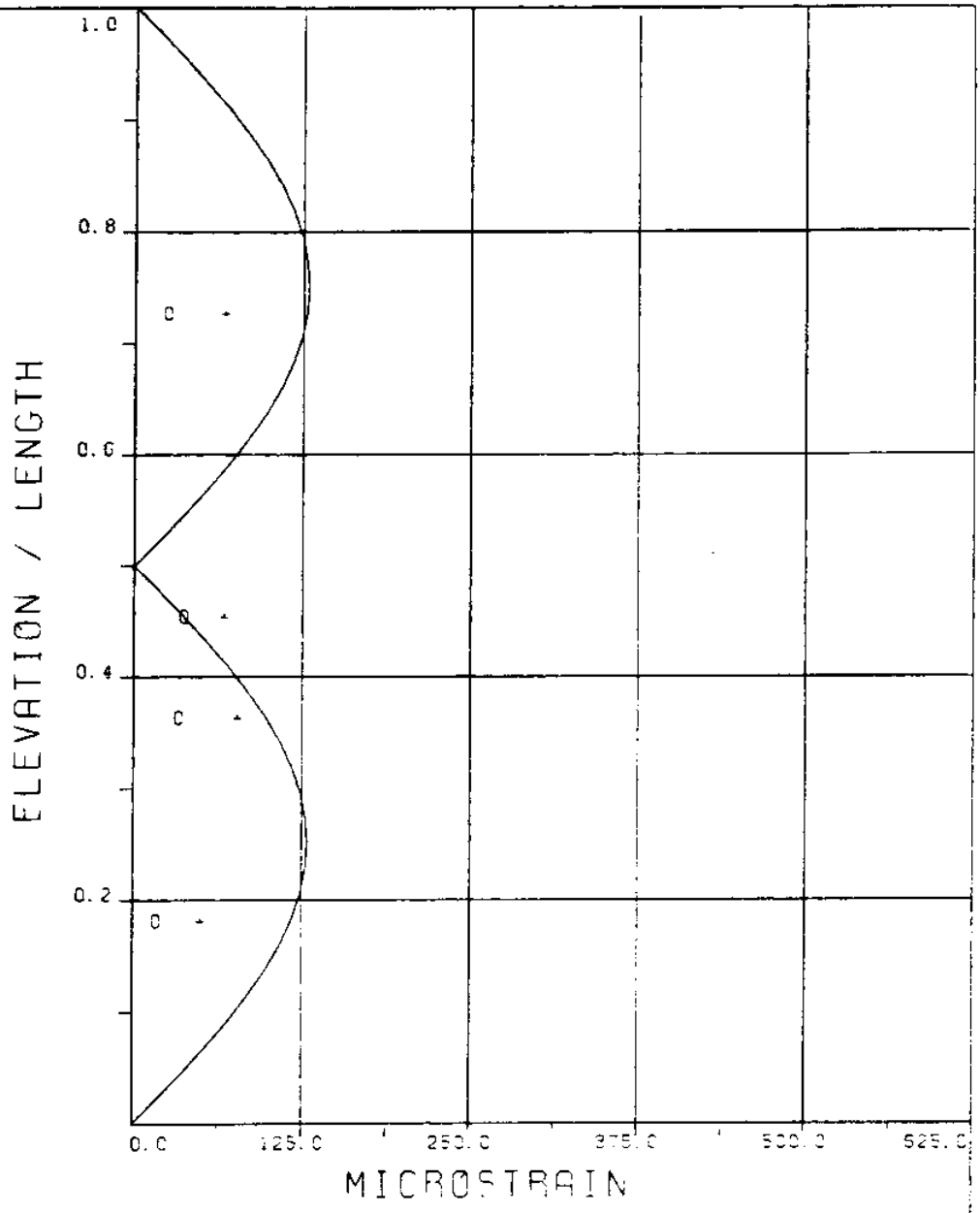

EXPERIMENT NUMBER 97

VC=300 A/DE=0.00

DYNAMIC RESPONSE AT F=FR IN PLANE B

——— THEORY c c c EXPERIMENT

MAXIMUM DYNAMIC RESPONSE IN PLANE B

——— THEORY + + + EXPERIMENT

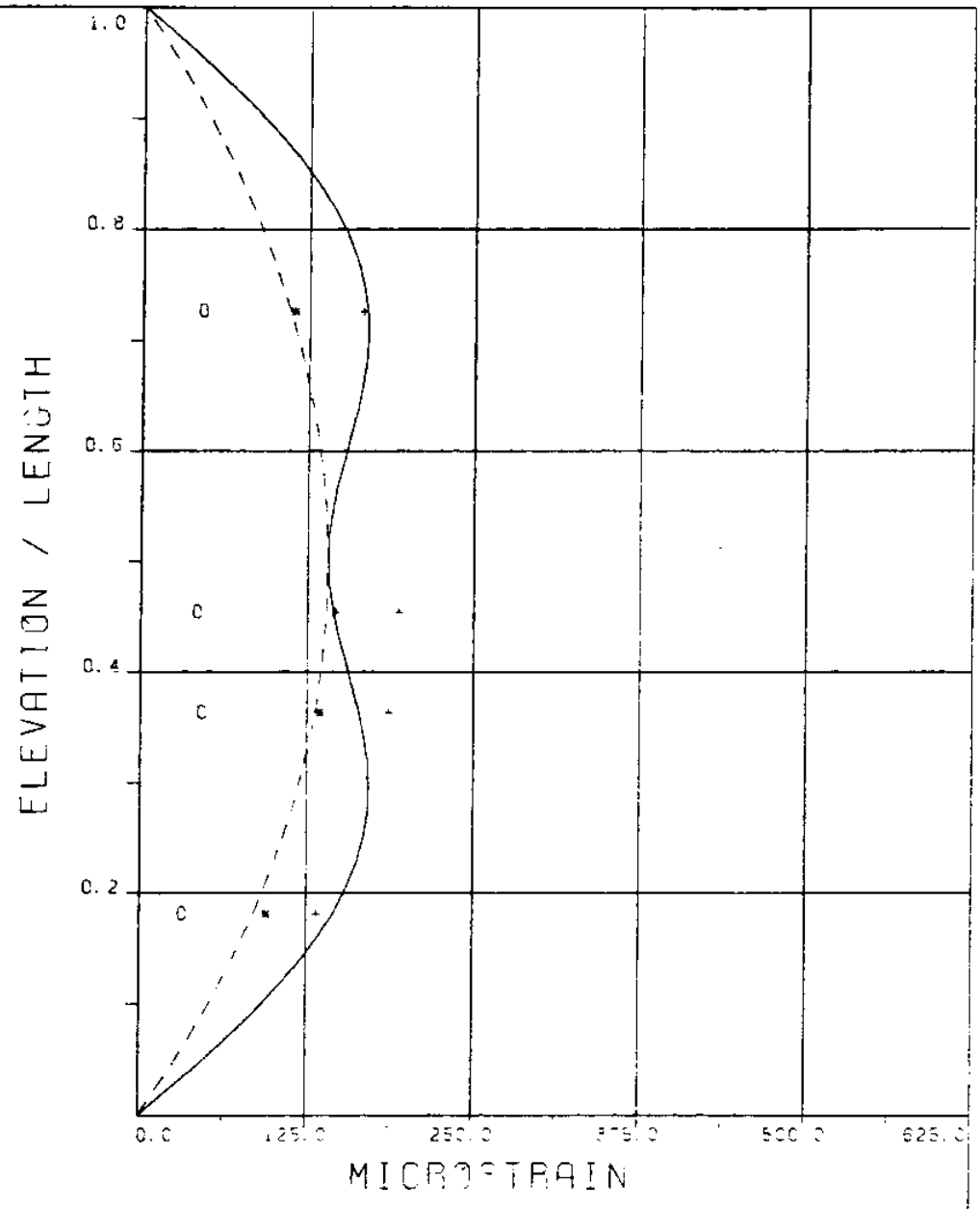

EXPERIMENT NUMBER 97

VC=300 A/DE=0.00

STATIC RESPONSE IN PLANE A

– – – – – THEORY * * * EXPERIMENT

MAXIMUM DYNAMIC RESPONSE IN PLANE A

o o o EXPERIMENT

MAXIMUM RESPONSE

_____ THEORY + + + EXPERIMENT

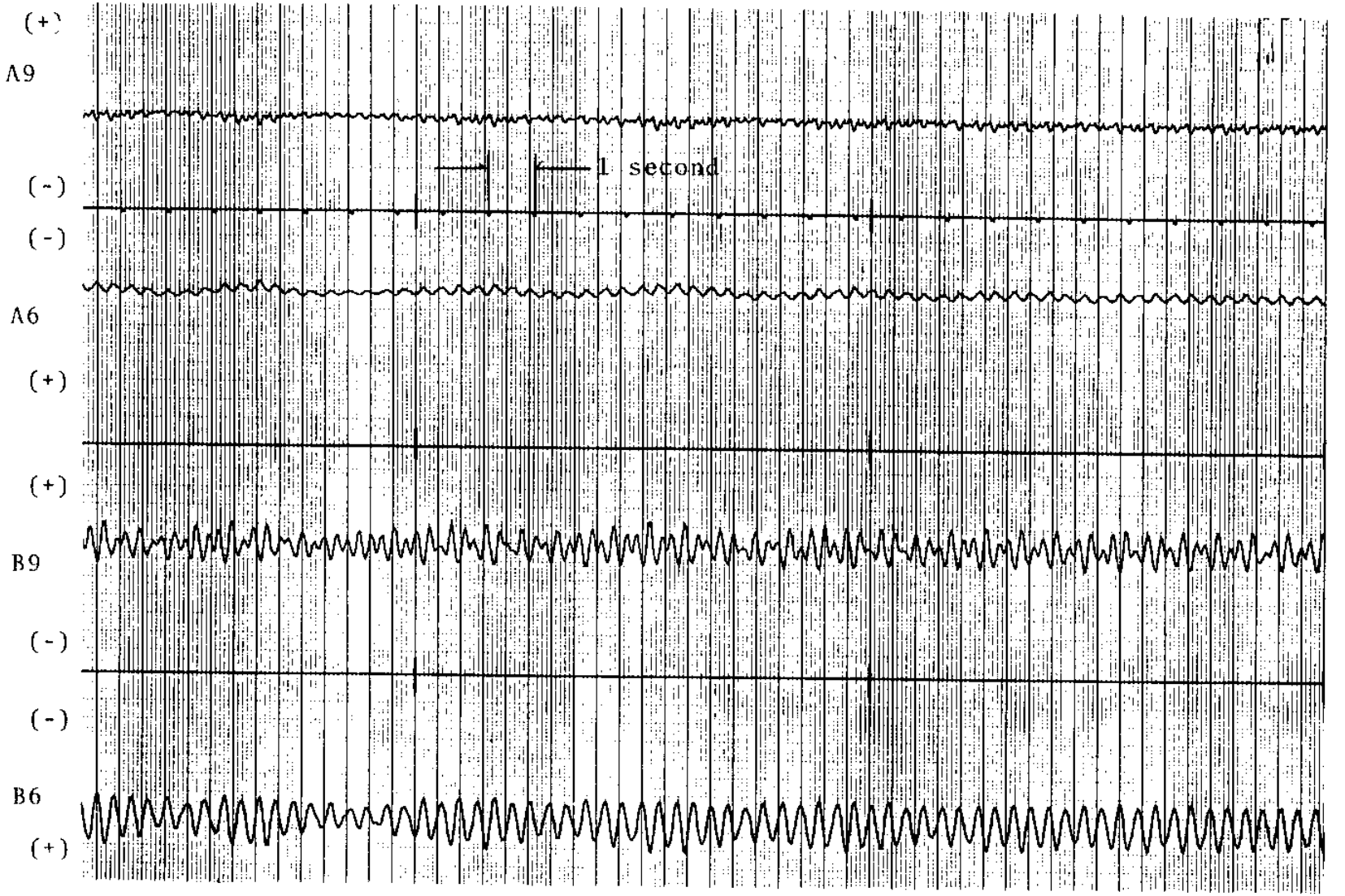

FIGURE 97Ta: A BRIDGES: 15.3 MICROSTRAIN/DIVISION; B BRIDGES 7.6 MICROSTRAIN/DIVISION

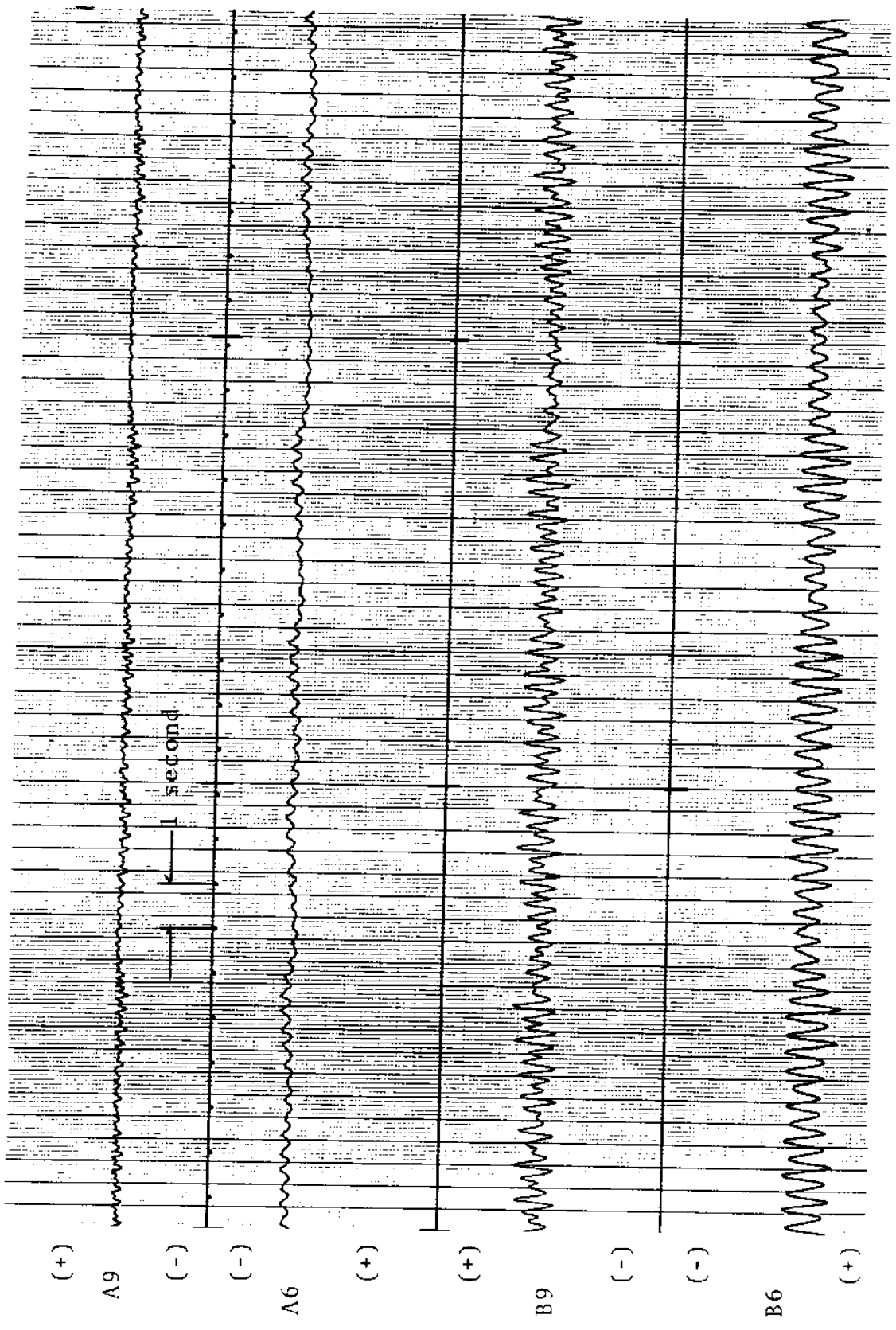

FIGURE 97b: A BRIDGES: 15.3 MICROSTRAIN/DIVISION
B BRIDGES: 7.6 MICROSTRAIN/DIVISION

EXPERIMENT 95

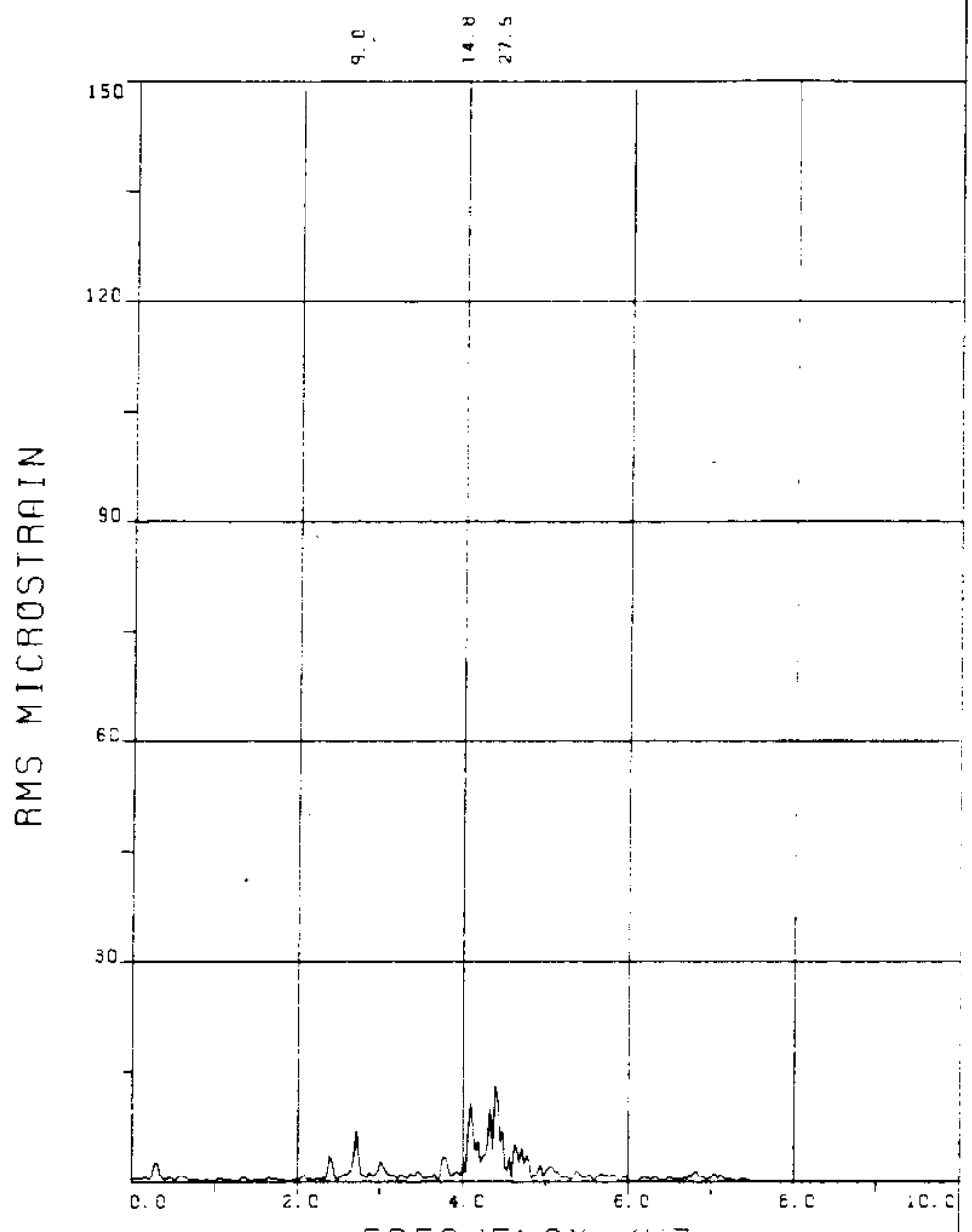

EXPERIMENT NUMBER 95

BRIDGE B9 ELEVATION=2L/11 BE=0.029

VC=350 A/DE=0.00

MEASURED RESPONSE IN MICROSTRAIN

TOTAL DYNAMIC RMS=34.2

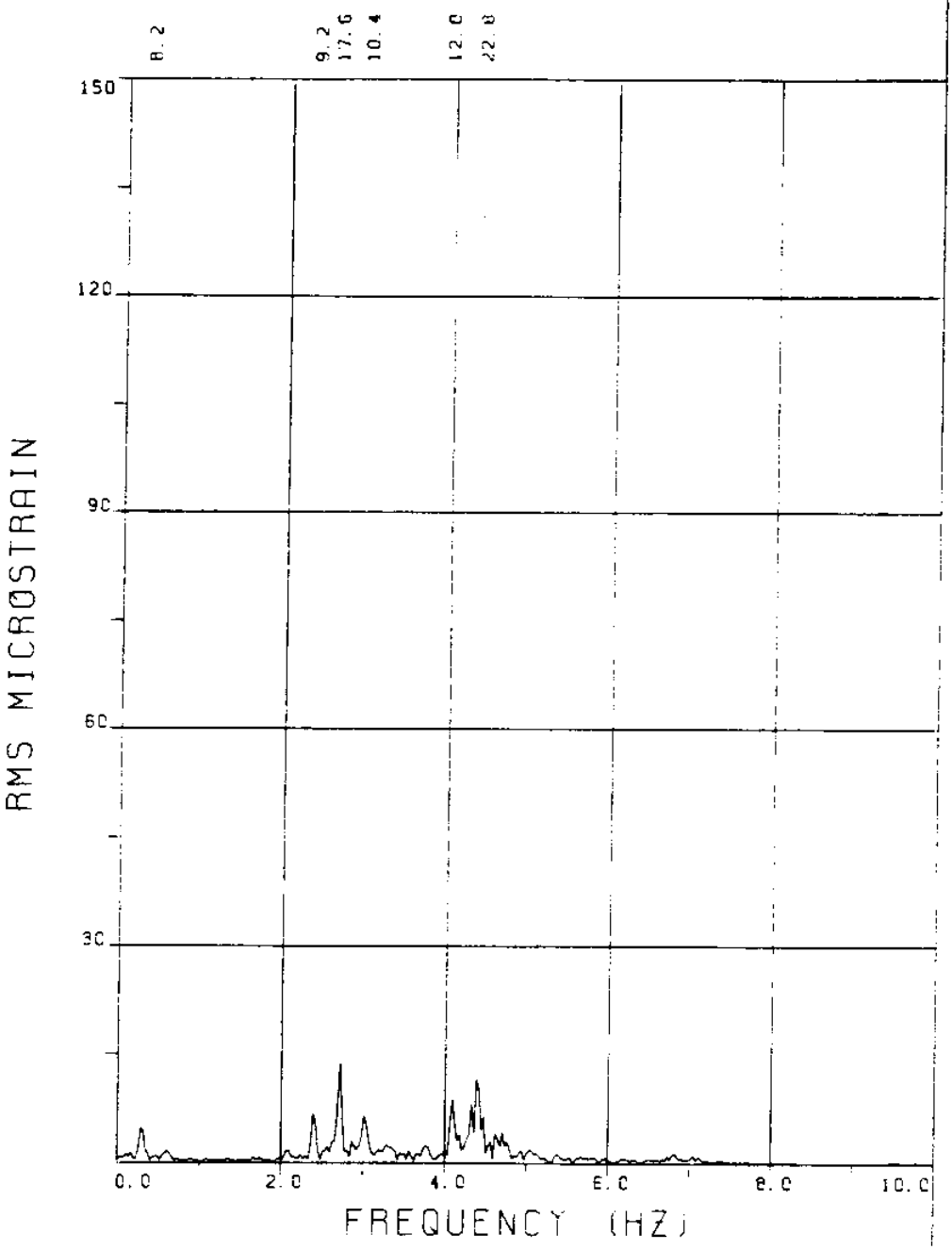

EXPERIMENT NUMBER 95

BRIDGE B7 ELEVATION=4L/11 BE=0.029

VC=350 A/DE=0.00

MEASURED RESPONSE IN MICROSTRAIN

TOTAL DYNAMIC RMS=37.0

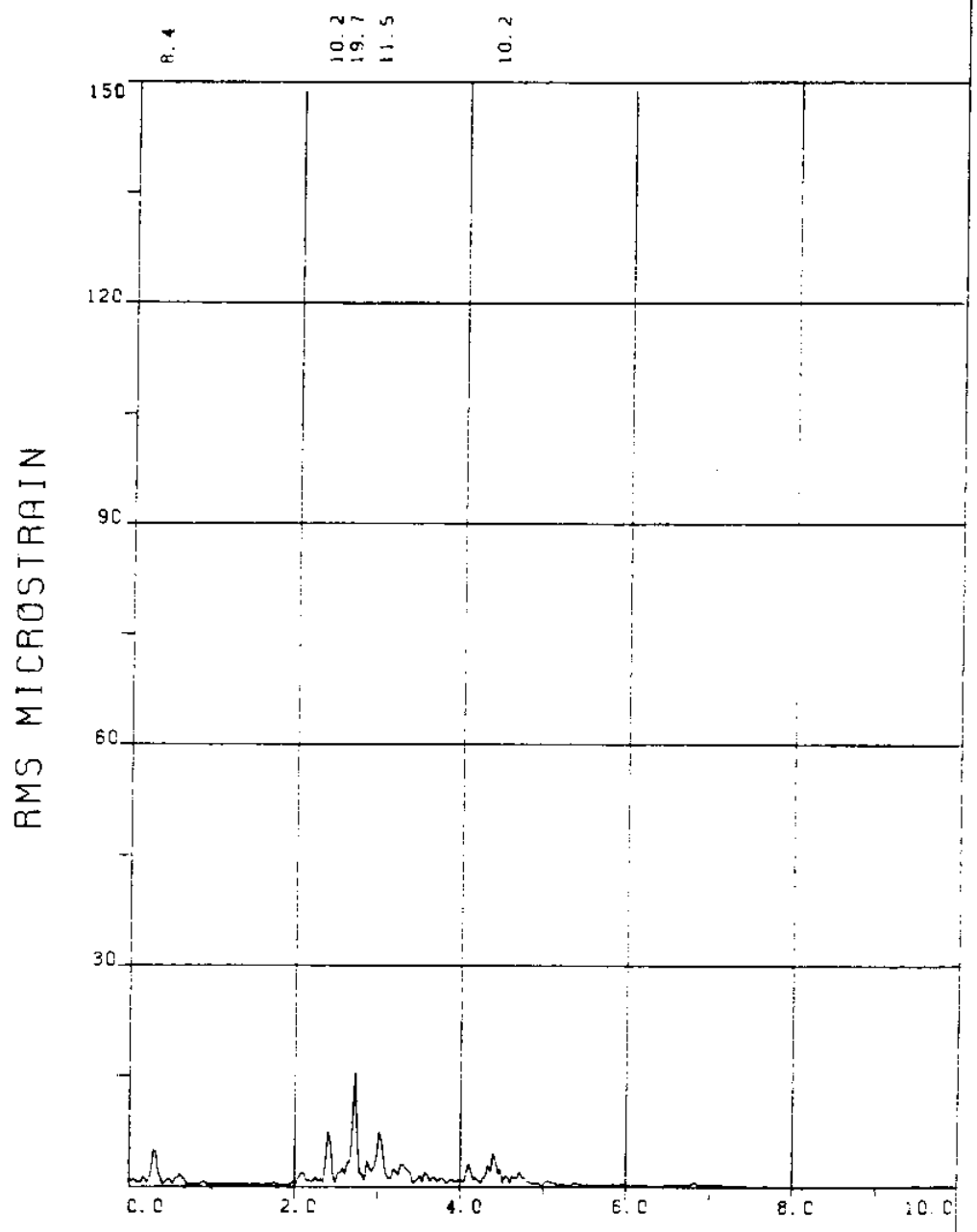

EXPERIMENT NUMBER 95

BRIDGE B6 ELEVATION=SL/11 BE=0.029

VC=350 A/DE=0.00

MEASURED RESPONSE IN MICROSTRAIN

TOTAL DYNAMIC RMS=30.8

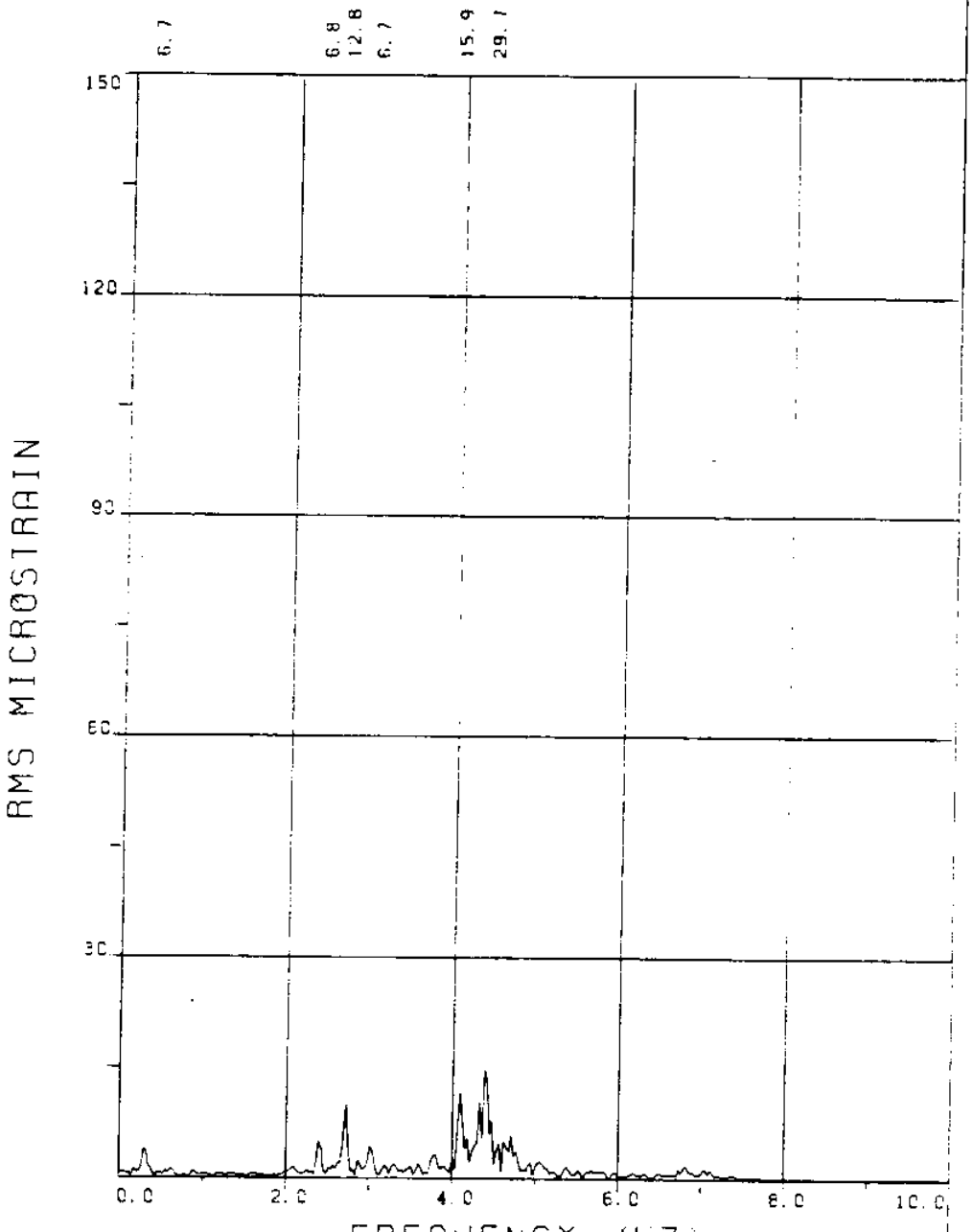

EXPERIMENT NUMBER 95

BRIDGE B3 ELEVATION=8L/11 BE=0.029

VC=350 A/DE=0.00

MEASURED RESPONSE IN MICROSTRAIN

TOTAL DYNAMIC RMS=39.2

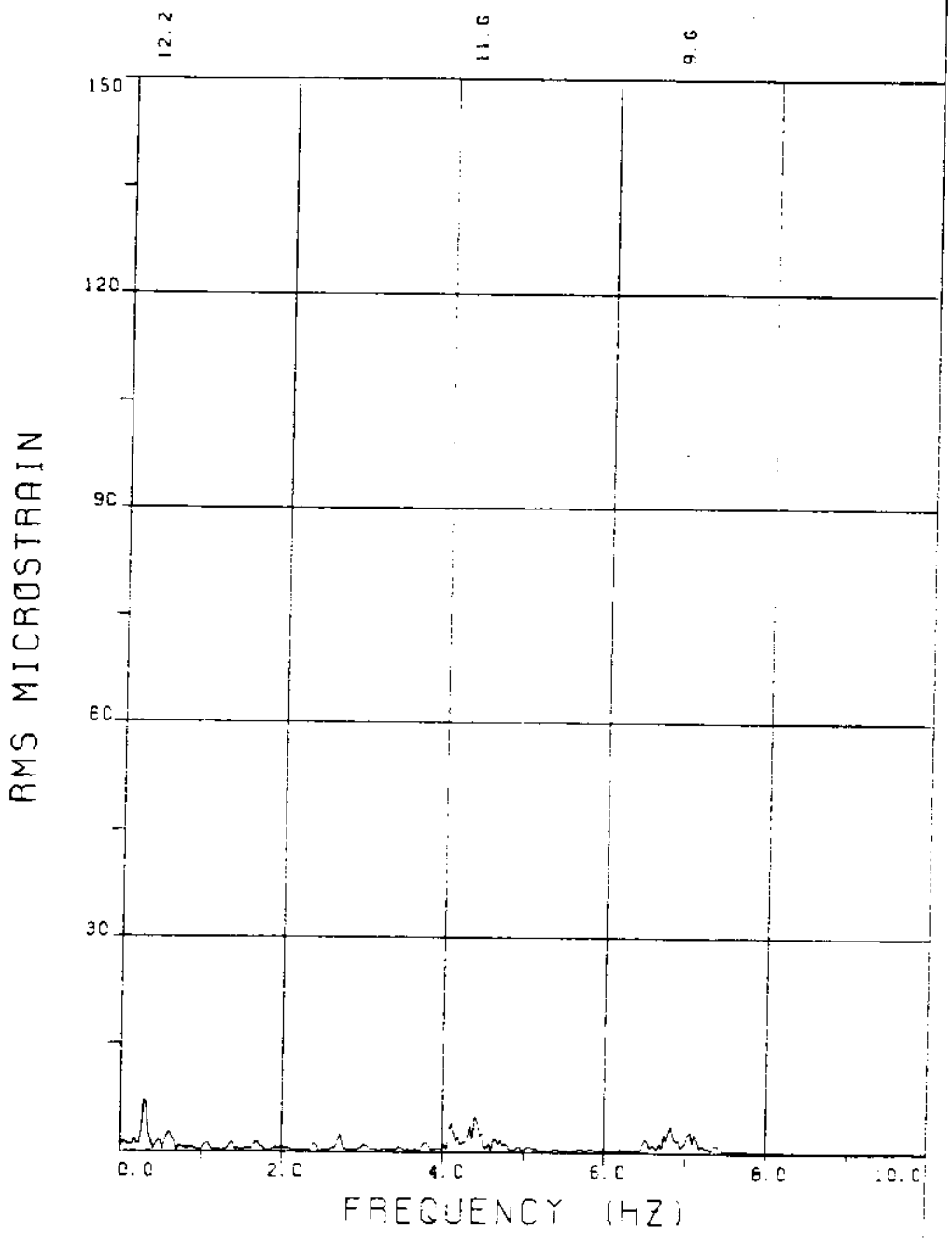

EXPERIMENT NUMBER 95

BRIDGE A9 ELEVATION=2L/11 BE=0.029

VC=350 A/DE=C.CO

MEASURED RESPONSE IN MICROSTRAIN

MEAN=139.6

TOTAL DYNAMIC RMS=20.3

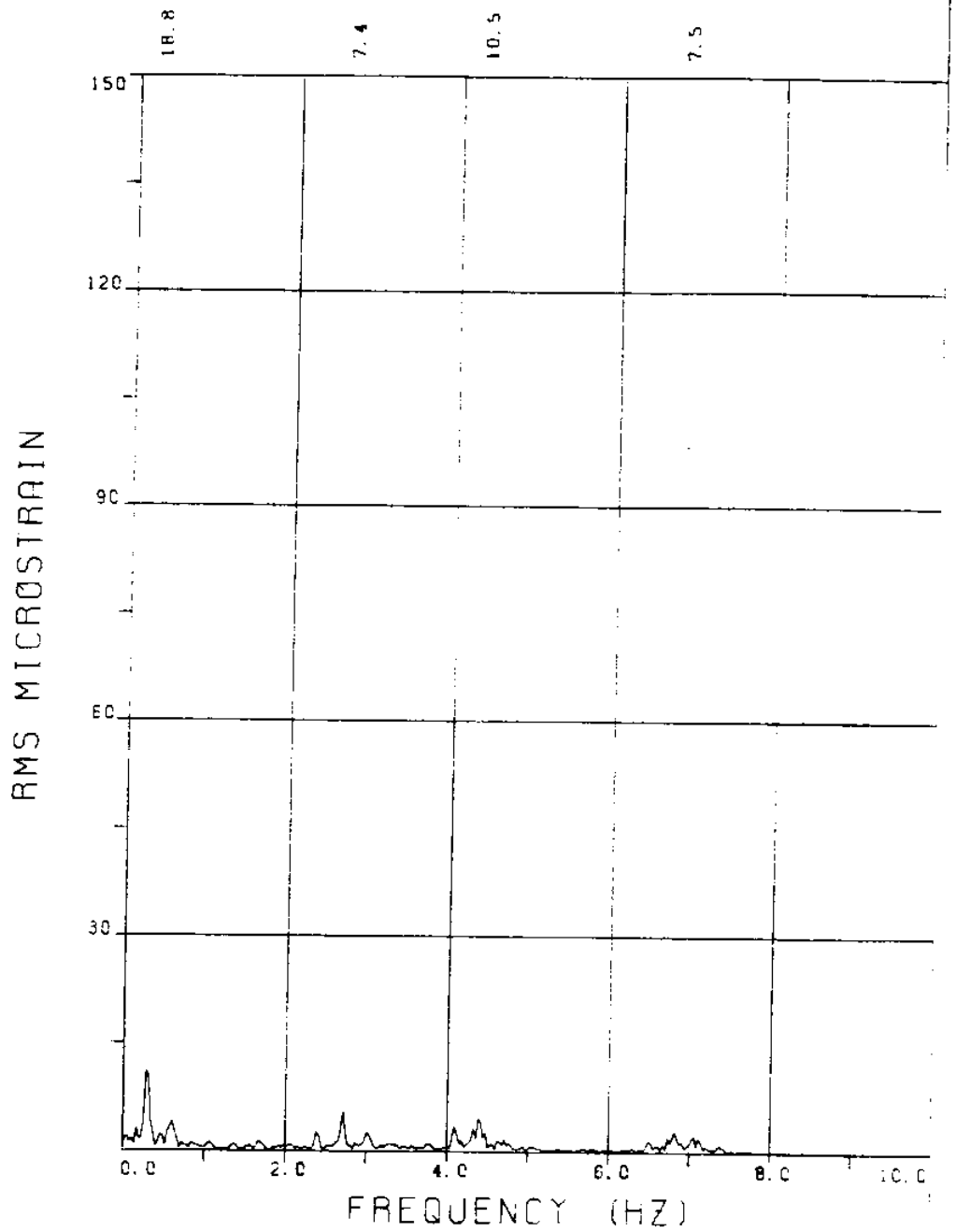

EXPERIMENT NUMBER 95

BRIDGE A7 ELEVATION=4L/11 BE=0.029

VC=350 A/DE=0.00

MEASURED RESPONSE IN MICROSTRAIN

MEAN=200.2

TOTAL DYNAMIC RMS=24.7

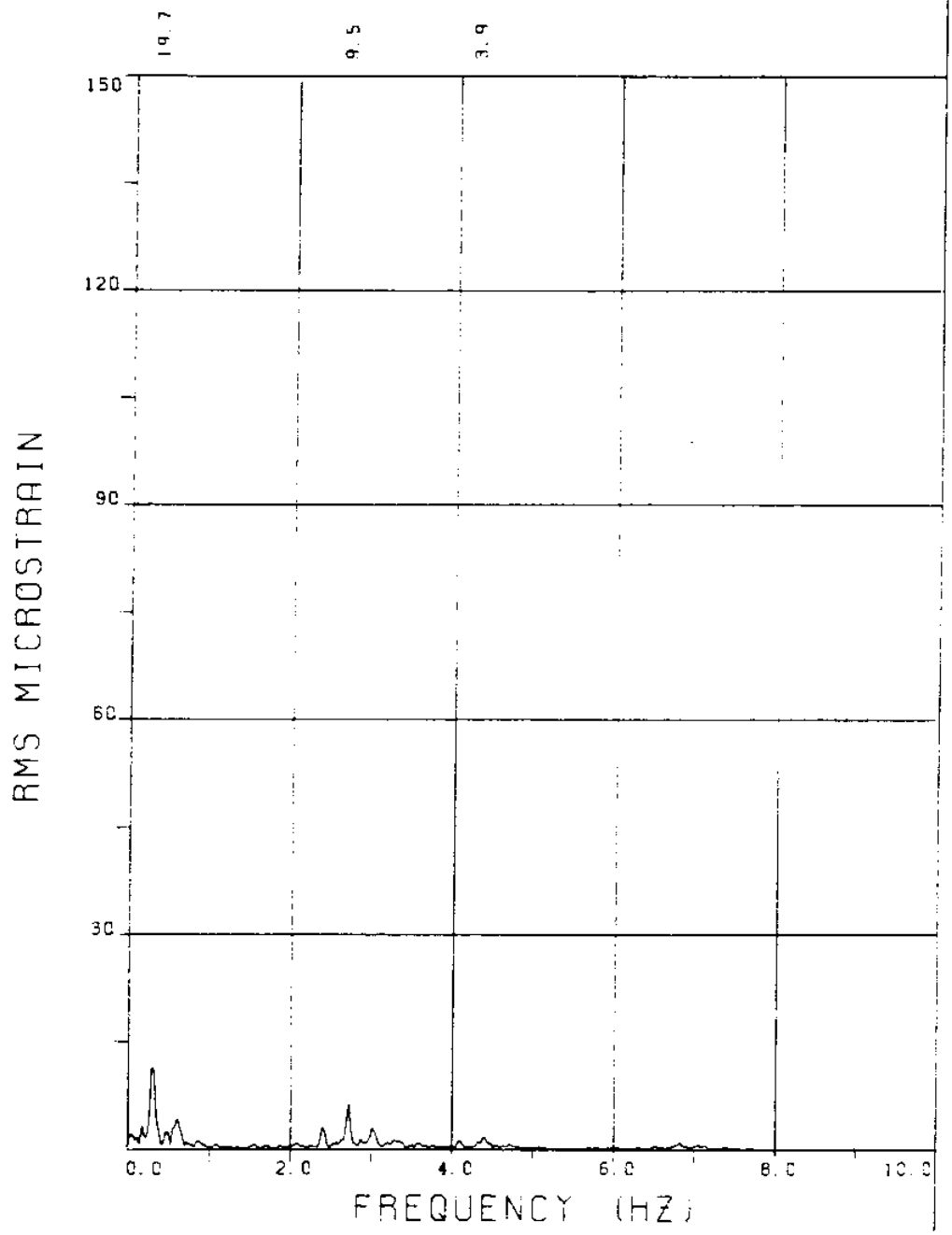

EXPERIMENT NUMBER 95

BRIDGE A6 ELEVATION=5L/11 BE=0.029

VC=350 A/DE=0.00

MEASURED RESPONSE IN MICROSTRAIN

MEAN=215.9

TOTAL DYNAMIC RMS=22.7

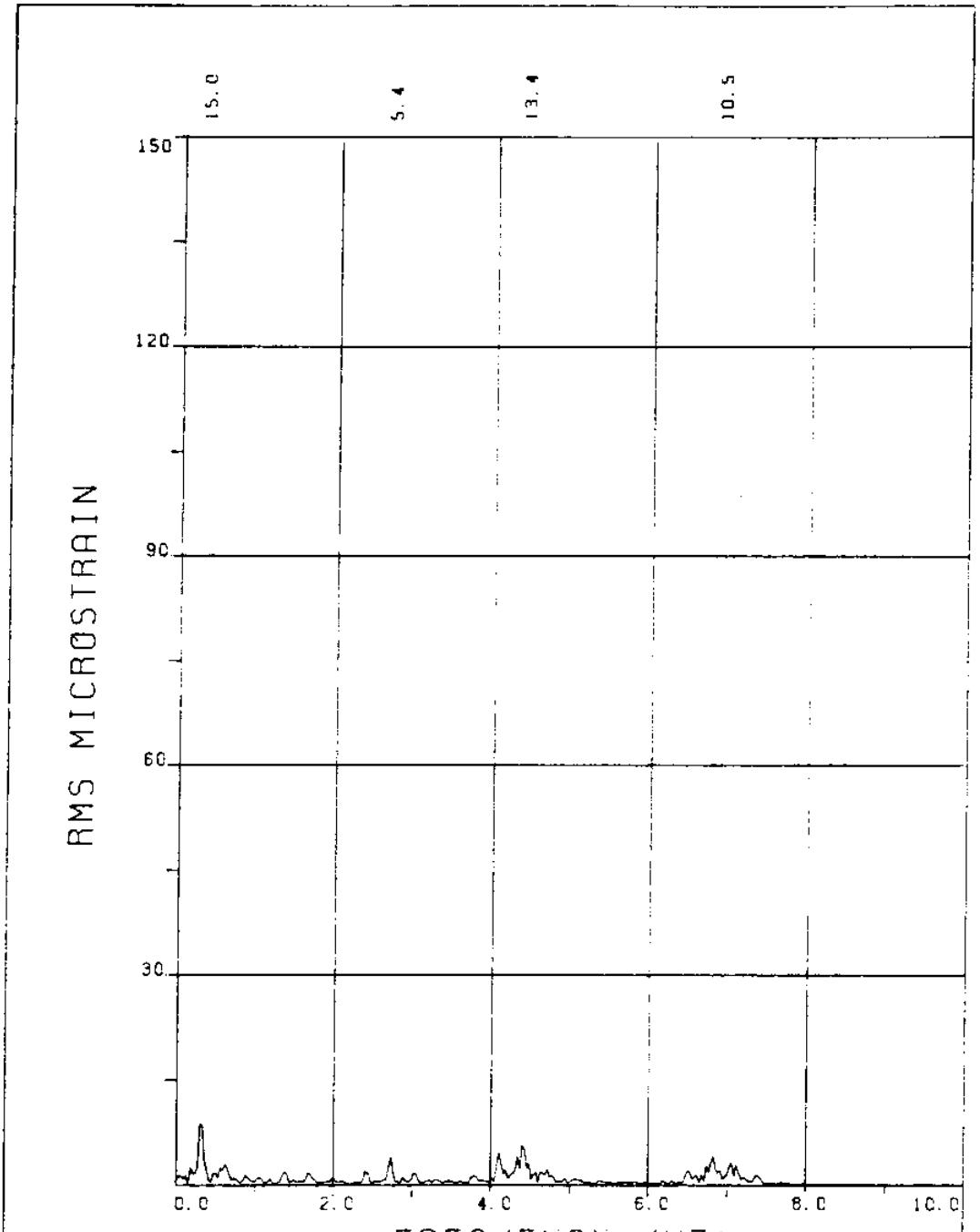

EXPERIMENT NUMBER 95

BRIDGE A3 ELEVATION=8L/11 BE=0.029

VC=350 A/DE=0.00

MEASURED RESPONSE IN MICROSTRAIN

MEAN=168.5

TOTAL DYNAMIC RMS=23.7

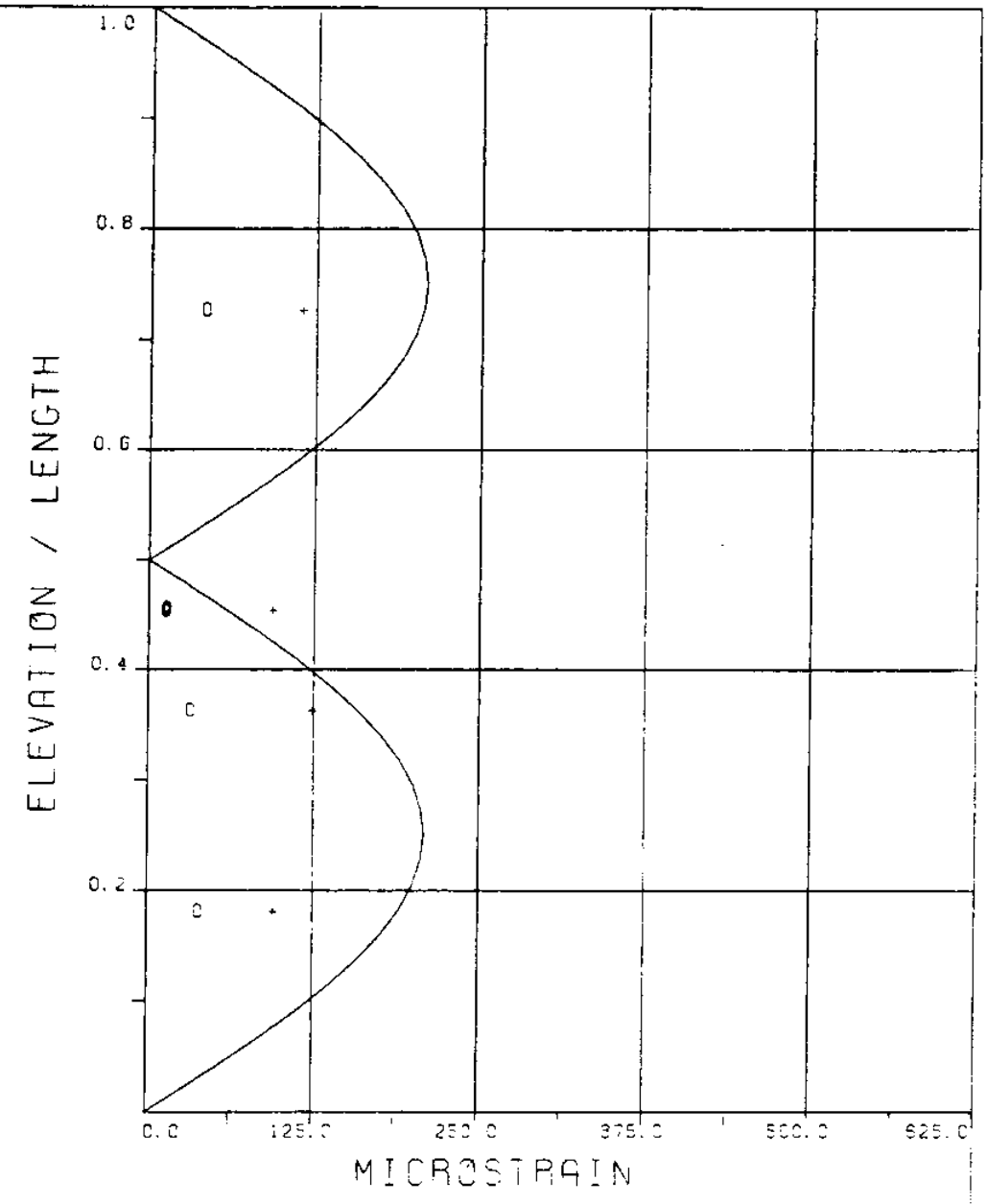

EXPERIMENT NUMBER 95

VC=350 A/DE=0.00

DYNAMIC RESPONSE AT F=FR IN PLANE B

——— THEORY o o o EXPERIMENT

MAXIMUM DYNAMIC RESPONSE IN PLANE B

——— THEORY + + + EXPERIMENT

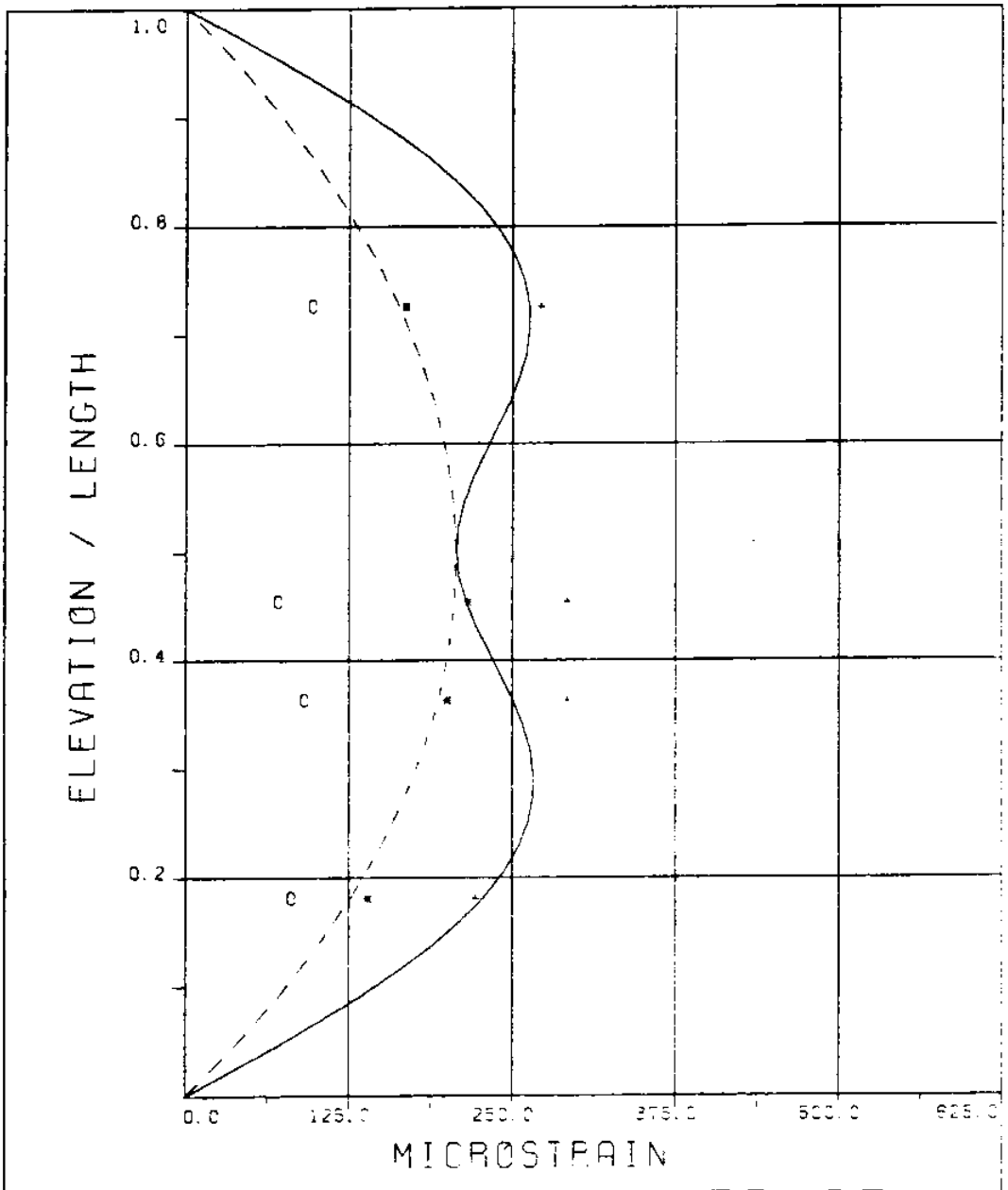

EXPERIMENT NUMBER 95

VC=350 A/DE=0.00

STATIC RESPONSE IN PLANE A

----- THEORY * * * EXPERIMENT

MAXIMUM DYNAMIC RESPONSE IN PLANE A

o o o EXPERIMENT

MAXIMUM RESPONSE

——— THEORY + + + EXPERIMENT

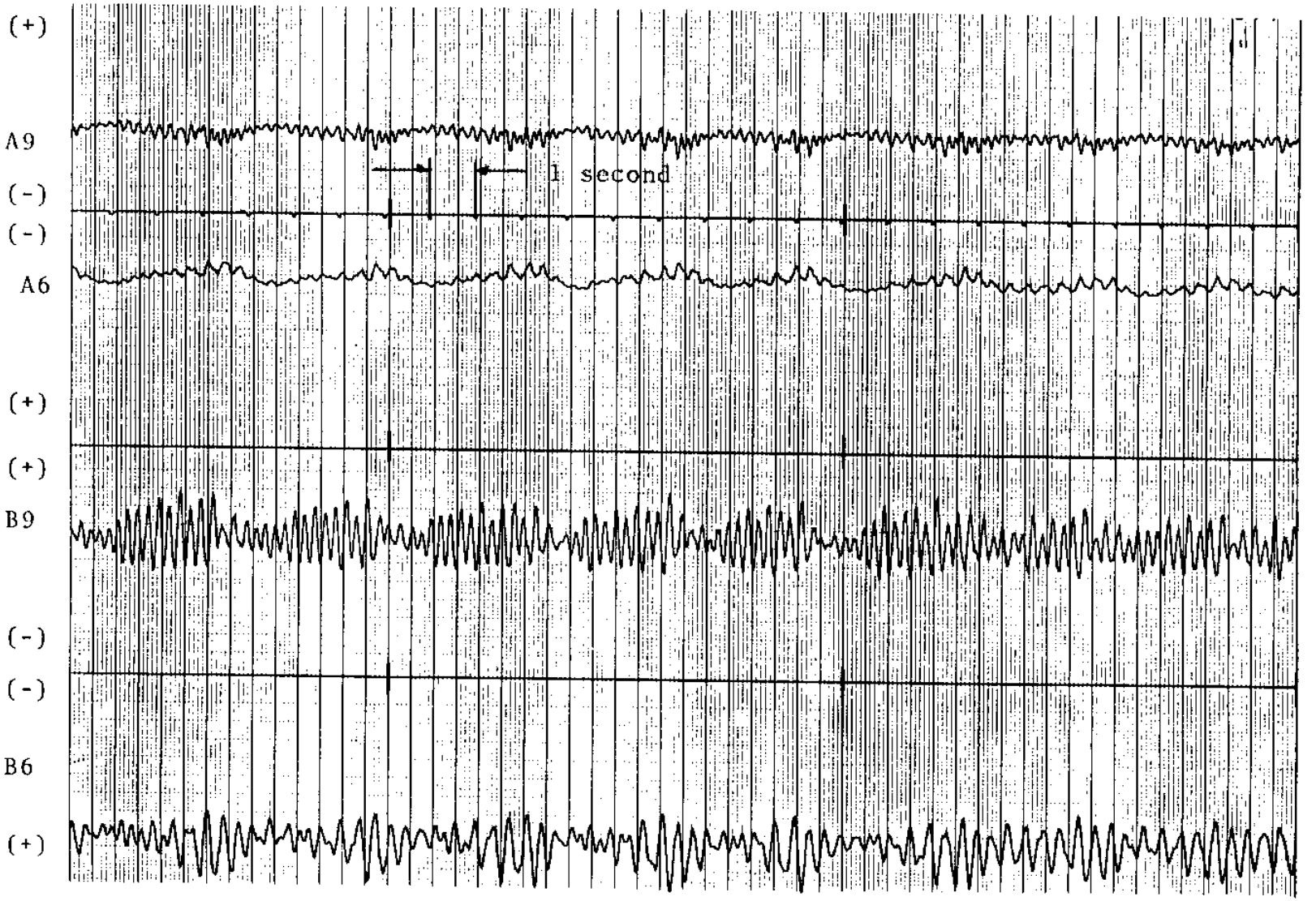

FIGURE 95Ta: A BRIDGES: 15.3 MICROSTRAIN/DIVISION; B BRIDGES: 7.6 MICROSTRAIN/DIVISION

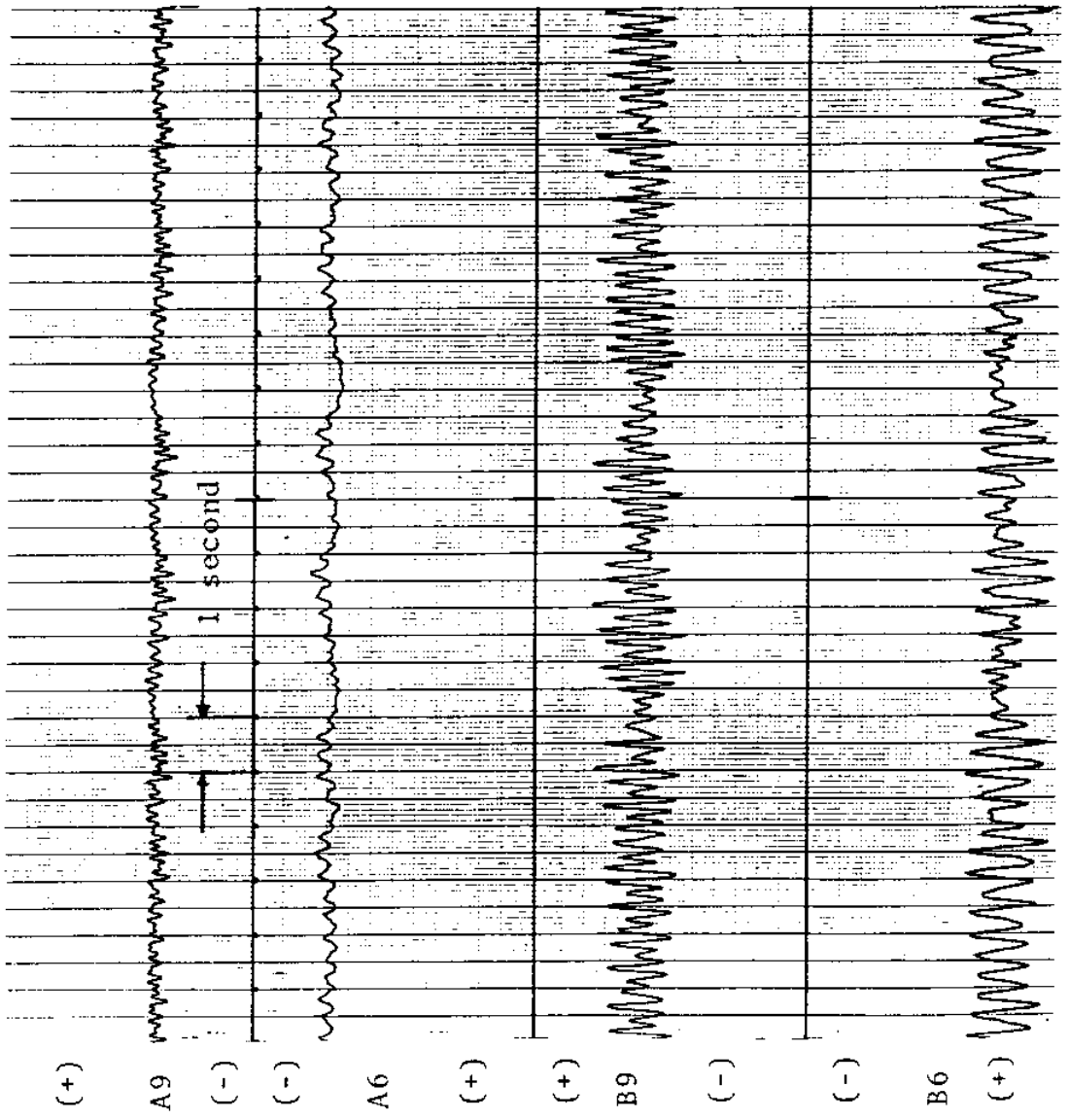

FIGURE 95Tb: A BRIDGES: 15.3 MICROSTRAIN/DIVISION
B BRIDGES: 7.6 MICROSTRAIN/DIVISION

EXPERIMENT 112

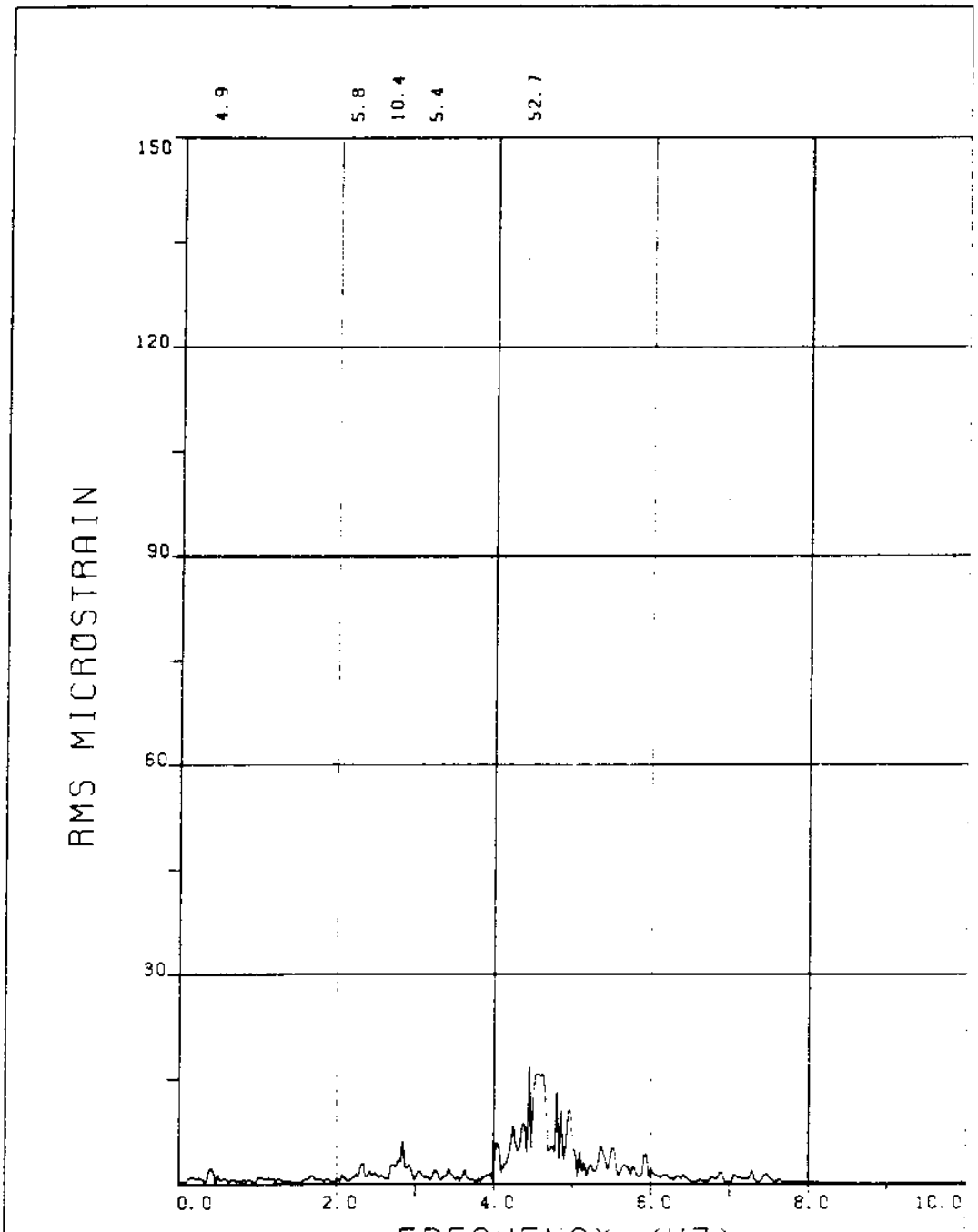

EXPERIMENT NUMBER 112

BRIDGE B9 ELEVATION=2L/11 BE=0.029

VC=385 A/DE=0.00

MEASURED RESPONSE IN MICROSTRAIN

TOTAL DYNAMIC RMS=57.2

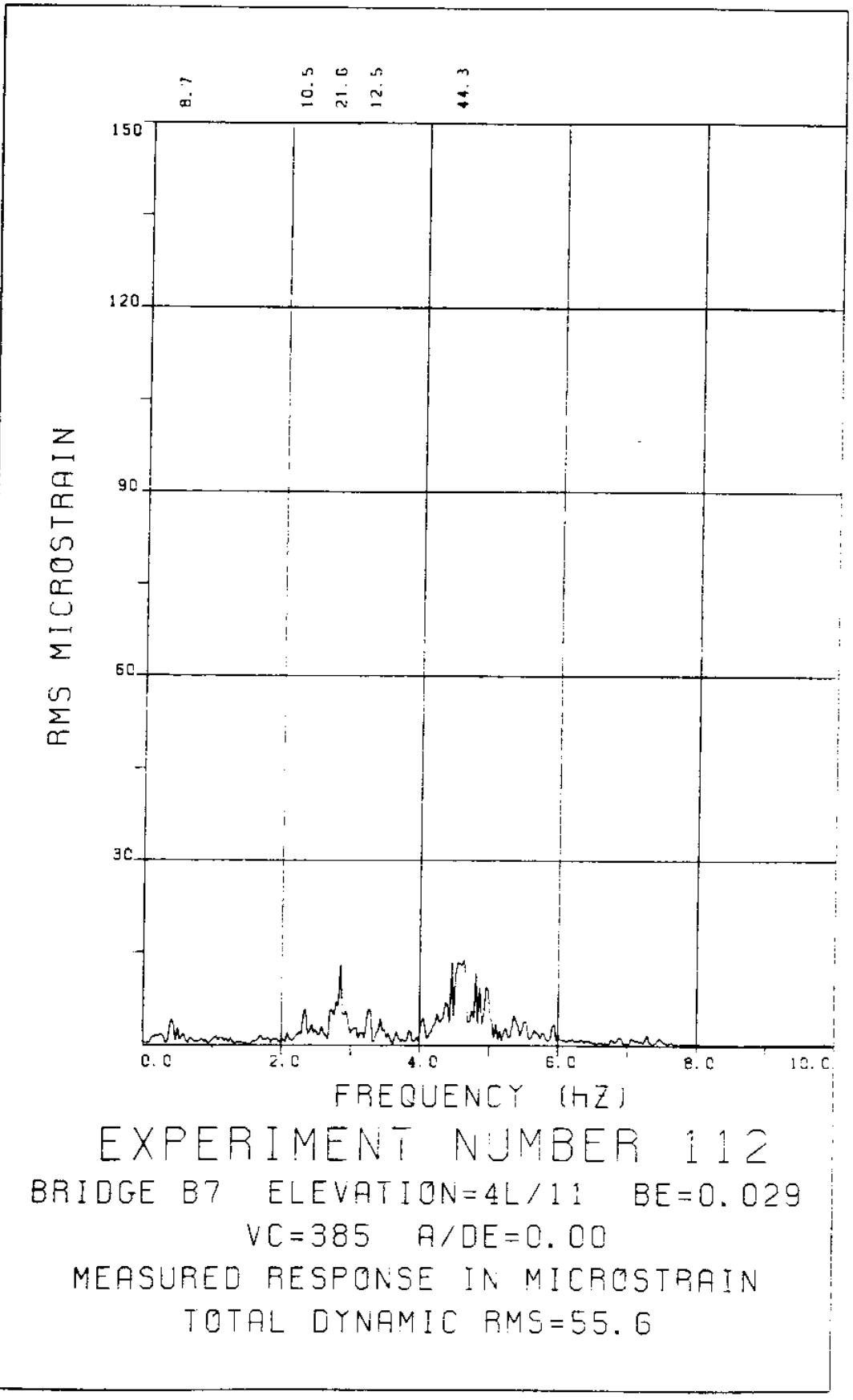
8.7
10.5
21.6
12.5
44.3
150
120
90
60
30
RMS MICROSTRAIN
0.0
2.0
4.0
6.0
8.0
10.0
FREQUENCY (HZ)
EXPERIMENT NUMBER 112
BRIDGE B7 ELEVATION=4L/11 BE=0.029
VC=385 A/DE=0.00
MEASURED RESPONSE IN MICROSTRAIN
TOTAL DYNAMIC RMS=55.6

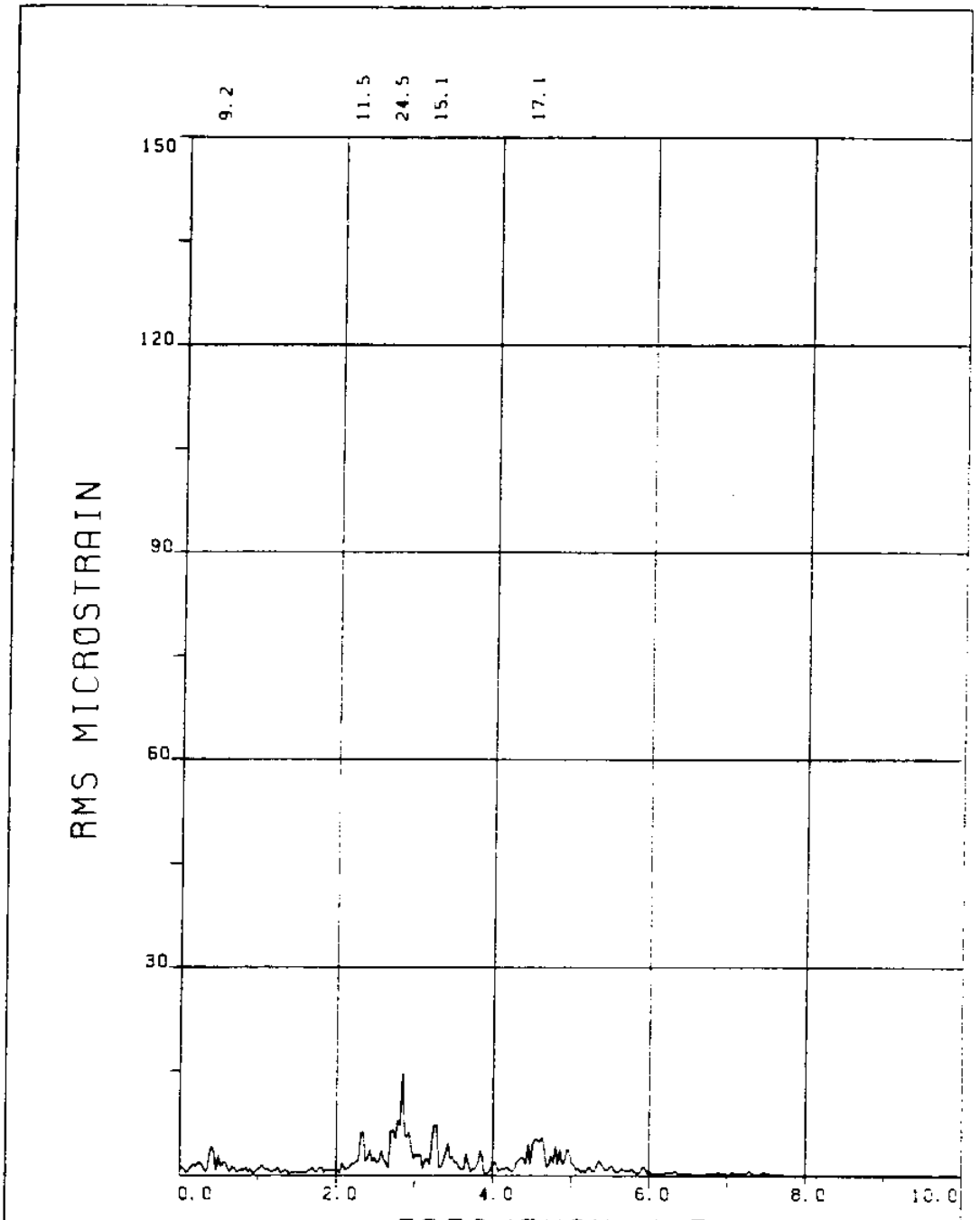

EXPERIMENT NUMBER 112

BRIDGE B6 ELEVATION=5L/11 BE=0.029

VC=385 A/DE=0.00

MEASURED RESPONSE IN MICROSTRAIN

TOTAL DYNAMIC RMS=39.5

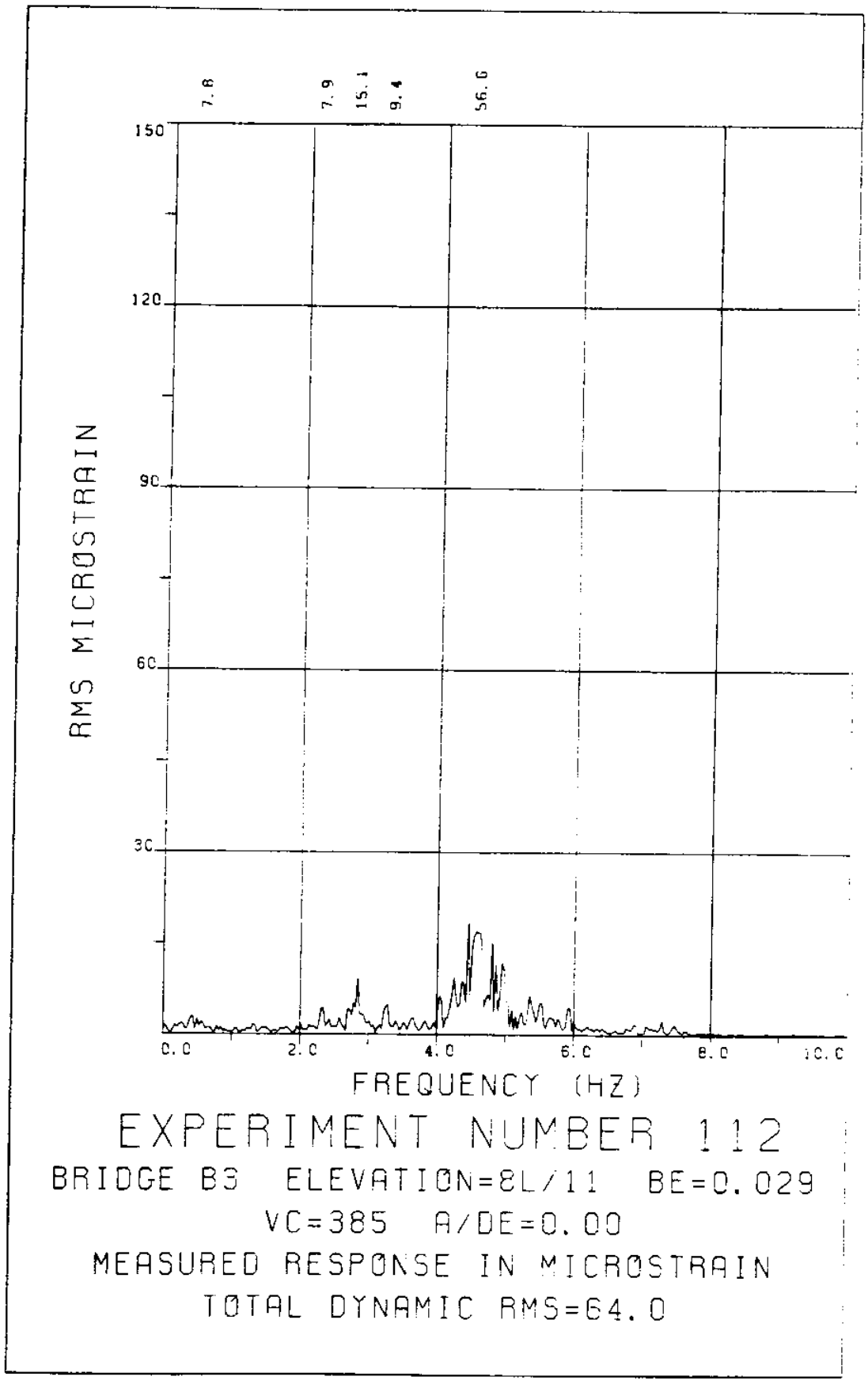

EXPERIMENT NUMBER 112

BRIDGE B3 ELEVATION=8L/11 BE=0.029

VC=385 A/DE=0.00

MEASURED RESPONSE IN MICROSTRAIN

TOTAL DYNAMIC RMS=64.0

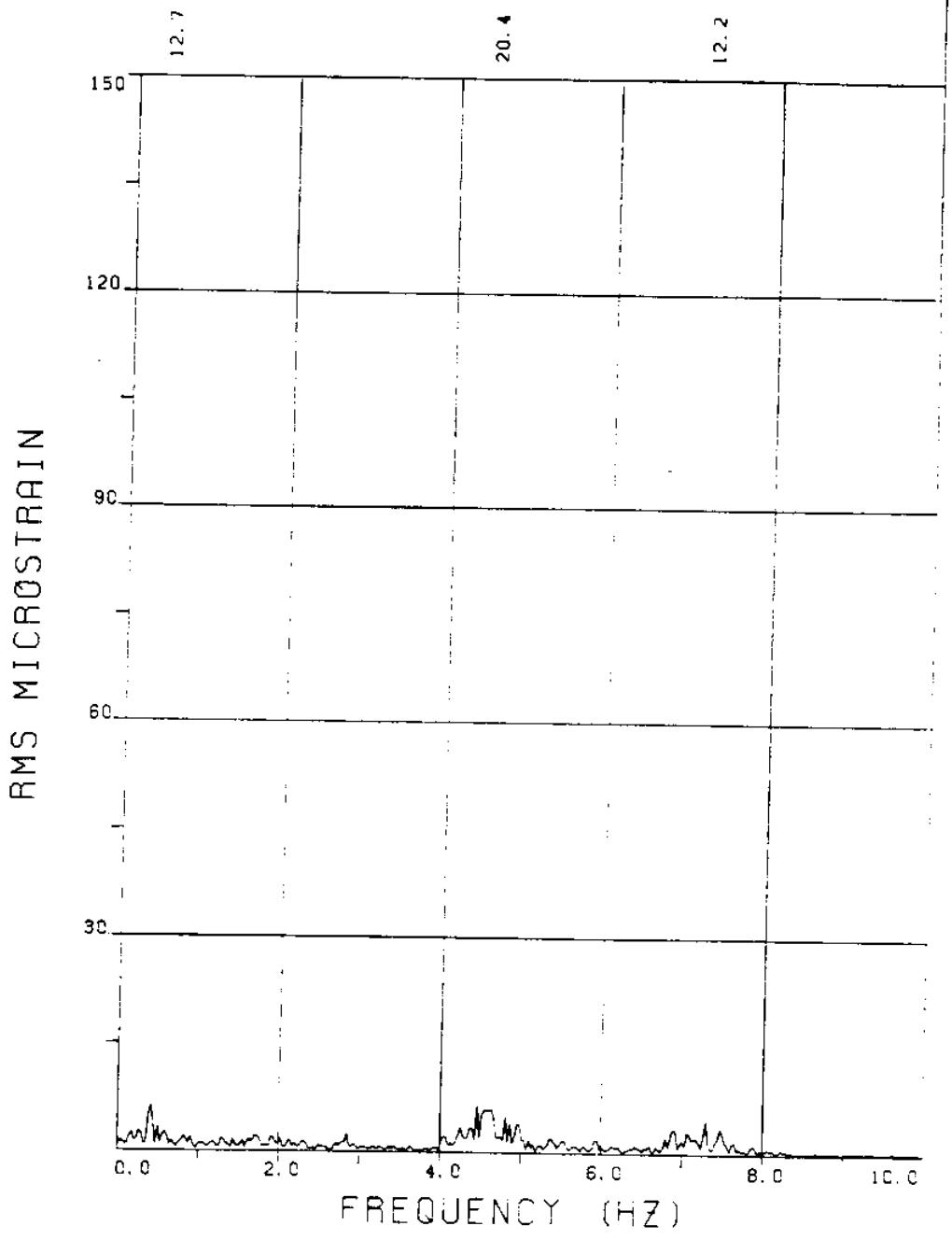

EXPERIMENT NUMBER 112

BRIDGE A9 ELEVATION=2L/11 BE=0.029

VC=385 A/DE=0.00

MEASURED RESPONSE IN MICROSTRAIN

MEAN=182.8

TOTAL DYNAMIC RMS=29.6

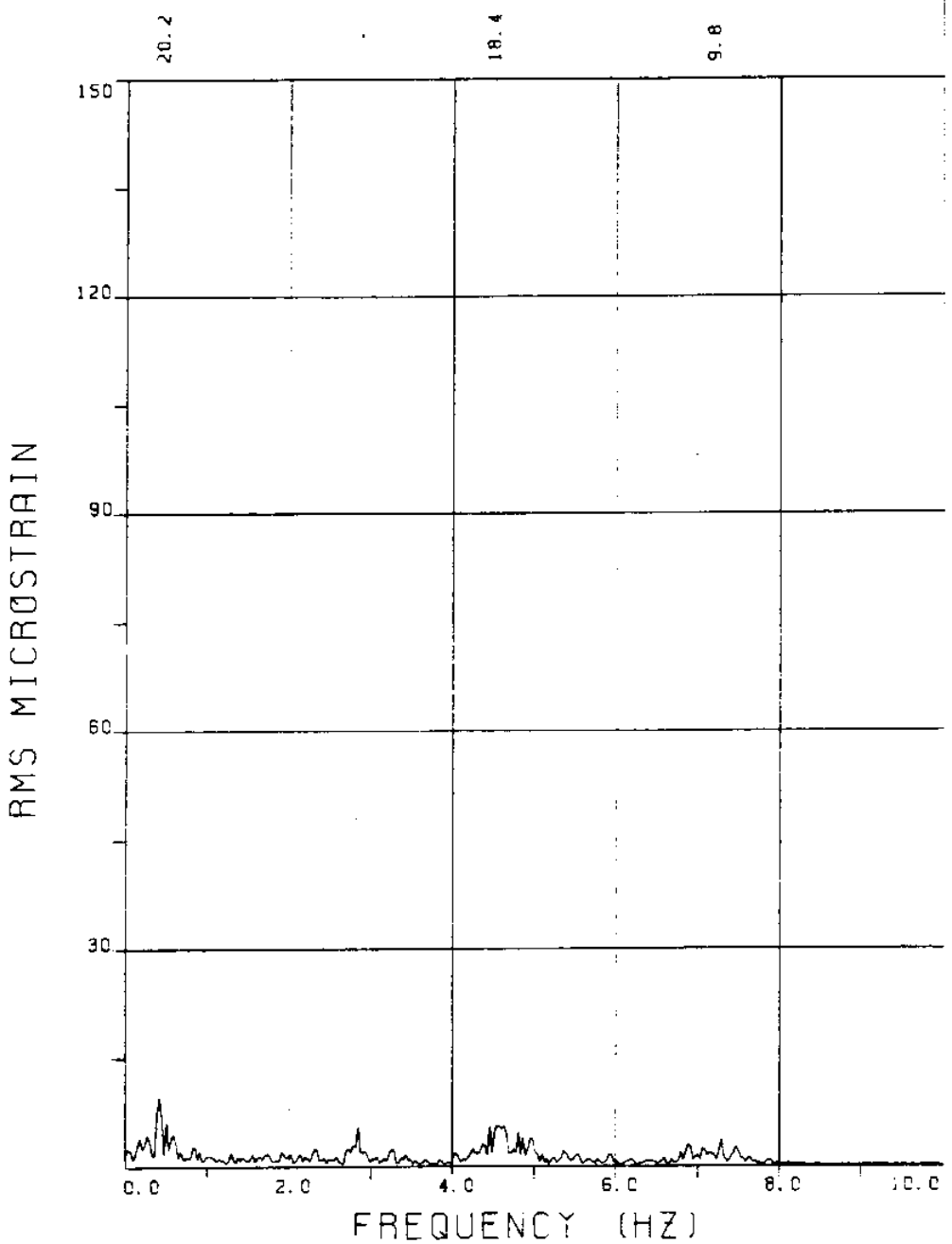

EXPERIMENT NUMBER 112

BRIDGE A7 ELEVATION=4L/11 BE=0.029

VC=385 A/DE=0.00

MEASURED RESPONSE IN MICROSTRAIN

MEAN=267.5

TOTAL DYNAMIC RMS=32.8

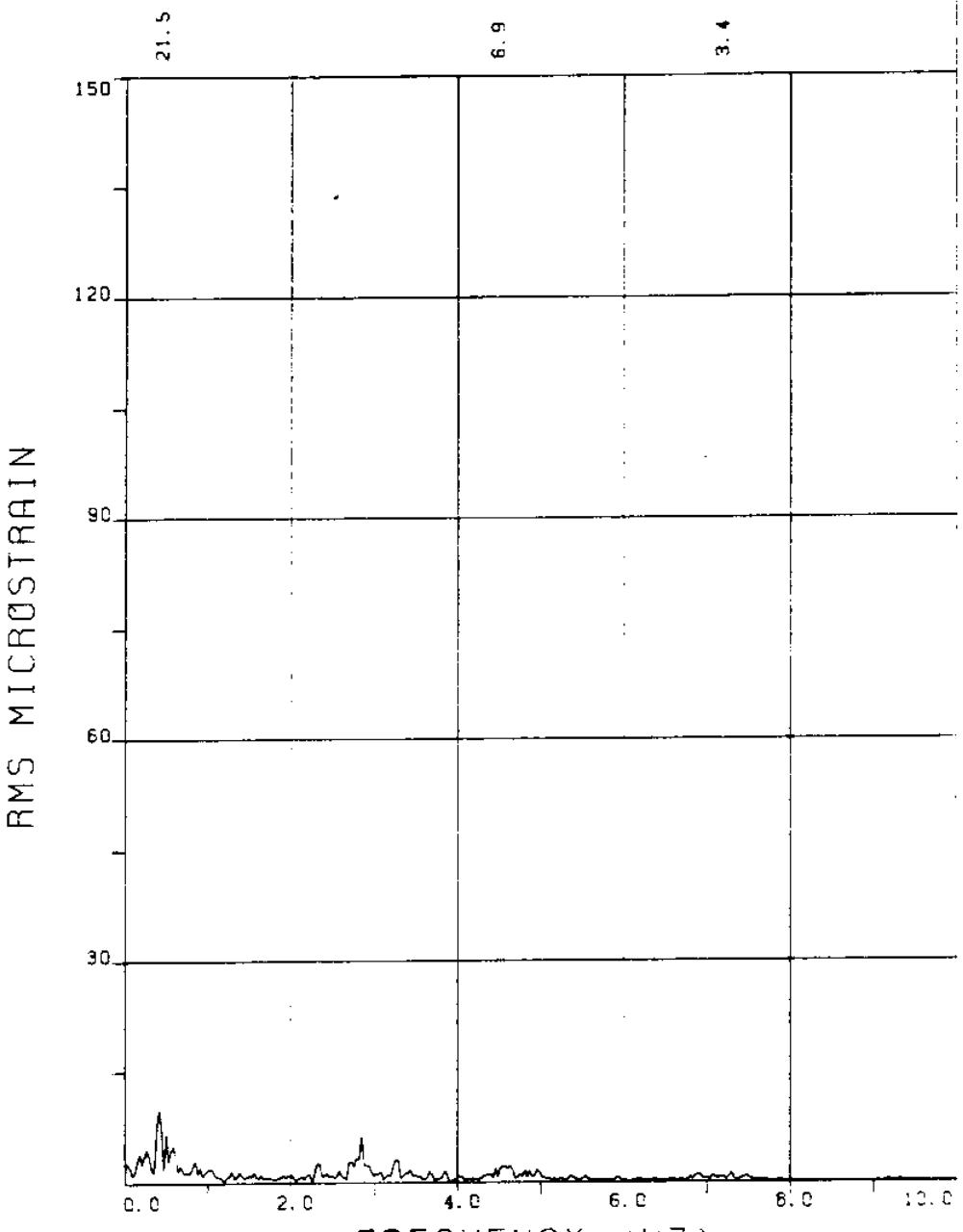

EXPERIMENT NUMBER 112

BRIDGE A6 ELEVATION=5L/11 BE=0.029

VC=385 A/DE=0.00

MEASURED RESPONSE IN MICROSTRAIN

MEAN=284.8

TOTAL DYNAMIC RMS=27.7

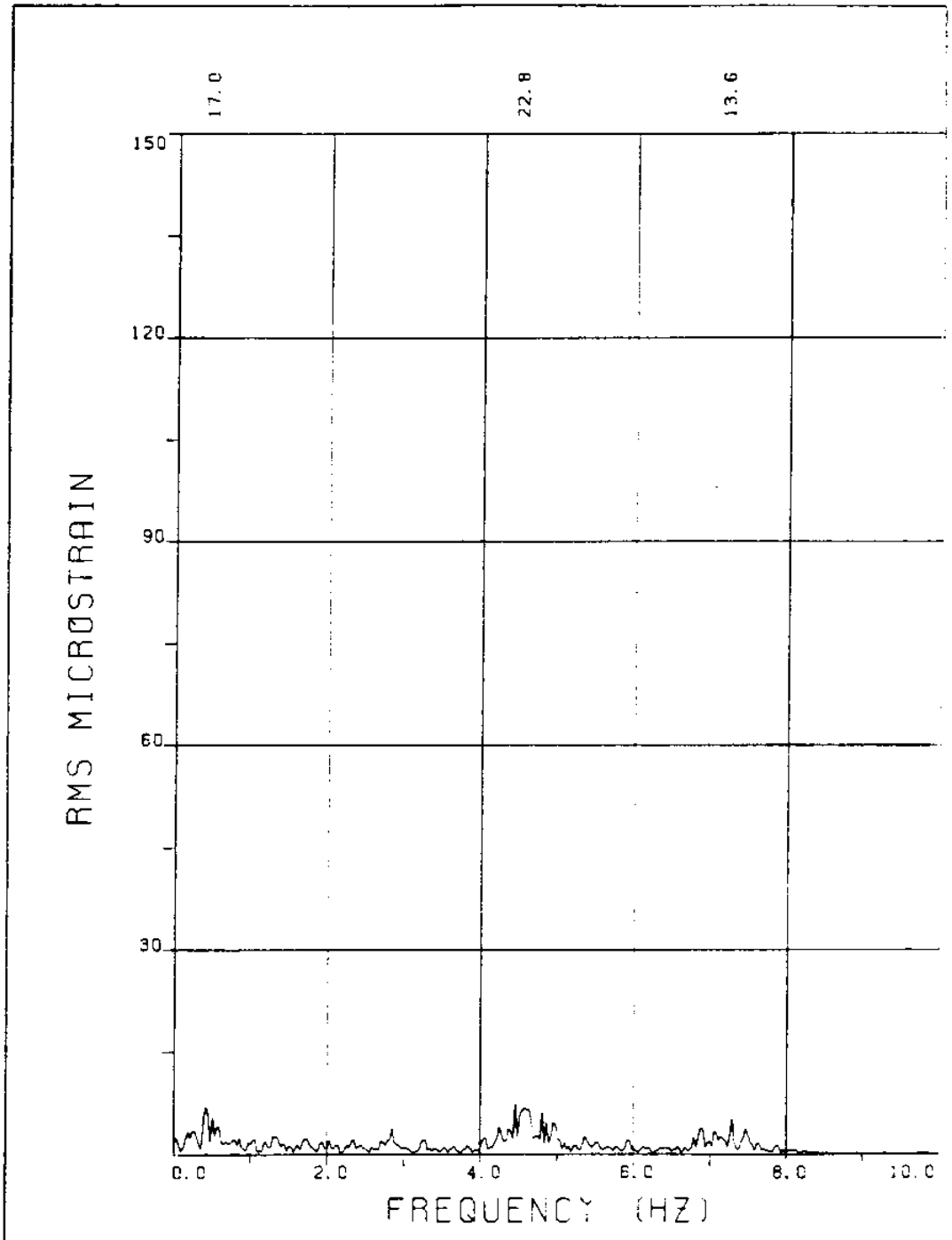

EXPERIMENT NUMBER 112

BRIDGE A3 ELEVATION=8L/11 BE=0.029

VC=385 A/DE=0.00

MEASURED RESPONSE IN MICROSTRAIN

MEAN=222.6

TOTAL DYNAMIC RMS=35.5

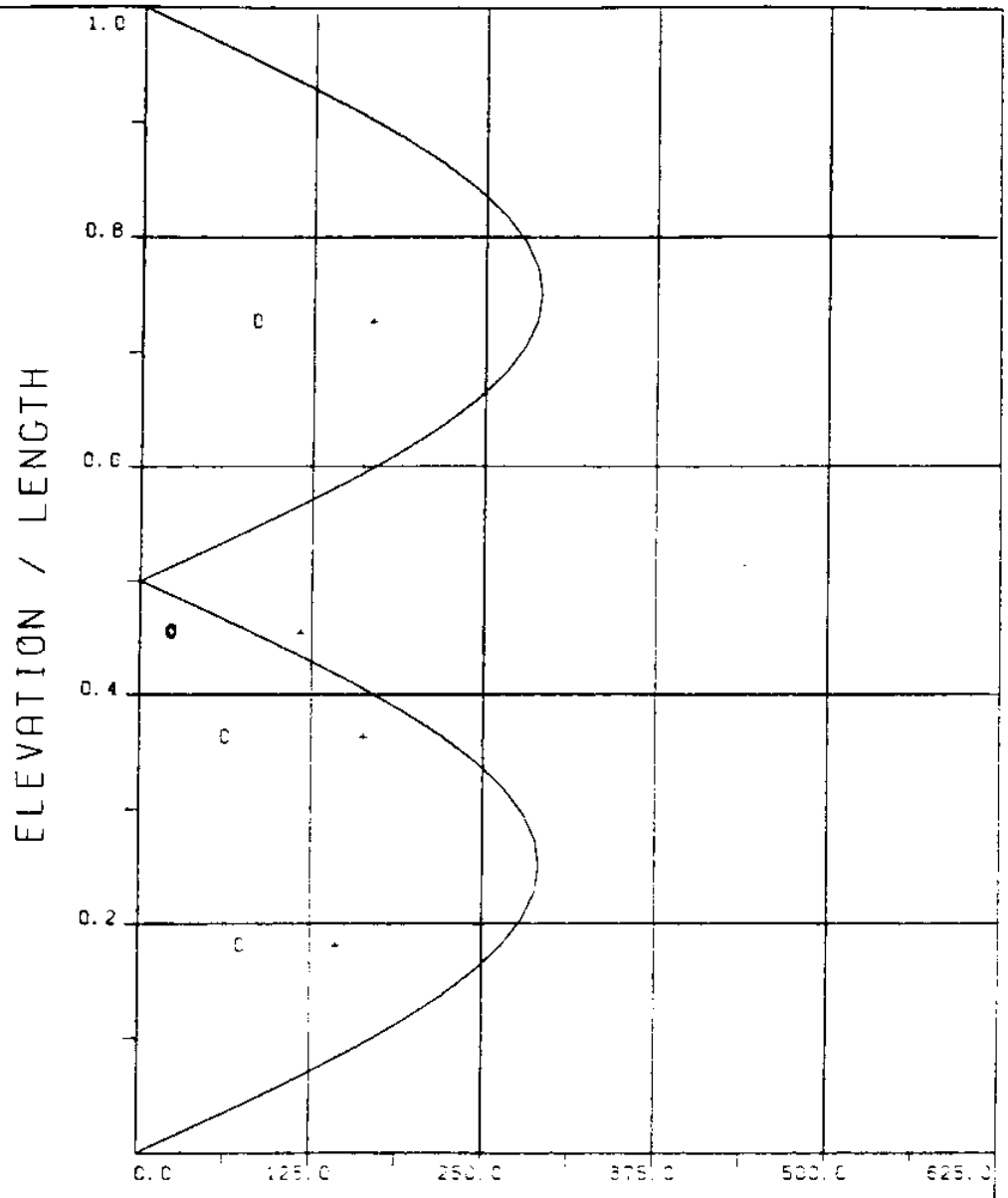

EXPERIMENT NUMBER 112

VC=385 A/DE=0.00

DYNAMIC RESPONSE AT F=FR IN PLANE B

——— THEORY o o o EXPERIMENT

MAXIMUM DYNAMIC RESPONSE IN PLANE B

——— THEORY + + + EXPERIMENT

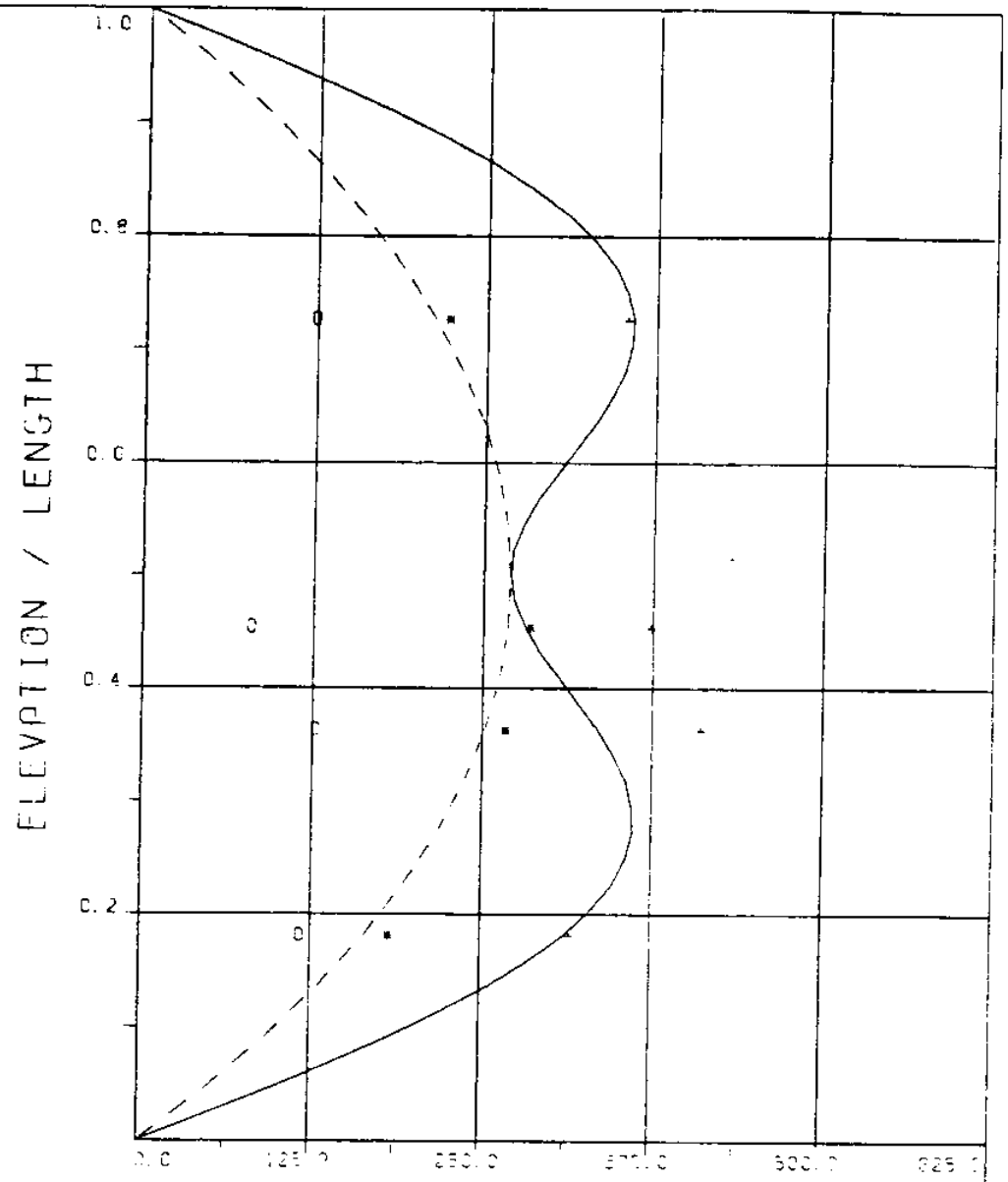

EXPERIMENT NUMBER 112

VC=350 A/DE=0.00

STATIC RESPONSE IN PLANE A

----- THEORY * * * EXPERIMENT

MAXIMUM DYNAMIC RESPONSE IN PLANE A

o o o EXPERIMENT

MAXIMUM RESPONSE

_____ THEORY + + + EXPERIMENT

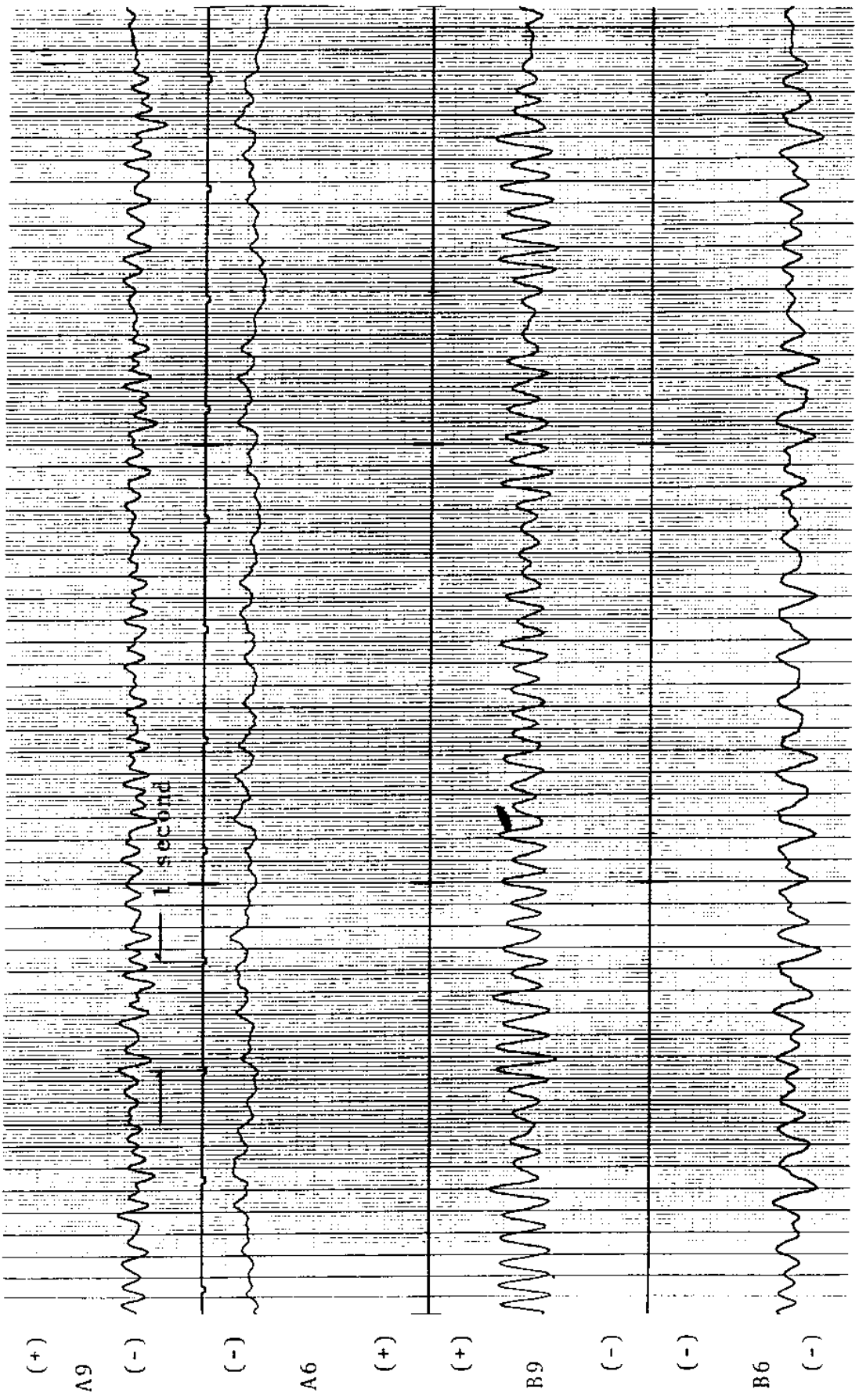

FIGURE 112Ta: A BRIDGES: 15.3 MICROSTRAIN/DIVISION
B BRIDGES: 7.6 MICROSTRAIN/DIVISION

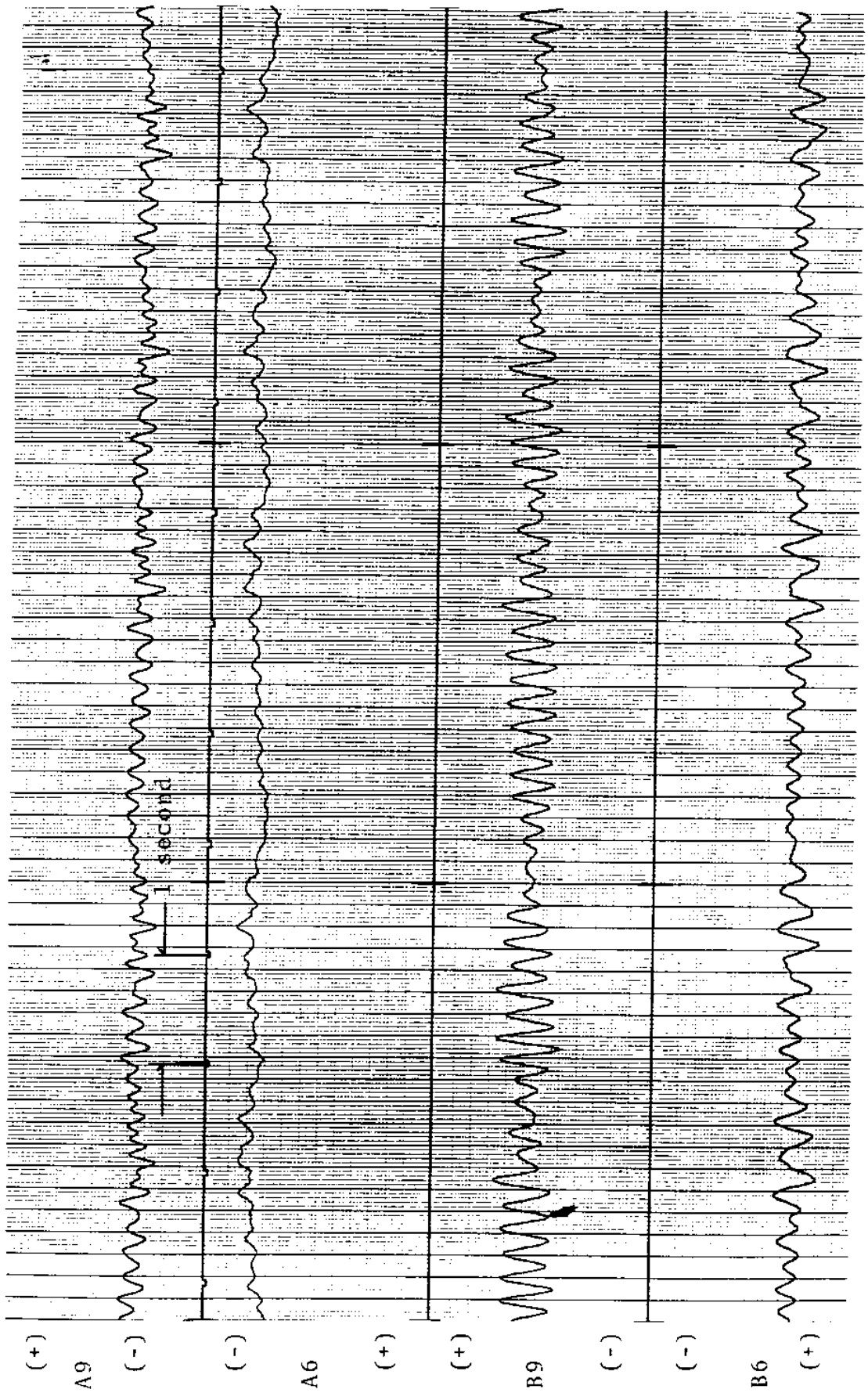

FIGURE 112Tb: A BRIDGES: 15.3 MICROSTRAIN/DIVISION
B BRIDGES: 7.6 MICROSTRAIN/DIVISION

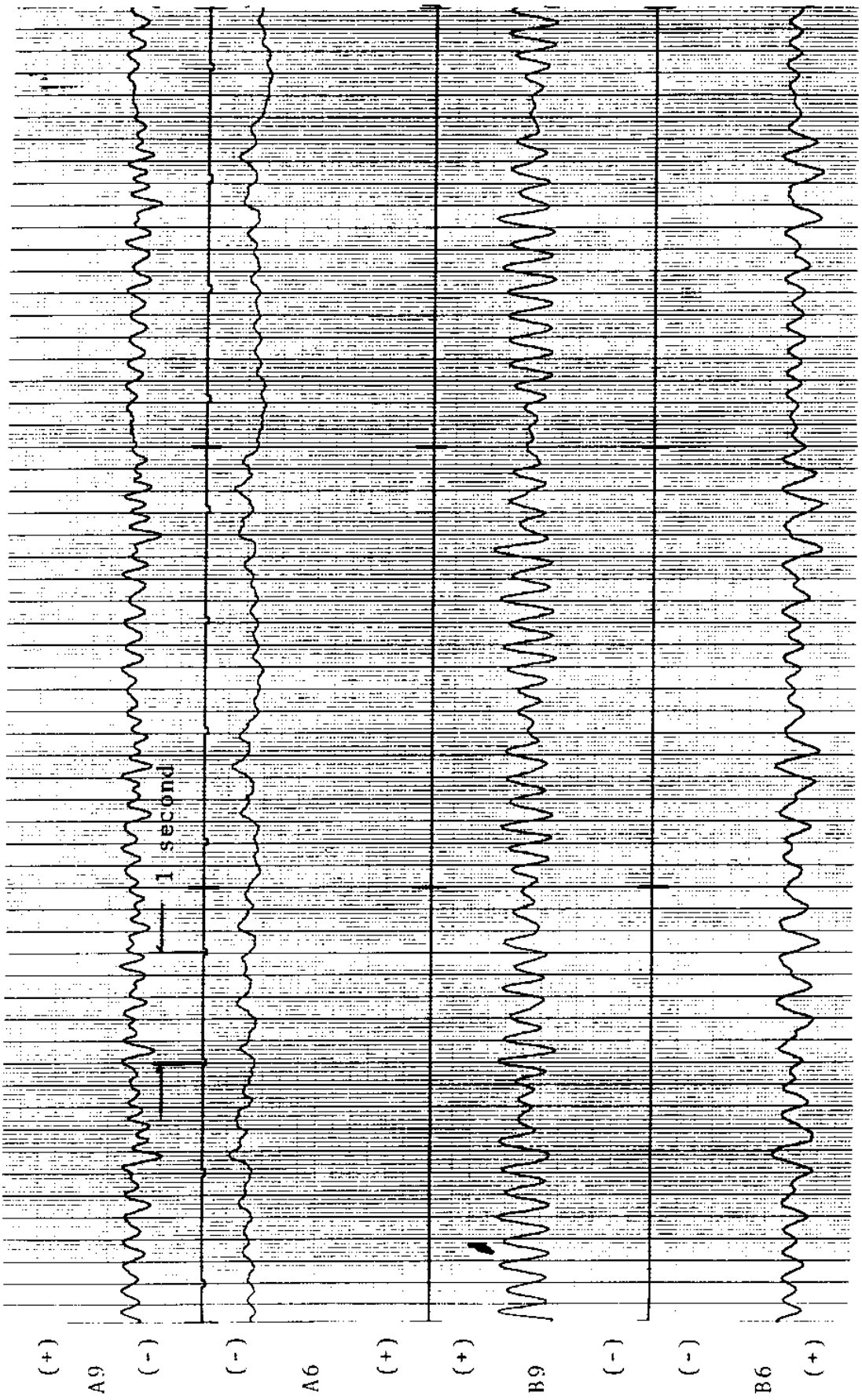

FIGURE 112Tc: A BRIDGES: 15.3 MICROSTRAIN/DIVISION
B BRIDGES: 7.6 MICROSTRAIN/DIVISION

EXPERIMENT 115

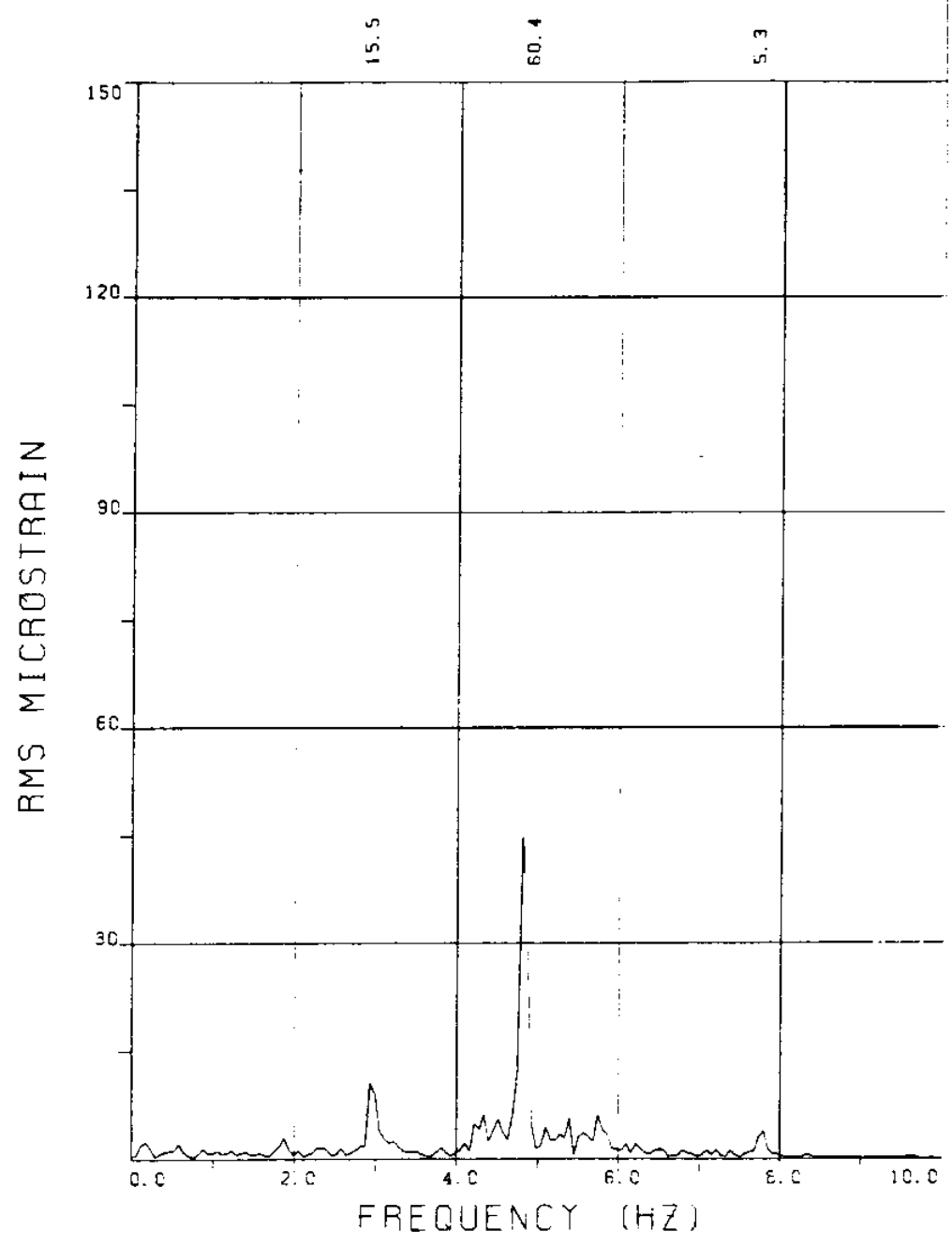

EXPERIMENT NUMBER 115

BRIDGE 89 ELEVATION=2L/11 BE=0.059

VC=410 A/DE=0.00

MEASURED RESPONSE IN MICROSTRAIN

TOTAL DYNAMIC RMS=65.6

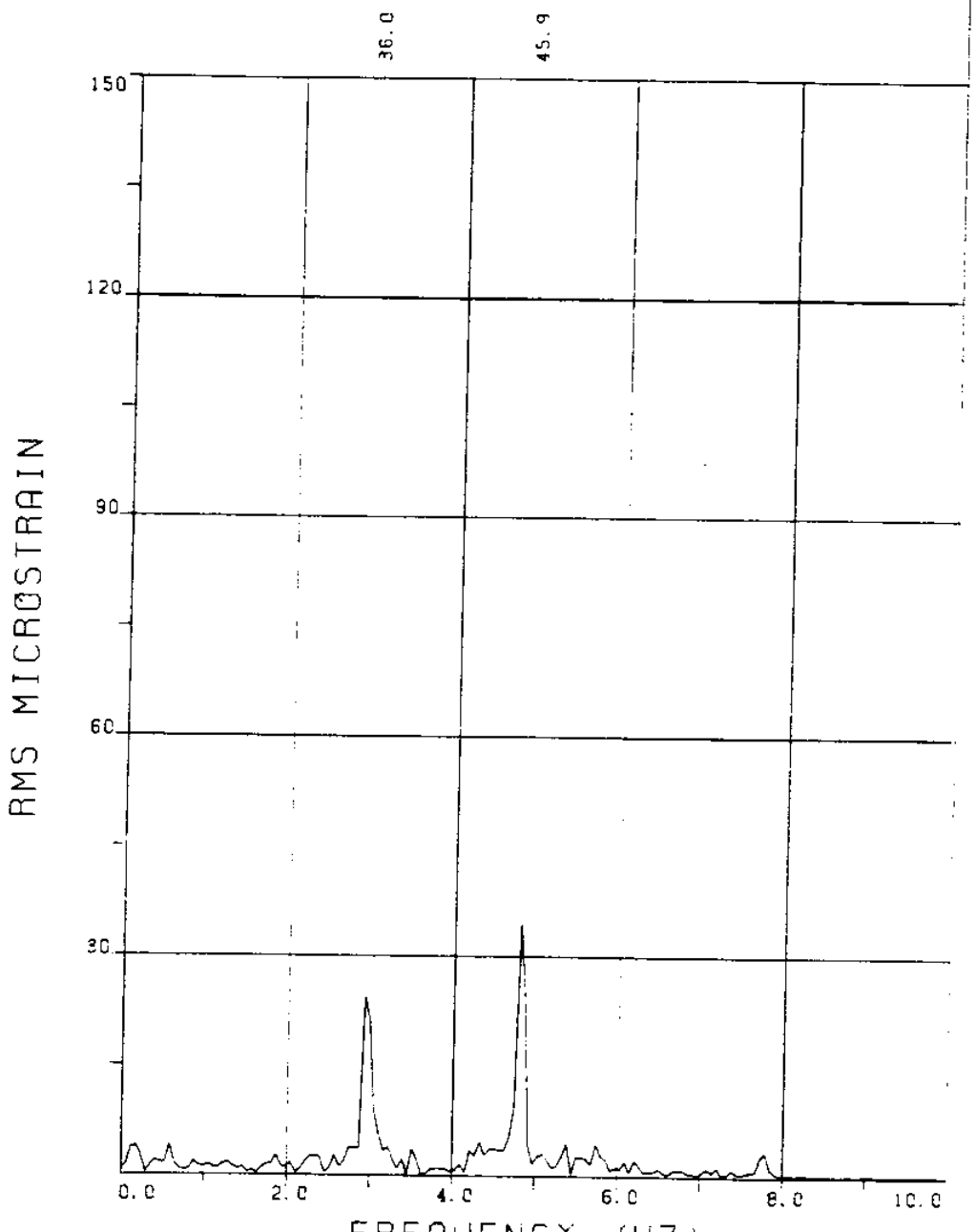

EXPERIMENT NUMBER 115

BRIDGE B7 ELEVATION=4L/11 BE=0.059

VC=410 A/DE=0.00

MEASURED RESPONSE IN MICROSTRAIN

TOTAL DYNAMIC RMS=60.8

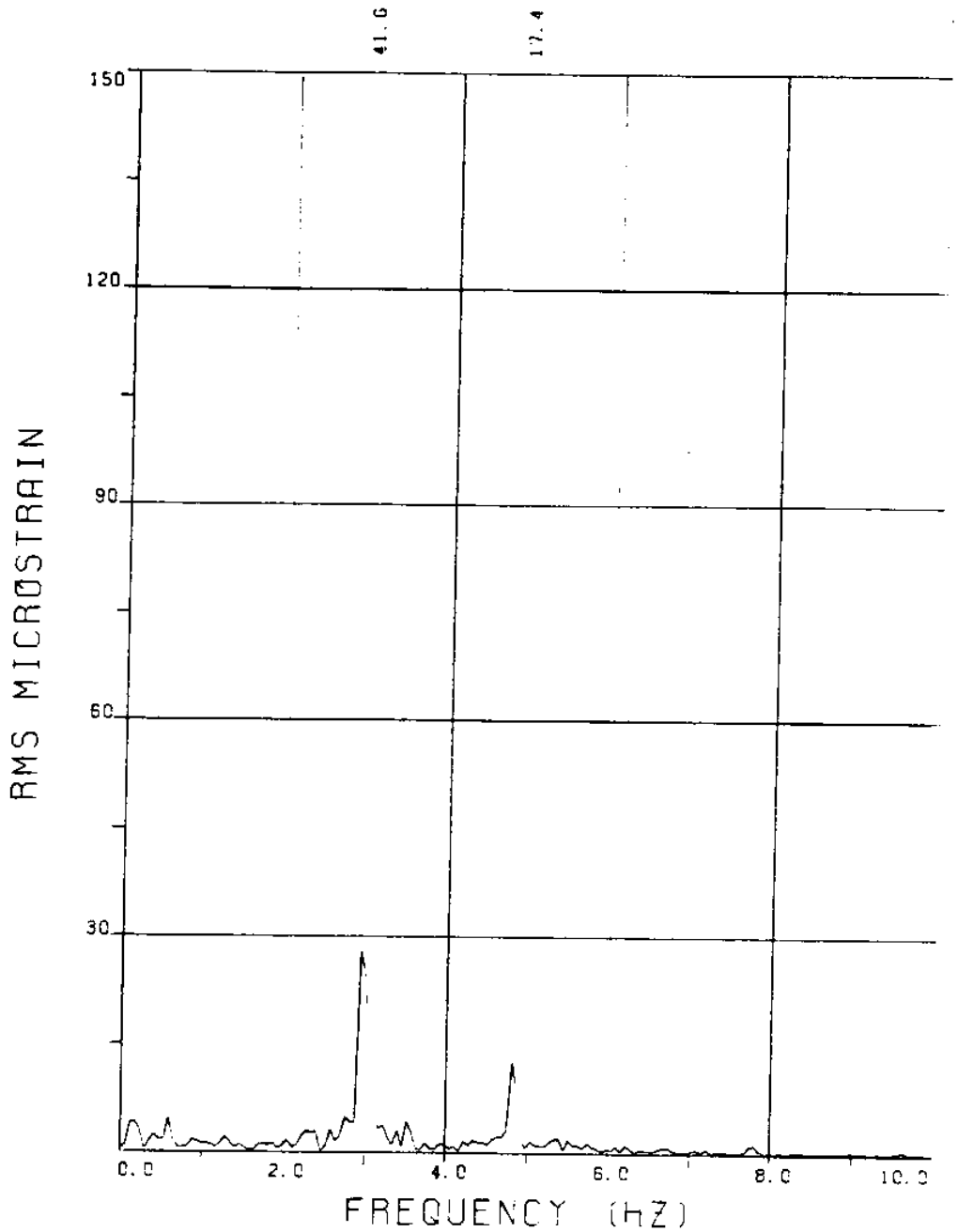

EXPERIMENT NUMBER 115

BRIDGE B6 ELEVATION=5L/11 BE=0.059

VC=410 A/DE=0.00

MEASURED RESPONSE IN MICROSTRAIN

TOTAL DYNAMIC RMS=45.9

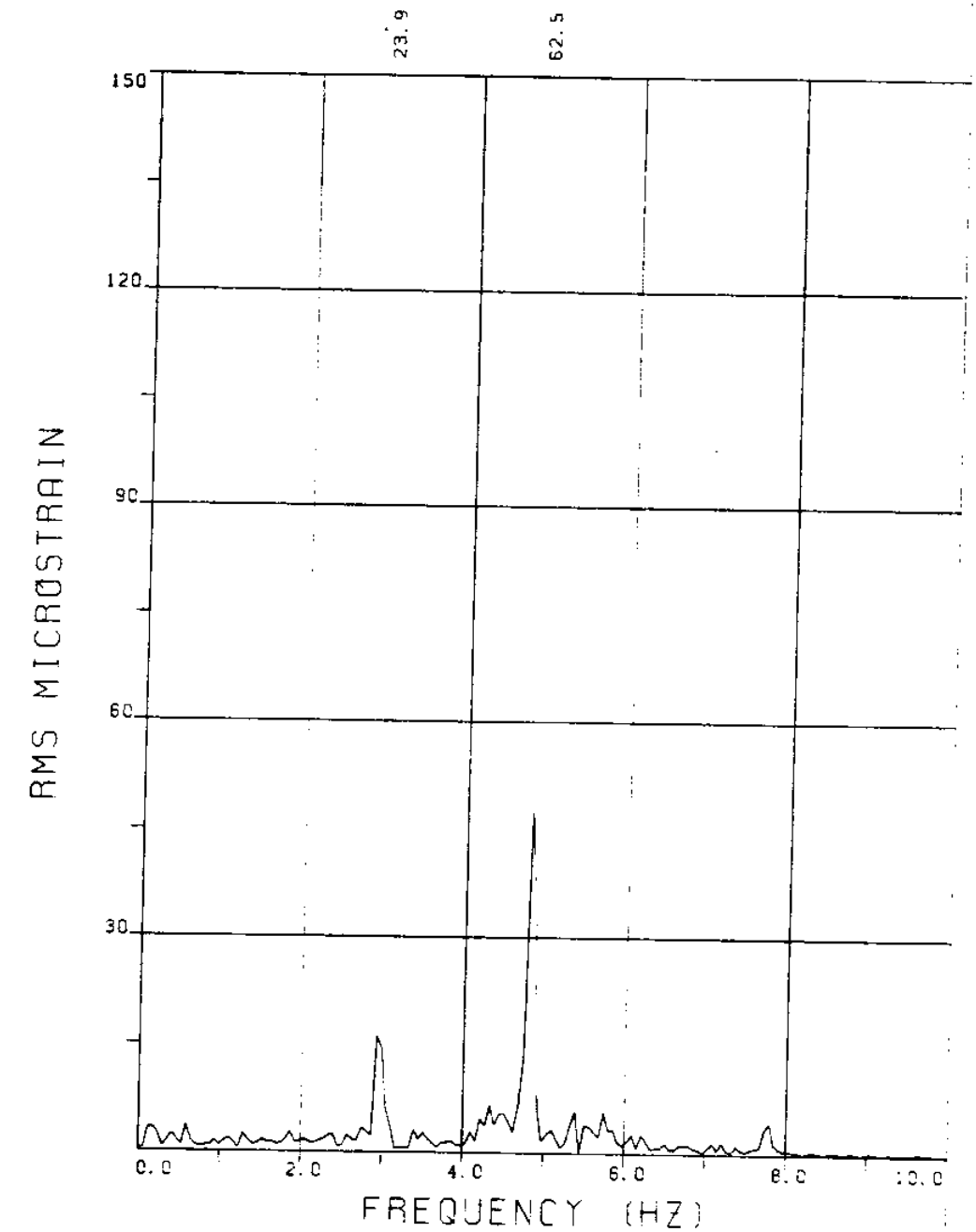

EXPERIMENT NUMBER 115

BRIDGE B3 ELEVATION=8L/11 BE=0.059

VC=410 A/DE=0.00

MEASURED RESPONSE IN MICROSTRAIN

TOTAL DYNAMIC RMS=71.3

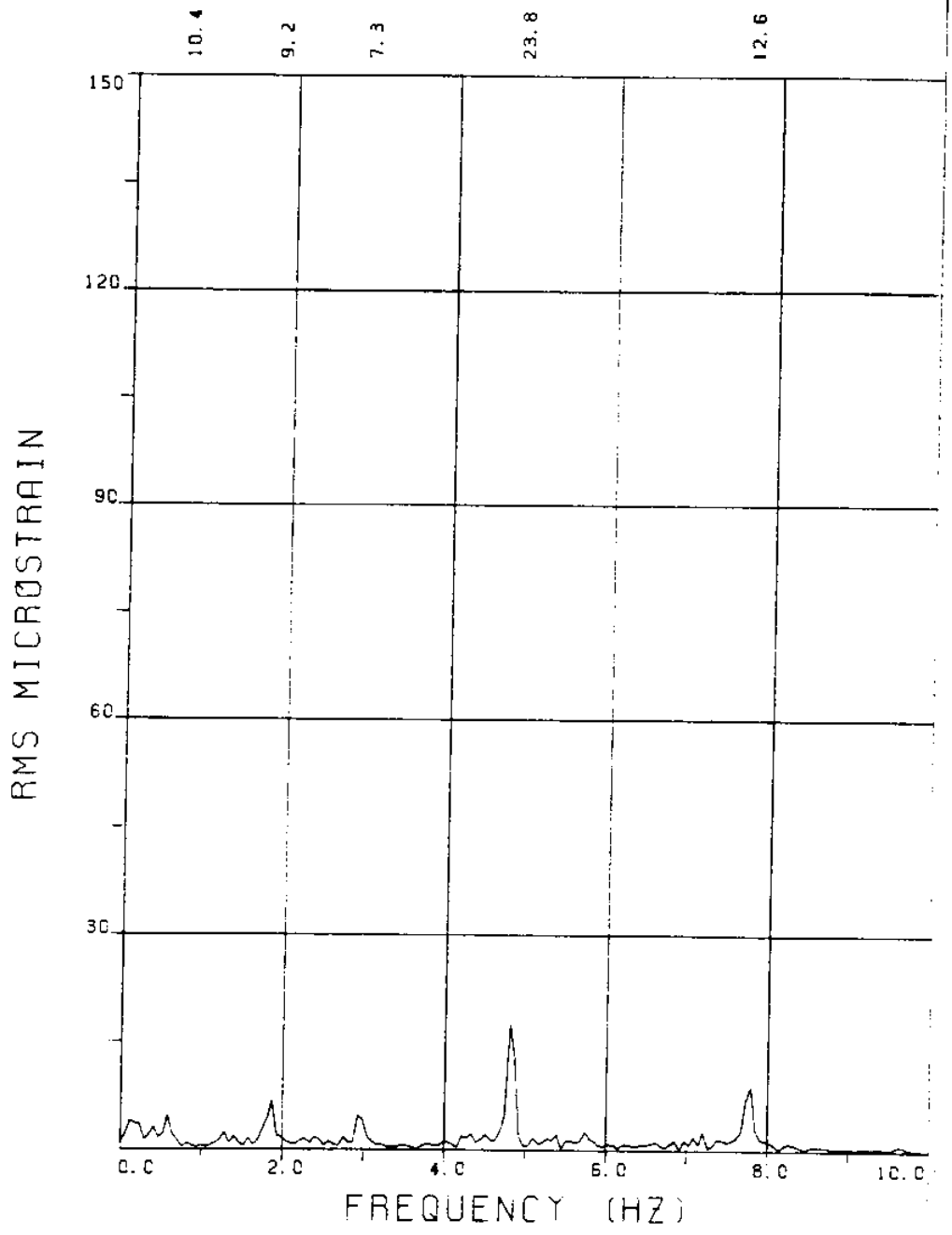

EXPERIMENT NUMBER 115

BRIDGE A9 ELEVATION=2L/11 BE=0.059

VC=410 A/DE=0.00

MEASURED RESPONSE IN MICROSTRAIN

MEAN=214.6

TOTAL DYNAMIC RMS=32.6

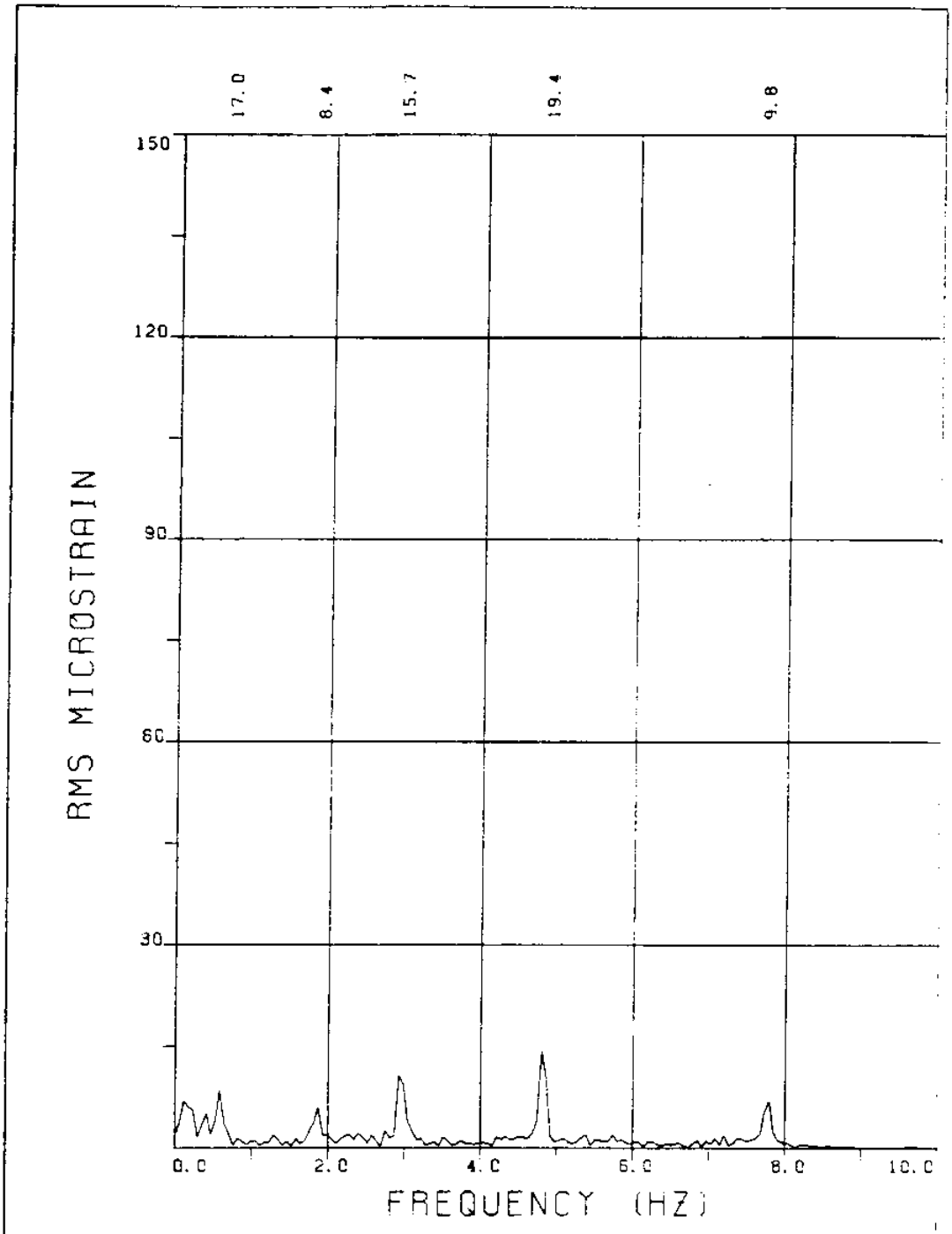

EXPERIMENT NUMBER 115

BRIDGE A7 ELEVATION=4L/11 BE=0.059

VC=410 A/DE=0.00

MEASURED RESPONSE IN MICROSTRAIN

MEAN=314.7

TOTAL DYNAMIC RMS=33.8

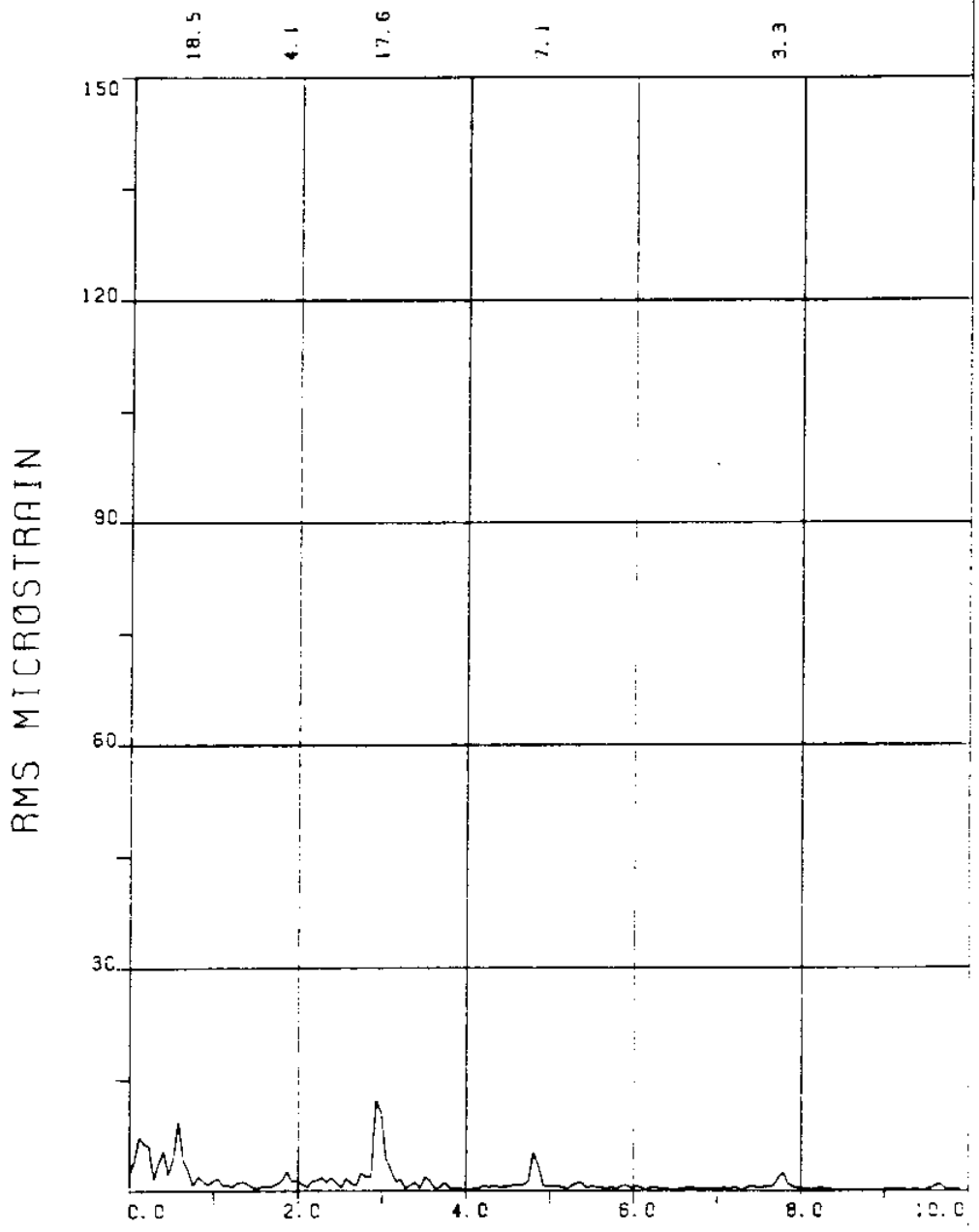

EXPERIMENT NUMBER 115

BRIDGE A6 ELEVATION=5L/11 BE=0.059

VC=410 A/DE=0.00

MEASURED RESPONSE IN MICROSTRAIN

MEAN=334.1

TOTAL DYNAMIC RMS=27.8

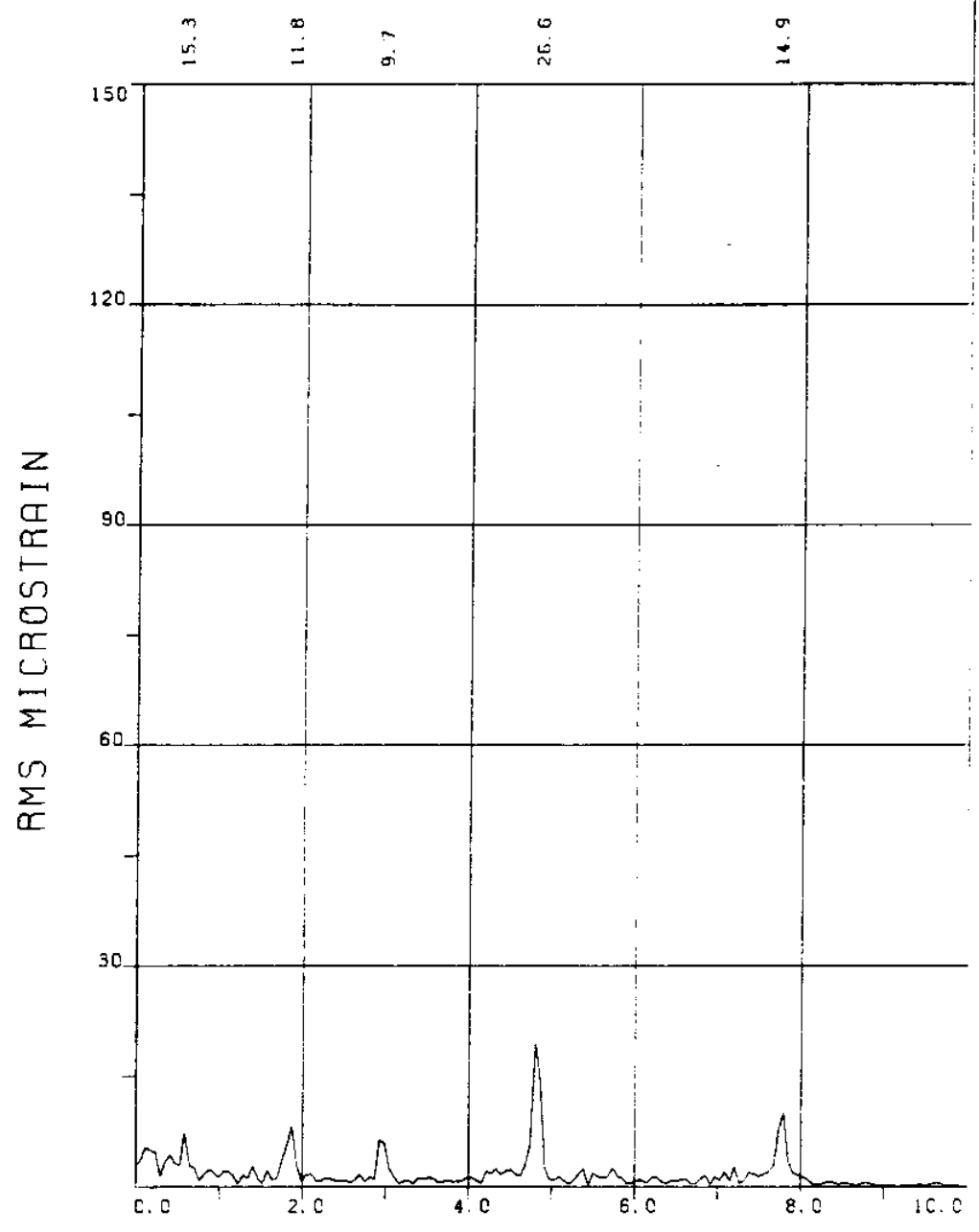

EXPERIMENT NUMBER 115

BRIDGE A3 ELEVATION=8L/11 BE=0.059

VC=410 A/DE=0.00

MEASURED RESPONSE IN MICROSTRAIN

MEAN=261.5

TOTAL DYNAMIC RMS=37.9

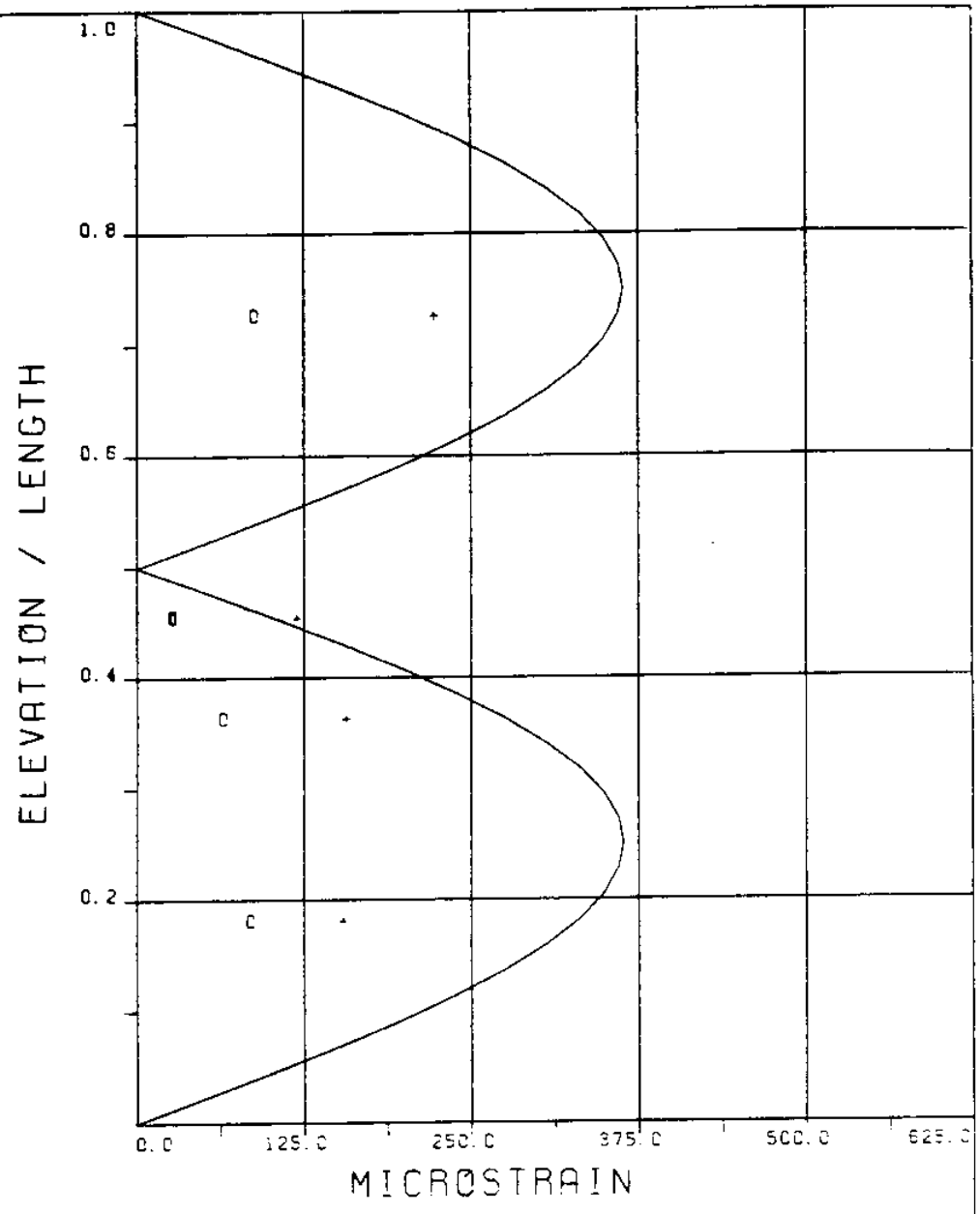

EXPERIMENT NUMBER 115

VC=410 A/DE=0.00

DYNAMIC RESPONSE AT F=FR IN PLANE B

——— THEORY o o o EXPERIMENT

MAXIMUM DYNAMIC RESPONSE IN PLANE B

——— THEORY + + + EXPERIMENT

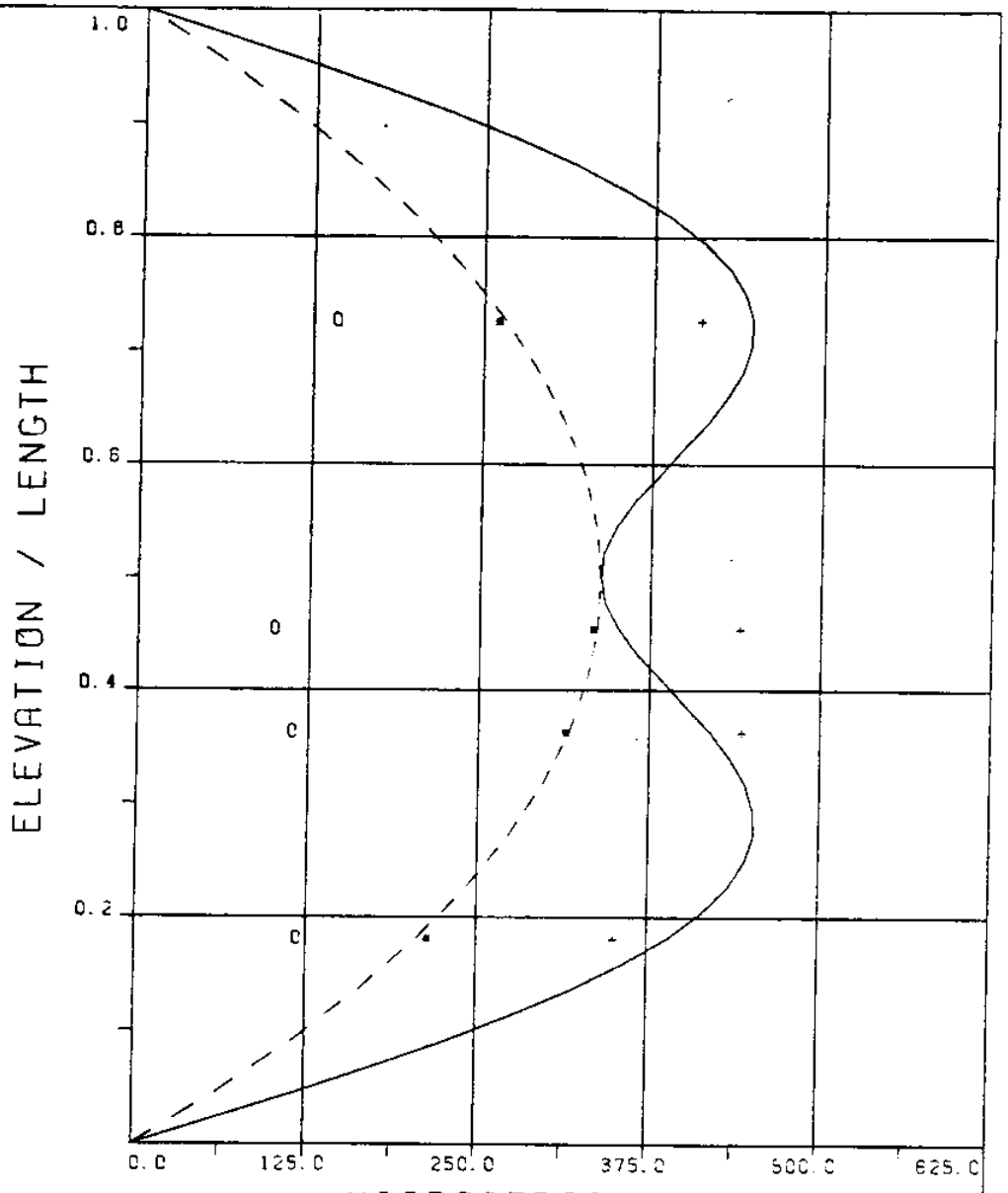

EXPERIMENT NUMBER 115

VC=410 A/DE=0.00

STATIC RESPONSE IN PLANE A

----- THEORY * * * EXPERIMENT

MAXIMUM DYNAMIC RESPONSE IN PLANE A

o o o EXPERIMENT

MAXIMUM RESPONSE

_____ THEORY + + + EXPERIMENT

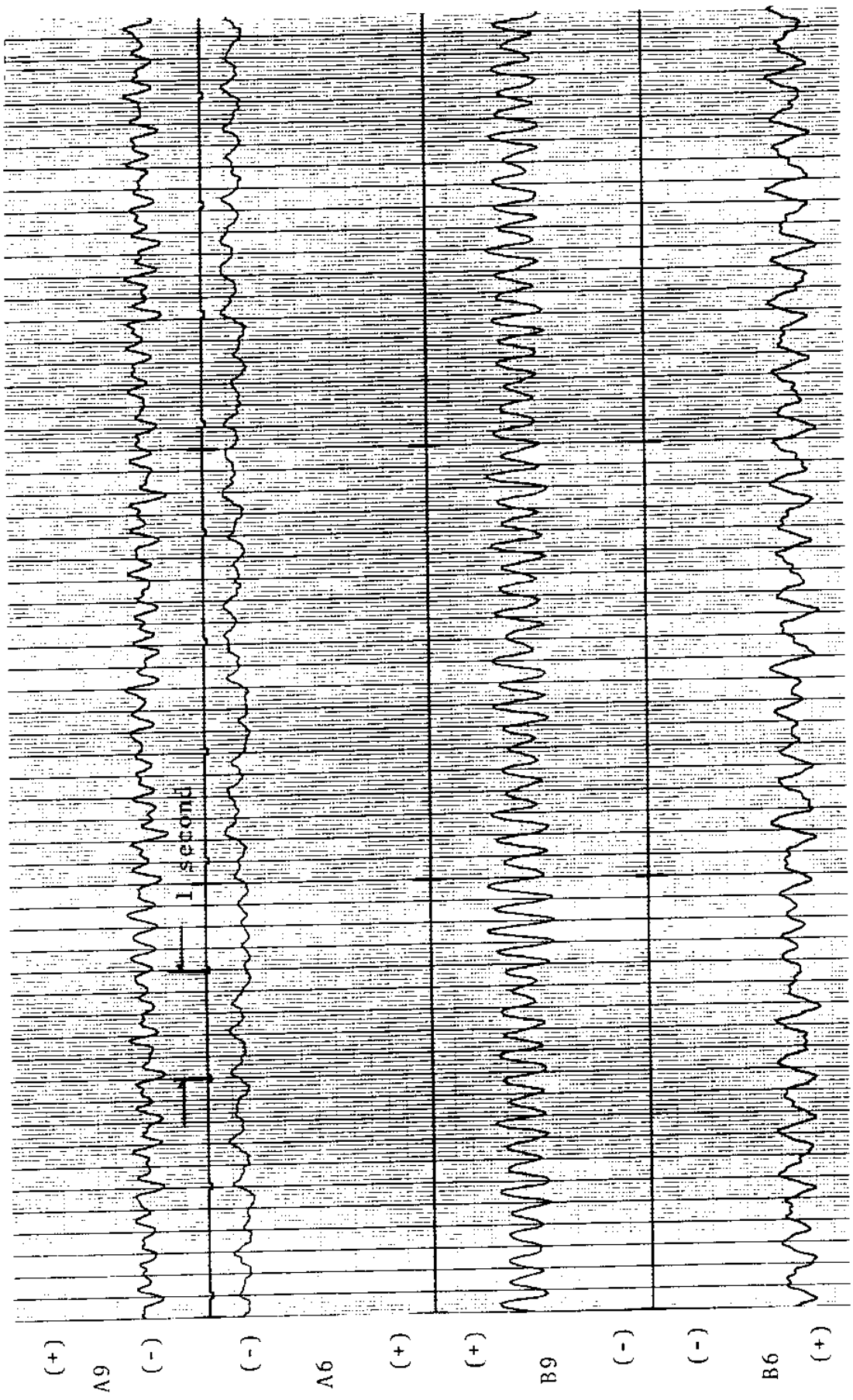

FIGURE 115Ta: ALL BRIDGES: 15.3 MICROSTRAIN/DIVISION

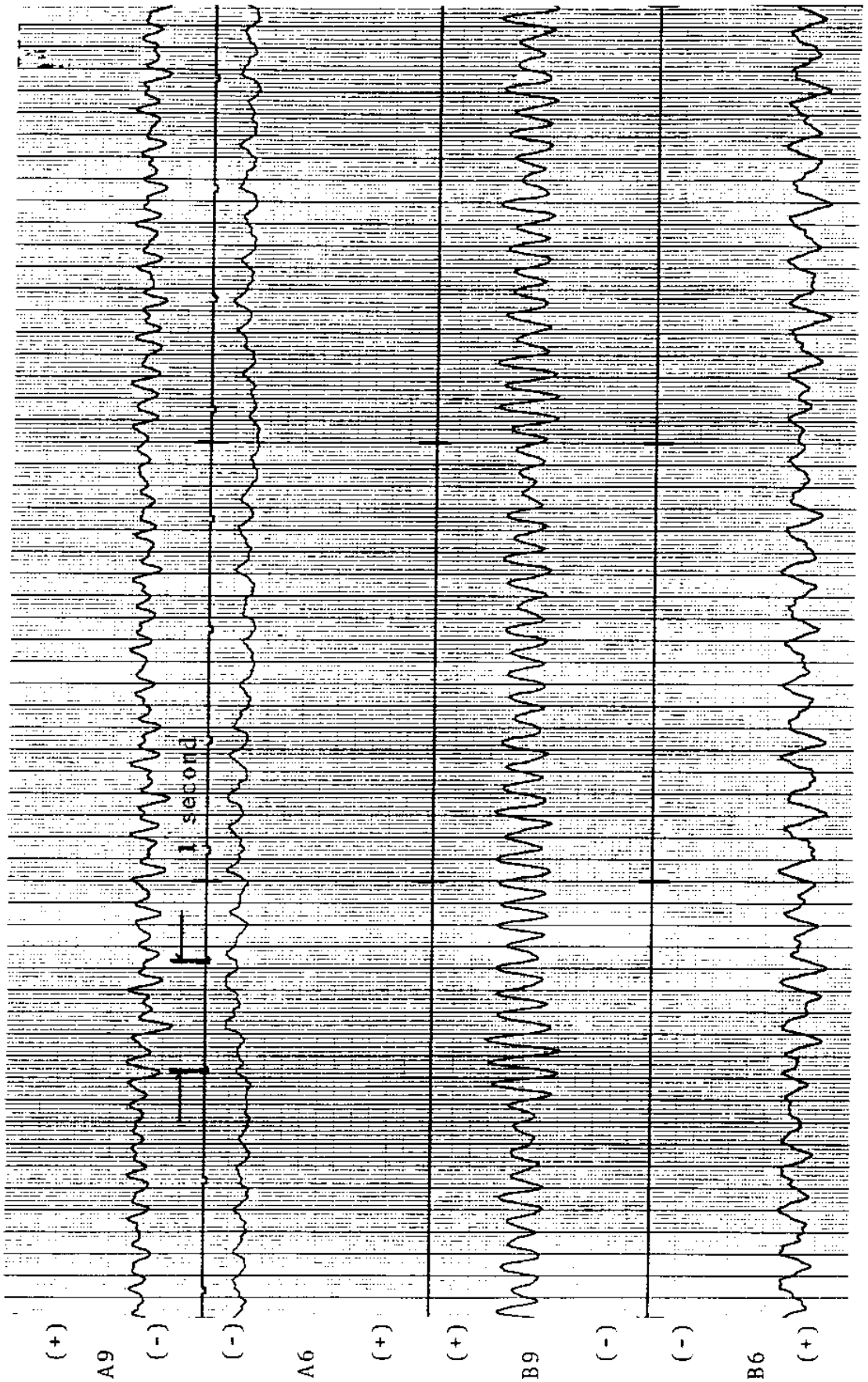

FIGURE 115Tb: ALL BRIDGES: 15.3 MICROSTRAIN/DIVISION

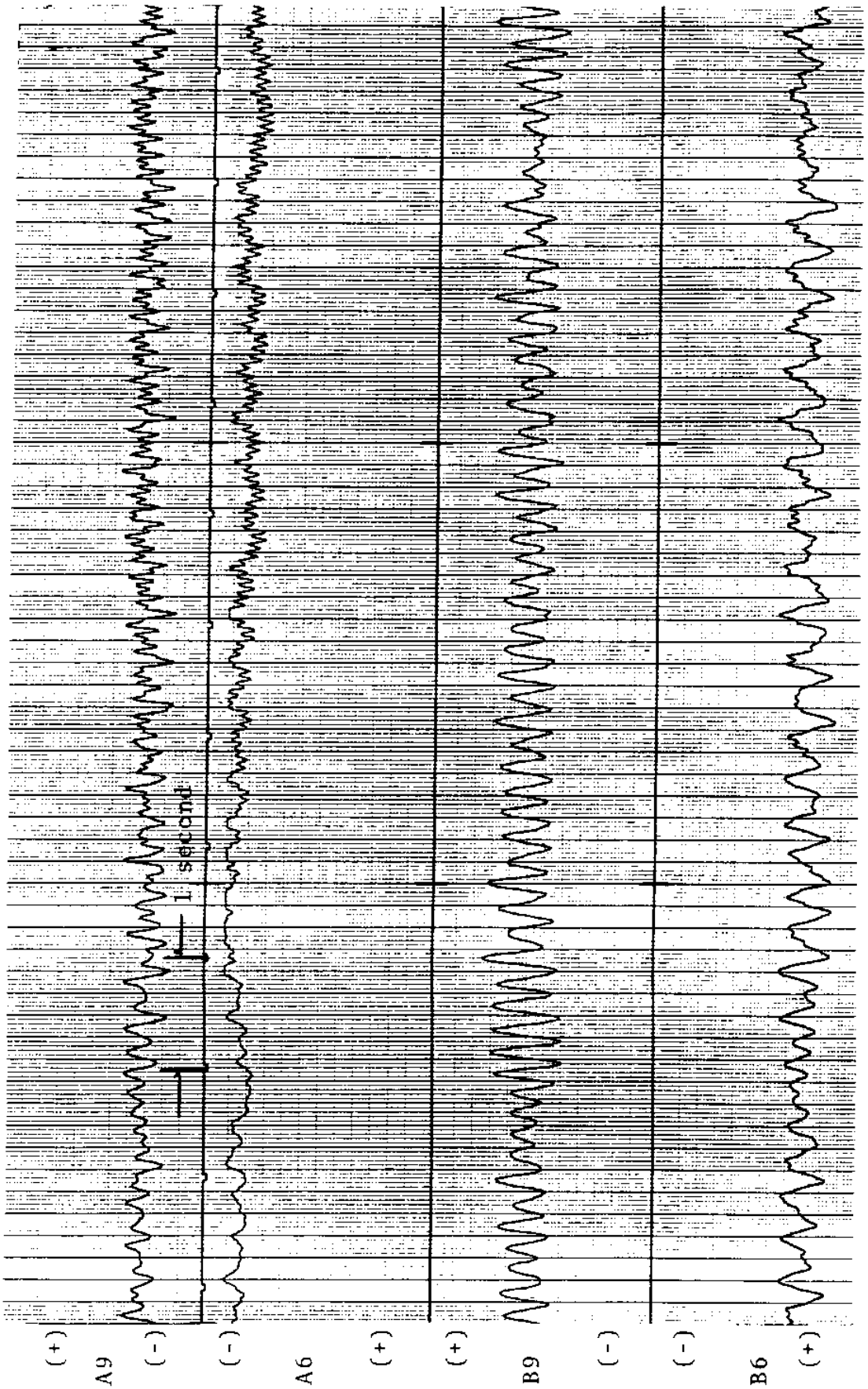

FIGURE 115Tc: ALL BRIDGES: 15.3 MICROSTRAIN/DIVISION

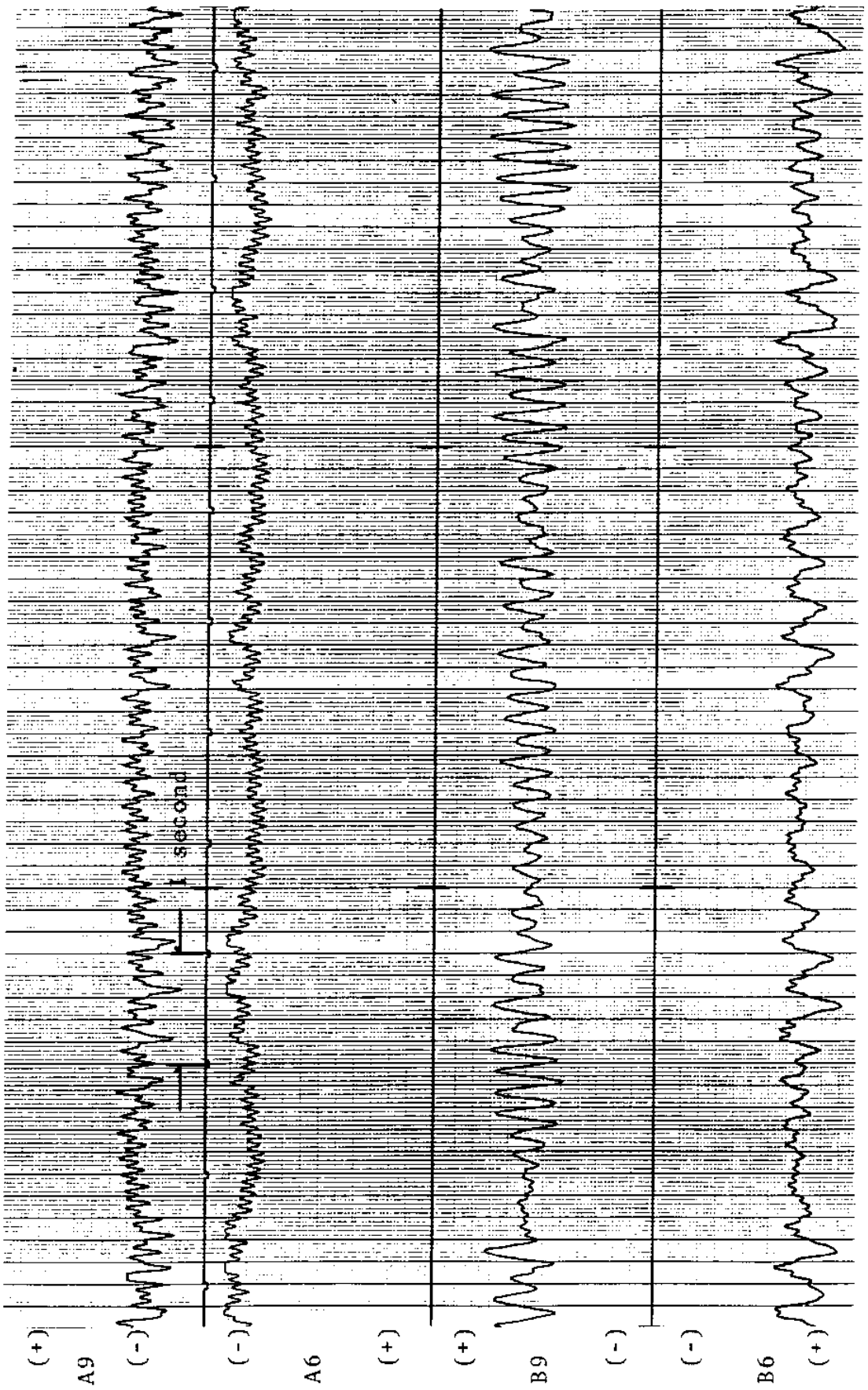

FIGURE 115Td: ALL BRIDGES: 15.3 MICROSTRAIN/DIVISION

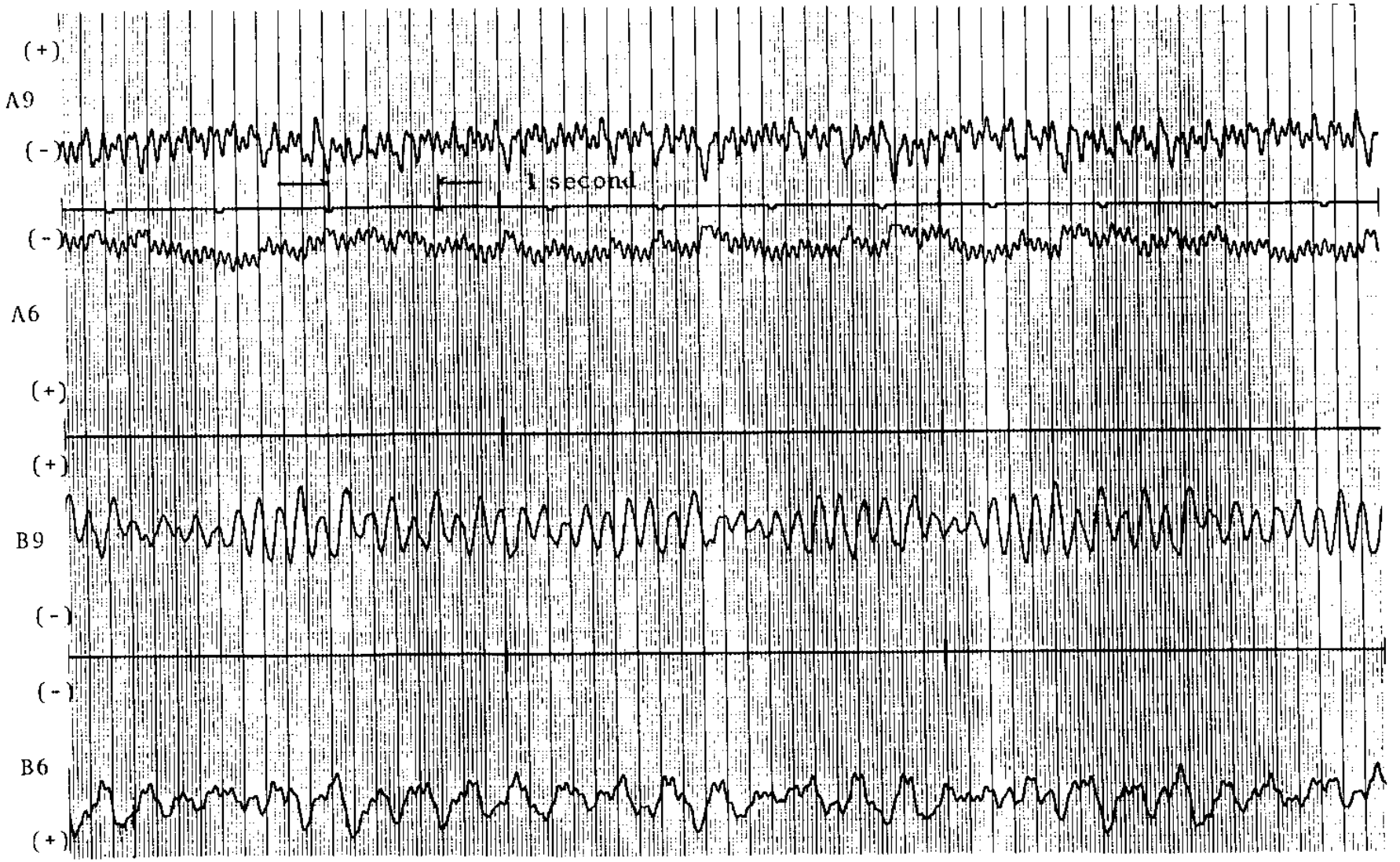

FIGURE 115Te: ALL BRIDGES: 15.3 MICROSTRAIN/DIVISION

EXPERIMENT 116

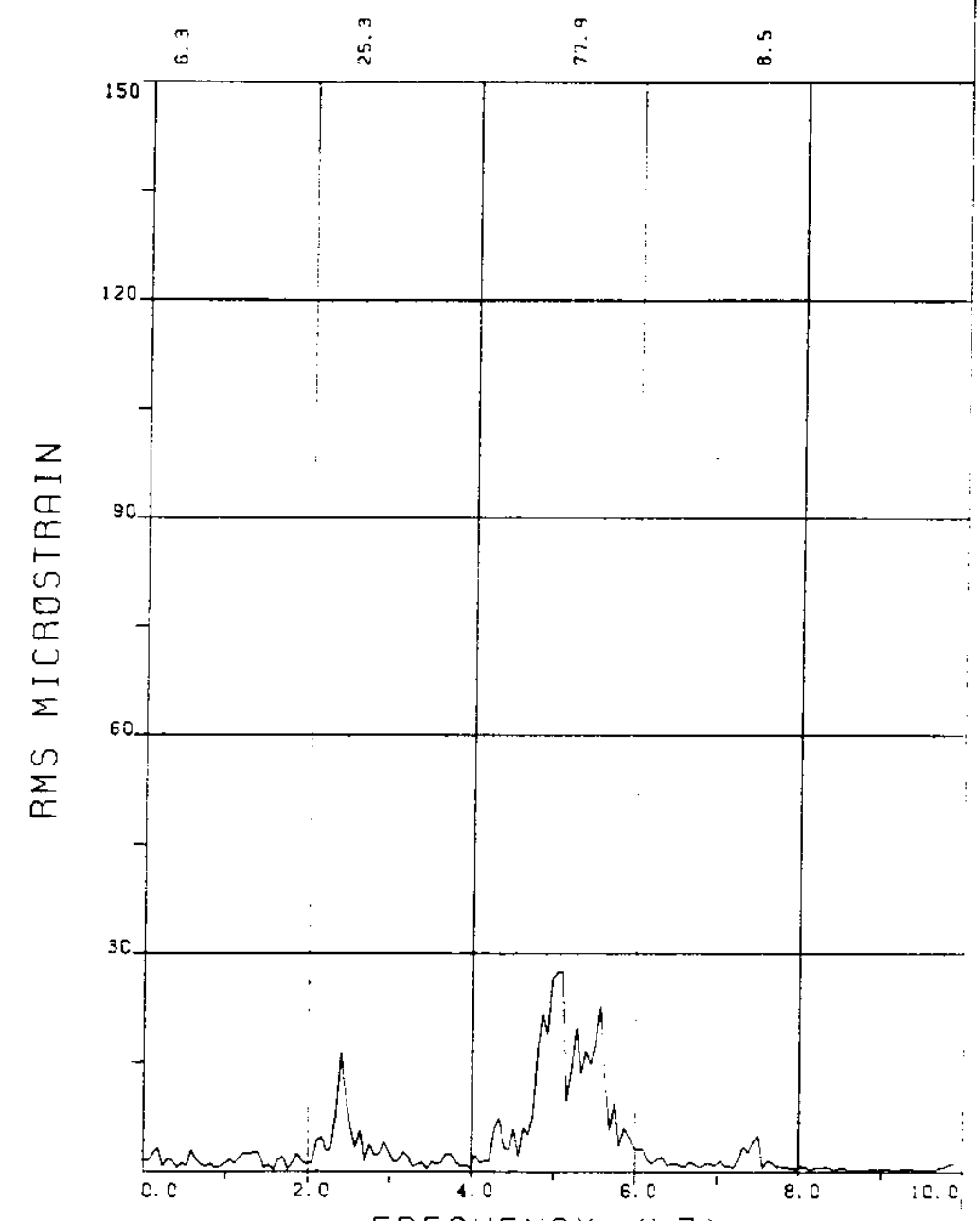

EXPERIMENT NUMBER 116

BRIDGE B9 ELEVATION=2L/11 BE=0.059

VC=430 A/DE=0.00

MEASURED RESPONSE IN MICROSTRAIN

TOTAL DYNAMIC RMS=82.4

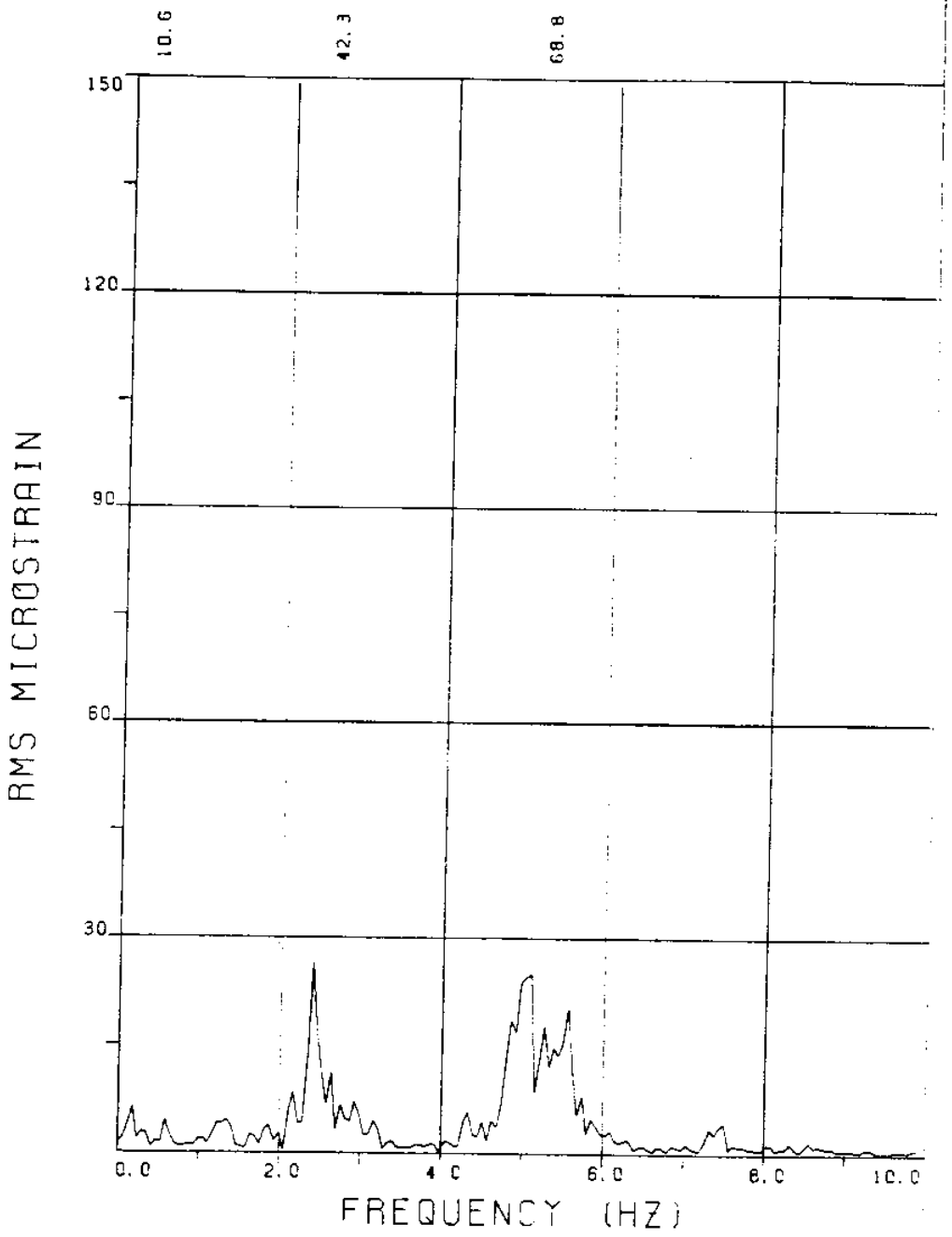

EXPERIMENT NUMBER 116

BRIDGE B7 ELEVATION=4L/11 BE=0.059

VC=430 A/DE=0.00

MEASURED RESPONSE IN MICROSTRAIN

TOTAL DYNAMIC RMS=83.1

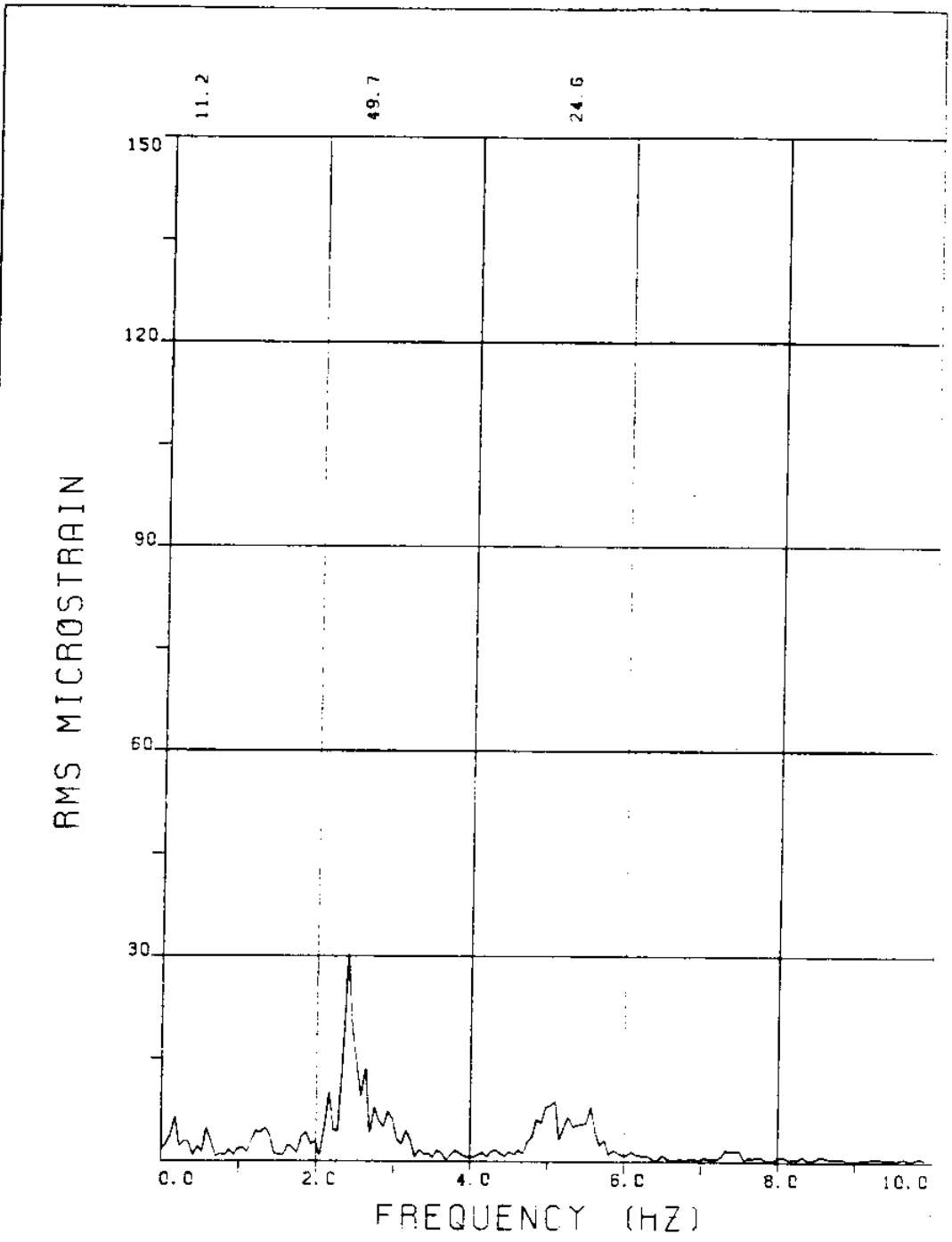

EXPERIMENT NUMBER 116

BRIDGE B6 ELEVATION=5L/11 BE=0.059

VC=430 A/DE=0.00

MEASURED RESPONSE IN MICROSTRAIN

TOTAL DYNAMIC RMS=60.4

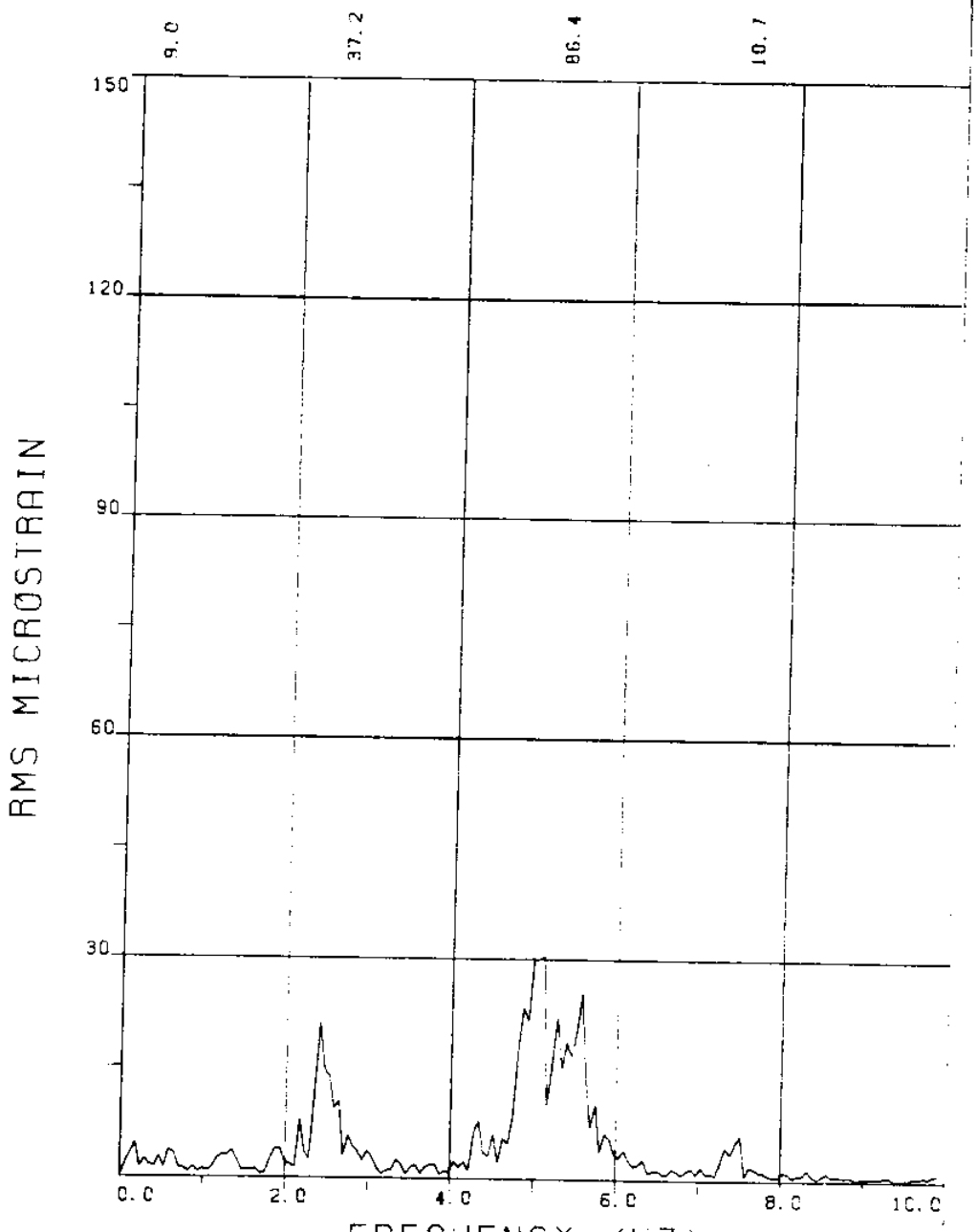

EXPERIMENT NUMBER 116

BRIDGE B3 ELEVATION=8L/11 BE=0.059

VC=430 A/DE=0.00

MEASURED RESPONSE IN MICROSTRAIN

TOTAL DYNAMIC RMS=93.9

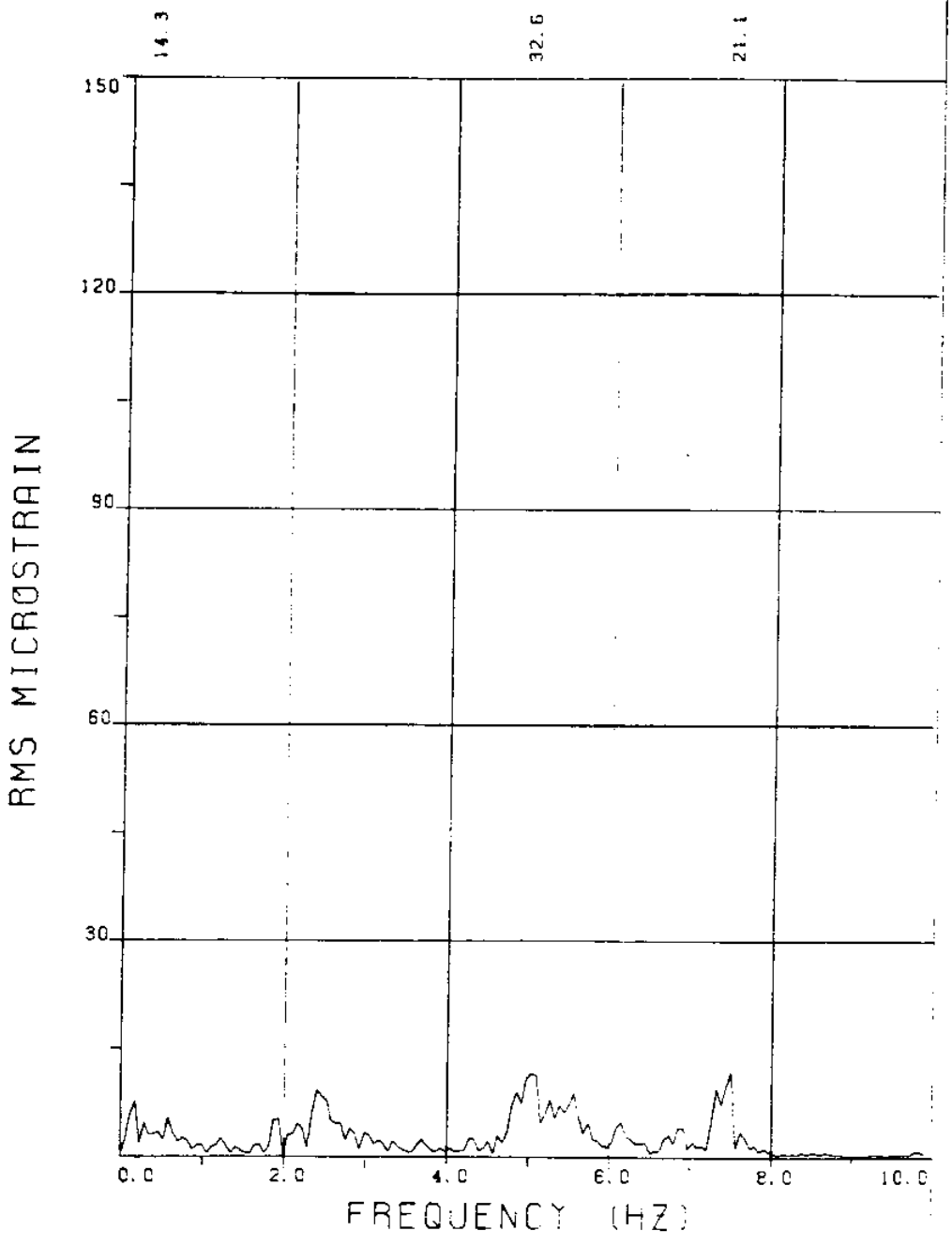

EXPERIMENT NUMBER 116

BRIDGE A9 ELEVATION=2L/11 BE=0.059

VC=430 A/DE=0.00

MEASURED RESPONSE IN MICROSTRAIN

MEAN=237.5

TOTAL DYNAMIC RMS=53.2

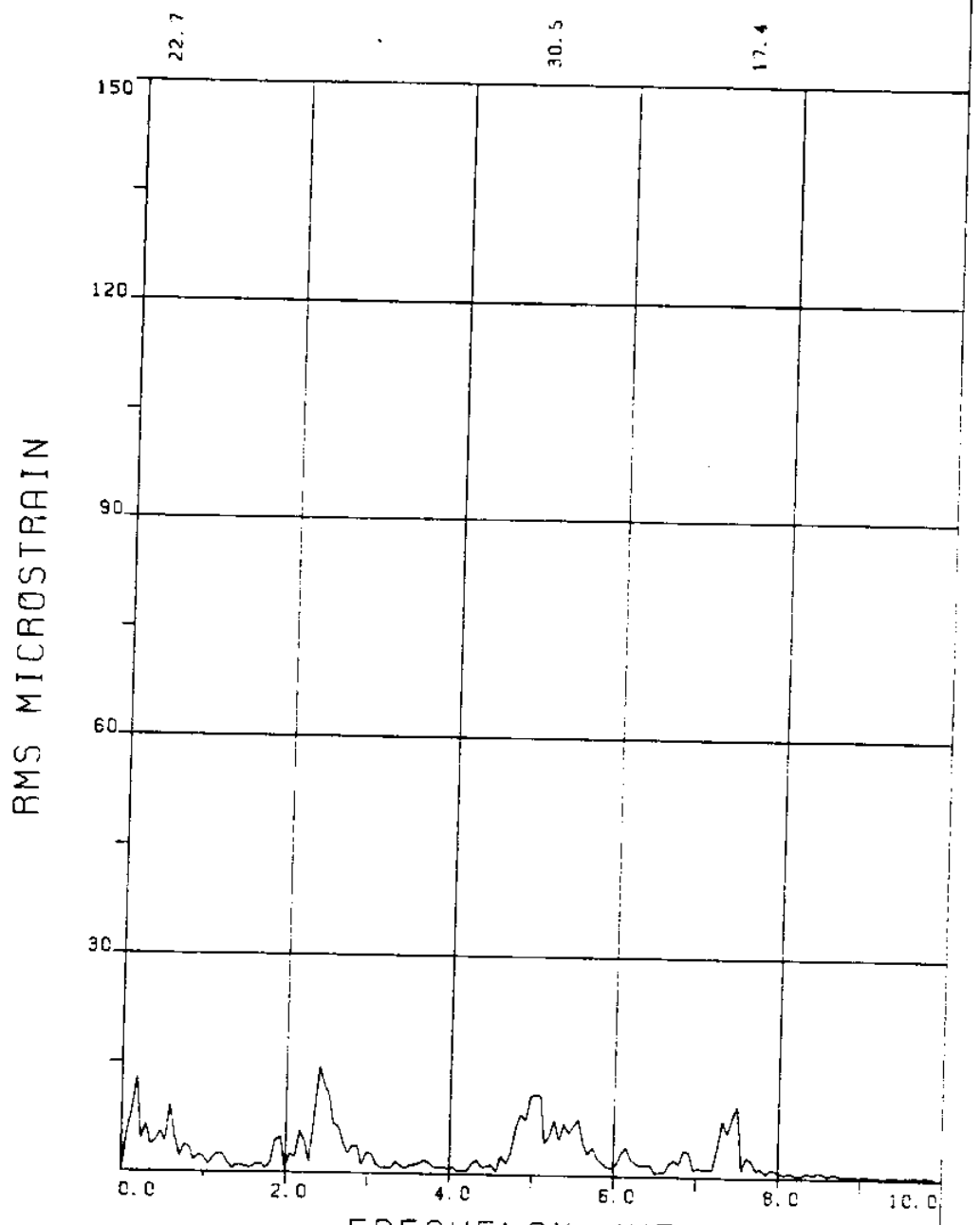

EXPERIMENT NUMBER 116

BRIDGE A7 ELEVATION=4L/11 BE=0.059

VC=430 A/DE=0.00

MEASURED RESPONSE IN MICROSTRAIN

MEAN=348.8

TOTAL DYNAMIC RMS=51.0

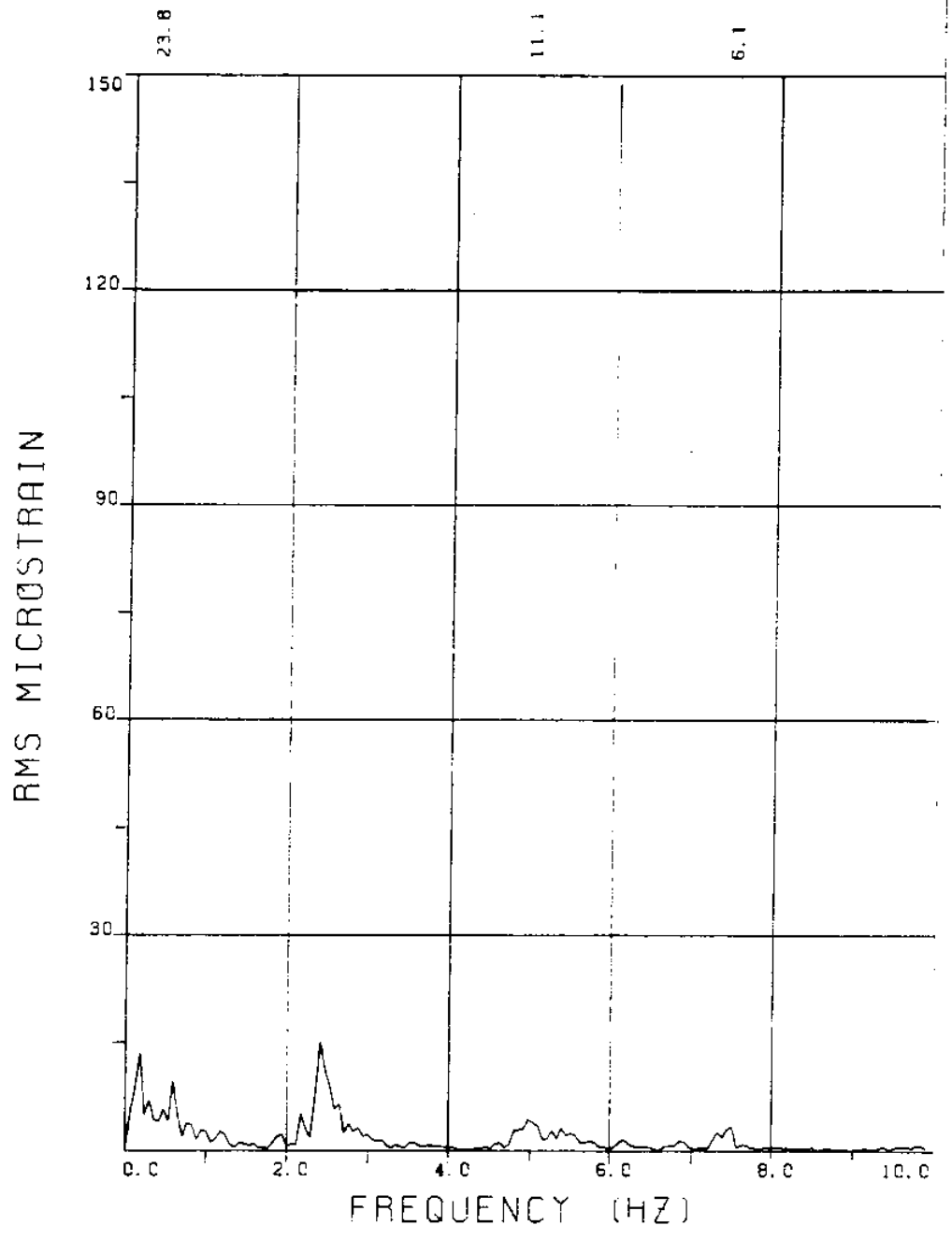

EXPERIMENT NUMBER 116

BRIDGE A6 ELEVATION=5L/11 BE=0.059

VC=430 A/DE=0.00

MEASURED RESPONSE IN MICROSTRAIN

MEAN=368.3

TOTAL DYNAMIC RMS=43.2

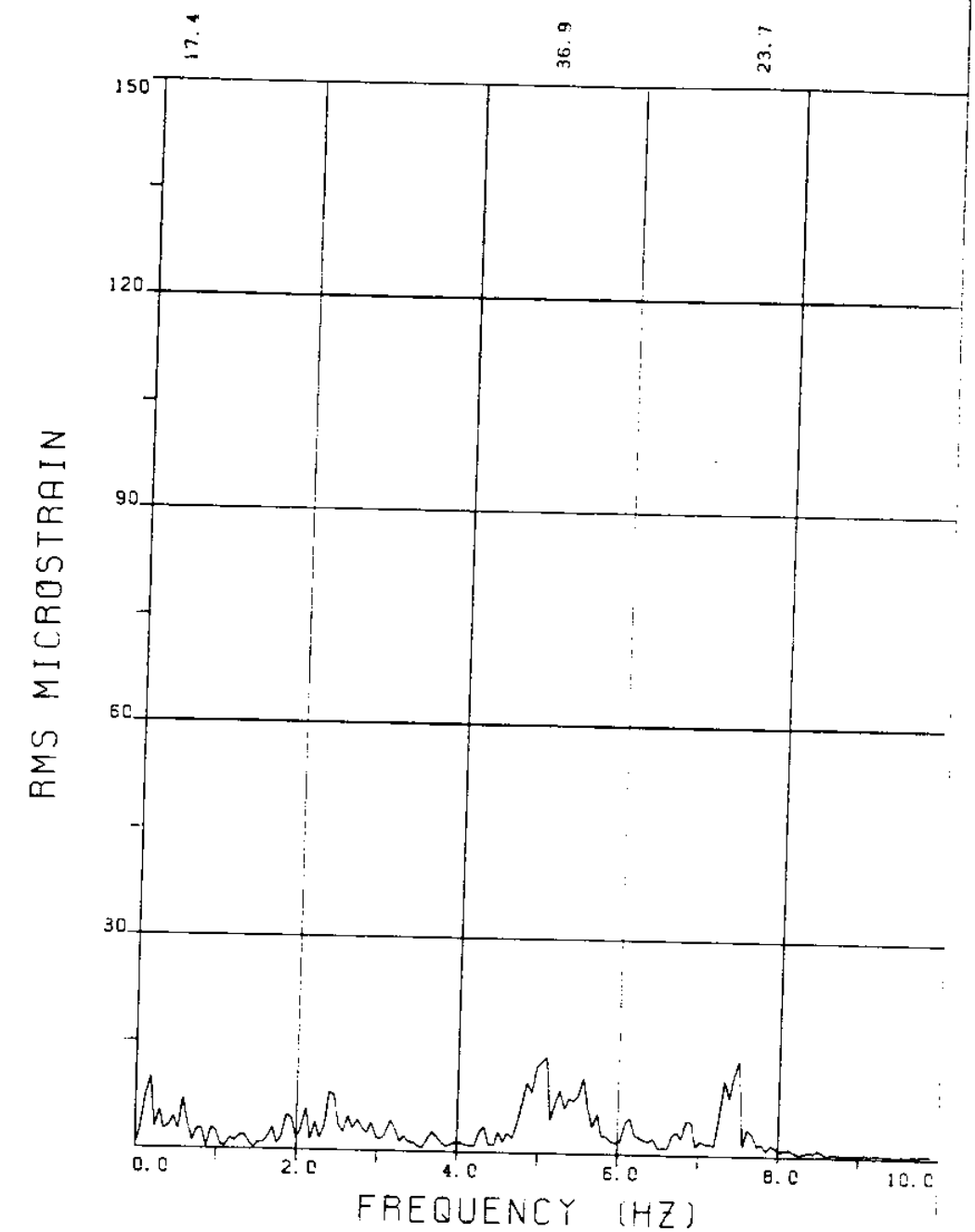

EXPERIMENT NUMBER 116

BRIDGE A3 ELEVATION=8L/11 BE=0.059

VC=430 A/DE=0.00

MEASURED RESPONSE IN MICROSTRAIN

MEAN=289.4

TOTAL DYNAMIC RMS=56.9

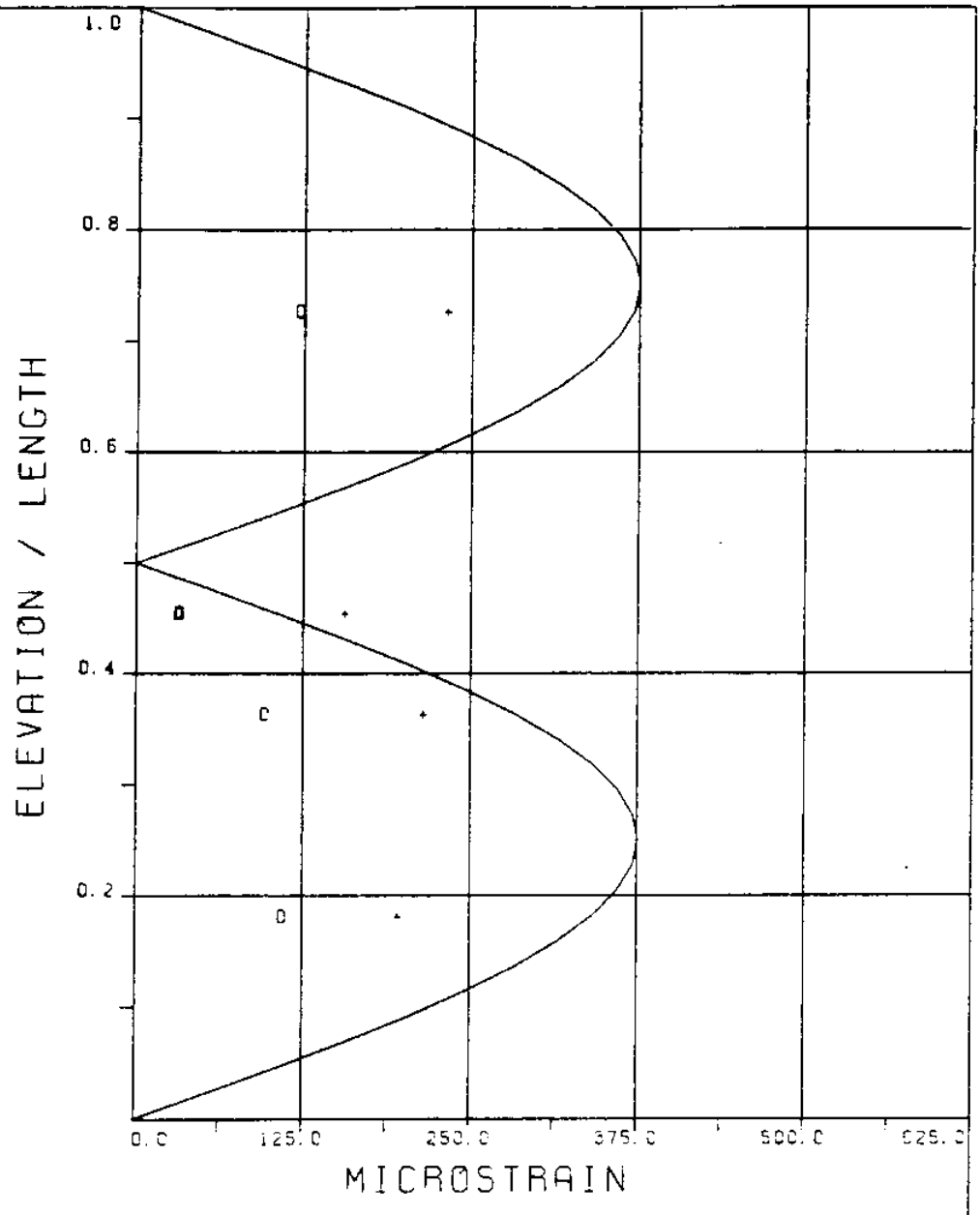

EXPERIMENT NUMBER 116

VC=430 A/DE=0.00

DYNAMIC RESPONSE AT F=FR IN PLANE B

——— THEORY o o o EXPERIMENT

MAXIMUM DYNAMIC RESPONSE IN PLANE B

——— THEORY + + + EXPERIMENT

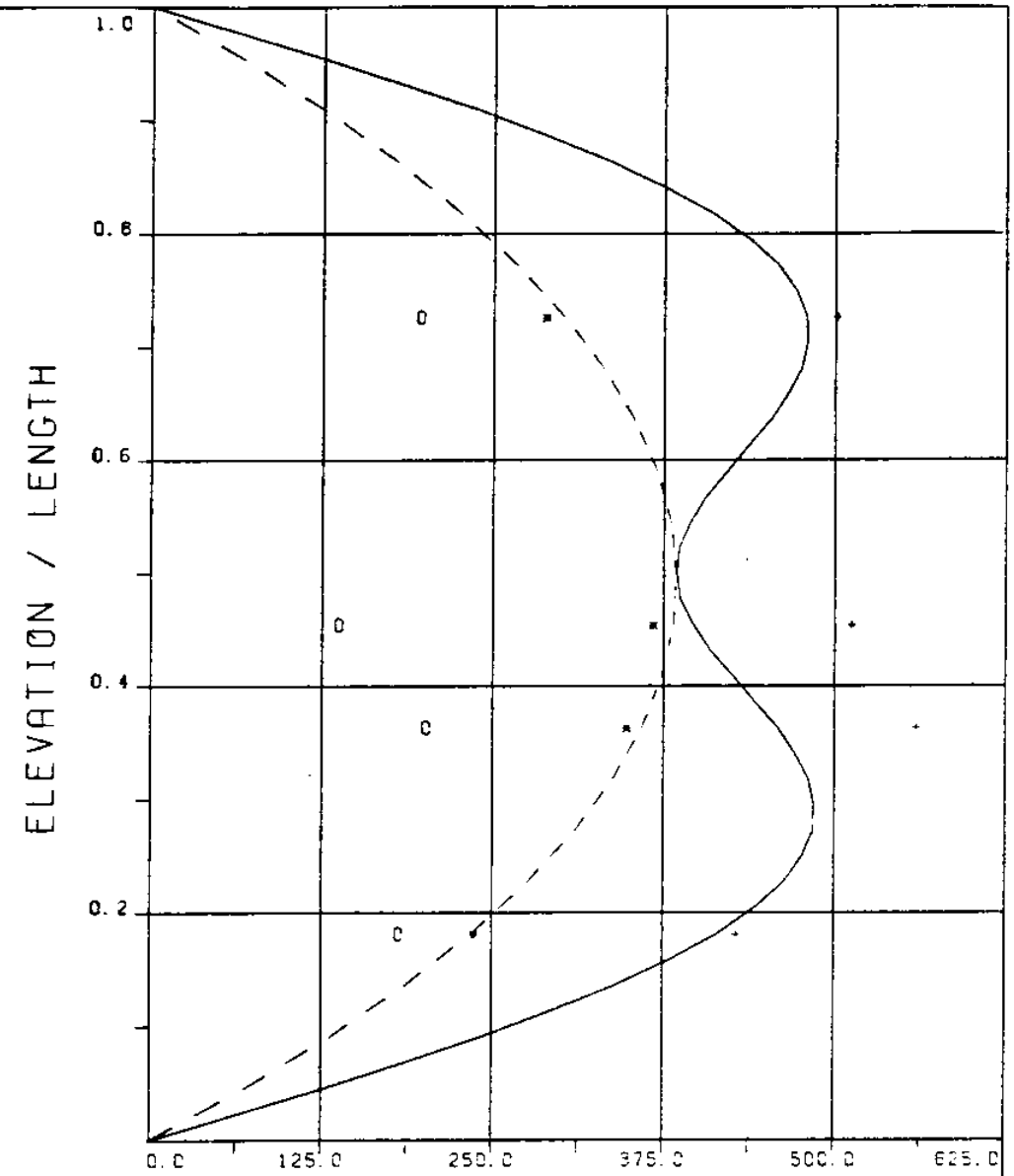

EXPERIMENT NUMBER 116

VC=430 A/DE=0.00

STATIC RESPONSE IN PLANE A

----- THEORY * * * EXPERIMENT

MAXIMUM DYNAMIC RESPONSE IN PLANE A

o o o EXPERIMENT

MAXIMUM RESPONSE

——— THEORY + + + EXPERIMENT

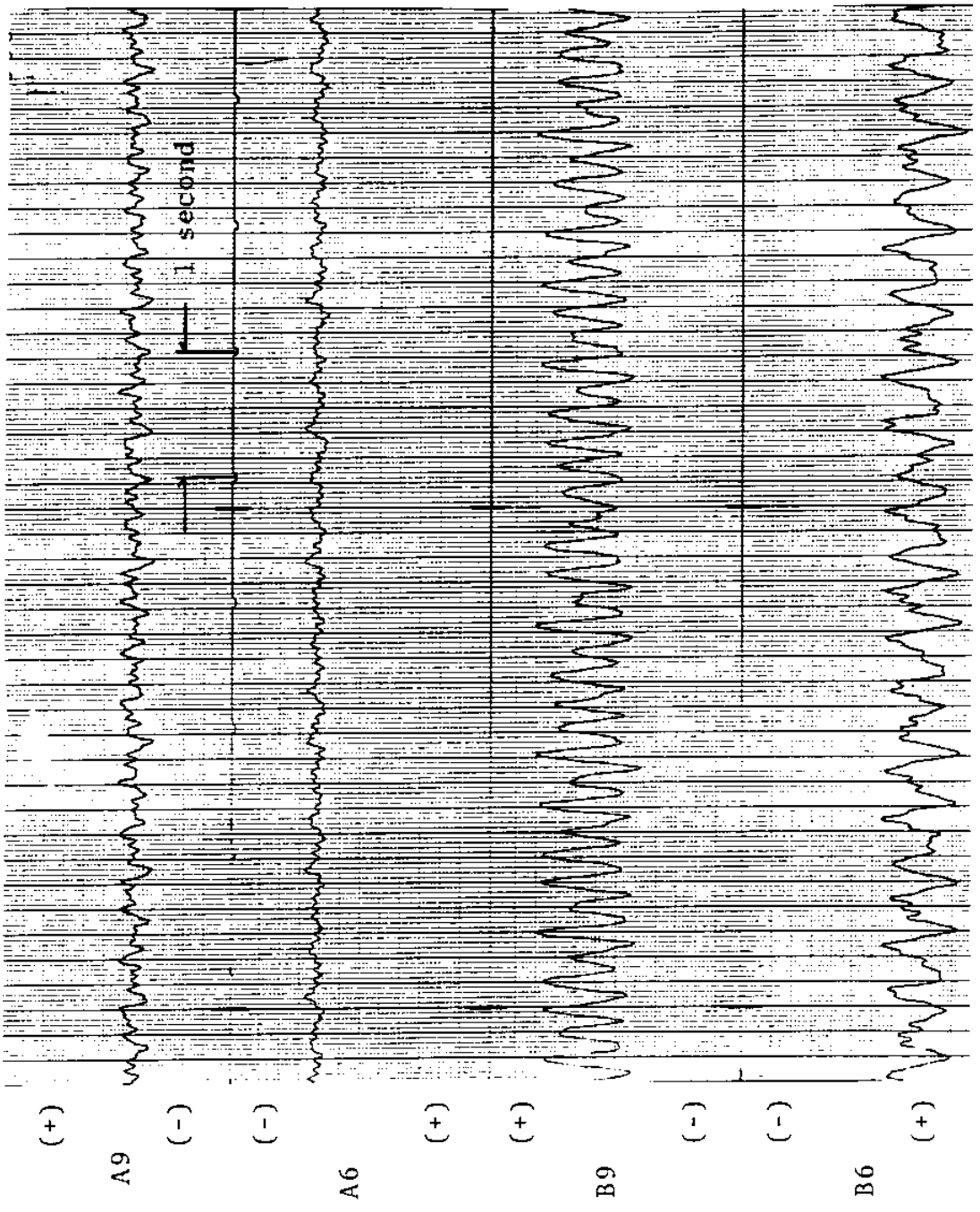

FIGURE 116Ta: A BRIDGES: 38.2 MICROSTRAIN/DIVISION
B BRIDGES: 15.3 MICROSTRAIN/DIVISION

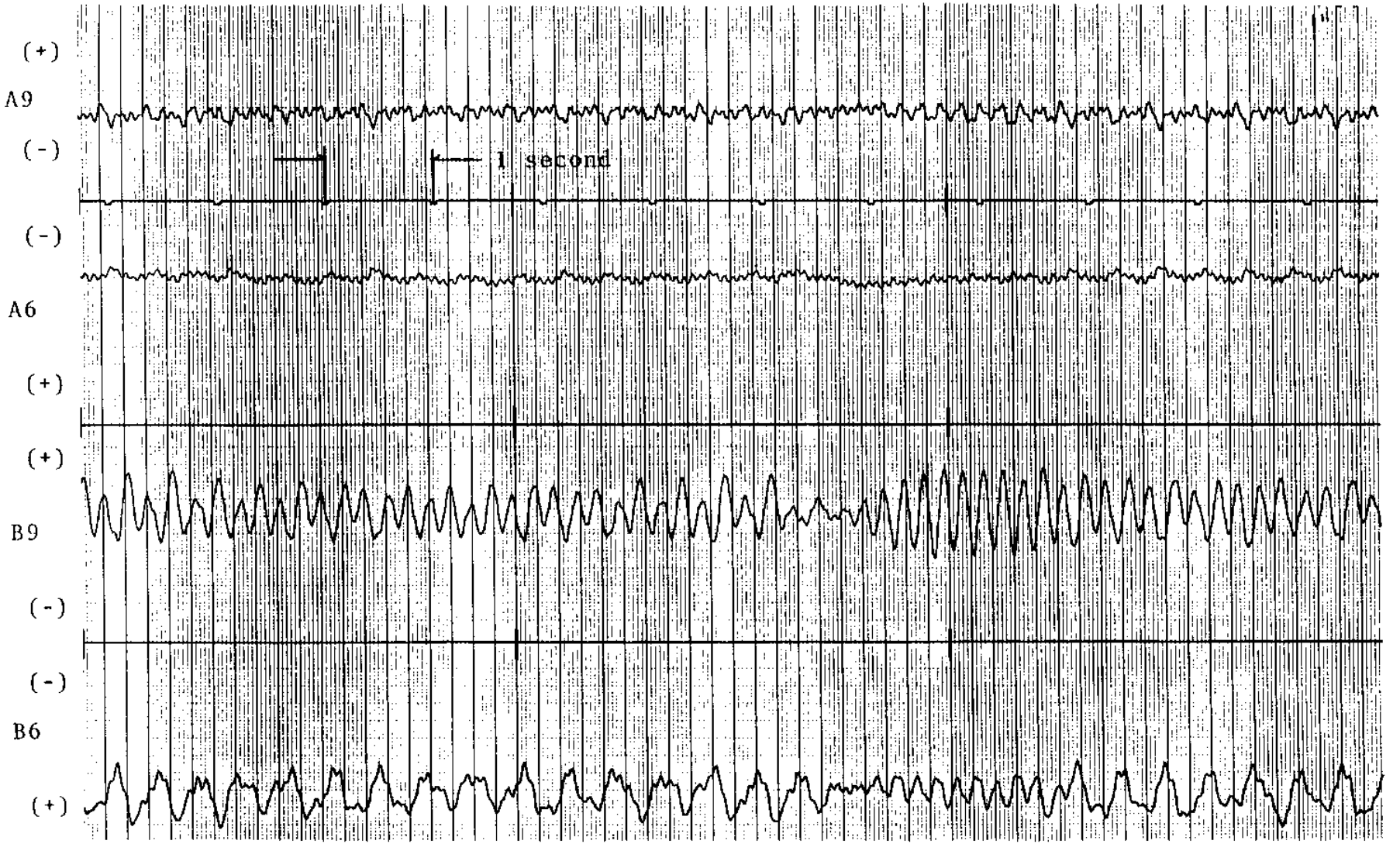

FIGURE 116Tb: A BRIDGES 38.2 MICROSTRAIN/DIVISION
B BRIDGES 15.3 MICROSTRAIN/DIVISION

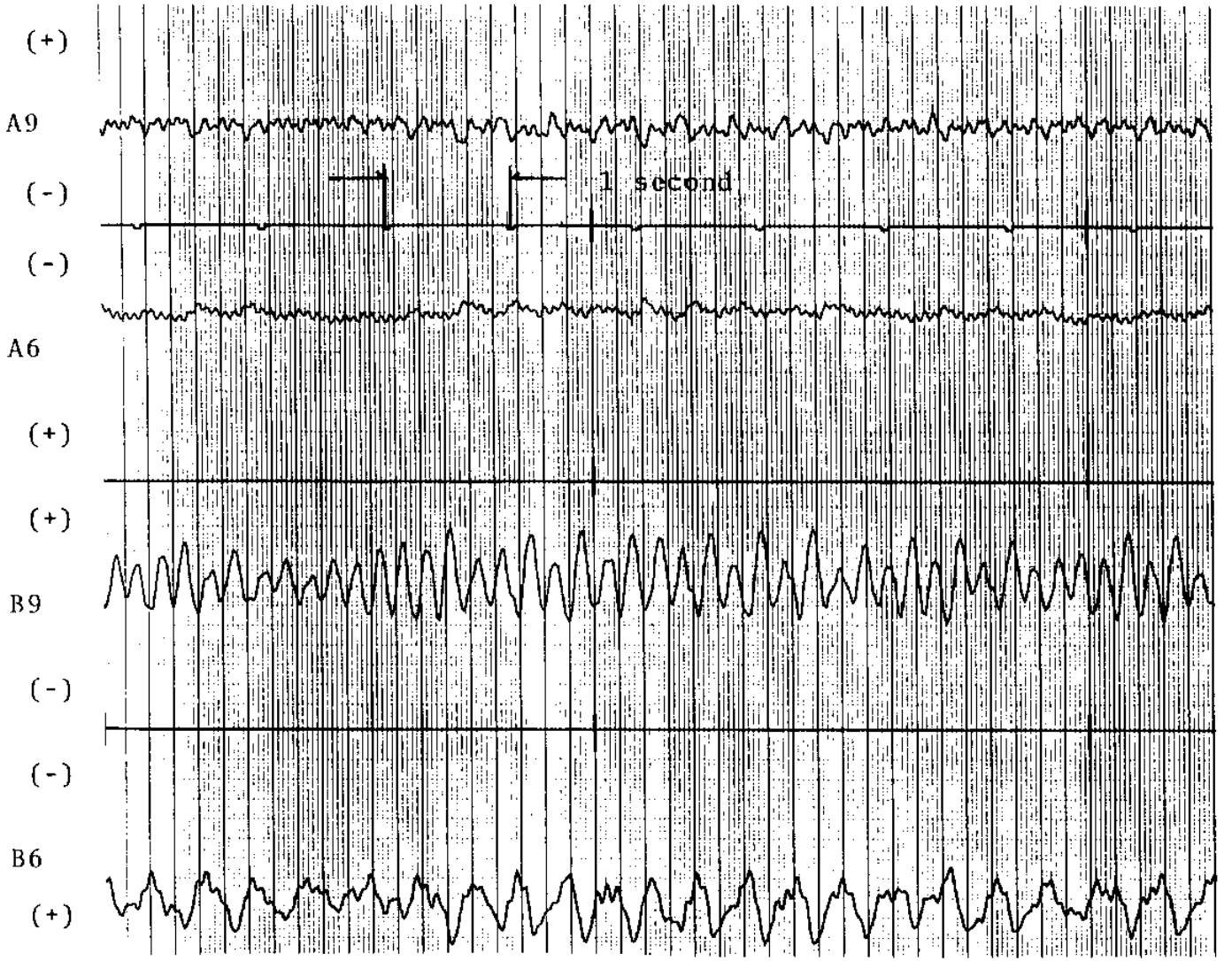

FIGURE 116Tc: A BRIDGES: 38.2 MICROSTRAIN/DIVISION
B BRIDGES: 15.3 MICROSTRAIN/DIVISION

EXPERIMENT 117

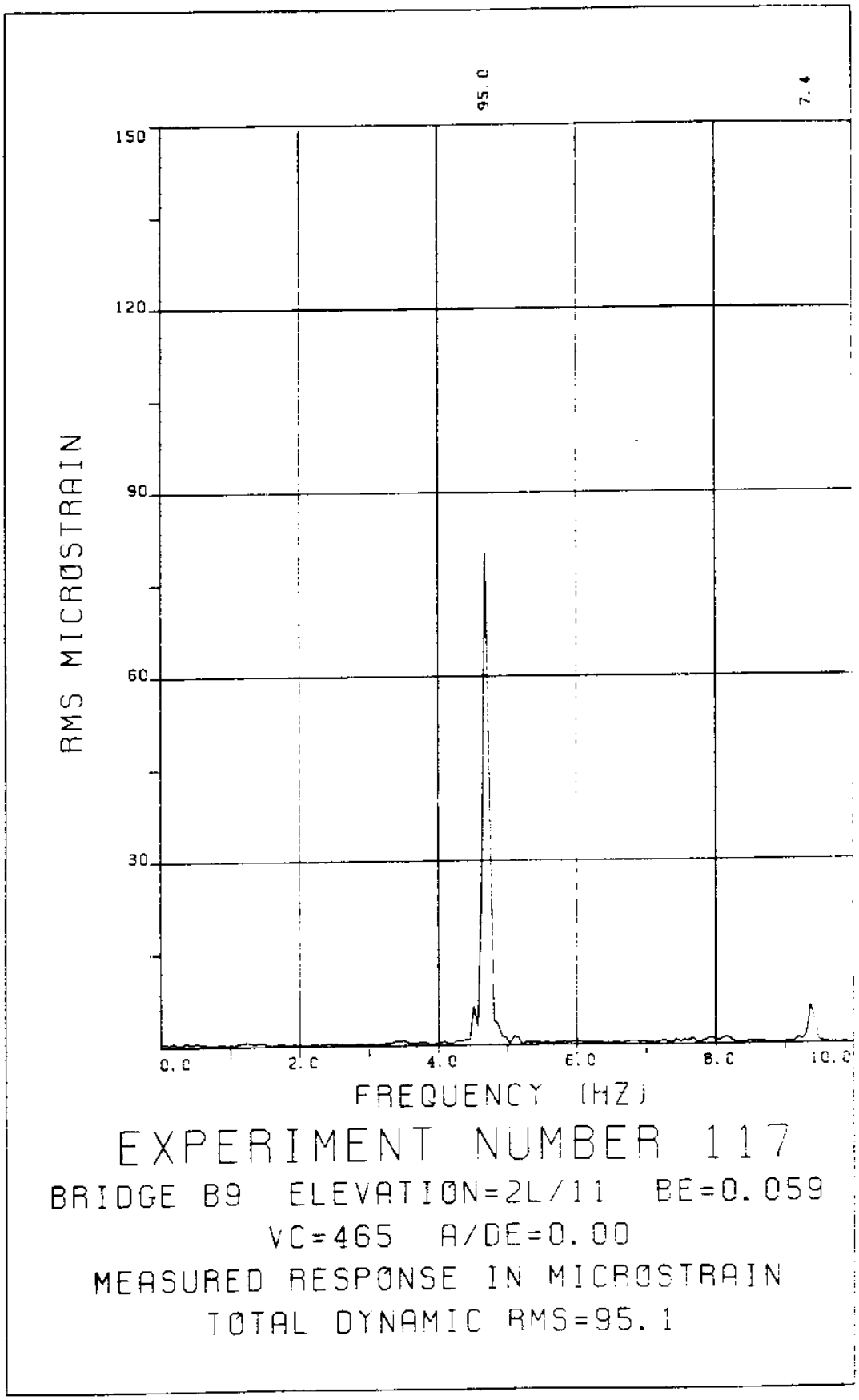

EXPERIMENT NUMBER 117

BRIDGE B9 ELEVATION=2L/11 BE=0.059

VC=465 A/DE=0.00

MEASURED RESPONSE IN MICROSTRAIN

TOTAL DYNAMIC RMS=95.1

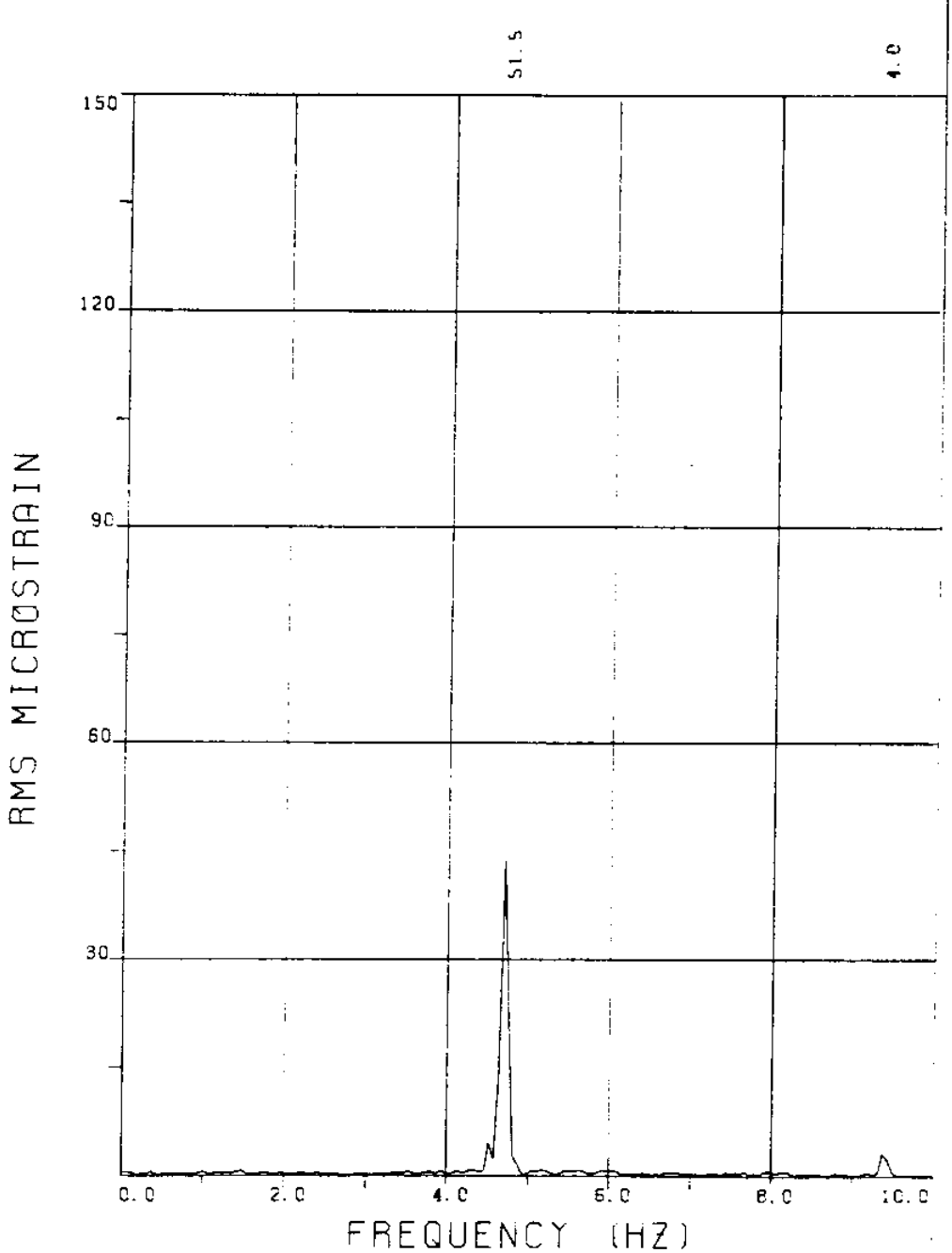

EXPERIMENT NUMBER 117

BRIDGE B7 ELEVATION=4L/11 BE=0.059

VC=465 A/DE=0.00

MEASURED RESPONSE IN MICROSTRAIN

TOTAL DYNAMIC RMS=53.1

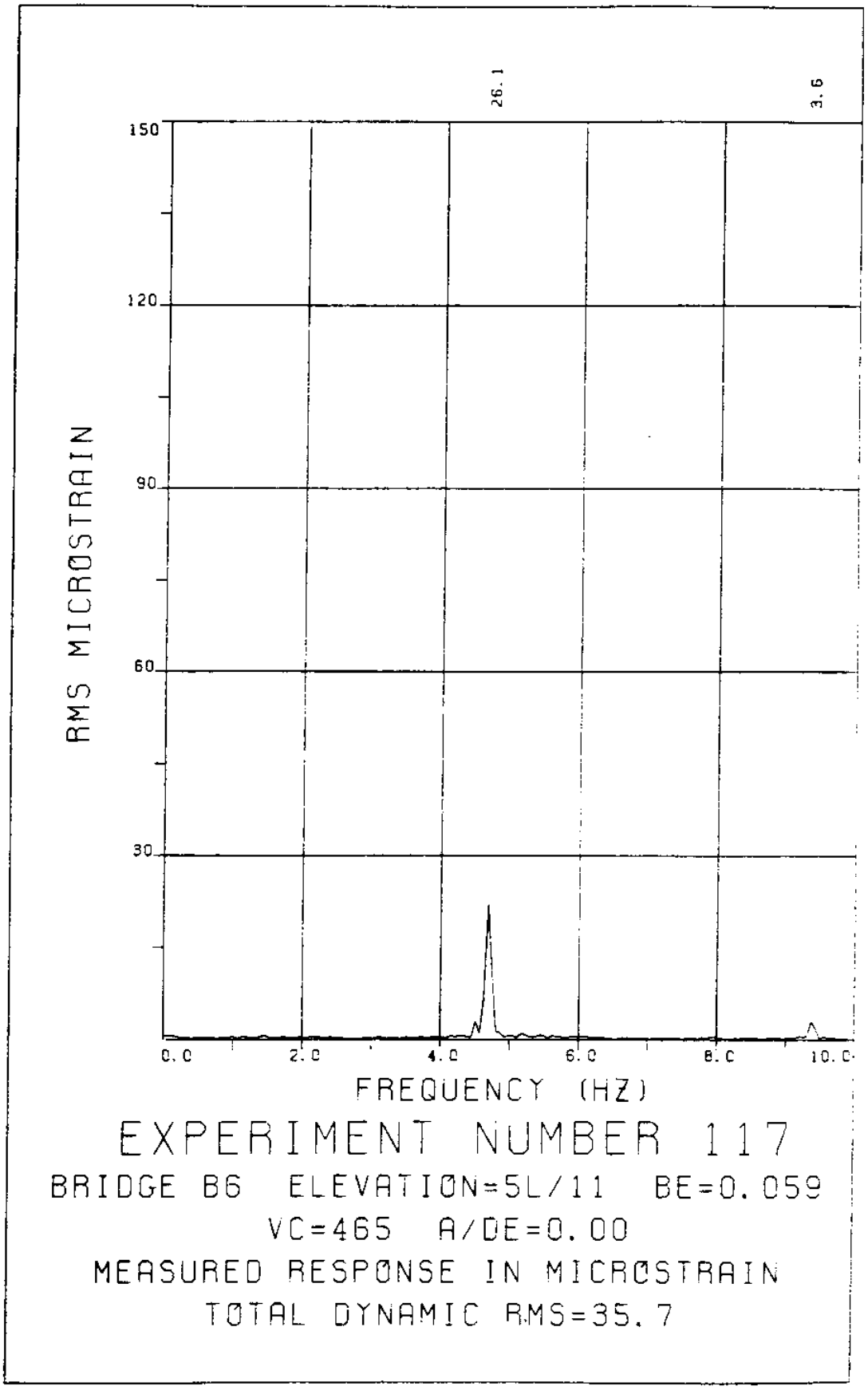

EXPERIMENT NUMBER 117

BRIDGE B6 ELEVATION=5L/11 BE=0.059

VC=465 A/DE=0.00

MEASURED RESPONSE IN MICROSTRAIN

TOTAL DYNAMIC RMS=35.7

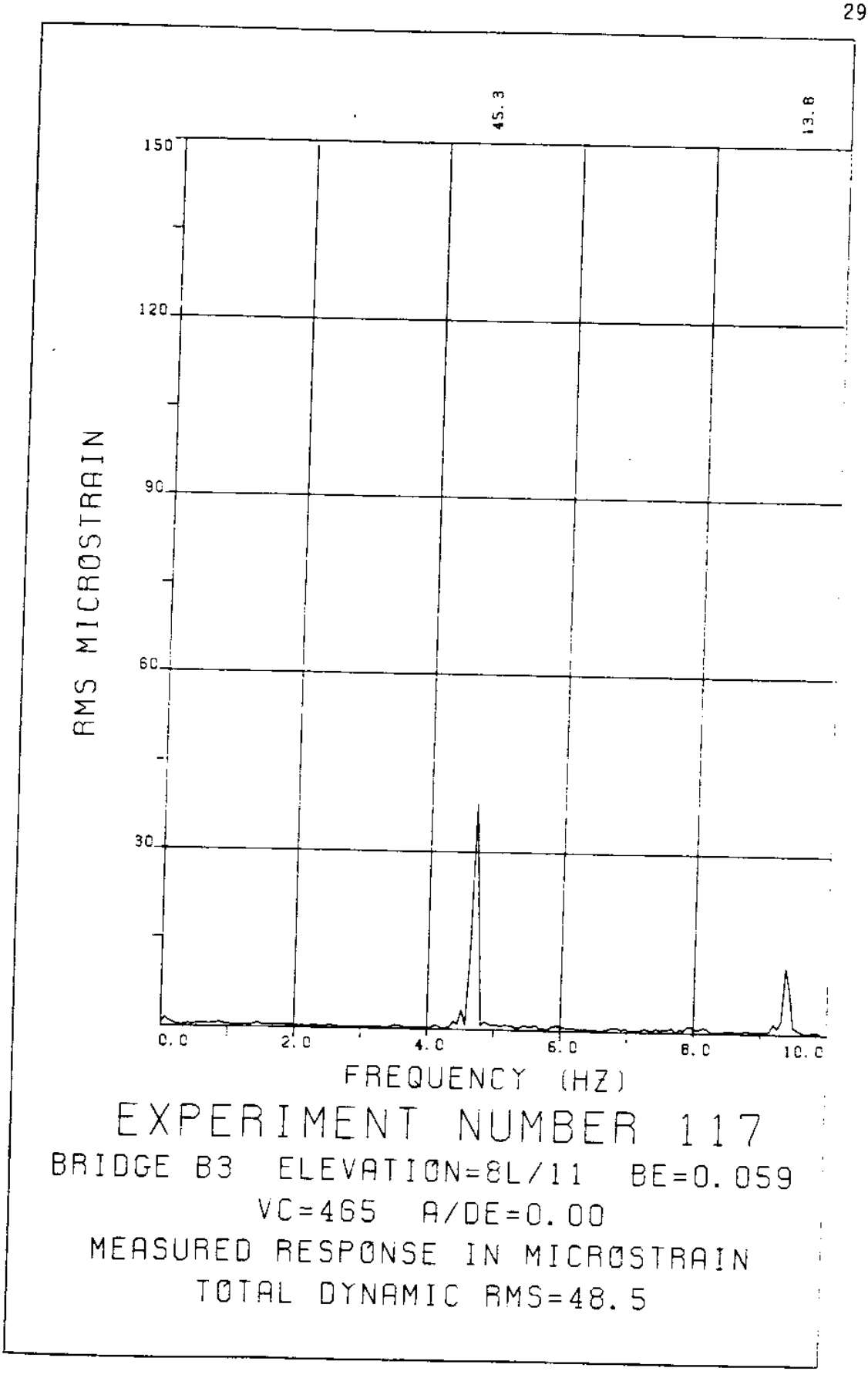

EXPERIMENT NUMBER 117

BRIDGE B3 ELEVATION=8L/11 BE=0.059

VC=465 A/DE=0.00

MEASURED RESPONSE IN MICROSTRAIN

TOTAL DYNAMIC RMS=48.5

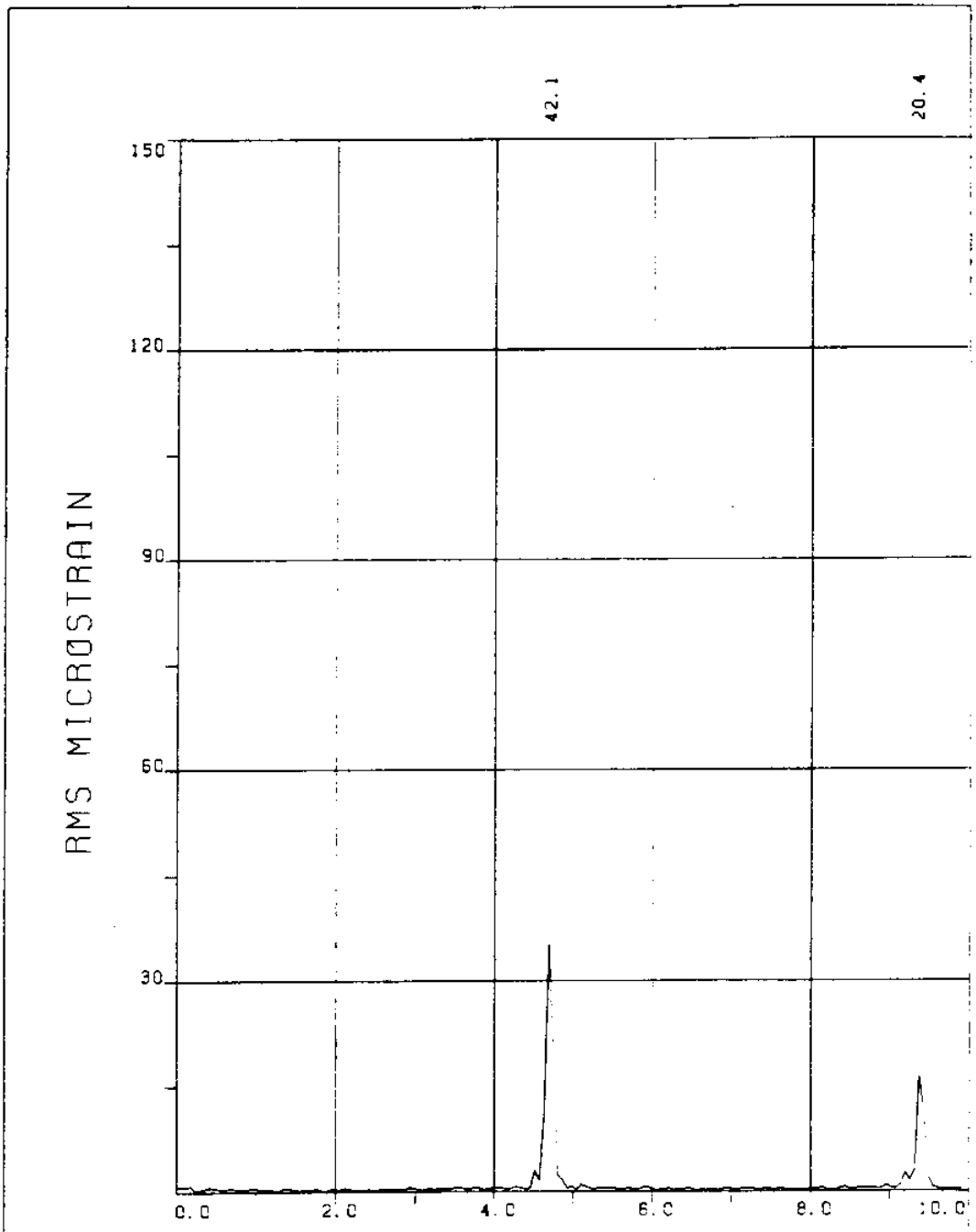

EXPERIMENT NUMBER 117

BRIDGE A9 ELEVATION=2L/11 BE=0.059

VC=465 A/DE=0.00

MEASURED RESPONSE IN MICROSTRAIN

MEAN=271.8

TOTAL DYNAMIC RMS=47.5

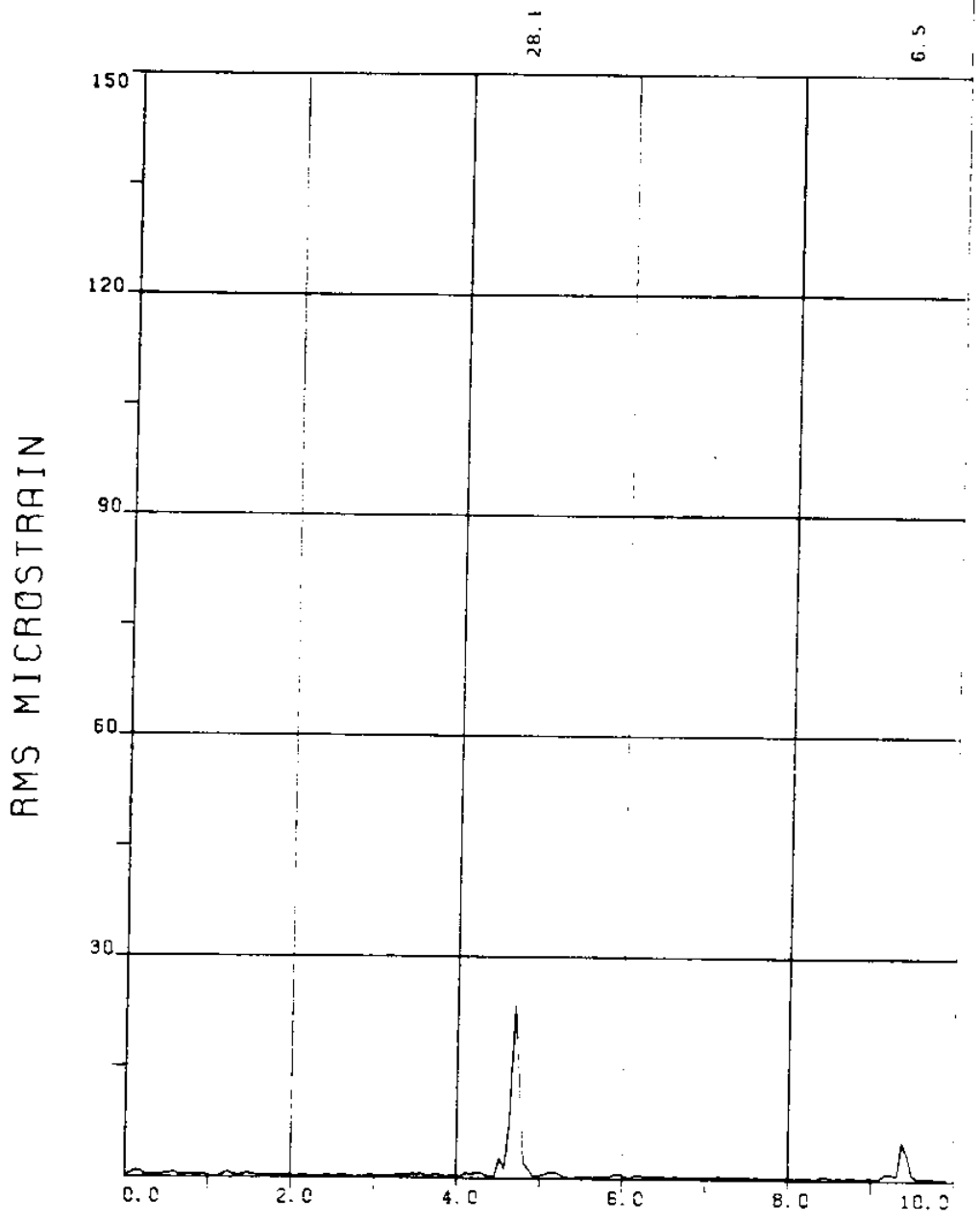

EXPERIMENT NUMBER 117

BRIDGE A7 ELEVATION=4L/11 BE=0.059

VC=465 A/DE=0.00

MEASURED RESPONSE IN MICROSTRAIN

MEAN=399.2

TOTAL DYNAMIC RMS=28.8

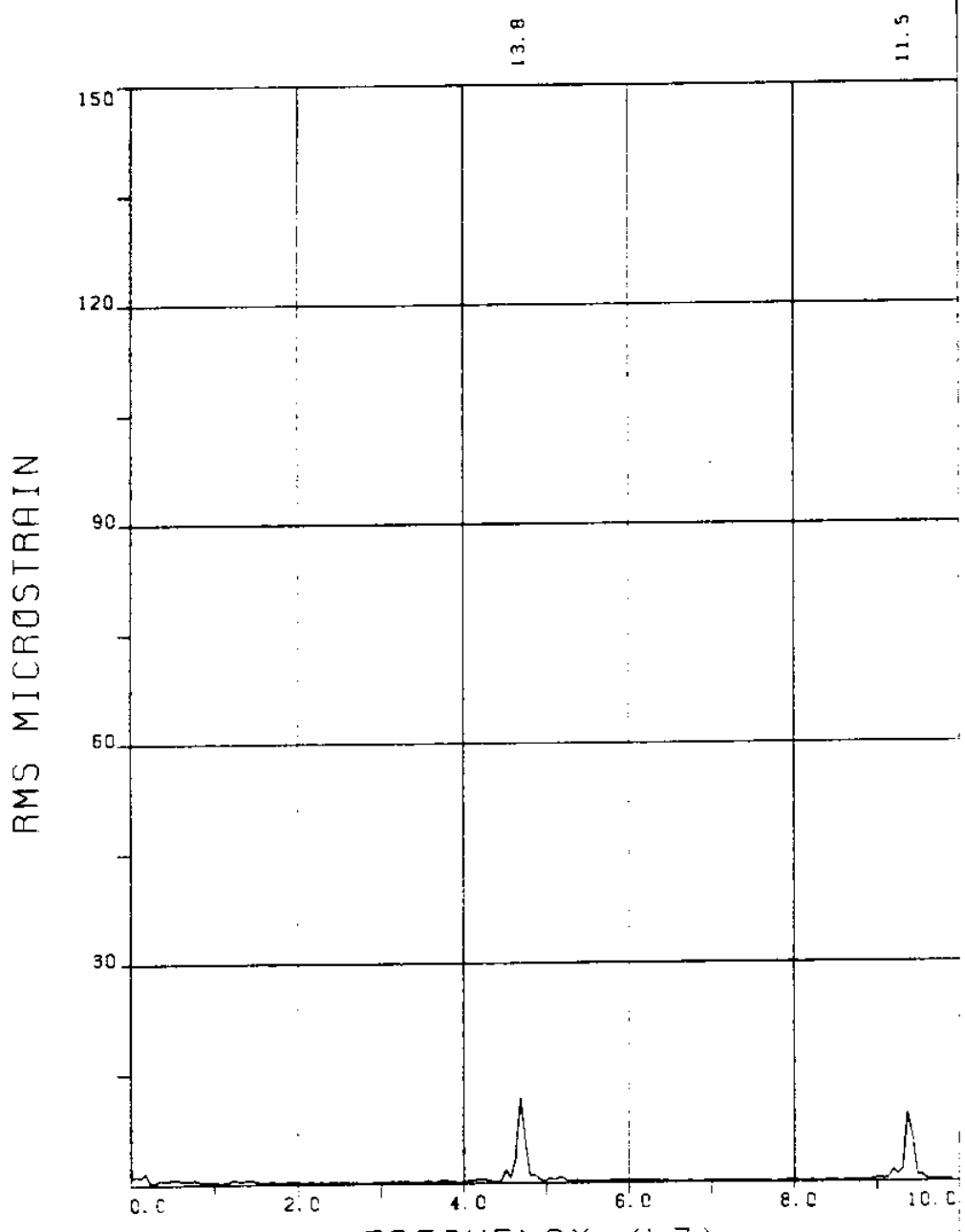

EXPERIMENT NUMBER 117

BRIDGE A6 ELEVATION=5L/11 BE=0.059

VC=465 A/DE=0.00

MEASURED RESPONSE IN MICROSTRAIN

MEAN=432.3

TOTAL DYNAMIC RMS=23.0

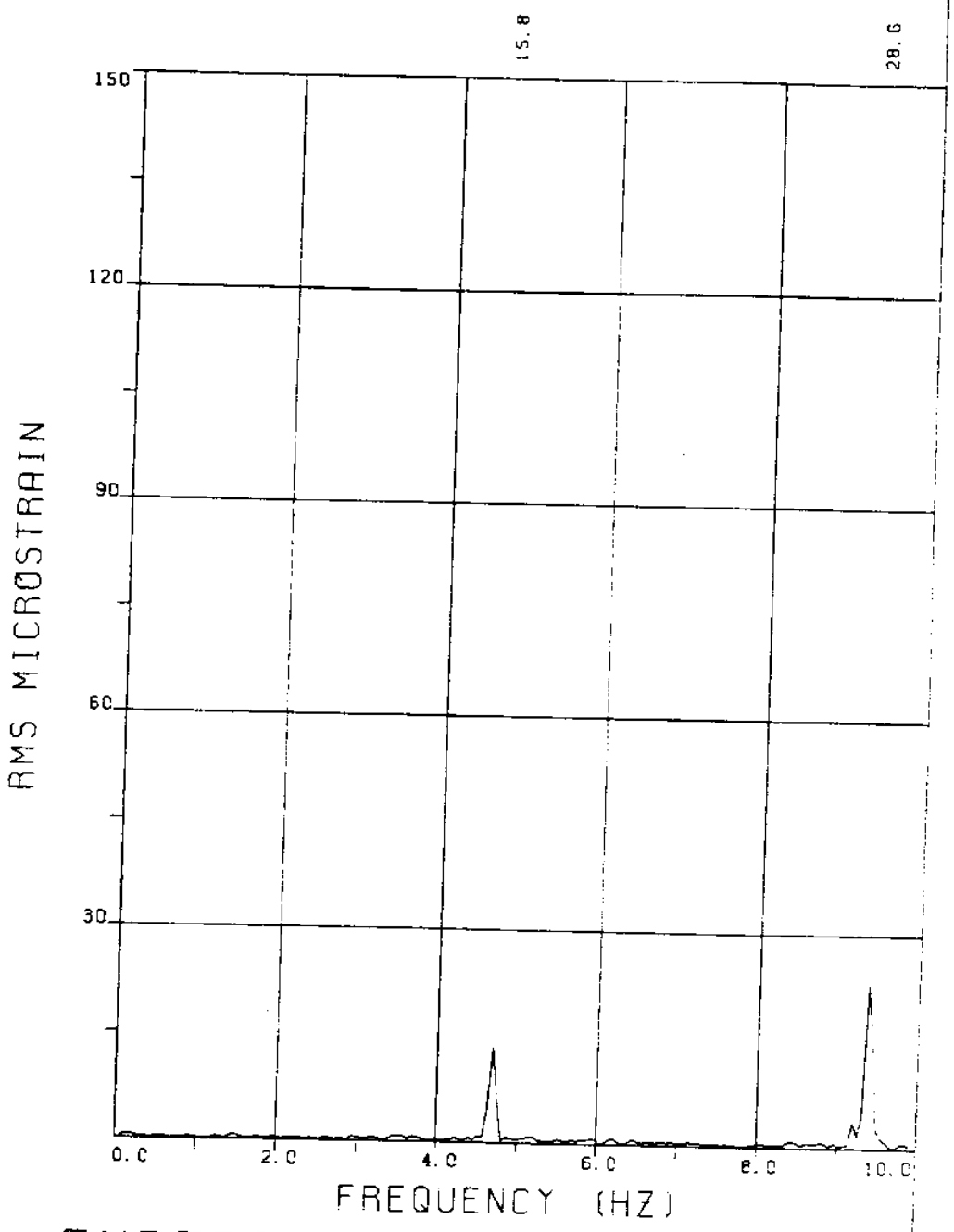

EXPERIMENT NUMBER 117

BRIDGE A3 ELEVATION=8L/11 BE=0.059

VC=465 A/DE=0.00

MEASURED RESPONSE IN MICROSTRAIN

MEAN=339.4

TOTAL DYNAMIC RMS=34.2

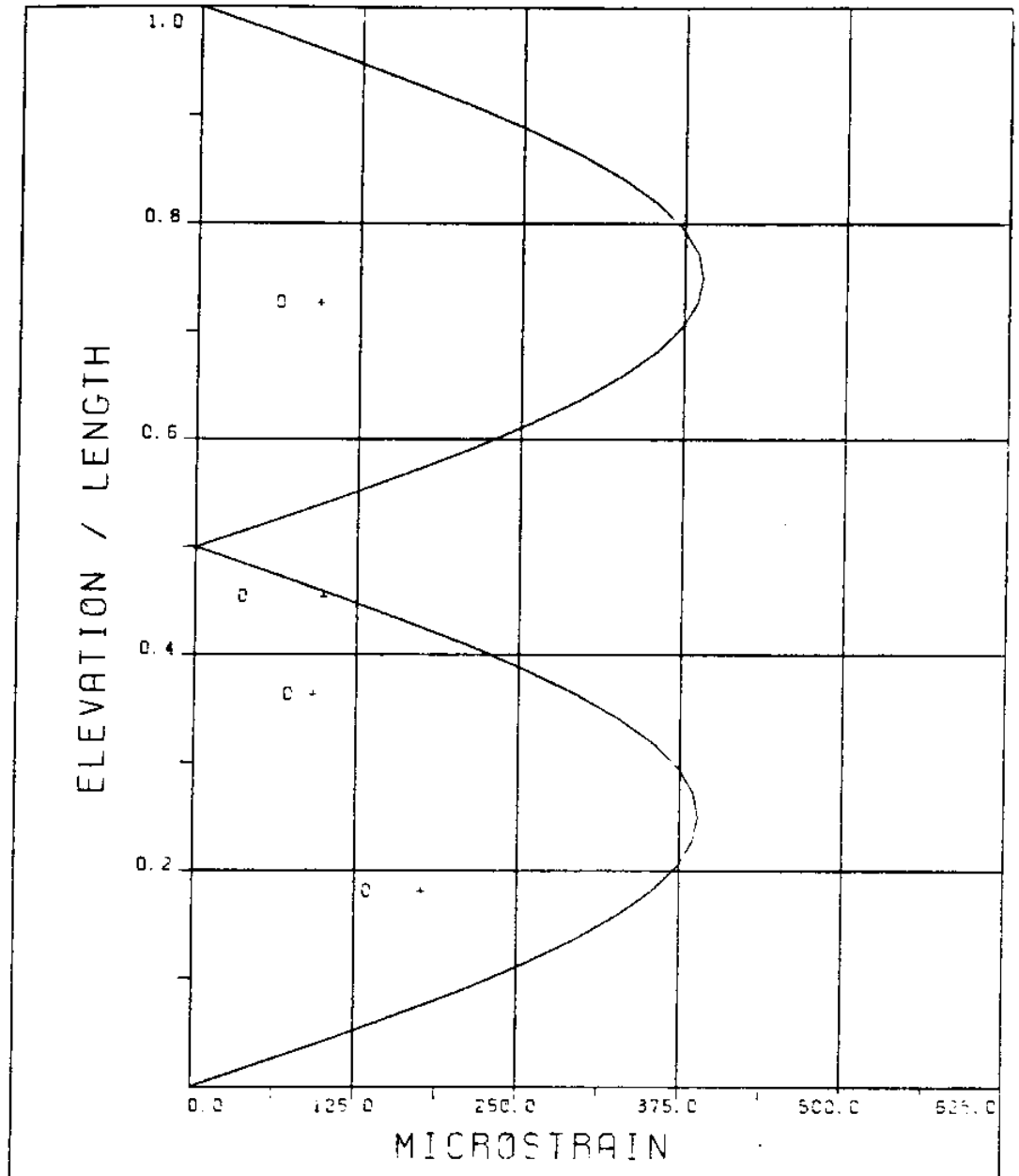

EXPERIMENT NUMBER 117

VC=465 A/DE=0.00

DYNAMIC RESPONSE AT F=FR IN PLANE B

——— THEORY o o o EXPERIMENT

MAXIMUM DYNAMIC RESPONSE IN PLANE B

——— THEORY + + + EXPERIMENT

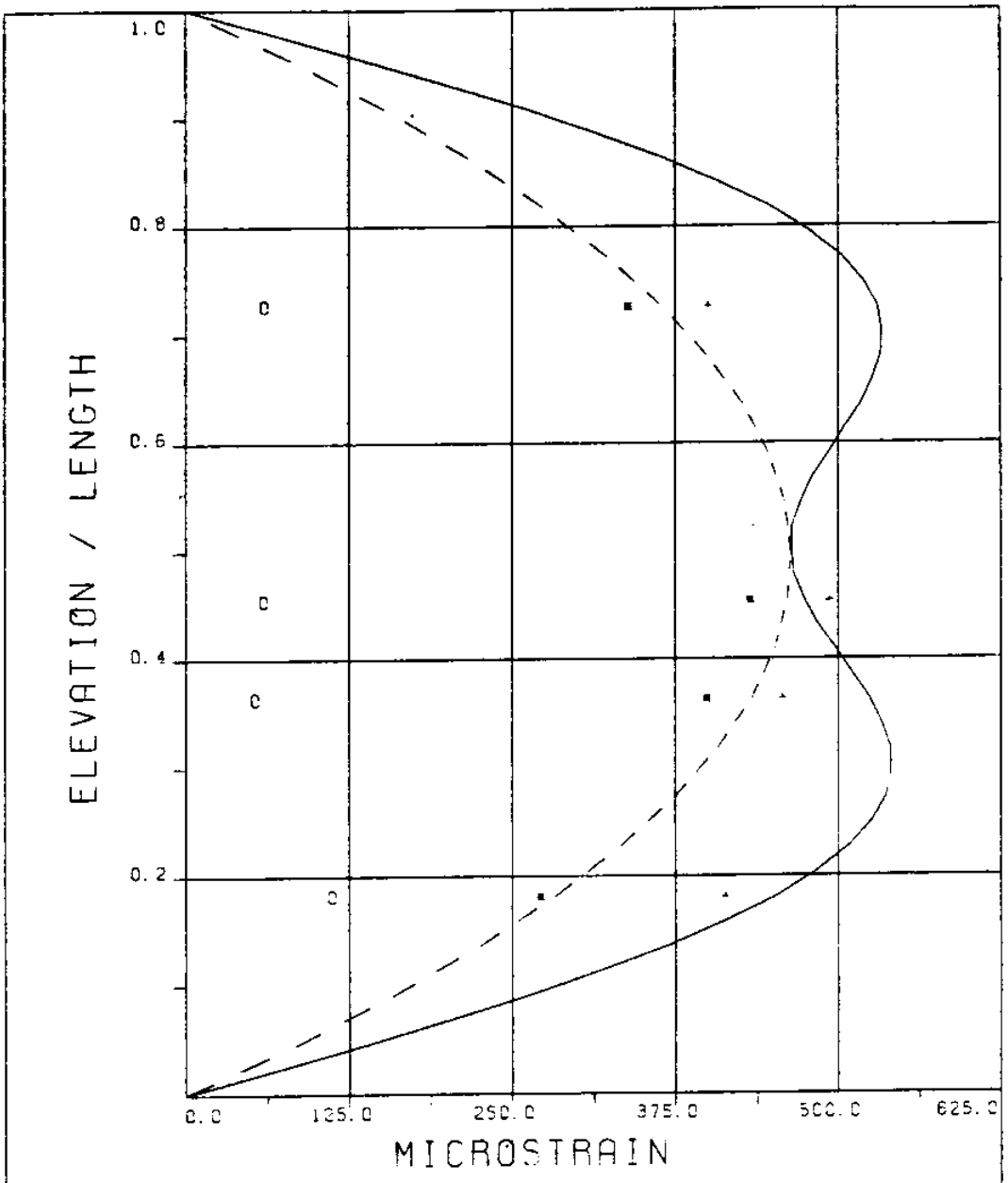

EXPERIMENT NUMBER 117

VC=465 A/DE=0.00

STATIC RESPONSE IN PLANE A

----- THEORY * * * EXPERIMENT

MAXIMUM DYNAMIC RESPONSE IN PLANE A

o o o EXPERIMENT

MAXIMUM RESPONSE

_____ THEORY + + + EXPERIMENT

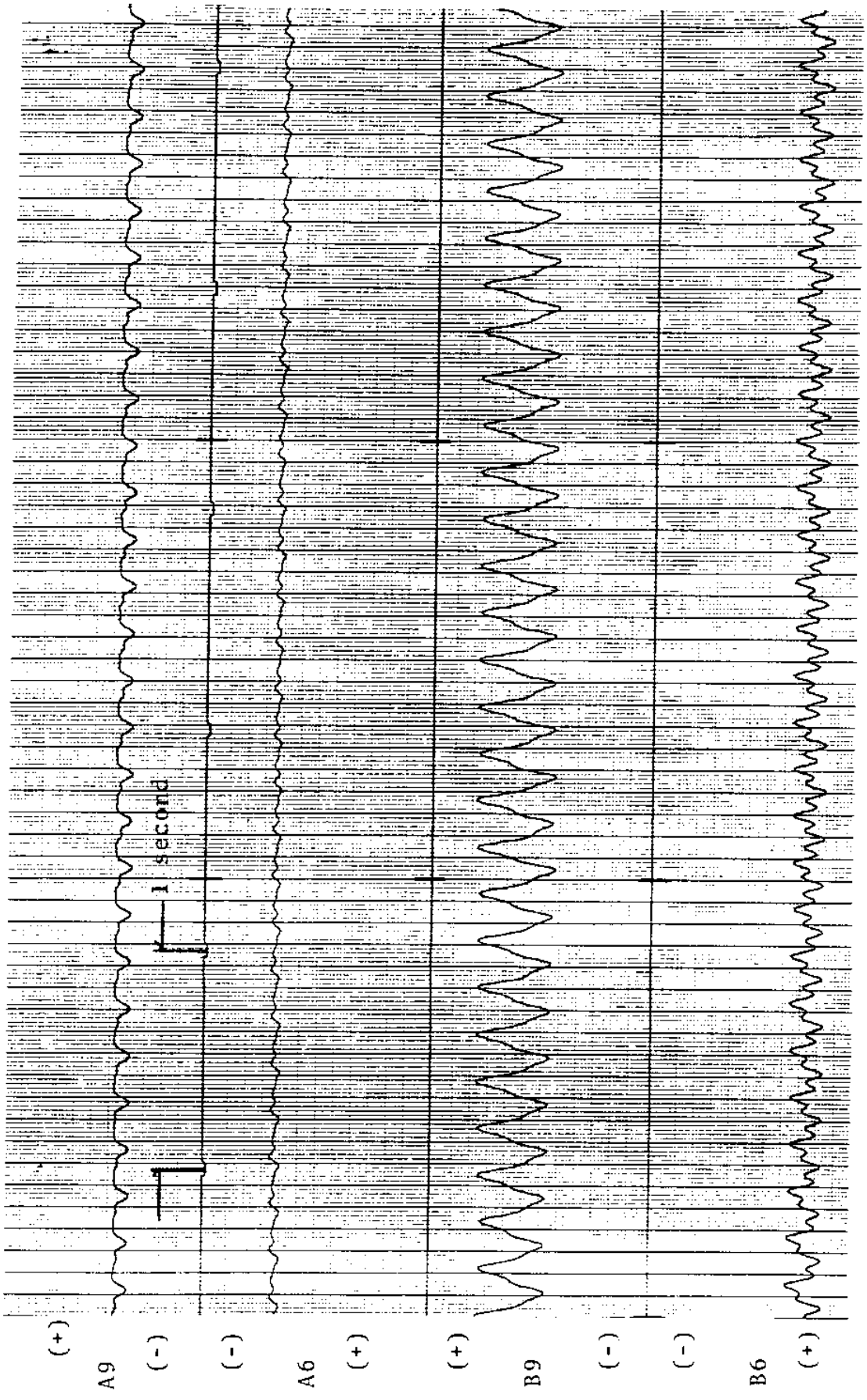

FIGURE 117Ta: A BRIDGES: 38.2 MICROSTRAIN/DIVISION
B BRIDGES: 15.3 MICROSTRAIN/DIVISION

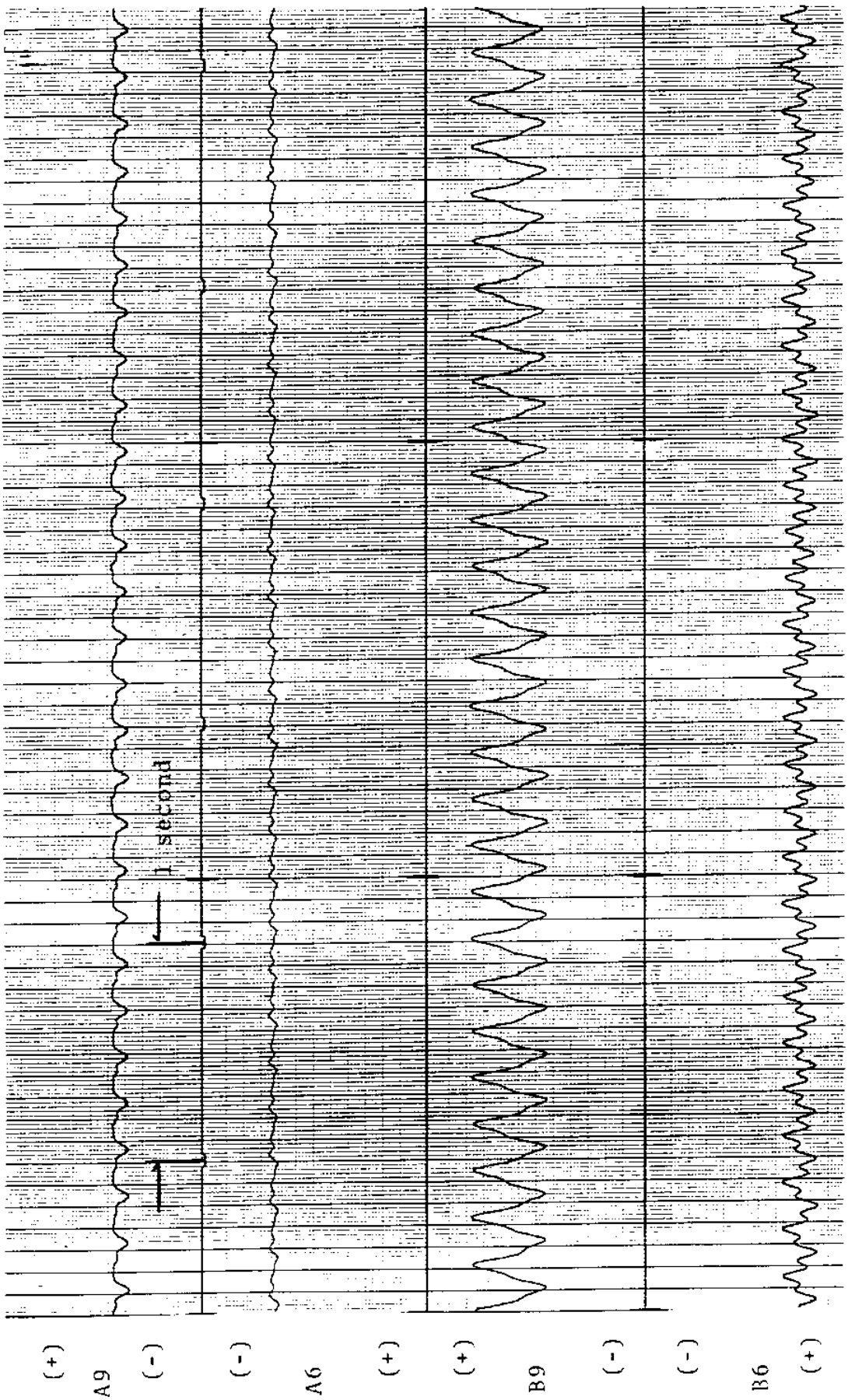

FIGURE 117Tb: A BRIDGES: 38.2 MICROSTRAIN/DIVISION
B BRIDGES: 15.3 MICROSTRAIN/DIVISION

4. REFERENCES

1. Bishop, R. E. D. and Hassan, A. Y., 1964, "The Lift and Drag Forces on a Circular Cylinder in a Flowing Fluid", Proceedings of the Royal Society, Series A, Vol. 277, pp. 32-50.

2. Dahlquist, G. and Björck, A., 1974, Numerical Methods, Prentice Hall, New Jersey.

3. Dean, R. B., Milligan, R. W. and Wootton, L. R., 1977, An Experimental Study of Flow Induced Vibrations, Atkins Research and Development, Epsom, Surrey, England, Report December 1977/1.

4. International Mathematical and Statistical Library (IMSL), Reference Manual, 1981, Edition 8, IMSL, Inc.

5. King, R., 1977, "A Review of Vortex Shedding Research and Its Application", Ocean Engineering, Vol. 4, pp. 141-171, London: Pergamon Press.

6. Mercier, J. A., 1973, Large Amplitude Oscillation of a Circular Cylinder in a Low Speed Stream, Ph.D. Thesis, Stevens Institute of Technology, Department of Mechanical Engineering, Ann Arbor, MI: University Microfilms Order No. UM74-884.

7. Moeller, M. J. and Leehey, P., 1982, "Measurements of Fluctuating Forces on an Oscillating Cylinder in a Cross Flow", Proceedings of the Third International Conference on the Behavior of Offshore Structures, August 1982, Vol. 2, pp. 681-689. New York: Hemisphere Publishing Co.

8. Patrikalakis, N. M., 1983, Theoretical and Experimental Procedures for the Prediction of the Dynamic Behavior of Marine Risers, Ph.D. Thesis, MIT, Department of Ocean Engineering.

9. Sarpkaya, T., 1977a, Transverse Oscillations of a Circular Cylinder in Uniform Flow, Naval Postgraduate School, Report No. NPS-69SL77071, Monterey, CA.

10. Sarpkaya, T., 1977b, "In-Line and Transverse Forces on Cylinders in Oscillatory Flow at High Reynolds Numbers", Journal of Ship Research, Vol. 21, No. 4, pp. 200-216.

11. Sarpkaya, T., 1979, "Vortex Induced Oscillations", Journal of Applied Mechanics, Vol. 46, pp. 241-258, June, 1979.

12. Staubli, T., 1983, "Calculation of the Vibration of an Elastically Mounted Cylinder Using Experimental Data from Forced Oscillation", Journal of Fluids Engineering, ASME Transactions, June 1983, Vol. 105, pp. 225-229.

13. Toebes, G. H., 1969, "The Unsteady Flow and Wake Near an Oscillating Cylinder", Journal of Basic Engineering, ASME Transactions, September 1969, pp. 493-505 and December, 1969, pp. 859-862.

14. Vandiver, J. K., 1983, "Drag Coefficients of Long Flexible Cylinders", Proceedings, 15th Offshore Technology Conference, Houston, TX, Vol. 1, Paper 4490.

15. Verley, R. L. P. and Moe, G., 1979, The Forces on a Cylinder Oscillating in a Current, Norwegian Institute of Technology, River and Harbour Laboratory, SINTEF Report No. STF60A79061.

APPENDIX A

Figure A-1: Rigid Cylinder Results

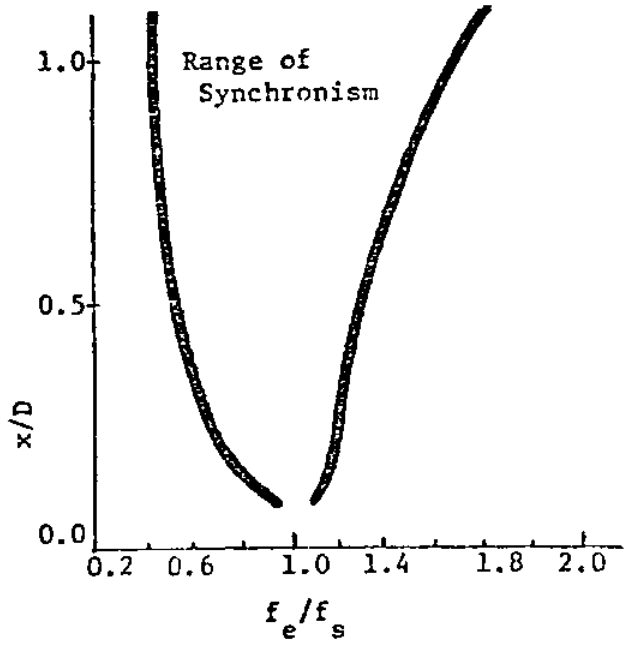

Range of Synchronism of Vortex Formation with Forced Oscillations Orthogonal to a Uniform Stream, adapted from Mercier (1973).

Figure A-2: Rigid Cylinder Results

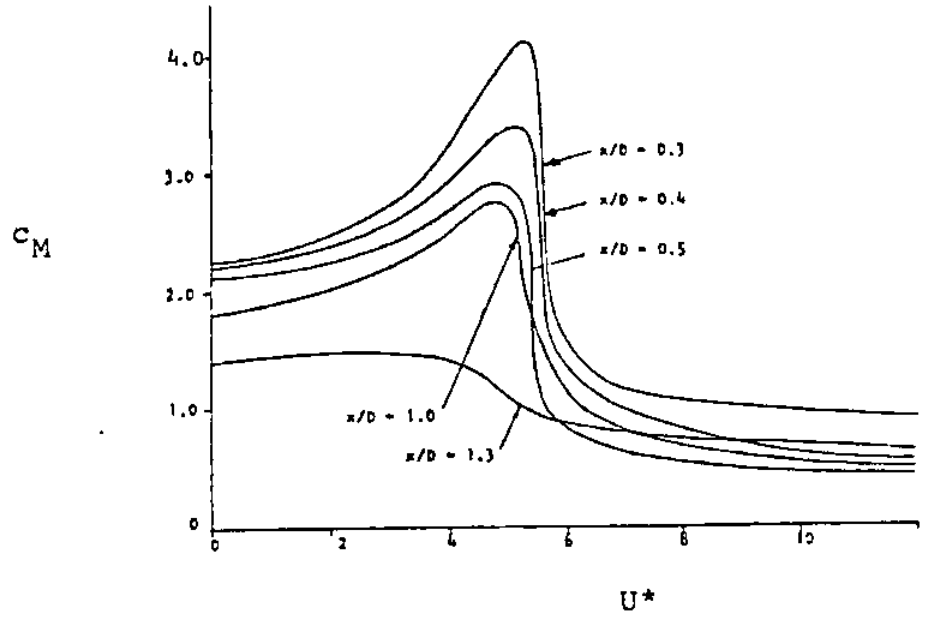

Inertia Coefficient c_M = Amplitude of Inertia Force Per Unit Length/$\rho A_o \omega^2 x+1$ as a Function of U^* Parametrically with Respect to x/D, for Sinusoid Oscillations Orthogonal to a Uniform Stream, Mercier (1973).

Nomenclature:

ρ Density of the Fluid

$A_o = \pi D^2/4$

D Cylinder Diameter

ω Circular Frequency of Oscillation

x Amplitude of Oscillation

$c_M = c_m + 1$

Figure A-3: Rigid Cylinder Results

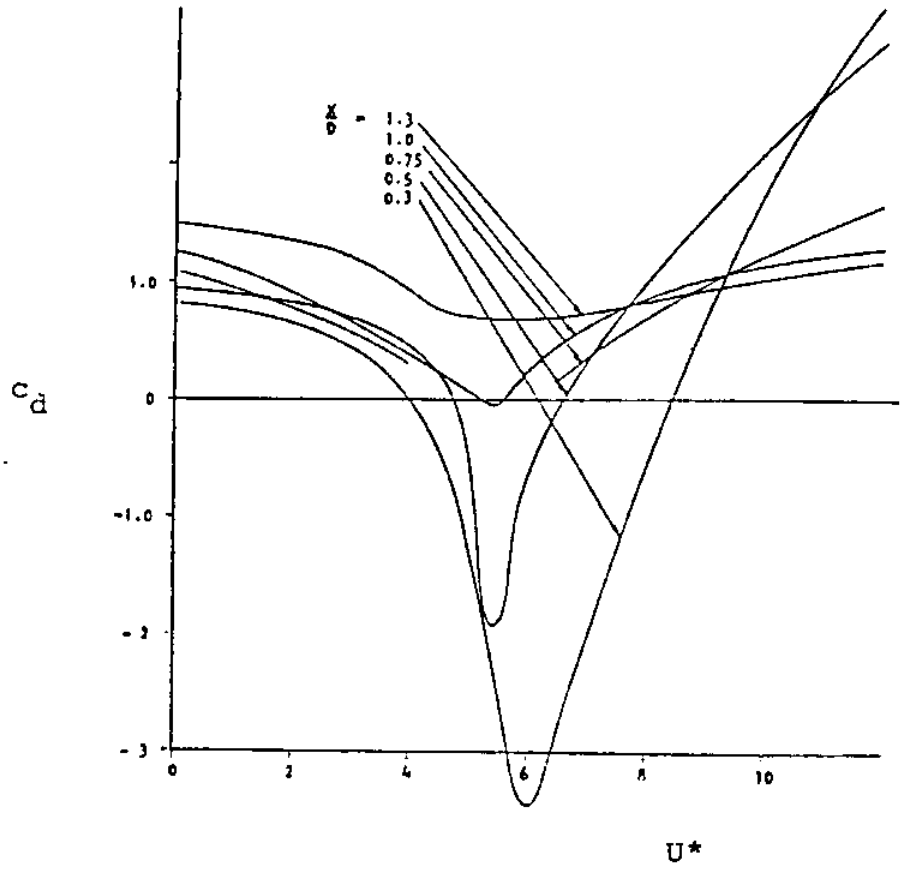

Drag Coefficient c_d = Amplitude of Drag Force Per Unit Length Parallel to the Oscillation/ $0.5\rho D\omega^2 x^2$ as a Function of U* Parametrically with Respect to x/D, for Sinusoid Oscillations Orthogonal to a Uniform Stream, Mercier (1973).

Figure A-4: Rigid Cylinder Results

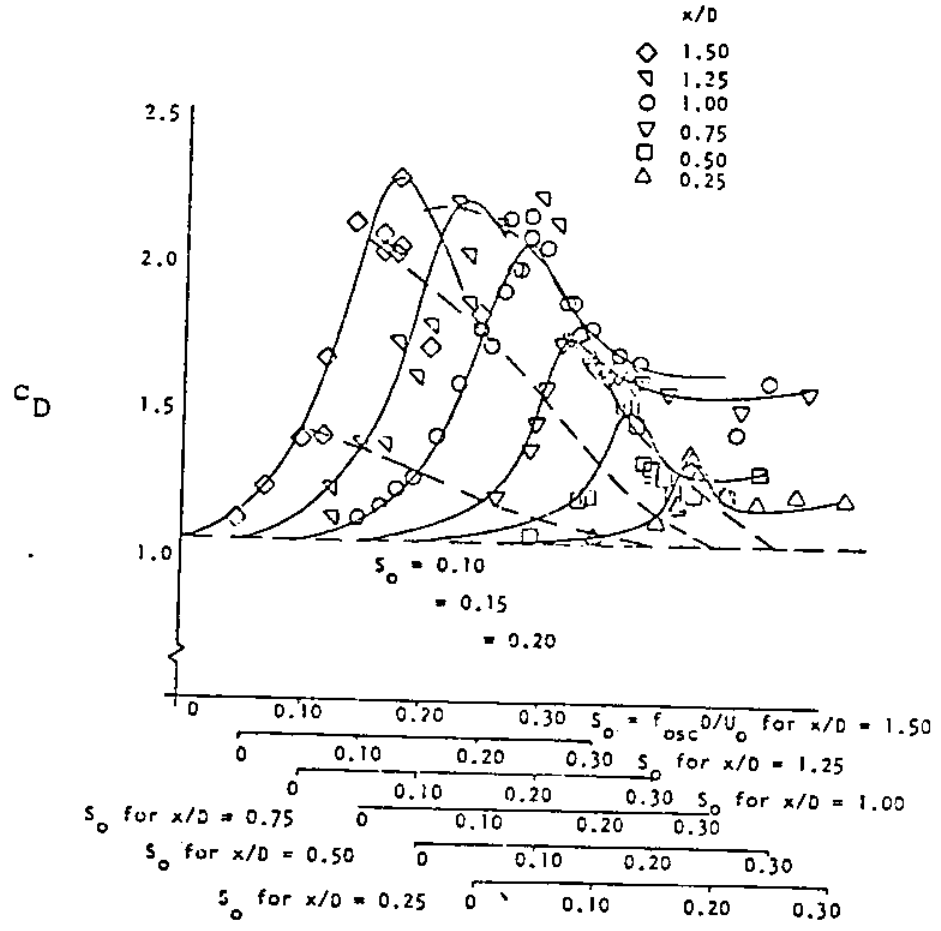

Average Drag Coefficient c_D = Average Drag Per Unit Length/$0.5\rho DV_c^2$ as a Function of S_o = $1/U^*$ Parametrically with Respect to x/D, for Sinusoid Oscillations Orthogonal to a Uniform Stream, Mercier (1973).

Figure A-5: Rigid Cylinder Results

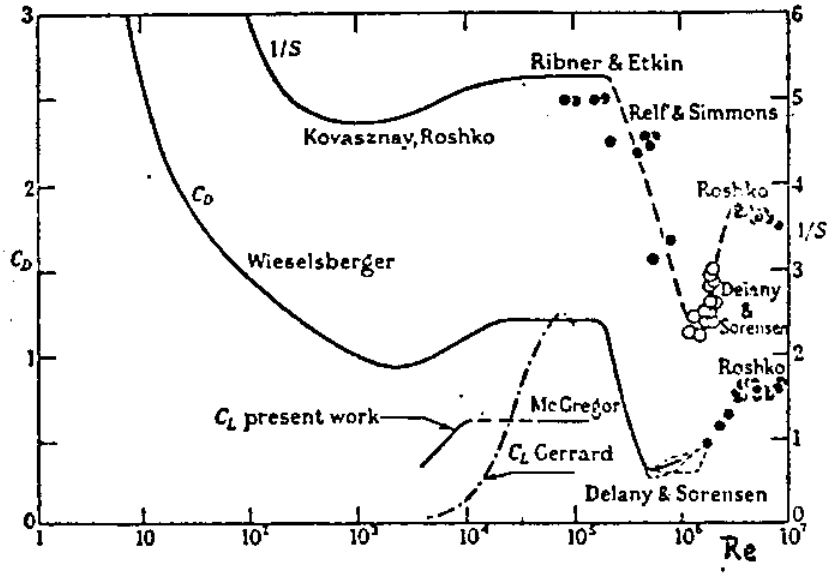

Average Drag Coefficient, Lift Coefficient and Strouhal Number for a Fixed Rigid Smooth Circular Cylinder in a Uniform Stream as a Function of Reynolds Number, Bishop and Hassan (1964).

APPENDIX B

PREDICTION OF THE RESPONSE OF A SPRING MOUNTED RIGID CYLINDER IN A UNIFORM STREAM USING RIGID CYLINDER EXPERIMENTS

Let us consider a rigid cylinder of mass M, diameter D_e, and length L, mounted on elastic springs of stiffness K, and dashpots of coefficient c, and permitted to respond orthogonally to a uniform stream. The basic assumption in the subsequent analysis is that the response motion $x(\hat{t})$ is monochromatic, i.e.:

$$x(\hat{t}) = A\sin(\hat{\omega}\hat{t}) \qquad (B.1)$$

with unknown amplitude, A, and circular frequency, $\hat{\omega}=2\pi f$. Under this assumption, estimates of the overall hydrodynamic force orthogonal to the stream $F^X(\hat{t})$, can be made from corresponding forced sinusoid motion rigid cylinder experiments using equation (1).

The displacement, $x(\hat{t})$, obeys the following equation:

$$Mx_{\hat{t}\hat{t}} + cx_{\hat{t}} + Kx = F^X(\hat{t}) \qquad (B.2)$$

where subscript $\hat{t}$ denotes derivative with respect to time.

Introducing equations (1) and (B.1) in equation (B.2), we find the following two simultaneous nonlinear equations to determine $U^*=2\pi V_c/\hat{\omega}D_e$ and non-zero values of $a=A/D_e$:

$$\frac{m+c_m}{U^{*2}} = \frac{m+1}{U^{*2}_n} \tag{B.3}$$

$$\frac{a\ c_d}{U^*} = -\frac{3\pi}{16}\ \frac{\delta[m+1]}{U^*_n} \tag{B.4}$$

where

m = $M/\rho A_e L$, mass to displaced fluid mass ratio;

A_e = $\pi D_e^2/4$, cross sectional area of the cylinder;

δ = $\pi\, c(KM_e)^{-1/2}$, a logarithmic decrement

U^*_n = $V_c/f_n D_e$, a reduced velocity based on the "natural frequency" f_n;

f_n = $(K/M_e)^{1/2}/2\pi$, and

M_e = $M + \rho A_e L$.

For a fixed value of V_c, equations (B.3) and (B.4) can be solved numerically for "a" and U*. Once "a" and U* are known, the average drag coefficient c_D can be determined, for example, from Figure A-4, taken from Mercier (1973).

It should be noted that equations (B.3) and (B.4) are similar in form to equations (25) and (26) respectively.

A comparison of the results of our procedure with a spring mounted rigid cylinder experiment is shown in Figure B-1. The experimental data shown in Figure B-1 are derived from Dean et al. (1977). Information about our theoretical prediction is given in Table B-1. The maximum calculated amplitude underpredicts the maximum measured amplitude by less than 16%. Possible explanation for this difference is that in our prediction, Reynolds number and aspect ratio were not scaled correctly. Another possible explanation is that the values of c_m and c_d from available rigid cylinder experiments are not very accurate. For example, rigid cylinder results from Mercier (1973) and Sarpkaya (1977a) show large discrepancies. As noted in Sarpkaya (1977a), lack of resolution led Mercier (1973) to occasionally fair his experimental data in a misleading way. Mercier's (1973) data have been digitized and used in our work because they extend to larger values of "a", which are of particular interest for large amplitude forced oscillations of flexible cylinders, Patrikalakis (1983). From Figure B-1 we also see that for $U_n^* \geq 5.75$ approximately, we have been unable to find a non-zero solution for "a" from equations (B.3) and (B.4). The most probable explanation for this is that our assumption for the response, see equation (B.1), is no longer valid.

An analysis similar to the one presented in this Appendix has been published concurrently by Staubli (1983) and corroborates our findings.

U_n^*	U^*	f (Hz)	a	c_m	c_d
3.75	4.78	1.69	0.23	3.46	-1.87
4.00	5.02	1.72	0.29	3.25	-1.46
4.25	5.07	1.80	0.37	2.67	-1.11
4.50	5.15	1.88	0.45	2.21	-0.86
4.75	5.29	1.93	0.63	1.95	-0.60
5.00	5.31	2.02	0.66	1.51	-0.55
5.25	5.32	2.12	0.69	1.11	-0.50
5.50	5.34	2.22	0.71	0.77	-0.47

Table B-1: Information about the Prediction of the Response of the Spring Mounted Cylinder of Figure B-1.

Figure B-1: Comparisons of Spring Mounted Rigid Cylinder Response with Theoretical Predictions

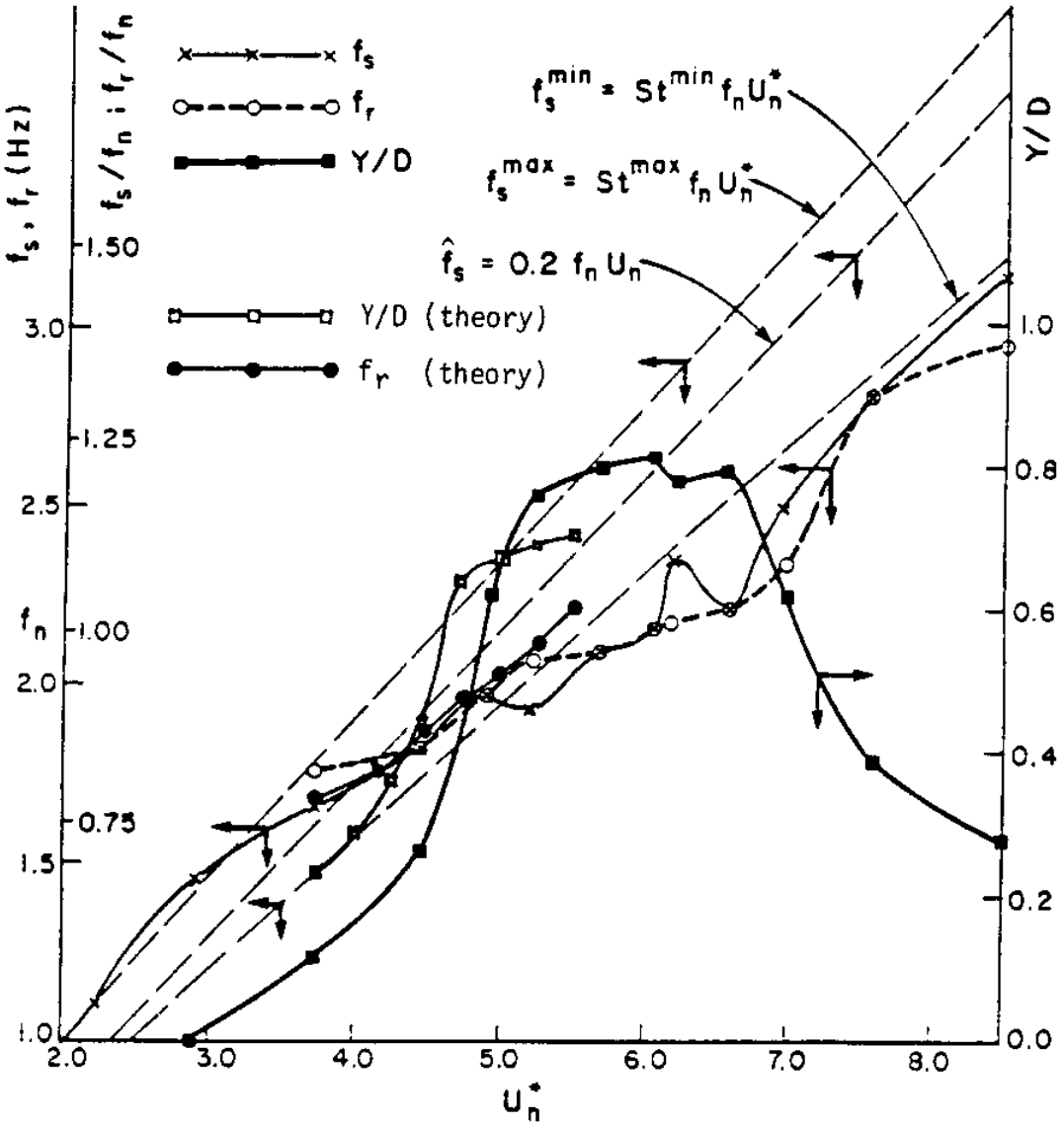

Plots of the Measured Vortex "Shedding" Frequency, f_s, the Measured and Calculated Response Frequency, f_r, and the Measured and Calculated Non-Dimensional Response Half Amplitude, Y/D, for a Smooth Spring Mounted Rigid Cylinder Oscillating Orthogonally to a Uniform Water Stream. Measured Data are Derived from Dean, et al. (1977). Model Characteristics: f_n=2.15 Hz, D=25.4 mm, m=2.93, $\lambda \simeq 13$, δ=0.147, K_s=0.91, Re≃2680 to 10370.

NOMENCLATURE FOR ADDITIONAL SYMBOLS SHOWN IN FIGURE B-1

$D = D_e$

$\lambda = L/D$

$K_s = 2\delta M_e/\rho D^2 L$

$Re = V_c D/\nu$

St^{max}, St^{min} Envelopes of Strouhal Number for a Fixed Rigid Cylinder in a Uniform Stream, Derived from Figure 2 of Chapter IV of Patrikalakis (1983).

$\hat{f}_s$ is the Frequency of Lift on a Fixed Rigid Cylinder in a Uniform Stream, Corresponding to a Strouhal Number, $St=\hat{f}_s D/V_c$, equal to 0.2.

f_s is the Vortex "Shedding" Frequency Measured in the Wake of the Spring Mounted Cylinder.

f_r is the Frequency of Primary Lift Motion of the Spring Mounted Rigid Cylinder.